AD_____

Award Number: W81XWH-06-2-0044

TITLE: The Development of Therapeutic and Diagnostic Countermeasures to WMD by the Advanced Medical Countermeasures Consortium

PRINCIPAL INVESTIGATOR: Milton G. Smith, M.D.

CONTRACTING ORGANIZATION: University of Michigan Medical School
Ann Arbor, MI 48109

REPORT DATE: September 2008

TYPE OF REPORT: Annual

PREPARED FOR: U.S. Army Medical Research and Materiel Command
Fort Detrick, Maryland 21702-5012

REPORT DOCUMENTATION PAGE

Form Approved
OMB No. 0704-0188

1. REPORT DATE *(DD-MM-YYYY)*	**2. REPORT TYPE**	**3. DATES COVERED** *(From - To)*
01-09-2008	Annual	21 AUG 2007 - 21 AUG 2008

4. TITLE AND SUBTITLE

The Development of Therapeutic and Diagnostic Countermeasures to WMD by the Advanced Medical Countermeasures Consortium

5a. CONTRACT NUMBER

5b. GRANT NUMBER
W81XWH-06-2-0044

5c. PROGRAM ELEMENT NUMBER

6. AUTHOR(S)
Milton G. Smith, M.D., Peter A. Ward, M.D.

E-Mail: pward@umich.edu

5d. PROJECT NUMBER

5e. TASK NUMBER

5f. WORK UNIT NUMBER

7. PERFORMING ORGANIZATION NAME(S) AND ADDRESS(ES)

University of Michigan
Ann Arbor, MI 48109-1274

8. PERFORMING ORGANIZATION REPORT NUMBER

9. SPONSORING / MONITORING AGENCY NAME(S) AND ADDRESS(ES)
U.S. Army Medical Research and Materiel Command
Fort Detrick, Maryland 21702-5012

10. SPONSOR/MONITOR'S ACRONYM(S)

11. SPONSOR/MONITOR'S REPORT NUMBER(S)

12. DISTRIBUTION / AVAILABILITY STATEMENT
Approved for Public Release; Distribution Unlimited

13. SUPPLEMENTARY NOTES
Project 2: Development of STIMAL to Protect Against CEES-induced Lung Injury in Rat

14. ABSTRACT

Acute lung injury in rats following airway delivery of CEES is associated with loss of distal lung barrier function (resulting in alveolar flooring) and an intense inflammatory response, which is lung-damaging. These acute lung injury parameters are attenuated by neutrophil depletion or complement blockade. Injuring the redox balance in lung after exposure to CEES by administration into lung of liposomes containing antioxidant compounds is highly protective even when delivery of liposomes is delayed by at least 1 hr. CEES-induced lung injury is progressive, as manifested by development of interstitial fibrosis which seems to peak at three weeks. Whether STIMAL will attenuate development of lung fibrosis is currently unknown.

15. SUBJECT TERMS
Parallel Synthesis: Biocatalytic Amplification; Drug Discovery; Chemotherapeutics; Lead Lead Optimization

16. SECURITY CLASSIFICATION OF:			**17. LIMITATION OF ABSTRACT**	**18. NUMBER OF PAGES**	**19a. NAME OF RESPONSIBLE PERSON**
a. REPORT	**b. ABSTRACT**	**c. THIS PAGE**			USAMRMC
U	U	U	UU	399	**19b. TELEPHONE NUMBER** *(include area code)*

Standard Form 298 (Rev. 8-98)
Prescribed by ANSI Std. Z39.18

Amaox, Ltd.

Overview of Work by the Advanced Medical Countermeasures Consortium 2006-08

Table of Contents

Amaox, Ltd.

Statement of work

Task 1- Telephone contact and/ or visitations with the investigators are done on a weekly basis (more frequently). These contacts with the investigators will be on going throughout the project by which real time integration and placement of information into the clinical context.

There was frequent telephone contact with all of the investigators.

Task 2- Develop experimental modifications based on newly gained information from the members of the group.

There was greater emphasis put on anthrax in the APC Biosensor experiments.
Persuant to one of the conversations that I had with Rick Rest (Drexel University) it was decided to titrate either the antioxidant levels or spores to examine the reductive effect of the antioxidants. This slight modification was important in elucidating the mechanism of action of the antioxidants.

Task 3- Continue guidance of the development of the APC Biosensor and STIMAL

This consistently was done through the life of the project.

Task 4- Act as an interface between governmental agencies and the Consortium
Communication has been established with the FDA, USAMRICD, USAMRIID, USDA and DTRA. These agencies were contacted in order to establish collaborations involving the developed technologies.
Task 5 -Assurance that reports and other paper work involving the consortium are done in a timely manner.
This has been done throughout the project.
Task 7- Supportive services for the investigators
As needed.
Task 8- Arrange for annual meetings for the Consortium
This was done in 2007 and 2008.
Task 9- Chair annual meetings
This was also done in 2007 and 2008.
Task 10- Design experimental goals for both technologies as it applies to the individual projects in each funding cycles
This was done at the beginning of the each funding cycle.

Amaox, Ltd.

Introduction

Most of the tests and treatments that are being developed as countermeasures to weapons of mass destruction (inclusive of biological, chemical and radiation) target a singular agent. There is merit to this approach, and it has served us well in past, but it does have shortcomings. That being said, a dilemma does exist in that there is an imbalance between the number of countermeasures which have been developed and the vast number of WMD. The existence of this inequity creates a significant vulnerability in civilian and military defenses.

One way in which the inequities between the number of WMD and the countermeasures could be addressed is to develop platform technologies that would have broad applications in treatments (Cowan et al., 2003) and diagnostics (Briese et al., 2005). The Advanced Medical Countermeasures Consortium has begun to address these inequities by developing two unique technologies that have broad applications. One of the countermeasures could be used as an ancillary treatment; the other would be a diagnostic countermeasure.

STIMAL, one of the two technologies, is a treatment. It consists of liposome encapsulated antioxidants that can be delivered topically, intravenously, or by aerosol. We have used both fat soluble and water soluble antioxidants encapsulated in liposomes. A differential effect in tissue protection has been observed depending on the isomer of vitamin E that was used in studies done with CEES (the mustard gas analogue, a chemical weapon). In the CEES exposed tissues STIMAL could decrease proinflammatory cytokines, oxidants, apoptosis and recruitment of inflammatory cells. Antioxidants also have an ameliorative effect on the germination of Bacillus anthracis spores.

Enhancement of antioxidants in the microenvironment induces cells to shift their redox potential to a more reductive state (Schafer and Buettner, 2001). In contrast, cells shift to an oxidative potential in areas of inflammation. The redox potential modulates redox sensitive components of the cells such as transcription factors or receptors. For instance, the transcription factor NFkB activity is down regulated with enhancement of intracellular antioxidant levels (Schafer and Buettner, 2001). In vitro studies using anthrax, antioxidants reduced spore receptors. These receptors appear to be responsible for inhibition of germination (manuscript in preparation- Rick Rest).

The APC Biosensor, the other technology, uses antigen presenting cells (APC-monocytes and dendritic cells) to diagnose disease. The APC Biosensor is anticipated to be most useful in diagnosing subclinical disease (e.g., infectious disease). Subclinical disease diagnosis detection has been problematic for military and civilian medicine alike. In general the state of the art diagnostic technologies are not adept at diagnosing subclinical infectious disease in man or animal. STIMAL and the APC Biosensor are two evolving technologies that may significantly impact biochemical defense.

Background

All of the vesicants induce an acute inflammatory reaction (Naghii, 2002; Ricketts et al., 2000) ; Sciuto, 1998; Segal and Lang, 2005; Sidell et al., 1997). A subcomponent of inflammation is oxidative stress (Bartsch and Nair, 2006). A consequence of oxidative stress (OS) is the oxidation of thiol groups, which is seen in all of the vesicant exposures (Carr et al., 2001; Pant et al., 2000; Vissers and Winterbourn, 1995).

Amaox, Ltd.

The oxidation of thiol groups disrupts redox balance, which can set into motion a cascade of events, such as apoptosis, oxidant production, and increased activity of redox regulated transcription factors (e.g., NFkB). In addition to the vesicants, there are other weapons of mass destruction that also induce OS radiation (Kang et al., 2006), bacterial infections (e.g. anthrax) (Hanna et al., 1994; Kuhn et al., 2006), viral infections (e.g. influenza (Ghezzi and Ungheri, 2004), and ricin (Kumar et al., 2003; Suntres et al., 2005) exposures. Sublethal oxidative stress induces varying degrees of damage in cellular organelles. Lethal oxidative stress occurs when antioxidant defenses completely fail, resulting in necrosis (Virag, 2005) or apoptosis (Haddad, 2004). Antioxidant defenses that are critical to the maintenance of redox balance are also discussed.

A significant component of acute inflammation is oxidative stress (OS) (Nonas et al., 2006). OS involves the production of oxidants and proinflammatory cytokines (PICS). It is defined as an imbalance of the antioxidant/oxidant ratio, which has a consequent effect on gene expression. Thiol groups that are part of intracellular proteins and glutathione are critical for the maintenance of redox homeostasis. The vesicants as a class are either oxidants themselves, or they indirectly produce oxidants.

Sulfur mustard is commonly referred to as an alkylating agent, but recent evidence has shown it to be a potent inducer of oxidants (Levitt et al., 2003; McClintock et al., 2006) . Additionally, its destructive effects are not localized to the site of application; remote cells and tissues also become affected. An important molecular target of SM is DNA. Sulfur mustard damages the DNA mainly by alkylating and cross-linking the purine bases (Fox and Scott, 1980). Cysteine groups are present on proteins sensitive to SM, resulting in covalently crosslinked dimers (Byrne et al., 1996). This cross-linking causes conformational change, or dysfunction of enzymes. The potent alkylating activity of SM is due to the formation of highly electrophilic ethylene episulphonium derivative (Gautam et al., 2006; Papirmeister et al., 1985). Sulfur mustard is known to be a radiomimetic and therefore shares several properties with radiation (Butler et al., 1950). Both radiation and mustards induce apoptosis, OS, and burns. Sulfur mustard is known to induce apoptosis by Ca^{2+} calmodulin and caspase dependent pathway (Rosenthal et al., 1998).

Anthrax

Early treatment of anthrax inhalation carries a high success rate. In contrast late treatment for systemic symptoms from inhalation of the spores has a 100% mortality rate (Dixon et al., 1999). The gastrointestinal route of infection carries a variable mortality rate but can approach 100%. Cutaneous infections are the most common clinical cases and have a high cure rate. Once systemic illness occurs the patient will have “flu like” symptoms which are chills, chough, aches, etc. In the advance stages of the disease a bacteremia occurs, progressing to shock and sudden death. The mechanism of actual death of the host is unknown, but is believed to but due to exotoxin complex secreted by B. anthracis (Hanna, 1998; Hanna et al., 1993). Entry to the host regardless of the route, the endospores are phagocytized by macrophages and transported to regional lymph nodes. Once in the lymph nodes the endospores become vegetative bacteria. The exotoxin components consist of lethal toxin (protective antigen-PA + lethal factor-LF) and edema factor. Injecting LeTx, a zinc metalloproteinase, induces shock when injected into animals. One of the ways it cripples the immune system is by inhibiting dendritic cell maturation (Agrawal et al., 2003) and kills macrophages (Friedlander et al., 1993). In vitro, low levels of LeTx activates macrophages to produce TNF and IL-6; at higher levels there is an excessive production of oxidants and was cytolytic (Hanna, 1999).

Stearns-Kurosawa, et. al. (Stearns-Kurosawa et al., 2006) observed in their primate model macroscopic, microscopic and molecular evidence of acute lung injury. Macroscopic findings were wide spread

hemorrhagic lesions, pleural fluid and frothy edematous fluid in the trachea. Microscopic examination revealed hemorrhagic lesions, intra-alveolar edema, neutrophilic influx and hyaline membrane formation. PIC were elevated in primate and patients exposed to BA. In the baboon model that Stearns-Kursawa et. al. it was found the MCP-1 and MIP-1 peaked at 2 hours (Stearns-Kurosawa et al., 2006). In contrast IL-8 peaked at 4 hours, whereas IL-12p70 remain elevated hours 2- 10 in the higher doses used of anthrax. Mouse macrophages (RAW264.7) exposed to lethal toxin and treated with NAC (N-acetyl-cystiene-an antioxidant) or methionine was resistant to cytolysis (cell death) (Hanna et al., 1994). Elevated PIC are likely are associated with acute lung injury seen in anthrax infected patients (Stearns-Kurosawa et al., 2006).

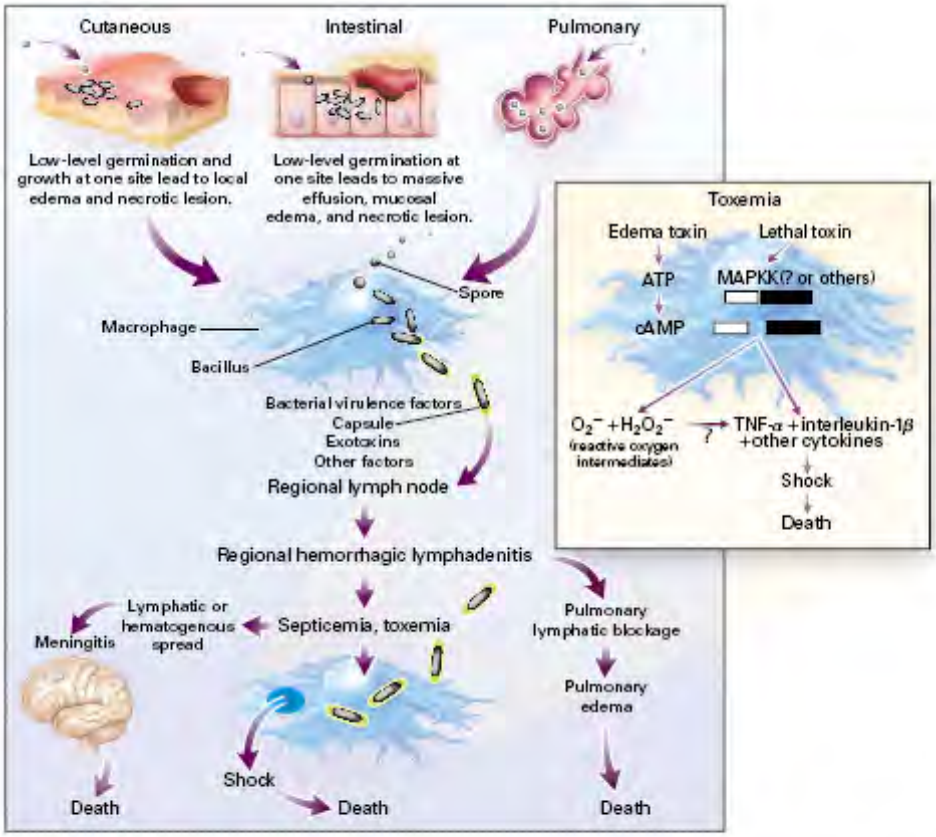

Figure 1. Pathophysiology of Anthrax.

Pathogenic *Bacillus anthracis* endospores reach a primary site in the subcutaneous layer, gastrointestinal mucosa, or alveolar spaces. For cutaneous and gastrointestinal anthrax, low-level germination occurs at the primary site, leading to local edema and necrosis. Endospores are phagocytosed by macrophages and germinate. Macrophages containing bacilli detach and migrate to the regional lymph node. Vegetative anthrax bacilli grow in the lymph node, creating regional hemorrhagic lymphadenitis. Bacteria spread through the blood and lymph and increase to high numbers, causing severe septicemia. High levels of exotoxins are produced that are responsible for overt symptoms and death. In a small number of cases, systemic anthrax can lead to meningeal involvement by means of lymphatic or hematogenous spread. In cases of pulmonary anthrax, peribronchial hemorrhagic lymphadenitis blocks pulmonary lymphatic drainage, leading to pulmonary edema. Death results from septicemia, toxemia, or pulmonary complications and can occur one to seven days after exposure.

The inset shows the effects of anthrax exotoxins on macrophages. Vegetative anthrax bacilli secrete two exotoxins that are active in host cells. Edema toxin is a calmodulin-dependent adenylate cyclase that increases intracellular levels of cyclic AMP (cAMP) on entry into most types of cell. This is believed to alter water homeostasis, resulting in massive edema. Lethal toxin is a zinc metalloprotease that causes a hyperinflammatory condition in macrophages, activating the oxidative burst pathway and the release of reactive oxygen intermediates, as well as the production of proinflammatory cytokines, such as tumor necrosis factor α (TNF-α) and interleukin-1β, that are responsible for shock and death. MAPKK denotes mitogen-activated protein kinase kinase.

Liposomes

Liposome encapsulation enables delivery of the antioxidants to area of inflammation in higher concentrations than would be possible with the free molecules. This has been a distinct advantage in consideration of the observed effects. These advantages have been seen in vivo and in vitro experiments in previous mustard studies as well as the newer studies with anthrax.

Diagnostics

The use of immune cells to diagnose infectious pathogens is a nascent technology with excellent promise (Mendis et al., 2005; Rubins et al., 2004). It presents the possibility of a vast improvement of our diagnostic capabilities in terms of earlier diagnosis and perhaps greater sensitivity as well. The AMCC has further refined the concept of the use of immune cells for subclinical diagnosis of infectious disease.

The APC Biosensor is composed of antigen presenting cells (monocytes and dendritic cells) that are harvested from the blood (man or animal) and then subjected to genomic/proteomic analysis. Approximately 15 of these APCs will undergo changes (the host pathogen reaction) that are reflective of the pathogen that is afflicting the host (a signature). APCs seek out areas of tissue that have a “danger” signal, which is increased mitotic activity, or viral/bacterial infections (Crawford et al., 2003). Once this signal is detected, dendritic cells initiate the early transcriptional changes, which lead to cell surface antigen expression and inflammatory mediator release (Crawford et al., 2003). These cellular modifications are required for recruitment of other inflammatory cells to the site of involvement and improved immune cell-to-cell contact. Dendritic cells possess pattern recognition receptors, which allow them to bind to and discriminate between various pathogens (Chaussabel et al., 2003; Huang et al., 2001). Discordant gene expression has been exhibited in dendritic cells and macrophages infected with bacteria, Candida, influenza, or different parasites (Appelmelk et al., 2003; Hofer et al., 2001; Huang et al., 2001; Pulendran et al., 2001). Dendritic cells are known to internalize virus; as well as harboring bacterial pathogens without killing the pathogen (Jantsch et al., 2003; Sundquist et al., 2004).

These changes in gene and protein expression represent key biological signatures, which can be used to identify persons, in the pre-symptomatic (not ill) state, who have been exposed to biological/chemical agent(s)- the high risk exposed individual; as well as persons who are in the early stages of developing symptoms. The same isolation technique of these cells may also allow isolation of the actual pathogen in parts or in total. Isolation of part or the whole pathogen by these techniques may predate symptoms by many hours or days (Das et al., 2008; Hammamieh et al., 2004).

Body

One of the cornerstones of the defense against the deployment of a biological and/or chemical weapon(s) is making a diagnosis in less than four hours. It is also essential to start treatment in patients that have no symptoms that have been in the proximity of the agent; or who are fully symptomatic. Currently there are few methods that can accomplish subclinical disease diagnosis for exposures to infectious disease or chemical weapons, even fewer that can perform the analysis rapidly. Another proviso necessary for an ideal diagnostic test is that it is be field deployable.

This criterion for the ideal robust diagnostic test would be that it be field deployable, rapid, handles both biochemical exposures, and detect subclinical disease. The use of the antigen presenting cells for potential diagnosis of these agents could conceivably be the best method for early diagnosis of these agents within four hours of presentation of the patient. Gene changes have been noted as early as 30 minutes after exposure for infectious agents (Das et al., 2008).

Both biological and chemical weapons produce an inflammatory response. Thus far this ubiquitous inflammatory response has not been specifically addressed by a treatment countermeasure. Hypothetically, if the inflammatory response was diminished it would decrease the tissue damage that is typically seen by a variety of agents. One method of addressing the inflammatory response, or specifically the oxidative stress component, would be to use antioxidants such as STIMAL. Based on the animal studies done thus far it appears that there is an ameliorative effect that would be synergistic with other drugs. There is more convincing evidence of an ameliorative effect in studies done with CEES. This evidence for both the chemical and biological agents provides a foundation for the possible development of a multithreat treatment countermeasure.

Key Research Accomplishments
STIMAL

Suntres- Northern Ontario
Toxicology studies
These studies were done in anticipation of the need for FDA approval for use of the drug. In vitro and in vivo studies using STIMAL did not show any toxicity. Arrangements have been made for STIMAL to undergo testing against phosgene and ricin. If STIMAL is efficacious in the phosgene studies, then development can be expedited since toxicity studies have already been done.

Rest-Drexel University
Anthrax
In vitro studies done at Drexel University demonstrated that BA germination was inhibited by using reducing agents such as NAC or glutathione. The apparent mechanism of action is a reduction of the GerK and GerL receptors found on the

spores. Also macrophages may be more efficient at killing anthrax when treated with reducing agents, such as NAC or glutathione. This line of research provides evidence that the enhancement of antioxidants in the microenvironment alters the redox state of spores and cells. The increased antioxidant levels shift the redox potential of spores/cells to the reductive state. In areas that are undergoing an acute inflammation, the environment would be more oxidative. It would stand to reason in when the redox potential of the microenvironment is oxidative this is likely to promote germination of spores and replication of the vegetative bacteria. These findings offer clues to the use of antioxidants as a therapeutic intervention in the earliest stages of anthrax exposure.

Merkel- FDA
In vivo
A Bacillus anthracis inhalation model was utilized. The antioxidant liposomes were injected by the intraperitoneal route and STIMAL was the only intervention tested. There was a statistically insignificant increase in longevity for the rats that were treated with STIMAL. STIMAL was the sole drug that was administered to the mice in these experiments.

Alibek- AFG Biosolutions
In vivo
Spores were injected by the intraperitoneal (IP) route. STIMAL was also injected IP at 4 and 8 hours after challenged with spores. This was a more detailed study than the one done at the FDA, and similar results were achieved. There was an increase in longevity when CIPRO was used in conjunction with STIMAL.
In both cases it is unknown whether further testing would improve the results.

CEES (2-chloroethyl ethyl sulfur)-chemical weapon

Stone- East Tennessee State University
In vitro model

In these experiments there was an attempt to discern the role of mast cells in the pathophysiology of CEES exposure.
Rat RBL-2H3 cells were exposed to CEES, and were found to actually inhibit degranulation. Non toxic levels of the calcium inophore A23187 enhanced the toxicity of low levels of CEES (0.02-0.2mM). The role of mast cells in CEES exposure remains unclear. This line of research will no longer be pursued.
Nitric oxide levels were measured and found to be generally low. Treatment with CEES reduced NO levels.

Redox Proteomics
In previous studies done with STIMAL it was shown to be protective. The exact mechanism of action for STIMAL was unknown. In an effort to elucidate that mechanism of action analysis of the oxidized proteins was undertaken. Tissues that had been exposed to sulfur mustard and CEES were exported from the other

Amaox, Ltd.

laboratories to Dr. Stone for analysis. 2-dimensional gel electrophoresis and mass spectrometry were used for analysis of those samples. These studies have begun to elucidate the role of oxidation of proteins in the pathophysiology of mustard and its analogue CEES.

Liposomes

Dr. Stone continues to produce the liposomes that are utilized by the group. Several preparations of liposomes were made, wherein the components (e.g. type of lipid, isomers of vitamin E were varied). It was found that the different isomers of vitamin had a differential effect on protection of tissues.

Das- Meharry Medical College

Guinea pig models were used previously used to demonstrate the protective effect of STIMAL in CEES exposures. In order to further elucidate the mechanism of action of action of CEES the transcription factor serum accelerator factor-1 or SAF-1 was analyzed. Within one hour of CEES exposure there was significant elevation of SAF-1 and decreases over a 30 day period. It is unknown if SAF-1 redox regulated. Further studies may show that STIMAL will down regulate SAF-1.

Crawford- Brigham and Women's Hospital

APC Biosensor-Diagnostics

The first human biomarkers for anthrax and Y. Pestis were developed.
Validation of these biomarkers are ongoing.
There is a clear difference the differences in gene up regulation in those APCs that are infected versus those that are not infected
Antigen presenting cells (APCs) exposed to anthrax produce inflammatory cytokines.
If these APCs could be completely suppressed by using STIMAL.

Reportable Outcomes

Invited speaker to the BARDA day industry conference August 3, 2007
Chaired the Annual Advanced Medical Countermeasures 2007 and 2008 Consortium conference.

Arrangements were made for Dr. Crawford to give a presentation to the JPEO. Dr. Crawford presented information on the APC Biosensor and its utility for diagnosing subclinical infectious disease. The information was well received by the audience of experts.

We have continued to be in discussions with DTRA on the potential use of the APC Biosensor.

Arrangements have been made for STIMAL to be tested against phosgene.

There have been discussions with Eric More and Benjamen Capascio on the potential use of the APC Biosensor to establish biomarkers for chemical weapons. We are seeking funding to establish a pilot project for biomarker discovery.

Amaox, Ltd.

The AMCC is currently collaborating with the FDA, USARICD, USAMRID and the USDA.

Manuscripts published during 2006 – 2008 and related to W81XWH-06-2-0044.

1) McClintock, S.D., Hoesel, L.M., Das, S.K., Till, G.O., Neff, T., Kunkel, R.G., **Smith, M.G.**, and Ward, P.A.: Attenuation of half sulfur mustard gas-induced acute lung injury in rats. J Appl Toxicol. 2006, 26:126-311.
2) **Smith, M.G.,** Stone, W., Guo, R.F., Ward, P.A., Suntres, Z., Mukherjee, S., and Das, S.K. Vesicants and Oxidative Stress. In Chemical Warfare Agents. Chemistry, Pharmacology, Toxicology, and Therapeutics, J.A. Romano, Jr., B.J. Lukey, H. Salem (eds). 2nd Edition, CRC Press, Boca Raton, FL. pp.247 – 312, 2007.
3) Hoesel, L.M., Flierl, M.A., Niederbichler, A.D., Rittirsch, D., Sarma, J.V., McClintock, S.D., Reuben, J.S., Pianko, M.J., Stone, W., Yang, H., **Smith, M.,** Ward, P.A.: Ability of anti-oxidant liposomes to prevent acute and progressive pulmonary injury. Antioxid Redox Signal. 2008, 10:973-981.
4) Das, S.K., Chatterjee, D., Mukherjee, S., Grimes, A., Shen, Y., **Smith, M.,** and Ghosh, S. (2006). Decrease in brain POMC mRNA expression and onset of obesity in guinea pigs exposed to 2-chloroethyl ethyl sulfide, a mustard analogue. Biochemical and biophysical research communications *339*, 55-58.
5) Mukhopadhyay, S., Mukherjee, S., **Smith, M**., and Das, S.K. (2008). Activation of MAPK/AP-1 signaling pathway in lung injury induced by 2-chloroethyl ethyl sulfide, a mustard gas analog. Toxicology letters.
6) Mukhopadhyay, S., Rajaratnam, V., Mukherjee, S., **Smith, M**., and Das, S.K. (2006). Modulation of the expression of superoxide dismutase gene in lung injury by 2-chloroethyl ethyl sulfide, a mustard analog. Journal of biochemical and molecular toxicology *20*, 142-149.
7) Paromov, V., Qui, M., Yang, H., **Smith, M**., and Stone, W.L. (2008). The influence of N-acetyl-L-cysteine on oxidative stress and nitric oxide synthesis in stimulated macrophages treated with a mustard gas analogue. BMC cell biology *9*, 33.
8) Viktor Paromov, **Milton Smith**, Zach Suntres, and William L. Stone "Sulfur mustard toxicity following dermal exposure: role of oxidative stress, and antioxidant therapy." Journal of Burns and Wounds 2007;7:e7
9) Qui, M., Paromov, V.M., Yang, H., **Smith, M**., and Stone, W.L. (2006). Inhibition of inducible Nitric Oxide Synthase by a mustard gas analog in murine macrophages. BMC cell biology 7, 39.

.

Amaox, Ltd.

Conclusion

The absence of a multithreat treatment and diagnostic countermeasures is a significant vulnerability to both civilian and military defense. STIMAL has shown promising results in the inhibition of Bacillus anthracis spore germination as well as increased efficiency of macrophage killing of vegetative bacteria. STIMAL has a salutary effect on CEES exposure in vitro and in vivo models. Use of STIMAL in the anthrax animal models has been less convincing. Nevertheless, in both instances of the use of STIMAL in completely different classes, one chemical and the other biological weapons of mass destruction, provide the foundation for a multithreat treatment countermeasure.

The discovery of the first human biomarkers for anthrax and Y. Pestis were derived from the exposures to antigen presenting cells (monocytes and dendritic cells). Identification of these biomarkers is a significant step forward in the development of a new diagnostic test. It is essential that other human biomarkers be developed for both chemical and biological weapons in order to facilitate rapid and robust diagnostic tools.

References

Agrawal, A., Lingappa, J., Leppla, S.H., Agrawal, S., Jabbar, A., Quinn, C., and Pulendran, B. (2003). Impairment of dendritic cells and adaptive immunity by anthrax lethal toxin. Nature *424*, 329-334.
Appelmelk, B.J., van Die, I., van Vliet, S.J., Vandenbroucke-Grauls, C.M., Geijtenbeek, T.B., and van Kooyk, Y. (2003). Cutting edge: carbohydrate profiling identifies new pathogens that interact with dendritic cell-specific ICAM-3-grabbing nonintegrin on dendritic cells. J Immunol *170*, 1635-1639.
Butler, J.A., Gilbert, L.A., and Smith, K.A. (1950). Radiomimetic action of sulphur and nitrogen "mustards" on deoxyribonucleic acid. Nature *165*, 714-716.
Byrne, M.P., Broomfield, C.A., and Stites, W.E. (1996). Mustard gas crosslinking of proteins through preferential alkylation of cysteines. Journal of protein chemistry *15*, 131-136.
Chaussabel, D., Semnani, R.T., McDowell, M.A., Sacks, D., Sher, A., and Nutman, T.B. (2003). Unique gene expression profiles of human macrophages and dendritic cells to phylogenetically distinct parasites. Blood *102*, 672-681.
Crawford, K., Stark, A., Kitchens, B., Sternheim, K., Pantazopoulos, V., Triantafellow, E., Wang, Z., Vasir, B., Larsen, C.E., Gabuzda, D., *et al.* (2003). CD2 engagement induces dendritic cell activation: implications for immune surveillance and T-cell activation. Blood *102*, 1745-1752.
Das, R., Hammamieh, R., Neill, R., Ludwig, G.V., Eker, S., Lincoln, P., Ramamoorthy, P., Dhokalia, A., Mani, S., Mendis, C., *et al.* (2008). Early indicators of exposure to biological threat agents using host gene profiles in peripheral blood mononuclear cells. BMC infectious diseases *8*, 104.
Dixon, T.C., Meselson, M., Guillemin, J., and Hanna, P.C. (1999). Anthrax. N Engl J Med *341*, 815-826.
Fox, M., and Scott, D. (1980). The genetic toxicology of nitrogen and sulphur mustard. Mutation research *75*, 131-168.
Friedlander, A.M., Bhatnagar, R., Leppla, S.H., Johnson, L., and Singh, Y. (1993). Characterization of macrophage sensitivity and resistance to anthrax lethal toxin. Infection and immunity *61*, 245-252.
Gautam, A., Vijayaraghavan, R., Sharma, M.J., and Ganesan, A.K. (2006). Comparative Toxicity Studies of Sulfur Mustard (2,2'-Dicholro Diethyl Sulfide) And Monofunctional Sulfur Mustard (2-Chloroethyl Ehtyl Sulfide), Administered Through Various Routes in Mice. Journal of Medical Chemical Biological Radiological Defense *4*http://www.jmedcbr.org/issue_0401/Vijay/Vijay_02_06.html

Hammamieh, R., Bi, S., Das, R., Neill, R., and Jett, M. (2004). Modeling of SEB-induced host gene expression to correlate in vitro to in vivo responses. Biosensors & bioelectronics *20*, 719-727.
Hanna, P. (1998). Anthrax pathogenesis and host response. Curr Top Microbiol Immunol *225*, 13-35.
Hanna, P. (1999). Lethal toxin actions and their consequences. J Appl Microbiol *87*, 285-287.
Hanna, P.C., Acosta, D., and Collier, R.J. (1993). On the role of macrophages in anthrax. Proc Natl Acad Sci U S A *90*, 10198-10201.
Hanna, P.C., Kruskal, B.A., Ezekowitz, R.A., Bloom, B.R., and Collier, R.J. (1994). Role of macrophage oxidative burst in the action of anthrax lethal toxin. Mol Med *1*, 7-18.
Hofer, S., Rescigno, M., Granucci, F., Citterio, S., Francolini, M., and Ricciardi-Castagnoli, P. (2001). Differential activation of NF-kappa B subunits in dendritic cells in response to Gram-negative bacteria and to lipopolysaccharide. Microbes and infection / Institut Pasteur *3*, 259-265.
Huang, Q., Liu, D., Majewski, P., Schulte, L.C., Korn, J.M., Young, R.A., Lander, E.S., and Hacohen, N. (2001). The plasticity of dendritic cell responses to pathogens and their components. Science (New York, NY *294*, 870-875.
Jantsch, J., Cheminay, C., Chakravortty, D., Lindig, T., Hein, J., and Hensel, M. (2003). Intracellular activities of Salmonella enterica in murine dendritic cells. Cellular microbiology *5*, 933-945.
Levitt, J.M., Lodhi, I.J., Nguyen, P.K., Ngo, V., Clift, R., Hinshaw, D.B., and Sweeney, J.F. (2003). Low-dose sulfur mustard primes oxidative function and induces apoptosis in human polymorphonuclear leukocytes. International immunopharmacology *3*, 747-756.
McClintock, S.D., Hoesel, L.M., Das, S.K., Till, G.O., Neff, T., Kunkel, R.G., Smith, M.G., and Ward, P.A. (2006). Attenuation of half sulfur mustard gas-induced acute lung injury in rats. J Appl Toxicol *26*, 126-131.
Mendis, C., Das, R., Hammamieh, R., Royaee, A., Yang, D., Peel, S., and Jett, M. (2005). Transcriptional response signature of human lymphoid cells to staphylococcal enterotoxin B. Genes and immunity *6*, 84-94.
Nonas, S., Miller, I., Kawkitinarong, K., Chatchavalvanich, S., Gorshkova, I., Bochkov, V.N., Leitinger, N., Natarajan, V., Garcia, J.G., and Birukov, K.G. (2006). Oxidized phospholipids reduce vascular leak and inflammation in rat model of acute lung injury. American journal of respiratory and critical care medicine *173*, 1130-1138.
Papirmeister, B., Gross, C.L., Meier, H.L., Petrali, J.P., and Johnson, J.B. (1985). Molecular basis for mustard-induced vesication. Fundam Appl Toxicol *5*, S134-149.
Pulendran, B., Kumar, P., Cutler, C.W., Mohamadzadeh, M., Van Dyke, T., and Banchereau, J. (2001). Lipopolysaccharides from distinct pathogens induce different classes of immune responses in vivo. J Immunol *167*, 5067-5076.
Rosenthal, D.S., Simbulan-Rosenthal, C.M., Iyer, S., Spoonde, A., Smith, W., Ray, R., and Smulson, M.E. (1998). Sulfur mustard induces markers of terminal differentiation and apoptosis in keratinocytes via a Ca2+-calmodulin and caspase-dependent pathway. The Journal of investigative dermatology *111*, 64-71.
Rubins, K.H., Hensley, L.E., Jahrling, P.B., Whitney, A.R., Geisbert, T.W., Huggins, J.W., Owen, A., Leduc, J.W., Brown, P.O., and Relman, D.A. (2004). The host response to smallpox: analysis of the gene expression program in peripheral blood cells in a nonhuman primate model. Proceedings of the National Academy of Sciences of the United States of America *101*, 15190-15195.
Stearns-Kurosawa, D.J., Lupu, F., Taylor, F.B., Jr., Kinasewitz, G., and Kurosawa, S. (2006). Sepsis and pathophysiology of anthrax in a nonhuman primate model. The American journal of pathology *169*, 433-444.
Sundquist, M., Rydstrom, A., and Wick, M.J. (2004). Immunity to Salmonella from a dendritic point of view. Cell Microbiol *6*, 1-11.

Financials
There was no change since the previous quarter.

Appendices

Book Chapter

Other articles are available upon request**.**

Second Edition

Chemical Warfare Agents

Chemistry, Pharmacology, Toxicology, and Therapeutics

Edited by

James A. Romano, Jr.
Brian J. Lukey
Harry Salem

CRC Press
Taylor & Francis Group
Boca Raton London New York

CRC Press is an imprint of the
Taylor & Francis Group, an **informa** business

CRC Press
Taylor & Francis Group
6000 Broken Sound Parkway NW, Suite 300
Boca Raton, FL 33487-2742

Printed in the United States of America on acid-free paper
10 9 8 7 6 5 4 3 2 1

International Standard Book Number-13: 978-1-4200-4661-8 (Hardcover)

Library of Congress Cataloging-in-Publication Data

Chemical warfare agents : chemistry, pharmacology, toxicology, and therapeutics / editors, James A. Romano Jr. and Brian J. Lukey. -- 2nd ed.
p. ; cm.
Rev. ed. of: Chemical warfare agents : toxicity at low levels / edited by Satu M. Somani, James A. Romano, Jr.
Includes bibliographical references and index.
ISBN 978-1-4200-4661-8 (alk. paper)
1. Chemical agents (Munitions) I. Romano, James A. II. Lukey, Brian J.
[DNLM: 1. Chemical Warfare Agents--poisoning. 2. Disaster Planning--methods. 3. Poisoning--prevention & control. 4. Poisoning--therapy. QV 663 C5177 2008]

RA648.C546 2008
363.17'9--dc22 2007027747

Visit the Taylor & Francis Web site at
http://www.taylorandfrancis.com

and the CRC Press Web site at
http://www.crcpress.com

12 Vesicants and Oxidative Stress

Milton G. Smith, William Stone, Ren-Feng Guo, Peter A. Ward, Zacharias Suntres, Shyamali Mukherjee, and Salil K. Das

CONTENTS

I. BACKGROUND

The primary treatment of vesicant exposure is decontamination and supportive therapies; there is only one vesicant that has an antidote. The paucity of the treatment options continues to confer their tactical advantage. The development of an ameliorative or antidote would accomplish, at a minimum, two goals: (1) effective treatment, if needed, and (2) decreased tactical advantage.

Vesicants are considered to be of low technology and are relatively simple to manufacture. Barrier protection gear, otherwise known as Mission Oriented Protective Posture (MOPP), provides significant protection if donned before exposure. During battlefield conditions, errors would be expected in the use of the MOPP gear because of stressful situations, tears in the suit, false positive or negative alarms, etc.

Vesicants share some common properties that are noteworthy in attempts to achieve a better understanding of their pathogenesis. One characteristic is that they all induce an acute inflammatory reaction (Sidell et al., 1997; Sciuto, 1998; Ricketts et al., 2000; Naghii, 2002; Segal and Lang, 2005), of which a subcomponent is oxidative stress (OS) (Bartsch and Nair, 2006). A consequence of OS is the oxidation of thiol groups, which is seen in all of the vesicant exposures (Vissers and Winterbourn, 1995; Pant et al., 2000; Carr et al., 2001).

The oxidation of thiol groups disrupts redox balance (defined later in this chapter), which can set into motion a cascade of events, such as apoptosis, oxidant production, and increased activity of redox-regulated transcription factors (e.g., nuclear factor kappa beta [NF-κB]). The occurrence of OS is not isolated to the vesicant class of weapons of mass destruction (WMD). Radiation (Kang et al., 2006), bacterial infections (e.g., anthrax) (Hanna et al., 1994; Kuhn et al., 2006), viral infections (e.g., influenza) (Ghezzi and Ungheri, 2004), and ricin (Kumar et al., 2003; Suntres et al., 2005) exposures also induce OS as part of the host pathogen response, which is acute inflammation.

Sublethal OS induces varying degrees of damage in cellular organelles. Lethal OS occurs when antioxidant defenses completely fail, resulting in necrosis (Virag, 2005) or apoptosis (Haddad, 2004). In this chapter, OS will be discussed as a concept, along with its occurrence in the organ systems that are most notably affected by the vesicants. Antioxidant defenses that are critical to the maintenance of redox balance are also discussed.

Achieving a deeper understanding of OS is important for the elucidation of all acute inflammatory disorders. The OS component of vesicant exposure has not been a focal point of research, by

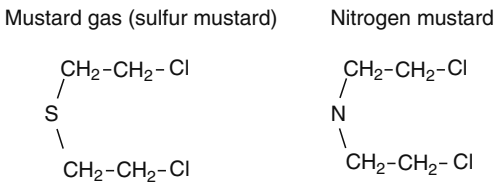

FIGURE 12.1 Chemical structure of sulfur and nitrogen mustards.

and large for vesicants or other WMD. It is hoped that this chapter will help to spur future research in the area.

II. INTRODUCTION

There are four primary vesicating agents–mustard, phosgene, chlorine, and Lewisite. Strategically, they are poor weapons because they are subject to being redirected by the wind. Sulfur mustards (SM) are considered to be one of the vesicants that cause the most concern. There are two types of mustards, sulfur- and nitrogen-based compounds (see Figure 12.1). The nitrogen mustards have been found to be unsuitable for warfare; therefore, there will be no further mention of them. Any further references to mustards will be to SM. Strategically, Lewisite is the least important since there is a proven antidote. British anti-Lewisite, the antidote for Lewisite, has been known for decades (Goldman and Dacre, 1989).

A significant component of acute inflammation is OS (Nonas et al., 2006). One aspect of OS is the production of oxidants and proinflammatory cytokines. It is defined as an imbalance of antioxidant/oxidant ratio, which has a consequent effect on gene expression. The maintenance of the antioxidant/oxidant ratio in the nonstressed cell would be termed redox homeostasis. Thiol groups that are part of intracellular proteins and glutathione (GSH) are critical for the maintenance of redox homeostasis. The vesicants as a class are either oxidants themselves, or they indirectly produce oxidants. Oxidants can be water soluble and fat soluble; therefore, they can arise in any compartment of the cell. They are able to attack any cellular structure, rendering them partially or completely dysfunctional.

The chemical WMD classified as vesicants cause blistering of the skin, which is why they are referred to as blistering agents. They incapacitate more so than kill the exposed person because burns occur on any tissue that it contacts. They all have prolonged systemic effects. The reader is referred to the individual sections of this book and other excellent reviews on the agents for a more detailed classic description of their effects, usage, and history (Goldman and Dacre, 1989; Naghii, 2002; Sciuto and Hurt, 2004; Segal and Lang, 2005). The agents themselves will be reviewed with the features of OS highlighted where information was available.

III. MUSTARD

Vesicants were first deployed against troops during World War I (WWI). They were used as recently as 1988 by Saddam Hussein against the Kurds in Halabja. SM (2-bis-chloroethyl ethyl chloride) is a straw-colored liquid that disseminates with a garlic-like odor on evaporation (Duke-Elder and MacFaul, 1972; Dahl et al., 1985). SM is composed of small, oily droplets with volatility significantly higher in warmer climates (e.g., the Middle East). At a temperature of 38°C, it can be present in the environment for 7 h, whereas at 10°C, it persists for 100 h. The density of mustards is 5.4-fold greater than air and tends to be found 6–12 inches above the ground. This ground-hugging characteristic causes it to sink into trenches and gullies. In WWI, soldiers frequently removed their masks in the morning, assuming that the mustard threat had subsided, and were unaware that the

mustard persisted in the environment. As the ambient temperature increased at sunrise, there was an increase in evaporation of the mustard at the ground-level atmosphere, and the soldiers would unknowingly inhale the newly evaporated gas. Mustard has a high freezing temperature (57°F). This freezing temperature can be reduced by mixing it with other agents, such as chlorobenzene or carbon tetrachloride (Borak and Sidell, 1992; Sidell et al., 1997). Similar reductions in freezing point can be accomplished by mixing it with Lewisite.

SM is commonly referred to as an alkylating agent, but recent evidence has shown it to be a potent inducer of oxidants (Levitt et al., 2003; McClintock et al., 2006). Mustard gas has a strong, irritating effect on living tissue and induces long-lasting, toxic effects (Safarinejad et al., 2001). Additionally, its destructive effects are not localized to the site of application; remote cells and tissues are also affected. SM damages DNA mainly by alkylating and cross-linking the purine bases (Fox and Scott, 1980). Cysteine groups in proteins make them sensitive to SM, resulting in covalently cross-linked dimers on exposure (Byrne et al., 1996). This cross-linking causes conformational change or dysfunction of enzymes. The potent alkylating activity of SM is due to the formation of highly electrophilic ethylene episulphonium derivative (Lundlum et al., 1984; Papirmeister et al., 1991). A portion of the inhalation pathogenesis of SM is due its cholinergic properties (mediating the action of acetylcholine) that stimulates both muscarinic and nicotinic receptors (Anslow, 1946).

On contact with human skin, 80% of the liquid evaporates and 20% penetrates (half remains on the skin and the other half is absorbed systemically). Systemic absorption results in partitioning to organs, such as the spleen, liver, and bone marrow (Langenberg et al., 1998). It is mutagenic and carcinogenic (Papirmeister et al., 1985; Somani and Babu, 1989; Wormser, 1991; Langenberg et al., 1998). The lethal dose for humans is 200 mg if ingested and 3 g with cutaneous exposure (Javadi et al., 2005). A property that has received little attention, but should be kept in mind, is that SM is also a radiomimetic, a property that is shared with other radiation-emitting agents. Additional properties that both radiation and mustards share are the inducement of apoptosis, burns, and OS.

A. Poly ADP-Ribose Polymerase

Alkylation of DNA by SM leads to the activation of poly ADP-ribose polymerase (PARP), which reduces the availability of oxidized nicotinamide adenine dinucleotide (NAD^+) and ATP in the cell (Fox and Scott, 1980). The consequent change in cellular bioenergetics leads to the inhibition of glycolysis, activation of hexosemonophosphate shunt, induction of plasminogen activator, and ultimately, production of skin lesions (Mol et al., 1989). Other alterations in cellular metabolism due to the loss of NAD^+ are microfilament architecture and function in keratinocytes (Papirmeister et al., 1985). PARP uses NAD^+ for a two-electron donor in an oxidation step to catalyze the polymerization of ADP-ribose units on target proteins to attach PARP. PARP has a multiplicity of functions, such as DNA damage sensor and repair chromatin modification, transcription, cell death pathways, insulator function, and mitotic apparatus function. These processes are important to several physiological and pathophysiological processes that involve genome maintenance, carcinogenesis, aging, inflammation, and neuronal function. Poly ADP-ribose polymerase-1 (PARP-1) is the most abundantly expressed member of the family of PARP proteins; it binds to DNA structures that have single and double strand breaks, crossovers, cruciforms, and supercoils (Kim et al., 2005). During normal cellular metabolism, the level of PARP-1 is very low. The enzymatic activity is greatly increased, as much as 500-fold, with allosteric activators, such as damaged and undamaged DNA occurrence (D'Amours et al., 1998, 1999; Kun and Bauer, 2001; Oei and Shi, 2001).

The attachment of PARP or PARrylation, in response to oxidation, alkylation, or ionizing radiation, is dramatic and immediate. At minimal levels of DNA damage, PARP-1 acts as a survival factor involved in DNA damage detections and repair. At high levels of DNA damage, PARP-1 promotes cell death (Burkle, 2001). Elevated levels of PARP in response to DNA damage canpromote necrosis secondary to exhaustion of cellular NAD^+ and ATP (cellular energy failure) (Decker and Muller, 2002; Bouchard et al., 2003). PARP-1 even facilitates apoptosis by a caspase-independent

apoptotic cell death via apoptosis inducing factor (AIF). AIF, a potent trigger of apoptosis, is a flavoprotein, which resides in the mitochondrial intermembrane (similar to cytochrome *c*). However, it is unclear what the exact trigger of AIF release is, but it could be the result of the depletion of NAD^+ due to excessive PARP synthesis and activity. PARP preferentially depletes cytosolic NAD^+ (Zong et al., 2004), which would be expected to affect the overall cellular bioenergetics.

B. Metabolites of Sulfur Mustard

The metabolites of SM are noteworthy because of their utilization of thiol compounds. These metabolites, in addition to OS, diminish the thiol cellular pool. Some metabolites occur by direct hydrolysis, but the majority are conjugates of GSH (Black et al., 1992; Black and Read, 1995); other metabolites are *N*-acetyl-L-cysteine (NAC) conjugates or methylthio/methylsulfhinyl derivatives. Enzymatic conjugation of alkylating agents utilizing GSH can occur through glutathione-S-transferase (GST); but alkylating agents can also combine directly with thiols (Moore and Ray 1983; Colvin et al., 1993). Spontaneous or enzymatic conjugation of alkylating agents occurs through an aziridium intermediate (Colvin et al., 1993).

C. Signaling

There are a multitude of activators of NF-κB, such as viral infections, bacterial infections, radiation, interleukin (IL)-1, and tumor necrosis factor (TNF). Most of the activators of NF-κB can be blocked with the use of antioxidants (Schulze et al., 1997). Other transcription factors, such as AP-1 (Xanthoudakis et al., 1994), MAF, and NRL (Kerppola and Curran, 1994), and NF-IL6 (Hsu et al., 1994) are regulated by oxygen-dependent mechanisms that cause redox cycling of cysteinyl residues.

NF-κB regulates many genes involved in inflammation, such as inducible nitric oxide synthase (iNOS), proinflammatory cytokines, IL-1, tumor necrosis factor-alpha (TNF-α), IL-6, chemokine, IL-8, E-selectin, vascular cell adhesion molecule 1 (ICAM-1), and granulocyte-macrophage colony stimulating factor (GM-CSF) (Brennan et al., 1995; Akira and Kishimoto, 1997; Barnes and Adcock, 1998; Rahman and MacNee, 1998; McClintock et al., 2002). Arroyo et al. (2000) found a dose-dependent increase in TNF-α, IL-6, and interleukin-1-beta (IL-1-beta) in SM-treated human keratinocyte cells.

Although inflammatory cytokine profiles differ depending on the skin models used (Ricketts et al., 2000; Sabourin et al., 2002), they were shown to be elevated in response to SM. In contrast, in guinea pig lungs exposed to 2-chloroethyl ethyl sulfide (CEES) (a mustards analog), the inflammatory cytokine TNF-α was found to be markedly elevated (Das et al., 2003). The inflammatory cytokines exacerbate the effects of CEES (Stone et al., 2003), which would imply that there is an amplification of the initial injury by the mustards. Lipopolysaccharide (LPS), a ubiquitous entity in our environment, also upwardly modulates the damage that CEES inherently causes to cells (Stone et al., 2003).

SM activates phospholipase A2 and liberates arachidonic acid by acting on linolenic acid found in cellular membranes. Activated neutrophils show an amplification of their respiratory burst in the presence of arachidonic acid (Bostan et al., 2003). Metabolites of arachidonic acid produce oxidants, which would be additional contributors to OS. Arachidonic acid itself and several of its metabolites, such as 12 HETE and 15 HETE, induce FOS and JUN expression (Haliday et al., 1991; Sellmayer et al., 1991; Rao et al., 1996).

One class of signaling pathways that has received considerable attention involves the action of cytokine-stimulated sphingomyelinase (SHM-ase) (Hannun and Obeid, 1997). Ceramide generated from SHM-ase activation plays a critical role in cytokine-mediated apoptosis, cellular differentiation, and senescence, each of which may be important in the inflammatory response.

Ceramide can be generated through several different pathways, such as synthesis within the cell, hydrolysis of SHM by SHM-ase, and breakdown of glycosphingolipids. The degradation of ceramide by acid ceramidase liberates sphingosine, a free fatty acid in the lysosomal compartment

(Alphonse et al., 2002). Ceramide can also be increased by the inhibition of ceramide breakdown by ceramidase and the inhibition of sphingomyelin synthase.

SHM-ase has been proposed as a key enzyme involved in stress-induced ceramide formation (Hannun and Obeid, 1997). Multiple pathways may be regulated, which in turn ultimately determine the levels of ceramide.

D. Tumor Necrosis Factor-Alpha Increases with CEES Exposure

A single, intratracheal injection (0.5 mg/kg body weight) of CEES in guinea pigs was done at different time points. The guinea pigs were dissected and the lung was removed after perfusion. The lung was lavaged and TNF-α concentrations were measured in lung lavage fluid, lung lavage macrophages, and in lung tissue. The level of TNF-α in lavage fluid was very low, whereas high levels accumulated in lung as well as in lung macrophages within 1 h of CEES exposure. The level of TNF-α decreased rapidly after 1 h and returned to normal levels within 24 h of CEES exposure (Figure 12.2a). Further studies revealed that the induction of TNF-α by CEES is dose dependent, and optimal TNF-α accumulation was observed at 2 mg/kg dose of CEES exposure (Figure 12.2b).

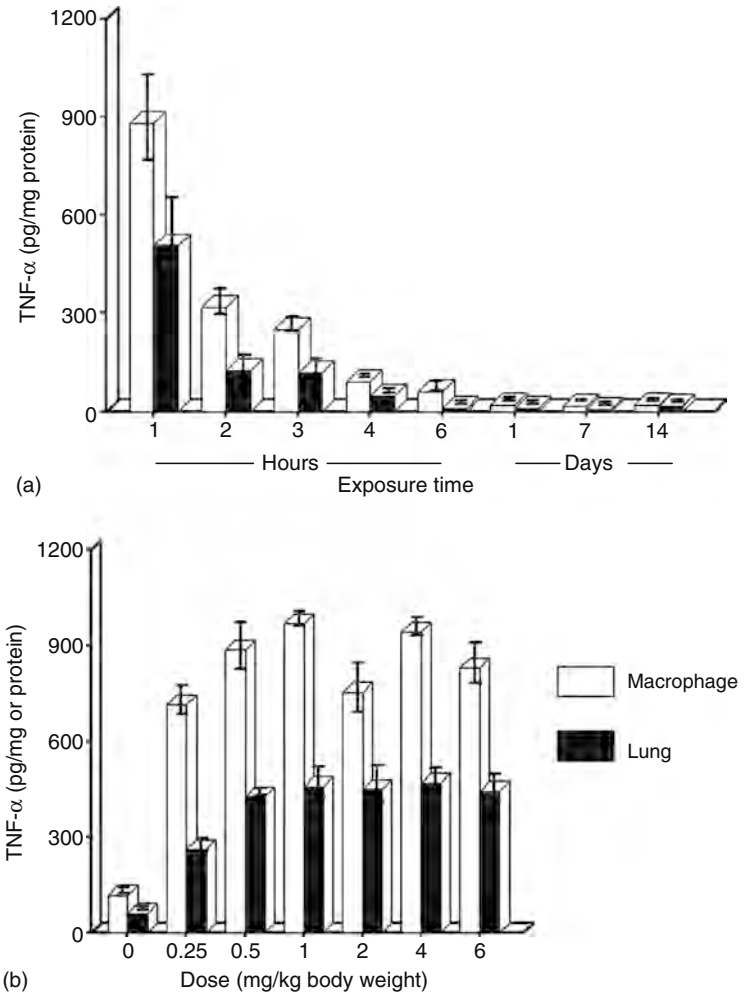

FIGURE 12.2 Accumulation of TNF-α in guinea pig lung and macrophages after exposure to CEES. (a) Time-dependent induction of TNF-α after intratracheal injection of CEES (0.5 mg/kg body weight). (b) Accumulation of TNF-α 1 h after exposure to CEES at different doses (ranging from 0.5 to 6.0 mg/kg body weight).

E. Activation of Sphingomyelinase Activities after CEES Exposure

Both the neutral and acid SHM-ase activities showed fourfold to fivefold increases after CEES treatment. The basal level of acidic SHM-ase activity (Figure 12.3b and d) was much higher than the basal level of neutral SHM-ase (Figure 12.3a and c).

Both neutral and acid SHM-ase activities started to increase, along with the increase of TNF-α; these activities reached a maximum peak between 4 and 6 h in the lung and between 3 and 4 h in macrophages. It is not known at this time whether this difference between lung and macrophages is functionally significant or not. The SHM-ase activities (both neutral and acidic) were found to be higher in lavage macrophages than those in the lung tissue. It is possible that macrophages are more sensitive to CEES than other cell types in the lung. The level of SHM-ase decreased rapidly and returned to near normal level within 24 h. It was also found that a 2 mg/kg dose of CEES is sufficient to reach the maximum level of both neutral and acid SHM-ase activity (Figure 12.3c and d).

F. Accumulation of Ceramide in Lungs after CEES Exposure

The ceramide accumulation after CEES exposure demonstrated a biphasic pattern. Within 1 h of CEES exposure, ceramide levels became very high and reached a peak accumulation within 2 h (Figure 12.4a). After 2 h, there was some decrease in the ceramide level, but then the level increased very high and remained almost to a steady state, even up to 14 days later (Figure 12.4a). CEES-induced ceramide accumulation was found to be saturated at 4 mg/kg dose of CEES. At 2 mg/kg dose of CEES, about 90% induction of ceramide was achieved (Figure 12.4b).

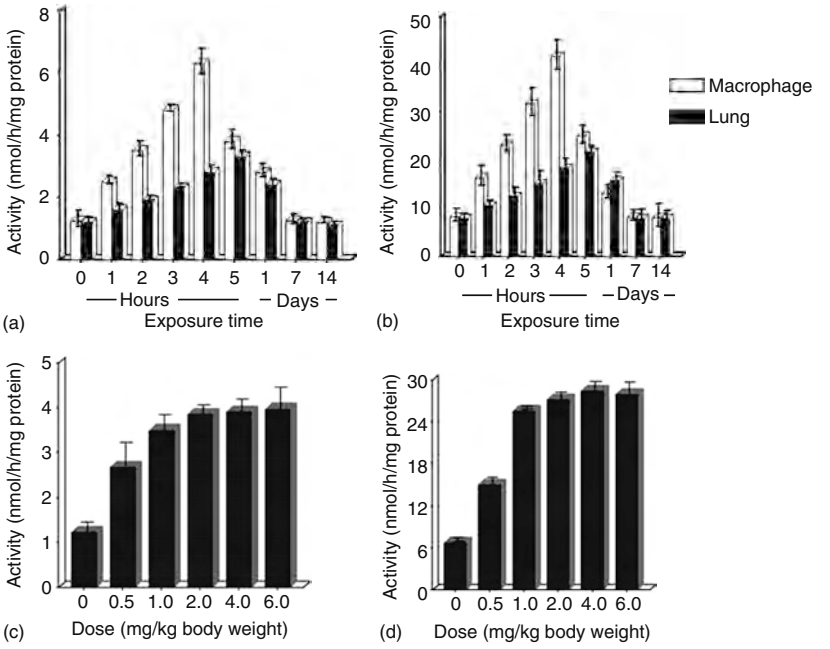

FIGURE 12.3 Activation of acid and neutral sphingomyelinase in guinea pig lung and macrophages following CEES exposure. Time course of induction of neutral (a) and acid (b) sphingomyelinase after intratracheal injection of CEES (0.5 mg/kg body weight). Accumulation of neutral (c) and acid (d) sphingomyelinase at 4 h after exposure to CEES at different doses (ranging from 0.5 to 6.0 mg/kg body weight).

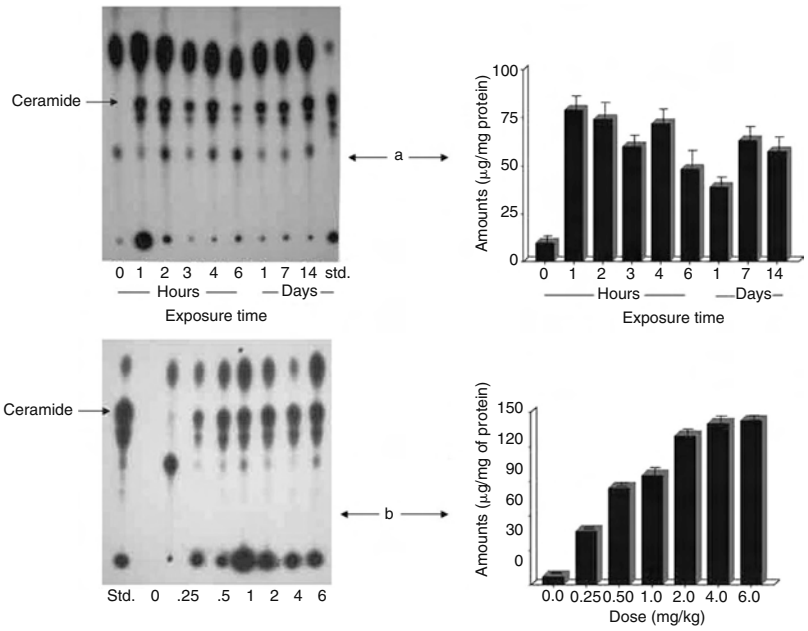

FIGURE 12.4 Accumulation of ceramide in guinea pig lung after CEES exposure. (a) Time course of induction of ceramide after intratracheal injection of CEES (0.5 mg/kg body weight). (b) Accumulation of ceramide at 1 h after exposure to CEES at different doses (ranging from 0.5 to 6.0 mg/kg body weight). In both cases (a and b), the left panel is the autoradiograph showing the accumulated ceramides, and the right panel represents the quantitative analysis of accumulated ceramide as determined by ^{32}P incorporation.

G. Activation of Nuclear Factor Kappa in Lungs after CEES Exposure

The activation of NF-κB was measured in the nuclear extracts of lungs after exposure to CEES. NF-κB, which is well known to inhibit TNF-α-mediated apoptosis, showed activation only up to 1–2 h after CEES exposure (Figure 12.5a). This may explain the biphasic effect of CEES on the lung.

After initial lung damage by TNF-α, within 2 h there was some recovery due to activation of NF-κB. After 2 h, the NF-κB level went down, ceramide level increased, and secondary lung damages were observed. Dose-dependent studies revealed that 4 mg/kg CEES was needed for the optimum activation of NF-κB (Figure 12.5b). Super shift assay using specific antibodies to p50 and p65 revealed that both the p50 and p65 subunits were activated in lung because of CEES exposure (Figure 12.5c).

H. Activation of Caspases after CEES Exposure

Activation of different caspases in guinea pig lung after the CEES exposure is shown in Figure 12.6. Within 1 h of exposure, some activation was observed for all four caspases, but the activity came back to the basal level within 2 h of exposure. The activity of caspase 2, caspase 3, caspase 8, as well as caspase 9 increased significantly between 4 and 6 h of exposure and then declined again. No activity for any of the caspases was observed at 24 h and thereafter. Here also, the activation of caspases was found to be optimum at 2 mg/kg body weight of CEES.

Our study clearly demonstrated the involvement of an SHM-ase/ceramide signal transduction pathway in the mustard gas-mediated lung injury. After intratracheal injection of CEES to guinea pigs, the TNF-α level increased sharply within 1 h of exposure. The TNF-α level started, declined after 1 h, and returned to basal level within 24 h.

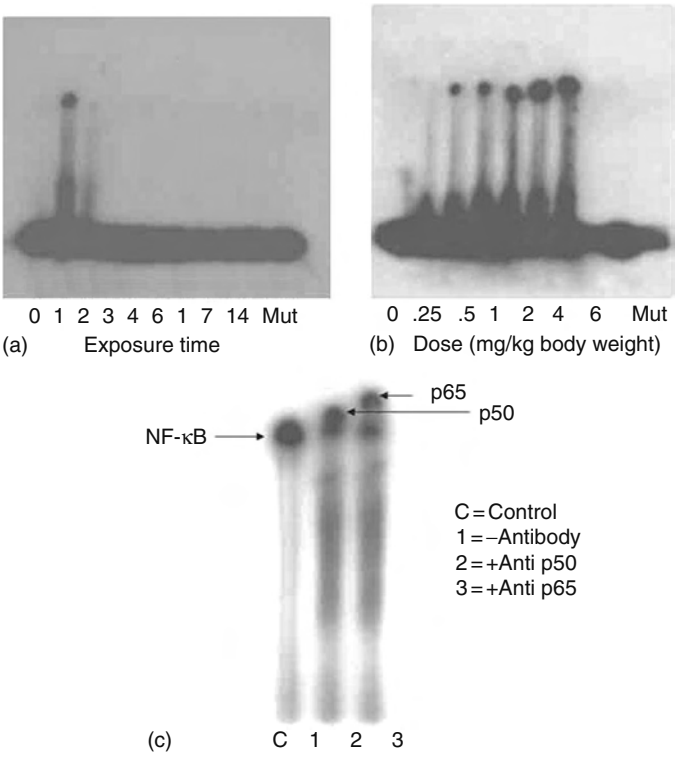

FIGURE 12.5 Activation of NF-κB in guinea pig lung following CEES exposure. (a) Time-dependent activation of NF-κB after intratracheal injection of CEES (0.5 mg/kg body weight), as observed by mobility shift assay. (b) Mobility shift assay showing the accumulation of NF-κB after 1 h of CEES exposure at different doses (ranging from 0.5 to 6.0 mg/kg body weight). (c) Supershift assay, using subunit specific antibodies, to identify the subunits (p50 and p65) of NF-κB activated due to CEES exposure in guinea pig lung.

Followed by the accumulation of TNF-α, both the acid and neutral SHM-ase activities were stimulated, peaking within 4–6 h after CEES exposure. Though both the acid and neutral SHM-ase activities were stimulated, the level of acid SHM-ase was found to be much higher after CEES exposure.

The higher levels of TNF-α, as well as both the acid and neutral SHM-ase activities in lung macrophages compared with those in lung tissue were expected because lung tissue consists of several types of cells, all of which were not responsive to CEES. We observed a biphasic effect of CEES on lung. After initial damage by TNF-α, there was some recovery due to activation of NF-κB within 2 h. This biphasic pattern was also observed in caspases activation.

Significant but small activation of caspase 2, caspase 3, caspase 8, and caspase 9 was observed within 1 h of CEES exposure. This activation of caspases declined thereafter and reappeared within 4–6 h, initiating the cell apoptosis in lung as observed by light as well as electron microscopy (unpublished observation). One explanation for this biphasic action of mustard gas is that NF-κB is activated by TNF-α through a phosphatidylcholine-specific phospholipase C/diacylglycerol (DAG)/protein kinase C (PKC) or phosphatidylcholine-specific phospholipase C/DAG/acid SHM-ase/ceramide model (Chatterjee et al., 2004).

These studies indicate that CEES exposure causes accumulation of TNF-α-activated SHM-ases, resulting in the production of ceramides and simultaneous activation of caspases and finally apoptosis. Ceramides are known to cause apoptosis via the activation of caspases (Alphonse et al., 2002; Hearps et al., 2002; Hetz et al., 2002).

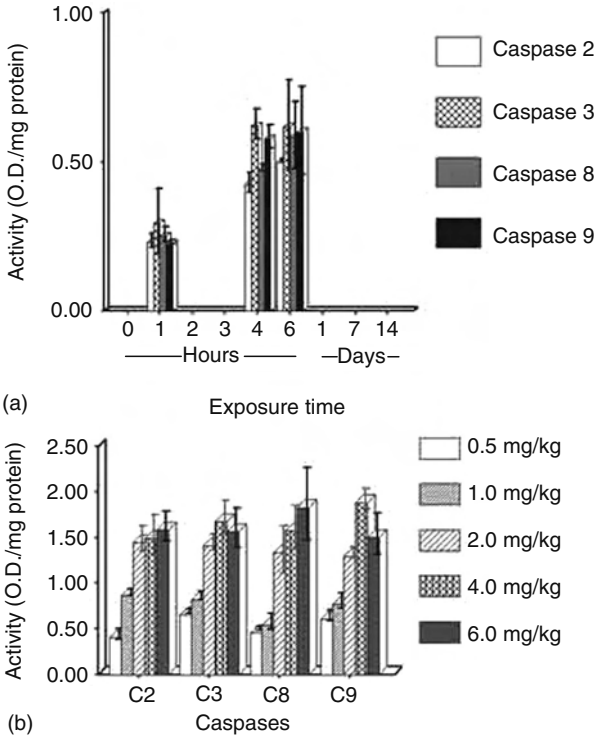

FIGURE 12.6 Activation of different caspases in guinea pig lung after CEES exposure. (a) Time course of activation of different caspases after intratracheal injection of CEES (0.5 mg/kg body weight). (b) Accumulation of different caspases at 4 h after exposure to CEES at different doses (ranging from 0.5 to 6.0 mg/kg body weight).

Our study also revealed that there was some initial damage of the lung tissue when exposed to CEES, but self-defense mechanisms of the lung played a significant role in the recovery from the damage and the prevention of any further damage. Furthermore, the present investigation enhances our understanding of mustard gas-mediated proapoptotic signaling pathways and characterizes the events of mustard gas-induced lung dysfunction.

Mustard gas exposure also causes inflammatory lung diseases, including acute respiratory distress syndrome (ARDS) (Calvet et al., 1994; Sohrabpour, 1984). A defective secretion of surfactant by alveolar type II cells has been implicated as one of the causative factors for the development of ARDS (Ansceschi, 1989). A major component of lung surfactant is DPPC (Stith and Das, 1982). The precursor of DPPC is normally 1-palmitoyl-2-oleolyl PC. DPPC is produced by deacylation and subsequent reacylation with palmitic acid at 2-position of glycerol moiety of the unsaturated phospholipid.

The CDP-choline pathway is the major pathway for the synthesis of PC in the lung, and cholinephosphotransferase (CPT) is a terminal enzyme in this pathway. Regulation of PC metabolism is one of the vital aspects of the cell cycle with implications in the control of cell proliferation as well as in apoptosis (Cui et al., 1996; Baburina and Jackowski, 1998).

PC is the most abundant phospholipid in mammalian cells, and it is synthesized via the CDP-choline pathway (Kent, 1995). CPT is the terminal enzyme of this pathway and plays a direct role in the final production of PC in the lung. This pathway is important for both cell proliferation and cell death (Ghosh et al., 2002; Ryan et al., 2003), and selective inhibition of this pathway has been shown to induce cellular apoptosis (Miquel et al., 1998). Any modulation in the expression and activity of this enzyme is expected to result in abnormal functioning of the cells.

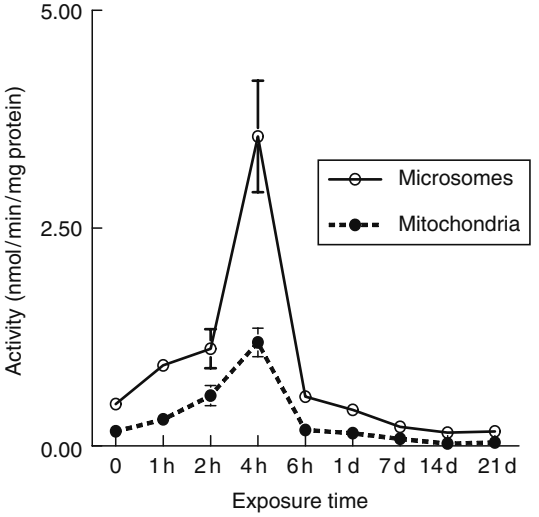

FIGURE 12.7 Time-dependent effects of 0.5 mg/kg body weight. CEES treatment on the mitochondrial and microsomal CPT activity. $N = 3$.

The time-dependent effects of CEES treatment showed a biphasic effect on CPT activity in both mitochondria and microsomes. The time-dependent studies indicated that a single infusion of CEES (0.5 mg/kg body weight) caused an increase in the activity for a short time after CEES exposure (up to 4 h), followed by a decrease (6 h onward) (Figure 12.7). The dose-dependent studies indicated that CEES treatment caused an initial increase in the CPT activity at low doses (0–2 mg/kg body weight), followed by a decrease at higher doses (4 and 6 mg/kg body weight) at incubation times of 1 and 4 h. This decrease was more acute in microsomes than in the mitochondria (Figure 12.8).

We have previously demonstrated that in addition to its predominant localization in the microsomes, CPT also exists in the mitochondria (Stith and Das, 1982; Sikpi and Das, 1987). Thus, it is possible that during the early stage of lung injury as observed in this study, cells try to repair the membrane damage by stimulating PC synthesis. Therefore, with increased CPT activity

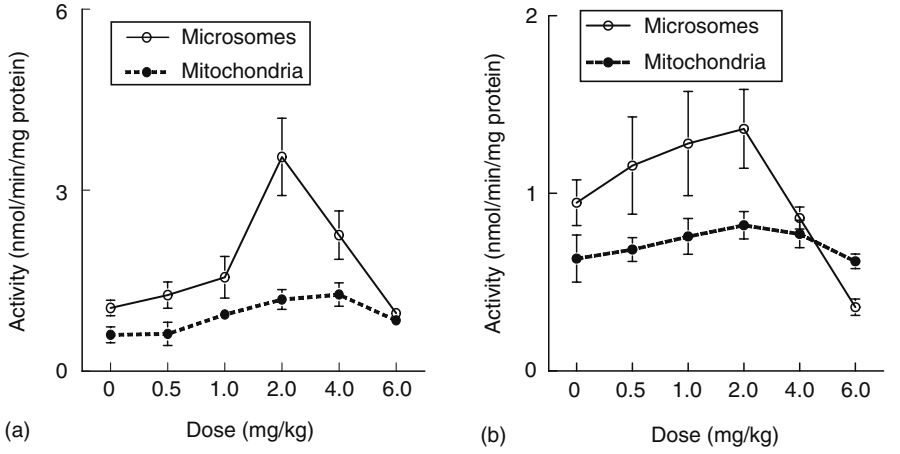

FIGURE 12.8 Dose-dependent effects of CEES on cholinephosphotransferase activity in mitochondria and microsomes. (a) After 1 h CEES treatment. (b) After 4 h CEES treatment. $N = 3$.

over time, lung cells lose their ability to repair membrane damage, as evident from decreased CPT activity in both mitochondria and microsomes isolated from lungs of CEES-treated animals (Figures 12.7 and 12.8). Hence, CEES has both short-term (stimulation) and long-term (inhibition) effects on lung CPT activity. Since CPT activity is crucial to the synthesis of surfactant, these effects may cause ARDS with long-term CEES exposure because of lack of surfactant synthesis.

I. Effects of Ceramide Treatment on Lung Microsomal CPT Activity

Ceramides are intracellular signaling molecules implicated in the induction of cellular apoptosis (Kolesnick and Krönke, 1998; Hannun and Luberto, 2000), and are known to induce several protein kinases and phosphatases (Mathias et al., 1991; Dobrowsky et al., 1993; Vietor et al., 1993). Ceramide analogs have been shown to inhibit PC synthesis (Bladergroen et al., 1999; Allan, 2000; Ramos et al., 2000; Vivekananda et al., 2001). Ceramides may directly affect the biosynthesis of PC and phosphatidylethanolamine (PE) by inhibiting the enzymes of the CDP-choline and CDP-ethanolamine pathways (Bladergroen et al., 1999; Awasthi et al., 2001; Ramos et al., 2002).

It has been reported that cells treated with ceramides may undergo programmed cell death, become growth arrested, or in rare cases, become stimulated to proliferate. The diversity of biological responses of cells to ceramides reflects the complexity of the role of these sphingolipids as second signal molecules (van Blitterswijk et al., 2003). Furthermore, ceramide treatment of lung cancer-derived A-549 cells promotes apoptosis in a caspase-dependent process (Kurinna et al., 2004).

Other laboratories have also shown that enzymes of the CDP-choline pathway for the production of PC in the cells, including CPT, show reduced activity when cells are incubated with cell-permeable C_2/C_6 ceramides (Bladergroen et al., 1999; Ramos et al., 2002), and it has been predicted that this inhibition may be due to the competitive inhibition by ceramides owing to the similarity in the structure to one of the substrates for CPT, DAG.

The downstream signal transduction events in lung following CEES exposure involve the induction of TNF-α, which in turn activates both acid and neutral SHM-ases, resulting in the subsequent accumulation of ceramides in the lung (Chatterjee et al., 2003, 2004). The level of ceramide was found to be ~60 μg/mg protein after 7 days (with 0.5 mg/kg body weight of CEES) and ~130 μg/mg protein for 2 mg/kg body weight of CEES (after 1 h; Figure 12.4).

When the lung microsomal fraction from control animals was incubated with C_2 ceramide at different concentrations (50, 100, and 200 μM) and time periods (0, 0.5, 1, and 6 h) before the assay for CPT activity, CPT activity decreased significantly in a time- and dose-dependent manner (Figure 12.9).

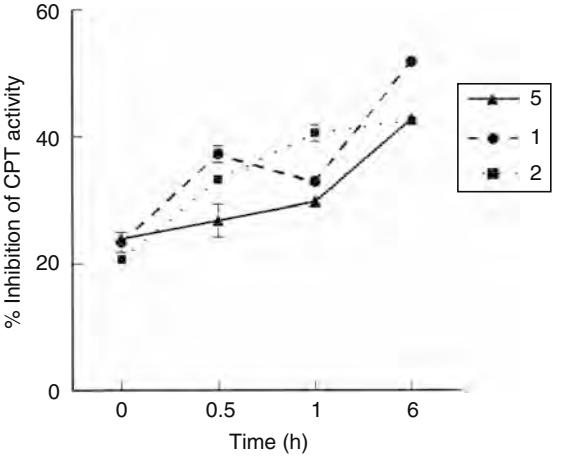

FIGURE 12.9 Effect of C_2 ceramide treatment on lung microsomal CPT activity. $N = 3$.

However, the effect was more pronounced when the microsomal fraction was preincubated with the ceramide before assay of the CPT activity. The degree of inhibition was increased with the increase in incubation time (0.5, 1, and 6 h). The highest inhibition (50%) was achieved after 6 h of incubation. However, only 20% inhibition was observed when ceramide was directly added into the assay mixture.

It has been shown that a 30% inhibition could be obtained in CPT activity when ceramides were directly added to the assay mixture at 50 μM concentrations (Bladergroen et al., 1999). Since this inhibition of 30% was less than the 64% obtained when cells were incubated directly, it would indicate competitive inhibition was not the only mechanism. In the present work, we found similar results with lung microsomal fraction, that is, with an increase in the incubation time with ceramides, the inhibition of the enzyme activity increases. Therefore, we support the observations by Bladergroen et al. (1999) that ceramide inhibition of CPT activity may be only partially through direct competitive inhibition with DAG; ceramide may act through interaction with other CPT enzyme inhibitors present in the microsomal fraction.

It is known that the short-chain ceramides often do not mimic the endogenous long-chain ceramides produced as a result of SHM-ase activity. However, the lipophilic nature of the both short- and long-chained ceramides makes these molecules likely candidates for altering biological processes as components of the lipid bilayer (Gidwani et al., 2003). We can therefore predict that ceramides accumulated in the lung because of exposure of CEES can alter the activity of the membrane-bound enzymes like CPT and can also act as a membrane perturbant.

This ceramide-induced membrane perturbation can result in mitochondrial release of cytochrome *c* and subsequent release of different caspases (Figure 12.6) (Gidwani et al., 2003; Chatterjee et al., 2004) as a part of the apoptotic pathway. Furthermore, CEES exposure (2.0 mg/kg body weight for 7 days) caused a significant decrease of both CPT activity (~1.5-fold; Figure 12.10) and gene expression (~1.7-fold; Figure 12.11) in the lung (Gidwani et al., 2003; Sinha Roy et al., 2005). This decrease in CPT activity was not associated with any mutation of the CPT gene. Thus, the inhibition of CPT activity as a chronic effect of CEES exposure may be directly responsible for the

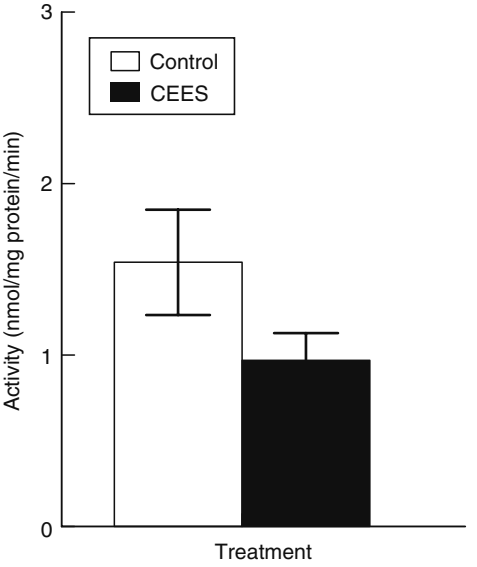

FIGURE 12.10 CPT enzyme activity in the lung microsomal fraction of 2 mg/kg body weight CEES (for 7 days) treated lung as compared with the control (only vehicle) showing significant decrease in activity. $p \leq 0.05$, $N = 3$.

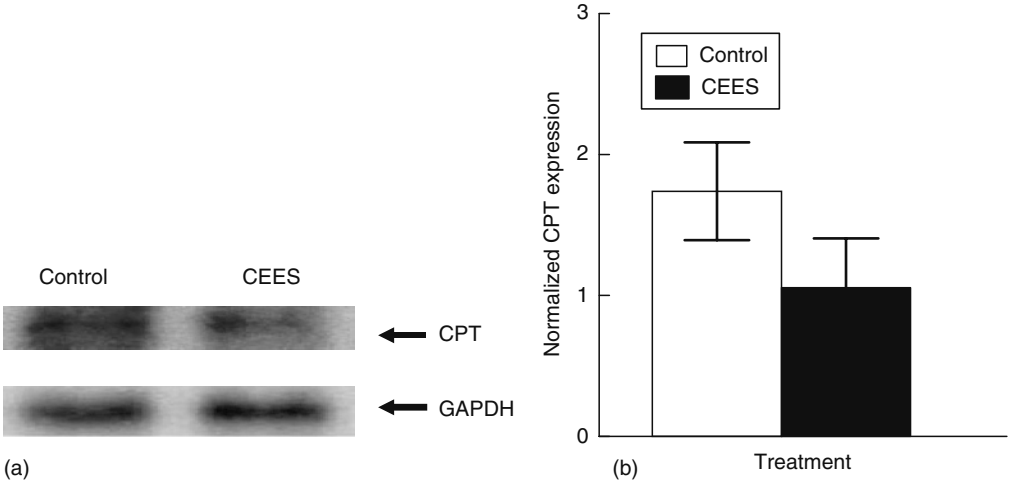

FIGURE 12.11 Northern blot analysis for the expression of the CPT gene. (a) One representative blot for CPT mRNA from control and CEES-treated guinea pig lung and same blot reprobed for GAPDH expression. (b) Graph showing downregulation of CPT expression as the result of mustards gas treatment normalized with GAPDH. $N = 3$.

reduction in the lung surfactant production, resulting in subsequent development of ARDS and pulmonary fibrosis, and is probably mediated by accumulation of ceramides.

J. CEES Induces Oxidative Stress

Stone et al. (2003) have found that OS and inflammatory agents play a key role in the toxicity of CEES. Both HD and CEES are known to provoke acute inflammatory responses in the skin (Blaha et al., 2000a, 2000b; Sabourin et al., 2002). It is interesting that RAW 264.7 macrophages stimulated with LPS or inflammatory cytokines are more susceptible to the cytotoxic effect of CEES than unstimulated macrophages. LPS (bacterial endotoxin) is a well-characterized inflammatory factor found in the cell wall of Gram-negative bacteria and is a ubiquitous natural agent found in the environment. LPS is present in serum, tap water, and dust. Military and civilian personnel would always have some degree of exposure to environmental LPS. Very low levels of LPS (20 ng/mL) were found to dramatically enhance the toxicity of CEES at concentrations greater than 400 μM (Stone et al., 2003). CEES alone is not toxic to RAW 264.7 macrophages at levels lower than about 500 μM (Stone et al., 2003).

LPS is known to trigger a variety of inflammatory reactions in macrophages and other cells having CD14 receptors (Wright et al., 1990; Downey and Han, 1998). In particular, LPS is known to stimulate the macrophage secretion of inflammatory cytokines such as TNF-α and IL-1-beta (Shapira et al., 1994). It is interesting, therefore, that both TNF-α and IL-1-beta were also found to enhance the cytotoxic effects of CEES but to a lesser extent than LPS (Stone et al., 2003). LPS stimulation of macrophages is known to involve the activation of protein phosphorylation by kinases as well as the activation of nuclear transcription factors such as NF-κB (Fujihara et al., 1994; Shapira et al., 1994, 1997; Chen et al., 1998). The activation of PKC by DAG is also a key event in LPS macrophage activation (Downey and Han, 1998). In vitro experiments have shown that the secretion of TNF-α and IL-1-beta by LPS-stimulated monocytes is dependent on PKC activation (Shapira et al., 1997; Coffey et al., 2000). Stone et al. (2003) also determined that phorbol myristate acetate (PMA) activation of PKC also enhanced CEES toxicity. These data suggest that the activation of PKC may play a key role in the molecular mechanism whereby LPS and inflammatory cytokines enhance the cytotoxicity of CEES (and potentially other vesicant weapons

as well). Evidence suggests that LPS (deRojas et al., 1995; Fu et al., 2001) as well as TNF-α (Ye et al., 1999) also stimulate the production of free radicals by macrophages. Collectively, this information supports the view that inflammatory factors and OS are key factors in understanding vesicant toxicity, and are important factors in designing effective countermeasures (Veness-Meehan et al., 1991; Yourick et al., 1991; Elsayed et al., 1992; Pant et al., 2000; Schlager and Hart, 2000; Kadar et al., 2001; Naghii, 2002; Levitt et al., 2003).

IV. CHLORINE

Chlorine is a pulmonary irritant that affects both the upper and the lower respiratory tracts. It is similar to SM in that its density is greater than that of air. Therefore, it characteristically hugs the ground, as does SM when deployed. It is only slightly water soluble; on contact with water or moisture, it forms hypochlorous acid (HClO) and hydrochloric acid (HCl). HClO is unstable and readily decomposes to oxygen-centered radicals. In animal models, 2000 ppm exposure will induce respiratory arrest. Subacute exposures of 9 ppm and acute exposures of 50 ppm can cause chemical pneumonitis (an inflammatory process) and bronchiolitis olbiterans (Segal and Lang, 2005).

The LD_{50} is in the range of 800–1000 ppm. HOCl, whether exogenously obtained from Cl_2 gas, or from an oxidative burst from neutrophils, the product reacts with a number of functional thiol groups present in enzymes (Winterbourn, 1985; Pullar et al., 2002). HOCl reactivity with thiol groups could inactivate such enzymes as GSH peroxidase and catalase (Aruoma and Halliwell, 1987). Inactivation of enzymes involved in antioxidant defense system renders the cell vulnerable to OS (a disruption of redox homeostasis).

Glutamylcysteine synthetase, cysteine, or methionine was 100 times more reactive to hypochlorous acid in comparison with amino acids that did not contain thiol groups (Folkes et al., 1995). Sublethal exposures to HOCl decreased GSH levels in several cell types (Vissers and Winterbourn, 1995; Pullar et al., 1999). In a study by Pullar et al. (1999) using human umbilical vein endothelial cells, doses of 25 nmol of HOCl and less were sublethal; when the exposure was done over 10 min, there was a concentration-dependent loss of intracellular GSH. Tissue exposure to HOCl resulted in a reduction of GSH. The metabolite of the HOCl interaction with GSH was an unexpected cyclic sulfonamide that was exported from the cell. The expected metabolites of glutathione disulfide (GSSH) and GSH sulfonic acid were actually minimal (Pullar et al., 2001). Inactivation of acetylcholinesterase by HOCl could be a contributory cause of airway hyperreactivity (den Hartog et al., 2002).

V. PHOSGENE

Phosgene ($COCl_2$), also referred to as carbonic dichloride, is extensively used as an industrial chemical. The gas dissolves slowly in water and is hydrolyzed to CO_2 and HCl. It produces little damage to the upper airway, although the lower airways sustain the bulk of the necrosis and inflammation. There is typically a delayed onset of symptoms in the pulmonary system occurring 1–24 h after the initial exposure. The respiratory symptoms of hypoxia (shortness of breath), and in extreme cases, respiratory arrest (discontinuation of spontaneous breathing), are apparently due to leaky alveolar capillaries and the resulting pulmonary edema (Noltkamper and Burgher, 2004); also contributory to the clinical symptoms are arachidonic acid mediators and lipid peroxides (Sciuto and Hurt, 2004).

In rodent models, phosgene elicits decreases in total GSH in lung tissue 48% within 45–60 min after exposure (Sciuto, 1998). Jaskot et al. (1991) confirmed similar results 2 years after the Sciuto publication. The concentration of phosgene exposure inversely affected the GSH levels (Jaskot et al., 1991). In gene expression studies in the inhalation mouse model, GSH regulation and redox regulation, in particular, were affected (Sciuto et al., 2005). A gene expression response can be seen as early as 30 min, wherein glutamate cysteine ligase increases and continues to increase at 8 h. Glutamate cysteine ligase continued to be elevated, approaching control levels in the 24–72 h time period. There was an upregulation of GST α-2, GSH peroxidase-2, glutamate, and γ-glutamyl

cysteine synthetase. At 4–12 h, GSH peroxidase-2, GSH reductase was elevated. GSH synthetase increased in the 4–24 h time frame. Further evidence of the crippling of the antioxidant defense system was the decreased SOD3 gene expression and enzyme activity. Similar results were found in independent experiments by Qin et al. (2004), as were reported by Sciuto in his examination of the antioxidant enzyme defense system. In the exposed rats, the antioxidant defense enzymes GST, superoxide dismutase (SOD), catalase, GSH peroxidase, and nitric oxide synthase in serum, blood, or liver were all increased. In contrast, the nitric oxide content was decreased. Similar changes in enzymes were also noted for other gaseous toxins, such as O_3 and NO_2 (Jaskot et al., 1991).

VI. LEWISITE

The Germans developed several arsenical-based warfare chemical agents circa 1917 (Goldman and Dacre, 1989). The allies, on the other hand, developed Lewisite (2-chlorovinydichloroarsine), adamsite (diphenylaminechloroarsine), methyldichloroarsine, and arsine. Lewisite is soluble in organic solvents; it is readily absorbed by rubber, paint, varnish, and porous materials. There are labile chlorine atoms, trivalent arsenic, carbons, and multiple bonds that make it quite reactive. Some of its reactions are due to nucleophilic substitution by water, hydrogen sulfide, thiols, and acid salts.

The reactions with thiol groups (e.g., those that are found in proteins) form an alkylarsine sulfide. Mustard gas, at the same LCt_{50}, induces vesication, whereas Lewisite does not. Apparently, Lewisite is more irritating initially to the pulmonary systems than mustard. The hydrolysis products are more persistent in soil in comparison with mustard. In ambient air, Lewisite is about 10 times more volatile than mustard.

The clinical sequelae after Lewisite absorption referred to as ''Lewisite Shock'' (L shock) are similar to that of severe burns. In dog models at high dosages, exposure resulted in retching, vomiting, extreme salivation, labored breathing, inflammation of the entire respiratory system, and pulmonary edema; respiratory distress was also common, and 80% died. Inhalation of 0.05 mg/L for 15 min results in intoxication and incapacitation for several weeks, whereas 0.5 mg/L for 5 min is lethal. The exact pathophysiology of the pulmonary symptoms seen is unknown, but is likely due to the dilatation of the capillaries. Apparently, the innate immune system is also compromised because of the occurrence of bronchopneumonia. In L shock, a hemolytic anemia can occur; however, it is unclear if this is due to an autoimmune reaction or OS (McMillan et al., 2004; Sato et al., 2006). Other complications of exposure are edema and bleeding that occur in the liver and kidneys (Wardell, 1941).

It is the arsenic in Lewisite that reacts with thiol groups to form alkylarsine sulfides, which is the basic reaction with thiol groups in tissues (Goldman and Dacre, 1989). The degree of enzyme dysfunction is dependent on the affinity of the enzyme to arsine. For example, it binds to the alpha and gamma thiol groups of lipoic acid, a component of pyruvate oxidase, which forms a stable six-membered ring (Stocken, 1949; Johnstone, 1963). Several other known enzymes are also inhibited–alcohol dehydrogenase, succinic oxidase, hexokinase, and succinate dehydrogenase (van Heyningen, 1941; Barron, 1947; Peters, 1946). Lewisite contact with skin results in the immediate elicitation of pain, in contrast to mustard, which would take 4–5 h (Wardell, 1941); it penetrates skin more rapidly than does mustard.

VII. ANTIDOTES OR AMELIORATIVE AGENTS

A. Lewisite

Partial protection was afforded by monothiols, such as cysteine or GSH, when tested against pyruvate oxidase (Goldman and Dacre, 1989), which was thought to be one of the prime targets of Lewisite. British anti-lewisite or 2,3-dimercaptopropanol preferentially binds with arsenicals over the thiol rings in proteins to form a nontoxic five-membered stable ring, which reverses the lesion induced by

Lewisite. British anti-lewisite is also effective against other heavy metals, such as gold, excessive copper deposition seen in Wilson's disease (El-Youssef, 2003), and mercury (Goldman and Dacre, 1989). Newer analogs of BAL have been synthesized to improve efficacy, such as DMSA, 2,3-dimercapto-1-propane sulfonic acid, and *N*-(2,3 dimercaptopropyl-phthalamidic acid) (DMPA).

B. Mustard

Elsayed et al. (1992) performed subcutaneous injections of CEES that resulted in increased GST activity, increased lipid peroxides, and depleted, reduced GSH in lung tissue (Elsayed et al., 1992). Similar findings occurred in the in vitro mouse model, a neuroblastoma–rat glioma hybrid cell line, in that there was a reduction in GSH as a function of time after exposure (Moore and Ray, 1983). Within the last 5 years, there has been a greater emphasis on the inhalation effects of SM.

Peter Ward and his group developed a rat instillation CEES model (McClintock et al., 2002). Leakage of radiolabeled albumin ([^{125}I] BSA) was used as a measure of lung damage, and the rats were sacrificed after 4 h after the installation of CEES into the rat lung with CEES. Neutrophil and complement depletion was found to significantly reduce the injury. Both enzymatic and nonenzymatic protocols were used to examine their ameliorative effect on the model. Dimethyl sulfoxide (DMSO) and dimethyl thiourea (DMTU) resulted in a 51% and 35% reduction in injury, respectively. The enzymatic antioxidants catalase and SOD exhibited 47% and 23% protection, respectively. In contrast, the antioxidant found in red wine, resveratrol (a phytoalexin), showed protection at 61%. Interestingly, the iron chelators 2,3-dihydroxybenzoic acid (DHBA) and deferoxamine mesylate (desferal) did not have any protective effect. NAC was administered 10 min before instillation of CEES. A dose–response curve was generated for 5, 10, 20, 30, and 40 mg/kg^{-1} body weight. All of the dosages of NAC were found to be protective. The dosage of NAC at 20 mg/kg^{-1} conferred the best protection out of all antioxidants at 70% protection. In vitro, the lethal effects of SM on L-cells were reduced by thiol reagents, namely, dithiothreitol and NAC (Walker, 1967; Walker and Smith, 1969). Several observations support the concept of a pathogenic role for toxic oxygen species in CEES-induced acute lung injury.

Other groups investigated the beneficial effects of agents that scavenge free radicals and other oxidant species (Wormser et al., 2000). They monitored the beneficial effects of those agents mainly by showing the recovery from damaged skin or by showing inhibition of the induction of proteolytic enzymes (Cowan et al., 1992; Cowan and Broomfield, 1993). Systemic and topical steroids administered revealed ameliorative properties in the rabbit SM skin model (Vogt et al., 1984).

The Das Group investigated the effects of orally administered antioxidants on signal transduction in the guinea pig model. A single dose of NAC could not block the CEES-induced lung injury at all. On the other hand, about 76% of lung injury could be blocked by long-term pretreatment (30 days) with NAC. No significant protection of lung injury was observed by pretreatment with either Ondrox (an over-the-counter antioxidant supplement as single-dose or 3 days pretreatment) or GSH (single; Table 12.1). Similarly, a single-dose treatment of NAC just before CEES exposure was found to be ineffective, whereas 76% of lung injury could be blocked by long-term pretreatment (30 days) with NAC. There was no significant protection of lung injury by pretreatment with either Ondrox (single-dose or 3 days pretreatment) or GSH (single dose).

A single-dose treatment of NAC just before CEES exposure was found to be ineffective, whereas 62% of TNF-α induction was inhibited by 3 days pretreatment with NAC. Long-term treatment with NAC gave more protection (inhibition of 73% of TNF-α induction). There was no protection for TNF-α accumulation by single dose of either Ondrox or GSH. Three days pretreatment with Ondrox and DMT could only block 13% and 8% of the TNF-α induction (Table 12.2). Additional support for an involvement of oxidants in the pathogenesis of CEES-induced acute lung injury was provided by the protective effects seen after treatment of CEES-exposed rat with NAC (McClintock et al., 2002). The protective effect of NAC was confirmed in the guinea pig lung model, as well as by others (Wormser et al., 1997).

TABLE 12.1
Effects of *N*-acetyl-L-Cysteine Pretreatment on CEES-Induced Lung Injury in Guinea Pigs

Treatment	Permeability Index
Control	0.20 ± 0.04
Control + NAC (3 days)	0.08 ± 0.01
CEES	2.01 ± 0.16
CEES + NAC (single dose)	2.07 ± 0.11
CEES + NAC (3 days)	0.62 ± 0.09[a]
CEES + NAC (30 days	0.48 ± 0.06[a]
CEES + Ondrox (single dose)	2.04 ± 0.03
CEES + Ondrox (30 days)	2.00 ± 0.08
CEES + GSH (single dose)	1.98 ± 0.10

Note: CEES was infused (6 mg/kg body weight) intratracheally into guinea pigs with or without pretreatment with NAC. NAC was given either in single dose (5 mg) by gavage directly into stomach 10 min before infusion of CEES or with drinking water (0.5 g/day/animal, for either 3 days or 30 days before CEES infusion). Information on treatment with ondrox and GSH is given in text. The lung injury was measured after 1 h of CEES exposure and expressed by permeability index, which is a measure of ^{125}I-BSA leakage from damaged blood vessels into lung tissue. Each group had six animals. Values are mean ± SE ($n = 6$).

[a] NAC supplementation in drinking water blocked the CEES-induced lung injury significantly ($p < 0.05$).

TABLE 12.2
Inhibition of CEES-Induced TNF-α Accumulation in Guinea Pig Lung by NAC Treatment

Treatment	Level of TNF-α (pg/mg Protein)
Control	20 ± 7
CEES	708 ± 38
CEES + NAC (single dose)	705 ± 24
CEES + NAC (3 days)	270 ± 40[a]
CEES + NAC (30 days)	190 ± 64[a]
CEES + Ondrox (single dose)	716 ± 22
CEES + Ondrox (3 days)	610 ± 54
CEES + DMT (3 days)	648 ± 62
CEES + GSH (single dose)	720 ± 41

Note: CEES was injected (4 mg/kg body weight) intratracheally into guinea pigs with or without pretreatment with NAC. NAC was given either in single dose (5 mg) by gavage directly into stomach 10 min before injection of CEES or with drinking water (0.5 g/day/animal, for either 3 days or 30 days before CEES injection). Information on treatment with ondrox, DMT and GSH is given in the text. TNF-α was measured after 1 h exposure of CEES. Values are mean TNF-α ± SE ($n = 6$).

[a] NAC supplementation in drinking water blocked the CEES-induced accumulation significantly (p of TNF-α < 0.05).

1. Effect of NAC on Signal Transduction

Short-term (3 days) and long-term (30 days) pretreatment with NAC blocked significantly the activation of acid (4% and 49%, respectively, Figure 12.12) and neutral (46% and 61%, respectively, Figure 12.12) SHM-ases and decreased the levels of ceramide by 71% and 77% (Table 12.3). However, pretreatment with a single dose of NAC did not inhibit the activity of either neutral or acid SHM-ase and accumulation of ceramide.

Exposure to CEES significantly inhibited ($p < 0.05$) the activity of SOD (31%), GSH peroxidase (67%), and catalase (25%) (Figure 12.13). Pretreatment of guinea pigs for 3 days with NAC before CEES infusion significantly ($p < 0.05$) decreased CEES-induced inhibition of SOD (from

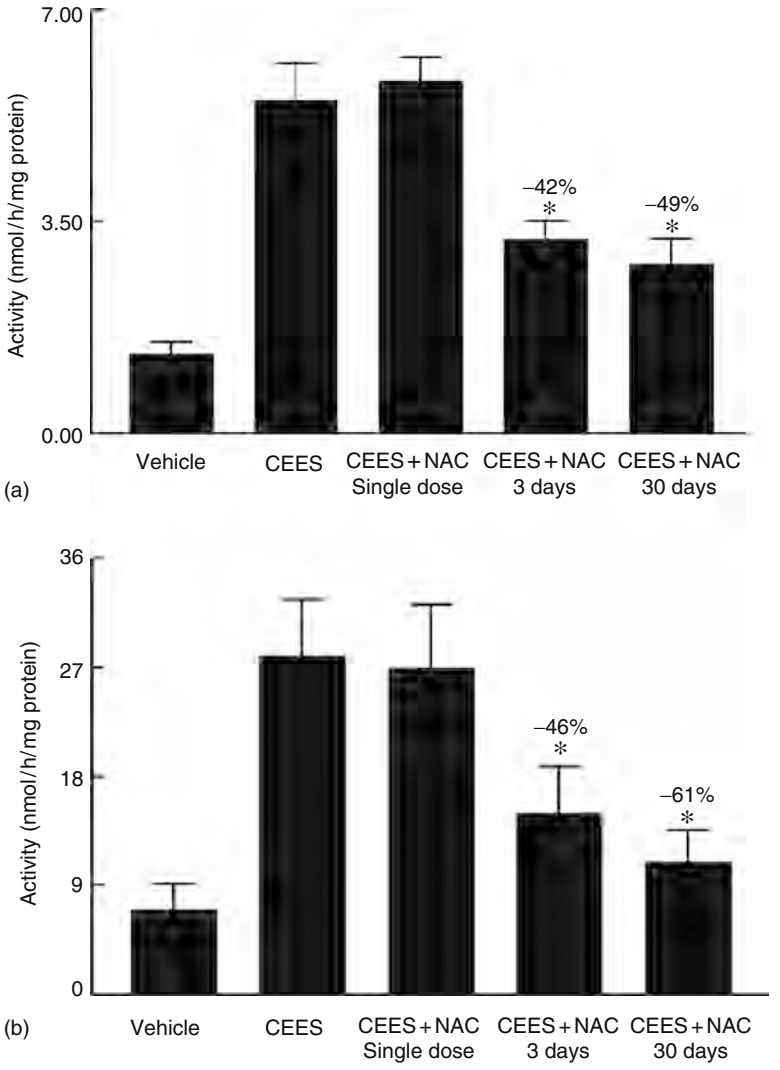

FIGURE 12.12 Inhibition of CEES-induced activation of neutral and acid sphingomyelinases in guinea pig lung by NAC treatment: Accumulation of neutral (a) and acid (b) sphingomyelinases at 4 h after exposure to CEES (4 mg/kg body weight) and their inhibition by 3 and 30 days pretreatment with NAC. Values are mean ± SE ($n = 6$). Pretreatment with single dose of NAC did not inhibit the activity of either neutral or acid sphingomyelinase. *Pretreatment with NAC for 3 and 30 days before CEES exposure caused a significant inhibition of both neutral and acid sphingomyelinases ($p < 0.05\%$).

TABLE 12.3
Inhibition of CEES-Induced Ceramide Accumulation in Guinea Pig Lung after NAC Treatment

Treatment	Levels of Ceramide (μg/mg Protein)
Control	9 ± 2
CEES	148 ± 14
CEES + NAC (single dose)	146 ± 10
CEES + NAC (3 days	39 ± 8[a]
CEES + NAC (30 days)	28 ± 12[a]

Note: CEES was infused (4 mg/kg body weight) intratracheally into guinea pigs with or without pretreatment with NAC. NAC was given either in single dose (5 mg) by gavage directly into stomach 10 min before infusion of CEES or with drinking water (0.5 g/day/animal, for either 3 days or 30 days before CEES infusion. Ceramide accumulations were assayed after 1 h of infusion of CEES. Values are mean ± SE ($n = 6$).

[a] NAC supplementation in drinking water blocked the CEES-induced accumulation of ceramide significantly ($p < 0.05$).

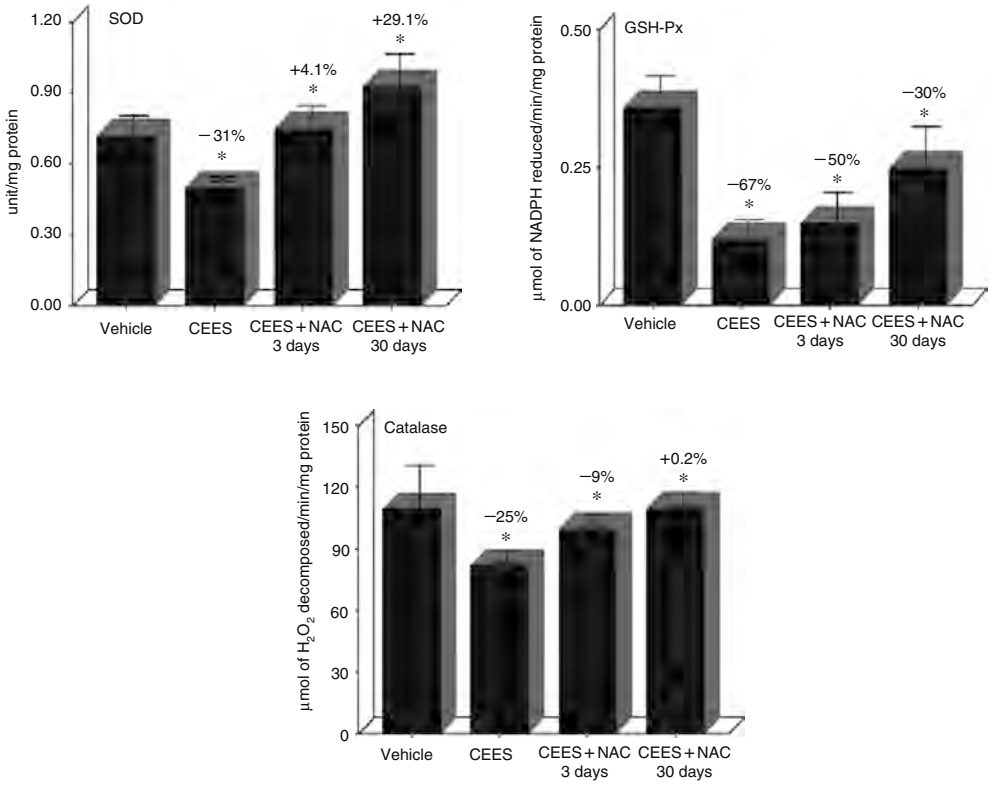

FIGURE 12.13 Effects of NAC pretreatment on the CEES-induced alterations in the free radical-metabolizing enzymes: Guinea pigs were infused with CEES (4 mg/kg body weight) intratracheally and the free radical-metabolizing enzymes (SOD, GSH pretreatment, catalase) were assayed in perfused lung after 4 h of CEES exposure. The samples were taken from guinea pigs with or without pretreatment with NAC for 3 days. *CEES exposure caused a significant decrease in the activity of SOD, GSH pretreatment, and catalase ($p < 0.05$). NAC treatment blocked the CEES-induced changes significantly ($p < 0.05$) for all enzymes.

31% decrease to 4.1% increase), GSH pretreatment (from 67% decrease to 50% decrease), and catalase (from 25% decrease to 9% decrease). Pretreatment of guinea pigs for 30 days with NAC provided additional resistance. For example, the activity of SOD was increased by 29% over the basal value, the activity of GSH pretreatment was decreased by only 30%, and the activity of catalase was brought back to the basal level.

Both short-term (3 days) and long-term (30 days) treatments significantly ($p < 0.05$) blocked the CEES-induced activation of NF-κB that was observed 1 h after CEES infusion (Figure 12.14a). Furthermore, pretreatment with NAC for 3 days also blocked the activation of caspase 2, caspase 3, caspase 8, and caspase 9 by 41%, 44%, 55%, and 51% (Figure 12.14b).

Protection by NAC from half-mustard, gas-induced, acute lung injury has also been demonstrated recently in rats by McClintock et al. (2006). However, in these studies, NAC was administered by liposome encapsulation directly into the lung as a method of treatment for acute exposure to mustard gas. The co-instillation with CEES of liposomes containing the pegylated (PEG)-catalase, PEG-superoxide, NAC, GSH, resvertrol, or combination greatly attenuated development of rat lung injury (McClintock et al., 2006). Thus, we suggest the following model for the action of NAC on CEES-induced guinea pig lung injury (Figure 12.15).

Morphological analysis indicates that animals exposed to CEES showed symptoms of a chemical burn within 1 h; however, the severity of damage progressively increased with time. At 21 days postexposure, severe bronchial constriction with occasional apoptotic nucleus and accumulation of viscid secretion of mucins were observed in CEES-treated animals. Furthermore, both polymorphonucleus (PMNs) and eosinophilic leukocytes migration were observed in both alveoli and bronchi. However, pretreatment with NAC protected the lung from all these changes remarkably, except mucin secretion (Figure 12.16). How CEES functions as a powerful oxidant and what lung cells are targets of CEES is unclear.

C. Antioxidant Liposomes

Another method of increasing antioxidant tissue levels is facilitated by using liposomes. Liposomal drug delivery is advantageous to using the oral route in that there is a multiplicity of possible administration routes. They can be used topically, orally (using the gastrointestinal tract), or delivered by aerosol to the lung.

Intact skin allows the passage of small lipophilic substances, but in most cases, efficiently retards the diffusion of water-soluble molecules. Lipid-insoluble drugs generally penetrate the skin slowly in comparison with their rates of absorption through other body membranes. Absorption of drugs through the skin may be enhanced by iontophoresis if the compound is ionized. Certain solvents (e.g., DMSO) may facilitate the penetration of drugs through the skin, but their use for therapeutic applications is controversial. In the formulation of topical dosage forms, attempts are being made to utilize drug carriers to ensure adequate localization or penetration of the drug within or through the skin in order to enhance the local and minimize the systemic effect. For dermatopharmacotherapy, there is a need for a drug delivery system that enhances the penetration of the active ingredient into the skin, localizes the drug at the site of action, and reduces percutaneous absorption. Antioxidant liposomes may prove very useful in this regard.

Liposomes are phospholipid vesicles composed of lipid bilayers enclosing an aqueous compartment. Hydrophilic molecules can be encapsulated in the aqueous spaces, and lipophilic molecules can be incorporated into the lipid bilayers. Liposomes, in addition to their use as artificial membrane systems, are used for the selective delivery of antioxidants and other therapeutic drugs to different tissues in sufficient concentrations to be effective in ameliorating tissue injuries (Stone et al., 2002). Antioxidant liposomes containing combinations of water- and lipid-soluble antioxidants may provide a unique therapeutic strategy for mustard gas exposure because (1) the antioxidants are nontoxic and could, therefore, be used at the earliest stages of exposure; (2) the liposomes themselves are composed of nontoxic, biodegradable, and reusable phospholipids;

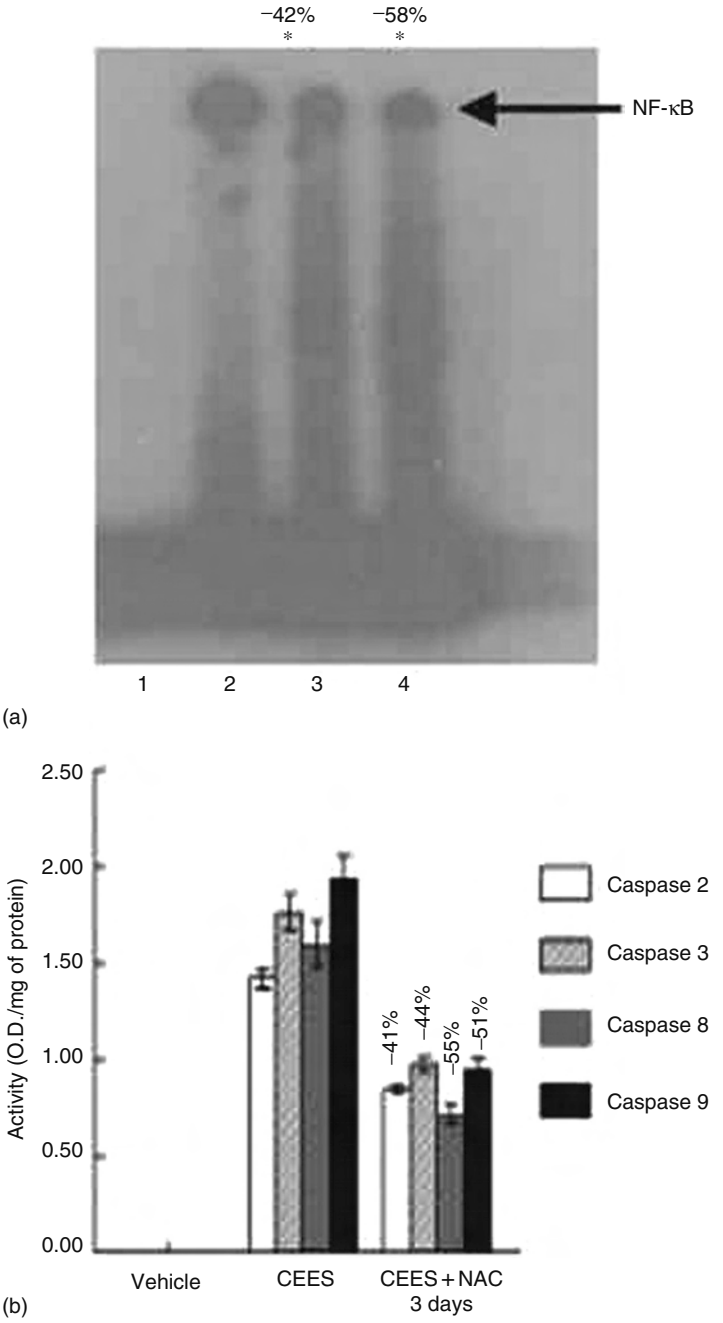

FIGURE 12.14 Inhibition of the activation of NF-κB (a) and different caspases (b) in guinea pig lung after CEES exposure by pretreatment with NAC. (a) Activation of NF-κB after 1 h of intratracheal infusion of CEES (4 mg/kg body weight) was monitored by mobility shift assay. The guinea pigs were treated with NAC either for 3 or for 30 days before CEES exposure. Panels 1, 2, 3, and 4 represent vehicle, CEES, CEES + NAC (3 days), and CEES + NAC (30 days), respectively. *NAC treatment caused a significant inhibition (46% and 58% for 3 and 30 days, respectively, $p < 0.05$) in the accumulation of NF-κB. (b) Accumulation of caspases 2, 3, 8, and 9 at 4 h after exposure to CEES (4 mg/kg body weight) and the prevention of these caspases activation by short-term pretreatment (3 days) with NAC. Values are mean ± SE ($n = 6$). *NAC treatment inhibited the activation of all caspases significantly ($p < 0.05$).

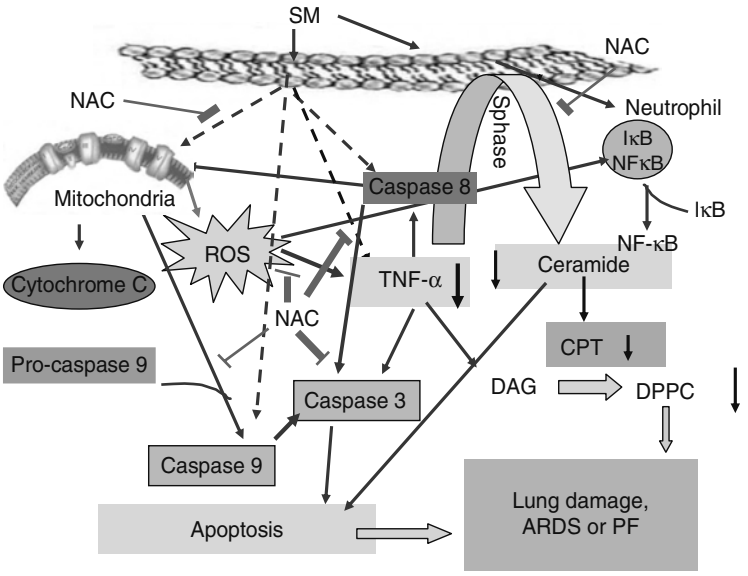

FIGURE 12.15 Proposed mechanism of action of NAC on CEES-induced lung injury.

(3) liposomes are preferentially taken up by the reticuloendothelial system which is an early target of mustards gas toxicity; (4) chemical antioxidants are relatively inexpensive and a wide range of commercial antioxidants are available; and (5) liposomes have low immunogenicity. Furthermore, results from several studies have clearly indicated that the liposomal antioxidant formulations exert a far superior protective effect compared with that of the free (unencapsulated) antioxidants, against OS-induced tissue injuries (Fan et al., 2000).

As shown in Figure 12.17, our preliminary data show that liposomes encapsulated with 5 mM GSH, a major intracellular chemical antioxidant, is effective at preventing CEES cytotoxicity to LPS-stimulated macrophages. We have also found that liposomes encapsulated with either 1 mM NAC (water-soluble antioxidant) or with 13.5 μM α-tocopherol are also effective in preventing CEES toxicity to stimulated macrophages (data not shown). Preliminary results from our ongoing collaborative research efforts have demonstrated that delivery of antioxidants as liposomal formulations were effective in protecting against CEES-induced cellular injury in an animal model.

D. Chlorine

Similar to phosgene, chlorine causes a delayed pulmonary edema. There is no specific antidote for chlorine gas inhalational exposure. Treatment for skin or eye contact is irrigation of the site. Inhalation of the gas can be treated supportively by the use of nebulized sodium bicarbonate and bronchodilators (Aslan et al., 2006). Modest improvement in animal models was obtained with the inhalation therapy using corticosteroids (Gunnarsson et al., 2000). Thiol-containing compounds are able to scavenge HOCl, which is suspected to be a significant metabolite of chlorine gas exposure (McKenzie et al., 1999). Enhancement of systemic levels of thiols by the use of orally administered NAC may be a consideration in life-threatening exposures to chlorine gas.

E. Phosgene

In experiments using agents as a prophylaxis, there is promise. Rats were exposed to phosgene in a whole-body chamber after 23 days of supplementation of vitamin E (α-tocopherol) or *N*-propyl gallate (nPG) (Sciuto and Moran, 2001). The vitamin E-fed rats did not show any survival

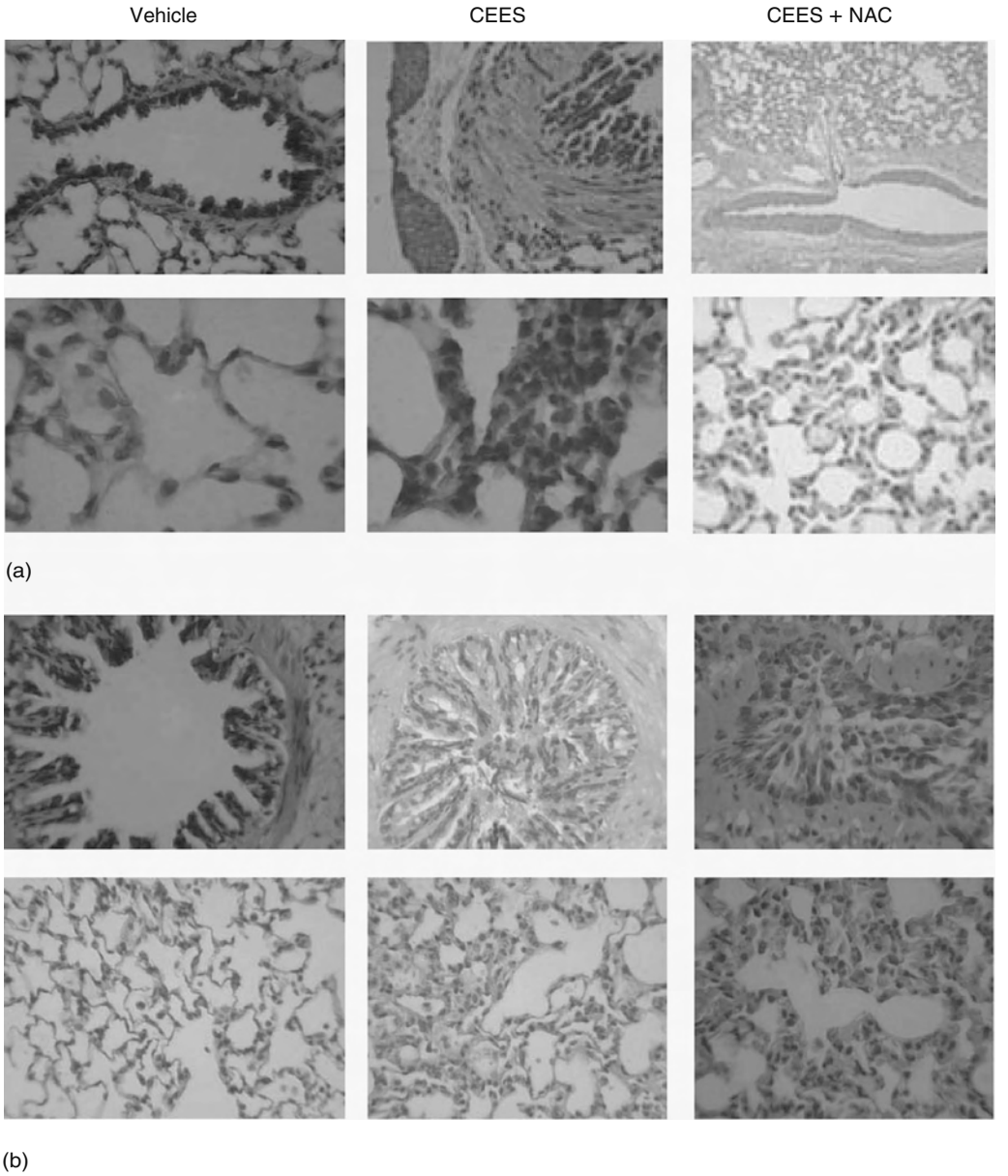

FIGURE 12.16 Histological analysis showing recovery from CEES-induced lung damage by pretreatment of NAC. Guinea pig lungs were examined under light microscope after 1 h (a) and after 21 days (b) of exposure to CEES (0.5 mg/kg body weight). Upper panel represents morphology of bronchi and lower panel represents morphology of the alveoli. Magnifications: 400×.

enhancement. The nPG-fed rats fed the lower doses of nPG (0.75%) showed the greatest increase in survival, and the higher dose of nPG (1.5%) was ineffective. In the lower dose of nPG, there was an obvious decrease in lipid peroxidation and increased lung tissue-reduced GSH. Gamma-tocopherol, in comparison with α-tocopherol, is a more potent anti-inflammatory agent and may have produced a much different result under the same experimental conditions that Sciuto and Moran (2001) performed (Jiang and Ames, 2003).

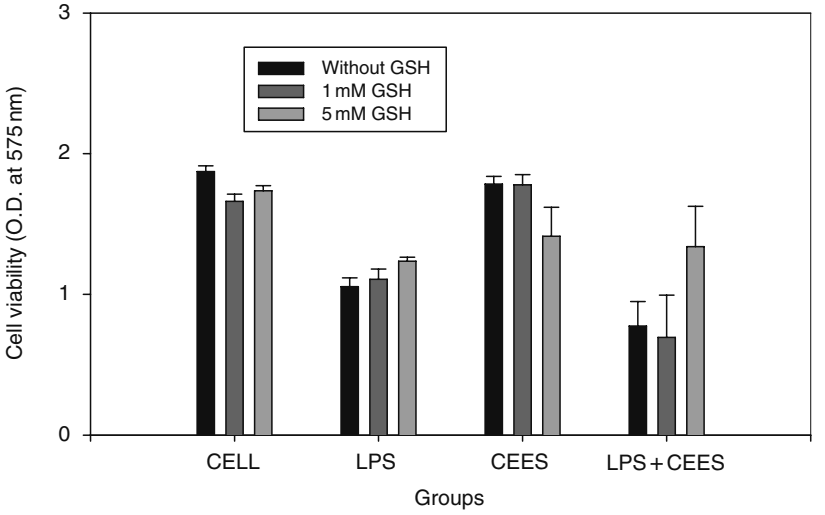

FIGURE 12.17 GSH-liposomes (5 mM) protect simulated macrophages from CEES toxicity.

Postexposure drugs used as a countermeasure to phosgene are more reflective of a clinical application or military theater exposures. The arachidonic acid analog 5-, 8-, 11-, and 14-eicosatetraynoic acid (ETYA) inhibits the release of arachidonic acid metabolites, which produce both leukotrienes and prostaglandins (Farrukh et al., 1988). ETYA used as a postexposure treatment in an in situ lung model resulted in less lung edema, as well as increased gluathione levels and lower lipid peroxidation levels. It is questionable as to whether ETYA possesses any antioxidant properties (Sciuto, 2000).

VIII. OXIDATIVE STRESS IN DIFFERENT ORGAN SYSTEMS

A. Lung

SM inhalation can produce hoarseness, laryngitis, acute airway obstruction, bronchopneumonia, pulmonary edema, and hemorrhage (Calvet et al., 1994). Bronchiolitis and dyspnea are common clinical findings. Examination of the pulmonary tree reveals a mild fibrosis in the parenchyma. Exaggerated fibroblast proliferation and increased collagen synthesis represent two critical events in the pathogenesis of this type of pulmonary fibrosis. The main initial changes are extreme hyperemia, exudation of inflammatory cells, cellular infiltration of the submucosa and detachment, necrosis, and cellular death of the respiratory epithelial lining (Chevillard et al., 1992).

Acute, heavy exposure to SM causes loss of the columnar cells of the upper respiratory tract, peribronchial edema, hyperemia of the blood vessels, cellular infiltrations in the submucosa, and intense vacuolization and disorganization of the cytoplasmic and nuclear structures (Emad and Rezaian, 1997, 1999). Pulmonary hemorrhage, pulmonary edema, and respiratory failure similar to ARDS may also occur. These cytotoxic effects are associated with acute thermal injury sustained by the airway mucosa and lead to scarring and development of stenosis of the tracheobronchial tree as was observed in 9.64% of the SM-exposed patients.

Cross-sectional study on the late pulmonary sequelae of SM-exposed veterans showed airway narrowing or stricture, asthma (10.65%), chronic bronchitis (58.88%), bronchiectasis (8.62%), and pulmonary fibrosis (PF; 12.18%) after 10 years. Crystal et al. (1984) recommended that SM be added to the various causes of interstitial lung diseases and PF (Crystal et al., 1984; DePaso and Winterbauer, 1991; Emad and Rezaian, 1997). The cellular constituents of bronchoalveolar (BAL)

fluid in patients with SM-induced PF are very similar to the cellular constituents seen in patients with idiopathic PF, and this finding indicates the presence of an ongoing active alveolitis in PF (Emad and Rezaian, 1997).

Under normal physiological conditions, airway lining fluids and extracellular spaces are maintained in a highly reduced state. Typically, the levels of antioxidants and oxidants in lung are balanced in favor of a reducing state (redox homeostasis). Decreases in antioxidants or increases in oxidants can disrupt this equilibrium and can cause OS. An imbalance in oxidant–antioxidant system has been recognized as one of the first changes that ultimately lead to inflammatory reactions (Crapo, 2003a).

An increased oxidizing environment can facilitate antigen-presenting cell (APC) maturation and T-cell activation, leading to the activation of the adaptive immune responses and, potentially, a hyperresponsive innate immune system. Thus, OS appears to play an important role in the pathogenesis of the asthmatic reaction. It is not surprising that OS occurs in many forms of lung disorders, such as pneumonia, adult respiratory distress syndrome, idiopathic pulmonary fibrosis, lung transplantation, chronic obstructive pulmonary disease, cystic fibrosis, bronchiectasis ischemia-reperfusion, and lung cancer (Bowler and Crapo, 2002; Crapo, 2003b; Rahman and Kelly, 2003; Rahman et al., 2004).

An oxidizing state in cells can initiate intracellular signaling cascades that lead to the production of inflammatory mediators. Stress kinases (JNK, ERK, p38) and transcription factors, such as NF-κB and AP-1, are known to be redox sensitive. On their activation, these signaling pathways lead to production of TNF-α, IL-1-beta, IL-6, IL-8, IL-12, adhesion molecules (VCAM-1, ICAM-1), and GM-CSF (Mastruzzo et al., 2002). In addition to protein expression, OS favors uncoiling of DNA, thereby increasing accessibility to transcription factor binding (Rahman et al., 2004). The presence of OS can also damage alveolar epithelial cells by the induction of apoptosis. The angiotensin-converting enzyme system is also known to be redox sensitive. OS facilitates the conversion of angiotensinogen into angiotensin II, which is a bioactive peptide with a broad range of activities, including the induction of apoptosis in epithelial cells and the activation of fibroblasts. Angiotensin II can also increase the lung levels of transforming growth factor (TGF)-α, which is a crucial factor in the development of fibrosis (Mastruzzo et al., 2002).

The maintenance of a reducing environment in lung is considered to be crucial in the lung function. A balance between intracellular and extracellular oxidants and antioxidants is a prerequisite for normal lung homeostasis. The lung has highly specialized and compartmentalized antioxidant defenses to protect against reactive oxygen species (ROS) and RNS. These include the following: (1) small molecular weight antioxidants (e.g., GSH, vitamins, uric acid); (2) mucins; (3) metal-binding proteins (transferrin, lactoferrin, metallothionein, etc.); (4) SODs (e.g., mitochondrial manganese SOD [MnSOD], intracellular copper zinc SOD [CuZnSOD], and extracellular SOD [ECSOD]); (5) a group of enzymes that decomposes hydrogen peroxide (H_2O_2) (numerous GSH-associated enzymes and catalase); (6) detoxification enzyme systems (e.g., GST); and (7) other redox-regulatory thiol proteins (e.g., thioredoxin–peroxiredoxin system and glutaredoxins) (Powis et al., 2000; Fattman et al., 2003; Kinnula and Crapo, 2003).

Reduced GSH appears to be one of the most important antioxidant defense systems. In the extravascular lung fluid that coats the alveolar epithelial surfaces, GSH is present in millimolar quantities. A decrease in the ratio between GSH and oxidized glutathione (GSSG) occurring during OS leads to the activation of a variety of cellular redox-sensitive signaling pathways. Antioxidant enzymes such as SOD and catalase also play an important role in the clearance of oxidative radicals in the lung. The primary oxidant-generating enzyme is nicotinamide adenosine dinucleotide phosphate (NADPH) oxidase in phagocytes such as alveolar macrophages and neutrophils. On activation, phagocytes generate superoxide anions, which lead to the production of H_2O_2 for host defense.

It is clear that a better understanding of the oxidative state in the lung is important for the diagnosis and treatment of lung diseases. There are many methods developed for the detection of free radicals from oxygen, ROS, and their by-products to assess the presence of OS. The techniques

include established standard protocols and advanced methodologies using HPLC, mass spectrometry, and electron paramagnetic resonance (EPR). The following sections describe the most frequently used methods to measure lung oxidative status.

1. Monitoring Oxidative Stress in Live Cells

ROS in live cells can be detected by using fluorogenic marker for ROS and observed under fluorescence microscopy. One of the frequently used markers is carboxy-H_2DCFDA, a permeable fluorogenic marker, which is oxidized during OS in live cells and emits bright green fluorescence (Wan et al., 2005).

2. Hydrogen Peroxide and Superoxide Radical Generation in Bronchoalveolar Fluids

H_2O_2 fluids in BAL can be measured by the simple assay for the detection of the presence of peroxides in both aqueous and lipid environments. The basis of these assays is the complexing of ferrous ion (Fe^{+2}) by H_2O_2 in the presence of xylenol orange. Peroxides oxidize Fe^{+2} to Fe^{+3}, and Fe^{+3} forms a colored complex with xylenol orange that can be read at 560 nm (Jones et al., 1995). Superoxide radical generation can be estimated by nitroblue-tetrazolium reduction assay (Libon et al., 1993).

3. Antioxidant Status in Lung

The antioxidant status in the lungs can be evaluated by lung levels of SOD and catalase and their activities. SOD activity can be assessed by the OxyScan SOD-525 assay, which measures the activity of all forms of SOD. The method is based on the SOD-mediated increase in the rate of autoxidation of 5,6,6a,11b-tetrahydro-3,9,10-trihydroxybenzo[c]fluorene in aqueous alkaline solution to yield a chromophore with maximum absorbance at 525 nm. Catalase activity can be determined by a two-step reaction scheme (Catalase-520 assay). First, catalase reacts with a known quantity of H_2O_2 to generate H_2O and O_2. In the presence of horseradish peroxidase (HRP), the remaining H_2O_2 reacts with 3,5-dichloro-2-hydroxybenzenesulfonic acid and 4-aminophenazone to form a chromophore with a color intensity. Lipid peroxidation levels in the lung can be measured by thiobarbutiric acid reactive substances assay (Erdincler et al., 1997). The GSH/GSSG ratio, a useful measure of OS, can also be determined by a colorimetric method by using Bioxytech GSH/GSSG-412.

4. Hydroxydeoxyguanosine, an Indicator of DNA Damage

The most common type of damage caused by ROS in the body is oxidative damage to DNA. Hydroxydeoxyguanosine (8-OHdG), a product of this type of DNA damage, is used as a biomarker for OS. It can be measured by the immunohistochemical procedure and a high-performance liquid chromatography system equipped with an electrochemical detector (HPLC-ECD) (Mei et al., 2003). More recently, it has been reported that capillary electrophoresis-mass spectrometry (CE/MS) can also be used for the analysis of 8-OHdG to study OS (Weiss and Lunte, 2000).

5. Direct Measurements of Oxygen Free Radicals

It is very difficult to directly measure oxygen-free radicals (OFRs) due to their short half-lives. To study these OFRs, radical spin-trapping agents have to be employed to facilitate the formation of stable radical adducts with the OFRs, for detection by EPR spectroscopy. Trapping agents are generally nitrone or nitroso-containing molecules, such as 5,5-dimethyl-1-pyrroline-*n*-oxide (DMPO), which react with OFRs to form stable nitroxide free radicals. These radical adducts can be analyzed by using EPR (Olea-Azar et al., 2003).

6. Exhaled Breath Condensate

Exhaled breath condensate collected by cooling or freezing the exhaled air is a totally noninvasive procedure. H_2O_2, leukotrienes, isoprostanes, and 3-nitrotyrosine are good candidates for OS assessments (Paredi et al., 2002). These products have been shown to elevate lung inflammation.

7. Analysis of Expired Air for Oxidation Products

Studies have shown that expired NO and CO can serve as biomarkers for OS, and ethane can serve as a marker of lipid peroxidation (Paredi et al., 2002). CO can be detected electrochemically, and it can also be measured by laser spectrophotometer and near-infrared CO analyzers. The levels of exhaled NO can be assessed by chemiluminescence. Ethane content can be detected using gas chromatography.

B. Skin

Skin is one of the major sites of damage after exposure to vesicant chemical weapons. In the case of SM, there is a latent period after exposure, followed by an erythematous rash within 4–8 h, and then blistering some 2–18 h later. Elsayed et al. (1992) found that a nonlethal, s.c. dose of the mustard analog chloroethyl 4-chlorobutyl sulfide (CECBS) in mice caused damage to distal tissues, such as the lung, that was consistent with free radical, mediated OS. These authors suggest that ''antioxidants could potentially modulate the response and reduce the damage'' (Elsayed et al., 1992). Although useful, animal models do not exactly mimic the development of SM injury to human skin. Nevertheless, the mouse ear model, the rabbit, the hairless guinea pig, the nude mouse, and the weanling swine have all been useful for studying the (1) pathophysiology; (2) molecular mechanism of action; and (3) efficacy of countermeasures for SM injury. Similarly, in vitro models have major limitations but have the advantage of being cost-effective and potentially very reproducible.

A synthetic human skin model, EpiDerm, showed considerable promise as an in vitro model. EpiDerm possessed all the main characteristic features of the native skin tissue, including the cuboidal appearance of the basal cell layer, the presence of the stratum spinosum and stratum granulosum with typical stellate-shaped keratohyalin granules, and the presence of numerous lamellar bodies that are extruded at the stratum granulosum–stratum corneum interface. The EpiDerm system has the potential for identifying and developing SM therapeutic agents but does have its limitations as well. In vivo, skin damage can be accompanied by the rapid leakage of serum and leukocyte infiltration but this cannot occur in the in vitro skin models.

The U.S. Army Research Institute of Environmental Medicine has used the EpiDerm model to study CEES-induced skin toxicity (Blaha et al., 2000a, 2000b, 2001). Blaha et al. (2000a), for example, studied the potential role of inflammatory cytokines on CEES-induced toxicity. Since CEES or SM is known to provoke an acute inflammatory response in skin, it is reasonable to assume that inflammatory cytokines are involved in this process and that EpiDerm would mimic the in vivo responses. Blaha et al. (2000a) found, however, that CEES depressed the levels of IL-1α and related cytokines. These authors concluded that the inflammatory responses seen in vivo are promoted by factors from sources other than keratinocytes (Blaha et al., 2000a). Stone et al. (2003, 2004) found that inflammatory cytokines dramatically enhance the toxicity of CEES in a macrophage model. It would be important, therefore, to determine if inflammatory cytokines increase CEES toxicity in the EpiDerm model. EpiDerm tissues in the presence of inflammatory cytokines may prove to be an excellent model to test the efficacy of countermeasures. Blaha et al. (2001) also demonstrated that CEES induces apoptosis in the EpiDerm model. This is a valuable observation since potential countermeasures could easily be tested for their antiapoptotic effects in this model.

1. Role of Skin Mast Cells in Vesicant Toxicity

Rikimaru et al. (1991) have used full-thickness human skin explants to study inflammatory mediators in response to topically applied SM. These investigators found that culture fluids from

the SM-treated skin contained increased levels of histamine, plasminogen-activating activity, and prostaglandin E2 compared with control explants. It was concluded that both mast cells and epidermal cells were apparently involved in early mediation of the inflammatory response to SM (Rikimaru et al., 1991). In contrast, Inoue et al. (1997) found that the inflammatory response of the mouse ear to SM did not differ in mast cell-deficient mice compared with normal mice. At present, there is no obvious explanation for the differences observed between the work of Rikimaru et al. (1991) and that of Inoue et al. (1997). It may well be that the mouse ear is not an optimal model for human skin. It is, however, critically important to determine if SM, or other toxic vesicants, degranulate mast cells, since this process could be a major source of inflammatory mediators.

C. Eyes

The eye is a complex sensory organ, which receives visual information from the environment. It encodes optical information into complex electrical signals, which are transmitted to the cortex for visual imagery through the optical nerve. The visual efficiency primarily depends on the optical clarity of the eye (e.g., cornea, crystalline lens, and intraocular media) and the neural integrity of the visual pathway (e.g., retina, optic nerve, and visual cortex).

The pathogenesis of most age-related eye disorders remain poorly understood. Significant evidence points to oxidative damage as a major factor in the initiation and progression of numerous age-related diseases (Kowluru and Kennedy, 2001; Algvere and Seregard, 2002; Hogg and Chakravarthy, 2004; Shichi, 2004; Ohia et al., 2005; Truscott, 2005). Generally, OS occurs when the level of ROS exceeds the ability of the cell to respond through antioxidant defenses leading to the modification and degradation of carbohydrates, membrane lipids, proteins, and nucleic acids (Gamaley and Klyubin, 1999; Kimura et al., 2005). H_2O_2, a relatively stable oxidant, is present at low concentrations in the normal eye and is found at elevated concentrations in some patients with maturity-onset cataract (Beatty et al., 2001; Ohia et al., 2005; Truscott, 2005). Oxidative damage has also been hypothesized to play a role in the pathogenesis of glaucoma, as the trabecular meshwork is exposed to high levels of OS arising from aerobic metabolism, high aqueous concentrations of H_2O_2, and photochemical reactions in the anterior segment (Shichi, 2004; Ohia et al., 2005). The retina is particularly susceptible to OS because of its high consumption of oxygen, its high proportion of polyunsaturated fatty acids (PUFAs), its abundance of photosensitizers and its exposure to visible light (Sickel, 1972; Beatty et al., 2001). In general, it is well known that the greater the oxygen content of tissues, the more susceptible they are to oxidative and photooxidative damage. The retina is supplied with oxygen by the blood with generally high oxygen content in different portions of the retinal tissues. The lipids present in the membranes of rods contain a high percentage of PUFAs, particularly docosahexanoic acid (DHA) (22:6ω-3), known to be the most highly PUFA in nature, making the retina inherently susceptible to lipid peroxidation (Sickel, 1972; Bazan, 1989; Beatty et al., 2001).

Although the eye is continuously exposed to OS, cells have numerous protective mechanisms to reduce the incidence of severe oxidative damage. Damage to the eye by increases in ROS is typically avoided because of a very efficient antioxidant system. It is further protected by pigments such as the kynurenines and melanin (Roberts, 2001). The major water-soluble antioxidants are GSH and ascorbic acid (Reddy and Giblin, 1984; Reddy, 1990; Delamere, 1996; Rose et al., 1998; Lou, 2003; Rahman and Kelly, 2003). Ascorbic acid, the most effective aqueous-phase antioxidant in human blood, is present in high concentrations in the lens, cornea, retinal pigment epithelium, and aqueous humor of humans (Delamere, 1996; Rose et al., 1998). GSH is a naturally occurring tripeptide and is found mostly concentrated in the lens epithelium; its concentration in the lens is as high as that seen in the liver. GSH acts as a reductant of peroxides either by a nonenzymatic reaction or by a reaction catalyzed by GSH peroxidase. GSH may be especially important in protecting the thiol groups of crystallins, preventing them from aggregating to form opaque clusters. Aging lenses or lenses under OS show an extensively diminished size of GSH pool, with some protein thiols

being S-thiolated by oxidized nonprotein thiols to form protein thiol-mixed disulfides, as protein-S-S-glutathione (PSSG), protein-S-S-cysteine (PSSC), or protein-S-S-gamma-glutamylcysteine (Megaw, 1984; Reddy and Giblin, 1984; Reddy, 1990; Rose et al., 1998; Beatty et al., 2000; Ganea and Harding, 2006).

The principal lipid-soluble antioxidants are vitamin E and the carotenoids (Hunt et al., 1984; Snodderly, 1995; Khachik et al., 1997; Beatty et al., 2001). Vitamin E is the major chain-breaking, lipid-soluble antioxidant in membranes, and is thus expected to play the most important role in minimizing effects of oxidation of PUFAs. Both vitamin E and the carotenoids scavenge free radicals, particularly hydroxyl radical and singlet oxygen. Vitamin E is recycled by redox coupling with vitamin C. The retina contains high quantities of α-tocopherol (outer segments of rod) and rod and retinal pigmented epithelium (RPE), and the concentrations within these tissues are very sensitive to dietary intake of the vitamin E (Hunt et al., 1984; Beatty et al., 2001). Vitamin E deficiency has been shown to result in retinal degeneration, excessive RPE lipofuscin levels, and a decrease in the PUFA content of rod outer segments and the RPE, suggesting that vitamin E protects against retinal oxidative damage (Hayes, 1974; Beatty et al., 2001). The antioxidant properties of the carotenoids are now well established, and they possess the ability to quench singlet oxygen and triplet sensitizers, interact with free radicals, and prevent lipid peroxidation. Of the many carotenoids circulating in human sera, only lutein and zeaxanthin are accumulated throughout the tissues of the eye, where they reach their highest concentration in the central retina (macula lutea). Lutein and zeaxanthin are more commonly referred to as macular pigments (Snodderly et al., 1984; Khachik et al., 1997).

SOD, catalase, and GSH peroxidase are antioxidant enzymes that play a significant role in protecting the retina from oxidative damage. GSH peroxidase is found in the retina and uses GSH as an electron donor to reduce fatty acid hydroperoxides, phospholipid hydroperoxides, cholesterol hydroperoxides, and H_2O_2 (Beatty et al., 2002; Ganea and Harding, 2006). SOD catalyzes the quenching of the superoxide anion to produce H_2O_2 and oxygen (Beatty et al., 2002; Lin et al., 2005). Catalase is an iron (Fe)-dependent enzyme that scavenges H_2O_2 either catalytically or peroxidatively. Catalase has been demonstrated in human neurosensory retina and RPE (Roberts, 2001; Beatty et al., 2002; Ohia et al., 2005).

1. Vesicant-Induced Ocular Injury and Oxidative Stress

The eyes are the organs most sensitive to vesicants, which cause cellular changes within minutes of contact; however, the onset of signs and symptoms to vesicant exposure may become evident several hours later. The time course of symptom development after exposure between SM and the nitrogen analogs is nearly the same. The initial contact of mustard gas with the eye for the most part does not cause pain and discomfort. Mild (12–70 $mg/m^3/min$) to moderate (100–200 $mg/m^3/min$) exposures might result in irritation, pain, swelling, and tearing that may occur within 3–12 h postexposure. Similar symptoms might appear 1–2 h after severe exposure (>200 $mg/m^3/min$) but the symptomatology might also include light sensitivity, severe pain, or temporary blindness. Physical findings include blepharospasm, periorbital edema, conjunctival injection, and inflammation of the anterior chamber (Solberg et al., 1997; Safarinejad et al., 2001; Banin et al., 2003; Javadi et al., 2005).

In the Iran–Iraq conflict, SM was heavily used and even now, about 30,000 victims still suffer from late effects of the agent, for example, chronic obstructive lung disease, lung fibrosis, recurrent corneal ulcer disease, chronic conjunctivitis, abnormal pigmentation of the skin, and several forms of cancer (Kehe and Szinicz, 2005). Evaluation of Iranian survivors with chronic or delayed-onset mustard gas keratitis revealed that mustard gas caused chronic and delayed destructive lesions in the ocular surface and cornea, leading to progressive visual deterioration and ocular irritation. Excised conjunctival and corneal specimens revealed a mixed inflammatory response without any specific features. Light microscopy of conjunctival specimens showed decreased goblet cell density, thickened epithelium, scarring in the substantia propria associated with plasmacytic and lymphocytic

infiltration, and dilated lymphatic vessels. Excised corneal buttons disclosed the absence of epithelium and Bowman's layer, stromal scarring, and vascularization. The pathophysiologic features of these changes are not clearly identified. Based on the clinical appearance of the lesions and the histopathologic findings, an immune-mediated component seems possible (Javadi et al., 2005).

In addition to their alkylating properties, mustards are now being recognized to mediate their toxic actions, at least in part, via the formation and action of ROS (Banin et al., 2003). A dramatic increase in copper levels and a decrease in ascorbic acid within the anterior chamber after ocular exposure to mustard compounds implicates the role of OS in mustard-induced eye injuries (McGahan and Bito, 1982; Kadar et al., 2001; Banin et al., 2003). Mustards are also known to rapidly inactivate sulfhydryl-containing proteins and peptides, such as GSH. These sulfhydryl compounds are critical in maintaining the appropriate oxidation–reduction state of cellular components, and GSH is also thought to be critical in reducing ROS in the cell and preventing peroxidation and loss of membrane integrity (Stadtman, 2001). Furthermore, the amelioration of mustard-induced ocular injuries by antioxidants is also evidence to implicate OS as a potential mechanism of injury (Banin et al., 2003; Morad et al., 2005).

Recognizing the fact that ROS play a role in the pathogenesis of mustard-induced ocular injuries, compounds that inhibit the formation of ROS or prevent their toxic effects would be beneficial in the treatment of mustard-induced ocular injuries. The topical application of low concentrations of Zn/DFO or Ga/DFO after corneal exposure to nitrogen mustards markedly reduced conjunctival, corneal, iris, and anterior chamber injury. In the cornea, the healing of epithelial erosions was faster, the long-term opacification was reduced, and the levels of neovascularization were lowered. In the anterior chamber, decreased inflammation and better maintenance of intraocular pressure were achieved. Cataractous changes were also notably milder (Banin et al., 2003).

A combination of topically applied Zn/DFO and dexamethasone, by virtue of their additive inhibitory effects on free radical formation and inflammation, reduced nitrogen mustard-induced injury to ocular anterior segment structures. Furthermore, the combination treatment of Zn/DFO and dexamethasone resulted in a speedier corneal reepithelization, less-severe corneal neovascularization, and the intraocular pressure was not as severely elevated as in the saline or the Zn/DFO- or dexamethasone-alone groups (Morad et al., 2005).

2. Redox Proteomics

OS induces free radical damage to biomolecules and alterations in redox-sensitive signaling pathways, both of which are key factors in understanding vesicant toxicology. In particular, small thiols, like GSH, are no longer viewed just as protective antioxidants but as redox regulators of proteins via glutathionylation or by oxidation of protein cysteine residue (Ghezzi and Ungheri, 2004). Redox proteomics is rapidly emerging as a very powerful tool for characterizing and identifying proteins based on their redox state (Ghezzi and Ungheri, 2004). This approach has not yet been applied to the study of vesicant toxicity, but studies should soon begin on exploring this area.

IX. OXIDATIVE STRESS: THE CONCEPT AND THE EFFECT ON GENE EXPRESSION

A. Definition of Oxidative Stress

Redox potential is defined by the half cell reduction potential that is created by redox couples that are primarily due to GSH, NAD^+ and nicotinamide dinucleotide phosphate. These couples are in ratios of the oxidized to reduced form of the molecules (NAD^+/NAD, $NADP^+$/NADPH, and GSSG/2GSH). The redox couples can be independent, as well linked to each other to form related couples. The redox environment is a reflection of these couples. These ratios can be measured by the Nernst equation, similar to a voltaic cell.

The Nernst equation is

$$E_h = E_0 + (RT/nF)\ln\{[\text{acceptor}]/[\text{donor}]\}$$

E_h is the electromotive force at a particular pH, its units are in volts or millivolts relative to a standard hydrogen electrode (1 atom H_2, 1M H^+). The electromotive force is a quantitative measurement of a redox-active molecule that donates or accepts electrons.

R is the gas constant, T is the absolute temperature, F is the Faraday's constant, and n is the number of electrons transferred. The steady state of E_h for a redox-active component depends on the kinetic of the transfer of the reduction and oxidation reactions. Under normal homeostatic conditions (absence of OS), the E_h for 2GSH/GSSG relatively reduces because of the NADPH-coupled GSSG reductase. During periods of OS, the E_h becomes more oxidized.

Under normal cellular conditions, the redox potential is reductive. In diseased conditions, wherein OS occurs, the redox potential becomes more oxidative. The redox potential is similar in different cell types, but varies according to the cellular processes: proliferation $E = -240$ mV, differentiation $E = -200$ mV, and apoptosis $E = -170$ mV (Kirlin et al., 1999).

An illustrative experimental example of a cell exposed to an oxidant was carried out by Kirlin et al. (1999). When they used HT29 cells (colon adenocarcinoma) and exposed them to sodium butyrate, it was found that there was an oxidant reaction that caused a drop from -260 to -200 mV in E_h. The 60 mV decrease resulted in a 100-fold change in protein dithiols:disulfide ratio. A correlation was noted between E_h, GST, and NADPH:quinone reductase Kirlin further indicated that the E_h provides two additional pieces of information (1) in reactions that use GSH as a reductant to maintain protein thiol/disulfides in their reduced form, it is an indicator of the reducing power quantitatively and (2) if the redox state is controlled by a GSH redox couple, it is an indication of the functional state of the protein (Kirlin et al., 1999).

B. Molecules that Influence the Redox Potential

GSH synthase, a tripeptide (glutamylcysteinylglycine), is not only a water-soluble antioxidant, but is also part of a redox buffer (Smith et al., 1996). It is found in all cells and is used for a multiplicity of cellular functions, such as protein and prostaglandin synthesis, detoxification, etc. Cytosolic concentrations of GSH range from 1 to 11 mm (Smith et al., 1996) and are 100–1000 times greater than the extracellular levels. Many proteins contain sulfhydryl groups because of their cysteine content. The content of thiols in proteins is greater than that of the pool of GSH (Torchinsky, 1981).

The intracellular compartment exchanges GSH with the cytosol (Griffith and Meister, 1985; Schnellmann et al., 1988; Fernandez-Checa et al., 1998). GSH concentrations within the nucleus are critical for maintaining the redox state of protein sulfhydryls that are necessary for DNA repair and expression (Arrigo, 1999). The endoplasmic reticulum has a more oxidizing environment than the cytosol or nucleus. GSH/GSSH in the endoplasmic reticulum is in the range of 1:1 to 3:1, in comparison with the cytosol (Hwang et al., 1992). The ratio of reduced GSH to GSSG influences a variety of cellular signaling processes, such as activation and phosphorylation of stress kinases (JNK, p38, PI-3K) via sensitive cysteine-rich domains, activation of SHM-ase ceramide pathway, and activation of AP-1 and NF-κB, with subsequent gene transcription (Singh et al., 1998; Arrigo, 1999; Mercurio and Manning, 1999a, 1999b).

1. Nicotinamide Adenosine Dinucleotide Phosphate

NADPH is usually involved in reductive (biosynthetic) reactions and serves as a source of electrons. In contrast, NAD is involved in oxidative reactions and serves as a sink for electrons. In cells and tissues, the ratio of $NADPH/NADP^+$ tends to be 1:10 and 1:1000. NADPH is considered the primary source of reducing equivalents for GSH.

2. Thioredoxin

Thioredoxin (TRX) is a pleiotropic polypeptide also known as T-cell leukemia-derived factor (Tagaya et al., 1989; Yodoi and Uchiyama, 1992). It has two redox-reactive cysteine residues in the reactive center (Cys-32 and Cys-35) (Holmgren, 1972, 1985, 1989; Buchanan et al., 1994). Reductases are used to donate electrons from NADPH to facilitate the reduction oxidation reaction between the dithiol or disulfide forms of TRX (Luthman and Holmgren, 1982; Watson et al., 2004).

TRX is responsible for the reduction of cysteine moieties in the DNA-binding sites of several transcription factors (Mathews, 1992; Okomoto, 1992), facilitates the refolding of disulfide-containing proteins, and regulates the DNA-binding activity of some transcription factors (e.g., NF-κB and Ref-1-dependent AP-1) (Sen, 1998; Arner and Holmgren, 2000). TRX facilitates gene expression in that it enables protein–nucleic acid interactions (Holmgren, 1985); it does so by reducing cysteine in the DNA-binding loop of several transcription factors (Matthews et al., 1992; Okamoto et al., 1992; Xanthoudakis et al., 1992, 1994). The redox state of TRX varies independently to that of GSH/GSSG. GSH forms intermolecular disulfides, whereas TRX is a protein that usually forms intramolecular disulfides. TRX assists in the control of apoptosis signal, regulating kinase-1 (ASK-1) (Saitoh et al., 1998).

C. Apoptosis

Apoptosis is induced, when tissue is exposed to SM by a calmodulin- and caspase-dependent pathway (Rosenthal et al., 1998; Sciuto and Hurt, 2004). Zhang et al. (2001) using Jurkat cells exposed to CEES, analyzed gene expression for death and survival pathways. The Akt (PKB) is an important kinase, which can block apoptosis and promote cell survival. It was downregulated in a dose-dependent manner. The antiapoptotic genes, Bcl family, were decreased: Bcl-2, 90%; bax, 80%; bcl-X_L, 67%; Bak and Mcl-1, 70%; and Bik, 57%. Caspases 3, 4, 6, 8, and 9 were upregulated. Crawford et al. (unpublished data) found that CEES-exposed human dendritic cells released cytochrome *c* before detectable levels of ROS generation. NAC was found to inhibit the release of cytochrome *c* and decrease apoptosis. The release of cytochrome *c* was likely due to the opening of the mitochondrial transport permeability transition pores, which is regulated by two redox couples, NADP and GSH (Dalton et al., 1999). It is well known that a portion of the toxicity of mustard is the depletion of NAD (Mol et al., 1989; Byers et al., 2000).

A depletion of GSH alone can act as an early activation of apoptotic signaling (Coffey et al., 2000; Coppola and Ghibelli, 2000; Armstrong and Jones, 2002). Conversion from the procaspase to an active enzyme requires a reduction of the cysteine residue (Hampton et al., 1998). OS can trigger caspase activity, but can also suppress it (Hampton et al., 1998).

Studies conducted by Celli et al. (1998) used BSO (buthionine sulfoximine) to deplete cells of GSH. There was a significant decrease in the Bcl levels and associated time-dependent increase in the number of cells undergoing apoptosis. Maintenance of GSH levels with GSH ethyl ester in the presence of BSO decreased apoptosis and prevented a decrease in Bcl-2 protein. The Celli study, if contrasted to Zhang et al. (2001), one begins to suspect that there may be a strong correlation between the loss of GSH and gene expression in CEES-exposed tissues.

The suppression of Bcl-2 expression induces the relocalization of GSH to the cytosol, whereas the overexpression of Bcl-2 induces a relocalization of GSH to the nucleus. There was a direct correlation between GSH levels and the Bcl-2 nuclear protein levels. It was concluded by Voehringer et al. (1998) that one of the functions of Bcl-2 is to promote the sequestration of GSH into the nucleus.

D. Gene Expression Controlled by Redox-State Transcription Factors

Redox homeostasis regulates activation and binding by transcription factors at the 5′ end of the target gene. In the transcription factors, cysteine residues are frequently located in their protein

sequence localized in their DNA-binding domain. The cysteine molecules are often essential for recognition of the binding site due to electrostatic interactions with specific DNA bases. Inhibition of the binding factor occurs if the cysteine is oxidized, which may be a consequence of an alteration of the tridimensional structure of the transcription factors. The function of several transcription factors could be impaired or inhibited because of oxidation of cysteine groups that result in inter- or intramolecular disulfide bonds (Arrigo, 1999). Several of the transcription factors undergo redox modification posttranslationally. NF-κB binding with DNA is augmented by TRX in vitro. Ref-1 is also modulated by redox compounds (e.g., TRX) (Hirota et al., 1997).

1. NF-κB

NF-κB regulates many genes, particularly those involved in immune and inflammatory responses (Baeuerle and Baltimore, 1996). Antioxidants, such as NAC, GSH, and cysteine, inhibit the activation of NF-κB (Mihm et al., 1995). TRX regulates the binding of NF-κB to DNA (Matthews et al., 1992).

2. Ref-1

In an oxidizing environment, Ref-1 facilitates the binding transcription factors to DNA by reduction of cysteine residues within the binding domains of these proteins (Xanthoudakis and Curran, 1992; Xanthoudakis et al., 1992; Walker et al., 1993). Under OS, cysteine 65 forms a disulfide bond with cysteine 93, which ceases the stimulatory activity of Rdf-1. Active Ref-1 is recycled by the contribution of hydrogen from TRX (Hirota et al., 1997).

3. Activator Protein-1

Activator protein-1 (ATP-1) binds to an enhancer element (Angel et al., 1987; Lee et al., 1987), and is modified by redox factor 1 (Ref-1), a DNA repair enzyme (Angel et al., 1987; Lee et al., 1987; Arrigo, 1999). It is present in the promoter region of several genes, which are implicated in cell proliferation and tumor promotion. Several growth factors, PKC activators, and intracellular redox activate it (Angel and Karin, 1991). It consists of c-Jun and c-Fos proteins, which are products of the c-jun and c-fos proto-oncogene. Agents that promote intracellular oxidants such as UV irradiation, H_2O_2, and mitogens induce c-fos and c-jun genes (Datta et al., 1992; Lo and Cruz, 1995). Antioxidants that have a phenolic group (e.g., d-α-tocopherol or butylated hydroxyltoluene) induce expression of c-fos and c-jun (Choi and Moore, 1993; Stauble et al., 1994). ATP-1 acts as a secondary antioxidant-responsive transcription factor (Meyer et al., 1993).

4. Heat Shock Transcription Factor

Heat shock transcription factor (HSF) is part of the family of heat shock factors that are activated and bind to DNA induced by OS. Several chemicals, heat shock, or conditions that generate abnormally folded proteins activate HSF1 conversion from a monomer to a trimer state (Liu et al., 1996). Iodoacetamide (IDAM), an alkylating agent, activates the transcription of Hsp 70 gene (Liu et al., 1996). The depletion of GSH induces oxidation of protein thiols, denaturation, and aggregation of proteins (Freeman et al., 1997). Alkylating agents that deplete GSH increase HSF1 (Liu et al., 1996) and induce trimerization of HSF1.

X. SUMMARY

Chlorine, phosgene, Lewisite, and SM all react with thiol groups as well as produce oxidants. The arsenic group in Lewisite has a high affinity to the alpha and gamma thiol groups of lipoic acid found in enzymes (e.g., pyruvate oxidase). Oxidants occur as part of the normal metabolism of cells (redox homeostasis). In the diseased state (e.g., exposure to a chemical agent), there is an acute

inflammatory response that is also inclusive of OS (redox imbalance). During significant OS, the oxidant burden exhausts the redox buffer of the cell (e.g., GSH/GSSH, NADP/NADPH, etc.) that consequently alters redox couples. The mitochondrial permeability transition pores (MPTPs) are directly regulated by the redox state. They are a cyclosporine A-sensitive, Ca^{2+}-dependent, and voltage-gated channel. There are two types. One is dependent on the GSH:GSSH ratio (Petronilli et al., 1994; Costantini et al., 1995); the other is a voltage-sensitive gate, regulated by the ratio of pyridine nucleotides (NAD^{+}NADP):($NADH^{+}$NADPH) and is independent of the reduced GSH (Reed and Savage, 1995; Costantini et al., 1996). MPTPs appear to be involved in the toxicity of several chemicals (Dalton et al., 1999). Opening of the pores results in energy uncoupling by a Ca^{2+}-dependent decrease of mitochondrial inner-membrane potential (Petronilli et al., 1994). The collapse of the membrane potential and the inhibition of oxidative phosphorylation result in diminished intracellular ATP. Consequently, there may be the release of inner-membrane cytochrome *c* to the cytosol, which may signal the initiation of apoptosis (Krippner et al., 1996).

In a comparison of SM to CEES done using a histological grading system, SM was shown to be about six times more potent than CEES (Dana Anderson, unpublished results). The doses that were used by our group in the in vivo models were found to be equivalent to those used at the U.S. Army Medical Research Institute of Chemical Defense. CEES increases the activity of the transcription factor NF-κB, and consequently, there is an increase in proinflammatory cytokine production (e.g., TNF-α). PARP activity increases dramatically in both CEES- (Crawford, unpublished results) and SM-exposed tissues (Bhat et al., 2006). Increased PARP activity affects the energy levels of the cell by oxidizing NADPH, which causes a redox imbalance ($NADP^{+}$/NADPH). The transcription factor NF-κB and caspases are increased in CEES- and SM-exposed tissues. In both CEES and SM exposures, there is a loss of GSH, likely due to direct interaction with thiols and OS. The combined loss of GSH, NADH, and NADPH has far-reaching ramifications on multiple cellular systems, particularly redox-regulated pathways.

A. Antidotes

Lewisite is the only vesicant with a proven antidote—British anti-lewisite (2,3-dimercaptopropanol). Increasing antioxidant levels have been found to be protective against the mustards analog, NAC. NAC, which we have used in our studies with CEES, is immediately clinically available. It is most commonly used for acetaminophen overdose. NAC has a long history of several gram quantities administered in several doses and has minimal adverse reactions. In the case of acetaminophen overdose, it is administered via the oral-gastric route, which increases hepatic GSH levels, and in turn, suppresses inflammatory cytokines (Dambach et al., 2006). Liposome encapsulation of both water- and fat-soluble antioxidants was proven to be more effective in the suppression of OS than the free molecule of NAC.

Antioxidants that are liposome encapsulated are advantageous in that they enhance delivery to sites at which inflammation occurs. In light of the common effect that the vesicants have on redox-regulated pathways and OS, it becomes a compelling reason for additional research. The down-regulation of OS may be a very significant step forward in developing treatment countermeasures against several vesicants and other WMD.

REFERENCES

Akira, S. and Kishimoto, T. (1997). NF-IL6 and NF-κB in cytokine gene regulation. *Adv Immunol* 65, 1–46.

Algvere, P.V. and Seregard, S. (2002). Age-related maculopathy: pathogenetic features and new treatment modalities. *Acta Ophthalmol Scand* 80, 136–43.

Allan, D. (2000). Lipid metabolic changes caused by short-chain ceramides and the connection with apoptosis. *Biochem J* 345 (Pt 3), 603–10.

Alphonse, G., Aloy, M.T., Broquet, P., Gerard, J.P., Louisot, P., Rousson, R., and Rodriguez-Lafrasse, C. (2002). Ceramide induces activation of the mitochondrial/caspases pathway in Jurkat and SCC61 cells

sensitive to gamma-radiation but activation of this sequence is defective in radioresistant SQ20B cells. *Int J Radiat Biol* 78, 821–35.

Angel, P. and Karin, M. (1991). The role of Jun, Fos and the AP-1 complex in cell-proliferation and transformation. *Biochim Biophys Acta* 1072, 129–57.

Angel, P., Baumann, I., Stein, B., Delius, H., Rahmsdorf, H.J., and Herrlich, P. (1987). 12-*O*-tetradecanoyl-phorbol-13-acetate induction of the human collagenase gene is mediated by an inducible enhancer element located in the 5′-flanking region. *Mol Cell Biol* 7, 2256–66.

Anslow, W.P. (1946). *Systemic Pharmacology and Pathology of Sulfur and Nitrogen Mustards*. Washington, DC: Office of Scientific Research and Development, National Defense Research Committee, Div. 9.

Ansceschi, M. (1989). The alveolar type II cells as a model for investigating the metabolism of surfactant phospholipids. *Eur Respir J* Suppl 3, 10s–12.

Armstrong, J.S. and Jones, D.P. (2002). Glutathione depletion enforces the mitochondrial permeability transition and causes cell death in Bcl-2 overexpressing HL60 cells. *FASEB J* 16, 1263–5.

Arner, E.S. and Holmgren, A. (2000). Physiological functions of thioredoxin and thioredoxin reductase. *Eur J Biochem* 267, 6102–9.

Arrigo, A.P. (1999). Gene expression and the thiol redox state. *Free Radic Biol Med* 27, 936–44.

Arroyo, C.M., Schafer, R.J., Kurt, E.M., Broomfield, C.A., and Carmichael, A.J. (2000). Response of normal human keratinocytes to sulfur mustards: cytokine release. *J Appl Toxicol* 20 Suppl 1, S63–72.

Aruoma, O.I. and Halliwell, B. (1987). Action of hypochlorous acid on the antioxidant protective enzymes superoxide dismutase, catalase and glutathione peroxidase. *Biochem J* 248, 973–6.

Aslan, S., Kandis, H., Akgun, M., Cakir, Z., Inandi, T., and Gorguner, M. (2006). The effect of nebulized $NaHCO_3$ treatment on ''RADS'' due to chlorine gas inhalation. *Inhal Toxicol* 18, 895–900.

Awasthi, S., Vivekananda, J., Awasthi, V., Smith, D., and King, R.J. (2001). CTP: phosphocholine cytidylyltransferase inhibition by ceramide via PKC-α, p38 MAPK, cPLA2, and 5-lipoxygenase. *Am J Physiol Lung Cell Mol Physiol* 281, L108–18.

Baburina, I. and Jackowski, S. (1998). Apoptosis triggered by 1-*O*-octadecyl-2-*O*-methyl-rac-glycero-3-phosphocholine is prevented by increased expression of CTP: phosphocholine cytidylyltransferase. *J Biol Chem* 273, 2169–73.

Baeuerle, P.A. and Baltimore, D. (1996). NF-κB: ten years after. *Cell* 87, 13–20.

Banin, E., Morad, Y. et al. (2003). Injury induced by chemical warfare agents: characterization and treatment of ocular tissues exposed to nitrogen mustard. *Invest Ophthalmol Vis Sci* 44(7): 2966–2972.

Barnes, P.J. and Adcock, I.M. (1998). Transcription factors and asthma. *Eur Respir J* 12, 221–34.

Barron, E.S., Miller, Z.B. et al. (1947). Reactivation by dithiols of enzymes inhibited by lewisite. *Biochem J* 41(1): 69–74.

Bartsch, H. and Nair, J. (2006). Chronic inflammation and OS in the genesis and perpetuation of cancer: role of lipid peroxidation, DNA damage, and repair. *Langenbecks Arch Surg* 391(5): 499–510.

Bazan, N.G. (1989). The metabolism of omega-3 polyunsaturated fatty acids in the eye: the possible role of docosahexaenoic acid and docosanoids in retinal physiology and ocular pathology. *Prog Clin Biol Res* 312, 95–112.

Beatty, S., Koh, H-H., Phil, M., Henson, D., and Boulton, M.E. (2000). The role of oxidative stress in the pathogenesis of age-related macular degeneration. *Surv Opthalmol* 45, 115–134.

Beatty, S., Murray, I.J., Henson, D.B., Carden, D., Koh, H., and Boulton, M.E. (2001). Macular pigment and risk for age-related macular degeneration in subjects from a Northern European population. *Invest Ophthalmol Vis Sci* 42, 439–46.

Bhat, K.R., Benton, B.J., and Ray, R. (2006). Poly (ADP-ribose) polymerase (PARP) is essential for sulfur mustards-induced DNA damage repair, but has no role in DNA ligase activation. *J Appl Toxicol* 26, 452–7.

Black, R.M. and Read, R.W. (1995). Biological fate of sulfur mustards, 1,1′-thiobis(2-chloroethane): identification of beta-lyase metabolites and hydrolysis products in human urine. *Xenobiotica* 25, 167–73.

Black, R.M., Brewster, K., Clarke, R.J., Hambrook, J.L., Harrison, J.M., and Howells, D.J. (1992). Biological fate of sulfur mustards, 1,1′-thiobis(2-chloroethane): isolation and identification of urinary metabolites following intraperitoneal administration to rat. *Xenobiotica* 22, 405–18.

Bladergroen, B.A., Bussiere, M., Klein, W., Geelen, M.J., Van Golde, L.M., and Houweling, M. (1999). Inhibition of phosphatidylcholine and phosphatidylethanolamine biosynthesis in rat-2 fibroblasts by cell-permeable ceramides. *Eur J Biochem* 264, 152–60.

Blaha, M., Bowers, W., Kohl, J., DuBose, D., and Walker, J. (2000a). Il-1-related cytokine responses of nonimmune skin cells subjected to CEES exposure with and without potential vesicant antagonists. *In Vitro Mol Toxicol* 13, 99–111.

Blaha, M., Bowers, W., Kohl, J., DuBose, D., Walker, J., Alkhyyat, A., and Wong, G. (2000b). Effects of CEES on inflammatory mediators, heat shock protein 70A, histology and ultrastructure in two skin models. *J Appl Toxicol* 20 Suppl 1, S101–8.

Blaha, M., Kohl, J., DuBose, D., Bowers, W., Jr., and Walker, J. (2001). Ultrastructural and histological effects of exposure to CEES or heat in a human epidermal model. *In Vitro Mol Toxicol* 14, 15–23.

Borak, J. and Sidell, F.R. (1992). Agents of chemical warfare: sulfur mustards. *Ann Emerg Med* 21, 303–8.

Bostan, M., Galatiuc, C., Hirt, M., Constantin, M.C., Brasoveanu, L.I., and Iordachescu, D. (2003). Phospholipase A2 modulates respiratory burst developed by neutrophils in patients with rheumatoid arthritis. *J Cell Mol Med* 7, 57–66.

Bouchard, V.J., Rouleau, M., and Poirier, G.G. (2003). PARP-1, a determinant of cell survival in response to DNA damage. *Exp Hematol* 31, 446–54.

Bowler, R.P. and Crapo, J.D. (2002). Oxidative stress in allergic respiratory diseases. *J Allergy Clin Immunol* 110, 349–56.

Brennan, F.M., Maini, R.N., and Feldmann, M. (1995). Cytokine expression in chronic inflammatory disease. *Br Med Bull* 51, 368–84.

Buchanan, B.B., Schurmann, P., Decottignies, P., and Lozano, R.M. (1994). Thioredoxin: a multifunctional regulatory protein with a bright future in technology and medicine. *Arch Biochem Biophys* 314, 257–60.

Burkle, A. (2001). PARP-1: a regulator of genomic stability linked with mammalian longevity. *Chembiochem* 2, 725–8.

Byers, S., Anderson, D., Brobst, D., and Cowan, F. (2000). Automated assay for nicotinamide adenine dinucleotide (NAD^+). *J Appl Toxicol* 20 Suppl 1, S19–22.

Byrne, M.P., Broomfield, C.A., and Stites, W.E. (1996). Mustards gas crosslinking of proteins through preferential alkylation of cysteines. *J Protein Chem* 15, 131–6.

Calvet, J.H., Jarreau, P.H., Levame M., D'Ortho, M.P., Lorino, H., Harf, A., and Macquin-Mavier, M.I. (1994). Acute and chronic effects of sulfur mustards intoxication in the guinea pig. *J Appl Physiol* 76, 681–8.

Carr, A.C., Hawkins, C.L., Thomas, S.R., Stocker, R., and Frei, B. (2001). Relative reactivities of *N*-chloramines and hypochlorous acid with human plasma constituents. *Free Radic Biol Med* 30, 526–36.

Celli, A., Que, F.G., Gores, G.J., and LaRusso, N.F. (1998). Glutathione depletion is associated with decreased Bcl-2 expression and increased apoptosis in cholangiocytes. *Am J Physiol* 275, G749–57.

Chatterjee, D., Mukherjee, S., Smith, M.G., and Das, S.K. (2003). Signal transduction events in lung injury induced by 2-chloroethyl ethyl sulfide, a mustards analog. *J Biochem Mol Toxicol* 17, 114–21.

Chatterjee, D., Mukherjee, S., Smith, M.G., and Das, S.K. (2004). Role of sphinomyelinase in the environmental toxin induced apoptosis of pulmonary cells. In: *In Lipids: Sphingolipid Metabolizing Enzymes*, eds. Dipak, Haldar, and Salil K Das, Research Signpost, pp. 117–139, Trivandum, Kerala, India.

Chen, C.C., Wang, J.K., and Lin, S.B. (1998). Antisense oligonucleotides targeting protein kinase C-alpha, -beta I, or -delta but not -eta inhibit lipopolysaccharide-induced nitric oxide synthase expression in RAW 264.7 macrophages: involvement of a nuclear factor kappa B-dependent mechanism. *J Immunol* 161, 6206–14.

Chevillard, M., Lainee, P., Robineau, P., and Puchelle, E. (1992). Toxic effects of sulfur mustards on respiratory epithelial cells in culture. *Cell Biol Toxicol* 8, 171–81.

Choi, H.S. and Moore, D.D. (1993). Induction of c-fos and c-jun gene expression by phenolic antioxidants. *Mol Endocrinol* 7, 1596–602.

Coffey, R.N., Watson, R.W., Hegarty, N.J., O'Neill, A., Gibbons, N., Brady, H.R., and Fitzpatrick, J.M. (2000). Thiol-mediated apoptosis in prostate carcinoma cells. *Cancer* 88, 2092–104.

Colvin, O.M., Friedman, H.S., Gamcsik, M.P., Fenselau, C., and Hilton, J. (1993). Role of glutathione in cellular resistance to alkylating agents. *Adv Enzyme Regul* 33, 19–26.

Coppola, S. and Ghibelli, L. (2000). GSH extrusion and the mitochondrial pathway of apoptotic signalling. *Biochem Soc Trans* 28, 56–61.

Costantini, P., Petronilli, V., Colonna, R., and Bernardi, P. (1995). On the effects of paraquat on isolated mitochondria. Evidence that paraquat causes opening of the cyclosporin A-sensitive permeability transition pore synergistically with nitric oxide. *Toxicology* 99, 77–88.

Costantini, P., Chernyak, B.V., Petronilli, V., and Bernardi, P. (1996). Modulation of the mitochondrial permeability transition pore by pyridine nucleotides and dithiol oxidation at two separate sites. *J Biol Chem* 271, 6746–51.

Cowan, F.M. and Broomfield, C.A. (1993). Putative roles of inflammation in the dermato-pathology of sulfur mustards. *Cell Biol and Toxicol* 9, 201–213.

Cowan, F.M., Broomfield, C.A., and Smith, W.J. (1992). Inhibition of sulfur mustards-increased protease activity by niacinamide, *N*-acetyl cysteine or dexamethasone. *Cell Biol Toxicol* 8, 129–138.

Crapo, J.D. (2003a). Oxidative stress as an initiator of cytokine release and cell damage. *Eur Respir J Suppl* 44, 4s–6s.

Crapo, J.D. (2003b). Redox active agents in inflammatory lung injury. *Am J Respir Crit Care Med* 168, 1027–8.

Crystal, R.G., Bitterman, P.B., Rennard, S.I., Hance, A.J., and Keogh, B.A. (1984). Interstitial lung diseases of unknown cause. Disorders characterized by chronic inflammation of the lower respiratory tract. *N Engl J Med* 310, 235–44.

Cui, Z., Houweling, M., Chen, M.H., Record, M., Chap, H., Vance, D.E., and Terce, F. (1996). A genetic defect in phosphatidylcholine biosynthesis triggers apoptosis in Chinese hamster ovary cells. *J Biol Chem* 271, 14668–71.

D'Amours, D., Germain, M., Orth, K., Dixit, V.M., and Poirier, G.G. (1998). Proteolysis of poly(ADP-ribose) polymerase by caspase 3: kinetics of cleavage of mono(ADP-ribosyl)ated and DNA-bound substrates. *Radiat Res* 150, 3–10.

D'Amours, D., Desnoyers, S., D'Silva, I., and Poirier, G.G. (1999). Poly(ADP-ribosyl)ation reactions in the regulation of nuclear functions. *Biochem J* 342 (Pt 2), 249–68.

Dahl, H., Gluud, B., Vangsted, P., and Norn, M. (1985). Eye lesions induced by mustards gas. *Acta Ophthamol Suppl* 173, 330–35.

Dalton, T.P., Shertzer, H.G., and Puga, A. (1999). Regulation of gene expression by reactive oxygen. *Annu Rev Pharmacol Toxicol* 39, 67–101.

Dambach, D.M., Durham, S.K., Laskin, J.D., and Laskin, D.L. (2006). Distinct roles of NF-κB p50 in the regulation of acetaminophen-induced inflammatory mediator production and hepatotoxicity. *Toxicol Appl Pharmacol* 211, 157–65.

Das, S.K., Mukherjee, S., Smith, M.G., and Chatterjee, D. (2003). Prophylactic protection by *N*-acetylcysteine against the pulmonary injury induced by 2-chloroethyl ethyl sulfide, a mustards analogue. *J Biochem Mol Toxicol* 17, 177–84.

Datta, R., Hallahan, D.E., Kharbanda, S.M., Rubin, E., Sherman, M.L., Huberman, E., Weichselbaum, R.R., and Kufe, D.W. (1992). Involvement of reactive oxygen intermediates in the induction of c-jun gene transcription by ionizing radiation. *Biochemistry* 31, 8300–6.

Decker, P. and Muller, S. (2002). Modulating poly (ADP-ribose) polymerase activity: potential for the prevention and therapy of pathogenic situations involving DNA damage and oxidative stress. *Curr Pharm Biotechnol* 3, 275–83.

Delamere, N.A. (1996). Ascorbic acid and the eye. *Subcell Biochem* 25, 313–29.

den Hartog, G.J., Vegt, E., van der Vijgh, W.J., Haenen, G.R., and Bast, A. (2002). Hypochlorous acid is a potent inhibitor of acetylcholinesterase. *Toxicol Appl Pharmacol* 181, 228–32.

DePaso, W.J. and Winterbauer, R.H. (1991). Interstitial lung disease. *Dis Mon* 37, 61–133.

deRojas Walker, T., Tamir, S., Ji, H., Wishnok, J.S., and Tannenbaum, S.R. (1995). Nitric oxide induces oxidative damage in addition to deamination in macrophage DNA. *Chem Res Toxicol* 8, 473–7.

Dobrowsky, R.T., Kamibayashi, C., Mumby, M.C., and Hannun, Y.A. (1993). Ceramide activates heterotrimeric protein phosphatase 2A. *J Biol Chem* 268, 15523–30.

Downey, J.S. and Han, J. (1998). Cellular activation mechanisms in septic shock. *Front Biosci* 3, d468–76.

Duke-Elder, S. and MacFaul, P.A. (1972). *Injuries, Part 2 Non-mechanical Injuries*, Henry Kimpton, London.

El-Youssef, M. (2003). Wilson disease. *Mayo Clin Proc* 78, 1126–36.

Elsayed, N.M., Omaye, S.T., Klain, G.J., and Korte, D.W., Jr. (1992). Free radical-mediated lung response to the monofunctional sulfur mustards butyl 2-chloroethyl sulfide after subcutaneous injection. *Toxicology* 72, 153–65.

Emad, A. and Rezaian, G.R. (1997). The diversity of the effects of sulfur mustards gas inhalation on respiratory system 10 years after a single, heavy exposure: analysis of 197 cases. *Chest* 112, 734–8.

Emad, A. and Rezaian, G.R. (1999). Immunoglobulins and cellular constituents of the BAL fluid of patients with sulfur mustards gas-induced pulmonary fibrosis. *Chest* 115, 1346–51.

Erdincler, D.S., Seven, A., Inci, F., Beger, T., and Candan, G. (1997). Lipid peroxidation and antioxidant status in experimental animals: effects of aging and hypercholesterolemic diet. *Clin Chim Acta* 265, 77–84.

Fan, J., Shek, P.N., Suntres, Z.E., Li, Y.H., Oreopoulos, G.D., and Rotstein, O.D. (2000). Liposomal antioxidants provide prolonged protection against acute respiratory distress syndrome. *Surgery* 128, 332–8.

Farrukh, I.S., Michael, J.R., Peters, S.P., Sciuto, A.M., Adkinson, N.F., Jr., Freeland, H.S., Paky, A., Spannhake, E.W., Summer, W.R., and Gurtner, G.H. (1988). The role of cyclooxygenase and lipoxygenase mediators in oxidant-induced lung injury. *Am Rev Respir Dis* 137, 1343–9.

Fattman, C.L., Schaefer, L.M., and Oury, T.D. (2003). Extracellular superoxide dismutase in biology and medicine. *Free Radic Biol Med* 35, 236–56.

Fernandez-Checa, J.C., Kaplowitz, N., Garcia-Ruiz, C., and Colell, A. (1998). Mitochondrial glutathione: importance and transport. *Semin Liver Dis* 18, 389–401.

Folkes, L.K., Candeias, L.P., and Wardman, P. (1995). Kinetics and mechanisms of hypochlorous acid reactions. *Arch Biochem Biophys* 323, 120–6.

Fox, M. and Scott, D. (1980). The genetic toxicology of nitrogen and sulfur mustards. *Mut Res* 75, 131–68.

Freeman, M.L., Huntley, S.A., Meredith, M.J., Senisterra, G.A., and Lepock, J. (1997). Destabilization and denaturation of cellular protein by glutathione depletion. *Cell Stress Chaperones* 2, 191–8.

Fu, Y., McCormick, C.C., Roneker, C., and Lei, X.G. (2001). Lipopolysaccharide and interferon-gamma-induced nitric oxide production and protein oxidation in mouse peritoneal macrophages are affected by glutathione peroxidase-1 gene knockout. *Free Radic Biol Med* 31, 450–9.

Fujihara, M., Connolly, N., Ito, N., and Suzuki, T. (1994). Properties of protein kinase C isoforms (beta II, epsilon, and zeta) in a macrophage cell line (J774) and their roles in LPS-induced nitric oxide production. *J Immunol* 152, 1898–906.

Gamaley, I.A. and Klyubin, I.V. (1999). Roles of reactive oxygen species: signaling and regulation of cellular functions. *Int Rev Cytol* 188, 203–55.

Ganea, E. and Harding, J.J. (2006). Glutathione-related enzymes and the eye. *Curr Eye Res* 31, 1–11.

Ghezzi, P. and Ungheri, D. (2004). Synergistic combination of *N*-acetylcysteine and ribavirin to protect from lethal influenza viral infection in a mouse model. *Int J Immunopathol Pharmacol* 17, 99–102.

Ghosh, A., Akech, J., Mukherjee, S., and Das, S.K. (2002). Differential expression of cholinephosphotransferase in normal and cancerous human mammary epithelial cells. *Biochem Biophys Res Commun* 297, 1043–8.

Gidwani, A., Brown, H.A., Holowka, D., and Baird, B. (2003). Disruption of lipid order by short-chain ceramides correlates with inhibition of phospholipase D and downstream signaling by FcepsilonRI. *J Cell Sci* 116, 3177–87.

Goldman, M. and Dacre, J.C. (1989). Lewisite: its chemistry, toxicology, and biological effects. *Rev Environ Contam Toxicol* 110, 75–115.

Griffith, O.W. and Meister, A. (1985). Origin and turnover of mitochondrial glutathione. *Proc Natl Acad Sci U S A* 82, 4668–72.

Gunnarsson, M., Walther, S.M., Seidal, T., and Lennquist, S. (2000). Effects of inhalation of corticosteroids immediately after experimental chlorine gas lung injury. *J Trauma* 48, 101–7.

Haddad, J.J. (2004). Redox and oxidant-mediated regulation of apoptosis signaling pathways: immuno-pharmaco-redox conception of oxidative siege versus cell death commitment. *Int Immunopharmacol* 4, 475–93.

Haliday, E.M., Ramesha, C.S., and Ringold, G. (1991). TNF induces c-fos via a novel pathway requiring conversion of arachidonic acid to a lipoxygenase metabolite. *EMBO J* 10, 109–15.

Hampton, M.B., Fadeel, B., and Orrenius, S. (1998). Redox regulation of the caspases during apoptosis. *Ann N Y Acad Sci* 854, 328–35.

Hanna, P.C., Kruskal, B.A., Ezekowitz, R.A., Bloom, B.R., and Collier, R.J. (1994). Role of macrophage oxidative burst in the action of anthrax lethal toxin. *Mol Med* 1, 7–18.

Hannun, Y.A. and Obeid, L.M. (1997). Mechanisms of ceramide-mediated apoptosis. *Adv Exp Med Biol* 407, 145–9.

Hannun, Y.A. and Luberto, C. (2000). Ceramide in the eukaryotic stress response. *Trends Cell Biol* 10, 73–80.

Hayes, K.C. (1974). Retinal degeneration in monkeys induced by deficiencies of vitamin E or A. *Invest Ophthalmol* 13, 499–510.

Hearps, A.C., Burrows, J., Connor, C.E., Woods, G.M., Lowenthal, R.M., and Ragg, S.J. (2002). Mitochondrial cytochrome *c* release precedes transmembrane depolarisation and caspase-3 activation during ceramide-induced apoptosis of Jurkat T cells. *Apoptosis* 7, 387–94.

Hetz, C.A., Hunn, M., Rojas, P., Torres, V., Leyton, L., and Quest, A.F. (2002). Caspase-dependent initiation of apoptosis and necrosis by the Fas receptor in lymphoid cells: onset of necrosis is associated with delayed ceramide increase. *J Cell Sci* 115, 4671–83.

Hirota, K., Matsui, M., Iwata, S., Nishiyama, A., Mori, K., and Yodoi, J. (1997). AP-1 transcriptional activity is regulated by a direct association between thioredoxin and Ref-1. *Proc Natl Acad Sci U S A* 94, 3633–8.

Hogg, R. and Chakravarthy, U. (2004). AMD and micronutrient antioxidants. *Curr Eye Res* 29, 387–401.

Holmgren, A. (1972). Tryptophan fluorescence study of conformational transitions of the oxidized and reduced form of thioredoxin. *J Biol Chem* 247, 1992–8.

Holmgren, A. (1985). Thioredoxin. *Annu Rev Biochem* 54, 237–71.

Holmgren, A. (1989). Thioredoxin and glutaredoxin systems. *J Biol Chem* 264, 13963–6.

Hsu, W., Kerppola, T.K., Chen, P.L., Curran, T., and Chen Kiang, S. (1994). Fos and Jun repress transcription activation by NF-IL6 through association at the basic zipper region. *Mol Cell Biol* 14, 268–76.

Hunt, D.F., Organisciak, D.T., Wang, H.M., and Wu, R.L. (1984). Alpha-tocopherol in the developing rat retina: a high pressure liquid chromatographic analysis. *Curr Eye Res* 3, 1281–8.

Hwang, C., Sinskey, A.J., and Lodish, H.F. (1992). Oxidized redox state of glutathione in the endoplasmic reticulum. *Science* 257, 1496–502.

Inoue, H., Asaka, T., Nagata, N., and Koshihara, Y. (1997). Mechanism of mustards oil-induced skin inflammation in mice. *Eur J Pharmacol* 333, 231–40.

Jaskot, R.H., Grose, E.C., Richards, J.H., and Doerfler, D.L. (1991). Effects of inhaled phosgene on rat lung antioxidant systems. *Fundam Appl Toxicol* 17, 666–74.

Javadi, M.A., Yazdani, S., Sajjadi, H., Jadidi, K., Karimian, F., Einollahi, B., Ja'farinasab, M.R., and Zare, M. (2005). Chronic and delayed-onset mustards gas keratitis: report of 48 patients and review of literature. *Ophthalmology* 112, 617–25.

Jiang, Q. and Ames, B.N. (2003). Gamma-tocopherol, but not alpha-tocopherol, decreases proinflammatory eicosanoids and inflammation damage in rats. *FASEB J* 17, 816–22.

Johnstone, R.M. (1963). Sulfhydryl Agents: Arsenicals. In *Metabolic Inhibitors* R.M. Hochester and J.H. Quastel (Eds.), New York: Academic Press, 99–118.

Jones, D.P., Maellaro, E., Jiang, S., Slater, A.F., and Orrenius, S. (1995). Effects of *N*-acetyl-L-cysteine on T-cell apoptosis are not mediated by increased cellular glutathione. *Immunol Lett* 45, 205–9.

Kadar, T., Turetz, J., Fishbine, E., Sahar, R., Chapman, S., and Amir, A. (2001). Characterization of acute and delayed ocular lesions induced by sulfur mustards in rabbits. *Curr Eye Res* 22, 42–53.

Kang, K.A., Zhang, R., Lee, K.H., Chae, S., Kim, B.J., Kwak, Y.S., Park, J.W., Lee, N.H., and Hyun, J.W. (2006). Protective effect of triphlorethol-A from Ecklonia cava against ionizing radiation in vitro. *J Radiat Res (Tokyo)* 47, 61–8.

Kehe, K. and Szinicz, L. (2005). Medical aspects of sulphur mustard poisoning. *Toxicology* 214(3): 198–209.

Kent, C. (1995). Eukaryotic phospholipid biosynthesis. *Annu Rev Biochem* 64, 315–43.

Kerppola, T.K. and Curran, T. (1994). Maf and Nrl can bind to AP-1 sites and form heterodimers with Fos and Jun. *Oncogene* 9, 675–84.

Khachik, F., Bernstein, P.S., and Garland, D.L. (1997). Identification of lutein and zeaxanthin oxidation products in human and monkey retinas. *Invest Ophthalmol Vis Sci* 38, 1802–11.

Kim, M.Y., Zhang, T., and Kraus, W.L. (2005). Poly(ADP-ribosyl)ation by PARP-1: 'PAR-laying' NAD^+ into a nuclear signal. *Genes Dev* 19, 1951–67.

Kimura, H., Sawada, T., Oshima, S., Kozawa, K., Ishioka, T., and Kato, M. (2005). Toxicity and roles of reactive oxygen species. *Curr Drug Targets Inflamm Allergy* 4, 489–95.

Kinnula, V.L. and Crapo, J.D. (2003). Superoxide dismutases in the lung and human lung diseases. *Am J Respir Crit Care Med* 167, 1600–19.

Kirlin, W.G., Cai, J., Thompson, S.A., Diaz, D., Kavanagh, T.J., and Jones, D.P. (1999). Glutathione redox potential in response to differentiation and enzyme inducers. *Free Radic Biol Med* 27(11–12): 1208–18.

Kolesnick, R.N. and Krönke, M. (1998). Regulation of ceramide production and apoptosis. *Annu Rev Physiol* 60, 643–65.

Kowluru, R.A. and Kennedy, A. (2001). Therapeutic potential of anti-oxidants and diabetic retinopathy. *Expert Opin Investig Drugs* 10, 1665–76.

Krippner, A., Matsuno-Yagi, A., Gottlieb, R.A., and Babior, B.M. (1996). Loss of function of cytochrome *c* in Jurkat cells undergoing fas-mediated apoptosis. *J Biol Chem* 271, 21629–36.

Kuhn, J.F., Hoerth, P., Hoehn, S.T., Preckel, T., and Tomer, K.B. (2006). Proteomics study of anthrax lethal toxin-treated murine macrophages. *Electrophoresis* 27, 1584–97.

Kumar, O., Sugendran, K., and Vijayaraghavan, R. (2003). Oxidative stress associated hepatic and renal toxicity induced by ricin in mice. *Toxicon* 41, 333–8.

Kun, E. and Bauer, P.I. (2001). Cell biological functions of PARP I: an overview. *Ital J Biochem* 50, 15–8.

Kurinna, S.M., Tsao, C.C., Nica, A.F., Jiffar, T., and Ruvolo, P.P. (2004). Ceramide promotes apoptosis in lung cancer-derived A549 cells by a mechanism involving c-Jun NH2-terminal kinase. *Cancer Res* 64, 7852–6.

Langenberg, J.P., van der Schans, G.P., Spruit, H.E., Kuijpers, W.C., Mars-Groenendijk, R.H., van Dijk Knijnenburg, H.C., Trap, H.C., van Helden, H.P., and Benschop, H.P. (1998). Toxicokinetics of sulfur mustards and its DNA-adducts in the hairless guinea pig. *Drug Chem Toxicol* 21 Suppl 1, 131–47.

Lee, W., Mitchell, P., and Tjian, R. (1987). Purified transcription factor AP-1 interacts with TPA-inducible enhancer elements. *Cell* 49, 741–52.

Levitt, J.M., Lodhi, I.J., Nguyen, P.K., Ngo, V., Clift, R., Hinshaw, D.B., and Sweeney, J.F. (2003). Low-dose sulfur mustards primes oxidative function and induces apoptosis in human polymorphonuclear leukocytes. *Int Immunopharmacol* 3, 747–56.

Libon, C., Forestier, F., Cotte-Laffitte, J., Labarre, C., and Quero, A.M. (1993). Effect of acute oral administration of alcohol on superoxide anion production from mouse alveolar macrophages. *J Leukoc Biol* 53, 93–8.

Lin, D., Barnett, M. et al. (2005). Expression of superoxide dismutase in whole lens prevents cataract formation. *Mol Vis* 11, 853–858.

Liu, H., Lightfoot, R., and Stevens, J.L. (1996). Activation of heat shock factor by alkylating agents is triggered by glutathione depletion and oxidation of protein thiols. *J Biol Chem* 271, 4805–12.

Lo, Y.Y. and Cruz, T.F. (1995). Involvement of reactive oxygen species in cytokine and growth factor induction of c-fos expression in chondrocytes. *J Biol Chem* 270, 11727–30.

Lou, M.F. (2003). Redox regulation in the lens. *Prog Retin Eye Res* 22, 657–82.

Ludlum, D.B., Tong, P.A., Mehata, J.R., Kirk, M.C., and Papirmeister, B. (1984). Formation of ethylthioethyl deoxy guanosine from the reaction of chloroethyl ethyl sulphide with deoxyguanosine. *Cancer Res*, 44, 12(1): 5698–5701.

Luthman, M. and Holmgren, A. (1982). Rat liver thioredoxin and thioredoxin reductase: purification and characterization. *Biochemistry* 21, 6628–33.

Mastruzzo, C., Crimi, N., and Vancheri, C. (2002). Role of oxidative stress in pulmonary fibrosis. *Monaldi Arch Chest Dis* 57, 173–6.

Mathias, S., Dressler, K.A., and Kolesnick, R.N. (1991). Characterization of a ceramide-activated protein kinase: stimulation by tumor necrosis factor alpha. *Proc Natl Acad Sci U S A* 88, 10009–13.

Matthews, J.R., Wakasugi, N., Virelizier, J.L., Yodoi, J., and Hay, R.T. (1992). Thioredoxin regulates the DNA binding activity of NF-κB by reduction of a disulphide bond involving cysteine 62. *Nucleic Acids Res* 20, 3821–30.

McClintock, S.D., Till, G.O., Smith, M.G., and Ward, P.A. (2002). Protection from half-mustards-gas-induced acute lung injury in the rat. *J Appl Toxicol* 22, 257–62.

McClintock, S.D., Hoesel, L.M., Das, S.K., Till, G.O., Neff, T., Kunkel, R.G., Smith, M.G., and Ward, P.A. (2006). Attenuation of half sulfur mustards gas-induced acute lung injury in rats. *J Appl Toxicol* 26, 126–31.

McKenzie, S.M., Doe, W.F., and Buffinton, G.D. (1999). 5-aminosalicylic acid prevents oxidant mediated damage of glyceraldehyde-3-phosphate dehydrogenase in colon epithelial cells. *Gut* 44, 180–5.

McMillan, D.C., Sarvate, S.D., Oatis, J.E., Jr., and Jollow, D.J. (2004). Role of oxidant stress in lawsone-induced hemolytic anemia. *Toxicol Sci* 82, 647–55.

Megaw, J.M. (1984). Glutathione and ocular photobiology. *Curr Eye Res* 3, 83–7.

Mei, N., Tamae, K., Kunugita, N., Hirano, T., and Kasai, H. (2003). Analysis of 8-hydroxydeoxyguanosine 5′-monophosphate (8-OH-dGMP) as a reliable marker of cellular oxidative DNA damage after gamma-irradiation. *Environ Mol Mutagen* 41, 332–8.

Mercurio, F. and Manning, A.M. (1999a). Multiple signals converging on NF-κB. *Curr Opin Cell Biol* 11, 226–32.

Mercurio, F. and Manning, A.M. (1999b). NF-κB as a primary regulator of the stress response. *Oncogene* 18, 6163–71.

Meyer, M., Schreck, R., and Baeuerle, P.A. (1993). H_2O_2 and antioxidants have opposite effects on activation of NF-κB and AP-1 in intact cells: AP-1 as secondary antioxidant-responsive factor. *EMBO J* 12, 2005–15.

Mihm, S., Galter, D., and Droge, W. (1995). Modulation of transcription factor NF kappa B activity by intracellular glutathione levels and by variations of the extracellular cysteine supply. *FASEB J* 9, 246–52.

Miquel, K., Pradines, A., Terce, F., Selmi, S., and Favre, G. (1998). Competitive inhibition of choline phosphotransferase by geranylgeraniol and farnesol inhibits phosphatidylcholine synthesis and induces apoptosis in human lung adenocarcinoma A549 cells. *J Biol Chem* 273, 26179–86.

Mol, M.A., van de Ruit, A.M., and Kluivers, A.W. (1989). NAD^+ levels and glucose uptake of cultured human epidermal cells exposed to sulfur mustards. *Toxicol Appl Pharmacol* 98, 159–65.

Moore, L., and Ray, P. (1983). Enhanced inhibition of hepatic microsomal calcium pump activity by CCl4 treatment of isopropanol-pretreated rats. *Toxicol Appl Pharmacol* 71, 54–8.

Morad, Y., Banin, E. et al. (2005) Treatment of ocular tissues exposed to nitrogen mustard: beneficial effects of zinc desferrioxamine combined with steroids. *Invest Ophthalmol Vis Sci* 46(5): 1640–1646.

Naghii, M.R. (2002). Sulfur mustards intoxication, oxidative stress, and antioxidants. *Mil Med* 167, 573–5.

Noltkamper, D. and Burgher, S.W. (2004). Toxicity, phosgene. *eMedicine*.

Nonas, S., Miller, I., Kawkitinarong, K., Chatchavalvanich, S., Gorshkova, I., Bochkov, V.N., Leitinger, N., Natarajan, V., Garcia, J.G., and Birukov, K.G. (2006). Oxidized phospholipids reduce vascular leak and inflammation in rat model of acute lung injury. *Am J Respir Crit Care Med* 173, 1130–8.

Oei, S.L. and Shi, Y. (2001). Poly(ADP-ribosyl)ation of transcription factor Yin Yang 1 under conditions of DNA damage. *Biochem Biophys Res Commun* 285, 27–31.

Ohia, S.E., Opere, C.A., and Leday, A.M. (2005). Pharmacological consequences of oxidative stress in ocular tissues. *Mutat Res* 579, 22–36.

Okamoto, T., Ogiwara, H., Hayashi, T., Mitsui, A., Kawabe, T., and Yodoi, J. (1992). Human thioredoxin/adult T cell leukemia-derived factor activates the enhancer binding protein of human immunodeficiency virus type 1 by thiol redox control mechanism. *Int Immunol* 4, 811–9.

Olea-Azar, C., Rigol, C., Mendizabal, F., Morello, A., Maya, J.D., Moncada, C., Cabrera, E., Di Maio, R., Gonzalez, M., and Cerecetto, H. (2003). ESR spin trapping studies of free radicals generated from nitrofuran derivative analogues of nifurtimox by electrochemical and Trypanosoma cruzi reduction. *Free Radic Res* 37, 993–1001.

Pant, S.C., Vijayaraghavan, R., Kannan, G.M., and Ganesan, K. (2000). Sulfur mustards induced oxidative stress and its prevention by sodium 2,3-dimercapto propane sulphonic acid (DMPS) in mice. *Biomed Environ Sci* 13, 225–32.

Papirmeister, B., Gross, C.L., Meier, H.L., Petrali, J.P., and Johnson, J.B. (1985). Molecular basis for mustards-induced vesication. *Fundam Appl Toxicol* 5, S134–49.

Papirmeister, B., Feister, A.J., Robinson, S.I., and Ford, R.D. (1991). *Mustards Gas. Toxic Mechanisms and Pharmacological Implications*, CRC Press, Boca Raton, FL.

Paredi, P., Kharitonov, S.A., and Barnes, P.J. (2002). Analysis of expired air for oxidation products. *Am J Respir Crit Care Med* 166, S31–7.

Peters, R.A., Sinclair, H.M. et al. (1946). An analysis of the inhibition of pyruvate oxidation by arsenicals in relation to the enzyme theory of vesication. *Biochem J* 40(4): 516–524.

Petronilli, V., Costantini, P., Scorrano, L., Colonna, R., Passamonti, S., and Bernardi, P. (1994). The voltage sensor of the mitochondrial permeability transition pore is tuned by the oxidation–reduction state of vicinal thiols. Increase of the gating potential by oxidants and its reversal by reducing agents. *J Biol Chem* 269, 16638–42.

Powis, G., Mustacich, D., and Coon, A. (2000). The role of the redox protein thioredoxin in cell growth and cancer. *Free Radic Biol Med* 29, 312–22.

Pullar, J.M., Winterbourn, C.C., and Vissers, M.C.M. (1999). Loss of GSH and thiol enzymes in endothelial cells exposed to sublethal concentrations of hypochlorous acid. *Am J Physiol Heart Circ Physiol* 277(4): H1505–12.

Pullar, J.M., Vissers, M.C., and Winterbourn, C.C. (2001). Glutathione oxidation by hypochlorous acid in endothelial cells produces glutathione sulfonamide as a major product but not glutathione disulfide. *J Biol Chem* 276, 22120–5.

Pullar, J.M., Winterbourn, C.C., and Vissers, M.C. (2002). The effect of hypochlorous acid on the expression of adhesion molecules and activation of NF-κB in cultured human endothelial cells. *Antioxid Redox Signal* 4, 5–15.

Qin, X.J., Hai, C.X., Liang, X., Wang, P., Chen, H.L., and Liu, R. (2004). [Effect of acute phosgene inhalation on antioxidant enzymes, nitric oxide and nitric-oxide synthase in rats]. *Zhonghua Lao Dong Wei Sheng Zhi Ye Bing Za Zhi* 22, 200–2.

Rahman, I. and Kelly, F. (2003). Biomarkers in breath condensate: a promising new non-invasive technique in free radical research. *Free Radic Res* 37, 1253–66.

Rahman, I. and MacNee, W. (1998). Role of transcription factors in inflammatory lung diseases. *Thorax* 53, 601–12.

Rahman, I., Marwick, J., and Kirkham, P. (2004). Redox modulation of chromatin remodeling: impact on histone acetylation and deacetylation, NF-κB and pro-inflammatory gene expression. *Biochem Pharmacol* 68, 1255–67.

Ramos, B., Salido, G.M., Campo, M.L., and Claro, E. (2000). Inhibition of phosphatidylcholine synthesis precedes apoptosis induced by C2-ceramide: protection by exogenous phosphatidylcholine. *Neuroreport* 11, 3103–8.

Ramos, B., El Mouedden, M., Claro, E., and Jackowski, S. (2002). Inhibition of CTP: phosphocholine cytidylyltransferase by C(2)-ceramide and its relationship to apoptosis. *Mol Pharmacol* 62, 1068–75.

Rao, G.N., Glasgow, W.C., Eling, T.E., and Runge, M.S. (1996). Role of hydroperoxyeicosatetraenoic acids in oxidative stress-induced activating protein 1 (AP-1) activity. *J Biol Chem* 271, 27760–4.

Reddy, V.N. (1990). Glutathione and its function in the lens–an overview. *Exp Eye Res* 50, 771–8.

Reddy, V.N. and Giblin, F.J. (1984). Metabolism and function of glutathione in the lens. *Ciba Found Symp* 106, 65–87.

Reed, D.J. and Savage, M.K. (1995). Influence of metabolic inhibitors on mitochondrial permeability transition and glutathione status. *Biochim Biophys Acta* 1271, 43–50.

Ricketts, K.M., Santai, C.T., France, J.A., Graziosi, A.M., Doyel, T.D., Gazaway, M.Y., and Casillas, R.P. (2000). Inflammatory cytokine response in sulfur mustards-exposed mouse skin. *J Appl Toxicol* 20 Suppl 1, S73–6.

Rikimaru, T., Nakamura, M., Yano, T., Beck, G., Habicht, G.S., Rennie, L.L., Widra, M., Hirshman, C.A., Boulay, M.G., Spannhake, E.W. et al. (1991). Mediators, initiating the inflammatory response, released in organ culture by full-thickness human skin explants exposed to the irritant, sulfur mustards. *J Invest Dermatol* 96, 888–97.

Roberts, J.E. (2001). Ocular phototoxicity. *J Photochem Photobiol B* 64(2–3): 136–143.

Rose, R.C., Richer, S.P., and Bode, A.M. (1998). Ocular oxidants and antioxidant protection. *Proc Soc Exp Biol Med* 217, 397–407.

Rosenthal, D.S., Simbulan Rosenthal, C.M., Iyer, S., Spoonde, A., Smith, W., Ray, R., and Smulson, M.E. (1998). Sulfur mustards induces markers of terminal differentiation and apoptosis in keratinocytes via a Ca^{2+}-calmodulin and caspase-dependent pathway. *J Invest Dermatol* 111, 64–71.

Ryan, A.J., McCoy, D.M., McGowan, S.E., Salome, R.G., and Mallampalli, R.K. (2003). Alveolar sphingolipids generated in response to TNF-alpha modifies surfactant biophysical activity. *J Appl Physiol* 94, 253–8.

Sabourin, C.L., Danne, M.M., Buxton, K.L., Casillas, R.P., and Schlager, J.J. (2002). Cytokine, chemokine, and matrix metalloproteinase response after sulfur mustards injury to weanling pig skin. *J Biochem Mol Toxicol* 16, 263–72.

Safarinejad, M.R., Moosavi, S.A., and Montazeri, B. (2001). Ocular injuries caused by mustards gas: diagnosis, treatment and medical defense. *Mil Med* 166, 67–70.

Saitoh, M., Nishitoh, H., Fujii, M., Takeda, K., Tobiume, K., Sawada, Y., Kawabata, M., Miyazono, K., and Ichijo, H. (1998). Mammalian thioredoxin is a direct inhibitor of apoptosis signal-regulating kinase (ASK) 1. *EMBO J* 17, 2596–606.

Sato, S., Furuta, K., Miyake, T., Mishiro, T., Kohge, N., Akagi, S., Uchida, Y., Rumi, M.A., Ishihara, S., Adachi, K., and Kinoshita, Y. (2006). Hemolytic anemia during 24 weeks of ribavirin and interferon-alpha2b combination therapy does not influence the cardiac function of patients with viral hepatitis C. *J Clin Gastroenterol* 40, 88–9.

Schlager, J.J. and Hart, B.W. (2000). Stress gene activity in HepG2 cells after sulfur mustards exposure. *J Appl Toxicol* 20, 395–405.

Schnellmann, R.G., Gilchrist, S.M., and Mandel, L.J. (1988). Intracellular distribution and depletion of glutathione in rabbit renal proximal tubules. *Kidney Int* 34, 229–33.

Schulze-Osthoff, K., Bauer, M.K., Vogt, M., and Wesselborg, S. (1997). Oxidative stress and signal transduction. *Int J Vitam Nutr Res* 67, 336–42.

Sciuto, A.M. (1998). Assessment of early acute lung injury in rodents exposed to phosgene. *Arch Toxicol* 72, 283–8.

Sciuto, A.M. (2000). Posttreatment with ETYA protects against phosgene-induced lung injury by amplifying the glutathione to lipid peroxidation ratio. *Inhal Toxicol* 12, 347–56.

Sciuto, A.M., and Hurt, H.H. (2004). Therapeutic treatments of phosgene-induced lung injury. *Inhal Toxicol* 16, 565–80.

Sciuto, A.M. and Moran, T.S. (2001). Effect of dietary treatment with n-propyl gallate or vitamin E on the survival of mice exposed to phosgene. *J Appl Toxicol* 21, 33–9.

Sciuto, A.M., Phillips, C.S., Orzolek, L.D., Hege, A.I., Moran, T.S., and Dillman, J.F., III. (2005). Genomic analysis of murine pulmonary tissue following carbonyl chloride inhalation. *Chem Res Toxicol* 18, 1654–60.

Segal, E. and Lang, E. (2005). Toxicity, chlorine gas. *eMedicine*.

Sellmayer, A., Uedelhoven, W.M., Weber, P.C., and Bonventre, J.V. (1991). Endogenous non-cyclooxygenase metabolites of arachidonic acid modulate growth and mRNA levels of immediate-early response genes in rat mesangial cells. *J Biol Chem* 266, 3800–7.

Sen, C.K. (1998). Redox signaling and the emerging therapeutic potential of thiol antioxidants. *Biochem Pharmacol* 55, 1747–58.

Shapira, L., Takashiba, S., Champagne, C., Amar, S., and Van Dyke, T.E. (1994). Involvement of protein kinase C and protein tyrosine kinase in lipopolysaccharide-induced TNF-alpha and IL-1 beta production by human monocytes. *J Immunol* 153, 1818–24.

Shapira, L., Sylvia, V.L., Halabi, A., Soskolne, W.A., Van Dyke, T.E., Dean, D.D., Boyan, B.D., and Schwartz, Z. (1997). Bacterial lipopolysaccharide induces early and late activation of protein kinase C in inflammatory macrophages by selective activation of PKC-epsilon. *Biochem Biophys Res Commun* 240, 629–34.

Shichi, H. (2004). Cataract formation and prevention. *Expert Opin Investig Drugs* 13, 691–701.

Sickel, W. (1972). *Retinal Metabolism in Dark and Light*, Springer-Verlag, Berlin.

Sidell, F., Urbanetti, J.S., Smith, W.J., and Hurst, C.G. (1997). Vesicants. In textbook of military medicine. Washington, DC: Borden Institute, Walter Reed Army Medical Center.

Sidell, F., Urbanetti, J.S., Smith, W.J., and Hurst, C.G. (1997). *Chapter 7 – Vesicants*.

Sikpi, M. and Das, S. (1987). Development of cholinephosphotransferase in guinea pig lung mitochondria and microsomes. *Biochim Biophys Acta* 899, 35–43.

Singh, I., Pahan, K., Khan, M., and Singh, A.K. (1998). Cytokine-mediated induction of ceramide production is redox-sensitive. Implications to proinflammatory cytokine-mediated apoptosis in demyelinating diseases. *J Biol Chem* 273, 20354–62.

Sinha Roy, S., Mukherjee, S., Kabir, S., Rajaratnam, V., Smith, M., and Das, S.K. (2005). Inhibition of cholinephosphotransferase activity in lung injury induced by 2-chloroethyl ethyl sulfide, a mustards analog. *J Biochem Mol Toxicol* 19, 289–97.

Smith, C.V., Jones, D.P., Guenthner, T.M., Lash, L.H., and Lauterburg, B.H. (1996). Compartmentation of glutathione: implications for the study of toxicity and disease. *Toxicol Appl Pharmacol* 140, 1–12.

Snodderly, D.M., Brown, P.K., Delori, F.C., and Auran, J.D. (1984). The macular pigment. I. Absorbance spectra, localization, and discrimination from other yellow pigments in primate retinas. *Invest Ophthalmol Vis Sci* 25, 660–673.

Snodderly, D.M. (1995). Evidence for protection against age-related macular degeneration by carotenoids and antioxidant vitamins. *Am J Clin Nutr* 62, 1448S-61.

Sohrabpour, H. (1984). Clinical manifestations of chemical agents on Iranian combatants during Iran–Iraq conflict. *Arch Belg* Suppl, 291–7.

Solberg, Y., Alcalay, M. et al. (1997). Ocular injury by mustard gas. *Surv Ophthalmol* 41(6): 461–466.

Somani, S.M. and Babu, S.R. (1989). Toxicodynamics of sulfur mustards. *Int J Clin Pharmacol Ther Toxicol* 27, 419–35.

Stadtman, E.R. (2001). Protein oxidation in aging and age-related diseases. *Ann NY Acad Sci* 928: 22–38.

Stauble, B., Boscoboinik, D., Tasinato, A., and Azzi, A. (1994). Modulation of activator protein-1 (AP-1) transcription factor and protein kinase C by hydrogen peroxide and D-alpha-tocopherol in vascular smooth muscle cells. *Eur J Biochem* 226, 393–402.

Stith, I.E. and Das, S.K. (1981). Pulmonary surfactant lipids: studies on cholinephosphotransferase in developing guinea pig lung. *Indian Biologist* 13, 120–8.

Stith, I.E. and Das, S.K. (1982). Development of cholinephosphotransferase in guinea pig lung and mitochondria and microsomes. *Biochem Biophys Acta* 714, 250–6.

Stocken, L.A. and Thompson, R.H.S. (1946c). British anti-lewisite. 3. Arsenic and thiol excretion in animals after treatment of lewisite burns. *Biochem J* 40: 548–554.

Stone, W.L., Mukherjee, S., Smith, M., and Das, S.K. (2002). Therapeutic uses of antioxidant liposomes. *Methods Mol Biol* 199, 145–61.

Stone, W.L., Qui, M., and Smith, M. (2003). Lipopolysaccharide enhances the cytotoxicity of 2-chloroethyl ethyl sulfide. *BMC Cell Biol* 4, 1.

Stone, W.L., Qui, M., Yang, H., and Smith, M. (2004). Lipopolysaccharide enhances the cytotoxicity of 2-chloroethyl ethyl sulfide. *Bioscience Proceedings* Chapter 236, 1–9.

Suntres, Z., Stone, W., and Smith, M.G. (2005). Ricin-induced tissue toxicity: the role of oxidative stress. *J Med CBR Def* 3, http://www.jmedcbr.org/Issue-0301/Suntres/Suntres_1205.html.

Tagaya, Y., Maeda, Y., Mitsui, A., Kondo, N., Matsui, H., Hamuro, J., Brown, N., Arai, K., Yokota, T., Wakasugi, H., and et al. (1989). ATL-derived factor (ADF), an IL-2 receptor/Tac inducer homologous to thioredoxin; possible involvement of dithiol-reduction in the IL-2 receptor induction. *EMBO J* 8, 757–64.

Torchinsky, Y.M. (1981). *Sulfur in Proteins*, Pergamon, Oxford, UK.

Truscott, R.J. (2005). Age-related nuclear cataract-oxidation is the key. *Exp Eye Res* 80, 709–25.

van Blitterswijk, W.J., van der Luit, A.H., Veldman, R.J., Verheij, M., and Borst, J. (2003). Ceramide: second messenger or modulator of membrane structure and dynamics? *Biochem J* 369, 199–211.

van Heyningen, R. (1941). The properties and -SH nature of hexokinase. *Report ETF*, Military Intelligence Division. Great Britain.

Veness-Meehan, K.A., Cheng, E.R., Mercier, C.E., Blixt, S.L., Johnston, C.J., Watkins, R.H., and Horowitz, S. (1991). Cell-specific alterations in expression of hyperoxia-induced mRNAs of lung. *Am J Respir Cell Mol Biol* 5, 516–21.

Vietor, I., Schwenger, P., Li, W., Schlessinger, J., and Vilcek, J. (1993). Tumor necrosis factor-induced activation and increased tyrosine phosphorylation of mitogen-activated protein (MAP) kinase in human fibroblasts. *J Biol Chem* 268, 18994–9.

Virag, L. (2005). Structure and function of poly(ADP-ribose) polymerase-1: role in oxidative stress-related pathologies. *Curr Vasc Pharmacol* 3, 209–14.

Vissers, M.C. and Winterbourn, C.C. (1995). Oxidation of intracellular glutathione after exposure of human red blood cells to hypochlorous acid. *Biochem J* 307 (Pt 1), 57–62.

Vivekananda, J., Smith, D., and King, R.J. (2001). Sphingomyelin metabolites inhibit sphingomyelin synthase and CTP: phosphocholine cytidylyltransferase. *Am J Physiol Lung Cell Mol Physiol* 281, L98–107.

Voehringer, D.W., McConkey, D.J., McDonnell, T.J., Brisbay, S., and Meyn, R.E. (1998). Bcl-2 expression causes redistribution of glutathione to the nucleus. *Proc Natl Acad Sci U S A* 95, 2956–60.

Vogt, R.F., Dannenberg, A.L., Schofiels, B., Hynes, N., and Papirmeister, B. (1984). Pathogenesis of skin caused by sulfur mustards. *Fundam Appl Toxicol* 4: 571–583.

Walker, I. (1967). *Protection of Animal Cells Against Mustards Gas by Pretreatment with Dithiothreitol*. Proceeding of the 5th International Congress Chemotherapy, Vienna.

Walker, I.G. and Smith, W. (1969). Protection of L-cells by thiols against the toxicity of sulfur mustards. *Can J Physiol Pharmacol* 47, 143–51.

Walker, L.J., Robson, C.N., Black, E., Gillespie, D., and Hickson, I.D. (1993). Identification of residues in the human DNA repair enzyme HAP1 (Ref-1) that are essential for redox regulation of Jun DNA binding. *Mol Cell Biol* 13, 5370–6.

Wan, X.S., Zhou, Z., Ware, J.H., and Kennedy, A.R. (2005). Standardization of a fluorometric assay for measuring oxidative stress in irradiated cells. *Radiat Res* 163, 232–40.

Wardell, B.L. (1941). Lewisite (M-1): Summary of physiologic and toxicologic data. *Report No. EATR 285*. Edgewood Arsenal, MD: Chemical Warfare Service.

Watson, W.H., Yang, X., Choi, Y.E., Jones, D.P., and Kehrer, J.P. (2004). Thioredoxin and its role in toxicology. *Toxicol Sci* 78, 3–14.

Weiss, D.J. and Lunte, C.E. (2000). Detection of a urinary biomaker for oxidative DNA damage 8-hydroxydeoxyguanosine by capillary electrophoresis with electrochemical detection. *Electrophoresis* 21, 2080–5.

Winterbourn, C.C. (1985). Comparative reactivities of various biological compounds with myeloperoxidase-hydrogen peroxide-chloride, and similarity of the oxidant to hypochlorite. *Biochim Biophys Acta* 840, 204–10.

Wormser, U. (1991). Toxicology of mustards gas. *Trends in Pharmacological Sciences* 12, 164–7.

Wormser, U., Brodsky, B., Green, B.S., Arad-Yellin, R., and Nyska, A. (1997). Protective effect of povidone-iodine ointment against skin lesions induced by sulfur mustards and by non-mustards vesicants. *Arch Toxicol* 71, 165–70.

Wormser, U., Brodsky, B., Green, B.S., Arad-Yellin, R., and Nyska, A. (2000). Protective effect of povidone iodine ointment against skin lesions induced by chemical and thermal stimuli. *J Appl Toxicol* 20 Suppl 1, S183–5.

Wright, S.D., Ramos, R.A., Tobias, P.S., Ulevitch, R.J., and Mathison, J.C. (1990). CD14, a receptor for complexes of lipopolysaccharide (LPS) and LPS binding protein. *Science* 249, 1431–3.

Xanthoudakis, S. and Curran, T. (1992). Identification and characterization of Ref-1, a nuclear protein that facilitates AP-1 DNA-binding activity. *EMBO J* 11, 653–65.

Xanthoudakis, S., Miao, G., Wang, F., Pan, Y.C., and Curran, T. (1992). Redox activation of Fos-Jun DNA binding activity is mediated by a DNA repair enzyme. *EMBO J* 11, 3323–35.

Xanthoudakis, S., Miao, G.G., and Curran, T. (1994). The redox and DNA-repair activities of Ref-1 are encoded by nonoverlapping domains. *Proc Natl Acad Sci U S A* 91, 23–7.

Ye, J., Wang, S., Leonard, S.S., Sun, Y., Butterworth, L., Antonini, J., Ding, M., Rojanasakul, Y., Vallyathan, V., Castranova, V., and Shi, X. (1999). Role of reactive oxygen species and p53 in chromium(VI)-induced apoptosis. *J Biol Chem* 274, 34974–80.

Yodoi, J. and Uchiyama, T. (1992). Diseases associated with HTLV-I: virus, IL-2 receptor dysregulation and redox regulation. *Immunol Today* 13, 405–11.

Yourick, J.J., Clark, C.R., and Mitcheltree, L.W. (1991). Niacinamide pretreatment reduces microvesicle formation in hairless guinea pigs cutaneously exposed to sulfur mustards. *Fundam Appl Toxicol* 17, 533–42.

Zhang, J., Johnston, G., Stebler, B., and Keller, E.T. (2001). Hydrogen peroxide activates NFkappaB and the interleukin-6 promoter through NFkappaB-inducing kinase. Antioxid Redox Signal, 3(3): 493–504.

Zong, W.X., Ditsworth, D., Bauer, D.E., Wang, Z.Q., and Thompson, C.B. (2004). Alkylating DNA damage stimulates a regulated form of necrotic cell death. *Genes Dev* 18, 1272–82.

REPORT DOCUMENTATION PAGE

Form Approved
OMB No. 0704-0188

1. REPORT DATE *(DD-MM-YYYY)*	2. REPORT TYPE	3. DATES COVERED *(From - To)*
15/09/2008	Annual	08/21/2007 – 08/20/2008

4. TITLE AND SUBTITLE

An Overview of the Continuation of the Work of the Mustard Gas Consortium for the Use of the Free and Liposome-Encapsulated Antioxidants as a Counter Measure to Mustards.

5a. CONTRACT NUMBER

5b. GRANT NUMBER
W81XWH-06-2-004

5c. PROGRAM ELEMENT NUMBER
PE 62384BP

6. AUTHOR(S)

Peter A. Ward, M.D.

5d. PROJECT NUMBER

5e. TASK NUMBER

5f. WORK UNIT NUMBER

7. PERFORMING ORGANIZATION NAME(S) AND ADDRESS(ES)

The Regents and the University of Michigan
DRDA – James R. Randolph
3003 South State St. Room 1040
Ann Arbor, MI 48109-1274

8. PERFORMING ORGANIZATION REPORT NUMBER

9. SPONSORING / MONITORING AGENCY NAME(S) AND ADDRESS(ES)
U.S. Army Medical Research and Material Command
Fort Detrick, MD 21702-5012

10. SPONSOR/MONITOR'S ACRONYM(S)

11. SPONSOR/MONITOR'S REPORT NUMBER(S)

12. DISTRIBUTION / AVAILABILITY STATEMENT
Approved for public release, distribution unlimited.

13. SUPPLEMENTARY NOTES

14. ABSTRACT

Acute lung injury in rats following airway delivery of CEES is associated with loss of distal lung barrier function (resulting in alveolar flooding) and an intense inflammatory response, which is lung-damaging. These acute lung injury parameters were attenuated by neutrophil depletion or complement blockade. The loss of redox balance in lung after exposure to CEES could be reversed by administration into lung of liposomes containing antioxidant compounds, which were highly protective even when delivery of liposomes was delayed by at least 1 hr. CEES-induced lung injury was progressive, as manifested by development of interstitial fibrosis which peaked at three weeks. The use of α, γ tocopherol liposomes did not attenuate the intensity of acute lung injury after CEES but markedly reduced the development of pulmonary fibrosis 3 weeks after exposure to CEES, as measured morphologically and biochemically (hydroxyproline content in lung homogenates). These data indicate that the development of acute lung injury or progressive lung injury after exposure to CEES proceeds by two different pathophysiological pathways, and that appropriate anti-oxidant liposome delivery attenuates both phases of injury.

15. SUBJECT TERMS
Lung injury, liposomes, anti-oxidants, fibrosis

16. SECURITY CLASSIFICATION OF:			17. LIMITATION OF ABSTRACT	18. NUMBER OF PAGES	19a. NAME OF RESPONSIBLE PERSON
a. REPORT	b. ABSTRACT	c. THIS PAGE			19b. TELEPHONE NUMBER *(include area code)*
U	U	U	U		

Table of Contents

Statement of Work

Our focus has been to understand the molecular mechanisms by which CEES induces both acute and progressive (fibrotic) lung injury, and how such injury may be averted. With respect to mechanisms, we now know that within hours after lung contact with CEES, there is an acute inflammatory response with buildup in lung of neutrophils (PMNs) and macrophages. With this is a surge of proinflammatory cytokines (IL-1α, TNFα, IL-6) and chemokines (MIP-2, MIP-1α, etc.) in bronchoalveolar lavage fluids. Oxidant and protease-induced injury of lung also occurs, chiefly due to the intense inflammatory response involving activated PMNs and macrophages. These events lead to severe damage of the lung vasculature and alveolar epithelial barriers, resulting in alveolar flooding, hemorrhage and fibrin deposition. We also know that the inflammatory response and resulting lung injury can be attenuated by PMN depletion or complement depletion prior to lung contact with CEES, indicating that much of the damage results from CEES triggering an intense acute inflammatory response. Our preliminary evidence suggests that all of these events are correlated with a surge within lung of proinflammatory mediators.

It is now well established by our work that antioxidant liposomes are highly protective against acute lung injury induced by CEES. Liposomes containing NAC, GSH or antioxidant enzymes (catalase, superoxide dismutase) are highly protective against the acute phase of injury after CEES, even if the airway (intratracheal) administration of liposomes is delayed by 60 min. The existence of the Advanced Medical Countermeasures Consortium has been invaluable for these studies, especially through collaborations with Dr. William Stone (East Tennessee University), who has provided many of the liposome preparations, and with Dr. Milton Smith (Amaox, Ltd.) who has provided guidance and coordination to the entire consortium. We have obtained evidence that lung exposure to CEES also results in progressive pulmonary fibrosis by three weeks. This irreversible outcome can be greatly attenuated by the use of liposomes obtaining α, γ tocopherol, which are administered intratracheally soon after lung exposure to CEES. Documentation of the protective effects of α, γ tocopherol is shown by morphological changes as well as biochemical (lung content of hydroxyproline) measurements. Interestingly, liposomes containing GSH or NAC, which are highly protective against the acute phase of injury, do not suppress the development of pulmonary fibrosis. Finally, we have shown that in vitro exposure of alveolar macrophages to CEES induces in vitro production of proinflammatory mediators (IL-1β, TNFα, IL-6, CINC-1), which is suppressed in vitro by antioxidant liposomes.

We intend to further pursue these observations according to the following questions:

1) What is the spectrum of proinflammatory cytokines and chemokines produced in lung after exposure to CEES?

2) Do protective antioxidant liposomes prevent *in vivo* activation of the transcription factor NFκB in lung tissues and in lung macrophages? Do these liposomes also reduce levels of cytokines and chemokines in lung after exposure to CEES?

3) Using lung macrophages, does *in vitro* cell exposure to LPS or CEES induce production of cytokines and chemokines, does this result in NFκB activation, and does the presence of antioxidant liposomes prevent such mediator production and NFκB activation?

Introduction

Over the past two years (summer 2006 – summer 2008), we have been involved in defining the mechanisms of 2-chloroethyl ethyl sulfide (CEES)-induced acute lung injury in rats and the ability of antioxidant liposomes (STIMAL) to attenuate acute lung injury as well as progressive lung injury (pulmonary fibrosis). Early on, we found that CEES induces acute lung injury (ALI) that features participation of the complement system as well as activation and mobilization of neutrophils (PMNs) and macrophages. The features of CEES-induced ALI are alveolar flooding, hemorrhage and fibrin deposition, all of which can be attenuated by complement depletion or depletion of blood PMNS (1) Overviews of the pathogenesis of ALI induced by CEES are provided (2,3), as well as in the Statement of Work (see above). Below, we summarize our recent progress.

Body

Anti-oxidant liposomes containing either anti-oxidant enzymes (superoxide dismutase or catalase), which will scavenge toxic oxygen products such as superoxide (O_2•) or H_2O_2, were highly protective in the CEES-induced ALI as were liposomes containing anti-oxidants such as GSH or N-acetyl cysteine (NAC). Instillation into lung of such liposomes as late as 60 min after exposure of lung to CEES still resulted in protection, suggesting that, in the field, aerosol administration of liposomes after exposure to mustard gas compounds might be protective (1).

In addition, we have shown that three weeks after exposure of rat lungs to CEES there is the onset of pulmonary fibrosis, as assessed morphologically and by increased lung content of hydroxyproline. Interestingly, intratracheal administration of liposomes containing α, γ tocopherol soon after exposure to CEES markedly attenuated the development of pulmonary fibrosis, but liposomes containing NAC or GSH were not protective (4).

Key Research Accomplishment

Listed above.

Reportable Outcomes

Presentations:

1. Invited presentation at NIH/NIAID Radiation Combined Injury Workshop, March 26-27, 2007, Bethesda, MD: "Factors affecting the outcomes of sepsis."
2. Advanced Medical Countermeasures Consortial Meeting, June 28, 2007, Crystal City, VA: "Protective effects of anti-oxidant liposomes in acute and progressive lung injury after CEES."
3. BARDA 2007 Industry Day Conference, August 3, 2007, Washington, DC: "Protective effects of anti-oxidant liposomes."
4. Invited platform presentation at Biosciences 2008 (Hunt Valley, MD), "Liposomal blockade of lung injury after exposure to 2-chloroethyl ethyl sulfide (CEES)", June 4, 2008.
5. Progress report, presented at Advanced Medical Countermeasures Consortium, Hunt Valley, (MD), June 4, 5, 2008.

Publications

Manuscripts published during 2006 – 2008 and related to W81XWH-06-2-0044.

1. McClintock, S.D., Hoesel, L.M., Das, S.K., Till, G.O., Neff, T., Kunkel, R.G., Smith, M.G., and **Ward, P.A**.: Attenuation of half sulfur mustard gas-induced acute lung injury in rats. J Appl Toxicol. 2006, 26:126-311.
2. Guo, R.F. and **Ward, P.A.:** Role of oxidants in lung injury during sepsis. Antioxidants and Redox Signaling 2007, 9:1-12.
3. Wrann, C.D., Tabriz, N.A., Barkhausen, T., Klos, A., van Griensven, M., Pape, H.C., Kendoff, D.O., Guo, R., **Ward, P.A.**, Krettek, C., Riedemann, N.C.: The phosphatidylinositol 3-kinase signaling pathway exerts protective effects during sepsis by controlling C5a-mediated activation of innate immune functions. J. Immunol. 2007; 178:5940-5948.
4. Smith, M.G., Stone, W., Guo, R.F., **Ward, P.A**., Suntres, Z., Mukherjee, S., and Das, S.K. Vesicants and Oxidative Stress. In Chemical Warfare Agents. Chemistry, Pharmacology, Toxicology, and Therapeutics, J.A. Romano, Jr., B.J. Lukey, H. Salem (eds). 2nd Edition, CRC Press, Boca Raton, FL. pp.247 – 312, 2007.
5. **Ward, P.A.**: New therapeutic approaches for influenza A H5N1 infected humans. (Invited Editorial) Crit Care Med. 2007; 35:1437-1438.
6. Hoesel, L.M., Flierl, M.A., Niederbichler, A.D., Rittirsch, D., Sarma, J.V., McClintock, S.D., Reuben, J.S., Pianko, M.J., Stone, W., Yang, H., Smith, M., **Ward, P.A**.: Ability of anti-oxidant liposomes to prevent acute and progressive pulmonary injury. Antioxid Redox Signal. 2008, 10:973-981.
7. Flierl, M.A., Rittirsch, D., Huber-Lang, M., Sarma, J.V., and **Ward, P.A.**: Catecholamines – Crafty weapons in the inflammatory arsenal of immune/inflammatory cells or opening Pandora's box? Mol Med. 2008, 14:195-204.
8. Rittirsch, D., Flierl, M.A., Day, D.E., Nadeau, B.A., McGuire, S.R., Hoesel, L.M., Ipaktchi, K., Zetoune, F.S., Sarma, J.V., Leng, L., Huber-Lang, M.S., Neff, T.A., Bucala, R., and **Ward, P.A.**: Acute lung injury induced by lipopolysaccharide is independent of complement activation. J Immunol. 2008 180:7664-7672.

Conclusion

It is now clear that CEES-induced lung injury is associated with both an acute phase (over the first few days following lung exposure to CEES) and a late phase (by 3 weeks) associated with pulmonary fibrosis. The acute phase of injury is an oxidant-mediated process that is associated with intensive inflammatory injury, causing a breach in the vascular and alveolar epithelial barriers. This results in a buildup of inflammatory cells, proteases and oxidants in the distal lung, resulting in alveolar flooding, hemorrhage, and fibrin deposition. Liposomes containing antioxidants (GSH, NAC) or antioxidant enzymes (catalase, SOD) were highly protective in this setting, even if their delivery was delayed for 60 min. after exposure to CEES. Very little is known about the late complication (pulmonary fibrosis), even though this outcome is well established to occur in humans subjected to inhalation of mustard gas. Our recent studies demonstrate that lung exposure to CEES induces a progressive pulmonary fibrosis that can be suppressed by the intratracheal administration of liposomes containing α, γ tocopherol (see publications and Statement of Work [above]).

References for Text

1. McClintock, S.D., Hoesel, L.M., Das, S.K., Till, G.O., Neff, T., Kunkel, R.G., Smith, M.G., and **Ward, P.A**.: Attenuation of half sulfur mustard gas-induced acute lung injury in rats. J Appl Toxicol. 2006, 26:126-311.
2. Smith, M.G., Stone, W., Guo, R.F., **Ward, P.A**., Suntres, Z., Mukherjee, S., and Das, S.K. Vesicants and Oxidative Stress. In Chemical Warfare Agents. Chemistry, Pharmacology, Toxicology, and Therapeutics, J.A. Romano, Jr., B.J. Lukey, H. Salem (eds). 2nd Edition, CRC Press, Boca Raton, FL. pp.247 – 312, 2007.
3. Guo, R.F. and **Ward, P.A.**: Role of oxidants in lung injury during sepsis. Antioxid Redox Signal. 2007 9:1991-2002.
4. Hoesel, L.M., Flierl, M.A., Niederbichler, A.D., Rittirsch, D., Sarma, J.V., McClintock, S.D., Reuben, J.S., Pianko, M.J., Stone, W., Yang, H., Smith, M., **Ward, P.A**.: Ability of anti-oxidant liposomes to prevent acute and progressive pulmonary injury. Antioxid Redox Signal. 2008, 10:973-981.

Appendices (available as PDF files)

Publications (above)

1. McClintock Paper – J Appl Toxicol. 2006, 26:126-311.
2. Ward Paper - Antioxidants and Redox Signaling 2007, 9:1-12.
3. Guo and Ward Review Chapter - J. Immunol. 2007; 178:5940-5948.
4. Wrann Paper - J. Immunol. 2007; 178:5940-5948.
5. Flierl Paper - Mol Med. 2008, 14:195-204.
6. Rittirsch Paper - J Immunol. 2008 180:7664-7672.
7. Hoesel Paper - Antioxid Redox Signal. 2008, 10:973-981.

ANTIOXIDANTS & REDOX SIGNALING
Volume 10, Number 5, 2008

DOI: 10.1089/ars.2007.1878

Original Research Communication

Ability of Antioxidant Liposomes to Prevent Acute and Progressive Pulmonary Injury

LASZLO M. HOESEL,[2] MICHAEL A. FLIERL,[1] ANDREAS D. NIEDERBICHLER,[2] DANIEL RITTIRSCH,[1] SHANNON D. MCCLINTOCK,[1] JAYNE S. REUBEN,[3] MATTHEW J. PIANKO,[1] WILLIAM STONE,[4] HONGSONG YANG,[4] MILTON SMITH,[5] J. VIDYA SARMA,[1] and PETER A. WARD[1]

ABSTRACT

We recently showed that acute oxidant-related lung injury (ALI) in rats after application of 2-chloroethyl ethyl sulfide (CEES) is attenuated by the airway instillation of antioxidants. We investigated whether intratracheal administration of antioxidant-containing liposomes immediately after instillation of CEES would attenuate short-term as well as long-term (fibrotic) effects of CEES-induced lung injury. In the acute injury model (4 h after injury), *N*-acetylcysteine (NAC)-containing liposomes were protective and reduced to baseline levels both the lung permeability index and the appearance of proinflammatory mediators in bronchoalveolar lavage fluids from CEES-exposed lungs. Similar results were obtained when rat alveolar macrophages were incubated *in vitro* with either CEES or lipopolysaccharide in the presence of NAC-liposomes. When lung fibrosis 3 weeks after CEES was quantitated by using hydroxyproline content, liposomes containing NAC or NAC + glutathione had no effects, but liposomes containing α/γ-tocopherol alone or with NAC significantly suppressed the increase in lung hydroxyproline. The data demonstrate that delivery of antioxidants *via* liposomes to CEES-injured lungs is, depending on liposomal content, protective against ALI, prevents the appearance of proinflammatory mediators in bronchoalveolar fluids, and suppresses progressive fibrosis. Accordingly, the liposomal strategy may be therapeutically useful in CEES-induced lung injury in humans. *Antioxid. Redox Signal.* 10, 973–981.

INTRODUCTION

OXIDANT-MEDIATED acute lung injury (ALI) is known to occur in a variety of conditions [including exposure to mustard gas and its derivatives such as 2-chloroethyl ethyl sulfide (CEES)] (8). CEES is a chemical agent that initiates cell injury associated with an imbalance between oxidants and antioxidants. On a subcellular level, it is known that sulfur mustard leads to an increase of gene expression involved in inflammation, apoptosis, and cell-cycle regulation (5). In addition to acute lung injury, lung exposure to sulfur mustard or its derivatives also leads to progressive lung injury, being represented by extensive interstitial fibrosis, which is well described in humans exposed to mustard gas compounds (18, 25) and in rats exposed to CEES (29). No specific therapy exists for the treatment of humans exposed to inhaled mustard gas compounds, although in the case of ALI in rats after exposure to CEES, we previously showed that protective strategies were associated with liposomes containing antioxidant enzymes (catalase, superoxide dismutase) or liposomes containing iron chelators or

Departments of Pathology[1] and Surgery,[2] University of Michigan Medical School, Ann Arbor, Michigan.
[3]Department of Biomedical Sciences, Baylor College of Dentistry The Texas A and M University System, Dallas, Texas.
[4]Department of Pediatrics, East Tennessee State University, Johnson City, Tennessee.
[5]AMAOX, Ltd., Melbourne, Florida.

nonspecific reducing agents (30). When given at the time of lung exposure to CEES, these agents reduced the intensity of acute lung injury (ALI), as defined by albumin leak into lung, by as much as 70%. Delayed instillation of these liposomes for as long as 90 min was still protective. These findings are consistent with the hypothesis that CEES upsets the redox balance in lung, leading to a loss of reducing equivalents in the lung (23, 26).

In a recent study, we showed that liposomes containing antioxidants, such as GSH or α-tocopherol given intratracheally at the time of injury, were also protective against ALI, as measured 4 h after airway instillation of CEES (29). Collectively, our studies have suggested that ALI occurring after airway exposure to CEES is associated with an intense lung-damaging inflammatory response featuring involvement of the complement system and neutrophils [polymorphonuclear leukocytes (PMNs)], both of which intensified inflammatory injury. In other words, exposure of lung to CEES triggered a lung-damaging inflammatory response. Instillation into CEES-exposed lungs of antioxidant liposomes was remarkably protective, even when liposomal delivery was delayed for 90 min after CEES instillation, suggesting that time for effective treatment of lungs may exist after exposure to CEES. Finally, it was also shown that CEES exposure of rat lung led to pulmonary fibrosis, although the effectiveness of antioxidant liposomes in that setting is not known.

Lipopolysaccharide (LPS), a major component of the cell wall of gram-negative bacteria, is known to trigger inflammatory reactions in lung similar to the effects of CEES (16, 51). Stimulation of macrophages by LPS results in activation of nuclear transcription factors [nuclear factor κB (NF-κB)] and release of proinflammatory cytokines (10, 20, 37, 38). Further, it has been shown that systemic administration of NAC may attenuate LPS-induced injury (15). In the context of CEES, LPS has been reported to enhance the cytotoxic effects of CEES (40). In the current study, we further explore the ability of antioxidant liposomes to protect against acute and progressive lung injury in rat lungs exposed to CEES. The data suggest that introduction of antioxidant interventions is protective in the lung.

MATERIALS AND METHODS

Chemicals

Except where noted, all chemicals and reagents were purchased from the Sigma Chemical Co. (St. Louis, MO).

Animal model

Adult male (275–325 g) specific pathogen-free Long-Evans rats (Harlan Co., Indianapolis, IN) were used in these studies. Intraperitoneal ketamine (100 mg/kg body weight) (Fort Dodge Animal Health, Fort Dodge, IA) was used for anesthesia, and intraperitoneal xylazine (13 mg/kg body weight) (Bayer Corp., Shawnee Mission, KS) for sedation. The experimental procedure for CEES-induced lung injury in rats was described previously (30). In brief, after induction of anesthesia, the trachea was surgically exposed, and a slightly curved P50 catheter was inserted into the trachea past the bifurcation to facilitate a unilateral, left-lung injury. A small volume of CEES (2 μl/rat; ~6 mg/kg) was solubilized in ethanol (58 μl/rat) and then added to a syringe containing Dulbecco's phosphate-buffered saline (DPBS) (340 μl/rat). This solution was injected *via* the intratracheal catheter into the left-lung mainstem bronchus. Animals were killed at indicated time points by exsanguinations *via* the inferior vena cava. All animal experiments were in accordance with the standards in The Guide for the Care and Use of Laboratory Animals, approved by the University Committee on Use and Care of Animals (UCUCA), and were supervised by veterinarians from the Unit for Laboratory and Animal Care of the University of Michigan Medical School.

Permeability index

The lung permeability index was determined as described later. Studies not requiring the use of a radiolabeled marker (^{125}I-BSA) proceeded identically, substituting DPBS (intravenously) for the radiomarker. For experiments where indicated, 0.5 mg bovine serum albumin (BSA) was mixed with 0.5 μCi ^{125}I-BSA, and the material (in 0.5 ml) was injected intravenously into rats. Animals were killed 4 h later, and the pulmonary arterial circulation was flushed with 10 ml of cold DPBS. The lungs were then surgically dissected, and the amount of radioactivity (^{125}I-labeled BSA) in lung parenchyma determined by gamma counting. For calculations of the permeability index, the amount of radioactivity remaining in perfused lungs was divided by the amount of radioactivity present in 1.0 ml of blood obtained from the inferior vena cava at the time of death, as described elsewhere (30). ^{125}I-BSA present in lung is a quantitative measure of the degree of vascular endothelial and alveolar epithelial damage, in which much of the ^{125}I-BSA can be lavaged from the distal airway compartment, indicating loss of the vascular and epithelial barrier function (24).

Liposome preparation

Dipalmitoylphosphatidylcholine (DPPC; Avanti Polar Lipids, Alabaster, AL) was dissolved 20 mg/ml in a 2:1 vol/vol chloroform/methanol solution. The DPPC solution was then dried under a thin stream of nitrogen in a round-bottom flask to form a thin lipid film on the walls of the tube. Once the film had been dried, the tube was then placed on a vacuum for at least 1 h to dry further and to remove any excess organic compounds from the lipid film.

The following compounds, being encapsulated within the liposomes, were prepared in Dulbecco's phosphate-buffered saline (DPBS), pH adjusted to 7.4. *N*-Acetylcysteine (NAC, 30 mg/ml), glutathione (GSH, 30 mg/ml), vitamin E (α + γ-tocopherol, each at 1.3 mg/ml) were then added to the lipid film. The tube was then vortexed to free the lipid film from the walls of the tube and then placed in a heated water bath (41°C). When sizing the liposomes, it was necessary to keep them at a temperature above their transition phase (41° C). Vortexing the liposomes once they were above the transition-phase temperature resulted in large multilamellar vesicles. To reduce the size of the liposomes and to produce uniform small unilamellar vesicles, the lipid suspension was then passed 10 times through polycarbonate membrane filters in a Liposofast Basic miniextruder (Avestin, Inc., Ottawa, Ontario, Canada). The resulting liposomes were uniform in size, measuring 100 nm in diame-

ter. It is well known that the pharmacokinetics of liposome uptake is dependent on particle-size distribution (11, 12). Uniformity and size of the liposomes was confirmed by light microscopy. Liposomes were injected intratracheally (volume of 100 μl per rat) through the same catheter setup immediately after the CEES instillation. This translates into 3 mg NAC, 3 mg GSH, and 0.13 mg α- or γ-tocopherol, respectively (the same doses apply where combinations of antioxidant agents were given). The same conditions were used when soluble NAC was used. *N*-Acetylcysteine (NAC, 30 mg/ml) was prepared in Dulbecco's phosphate-buffered saline (DPBS); pH adjusted to 7.4 and 100 μl of the suspension per rat was injected intratracheally.

Cytokine measurements in bronchoalveolar lavage fluid

To determine the concentration of various inflammatory cytokines in the lungs, bronchoalveolar lavage fluids (BALFs) were obtained selectively from the left, (injured) lung lobe at indicated time points after administration of CEES. After centrifugation, IL-1β, IL-6, TNF-α, and CINC-1 were measured in the supernatant fluids by using commercially available ELISA kits and by following the manufacturer's instructions (R&D Systems, Minneapolis, MN).

In vitro *stimulation of alveolar macrophages*

Alveolar macrophages were obtained from normal rat lungs by bronchoalveolar lavage. After pooling, gentle centrifugation and counting of the cells (with a yield of $\sim 10 \times 10^6$ cells per lung), macrophages resuspended in RPMI medium containing 0.5% BSA were incubated for 1 h to allow for settling. To create an *in vitro* situation similar to the *in vivo* CEES model, 2.5×10^6 cells/ml media were incubated with 500 μM CEES with or without antioxidant liposomes (50 μl) for 4 h. In additional experiments, plated macrophages were incubated with 100 ng/ml lipopolysaccharide (LPS) from *Escherichia coli* (serotype O111:B4) and 50 μl liposomes. After centrifugation, IL-1β, IL-6, TNF-α, and CINC-1 were measured in the supernatants by using commercially available ELISA kits and by following the manufacturer's instructions (R&D Systems, Minneapolis, MN).

Hydroxyproline assays

Hydroxyproline is a modified amino acid found at a uniquely high percentage in collagen. Therefore, we determined hydroxyproline content of the lungs as a quantitative measure of collagen deposition, as described previously. Although the accuracy of this assay may potentially be affected by proteins containing collagen-like motifs (*e.g.*, surfactant), its usefulness for determining tissue collagen content has been established and well accepted (31). Rats were killed 3 weeks after exposure to CEES, and the pulmonary circulation was flushed with 10 ml cold DPBS. The left (injured) lung was surgically removed. The isolated lobes were homogenized in 1 ml of PBS, and hydrolyzed by the addition of 1 ml of 12N HCl. Samples were then baked at 110°C for 12 h. Aliquots were then assayed by adding chloramine-T solution for 20 min followed by development with Ehrlich's reagent at 65°C for 15 min, as previously described (47). Absorbance was measured at 550 nm, and the amount of hydroxyproline was determined against a standard curve generated by using known concentrations of pure hydroxyproline.

Morphologic assessment of lung injury

Morphologically to assess lung injury, lungs were fixed by gentle intratracheal instillation of 10 ml buffered (pH 7.2) formalin (10%) at the indicated time points after airway instillation of CEES. Tissues were embedded in paraffin. Lung sections were then obtained for histologic examination by using hematoxylin and eosin stain. In addition, lung sections were stained with Masson trichrome to assess deposition of fibrin and collagen (28).

Statistical analysis

Results are presented as mean ± SEM in the text and figures. Groups ($n = 5$ rats) were subjected to one-way analysis of variance (ANOVA), and when significance was found, Tukey's *post hoc* test was applied. A value of $p < 0.05$ was considered significant.

RESULTS

Protective effects of NAC-containing liposomes in ALI

Because NAC-containing liposomes are known to protect against acute (4-h) CEES-induced injury in rat lungs when

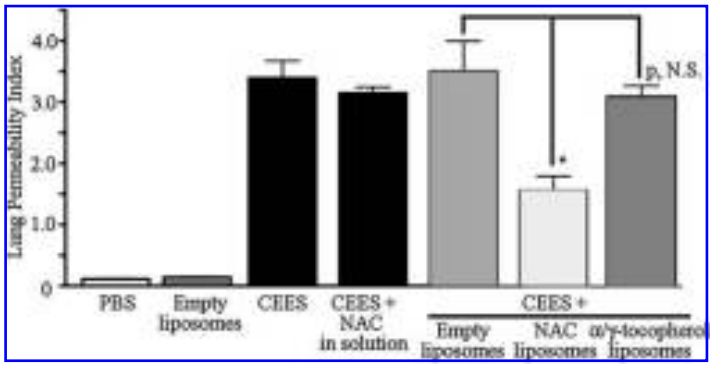

FIG. 1. Permeability indices in rat lungs 4 h after airway delivery of PBS (control) or empty liposomes, or CEES (6 mg/kg) in the absence of liposomes or in the presence of empty liposomes, NAC-containing (30 mg/ml), or α/γ-tocopherol-containing (1.3 mg/ml) liposomes. An additional group of animals received soluble NAC dissolved in PBS (fourth bar, CEES + NAC in solution) by using the same conditions used for preparation of NAC-liposomes. The permeability index was the ratio of ^{125}I-albumin in left lung parenchyma to the radioactivity present in 1.0 ml blood (vena cava) obtained at the time of death. For each bar, $n = 6$ animals. *$p < 0.05$.

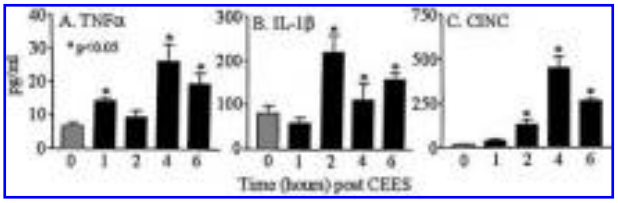

FIG. 2. Appearance of TNF-α, IL-1β, and CINC-1 (as measured by ELISA) in BAL fluids from the left (injured) lung as a function of time after intratracheal instillation of CEES into rat lungs. For each bar, $n = 6$ animals. *$p < 0.05$ when compared with 0 time values.

given intratracheally immediately after instillation of CEES (29), experiments were designed to assess the protective effects of empty liposomes, NAC in solution (PBS), NAC-liposomes, and α/γ-tocopherol liposomes. As shown in Fig. 1, control lungs (receiving PBS or empty liposomes) showed very little evidence of albumin leak (permeability index), with values <0.15. CEES caused an intense leak of serum albumin, with the permeability index ~3.4, whereas CEES instillation followed by NAC in PBS (pH 7.4) showed a very modest reduction in the permeability index (<10%). Empty liposomes or liposomes loaded with α/γ-tocopherol, given into the upper airways immediately after CEES, did not reduce the permeability index (same as with CEES alone), whereas in the case of NAC-liposomes, a 59% reduction in the permeability index was found ($p < 0.05$).

Time course for mediators in BAL fluids after CEES

To establish the time course for appearance of inflammatory mediators in BAL fluids from rats given CEES into the left lung at time 0, BAL samples were obtained at 0, 1, 1.5, 2, 4, and 6 h after CEES administration. Mediators were measured with ELISA (Fig. 2). Time courses for TNF-α, IL-1β, and CINC-1 indicated that, as a general rule, these proinflammatory mediators peaked between 2 and 4 h after instillation of CEES into rat lungs. For subsequent experiments, the 4-h time point was selected.

Reductions in BAL Mediators in CEES lungs after antioxidant liposomes

We previously showed that liposomes containing NAC prevent the ALI that follows airway administration of CEES (30). CEES was used to induce ALI in the absence of liposomes or in the presence of empty liposomes or NAC-containing liposomes, the last of which are known to be protective in the ALI CEES model (29). In the current studies, we sought to determine to what extent protective liposomes would affect BAL levels of cytokines and chemokines. BAL fluids were obtained 4 hours after airway administration of CEES in the absence or presence of empty liposomes or NAC-liposomes, as indicated in Fig. 3. CEES caused ~20-fold, fourfold, 2.5-fold, and 1.6-fold increases in CINC-1, IL-1β, IL-6, and TNF-α, respectively, in BAL fluids. The presence of empty liposomes with CEES caused little or no change when compared with the values found with CEES alone. Conversely, NAC-liposomes caused the levels of BAL mediators to decrease to virtually baseline levels in all cases.

Effects of antioxidant liposomes on in vitro *production of cytokines and chemokines by lung macrophages*

Two different *in vitro* experiments were used in which alveolar macrophages (2.5×10^{-6}/ml) from normal rat lungs were

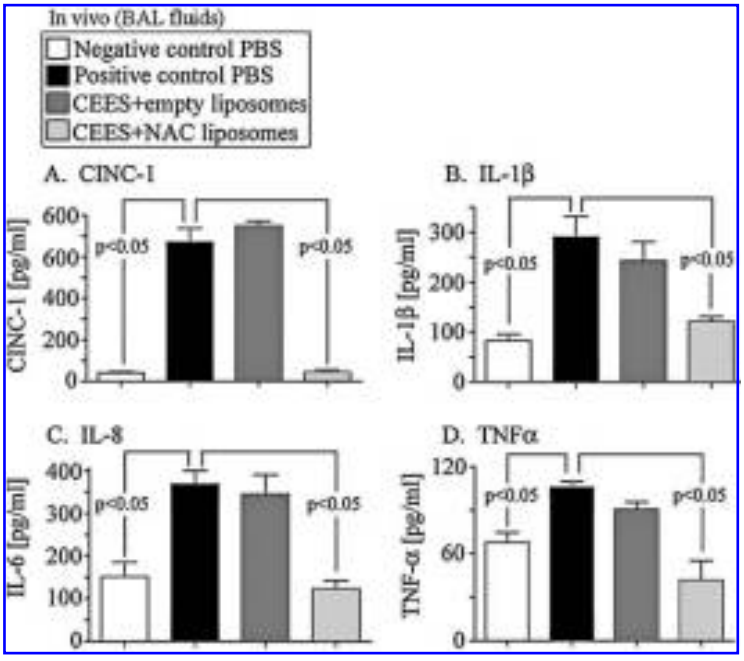

FIG. 3. Levels of rat CINC-1 (A), IL-1β (B), IL-6 (C), and TNF-α (D) in BAL fluids from left lung 4 h after instillation of PBS (control) or CEES. As indicated, CEES was instilled, followed by airway instillation of empty liposomes (lips) or NAC-liposomes. For each bar, $n = 8$ animals.

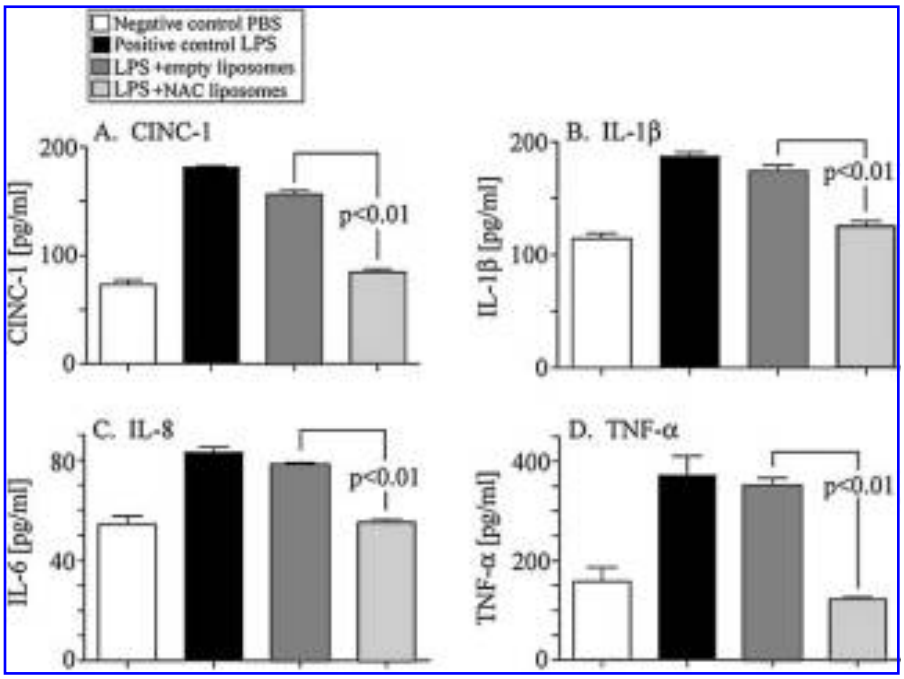

FIG. 4. Effects of LPS and liposomes on levels of proinflammatory mediators in 4-h culture fluids of alveolar macrophages (2.5×10^6) incubated with PBS (negative control) or with LPS (100 ng/ml) alone (positive control), or with empty liposomes or NAC-containing liposomes. Mediators CINC-1 (**A**), IL-1β (**B**), IL-6 (**C**), and TNF-α (**D**) were measured with ELISA. Each sample was measured in quadruplicate. For each bar, $n = 6$ animals.

used. In the first set of experiments, cells were exposed to LPS (100 ng/ml) for 4 hours in the absence or presence of empty or NAC-liposomes. Supernatant fluids were then measured for the presence of proinflammatory mediators, as shown in Fig. 4. In each case, LPS addition in the absence or presence of empty liposomes induced a substantial increase (over negative controls) of CINC-1, IL-1β, IL-6, and TNF-α. The presence of NAC-liposomes caused the mediator levels to decrease to baseline levels. Addition of empty liposomes did not induce mediator release from nonstimulated alveolar macrophages (data not shown).

In the second set of *in vitro* experiments (Fig. 5), the effect of CEES alone or in the presence of empty or NAC-containing liposomes on mediator release from alveolar macrophages was assessed. Empty liposomes did not perturb the levels of mediators released, remaining at baseline levels in nonstimulated

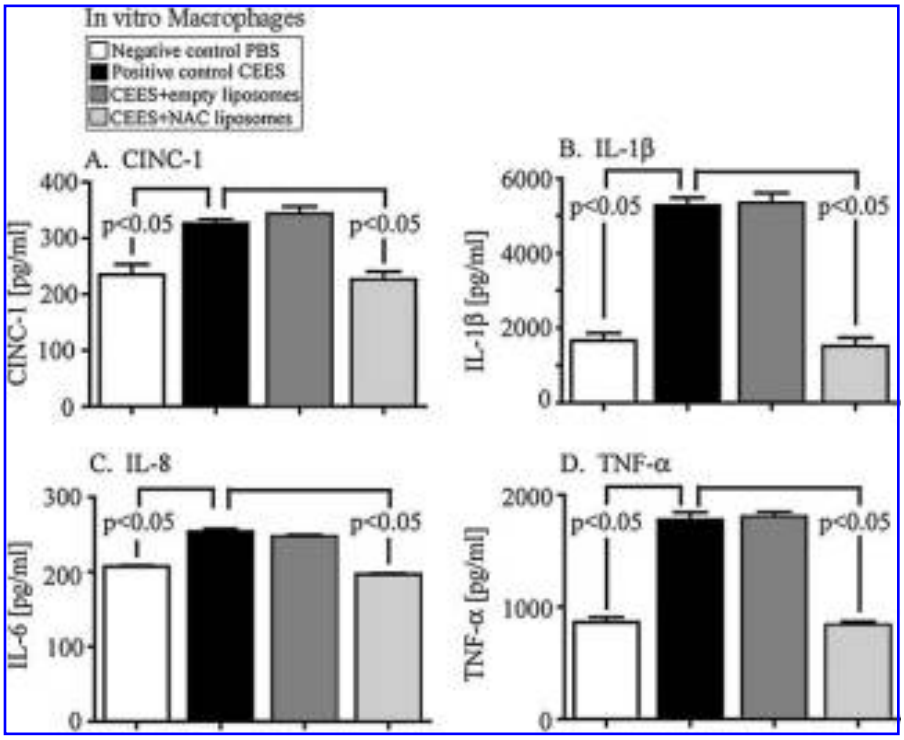

FIG. 5. *In vitro* effects of CEES and liposomes on levels of proinflammatory mediators in 4-h culture fluids of alveolar macrophages (2.5×10^6) incubated with PBS (negative control), CEES (500 μM) alone (positive control), or with empty liposomes or NAC-containing liposomes. Mediators CINC-1 (**A**), IL-1β (**B**), IL-6 (**C**), and TNF-α (**D**) were measured with ELISA. Each sample was measured in quadruplicate. For each bar, $n = 6$ animals.

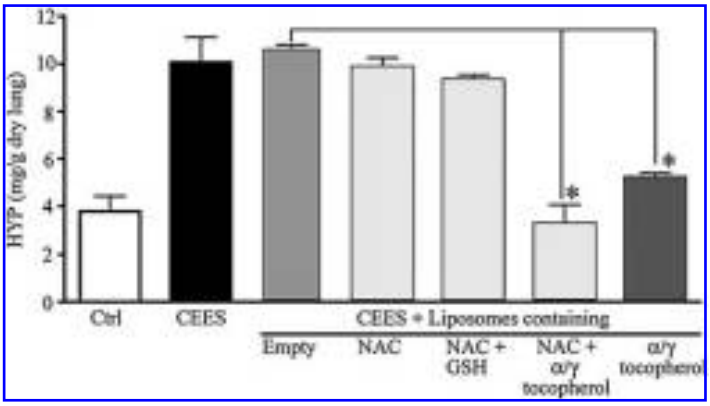

FIG. 6. Collagen levels (as measured by hydroxyproline content) in left lung homogenates 3 weeks after airway instillation of PBS (control) or CEES alone or together with empty liposomes or liposomes containing NAC, NAC + GSH, NAC + α, γ-tocopherol, or α, γ-tocopherol alone. For each bar, $n = 8$ animals. *$p < 0.05$ when compared with the CEES group.

macrophages (data not shown). Furthermore, in all cases, the addition of empty liposomes had no effect on mediator release when compared with CEES-stimulated macrophages not otherwise manipulated (Fig. 5). In contrast, the addition of NAC-containing liposomes to CEES-stimulated macrophages caused total suppression of the increase in levels of IL-6, IL-1β, TNF-α, and CINC-1 release, declining to levels equivalent to negative controls. Clearly, NAC-liposomes suppress release of proinflammatory mediators *in vitro* and *in vivo* after exposure of alveolar macrophages to either CEES (Fig. 5) or LPS (Fig. 4). The mechanisms by which CEES induces release of proinflammatory mediators from alveolar macrophages and the protective effects of NAC-liposomes are not known but may be linked to NF-κB activation or suppressed NF-κB activation.

Ability of anti-oxidant liposomes to protect from CEES-induced pulmonary fibrosis

We recently showed that CEES administration into rat lung induces intense pulmonary fibrosis within 3 weeks, as defined by histologic changes (29). In the current studies, we assessed whether antioxidant liposomes would prevent this outcome. Accordingly, CEES was administered into rat lungs in the absence of liposomes or together with empty liposomes or liposomes containing NAC, NAC + GSH, or NAC + α/γ-tocopherol or α/γ-tocopherol alone. Three weeks later, lungs were obtained, and collagen content (hydroxyproline, HYP) was assessed, as described earlier (31). As shown in Fig. 6, hydroxyproline content (mg/gm dry lung) increased 2.5-fold 3 weeks after CEES exposure of lungs in the absence of liposomes or in the presence of empty liposomes or liposomes containing NAC or NAC + GSH. No protective effects on hydroxyproline build-up were found. Strikingly, when liposomes containing NAC + α/γ-tocopherol were used, the build-up of hydroxyproline was completely abrogated ($p < 0.05$). Liposomes containing only α/γ-tocopherol also suppressed HYP buildup but not to the same extent as when α/γ-tocopherol liposomes were used ($p < 0.05$).

Morphologic correlates in lung

As shown in Fig. 7, sham lungs demonstrated normal architecture (A), whereas lungs exposed 3 weeks earlier to CEES showed extensive interstitial fibrosis (shown by blue staining in Masson-trichrome–stained sections), inflammatory cell infiltrates (neutrophils and mononuclear cells), and alveolar collapse (B). In contrast, CEES-exposed lungs from rats also given liposomes with NAC and α/γ-tocopherol had preservation of alveolar spaces and limited inflammatory cellular infiltrates, both in alveolar walls and in alveolar spaces (C). These data support the biochemical data shown in Fig. 6.

DISCUSSION

These studies establish that antioxidant liposomes can protect against CEES-induced ALI in rats after airway instillation of appropriate liposomes. ALI, as defined by breakdown of the vascular endothelial and alveolar epithelial barriers with leak of ^{125}I-albumin into lung parenchyma, occurred in rats after airway exposure to CEES. In the setting of CEES, development of ALI is related to complement activation, PMN influx, generation predominantly by activated lung macrophages of proinflammatory cytokines and chemokines, and release of oxidants and proteases from PMNs and macrophages (9, 50). In other words, ALI caused by exposure to CEES is fundamentally caused by triggering of an extremely robust intrapulmonary inflammatory response, which is complement dependent (5). The vascular (endothelial) and airway (alveolar epithelial) barriers are breached by this intense inflammatory response, resulting in alveolar flooding and hemorrhage. It is possible that interaction of CEES with endothelial and epithelial cells also directly results in tissue damage (32). Some of the mechanisms of CEES-induced cell injury have recently been established. CEES is an alkylating agent and has variably toxic, mutagenic, carcinogenic, and teratogenic effects. However, the mechanisms of its delayed toxic effects (retardation in the rate of cell division, disruption of mitoses, chromosomal breakages, and other abnormalities of chromosomes) and of its carcinogenic actions are not understood (5). A review of the evidence linking sulfur mustard to oxidative stress has been described (32). Direct evidence for free radical formation in rat lung lavage after inhalation of sulfur mustard vapor has been obtained by using electron paramagnetic resonance (EPR) and spin-trapping techniques (1). These studies show a rapid formation of ascorbyl radicals followed by the formation of carbon-centered radicals. Evidence for free radical–mediated lung damage in CEES-exposed mice (*i.e.*, increased lipid peroxidation, as well as decreased GSH and increased oxidized GSH) has also been described) (17). Interestingly, it has been shown that CEES is

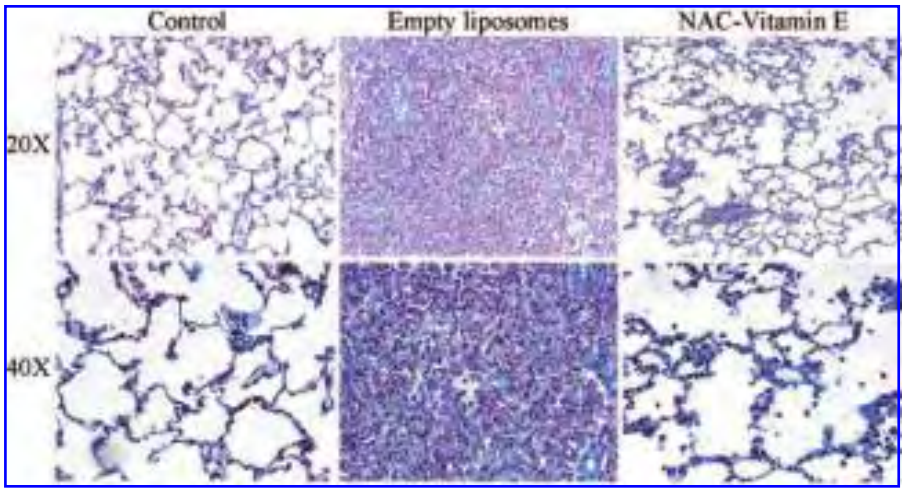

FIG. 7. Histologic features of control lung (airway instillation of PBS), CEES lung with empty liposomes, or CEES lung with liposomes containing NAC + α/γ-tocopherol (vitamin E). Lungs were obtained 3 weeks after airway instillation of CEES. (Masson Trichome staining of paraffin-embedded sections, 20× and 40× magnification).

an alkylating agent that will react with nonprotein thiols (NAC or GSH) as well as protein thiol groups. Mustard gas is known to form metabolites (by the β-lyase pathway) derived from its covalent conjugation with GSH. Sulfur mustard metabolites from the glutathione (GSH)/β-lyase pathway are specific markers for exposure to sulfur mustard (6, 7). This may represent another mechanism by which antioxidant liposomes protect against CEES-induced lung injury.

In the setting of our lung-injury model, all of these changes result in acute lung injury (4 h), followed by alveolar collapse and interstitial pulmonary fibrosis 3 weeks later. These outcomes can be averted by liposomes that contain the combination of NAC and α/γ-tocopherol or α/γ-tocopherol alone, whereas liposomes containing α/γ-tocopherol did not attenuate the acute lung injury. In contrast, liposomes containing NAC or NAC + GSH did not attenuate long-term fibrosis (3 weeks) but proved to be efficacious in protecting against CEES-induced ALI (4 h). Why liposomes containing certain antioxidants or combinations thereof are effective in the acute injury but not in the long-term injury, and *vice versa*, is not clear. It seems that tocopherol and NAC affect different aspects of the acute reaction, whereas tocopherol is more effective in preventing the progression to fibrosis. One possible explanation might be the hydrophobic nature of α/γ-tocopherol, which allows insertion into membranes (cell membrane, endoplasmatic reticulum, and mitochondrial membranes), producing a relatively long-lasting effect, whereas internalization of NAC might lead to a relatively short life span (48). Similar to our results, it has been reported that the instillation of liposomes containing both GSH and α-tocopherol (but not GSH alone) resulted in the highest level of GSH retention in lung tissue, suggesting an effective antioxidant formulation for treating oxidative lung injury (43). In addition, it has been shown that tocopherol may also modulate signal-transduction pathways (2, 35, 52). Precisely what products of the macrophage can be linked to the development of pulmonary fibrosis after lung exposure to CEES remains to be defined, but a likely candidate mediator known to be released by macrophages is TGF-β (4). The protective effects of NAC-liposomes after acute exposure of lung to CEES liposomes may be associated with the dramatic disappearance of proinflammatory mediators in BAL fluids appearing after exposure to CEES (Fig. 3). Suppression of mediator appearance may be related to the ability of intracellular NAC to suppress NF-κB activation within macrophages, preventing generation of proinflammatory mediators. However, it should be noted that we did not directly measure a "restoration of redox balance," but other investigators, by using *in vitro* model systems, have shown that NAC protects against CEES toxicity by blocking the CEES-induced loss of intracellular GSH (22). We therefore assume that the administration of antioxidant liposomes affects the redox status in lung cells. It remains to be shown in future experiments whether antioxidant agents indeed restore the redox balance within the different lung cells.

Liposomal use for drug delivery has been studied extensively [reviewed in (13)]. The main cellular targets for lung oxidant stress are epithelial cells lining the alveoli (including type I and II alveolar cells), endothelial cells lining the pulmonary capillaries, and alveolar macrophages. Liposomal drugs may be administered orally, intravenously, or intratracheally, but only the latter two routes improve drug delivery (13). Intravenously administered liposomal drugs may be absorbed by pulmonary endothelial cells, but providing effective methods of drug delivery is still challenging.

For intratracheal instillation, the uptake and subcellular distribution of liposomal α-tocopherol (but not γ-tocopherol) in lung tissue was examined (41). Recovery of α-tocopherol in the lung was maximal 1 hour after liposomal instillation and resulted in a 16-fold increase in pulmonary total α-tocopherol concentration 72 h after instillation. α-Tocopherol was recovered largely from cytosolic, nuclear, microsomal, and mitochondrial fractions, providing evidence that α-tocopherol levels present in the membranes of these subcellular fractions were sufficient to protect against oxidant-induced lipid peroxidation. Evidence suggests that liposomes given into the airways are avidly taken up by phagocytes of the reticuloendothelial system (21, 27, 39, 46). Once internalized, they release their contents intracellularly (34, 36). In addition, alveolar types I and II as well as pulmonary endothelial cells have been shown to be able to internalize intratracheally administered liposomes (3, 33). In the current studies, we focused on alveolar macrophages (which are the chief sources of lung cytokines and chemokines) being affected by NAC-liposomes (Fig. 3); however, to what extent other lung cells such as alveolar epithelial cells have been altered remains to be determined.

The implications from the current studies (especially *in vitro* data) are that liposomal delivery most likely enhances a reduc-

ing environment in lung macrophages, which may be otherwise compromised when these cells come into contact with CEES or LPS. Delivery of NAC in liposomes may be protective in the setting of CEES-induced lung injury by phagocytosis of liposomes into lung macrophages and possibly by other lung cells as well (21, 27, 39). Once ingested by macrophages, the liposomal contents are released into the interior of the macrophages (34, 36). NAC may be distributed into the cytosol component, whereas α/γ-tocopherol is distributed into membranes within cells (see earlier). Phosphonate-containing liposomes have been used in rodents selectively to deplete the lung of macrophages, whereas other types of lung cells are not affected (49). It seems in the CEES model of ALI that the release of proinflammatory mediators (cytokines and chemokines) from lung macrophages is blocked by the use of NAC-liposomes, subsequently resulting in intracellular release of NAC and blockade of NF-κB activation within macrophages. However, it seems plausible that an attenuated oxidative stress within macrophages may also indirectly result in protection of adjacent alveolar epithelial and endothelial cells. Whether the use of other liposomes with antioxidant properties (*e.g.*, GSH, α/γ-tocopherol) would also suppress the release into CEES-treated lungs of proinflammatory mediators remains to be determined, but it seems likely, because such liposomes protect against ALI after airway exposure (44). As suggested earlier, it is likely that NAC liposomes are phagocytized by lung macrophages, resulting in release of NAC into the cytosol, resulting in blockade of NF-κB activation, which is required for production and release of mediators by macrophages. The trigger in this situation is likely CEES, which causes NF-κB activation in macrophage-type cells (9, 14).

Lipopolysaccharide (LPS) is known to induce acute lung injury with features similar to changes in CEES-induced acute lung injury (50). Because both types of injury result in an inflammatory response and its accompanying oxidative stress, we extended our experiments to *in vitro* exposure of alveolar macrophages to LPS or CEES (Figs. 3 and 4). *In vivo* experiments have shown that administration of liposomes containing NAC or α-tocopherol protects rats from ALI induced by LPS or paraquat (19, 42, 44, 45). We show in this report that liposomes containing NAC significantly suppressed the release of proinflammatory cytokines from alveolar macrophages exposed to either LPS or CEES, suggesting similar pathways being activated under both conditions. This confirms the *in vivo* data (Fig. 3), underscoring the hypothesis that augmentation of the pulmonary antioxidant status can attenuate both LPS- and CEES-induced oxidative stress.

Taken together, restoration of the redox balance may be crucial in the setting of ALI induced by CEES for attenuation of early, acute injury, and may also set the stage for attenuating the long-term effects of CEES (pulmonary fibrosis). Liposome-mediated delivery of antioxidant agents, particularly NAC and α/γ-tocopherol, is a powerful tool to diminish CEES-induced acute and long-term lung injury.

ABBREVIATIONS

ALI, acute lung injury; ANOVA, analysis of variance; BALF, bronchoalveolar lavage fluid; BSA, bovine serum albumin; ^{125}I-BSA, iodine 125–labeled bovine serum albumin; CINC-1, cytokine-induced neutrophil chemoattractant-1; CEES, chloroethyl ethyl sulfide; DPBS, Dulbecco's phosphate-buffered saline; DPPC, dipalmitoylphosphatidylcholine; ELISA, enzyme-linked immunosorbent assay; GSH, glutathione; HYP, hydroxyproline; IL-1β, interleukin-1β; IL-6, interleukin-6; LPS, lipopolysaccharide; NAC, *N*-acetylcysteine; NF-κB, nuclear factor κ-B; PMN, polymorphonuclear leukocyte; RPMI, Roswell Park Memorial Institute; TGF-β, transforming growth factor-β; TNF-α, tumor necrosis factor-α.

ACKNOWLEDGMENTS

This work was supported by DOD grants DAMD17-03-2-0054 and W81XWH-06-2-0044 and NIH grants GM-029507 and HL-31963.

REFERENCES

1. Anderson DR, Yourick JJ, Arroyo CM, Young GD, and Harris LW. Use of EPR spin-trapping techniques to detect radicals from rat lung lavage fluid following sulfur mustard vapor exposure. *Med Defense Biosci Rev Proc* 1: 113–121, 1993.
2. Azzi A, Gysin R, Kempna P, Munteanu A, Negis Y, Villacorta L, Visarius T, and Zingg JM. Vitamin E mediates cell signaling and regulation of gene expression. *Ann N Y Acad Sci* 1031: 86–95, 2004.
3. Baker RR, Czopf L, Jilling T, Freeman BA, Kirk KL, and Matalon S. Quantitation of alveolar distribution of liposome-entrapped antioxidant enzymes. *Am J Physiol* 263: L585–L594, 1992.
4. Bartram U and Speer CP. The role of transforming growth factor beta in lung development and disease. *Chest* 125: 754–765, 2004.
5. Bignold LP. Alkylating agents and DNA polymerases. *Anticancer Res* 26: 1327–1336, 2006.
6. Black RM, Brewster K, Clarke RJ, Hambrook JL, Harrison JM, and Howells DJ. Biological fate of sulphur mustard, 1,1'-thiobis(2-chloroethane): isolation and identification of urinary metabolites following intraperitoneal administration to rat. *Xenobiotica* 22: 405–418, 1992.
7. Boyer AE, Ash D, Barr DB, Young CL, Driskell WJ, Whitehead RD Jr, Ospina M, Preston KE, Woolfitt AR, Martinez RA, Silks LA, and Barr JR. Quantitation of the sulfur mustard metabolites 1,1'-sulfonylbis[2-(methylthio)ethane] and thiodiglycol in urine using isotope-dilution gas chromatography-tandem mass spectrometry. *J Analyt Toxicol* 28: 327–332, 2004.
8. Calvet JH, Jarreau PH, Levame M, D'Ortho MP, Lorino H, Harf A, and Macquin-Mavier I. Acute and chronic respiratory effects of sulfur mustard intoxication in guinea pig. *J Appl Physiol* 76: 681–688, 1994.
9. Chatterjee D, Mukherjee S, Smith MG, and Das SK. Signal transduction events in lung injury induced by 2-chloroethyl ethyl sulfide, a mustard analog. *J Biochem Mol Toxicol* 17: 114–121, 2003.
10. Chen CC, Wang JK, and Lin SB. Antisense oligonucleotides targeting protein kinase C-alpha, -beta I, or -delta but not -eta inhibit lipopolysaccharide-induced nitric oxide synthase expression in RAW 264.7 macrophages: involvement of a nuclear factor kappa B-dependent mechanism. *J Immunol* 161: 6206–6214, 1998.
11. Chono S, Tanino T, Seki T, and Morimoto K. Influence of particle size on drug delivery to rat alveolar macrophages following pulmonary administration of ciprofloxacin incorporated into liposomes. *J Drug Target* 14: 557–566, 2006.
12. Chono S, Tanino T, Seki T, and Morimoto K. Uptake characteristics of liposomes by rat alveolar macrophages: influence of particle size and surface mannose modification. *J Pharm Pharmacol* 59: 75–80, 2007.

13. Christofidou-Solomidou M and Muzykantov VR. Antioxidant strategies in respiratory medicine. *Treat Respir Med* 5: 47–78, 2006.
14. Das SK, Mukherjee S, Smith MG, and Chatterjee D. Prophylactic protection by *N*-acetylcysteine against the pulmonary injury induced by 2-chloroethyl ethyl sulfide, a mustard analogue. *J Biochem Mol Toxicol* 17: 177–184, 2003.
15. Davreux CJ, Soric I, Nathens AB, Watson RW, McGilvray ID, Suntres ZE, Shek PN, and Rotstein OD. *N*-Acetyl cysteine attenuates acute lung injury in the rat. *Shock* 8: 432–438, 1997.
16. Downey JS and Han J. Cellular activation mechanisms in septic shock. *Front Biosci* 3: d468–d476, 1998.
17. Elsayed NM and Omaye ST. Biochemical changes in mouse lung after subcutaneous injection of the sulfur mustard 2-chloroethyl 4-chlorobutyl sulfide. *Toxicology* 199: 195–206, 2004.
18. Emad A and Rezaian GR. Immunoglobulins and cellular constituents of the BAL fluid of patients with sulfur mustard gas-induced pulmonary fibrosis. *Chest* 115: 1346–1351, 1999.
19. Fan J, Shek PN, Suntres ZE, Li YH, Oreopoulos GD, and Rotstein OD. Liposomal antioxidants provide prolonged protection against acute respiratory distress syndrome. *Surgery* 128: 332–338, 2000.
20. Fujihara M, Connolly N, Ito N, and Suzuki T. Properties of protein kinase C isoforms (beta II, epsilon, and zeta) in a macrophage cell line (J774) and their roles in LPS-induced nitric oxide production. *J Immunol* 152: 1898–1906, 1994.
21. Gonzalez-Rothi RJ, Straub L, Cacace JL, and Schreier H. Liposomes and pulmonary alveolar macrophages: functional and morphologic interactions. *Exp Lung Res* 17: 687–705, 1991.
22. Han S, Espinoza LA, Liao H, Boulares AH, and Smulson ME. Protection by antioxidants against toxicity and apoptosis induced by the sulphur mustard analog 2-chloroethylethyl sulphide (CEES) in Jurkat T cells and normal human lymphocytes. *Br J Pharmacol* 141: 795–802, 2004.
23. Husain K, Dube SN, Sugendran K, Singh R, Das Gupta S, and Somani SM. Effect of topically applied sulphur mustard on antioxidant enzymes in blood cells and body tissues of rats. *J Appl Toxicol* 16: 245–248, 1996.
24. Johnson KJ and Ward PA. Acute immunologic pulmonary alveolitis. *J Clin Invest* 54: 349–357, 1974.
25. Khateri S, Ghanei M, Keshavarz S, Soroush M, and Haines D. Incidence of lung, eye, and skin lesions as late complications in 34,000 Iranians with wartime exposure to mustard agent. *J Occup Environ Med* 45: 1136–1143, 2003.
26. Kopff M, Zakrzewska I, Strzelczyk M, Klem J, and Dubiecki W. Superoxide dismutase and catalase activity in psoriatic patients treated topically with ointment containing 2-chloroethyl-3-chloropropyl sulfide. *Pol J Pharmacol* 46: 439–444, 1994.
27. Lentsch AB, Czermak BJ, Bless NM, Van Rooijen N, and Ward PA. Essential role of alveolar macrophages in intrapulmonary activation of NF-kappaB. *Am J Respir Cell Mol Biol* 20: 692–698, 1999.
28. Luna L. *Manual histology staining methods: AFIP*. New York: McGraw-Hill, 1968.
29. McClintock SD, Hoesel LM, Das SK, Till GO, Neff T, Kunkel RG, Smith MG, and Ward PA. Attenuation of half sulfur mustard gas-induced acute lung injury in rats. *J Appl Toxicol* 26: 126–131, 2006.
30. McClintock SD, Till GO, Smith MG, and Ward PA. Protection from half-mustard-gas-induced acute lung injury in the rat. *J Appl Toxicol* 22: 257–262, 2002.
31. Moore BB, Coffey MJ, Christensen P, Sitterding S, Ngan R, Wilke CA, McDonald R, Phare SM, Peters-Golden M, Paine R 3rd, and Toews GB. GM-CSF regulates bleomycin-induced pulmonary fibrosis via a prostaglandin-dependent mechanism. *J Immunol* 165: 4032–4039, 2000.
32. Naghii MR. Sulfur mustard intoxication, oxidative stress, and antioxidants. *Mil Med* 167: 573–575, 2002.
33. Poelma DL, Zimmermann LJ, Scholten HH, Lachmann B, and van Iwaarden JF. In vivo and in vitro uptake of surfactant lipids by alveolar type II cells and macrophages. *Am J Physiol Lung Cell Mol Physiol* 283: L648–L654, 2002.
34. Popescu MC, Swenson CE, and Ginsberg RS. Liposome-mediated treatment of viral, bacterial and protozoal infections. In: *Liposomes: from biophysics to therapeutics*, edited by Ostro MJ. New York: Marcel Dekker, 1987, pp 219–251.
35. Rimbach G, Minihane AM, Majewicz J, Fischer A, Pallauf J, Virgli F, and Weinberg PD. Regulation of cell signalling by vitamin E. *Proc Nutr Soc* 61: 415–425, 2002.
36. Roerdink F, Regts J, Daemen T, Bakker-Woudenberg I, and Scherphof G. Liposomes as drug carriers to liver macrophages: fundamentals and therapeutic aspects. In: *Targeting of drugs with synthetic systems*, edited by Senior J and Poste G. New York: Plenum Press, 1986, pp 193–206.
37. Shapira L, Sylvia VL, Halabi A, Soskolne WA, Van Dyke TE, Dean DD, Boyan BD, and Schwartz Z. Bacterial lipopolysaccharide induces early and late activation of protein kinase C in inflammatory macrophages by selective activation of PKC-epsilon. *Biochem Biophys Res Commun* 240: 629–634, 1997.
38. Shapira L, Takashiba S, Champagne C, Amar S, and Van Dyke TE. Involvement of protein kinase C and protein tyrosine kinase in lipopolysaccharide-induced TNF-alpha and IL-1 beta production by human monocytes. *J Immunol* 153: 1818–1824, 1994.
39. Shephard EG, Joubert JR, Finkelstein MC, and Kuhn SH. Phagocytosis of liposomes by human alveolar macrophages. *Life Sci* 29: 2691–2698, 1981.
40. Stone WL, Qui M, and Smith M. Lipopolysaccharide enhances the cytotoxicity of 2-chloroethyl ethyl sulfide. *BMC Cell Biol* 4: 1, 2003.
41. Suntres ZE, Hepworth SR, and Shek PN. Pulmonary uptake of liposome-associated alpha-tocopherol following intratracheal instillation in rats. *J Pharm Pharmacol* 45: 514–520, 1993.
42. Suntres ZE and Shek PN. Alleviation of paraquat-induced lung injury by pretreatment with bifunctional liposomes containing alpha-tocopherol and glutathione. *Biochem Pharmacol* 52: 1515–1520, 1996.
43. Suntres ZE and Shek PN. Incorporation of alpha-tocopherol in liposomes promotes the retention of liposome-encapsulated glutathione in the rat lung. *J Pharm Pharmacol* 46: 23–28, 1994.
44. Suntres ZE and Shek PN. Prophylaxis against lipopolysaccharide-induced acute lung injury by alpha-tocopherol liposomes. *Crit Care Med* 26: 723–729, 1998.
45. Suntres ZE and Shek PN. Treatment of LPS-induced tissue injury: role of liposomal antioxidants. *Shock* 6(suppl 1): S57–S64, 1996.
46. Thepen T, Van Rooijen N, and Kraal G. Alveolar macrophage elimination in vivo is associated with an increase in pulmonary immune response in mice. *J Exp Med* 170: 499–509, 1989.
47. Thrall RS, McCormick JR, Jack RM, McReynolds RA, and Ward PA. Bleomycin-induced pulmonary fibrosis in the rat: inhibition by indomethacin. *Am J Pathol* 95: 117–130, 1979.
48. Traber MG and Atkinson J. Vitamin E, antioxidant and nothing more. *Free Radic Biol Med* 43: 4–15, 2007.
49. Van Rooijen N and Sanders A. Liposome mediated depletion of macrophages: mechanism of action, preparation of liposomes and applications. *J Immunol Methods* 174: 83–93, 1994.
50. Ward PA. Role of complement, chemokines, and regulatory cytokines in acute lung injury. *Ann N Y Acad Sci* 796: 104–112, 1996.
51. Wright SD, Ramos RA, Tobias PS, Ulevitch RJ, and Mathison JC. CD14, a receptor for complexes of lipopolysaccharide (LPS) and LPS binding protein. *Science* 249: 1431–1433, 1990.
52. Zingg JM and Azzi A. Non-antioxidant activities of vitamin E. *Curr Med Chem* 11: 1113–1133, 2004.

Address reprint requests to:
Peter A. Ward, M.D.
Department of Pathology
University of Michigan Medical School
1301 Catherine Road
Ann Arbor, MI 48109-0602

E-mail: pward@umich.edu

Date of first submission to ARS Central, August 13, 2007; date of final revised submission, November 14, 2007; date of acceptance, November 15, 2007.

Acute Lung Injury Induced by Lipopolysaccharide Is Independent of Complement Activation[1]

Daniel Rittirsch,* Michael A. Flierl,* Danielle E. Day,* Brian A. Nadeau,* Stephanie R. McGuire,* Laszlo M. Hoesel,*† Kyros Ipaktchi,† Firas S. Zetoune,* J. Vidya Sarma,* Lin Leng,¶ Markus S. Huber-Lang,§ Thomas A. Neff,‡ Richard Bucala,¶ and Peter A. Ward[2]*

Although acute lung injury (ALI) is an important problem in humans, its pathogenesis is poorly understood. Airway instillation of bacterial LPS, a known complement activator, represents a frequently used model of ALI. In the present study, pathways in the immunopathogenesis of ALI were evaluated. ALI was induced in wild-type, $C3^{-/-}$, and $C5^{-/-}$ mice by airway deposition of LPS. To assess the relevant inflammatory mediators, bronchoalveolar lavage fluids were evaluated by ELISA analyses and various neutralizing Abs and receptor antagonists were administered in vivo. LPS-induced ALI was neutrophil-dependent, but it was not associated with generation of C5a in the lung and was independent of C3, C5, or C5a. Instead, LPS injury was associated with robust generation of macrophage migration inhibitory factor (MIF), leukotriene B_4 (LTB4), and high mobility group box 1 protein (HMGB1) and required engagement of receptors for both MIF and LTB4. Neutralization of MIF or blockade of the MIF receptor and/or LTB4 receptor resulted in protection from LPS-induced ALI. These findings indicate that the MIF and LTB4 mediator pathways are involved in the immunopathogenesis of LPS-induced experimental ALI. Most strikingly, complement activation does not contribute to the development of ALI in the LPS model. *The Journal of Immunology,* **2008, 180: 7664–7672.**

To investigate the molecular mechanisms of acute lung injury (ALI),[3] which is a major problem in humans, various experimental models of ALI have been used, the most common being the endotoxin (bacterial LPS) model. In experimental ALI, the lung parenchyma is damaged by the generation and release of proteases and reactive oxygen and nitrogen species produced by activated lung macrophages and transmigrated neutrophils in the interstitial and alveolar compartments. The end results are microvascular injury and diffuse alveolar damage with intrapulmonary hemorrhage, edema, and fibrin deposition (1, 2), which are also features in patients with ALI and the acute respiratory distress syndrome (ARDS) (3, 4).

Clinical studies (5, 6) as well as experimental studies (4, 7) have suggested an important role for complement activation products in the pathophysiology of ALI/ARDS. For the full development of injury in other experimental ALI models (e.g., intrapulmonary IgG immune complex deposition), local activation of complement is usually required (7). In particular, generation of C5a amplifies production of proinflammatory cytokines (7–10), leading to intrapulmonary accumulation and activation of neutrophils and macrophages.

However, in the LPS-induced model of ALI, it is not clear to what extent activation of the complement system contributes to the development of lung injury, even though LPS is known to be an activator of the complement system via the classical and the alternative pathways (11–13). As a so-called pathogen-associated molecular pattern, LPS is recognized by TLR4, which is up-regulated on bronchial epithelial cells and lung macrophages during LPS-induced ALI and is considered to play a crucial role in innate immune responses (14, 15). The interaction of LPS with TLR4 ultimately leads to release of proinflammatory mediators and the subsequent recruitment of leukocytes into lungs (3, 10, 14, 16, 17).

Because the role of complement activation and its contribution to the development of experimental ALI after LPS challenge is unclear, the immunopathogenesis of the LPS model of ALI was investigated for specific mediator pathways involved in events leading to lung injury. LPS-induced ALI was neutrophil-dependent and required participation of macrophage migration inhibitory factor (MIF) and leukotriene B_4 (LTB4). Unexpectedly, the development of ALI after LPS administration was independent of complement activation.

Materials and Methods

Animals

Adult male (22–25 g) specific pathogen-free C57BL/6 mice were used in these studies. Additionally, lung injury was used in $C3^{-/-}$ (on a C57BL/6 genetic background) (18), $C5^{+/+}$, and $C5^{-/-}$ mice (congenic strains B10.D2/oSn and B10.D2/nSn, respectively) (19). All studies were done in accordance with the University of Michigan committee on the use and care of animals.

*Department of Pathology and †Department of Traumatology, University of Michigan Medical School, Ann Arbor, MI 48109; ‡Department of Anesthesiology, University Hospital Zurich, Zurich, Switzerland; §Department of Traumatology, Hand, Plastic, and Reconstructive Surgery, University Hospital Ulm, Ulm, Germany; and ¶Department of Medicine and Pathology, Yale University School of Medicine, The Anlyan Center, New Haven, CT 06520

Received for publication August 23, 2007. Accepted for publication April 3, 2008.

The costs of publication of this article were defrayed in part by the payment of page charges. This article must therefore be hereby marked *advertisement* in accordance with 18 U.S.C. Section 1734 solely to indicate this fact.

[1] This work was supported by National Institutes of Health Grants GM-29507 and HL-31963 (to P.A.W.), AI43210 (to R.B.), and Deutsche Forschungsgemeinschaft Grant HU 823/2-2 (to M.S.H.-L.).

[2] Address correspondence and reprint requests to Dr. Peter A. Ward, Department of Pathology, University of Michigan Medical School, 1301 Catherine Road, Ann Arbor, MI 48109. E-mail address: pward@umich.edu

[3] Abbreviations used in this paper: ALI, acute lung injury; ARDS, acute respiratory distress syndrome; BAL, bronchoalveolar lavage; HMGB1, high mobility group box 1 protein; KC, CXCL1; LIX, LPS-induced CXC chemokine; LTB4, leukotriene B_4; MIF, migration inhibitory factor; MPO, myeloperoxidase; WT, wild type.

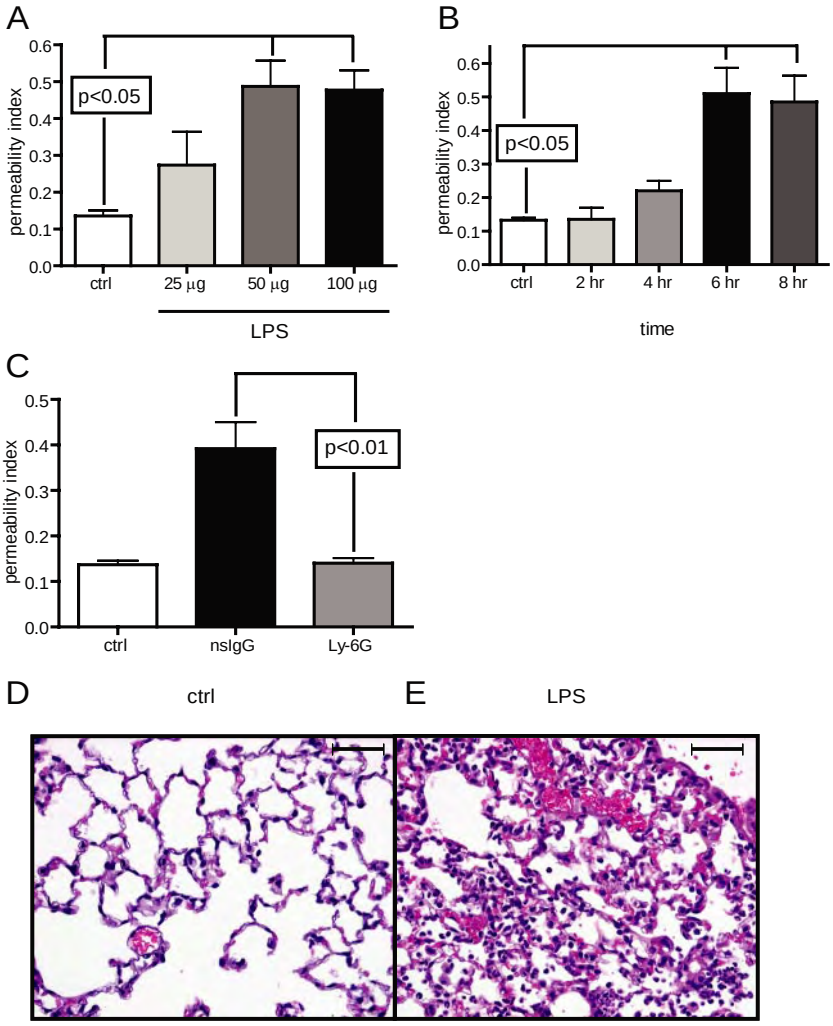

FIGURE 1. Parameters of acute lung injury as reflected by leak of ^{125}I-albumin into lung parenchyma (permeability index) as a function of the dose (25–100 μg) of LPS used (*A*) or as a function of time (0–8 h) after LPS administration (*B*). *C*, Effects of systemic neutrophil depletion on LPS-induced ALI. For each bar, $n \geq 5$ mice. Histologic features in control lung (*D*) and lungs injured by deposition of LPS (*E*). H&E, ×40 (scale bar = 100 μm).

LPS lung injury

For LPS lung injury, unless otherwise indicated, 50 μg LPS from *Escherichia coli* (serotype O111:B4; Sigma-Aldrich) in 40 μl PBS was given intratracheally. Sham-operated animals underwent the same procedure with intratracheal injection of PBS. Permeability index as a quantitative marker for vascular leakage was determined as described elsewhere (20). For retrieval of bronchoalveolar lavage (BAL) fluids, airways were flushed with 0.8 ml PBS. If not otherwise noted, the permeability index was determined and BAL fluids were collected 6 h after lung injury induction.

Neutrophil depletion

Neutropenia was induced using monoclonal anti-mouse Ly-6G Ab (RB6–8C5; eBioscience). Control animals received injections of nonspecific ChromPure Rat IgG (nsIgG; Jackson ImmunoResearch Laboratories). Mice were given a single injection of 25 μg Ly-6G Ab or nsIgG in 100 μl of sterile saline i.v. 24 h before lung injury induction (21).

Lung myeloperoxidase (MPO) activity in lung extracts

After 6 h, mouse lungs were perfused through the right ventricle with 2 ml PBS, snap frozen in liquid nitrogen, and stored at −80°C. To measure MPO activity, whole lungs were homogenized in 50 mmol/L potassium phosphate buffer containing 0.5% hexadecyltrimethylammonium bromide and 5 mmol/L EDTA. After centrifugation at 12,000 × *g* for 10 min at 4°C, the supernatant fluids were incubated in a 50 mmol/L potassium phosphate buffer containing the substrate, H_2O_2 (1.5 mol/L) and *o*-dianisidine dihydrochloride (167 μg/ml; Sigma-Aldrich). The enzymatic activity was determined spectrophotometrically by measuring the change in absorbance at 460 nm over 3 min (Molecular Devices) (10).

Leukocyte count in BAL fluids

Immediately after collection of BAL fluids, RBC were lysed with 1% acetic acid and total white cell count of each BAL sample was determined using a Neubauer hemocytometer (Hauser Scientific). Cell differentials were analyzed (300 cells for each experimental condition) after cytospin centrifugation (500 × *g*, 3 min), methanol fixation (10 min), and Pappenheim's staining.

Anti-C5a treatment

Rabbit anti-rat C5a IgG (40 μg) (22) or nonspecific rabbit IgG (40 μg) (Jackson ImmunoResearch Laboratories) was given intratracheally together with LPS.

Blockade of MIF or MIF receptor

Neutralizing mAb against mouse MIF was purified from mouse ascites fluids (ImmunoPure IgG purification kit, Pierce). Ten to 80 μg anti-MIF mAb (IgG1) or irrelevant mouse IgG1 (Jackson ImmunoResearch Laboratories) was mixed with LPS. For blockade of the MIF receptor, mice were treated with ISO-1 (35 mg/kg body weight i.p.; Calbiochem) or vehicle (aqueous 5% DMSO) 30 min before lung injury induction.

Blockade of LTB4 receptor

For in vivo blockade of the LTB4 receptor BLT1, the synthetic receptor antagonist U-75302 (BIOMOL) or vehicle (DMSO) was given intratracheally together with endotoxin (23).

ELISA for mouse C5a and C3a

To measure the concentration of mouse C5a in BAL fluids, ELISA plates were coated with purified monoclonal anti-mouse C5a IgG (BD Pharmingen, capture Ab, 5 μg/ml). After blocking, BAL fluids and recombinant mouse C5a (as standards) were applied and biotinylated monoclonal anti-mouse C5a Ab was used subsequently (BD Pharmingen, detection Ab, 500 ng/ml) followed by incubation with streptavidin-peroxidase (400 ng/ml). *O*-phenylenediamine dihydrochloride was then added, the color reaction

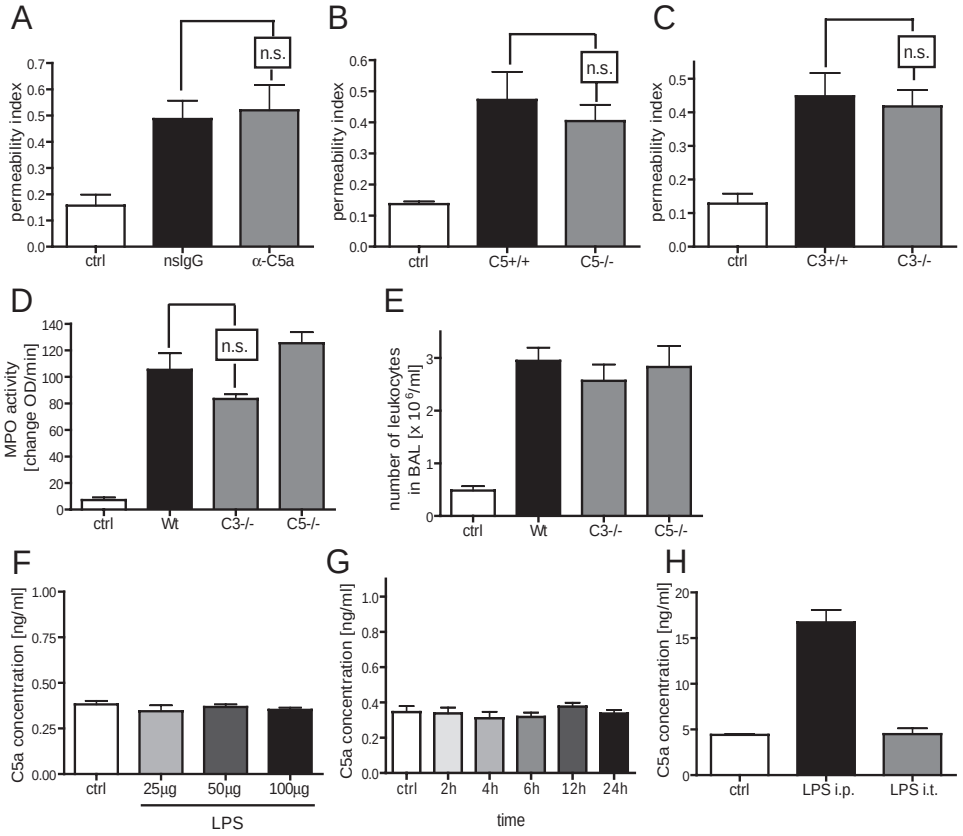

FIGURE 2. *A*, Effects of anti-C5a (40 μg IgG) administered intratracheally on ALI in the LPS model (50 μg). Lung injury induced by LPS in $C5^{-/-}$ mice (*B*) or $C3^{-/-}$ mice (*C*). Lung MPO content in WT and C3- and C5-deficient mice (*D*). *E*, Number of leukocytes in BAL from $C3^{-/-}$ and $C5^{-/-}$ mice in comparison to WT animals with ALI. *F*, BAL C5a content in LPS-injured lungs as a function of dose of LPS, as measured at 6 h. *G*, Time-course for BAL C5a content (determined by ELISA) after airway deposition of 50 μg LPS. *H*, Plasma C5a levels after intraperitoneal vs intratracheal administration of LPS. For each bar, $n \geq 5$ mice.

was stopped with 3 M sulfuric acid, and the absorbance was read at 490 nm (24).

ELISA for mouse IL-6, TNF-α, LPS-induced CXC chemokine (LIX), CXCL1 (KC), MIP-2, high mobility group box 1 protein (HMGB1), MIF, and LTB4

For measurement of IL-6, TNF-α, MIP-2, LIX,and KC in BAL fluids, ELISA kits (DuoSet, R&D Systems) were used according to the manufacturer's protocol. For quantification of HMGB1 in BAL fluids, a commercially available ELISA assay (Shino-Test) was used. Measurement of MIF was done using purified rabbit anti-MIF IgG (5 μg/ml, Cell Sciences). As detection Ab, purified rabbit anti-MIF IgG was biotinylated using the EZ-link NHS-PEO solid-phase biotinylation kit (Pierce). After washing and blocking of wells, BAL fluids or standards (recombinant mouse MIF, R&D Systems) were applied in various dilutions. Biotinylated detection Ab (500 ng/ml) was added and development was performed as described above (ELISAs for C5a and C3a). LTB4 concentrations in BAL fluids were determined by using a commercially available ELISA kit (Cayman Chemical).

Statistical analysis

All values were expressed as means ± SEM. Data sets were analyzed by one-way ANOVA followed by Tukey multiple comparison test with GraphPad Prism 4 software (GraphPad Software). Results were considered statistically significant when $p < 0.05$.

Results

Characterization of lung injury after deposition of LPS

Lung injury as defined by the permeability index (albumin leak) was studied as a function of dose of LPS, which was administered directly into the airways of mice. As shown in Fig. 1*A*, the dose of the inflammatory stimulus was related to an increase in the permeability index. There was no significant difference in the permeability index between the 50 μg and the 100 μg dose. In all subsequent experiments, unless otherwise indicated, the dose of LPS used was 50 μg. The injury peaked 6 h after LPS administration (Fig. 1*B*). In the current study we used the mAb Ly-6G to induce >95% depletion of blood neutrophils (without affecting the number of blood monocytes), as recently described (21). The permeability index rose to a level of 0.39 ± 0.06 6 h after intratracheal instillation of 50 μg LPS, as contrasted to a value of 0.14 ± 0.01 in the uninjured lungs (Fig. 1*C*). In neutrophil-depleted mice (Ly-6G), the permeability index remained at baseline (0.14 ± 0.01), indicating that for LPS to induce lung injury blood neutrophils must be available (Fig. 1*C*).

The histological patterns of ALI due to LPS are shown in Fig. 1, *D* and *E*. Fig. 1*D* depicts a control lung, in which PBS was

Table I. *Cytokine/chemokine concentrations in BAL fluids (pg/ml)*[a]

Cytokine/Chemokine	Control PBS	WT LPS	$C3^{-/-}$ LPS[b]	$C5^{-/-}$ LPS[b]
IL-6	69.12 ± 11.63	1200 ± 161.4	1491 ± 195.1	1797 ± 242.2
TNF-α	396.2 ± 41.65	5028 ± 472.6	3763 ± 332.2	5404 ± 728.5
MIP-2	15.44 ± 1.577	764.3 ± 191.0	1124 ± 207.5	927.9 ± 385.1
KC	87.7 ± 12.1	4671 ± 1609	7583 ± 832.1	2158 ± 668.8
LIX	300.8 ± 10.3	1262 ± 73	953.9 ± 67.84	1132 ± 234.8

[a] $n \geq 5$ for each group.
[b] All values in column are not significant when compared with WT LPS data.

Table II. *Mediator concentrations in BAL fluids*[a]

Mediator	Control PBS	LPS	Unit
HMGB1	48.4 ± 1.3	141.3 ± 22.7*	ng/ml
MIF	0.6 ± 0.2	4.6 ± 0.8*	μg/ml
LTB4	n.d.	426.2 ± 38.5*	pg/ml

[a] $n \geq 5$ for each group. All p values are based on comparison to control PBS data. *, $p < 0.05$. n.d., Not detectable.

administered intratracheally. The lung was essentially normal in appearance. In Fig. 1*E*, LPS-induced ALI was characterized by interstitial and intraalveolar deposits of neutrophils and fibrin, prominence of alveolar macrophages, and intraalveolar hemorrhage.

Complement activation is not required in the LPS model of ALI

Previous studies have shown a requirement for C5 for the full expression of lung injury following deposition of IgGIC in mouse lung (24). Contrarily, in LPS-induced ALI blockade of C5a with 40 μg anti-C5a-IgG, which was given together with the LPS, did not suppress lung injury (Fig. 2*A*), nor was there reduced injury in the absence of C5 (Fig. 2*B*) or C3 (Fig. 2*C*). In accord, the absence of C3 or C5 neither affected accumulation of leukocytes in lung as indicated by assessment of lung myeloperoxidase activity (Fig. 2*D*) nor their appearance in the alveolar space (Fig. 2*E*). Using a self-developed ELISA with which C5a has been detected in mouse BAL fluids (24), no increase of C5a in BAL was found as a function of the dose (25–100 μg) of LPS used (Fig. 2*F*) or as a function of time (0–24 h) after LPS administration (Fig. 2*G*). Additionally, there was no increase in C5a plasma levels after intratracheal injection of LPS, indicating that systemic complement activation in terms of a possible LPS clearance mechanism does not occur during ALI (Fig. 2*H*). In contrast, in wild-type mice (WT) injected i.p. with 10 μg LPS in 200 μl PBS, C5a plasma levels rose 4-fold as compared with WT mice not given LPS (Fig. 2*H*), indicating that the LPS used in the present study is capable of activating mouse complement if given i.p. Collectively, these data suggest that ALI following airway deposition of LPS is complement-independent.

Appearance of proinflammatory mediators in experimental ALI

The levels of proinflammatory mediators were quantitated in BAL fluids after airway deposition of LPS. The lung cytokines IL-6 and TNF-α and the chemokines MIP-2, KC, and LIX, which are chiefly derived from lung macrophages in a NF-κB-dependent fashion, are known to play important roles in ALI (25, 26). It has

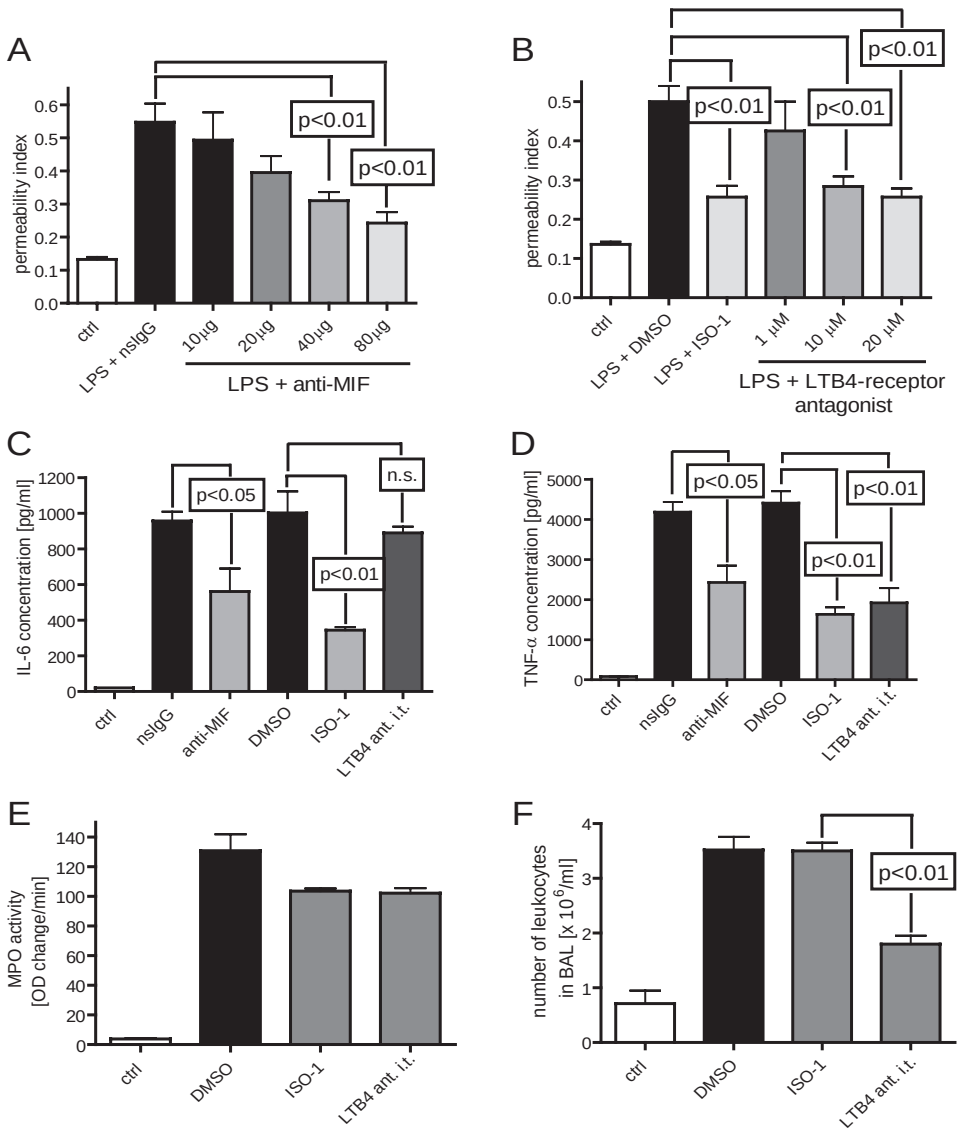

FIGURE 3. *A*, Intensity of lung injury (measured as permeability index) in the LPS model with isotype-matched IgG1 or with anti-MIF mAb (each at 40 μg mixed with LPS). *B*, Effects of ISO-1 (the MIF receptor antagonist, 35 mg/kg body weight, administered i.p. 30 min before lung injury induction) or the LTB4 receptor antagonist (1–20 μM) after admixture with the intratracheally administered LPS. Effects of MIF or LTB4 blockade on the buildup of IL-6 (*C*) and TNF-α (*D*). For the interventions indicated in *C* and *D*, 40 μg neutralizing mAb to mouse MIF or 20 μM of the LTB4 receptor antagonist was mixed with the LPS; when the MIF receptor antagonist (ISO-1) was used, 35 mg/kg body weight was injected i.p. 30 min before intratracheal administration of 50 μg LPS. *E*, Lung MPO content in LPS-injured lungs of the LPS-treated animals of the ISO-1 (35 mg/kg body weight) or the LTB4 receptor antagonist (20 μM). *F*, Effects of MIF or LTB4 blockade on the total white cell count in BAL fluids. For each bar, $n \geq 5$ mice.

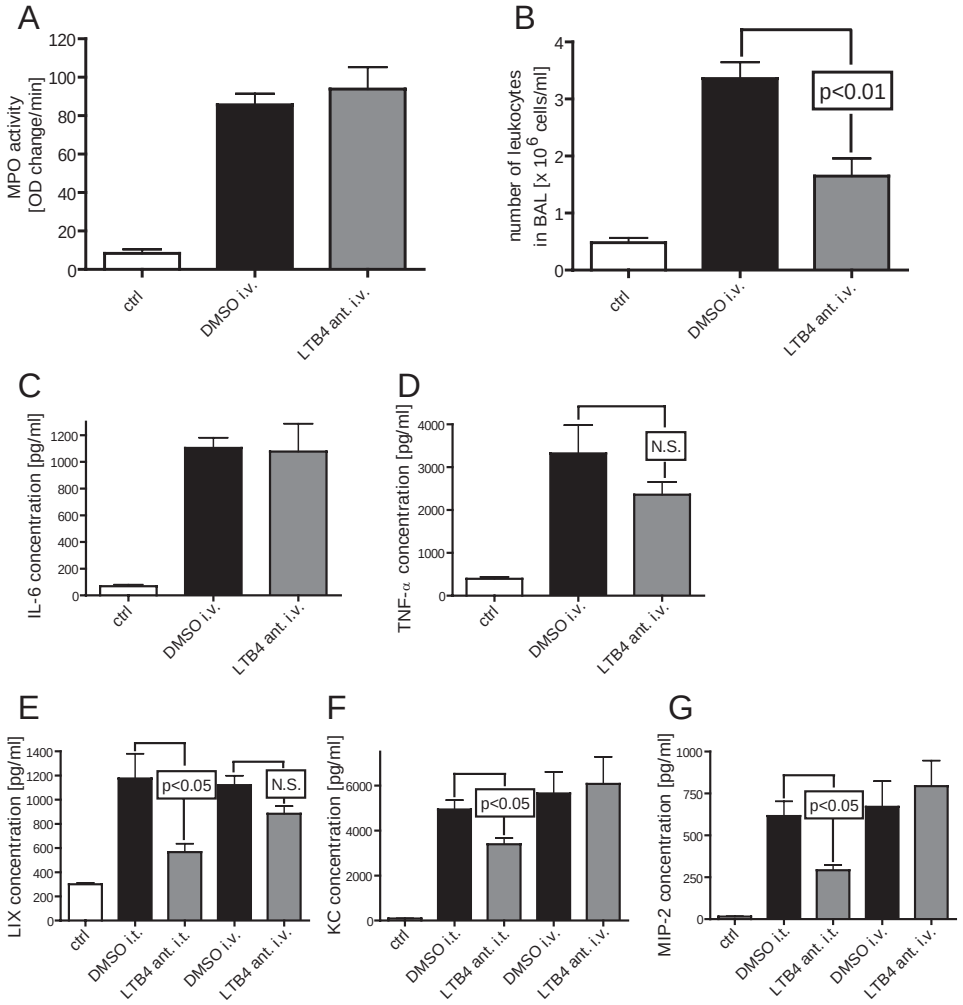

FIGURE 4. Effects of LTB4 blockade by the LTB4 antagonist when administered i.v. in comparison to intratracheal administration on lung MPO content (*A*) and appearance of leukocytes in BAL fluids (*B*). Levels of IL-6 (*C*) and TNF-α (*D*) in BAL fluids after i.v. application of the LTB4 antagonist. Concentrations of the chemoattractants LIX (*E*), KC (*F*), and MIP-2 (*G*) in BAL fluids after i.v. vs intratracheal administration of the LTB4 antagonist in lung injury. For each bar, $n \geq 5$ mice.

been shown that PMN recruitment is mediated by neutrophil chemoattractants such as KC, MIP-2, and LIX. In particular, PMN infiltration into lung following exposure to LPS is dependent on interaction of CXCR2 with its ligands (e.g., KC, MIP-2) (26). As shown in Table I, the cytokine/chemokine levels were substantially elevated in BAL fluids of LPS-injured lungs of WT mice. As is evident, there was no difference in cytokine/chemokine levels in BAL fluids from $C3^{-/-}$ or $C5^{-/-}$ mice when compared with WT mice with lung injury. Consistent with the findings described above (Fig. 2), these data support the conclusion that complement is not required for the full inflammatory response during LPS-induced ALI.

Requirements for MIF and LTB4 in the LPS model of ALI

BAL fluids from WT mice after LPS-induced lung injury were screened for the mediators HMGB1, MIF, and LTB4, which have been described to play important roles in the pulmonary inflammatory response (16, 27, 28). HMGB1, which is known to be a distal mediator in ALI and the blockade of which has shown protective effects in the LPS model (16), showed a robust increase in BAL fluids after LPS administration (Table II). MIF was also found at increased levels in BAL fluids from LPS-injured lungs as compared with the PBS controls (Table II). Finally, measurement of LTB4 in BAL fluids revealed no detectable levels in controls, but readily detectable levels of LTB4 in LPS-injured lungs (Table II), suggesting that LTB4, HMGB1, and MIF contribute to the development of LPS-induced lung injury.

Because no complement requirement could be demonstrated in the LPS model (Fig. 2) and MIF and LTB4 levels were robustly elevated in LPS-induced ALI (Table II), the possible roles of these mediators in the development of ALI were evaluated. In particular, we were interested in whether these mediators might be required for PMN recruitment, which was found to be necessary for the development of lung injury (Fig. 1*C*). As shown in Fig. 3, neutralization of MIF (10–80 μg anti-MIF IgG intratracheally) reduced the index of lung injury as a function of dose (Fig. 3*A*), while intraperitoneal administration of the MIF receptor antagonist ISO-1 also significantly suppressed injury (Fig. 3*B*). When the LTB4 receptor antagonist (1–20 μM) was administered intratracheally together with LPS, there was a dose-dependent reduction in the permeability index (Fig. 3*B*). We assessed how neutralization of MIF, blockade of the MIF receptor, or blockade of the LTB4 receptor (20 μM) might affect production of IL-6 and TNF-α. In Fig. 3*C*, protective interventions with anti-MIF or ISO-1 reduced the BAL levels of IL-6 by 48 and 71%, respectively. In contrast, the use of the LTB4 receptor antagonist did not significantly reduce the levels of IL-6. When BAL levels of TNF-α were determined, using the same BAL samples used for IL-6 assays, similar data were obtained, except for mice treated with the LTB4 receptor antagonist in which TNF-α levels were also significantly suppressed (Fig. 3*D*). In summary, these data suggest that MIF and LTB4 promote production of proinflammatory cytokines during ALI induced by LPS.

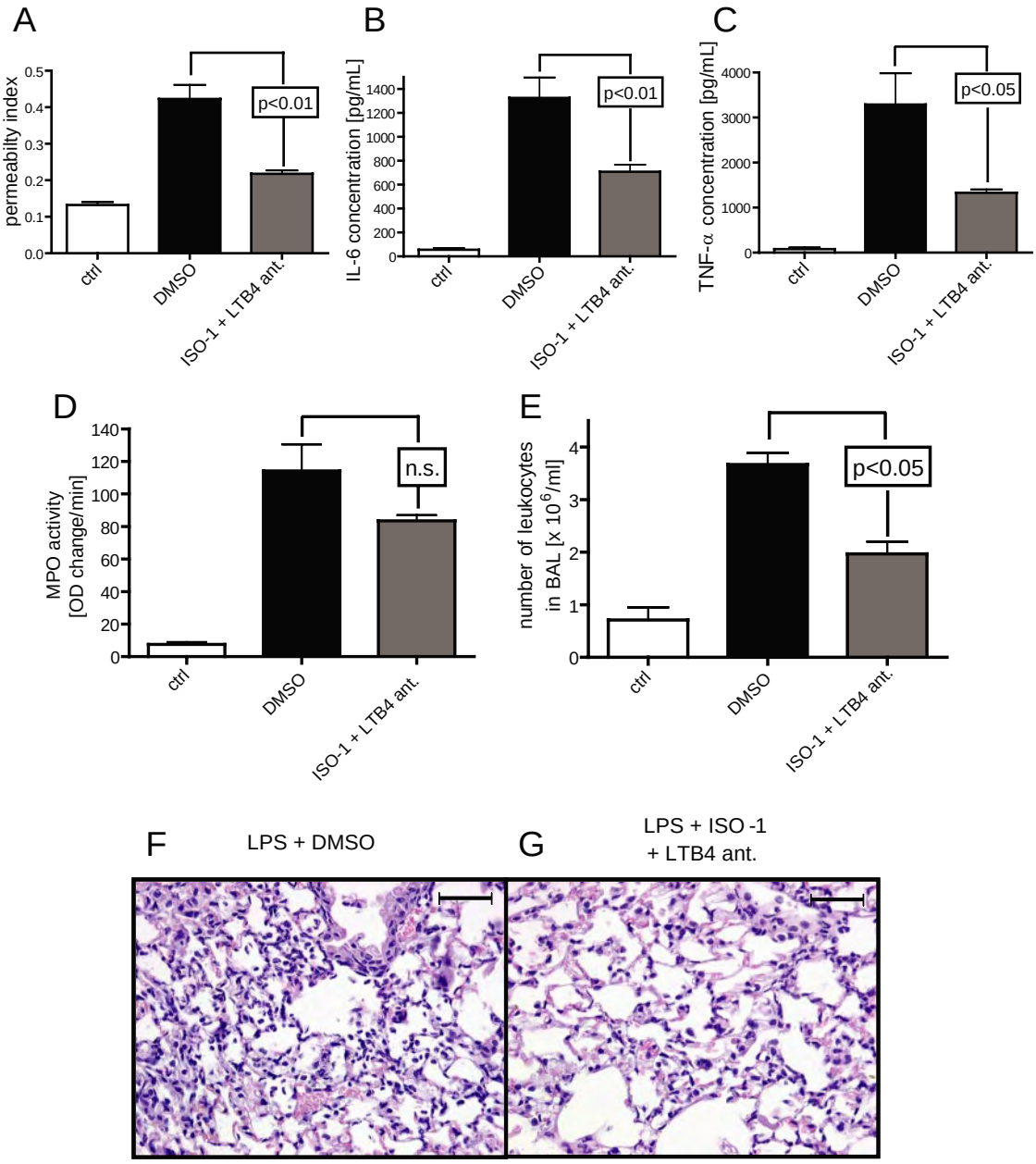

FIGURE 5. *A*, Effects of a dual blockade of MIF (ISO-1; 35 mg/kg body weight) and LTB4 (receptor antagonist; 20 μM) on LPS-induced ALI. Intensity of lung injury as determined by lung permeability. Levels of proinflammatory cytokines IL-6 (*B*) and TNF-α (*C*) in the combined presence of ISO-1 and the LTB4 antagonist. *D*, Buildup of lung MPO after intratracheal LPS administration and ISO-1 + LTB4 antagonist. *E*, Total leukocyte count in BAL fluids. For each bar, $n \geq 5$ mice. Effect of the LTB4 antagonist + ISO-1 on lung histology (*G*) in comparison to deposition of LPS + DMSO (*F*). H&E, $\times$40 (scale bar = 100 μm).

Finally, lung MPO levels after LPS administration were assessed (Fig. 3*E*). When the protective interventions (ISO-1, LTB4 receptor antagonist) were used with the doses described above, minor reductions in MPO content were found, but these were not significantly different from MPO content in LPS lungs that were not otherwise manipulated. However, the number of leukocytes in BAL fluids was significantly reduced in the presence of the LTB4 antagonist, but not when ISO-1 was administered (Fig. 3*F*). In all groups treated with LPS, there was no difference in cell differentials, with predominantly PMNs and 10–15% macrophages (data not shown). Collectively, these data suggest that protective interventions directed at receptors for MIF or LTB4 reduce the development of ALI but do not interfere with neutrophil accumulation in lung after administration of LPS. LTB4 appears to promote transmigration of PMNs into the alveolar space, while MIF seems to accentuate proinflammatory mediator release from macrophages and neutrophils rather than interfering with their migration.

Similar to the results displayed in Fig. 3, *E* and *F*, where the LTB4 antagonist was given intratracheally, i.v. administration of the antagonist did not alter buildup of lung MPO (Fig. 4*A*), but resulted in reduced numbers of leukocytes present in the airway compartment (Fig. 4*B*). In accord with Fig. 3*C* (intratracheal application), i.v. treatment with the LTB4 antagonist also did not affect the secretion of IL-6 (Fig. 4*C*). TNF-α levels in BAL fluids were not substantially reduced by LTB4 blockade when the antagonist was injected i.v. (Fig. 4*D*), although intratracheal administration significantly suppressed TNF-α production (Fig. 3*D*). A similar pattern was found for the chemokines LIX, KC, and MIP-2,

with the latter two being ligands for CXCR2, which is known to mediate PMN recruitment into lungs. Only intratracheal administration of the LTB4 antagonist resulted in decreased chemokine levels in BAL fluids of LPS-injured mice, whereas its i.v. application had no effect on local chemokine production (Fig. *4E–G*). In summary, these data suggest that LTB4 might trigger the release of chemoattractants from alveolar macrophages rather than directly recruiting PMNs into the lung. However, leukocyte transmigration into the alveolar space seems to depend on direct interaction of LTB4 with the recruited cells because the number of leukocytes was significantly reduced, regardless of whether the LTB4 antagonist was administered via the intratracheal or the i.v. route.

Dual inhibition of LTB4 and MIF in the LPS model of ALI

When blockade of MIF was used together with inhibition of LTB4 (Fig. 5), the intensity of lung injury was reduced to an extent similar to that found when either antagonist was administered alone (70% reduction vs 67% by ISO-1 or LTB4 antagonist, respectively) (Fig. 5*A*). Moreover, concentrations of IL-6 (Fig. 5*B*) and TNF-α (Fig. 5*C*) in BAL fluids were significantly suppressed in the presence of ISO-1 and the LTB4 antagonist, but they were still elevated in comparison to control animals. Dual inhibition of MIF and LTB4 failed to significantly reduce the buildup of lung MPO (Fig. 5*D*). In contrast, as in the case of the single inhibition of LTB4 (Fig. 3*F*), the number of leukocytes in BAL fluids was clearly lower when the LTB4 antagonist + ISO-1 were given (Fig. 5*E*), but without any further accentuation of this effect by the additional blockade of MIF. These findings were underpinned by lung histology. In the presence of the LTB4 antagonist and ISO-1, the bulk of PMNs only accumulated in the lung interstium (Fig. 5*G*), whereas in LPS-injured lungs without inhibitors, PMNs were also present in the alveolar compartment (Fig. 5*F*). Taken together, these data suggest that MIF and LTB4 promote lung injury via different mechanisms and that dual inhibition of both mediators does not result in a synergistic effect on the attenuation of inflammatory response.

Discussion

ALI and ARDS, as well as chronic obstructive pulmonary disease, represent fundamentally disordered inflammation in the lung and continue to be prevalent clinical problems (2). Despite extensive efforts in both the clinical and laboratory settings, the molecular mechanisms of these inflammatory disorders are poorly understood. LPS and related products are known to be present in BAL fluids from patients with ARDS (29). Therefore, lung injury induction by LPS in rodents represents a frequently used ALI model, mimicking many features of ALI/ARDS in humans. In this study, the LPS model was evaluated for immunopathological events leading to lung injury.

It is well established that following the intrapulmonary deposition of IgG immune complexes, generation of C5a plays an important role in the pathogenesis of ALI (7, 24). However, activation of the complement system was not required for the full development of LPS-induced lung injury suggesting that there is differential regulation of local complement activation in the lung depending on the nature of the inflammatory stimulus. In the present study, neither the blockade of C5a nor the absence of C5 or C3 influenced the intensity of lung injury in the LPS model, and no increase of BAL C5a was found after LPS administration (Fig. 2). This is in accord with an earlier report (30), but contrasts with a recent publication that describes altered complement levels and expression in LPS-induced ALI (31). However, in the latter report, only the expression of nonactivated complement proteins was presented, making it far from certain if activation of the complement cascade actually occurred. In another conflicting report, C3 and C5b-9 deposition on the endothelium of pulmonary vessels has been reported, but complement depletion had no effect on lung MPO activity and TNF-α levels, which again raises the question of whether complement activation had effectively proceeded (32). In various studies, patients with ARDS showed evidence for complement activation, the extent of which correlated with the degree and outcome of ARDS (5, 6, 33). In contrast, in another study published some years ago, C5a could not be detected in BAL fluids from patients with ARDS using the methods available at that time (34). Although hepatic production is the main source for complement proteins, virtually all complement proteins can be locally synthesized in the lung by type II alveolar pneumocytes, alveolar macrophages, and lung fibroblasts (35, 36). However, while the total pulmonary complement protein concentration is comparable to levels found in serum, its activity in normal lung is markedly reduced due to the complement-inhibitory activity of surfactant protein A and C1 inhibitor, both being abundantly present and active in the lung (37, 38). Reduced lung activity of both surfactant protein A and C1 inhibtor can be related to the development of ARDS in humans (39, 40). In other words, pulmonary activation of the complement system underlies a complex and distinct regulation. Therefore, presence of complement proteins in the lung does not necessarily imply their local activation.

There is also diverse information regarding the role of the complement system in the setting of endotoxemia. The febrile response induced by infusion of LPS seems related to generation of C5a, and endotoxic $C5^{-/-}$ mice had reduced evidence for organ failure when compared with $C5^{+/+}$ mice (41, 42). In contrast, C3- and C4-deficient mice infused with LPS showed greatly increased mortality, suggesting that systemic in vivo clearance of LPS requires C3 and C4 (43). In line with the above-mentioned observations, in this study robust complement activation (as indicated by increased plasma levels of C5a) only occurred when LPS was injected i.p., but not when it was administered via the intratracheal route (Fig. 2*F–H*). These observations suggest that complement may be necessary for systemic clearance of LPS from the blood compartment in vivo, but not in the local setting of the lung as described in this report, where LPS failed to induce activation of the complement system. In other words, different mechanisms of endotoxin clearance might be involved that are dependent on the entry route of LPS.

Finally, although our data strongly suggest that the complement activation does not contribute in the development of ALI after LPS exposure, we were able to identify MIF and LTB4 as key mediators in the pathogenesis of LPS-induced ALI. MIF has been found in BAL fluids from humans with ARDS and may play a role in sustaining the pulmonary inflammatory response (27). In the present study we sought to evaluate the role of MIF in experimental ALI. MIF functions as a pleiotropic proinflammatory protein and plays a key role in systemic and local inflammatory responses (44). It is abundantly produced by monocytes/macrophages, can induce and enhance the production of other cytokines, and regulates apoptosis of leukocytes (44–46). Previous studies suggest the participation of MIF in neutrophil accumulation in lung after intraperitoneal injection of LPS (47). Intratracheal administration of neutralizing mAb to MIF or use of the MIF receptor antagonist ISO-1 attenuated the capillary leak and tissue damage in ALI. Blockade of MIF suppressed proinflammatory cytokine release in LPS-induced ALI, but did not interfere with PMN accumulation or their transmigration into the alveolar space. The chief effects of MIF in experimental ALI may be enhancement of the proinflammatory response (27), up-regulation of TLR4 (48), glucocorticoid antagonism (27), or a combination of all the above.

Because of its importance in the pathogenesis of airway hyperresponsiveness, the role of LTB4 and interaction with its receptor (BLT1) in acute lung injury was evaluated (28). LTB4 is a chemotactic factor for neutrophils and appears to be responsible for neutrophil accumulation in lung tissue during acute asthmatic exacerbation (49, 50). Additionally, LTB4 enhances the release of active oxygen species and the respiratory burst of neutrophils via its priming effects (51, 52). In the present LPS model, LTB4 levels in BAL fluids were substantially elevated when compared with noninjured lungs. Furthermore, blockade of the LTB4 receptor BLT1 strikingly reduced lung injury. Interestingly, these protective effects in the LPS model were not linked to altered accumulation of neutrophils based on lung MPO content, which does not distinguish between interstitial and intraalveolar PMNs. However, the transmigration of PMNs from the interstitium to the airway compartment seems to be LTB4-dependent (Figs. 3 and 4). These findings are consistent with previous studies describing that intratracheal instillation of LTB4, which is also a major product of alveolar macrophages, can recruit active PMNs into airspace (53, 54). Although the precise mechanisms involved are largely unknown, reactive oxygen species and the expression of neutrophil elastase seem to be involved in the regulation of transepithelial migration of PMNs into the alveolar compartment in response to LTB4 (54, 55).

In summary, the immunopathogenesis of LPS-induced ALI underlies a complex regulation regarding mediators and pathways involved in neutrophil mobilization and priming. Most strikingly, LPS-induced ALI is independent of activation of the complement system and, instead, is orchestrated by MIF and LTB4.

Acknowledgments

We thank Beverly Schumann and Sue Scott for excellent secretarial assistance in preparation of the manuscript.

Disclosures

The authors have no financial conflicts of interest.

References

1. Johnson, K. J., and P. A. Ward. 1974. Acute immunologic pulmonary alveolitis. *J. Clin. Invest.* 54: 349–357.
2. Flierl, M. A., D. Rittirsch, L. M. Hoesel, H. Gao, M. Huber-Lang, and P. A. Ward. 2006. Acute lung injury: a challenging transfer from bench to bedside. *Med. Hypothesis Res.* 3: 727–738.
3. Kabir, K., J. P. Gelinas, M. Chen, D. Chen, D. Zhang, X. Luo, J. H. Yang, D. Carter, and R. Rabinovici. 2002. Characterization of a murine model of endotoxin-induced acute lung injury. *Shock* 17: 300–303.
4. Ward, P. A. 1996. Rous-Whipple Award lecture: role of complement in lung inflammatory injury. *Am. J. Pathol.* 149: 1081–1086.
5. Hammerschmidt, D. E., L. J. Weaver, L. D. Hudson, P. R. Craddock, and H. S. Jacob. 1980. Association of complement activation and elevated plasma-C5a with adult respiratory distress syndrome: pathophysiological relevance and possible prognostic value. *Lancet* 1: 947–949.
6. Solomkin, J. S., L. A. Cotta, P. S. Satoh, J. M. Hurst, and R. D. Nelson. 1985. Complement activation and clearance in acute illness and injury: evidence for C5a as a cell-directed mediator of the adult respiratory distress syndrome in man. *Surgery* 97: 668–678.
7. Mulligan, M. S., E. Schmid, B. Beck-Schimmer, G. O. Till, H. P. Friedl, R. B. Brauer, T. E. Hugli, M. Miyasaka, R. L. Warner, K. J. Johnson, and P. A. Ward. 1996. Requirement and role of C5a in acute lung inflammatory injury in rats. *J. Clin. Invest.* 98: 503–512.
8. Warren, J. S., K. R. Yabroff, D. G. Remick, S. L. Kunkel, S. W. Chensue, R. G. Kunkel, K. J. Johnson, and P. A. Ward. 1989. Tumor necrosis factor participates in the pathogenesis of acute immune complex alveolitis in the rat. *J. Clin. Invest.* 84: 1873–1882.
9. Shanley, T. P., J. L. Foreback, D. G. Remick, T. R. Ulich, S. L. Kunkel, and P. A. Ward. 1997. Regulatory effects of interleukin-6 in immunoglobulin G immune-complex-induced lung injury. *Am. J. Pathol.* 151: 193–203.
10. Speyer, C. L., H. Gao, N. J. Rancilio, T. A. Neff, G. B. Huffnagle, J. V. Sarma, and P. A. Ward. 2004. Novel chemokine responsiveness and mobilization of neutrophils during sepsis. *Am. J. Pathol.* 165: 2187–2196.
11. Oishi, K., N. L. Koles, G. Guelde, and M. Pollack. 1992. Antibacterial and protective properties of monoclonal antibodies reactive with *Escherichia coli* O111:B4 lipopolysaccharide: relation to antibody isotype and complement-fixing activity. *J. Infect. Dis.* 165: 34–45.
12. Mintz, C. S., D. R. Schultz, P. I. Arnold, and W. Johnson. 1992. *Legionella pneumophila* lipopolysaccharide activates the classical complement pathway. *Infect. Immun.* 60: 2769–2776.
13. Vukajlovich, S. W., J. Hoffman, and D. C. Morrison. 1987. Activation of human serum complement by bacterial lipopolysaccharides: structural requirements for antibody independent activation of the classical and alternative pathways. *Mol. Immunol.* 24: 319–331.
14. Medzhitov, R., and C. Janeway, Jr. 2000. Innate immune recognition: mechanisms and pathways. *Immunol. Rev.* 173: 89–97.
15. Saito, T., T. Yamamoto, T. Kazawa, H. Gejyo, and M. Naito. 2005. Expression of Toll-like receptor 2 and 4 in lipopolysaccharide-induced lung injury in mouse. *Cell Tissue Res.* 321: 75–88.
16. Abraham, E., J. Arcaroli, A. Carmody, H. Wang, and K. J. Tracey. 2000. HMG-1 as a mediator of acute lung inflammation. *J. Immunol.* 165: 2950–2954.
17. Reutershan, J., A. Basit, E. V. Galkina, and K. Ley. 2005. Sequential recruitment of neutrophils into lung and bronchoalveolar lavage fluid in LPS-induced acute lung injury. *Am. J. Physiol.* 289: L807–L815.
18. Circolo, A., G. Garnier, W. Fukuda, X. Wang, T. Hidvegi, A. J. Szalai, D. E. Briles, J. E. Volanakis, R. A. Wetsel, and H. R. Colten. 1999. Genetic disruption of the murine complement C3 promoter region generates deficient mice with extrahepatic expression of C3 mRNA. *Immunopharmacology* 42: 135–149.
19. Wheat, W. H., R. Wetsel, A. Falus, B. F. Tack, and R. C. Strunk. 1987. The fifth component of complement (C5) in the mouse: analysis of the molecular basis for deficiency. *J. Exp. Med.* 165: 1442–1447.
20. Neff, T. A., R. F. Guo, S. B. Neff, J. V. Sarma, C. L. Speyer, H. Gao, K. D. Bernacki, M. Huber-Lang, S. McGuire, L. M. Hoesel, et al. 2005. Relationship of acute lung inflammatory injury to Fas/FasL system. *Am. J. Pathol.* 166: 685–694.
21. Hoesel, L. M., T. A. Neff, S. B. Neff, J. G. Younger, E. W. Olle, H. Gao, M. J. Pianko, K. D. Bernacki, J. V. Sarma, and P. A. Ward. 2005. Harmful and protective roles of neutrophils in sepsis. *Shock* 24: 40–47.
22. Huber-Lang, M. S., J. V. Sarma, S. R. McGuire, K. T. Lu, R. F. Guo, V. A. Padgaonkar, E. M. Younkin, I. J. Laudes, N. C. Riedemann, J. G. Younger, and P. A. Ward. 2001. Protective effects of anti-C5a peptide antibodies in experimental sepsis. *FASEB J.* 15: 568–570.
23. Noiri, E., T. Yokomizo, A. Nakao, T. Izumi, T. Fujita, S. Kimura, and T. Shimizu. 2000. An in vivo approach showing the chemotactic activity of leukotriene B(4) in acute renal ischemic-reperfusion injury. *Proc. Natl. Acad. Sci. USA* 97: 823–828.
24. Huber-Lang, M., J. V. Sarma, F. S. Zetoune, D. Rittirsch, T. A. Neff, S. R. McGuire, J. D. Lambris, R. L. Warner, M. A. Flierl, L. M. Hoesel, et al. 2006. Generation of C5a in the absence of C3: a new complement activation pathway. *Nat. Med.* 12: 682–687.
25. Kelley, J. 1990. Cytokines of the lung. *Am. Rev. Respir. Dis.* 141: 765–788.
26. Reutershan, J., M. A. Morris, T. L. Burcin, D. F. Smith, D. Chang, M. S. Saprito, and K. Ley. 2006. Critical role of endothelial CXCR2 in LPS-induced neutrophil migration into the lung. *J. Clin. Invest.* 116: 695–702.
27. Donnelly, S. C., C. Haslett, P. T. Reid, I. S. Grant, W. A. Wallace, C. N. Metz, L. J. Bruce, and R. Bucala. 1997. Regulatory role for macrophage migration inhibitory factor in acute respiratory distress syndrome. *Nat. Med.* 3: 320–323.
28. Miyahara, N., S. Miyahara, K. Takeda, and E. W. Gelfand. 2006. Role of the LTB4/BLT1 pathway in allergen-induced airway hyperresponsiveness and inflammation. *Allergol. Int.* 55: 91–97.
29. Martin, T. R., G. D. Rubenfeld, J. T. Ruzinski, R. B. Goodman, K. P. Steinberg, D. J. Leturcq, A. M. Moriarty, G. Raghu, R. P. Baughman, and L. D. Hudson. 1997. Relationship between soluble CD14, lipopolysaccharide binding protein, and the alveolar inflammatory response in patients with acute respiratory distress syndrome. *Am. J. Respir. Crit. Care Med.* 155: 937–944.
30. Burrell, R., R. C. Lantz, and D. E. Hinton. 1988. Mediators of pulmonary injury induced by inhalation of bacterial endotoxin. *Am. Rev. Respir. Dis.* 137: 100–105.
31. Bolger, M. S., D. S. Ross, H. Jiang, M. M. Frank, A. J. Ghio, D. A. Schwartz, and J. R. Wright. 2007. Complement levels and activity in the normal and LPS-injured lung. *Am. J. Physiol.* 292: L748–L759.
32. Rabinovici, R., C. G. Yeh, L. M. Hillegass, D. E. Griswold, M. J. DiMartino, J. Vernick, K. L. Fong, and G. Feuerstein. 1992. Role of complement in endotoxin/platelet-activating factor-induced lung injury. *J. Immunol.* 149: 1744–1750.
33. Pittet, J. F., R. C. Mackersie, T. R. Martin, and M. A. Matthay. 1997. Biological markers of acute lung injury: prognostic and pathogenetic significance. *Am. J. Respir. Crit. Care Med.* 155: 1187–1205.
34. Parsons, P. E., A. A. Fowler, T. M. Hyers, and P. M. Henson. 1985. Chemotactic activity in bronchoalveolar lavage fluid from patients with adult respiratory distress syndrome. *Am. Rev. Respir. Dis.* 132: 490–493.
35. Hetland, G., E. Johnson, and U. Aasebo. 1986. Human alveolar macrophages synthesize the functional alternative pathway of complement and active C5 and C9 in vitro. *Scand. J. Immunol.* 24: 603–608.
36. Strunk, R. C., D. M. Eidlen, and R. J. Mason. 1988. Pulmonary alveolar type II epithelial cells synthesize and secrete proteins of the classical and alternative complement pathways. *J. Clin. Invest.* 81: 1419–1426.
37. Watford, W. T., J. R. Wright, C. G. Hester, H. Jiang, and M. M. Frank. 2001. Surfactant protein A regulates complement activation. *J. Immunol.* 167: 6593–6600.
38. Watford, W. T., A. J. Ghio, and J. R. Wright. 2000. Complement-mediated host defense in the lung. *Am. J. Physiol.* 279: L790–L798.

39. Seeger, W., A. Gunther, H. D. Walmrath, F. Grimminger, and H. G. Lasch. 1993. Alveolar surfactant and adult respiratory distress syndrome: pathogenetic role and therapeutic prospects. *Clin. Invest.* 71: 177–190.
40. Carvalho, A. C., S. DeMarinis, C. F. Scott, L. D. Silver, A. H. Schmaier, and R. W. Colman. 1988. Activation of the contact system of plasma proteolysis in the adult respiratory distress syndrome. *J. Lab. Clin. Med.* 112: 270–277.
41. Li, S., S. A. Boackle, V. M. Holers, J. D. Lambris, and C. M. Blatteis. 2005. Complement component C5a is integral to the febrile response of mice to lipopolysaccharide. *Neuroimmunomodulation* 12: 67–80.
42. Barton, P. A., and J. S. Warren. 1993. Complement component C5 modulates the systemic tumor necrosis factor response in murine endotoxic shock. *Infect. Immun.* 61: 1474–1481.
43. Fischer, M. B., A. P. Prodeus, A. Nicholson-Weller, M. Ma, J. Murrow, R. R. Reid, H. B. Warren, A. L. Lage, F. D. Moore, Jr., F. S. Rosen, and M. C. Carroll. 1997. Increased susceptibility to endotoxin shock in complement C3- and C4-deficient mice is corrected by C1 inhibitor replacement. *J. Immunol.* 159: 976–982.
44. Nishihira, J. 2000. Macrophage migration inhibitory factor (MIF): its essential role in the immune system and cell growth. *J. Interferon Cytokine Res.* 20: 751–762.
45. Leng, L., and R. Bucala. 2005. Macrophage migration inhibitory factor. *Crit. Care Med.* 33: S475–S477.
46. Kudrin, A., M. Scott, S. Martin, C. W. Chung, R. Donn, A. McMaster, S. Ellison, D. Ray, K. Ray, and M. Binks. 2006. Human macrophage migration inhibitory factor: a proven immunomodulatory cytokine? *J. Biol. Chem.* 281: 29641–29651.
47. Makita, H., M. Nishimura, K. Miyamoto, T. Nakano, Y. Tanino, J. Hirokawa, J. Nishihira, and Y. Kawakami. 1998. Effect of anti-macrophage migration inhibitory factor antibody on lipopolysaccharide-induced pulmonary neutrophil accumulation. *Am. J. Respir. Crit. Care Med.* 158: 573–579.
48. Roger, T., J. David, M. P. Glauser, and T. Calandra. 2001. MIF regulates innate immune responses through modulation of Toll-like receptor 4. *Nature* 414: 920–924.
49. Rae, S. A., and M. J. Smith. 1981. The stimulation of lysosomal enzyme secretion from human polymorphonuclear leucocytes by leukotriene B4. *J. Pharm. Pharmacol.* 33: 616–617.
50. Lamblin, C., P. Gosset, I. Tillie-Leblond, F. Saulnier, C. H. Marquette, B. Wallaert, and A. B. Tonnel. 1998. Bronchial neutrophilia in patients with noninfectious status asthmaticus. *Am. J. Respir. Crit. Care Med.* 157: 394–402.
51. Suda, N., I. Morita, T. Kuroda, and S. Murota. 1992. Priming effects of leukotriene B4 on endothelial cell injury induced by TPA-activated leukocytes. *Inflammation* 16: 307–314.
52. Sibelius, U., K. Hattar, S. Hoffmann, K. Mayer, U. Grandel, A. Schenkel, W. Seeger, and F. Grimminger. 2002. Distinct pathways of lipopolysaccharide priming of human neutrophil respiratory burst: role of lipid mediator synthesis and sensitivity to interleukin-10. *Crit. Care Med.* 30: 2306–2312.
53. Martin, T. R., B. P. Pistorese, E. Y. Chi, R. B. Goodman, and M. A. Matthay. 1989. Effects of leukotriene B4 in the human lung: recruitment of neutrophils into the alveolar spaces without a change in protein permeability. *J. Clin. Invest.* 84: 1609–1619.
54. Woo, C. H., M. H. Yoo, H. J. You, S. H. Cho, Y. C. Mun, C. M. Seong, and J. H. Kim. 2003. Transepithelial migration of neutrophils in response to leukotriene B_4 is mediated by a reactive oxygen species-extracellular signal-regulated kinase-linked cascade. *J. Immunol.* 170: 6273–6279.
55. Young, R. E., M. B. Voisin, S. Wang, J. Dangerfield, and S. Nourshargh. 2007. Role of neutrophil elastase in LTB4-induced neutrophil transmigration in vivo assessed with a specific inhibitor and neutrophil elastase deficient mice. *Br. J. Pharmacol.* 151: 628–637.

JOURNAL OF APPLIED TOXICOLOGY
J. Appl. Toxicol. 2006; **26**: 126–131
Published online 26 October 2005 in Wiley InterScience (www.interscience.wiley.com). DOI: 10.1002/jat.1115

Attenuation of half sulfur mustard gas-induced acute lung injury in rats

Shannon D. McClintock,[1] Laszlo M. Hoesel,[1] Salil K. Das,[2] Gerd O. Till,[1] Thomas Neff,[1] Robin G. Kunkel,[1] Milton G. Smith[1] and Peter A. Ward[1,*]

[1] The University of Michigan Medical School, Department of Pathology, Ann Arbor, MI 48109, USA
[2] Meharry Medical School, Department of Biochemistry, Nashville, TN, USA
[3] Amaox, Ltd, Paw Paw, MI 49079, USA

Received 12 January 2005; Revised 29 June 2005; Accepted 9 August 2005

ABSTRACT: Airway instillation into rats of 2-chloroethyl ethyl sulfide (CEES), the half molecule of sulfur mustard compound, results in acute lung injury, as measured by the leak of plasma albumin into the lung. Morphologically, early changes in the lung include alveolar hemorrhage and fibrin deposition and the influx of neutrophils. Following lung contact with CEES, progressive accumulation of collagen occurred in the lung, followed by parenchymal collapse. The co-instillation with CEES of liposomes containing pegylated (PEG)-catalase (CAT), PEG-superoxide dismutase (SOD), or the combination, greatly attenuated the development of lung injury. Likewise, the co-instillation of liposomes containing the reducing agents, N-acetylcysteine (NAC), glutathione (GSH), or resveratrol (RES), significantly reduced acute lung injury. The combination of complement depletion and airway instillation of liposomes containing anti-oxidant compounds maximally attenuated CEES-induced lung injury by nearly 80%. Delayed airway instillation of anti-oxidant-containing liposomes (containing NAC or GSH, or the combination) significantly diminished lung injury even when instillation was delayed as long as 1 h after lung exposure to CEES. These data indicate that CEES-induced injury of rat lungs can be substantially diminished by the presence of reducing agents or anti-oxidant enzymes delivered via liposomes. Copyright © 2005 John Wiley & Sons, Ltd.

KEY WORDS: CEES; anti-oxidant liposomes; neutrophils; fibrosis; macrophages

Introduction

As is well known, mustard gas [bis (2-chloroethyl ethyl) sulfide], also known as sulfur mustard (HD), has long been known to be a vesicant in humans and, when inhaled, causes extreme lung damaging reactions (Eisenmenger *et al*., 1991; Khateri *et al*., 2003; Lakshmana Rao *et al*., 1999). In human survivors, progressive lung dysfunction due to pulmonary fibrosis is well documented (Emad and Rezaian, 1999). Not unexpectedly, HD is radiomimetic, teratogenic and mutagenic (Angelov *et al*., 1996; Dube *et al*., 1998). Currently, there is no effective therapy for either the vesicant-inducing properties of HD or for the outcomes that can lead to acute and progressive lung injury and death.

2-Chloroethyl ethyl sulfide (CEES) is less toxic than HD and can be used in the absence of facilities required for HD studies. In rats CEES has been shown to induce acute lung injury in a dose-dependent and time-dependent manner (McClintock *et al*., 2002). CEES-induced acute lung injury is complement- and neutrophil-dependent, suggesting that some of the CEES-induced injury is due to engagement of the inflammatory response in lung in an unknown manner (McClintock *et al*., 2002). Furthermore, lung injury is attenuated after intravenous treatment with the anti-oxidant, N-acetylcysteine (NAC), or airway delivery of anti-oxidants or anti-oxidant enzymes (McClintock *et al*., 2002). These data have suggested that CEES compromises the redox potential in the lung, putting it at risk of oxidant-mediated injury.

Liposomal delivery of drugs or chemical compounds is a way to achieve high tissue levels of a desired compound (Fan *et al*., 2000; Freeman *et al*., 1985; Suntres and Shek, 1996). In the lung, airway delivery of liposomes results in macrophage uptake of liposomes by a phagocytic pathway (Gonzalez-Rothi *et al*., 1991; Shephard *et al*., 1981; Sone *et al*., 1980). As far as is known, liposomes are not internalized by any other lung cells. The current studies demonstrated that liposomes containing anti-oxidants or anti-oxidant enzymes cause a reduction in acute lung injury in rats following airway delivery of CEES. Furthermore, delivery of such liposomes, when delayed 1 h after CEES administration, still provides significant attenuation of acute lung injury.

* Correspondence to: Dr Peter A. Ward, The University of Michigan Medical School, Department of Pathology, 1301 Catherine Rd, Ann Arbor, MI 48109, USA.
E-mail: pward@umich.edu
Contract/grant sponsor: USAMRMC DAMD; Contract/grant number: 17-03-2-0054.

These findings may have important therapeutic implications for HD-induced acute lung injury in humans.

Materials and Methods

Chemicals

Except where noted, all chemicals and reagents were purchased from the Sigma Chemical Co. (St Louis, MO).

Animal Model

Adult male (275–325 g) specific pathogen-free Long-Evans rats (Harlan Co., Indianapolis, IN) were used in these studies. Intraperitoneal ketamine (100 mg kg^{-1} body weight) (Fort Dodge Animal Health, Fort Dodge, IA) was used for anesthesia and intraperitoneal xylazine (13 mg kg^{-1} body weight) (Bayer Corp. Shawnee Mission, KS) was used for sedation when required (delayed time point liposome administration). The experimental procedure for CEES-induced lung injury in rats has been described previously (McClintock *et al*., 2002). Briefly, after induction of anesthesia, ^{125}I-labeled bovine serum albumin (^{125}I-BSA, 0.5 μCi per rat) was injected intravenously as a quantitative marker for vascular leakage. The trachea was then surgically exposed and a slightly curved P50 catheter was inserted into the trachea past the bifurcation so as to facilitate a unilateral, left-lung injury. A small volume of CEES (2 μl per rat; about 6 mg kg^{-1}) was solubilized in ethanol (58 μl per rat) and then added to a syringe containing Dulbecco's phosphate buffered saline (DPBS) (340 μl per rat). This solution was injected via the intratracheal catheter, into the left lung main stem bronchus. Studies, not requiring the usage of a radiolabeled marker, proceeded identically substituting DPBS for the radioactive injection. For all studies, except the time response experiment, animals were killed 4 h later, the pulmonary arterial circulation was flushed with 10 ml of cold DPBS, the lungs were surgically dissected, placed in counting vessels, and the amount of radioactivity (^{125}I-labeled BSA) determined by gamma counting. For calculations of the permeability index, the amount of radioactivity (^{125}I-labeled BSA) remaining in the lungs in which the vasculature was perfused with saline was divided by the amount of radioactivity present in 1.0 ml of blood obtained from the inferior vena cava at the time of killing as described elsewhere (McClintock *et al*., 2002). ^{125}I-BSA present in the lung after thorough flushing of the vasculature is a quantitative measure of the degree of vascular endothelial and alveolar epithelial damage, in which much of the ^{125}I-BSA can be lavaged from the distal airway compartment, indicating the loss of the vascular and epithelial barriers (Johnson and Ward, 1974).

All animal experiments were in accordance with the standards in The Guide for the Care and Use of Laboratory Animals, and were supervised by veterinarians from the Unit for Laboratory and Animal Care of the University of Michigan Medical School.

Complement Depletion

Cobra venom factor (CVF) was purified from crude, lyophilized cobra venom (*Naja atra*) by ion exchange chromatography (Ballow and Cochrane, 1969). Complement depletion of experimental animals was achieved by intraperitoneal injections of 25 units of CVF per rat at time zero and 24 h later, resulting in undetectable levels of serum hemolytic complement activity as confirmed by CH50 assay (Mayer, 1961). Experiments were performed 24 h after the second CVF injection.

Liposome Preparation

Dipalmitoylphosphatidylcholine (DPPC, Avanti Polar Lipids) was dissolved 20 mg ml^{-1} in a 2 : 1 v/v chloroform/methanol solution. When α-tocopherol (αT) was also included in the liposomes, it was added just after the chloroform/methanol solvent to provide a 7 : 3 molar ratio (DPCC : α-T) after first being carefully dissolved in a small volume of ethanol. The DPPC or (DPPC : α-T) solution was then dried under a thin stream of nitrogen in a round bottom flask to form a thin lipid film on the walls of the tube. Once the film had been dried, the tube was then placed on a vacuum for at least 1 h to further dry and remove any excess organic compounds from the lipid film.

The compounds being encapsulated in the liposomes were exclusively prepared in Dulbecco's phosphate buffered saline (DPBS), pH adjusted to 7.4 and then added to the lipid film. The tube was then vortexed to free the lipid film from the walls of the tube, and then placed in a heated water bath (41 °C). When sizing the liposomes, it is necessary to keep them at a temperature above their transition phase. The transition phase temperature for DPPC is 41 °C. Vortexing the liposomes once they are above the transition phase temperature results in large multilamellar vesicles. To reduce the size of the vesicles and to produce uniform small unilamellar vesicles, the lipid suspension was then passed ten times through polycarbonate membrane filters in a Liposofast Basic mini extruder available from Avestin, Inc. (Ottawa, Ontario). The resulting liposomes were uniform in size measuring 100 nm in diameter. According to the manufacturer, the use of an extruder is an efficient method for producing liposomes that are of relatively uniform size. Liposomes were checked via light microscopy for uniformity and size. Liposomes were injected intratracheally in a volume

of 100 µl per rat through the same catheter setup used for CEES instillation at the time point designated by each individual experimental protocol.

Morphological Assessment of Lung Injury

In order morphologically to assess lung injury, lungs were fixed by intratracheal instillation of 10 ml buffered (pH 7.2) formalin (10%) at the indicated time points following airway instillation of CEES. Lung sections were then obtained for histological examination by staining with hematoxylin and eosin. In addition, lung sections were stained with trichrome in order to assess the deposition of fibrin and collagen (Luna, 1968).

Statistical Analysis

The results are presented as mean ± SEM in the text and figures. Groups ($n \geq 5$) were subjected to one-way analysis of variance and when significance was found, Student's *t*-test with the Bonferroni correction for multiple comparisons was applied. A value of $P < 0.05$ was considered significant.

Results

Histopathologic Features of Lung Response to CEES

Following airway instillation of CEES into rat lungs, tissues were obtained at 0, 6, 12 and 24 h as well 3 and 6 days and 6 weeks after exposure to CEES. Lung sections were stained with trichrome stain to evaluate lung deposition of fibrin and collagen. Composite results are shown in Fig. 1 (frames A–I). At time 0, trichrome stains revealed the usual perivascular and septal evidence of collagen (frames A, B). As early as 6 h, increased evidence of trichrome stained deposition in alveolar walls was likely related to fibrin deposition (frame C). By 24 h after lung instillation of CEES, dense interstitial and intra-alveolar accumulations of trichrome positive (blue dye) were evident throughout the affected lungs, suggestive of increased deposition of fibrin and collagen fibers (frame D). Intra-alveolar hemorrhage, edema and intra-alveolar accumulation of macrophages and mononuclear cells were found at 24 h (frame E). By 3 days, dense interstitial deposits of fibrin and collagen occurred (frame F). By day 6, extensive confluent collagen deposits were found in the lung, together with a collapse of alveolar

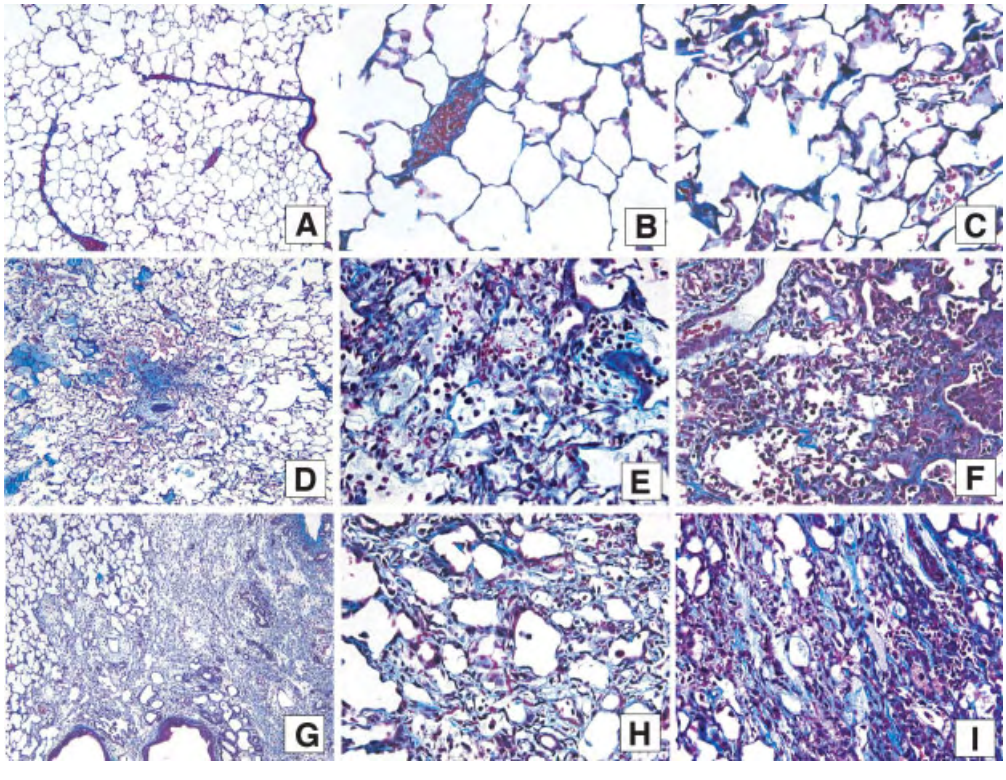

Figure 1. Tissue sections of lungs with trichrome stain. Lungs were obtained after airway instillation of CEES at time 0 (A, B, 10× and 40×); 6 h (C, 40×); 24 h (D, E, 10× and 40×); 3 days (F, 10×), 6 days (G, 10× and H, 40×); and 3 weeks (I, 40×). All tissue sections were reacted with trichrome stain

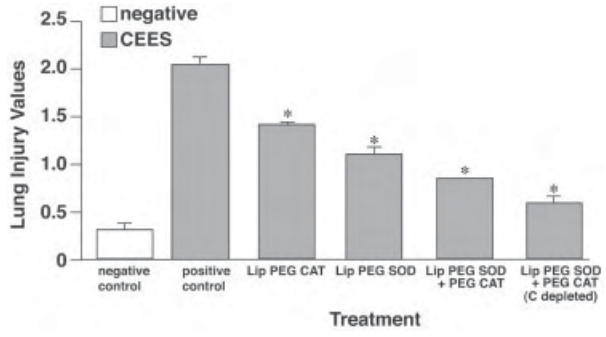

Figure 2. Attenuative effects of liposomes loaded with anti-oxidant enzymes. Rats received either saline followed by unloaded liposomes (negative control), CEES followed by airway delivery of unloaded liposomes (positive control), or CEES with liposomes containing either pegylated (PEG)-CAT or PEG-SOD, individually or the combination, or the combination of liposomes in complement depleted animals induced by the earlier intraperitoneal injection of purified cobra venom factor. Liposomes were administered immediately after CEES instillation. For each bar $n \geq 6$. Lung injury values are represented by the leak of ^{125}I-albumin from the vascular compartment into the airway compartment 4 h after airway delivery of CEES (see text). * Represents P values of <0.05 when compared with the positive control group

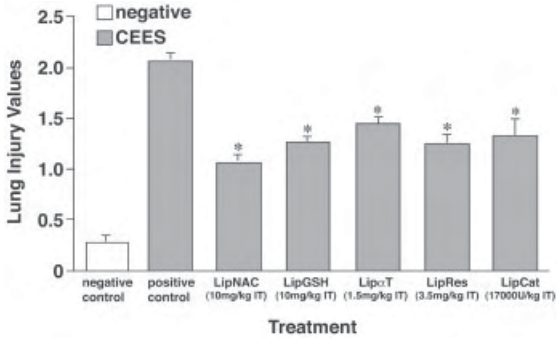

Figure 3. Attenuative effects of liposomes loaded with reducing agents in CEES lung injury. The positive and negative controls are similar to those described in Fig. 1. When used, liposomes were injected intratracheally immediately after the airway instillation of CEES. Lung injury was determined by the permeability index. αT, α-tocopherol

structures and the appearance of honeycombing (frames G, H). By week 3, little recognizable lung structure remained in the face of dense collagen deposits and parenchymal collapse, together with numerous interstitial macrophages and mononuclear cells (frame I).

Attenuation of CEES-Induced Acute Lung Injury by Anti-Oxidant Enzymes in Liposomes

As shown in Fig. 2, the airway instillation of CEES together with unloaded liposomes resulted 4 h later in approximately a 10-fold increase in lung injury, as defined by the leakage of ^{125}I-albumin from blood into the lung. When instilled into the lung immediately after CEES, polyethyleneglycol (PEG)-linked catalase-containing liposomes (LIP-PEG-CAT) attenuated injury by 40%. Liposomes containing PEG-superoxide dismutase (PEG-SOD) diminished injury by 57%. The combination of PEG-SOD and PEG-CAT in liposomes further reduced injury by 71%. With the combination of PEG-SOD and PEG-CAT liposomes given to complement-depleted animals, the injury was reduced by 86%. These data indicate that anti-oxidant enzymes have powerful attenuative effects on CEES-induced acute lung injury. Since, as described above, airway delivery of liposomes results in their phagocytosis by lung macrophages, it seems likely that the attenuative effects of liposomes containing anti-oxidant enzymes are due to the bolstering of anti-oxidant defenses in lung macrophages.

Attenuative Effects of Liposomes Containing Reducing Agents

In an additional set of experiments (shown in Fig. 3), there was approximately a 10-fold increase in leakage of albumin from the circulation into the lungs of animals receiving airway instillation of CEES 4 h earlier together with unloaded liposomes. When liposomes containing NAC (Lip-NAC) were instilled immediately after CEES, injury was attenuated by 60%. Liposomes containing glutathione (GSH) led to a 48% reduction in lung injury. Liposomes containing α-tocopherol (αT) reduced injury by 37%. Liposomes containing the reducing agent present in red wine, resveratrol (RES), reduced injury by 48%, while liposomes containing PEG-CAT reduced injury by 44%. These data indicate that reducing agents presented in liposomes have significantly attenuative effects against CEES-induced acute lung injury. The data also indicate that the non-derivatized form of catalase (CAT) also has attenuative effects when given within liposomes.

Additive Effects of Complement Depletion and Liposomes Containing Reducing Agents

Previous studies in our laboratory have shown that complement depletion resulted in a 43% reduction of lung injury (McClintock *et al*., 2002). As shown in Fig. 4, approximately a 10-fold increase in the leakage of ^{125}I-albumin into the lungs occurred following instillation of CEES together with unloaded liposomes. When the animals were complement (C) depleted, the instillation

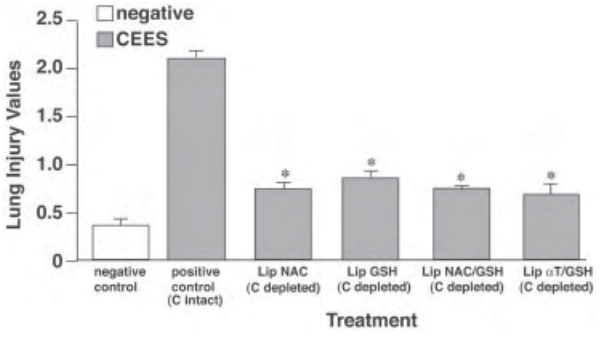

Figure 4. Enhanced effects of anti-oxidant containing liposomes in complement depleted rats. The negative and positive control groups are similar to those described in Fig. 1. Complement depletion was induced in four groups of animals by the prior intraperitoneal injection of purified cobra venom factor (CVF). Liposomes containing the various anti-oxidant compounds were given immediately after airway instillation of CEES. For each group, $n \geq 6$

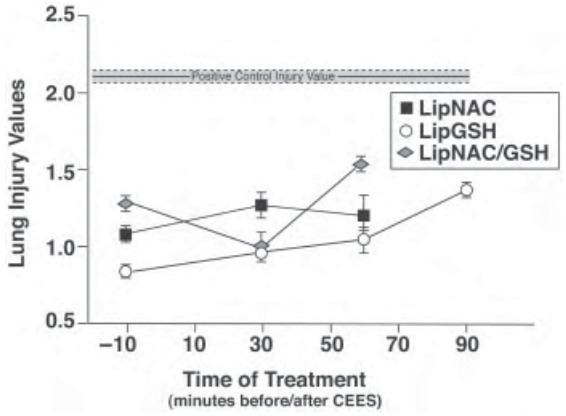

Figure 5. Attenuative effects of anti-oxidant containing liposomes when airway instillation was given at various time points before or after airway delivery of CEES. The dotted line near the top represents the positive control value. Lung injury values (permeability indices) in the negative control are not shown but were <0.5, as described in Figs 1–3

of liposomes containing NAC reduced injury by 79%, those containing GSH reduced injury by 72% in complement-depleted rats, liposomes containing the combination of NAC and GSH reduced injury by 78% in complement-depleted rats. Complement-depleted animals receiving liposomes containing αT together with GSH showed an 82% reduction in lung injury as measured by leakage of albumin from the blood. Thus, the combination of complement depletion and anti-oxidant liposomes seems significantly to attenuate CEES-induced acute lung injury in an additive manner.

Effects of Delayed Lung Instillation of Anti-Oxidant Liposomes

As shown in Fig. 5, in CEES treated animals instillation of liposomes containing reducing agents was done either 10 min before the airway instillation of CEES or at 30, 60 and, in one case, 90 min following the airway instillation of CEES. As shown in Fig. 5, over the course of the first 60 min after instillation of CEES, there were significant attenuative effects of liposomes containing NAC or GSH, or the combination. Under these circumstances, injury was reduced between 55% and 77%, respectively. In the case of liposomes containing the combination of NAC and GSH, even when delivery was delayed until 90 min following instillation of CEES, there was a 55% reduction in the development of acute lung injury. These data indicate that delayed airway administration of anti-oxidant-containing liposomes results in significant reduction of CEES-induced lung injury, even when delivery is delayed by at least an hour following exposure of lungs to CEES.

Discussion

The data described in this report indicate that CEES instillation into the lung produces acute lung injury in a manner that seems related to the loss of the redox balance in the lung, although this has not been demonstrated directly. This conclusion is based on the attenuative effects of reducing agents (NAC, GSH, αT, resveratrol) or anti-oxidant enzymes (SOD, CAT) or various combinations, all presented in liposomes alone or in combination. Since it is well known that liposomes given into the airways are phagocytized by macrophages and internalized (Gonzalez-Rothi *et al*., 1991; Lentsch *et al*., 1999; Shephard *et al*., 1981), the implications from the current studies are that liposomal delivery selectively enhances a reducing environment in lung macrophages, which may be compromised when these cells came into contact with CEES.

The morphological features described in this report are consistent with our earlier report of an accumulation of myeloperoxidase (MPO) in the lung after CEES instillation (McClintock *et al*., 2002). The presence of alveolar hemorrhage and edema implies a severe disruption of vascular and distal airway barrier. These changes are consistent with the concept that CEES induces an acute lung-damaging inflammatory response that is complement-dependent. Beneficial effects of neutrophil and complement depletion as demonstrated previously indicate that the inflammatory response to CEES contributes to the development of lung injury (McClintock *et al*., 2002). Masson's trichrome staining revealed an accumulation of fibrin and/or collagen within the alveolar spaces. Deposition of fibrin reflects a nonspecific reaction to tissue damage. It remains to be shown

that CEES-exposure causes rapid development of interstitial fibrosis, as confirmed biochemically by collagen accumulation. It is hypothesized that epithelial and endothelial damage following CEES-exposure results in disruption of tissues, resulting in collagen accumulation in the interstitial and alveolar spaces. It appears likely that following lung exposure to CEES collagen deposition occurs in a widespread manner, resulting in parenchymal collapse and the honeycombing changes that occur in humans with pulmonary fibrosis. Numerous macrophages and mononuclear cells in areas of collagen deposition in the lung may be associated with the release of mediators (such as TGF_{β}) that promote lung production of collagen.

How CEES functions as a powerful oxidant and what lung cells are targets of CEES is unclear. The extensive leakage of albumin into the lung after exposure to airway administration of CEES infers that the blood–gas barrier has been seriously compromised, causing a functional impairment (or destruction) of both vascular endothelial and alveolar epithelial cells. The subsequent alveolar flooding with plasma components leaking into the distal airway compartment could seriously compromise blood–gas exchange, resulting in hypoxia.

The permeability index after instillation of CEES and empty liposomes was found to be similar to CEES instillation alone (as reported in McClintock *et al*., 2002) implying that empty liposomes do not cause any lung damage by themselves. The fact that the combination of complement depletion and liposomal delivery of GSH or NAC enhances the attenuation when compared with the use of either type of liposomes given to complement-intact rats (Figs 3 and 4) suggests that it may be both the loss of reducing potential in the lung as well as an engagement of complement activation products (e.g. C5a) that leads to intense acute lung injury. Whether complement activation products are directly responsible for lung injury or are functioning to enhance cytokine and chemokine expression remains to be determined. In a recent study it was shown that neutrophil depletion prior to CEES delivery was also capable of reducing CEES-induced lung injury (McClintock *et al*., 2002), suggesting that activated neutrophils enter into the sequence of destructive events after CEES instillation into the lung.

A matter of considerable interest is that delayed delivery (for as long as 60 min) of liposomes containing NAC or GSH, or the combination, into lungs after CEES instillation still provides substantial attenuation from the massive leak of albumin into the lung. It should be noted that there is not much increased albumin leak into the lung in the first 60 min after administration of CEES (McClintock *et al*., 2002). In fact, compared with values at 1 h, the permeability index at 2, 4 and 6 h after instillation of CEES rose 2 fold, 2.9 fold, 7.7 fold and 16.2 fold, respectively, when compared with uninjured lung values. Accordingly, the development of extensive lung injury after airway instillation of CEES requires considerable time for full development of lung injury. This would be in accord with the concept that CEES triggers in the lung an acute inflammatory response, which itself serves to cause lung damage. Since this sequence requires several hours before the large increases in lung permeability (albumin leak into lung) are seen, this may explain why delayed administration of anti-oxidant liposomes can still bring about significant attenuative effects. Understanding more fully the molecular events that lead to CEES-induced intense acute lung injury may provide even better strategies for effective therapeutic intervention after exposure of lung to HD and related compounds.

References

Angelov A, Belchen L, Angelov G. 1996. Experimental sulfur mustard gas poisoning and protective effect of different medicines in rats and rabbits. *Indian Vet. J.* **73**: 546–551.

Ballow M, Cochrane CG. 1969. Two anticomplementary factors in cobra venom: hemolysis of guinea pig erythrocytes by one of them. *J. Immunol.* **103**: 944–952.

Dube SN, Husain K, Sugendran K, Vijayaraghavan R, Somani SM. 1998. Dose response of sulphur mustard: behavioral and toxic signs in rats. *Indian J. Physiol. Pharmacol.* **42**: 389–394.

Eisenmenger W, Drasch G, von Clarmann M, Kretschmer E, Roider G. 1991. Clinical and morphological findings on mustard gas [bis(2-chloroethyl)sulfide] poisoning. *J. Forensic Sci.* **36**: 1688–1698.

Emad A, Rezaian GR. 1999. Immunoglobulins and cellular constituents of the BAL fluid of patients with sulfur mustard gas-induced pulmonary fibrosis. *Chest* **115**: 1346–1351.

Fan J, Shek PN, Suntres ZE, Li YH, Oreopoulos GD, Rotstein OD. 2000. Liposomal antioxidants provide prolonged protection against acute respiratory distress syndrome. *Surgery* **128**: 332–338.

Freeman BA, Turrens JF, Mirza Z, Crapo JD, Young SL. 1985. Modulation of oxidant lung injury by using liposome-entrapped superoxide dismutase and catalase. *Fed. Proc.* **44**: 2591–2595.

Gonzalez-Rothi RJ, Straub L, Cacace JL, Schreier H. 1991. Liposomes and pulmonary alveolar macrophages: functional and morphologic interactions. *Exp. Lung Res.* **17**: 687–705.

Johnson KJ, Ward PA. 1974. Acute immunologic pulmonary alveolitis. *J. Clin. Invest.* **54**: 349–357.

Khateri S, Ghanei M, Keshavarz S, Soroush M, Haines D. 2003. Incidence of lung, eye, and skin lesions as late complications in 34,000 Iranians with wartime exposure to mustard agent. *J. Occup. Environ. Med.* **45**: 1136–1143.

Lakshmana Rao PV, Vijayaraghavan R, Bhaskar AS. 1999. Sulphur mustard induced DNA damage in mice after dermal and inhalation exposure. *Toxicology* **139**: 39–51.

Lentsch AB, Czermak BJ, Bless NM, Van Rooijen N, Ward PA. 1999. Essential role of alveolar macrophages in intrapulmonary activation of NF-kappaB. *Am. J. Respir. Cell Mol. Biol.* **20**: 692–698.

Luna L. 1968. *Manual of Histologic Staining Methods of the AFIP*, 3rd edn. McGraw-Hill: New York.

Mayer MM. 1961. Complement and complement fixation. In *Experimental Immunochemistry*, Kabat EA, Mayer MM (eds). Springfield: Thomas, 133–240.

McClintock SD, Till GO, Smith MG, Ward PA. 2002. Protection from half-mustard-gas-induced acute lung injury in the rat. *J. Appl. Toxicol.* **22**: 257–262.

Shephard EG, Joubert JR, Finkelstein MC, Kuhn SH. 1981. Phagocytosis of liposomes by human alveolar macrophages. *Life Sci.* **29**: 2691–2698.

Sone S, Poste G, Fidler IJ. 1980. Rat alveolar macrophages are susceptible to activation by free and liposome-encapsulated lymphokines. *J. Immunol.* **124**: 2197–2202.

Suntres ZE, Shek PN. 1996. Treatment of LPS-induced tissue injury: role of liposomal antioxidants. *Shock* **6** (Suppl 1): S57–S64.

Catecholamines—Crafty Weapons in the Inflammatory Arsenal of Immune/Inflammatory Cells or Opening Pandora's Box§?

Michael A Flierl,[1] Daniel Rittirsch,[1] Markus Huber-Lang,[2] J Vidya Sarma,[1] and Peter A Ward[1]

[1]Department of Pathology, University of Michigan Medical School, Ann Arbor, MI, USA; [2]Departments of Traumatology, Hand, Plastic, and Reconstructive Surgery, University of Ulm Medical School, 89075 Ulm, Germany

It is well established that catecholamines (CAs), which regulate immune and inflammatory responses, derive from the adrenal medulla and from presynaptic neurons. Recent studies reveal that T cells also can synthesize and release catecholamines which then can regulate T cell function. We have shown recently that macrophages and neutrophils, when stimulated, can generate and release catecholamines *de novo* which, then, in an autocrine/paracrine manner, regulate mediator release from these phagocytes via engagement of adrenergic receptors. Moreover, regulation of catecholamine-generating enzymes as well as degrading enzymes clearly alter the inflammatory response of phagocytes, such as the release of proinflammatory mediators. Accordingly, it appears that phagocytic cells and lymphocytes may represent a major, newly recognized source of catecholamines that regulate inflammatory responses.

Online address: http://www.molmed.org
doi: 10.2119/2007-00105.Flierl

INTRODUCTION

Norepinephrine and epinephrine are key hormones to prepare the body for one of its most primeval reactions: the "fight or flight" response. Catecholamines (CAs) increase the contractility and conduction velocity of cardiomyocytes, leading to increased cardiac output and a rise in blood pressure, which leads to increased vascular tone and resistance. This results in an increased "pre-load" in the right atrium, causing the heart rate to drop due to the Starling-mechanism. Moreover, catecholamines facilitate breathing (bronchi become dilated), and the body's metabolic reserves are mobilized (lipolysis and glycogenolysis) to provide vital energy. Past concepts held the adrenal medulla and the nervous system to be responsible for the production, storage, and release of catecholamines. Recent findings suggest that such assertions need to be re-evaluated. Because the brain and the immune system are some of the body's major adaptive systems (1) and communicate with each other extensively in an attempt to regulate body homeostasis (2), a common "language" is needed to facilitate this crosstalk. Key systems involved in this crosstalk are the hypothalamic-pituitary-adrenal (HPA) axis and the autonomic nervous system, consisting of the adrenergic sympathetic nervous system, the vagus-mediated parasympathetic nervous system, and the enteric nervous system (1-3). Over many decades, an increasing body of evidence has accumulated demonstrating that lymphocytes and phagocytes not only are capable of synthesizing and releasing neuropeptides, but also neurotransmitters and hormones. Furthermore, these cells express adrenergic and cholinergic functions. Thus, coexisting in the nervous as well as in the immune system, these mediators become an universal language of a neuro-endocrine-immune modulating network (4), which enables the nervous, endocrine, and immune system to regulate and fine-tune their functional responses positively or negatively, and thereby allows the body to adapt rapidly to various changes of internal and external environments. We are beginning now to understand that catecholamines are an integral part, and potent modulators, of these neuro-endocrine-immune/inflammatory interactive networks. Through direct communication via sympathetic nerve fibers that innervate lymphoid organs (5), catecholamines can modulate mouse lymphocyte proliferation, differentiation, (6) and cytokine pro-

Footnote §: *Zeus ordered Hephaestus to create the first woman on earth, Pandora. She was bestowed with exceptional beauty and many talents by the Greek Gods. When Prometheus stole fire from heaven, furious Zeus provided Pandora with a jar (Pandora's box) and gave her to Epimetheus, Prometheus' brother. Not under any circumstances was she to open that box, but intrigued by natural inquisitiveness, she did, and all evil contained escaped and spread over the earth. The only thing remaining at the bottom of the box was Hope.*

Address correspondence and reprint requests to *Peter A. Ward, M.D., Department of Pathology, The University of Michigan Medical School, 1301 Catherine Road, Ann Arbor, Michigan 48109-0602. Phone: 734-647-2921, Fax: 734-763-4782; E-mail: pward@umich.edu.*
Submitted October 18, 2007; Accepted for publication December 3, 2007; Epub (www.molmed.org) ahead of print December 5, 2007.

duction of rodent Th cells (7) and human peripheral blood mononuclear cells (PBMCs) (8). These interactions are facilitated by adrenergic receptors expressed on murine lymphocytes (7), rat natural killer (NK) cells (9), rodent macrophages and neutrophils (10,11), and human PBMCs (12). Consequently, we need to understand better the sources, distribution, and roles of catecholamines and their receptors in immunity and inflammation.

IMMUNE CELLS—A NEW, DIFFUSELY EXPRESSED ADRENERGIC ORGAN

The first evidence that catecholamines might originate from sources other than neuronal or endocrine tissue was reported more than ten years ago when the presence of endogenous catecholamines was reported in human lymphocytes (13). Lymphocytes were described not only to contain intracellular levels of catecholamines, but these catecholamines were secreted, negatively regulating lymphocyte proliferation, differentiation, and apoptosis via an autocrine loop in mice and humans (13,14). Shortly thereafter, parallel experiments identified dopamine and norepinephrine in human PBMCs (15,16). In line with these findings, additional studies confirmed the presence of catecholamines in various other cells, including murine bone marrow derived mast cells (17), rodent macrophages and neutrophils (11,18), and in a macrophage cell line (19). Surprisingly high levels of the epinephrine-synthesizing enzyme, phenylethanolamine-*N*-methyl transferase (PNMT), were found in the thymus of young mice, which were comparable to levels in the brainstem (Figure 1A; 20). Interestingly, PNMT levels were found to be two-fold higher in the lymphocyte-harboring cortex of the thymus than in the medulla. Low PNMT activity and PNMT mRNA also could be detected in the marginal zone of the white pulp of the spleen (20), which contains significant amounts of lymphocytes also, suggesting the presence of epinephrine-generating cell population(s) in lymphoid organs. As the morphology of these findings correlate perfectly with the lymphocyte-rich sites of lymphoid organs, it is reasonable to assume that the epinephrine-producing cell population might be lymphocytes. The mere presence of catecholamines in cells, however, left the unanswered question as to whether these catecholamines originated from extracellular sources and simply were taken up actively and stored by lymphocytes and phagocytes or whether such cells might have synthesized catecholamines *de novo*. Affirmation of the presence of the intracellular machinery for catecholamine production in human lymphocytes was obtained indirectly when human hematopoietic cell lines and human T and B cell hybridomas were cultured over a long period of time, with subsequent detection of catecholamines inside the cells. Based on the cell culture protocols, it was highly unlikely that these intracellular catecholamines could have originated from extracellular sources (21).

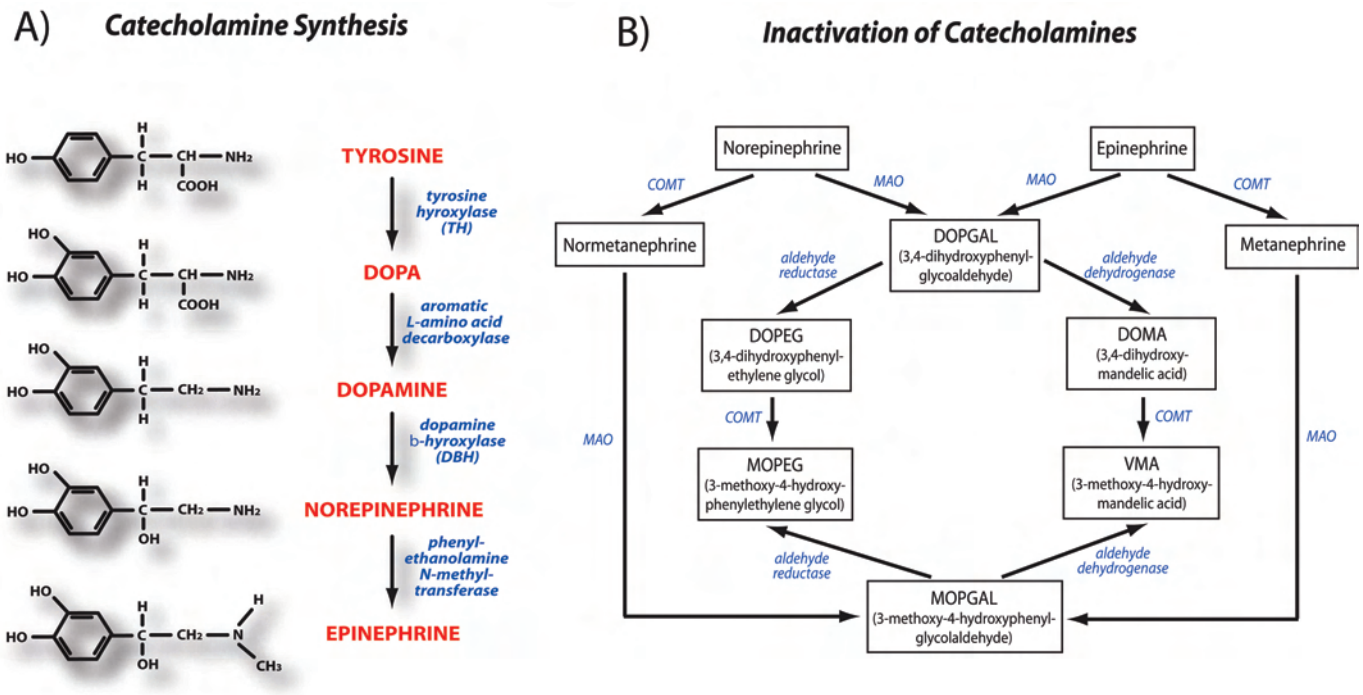

Figure 1. Pathways for synthesis of catecholamines (A) and various metabolizing pathways of catecholamines (B).

Evidence for *de novo* Synthesis, Storage, Release, and Inactivation of Catecholamines by Immune/ Inflammatory Cells

Synthesis. The synthesis of catecholamines relies on two key enzymes: tyrosine-hydroxylase (TH), which is known to be the rate-limiting step in catecholamine synthesis, and dopamine-β-hydroxylase (DBH), which converts dopamine to norepinephrine (3; Figure 1A). The intracellular presence of these hydroxylases and changes in expression of these enzymes strongly implies the ability of cells to synthesize catecholamines *de novo*. Recently, rat phagocytes were found to contain mRNA for both TH and DBH, which clearly were inducible by cell contact with bacterial lipopolysaccharide (LPS) (11). In parallel, rat lymphocytes (22,23) and human PBMCs (24) contain inducible mRNA for these catecholamine-generating enzymes, upregulation of which results in increased levels of dopamine, norepinephrine, and epinephrine when rat lymphocytes were stimulated (22). In contrast, pharmacological inhibition of TH and DBH in rat and human lymphocytes decreased intracellular catecholamine levels in a dose-dependent manner (22,25). Blockade of the conversion of dopamine to norepinephrine (by DBH-inhibition) increased intracellular levels of dopamine and other norepinephrine precursor molecules in human PBMCs (25). Therefore, it is not surprising that the addition of tyrosine and *L*-DOPA to lymphocyte cultures increases catecholamine levels in these cells in a dose-dependent manner (25). Shortly after exposure of human PBMCs to [^{3}H]-*L*-DOPA, [^{3}H]-norepinephrine, and [^{3}H]-dopamine were detected in these cells, suggesting an active uptake mechanism of catecholamine-precursor molecules from the extracellular fluids into human PBMCs (25). Interestingly, these metabolic events are highly selective, because, in contrast to *L*-dopa, *D*-dopa failed to alter catecholamine synthesis in human PBMCs (25). However, human PBMC presents a highly heterogenous group of cells (lymphocytes, monocytes, etc.), making it difficult to draw definitive conclusions about its various cell types.

In summary, these findings suggest that, like neurons and endocrine cells, lymphocytes actively transport tyrosine and *L*-dopa from extracellular sources into the cell to produce catecholamines via catalysis by TH and DBH. Thus, it now is becoming clear that lymphocytes and phagocytes not only possess the ability to produce, store, release, and reuptake catecholamines *de novo*, but that these cells also are capable of exquisitely regulating their catecholamine-synthesis in response to various extracellular stimuli. But, the question remains: how significant is the relative abundance of immune cell-derived catecholamines in comparison to the main catecholamine-producing organ, the adrenal medulla or presynaptic neurons? The adrenomedullary baseline production of epinephrine and norepinephrine in rodents is about 730pg/mL/min and 102pg/mL/min, respectively (26). In a recent study, 10^7 rat neutrophils produced about 100pg/mL and 20pg/mL while 10^7 rat macrophages released nearly 375pg/mL of epinephrine and 50pg/mL of norepinephrine when stimulated with 50ng/mL LPS (11). However, it is important to note that the kinetics of phagocytic catecholamine release is biphasic due to release of stored material versus *de novo* biosynthesis (11). This means that, during inflammatory processes, phagocytic catecholamine levels are linked to a very delicate and dynamic regulation within a local milieu, making it difficult to determine precisely the relative contributions to catecholamines by phagocytes as opposed to the adrenal medulla during inflammation. There do not appear to be definitive publications describing the amount of catecholamines secreted by lymphocytes or presynaptic neurons.

Storage and release of catecholamines. Catecholamines are found throughout adrenergic neurons, but the highest concentrations of these biogenic amines are found in the peripheral presynaptic nerve terminals where these amines are stored in membrane-bound granules and protected from enzymatic destruction (27,28). After depolarizing stimulation of these neurons, rapid secretory release of stored catecholamines occurs. One of the main modes to remove catecholamines that have been released by presynaptic neurons is cellular reuptake of these amines (*see* below). In neurons, this process is known to be inhibited by reserpine. In rodent and human lymphocytes, trace amounts of intracellular catecholamines have been found. In the resting rodent lymphocyte, norepinephrine was the highest content (2.53×10^{-20} M/cell), followed by dopamine (1.29×10^{-20} M/cell) and epinephrine (1.00×10^{-20} M/cell) (22). To date, it seems unclear which role these intracellular baseline catecholamine stores play, because it is only after mitogen stimulation such as phytohaemagglutinin (PHA) (29), concanavalin A (conA) (22), or lipopolysaccharide (LPS) (11), that lymphocyte- or phagocyte-derived catecholamines increase to significant amounts for secretion, affecting cells in an autocrine/ paracrine fashion. Incubation of human PBMCs with reserpine markedly reduced intracellular accumulation of catecholamines, while catecholamine levels in culture supernatant fluids significantly increased (21), suggesting that human PBMCs employ a mechanism similar to neurons, resulting in catecholamine release followed by reuptake. Moreover, studies have revealed that, in accordance with chromaffin cells from the adrenal medulla, secretion of norepinephrine by human lymphocytes depends on acetylcholine and calcium (30,31). Acetylcholine (ACh) facilitated norepinephrine release from peripheral human lymphocytes, as did inflow of calcium into human lymphocytes. Yet, in clear contrast to mechanisms employed by chromaffin cells, blockade of nicotinergic receptors on lymphocytes blocked ACh-induced release of norepinephrine release only by about 50% and blocking of Ca^{2+}-channels attenuated the ACh-induced norepinephrine release by no more than 30% (30,31). Therefore, it is clear that we lack a detailed understand-

ing of the molecular mechanisms involved in catecholamine release by lymphocytes. A recent report identified interferons (IFNs) as molecular regulators of catecholamine synthesis in human PBMCs (29). When human PBMCs were stimulated with phytohaemagglutinin, catecholamine production and release was increased by addition of IFNβ, while the opposite was the case when stimulated PBMCs were exposed to IFNγ which reduced even the mRNA expression of TH. In turn, stimulation with norepinephrine caused mouse Th1 cells to produce two- to four-fold more IFNγ(6), suggesting a negative feedback loop of IFNγ on norepinephrine production. Thus, IFNs seem to emerge as the first physiological compounds that mediate production of catecholamines by human PBMCs. However, PBMCs are a highly heterogenous population of various cell types, making it difficult to draw definitive conclusions from these findings. Thus, achieving a more complete comprehension of the involvement of various ion channels, neurotransmitters, and other mediators triggering catecholamine-release clearly is needed.

Reuptake and degradation of catecholamines by immune/inflammatory cells. Following release of epinephrine and norepinephrine, their activities are terminated by (1) reuptake into nerve terminals, (2) dilution into extracellular fluids and uptake at extraneuronal sites, and (3) metabolic transformation (inactivation) of these catecholamines (32). Two enzymes are essential in the initial steps of metabolic inactivation (Figure 1B): monoamine oxidase (MAO) and catechol-*O*-methyl transferase (COMT) (33,34). MAO and COMT produce physiologically inactive catecholamine-metabolites, but neither of these enzymes plays an important role in the rapid termination of the physiological actions of secreted catecholamines. Rather, this is achieved by active reuptake into presynaptic nerve terminals (27). Human lymphocytes also have been shown to express some of these reuptake transporters. Dopamine-specific binding sites, as well as a dopamine-selective reuptake system, have been demonstrated on human lymphocyte membranes (35,36). Selective blockade of these monoamine transporters suppressed both the dopamine binding to the specific sites and the uptake of [^{3}H]-dopamine. Dopamine-transporter (DAT) mRNA, DAT immunoreactivity, and vesicular monoamine transporter immunoreactivity have been detected on cell membranes and in vesicle-like structures of human lymphocytes (37,38), suggesting DAT on lymphocytes similar to that on neurons. There is some evidence that, in addition to DATs, human PBMCs also may express a norepinephrine transporter (NAT), which would allow for active uptake of catecholamines (12). Nevertheless, the presence of NAT on immune cells remains debatable and additional confirmation is needed for definitive proof (39,40).

As mentioned above, the physiological actions of released catecholamines are terminated primarily by rapid cellular reuptake. Yet, their final intracellular inactivation still relies on the mitochondria-bound MAO and the cytosolic COMT. Several studies have demonstrated the presence of MAO and COMT in human lymphocytes (34,41). Furthermore, metabolites of dopamine, norepinephrine, and epinephrine have been detected in rat lymphocytes (21). Recently, both mRNA and protein for MAO and COMT were found in rat macrophages and rat neutrophils and could be induced by LPS (11). When MAO was inhibited by pargyline, the content of intracellular dopamine, norepinephrine, and epinephrine levels increased in activated human and rat lymphocytes, while intracellular catecholamine metabolites decreased (12,22). Thus, immune cells seem to possess not only the full cellular machinery for *de novo* synthesis, release, and inactivation of catecholamines, but also are capable of intracellular catecholamine-inactivation by MAO and COMT, utilizing the same classical metabolic pathway described in nervous and endocrine systems.

Modulation of Immune/Inflammatory Cell Functions by Catecholamines

Endogenous catecholamines as modulators of immune/inflammatory cells. There is a large body of evidence indicating that, in addition to being crucial neurotransmitters and hormones, catecholamines are important immunomodulators during health and disease (3,42-45; Figure 2). Surprisingly, first reports of the immunomodulating functions of catecholamines were published as early as 1904, describing a robust leukocytosis following subcutaneous administration of epinephrine (46). However, it was not until the mid 1990s that it was reported that lymphocyte-derived catecholamines modulate lymphocyte functions in an autocrine and paracrine manner, providing these cells with a potent tool to fine tune their actions and crosstalk with nearby cells (13). Because the expression of TH and DBH mRNA has been found to be inducible by various stimuli when compared with non-stimulated lymphocytes, it seems likely that the catecholamine synthesis in lymphocytes and phagocytes depends on the functional state of these cells, and that there are diverse cell triggers (11,19,22,23). These auto-regulatory interactions between endogenous catecholamines and immune/inflammatory cells can alter a wide array of cell functions, in part through adrenoceptors or dopaminergic receptors expressed on these cells (10,11,47,48) (*see* below). For instance, it has been observed that the neurotransmitter dopamine, at physiological concentrations, inhibits the proliferation (by downregulating tyrosine kinases) (49-51) and the cytotoxicity of human $CD4^+$ and $CD8^+$ T cells in vitro by acting through the D1/D5, D2, and D3 receptors, making dopamine an important regulator of human T cell functions (52,53). Moreover, exposure of human PBMCs to norepinephrine triggered a very distinct profile of mRNA expression and cytokine production in individual lymphocyte populations, augmenting Th1 (IL-2) and Th2 (IL-4, IL-5, IL-13) type cytokine production, while expression of MIP-1α and

MCP-1 mRNA remained unaffected (8). Similar results were obtained when cells were exposed to dopamine. Thus, it seems likely that catecholamines very selectively activate different lymphocyte subpopulations, leading to a pattern of very distinct expression of inflammatory mediators. It also was demonstrated that catecholamines activate resting T cells by stimulating the release of pro- and anti-inflammatory mediators and alter the expression of surface integrins.

Regulation of immune cell-derived catecholamines. Immune cells seem to regulate their activity and the function of surrounding cells via endogenous catecholamines by two different mechanisms: (a) released catecholamines act in an autocrine/paracrine feedback fashion and (b) catecholamines produced by the adrenal medulla directly activate and modulate intracellular functions of immune/inflammatory cells.

Receptor-mediated autocrine/paracrine mechanisms. It is well established now that immune/inflammatory cells express multiple receptors for catecholamines. Numerous types of adrenergic receptors have been identified on human and rodent PBMCs, macrophages, neutrophils, and lymphocytes (10,11,48,54,55). Dopamine receptor subtypes also have been described on these cells (50,56,57). Adrenoceptors are G-protein coupled, seven-transmembrane spanning receptors (58). Upon interaction with their ligand, intracellular second messengers such as cyclic AMP, calcium ions, diacylglycerol, and inositol 1,4,5-triphosphate become activated and/or inhibited. Therefore, secreted endogenous catecholamines are able to activate the releasing cell itself as well as nearby cells in an autocrine/paracrine manner, stimulating cellular adrenergic/dopaminergic receptors, activating intracellular second messengers, and ultimately regulating cell functions (18,59). Rodent phagocytes have been demonstrated to regulate their release of inflammatory mediators via autocrine/paracrine interactions of endogenous catecholamines with adrenergic receptors expressed on their cell surfaces (10,11,18). Blockade of α- and β-adrenoceptors on human or rodent macrophages, neutrophils, and lymphocytes significantly inhibited the cytokine/chemokine production of these cells (10,11,18,60). These findings make it tempting to speculate that the inflammatory cytokine/chemokine network might be one of the important mediator systems tightly controlled by catecholamines via adrenergic receptors. Yet, it remains to be determined if catecholamine secretion by immune cells is a ubiquitous phenomenon or if it is, rather, an ultimate weapon of immune cells facing overpowering pathogenic insults. The physiological counterpart of the adrenergic system, the cholinergic system, also is known to be an integral part of human macrophage and lymphocyte regulation. Human macrophages are known to control their cytokine release via interactions of acetylcholine with nicotinic acetylcholine receptors expressed on cell membranes (61,62). Stimulation of the α7 subunit of the nicotinic acetylcholine receptors on macrophages greatly inhibited production of tumor necrosis factor (TNF)α, interleukin- (IL-)1β, HMGB1 (and other cytokines), by transducing a cellular signal that inhibits the nuclear activity of NF-κB and activates the transcription factor STAT3 via phosphorylation by JAK2 (63). Human peripheral blood lymphocytes also have been shown to express various cholinergic products including acetylcholine, choline acetyltransferase (ChAT), acetylcholinesterase (AChE), and vesicular acetylcholine transporter (VAChT), as well as M_2-M_5 muscarinic cholinergic receptors (38). As evaluated by confocal microscopy, acetylcholine and VAChT were clustered in punctiform intracellular areas (which most likely correspond to cytoplasmic storage vesicles), while ChAT and AChE were spread diffusely throughout the cytoplasm. As expected, muscarinic receptors were localized in the cell membranes (38). To date, however, it is not clear how these lymphocytic cholinergic markers may contribute to the regulation of immune functions.

Receptor-independent intracellular regulatory mechanisms. Following termination of their actions and cellular reuptake, catecholamines are oxidized intracellularly by the mitochondrion-associated MAO and the ubiquitous cytosolic COMT. During inactivation, catecholamines are degraded into various products including large quantities of reactive oxygen species and other cytotoxic oxidative metabolites, which are known to induce cellular apoptosis in mouse lymphocytes, human PBMCs, and PC12 cell lines (14,64-67). Newly synthesized intracellular catecholamines might not be released immediately but stored inside the cells, which may put cells in jeopardy of receptor-independent and oxidative stress-induced apoptosis (39). This theory is supported by the finding that stress-induced apoptosis can be blocked by the anti-oxidant ascorbic acid (19). Therefore, it seems likely that catecholamines use intracellular oxidative mechanisms to exert autoregulatory functions on immune cells. Even more importantly, a catecholamine-specific transporter has been described on nuclear membranes of lymphocytes, which actively transports catecholamines from the cytoplasm into the cell nucleus where catecholamines interact with nuclear receptors such as steroid receptors (16,68), influence transcription processes via interaction with nuclear factor (NF-)κB, and modulate apoptosis (69) by facilitating the expression of proto-oncogene *Bax* while attenuating *Bcl-2* expression (16,17). It is noteworthy that the mitochondria-associated MAO and the cytosolic COMT fail to enter the nucleus, posing the important but so far unanswered question of how and by what mechanism intranuclear actions of catecholamines are terminated.

IMMUNE CELL-DERIVED CATECHOLAMINES DURING SHOCK AND SEPSIS

Foolishly Unlocking Pandora's Box?

Even though catecholamines are used frequently, sometimes even as last-resort

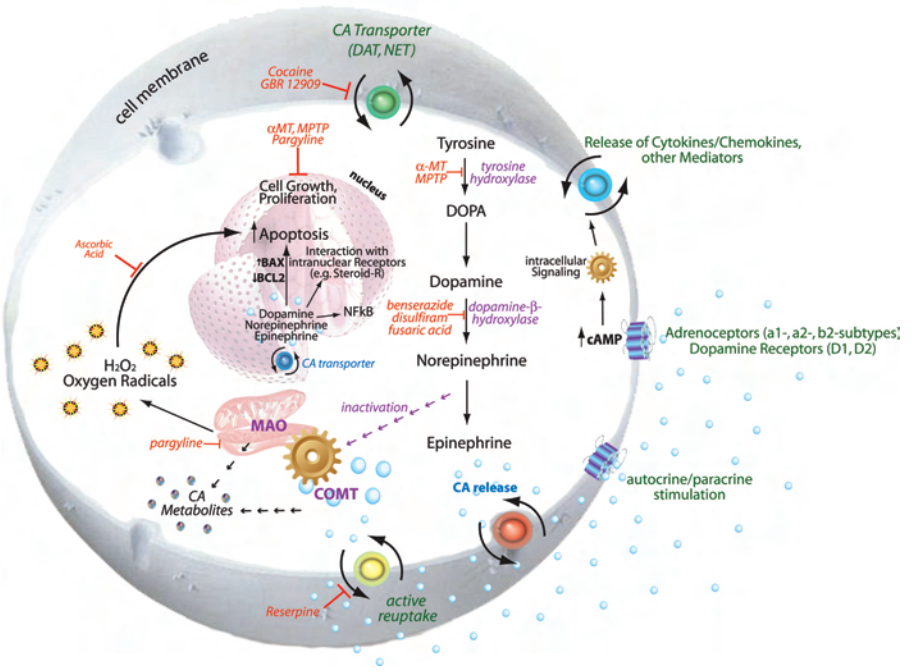

Figure 2. Summary of the various interactions between catecholamines and lymphocytes/phagocytes. Most of these actions have been demonstrated in lymphocytes (*see* text).

drugs to stabilize cardiovascular functions in the critically ill patient, there are several potentially fatal consequences of lymphocyte/phagocyte-derived or exogenously administered catecholamines, in addition to the above described immunomodulatory properties, that need to be taken into account.

Shock. The state of shock leads to a strong activation of the sympathetic nervous system resulting in a massive increase of circulating catecholamines. When endogenous catecholamine-release fails to stabilize cardiovascular parameters, therapeutic catecholamines frequently are administered. Therefore, it is essential to understand the immunomodulatory effects of endogenously released or administered catecholamines in the setting of shock. As expected, hemorrhagic shock induces a robust increase of circulating epinephrine and norepinephrine in an experimental animal model (70). While these increases were paralleled by an elevated number of circulating natural killer (NK) cells and an elevated $CD4/CD8^-$ ratio, levels of circulating $CD8^+$ lymphocytes significantly decreased. Moreover, an increased rate of splenocyte apoptosis was noted 24 h after induction of hemorrhage. All of these effects could be abolished by administration of nonselective or β_1-selective adrenergic blockade without affecting serum cytokine concentrations of TNFα or IL-10 (70). In addition, when noradrenergic neurons were depleted within the central nervous system, cellular cytokine release was affected significantly during hemorrhagic shock (71-73). Thus, hemorrhagic shock leads to vigorous increases in circulating catecholamines, which finally modulate immune cell functions via adrenergic receptors expressed on these cells. Surprisingly, it has been shown that massive, trauma-induced activation of the sympathetic nervous system with subsequent robust release of norepinephrine leads to increased in vivo growth of bacteria within the gastrointestinal system in an experimental animal model, which most likely contributes to the high incidence of systemic bacterial inflammation and sepsis following trauma hemorrhage (74). Most importantly (or shockingly), it was discovered that catecholamines *directly* stimulate bacterial growth. It was reported that catecholamines enhanced growth of several gram-negative bacteria and the production of bacterial growth factor in cultured *E. coli* (75-77). However, to date, it is unclear under precisely what conditions catecholamines inhibit or augment bacterial growth, because norepinephrine and epinephrine failed to demonstrate uniform effects on bacterial growth (78).

Sepsis and septic shock. One of the most challenging subtypes of shock clinically is the septic shock, which is characterized by impaired functions of heart and vessel tone, despite high concentrations of circulating catecholamines (79). Yet, administration of catecholamines often becomes the choice of last resort to maintain blood pressure in patients with septic shock (80). In an experimental model of sepsis, infusion of epinephrine was associated with profound alterations of cellular immune functions analogous to those observed in hemorrhagic shock: all lymphocyte subsets decreased, while the splenocyte apoptosis rate and number of circulating NK cells increased (81). Moreover, splenocyte proliferation and cytokine release was inhibited, whereas apoptosis-rate of splenic lymphocytes was increased (81). In parallel, infusion of dopamine decreased the survival rate of septic mice. Thus, there seems to be a universal pattern for catecholamine effects during sepsis, which might be modulated by cellular adrenoceptors: splenocytes are driven into apoptosis, lymphocyte counts decrease (perhaps due to apoptosis), while NK cell numbers increase. Dopamine is another commonly used drug to prevent renal failure and treat moderate hypotension in the critically ill (82). Dopamine also is an agonist of α- and β-adrenergic receptors, but exerts its effects mainly via

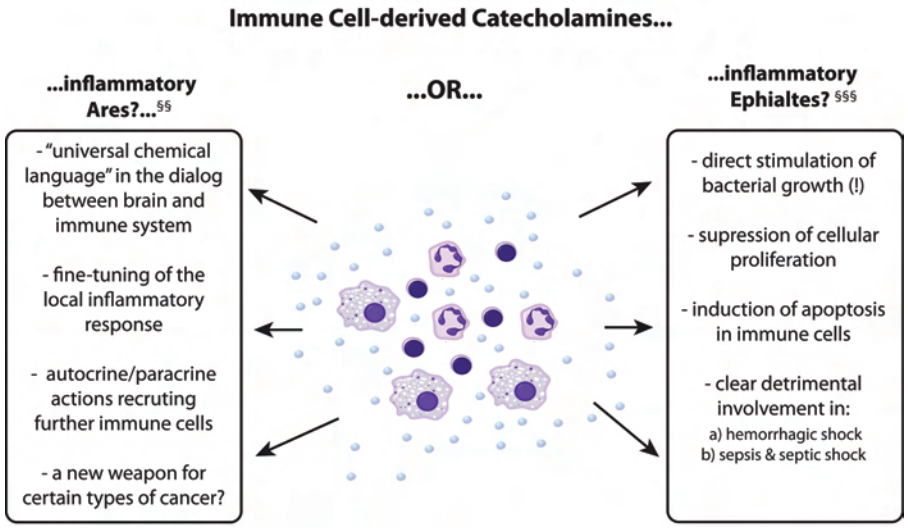

Figure 3. Lymphocyte- and phagocyte-derived catecholamines seem to be a double-edged sword. Some of these bidirectional actions during inflammation are listed.

specific dopaminergic receptors that can be found on a large number of cells including lymphocytes (83). In physiological concentrations, dopamine inhibits the proliferation and cytotoxicity of human $CD4^+$ and $CD8^+$ lymphocytes in vivo and in vitro via the dopamine receptors (52,84-86), paralleling the adverse effects of epinephrine and norepinephrine.

Lately, the gut has also been identified as an alternate source of catecholamines during sepsis in rodents, releasing norepinephrine into the portal vein and thereby altering the functional state of hepatocytes and Kupffer cells, unexpectedly contributing to hepatocellular dysfunction during sepsis (87-90). This mechanism also seems to be mediated via α_2-adrenoceptors (88).

Unfortunately, there are only a few human studies investigating the immunomodulatory effects of catecholamines in septic patients. Yet, evidence now is emerging that the pro- and anti-inflammatory "cytokine-/chemokine storm" occurring in septic patients seems to be modulated, at least in part, by epinephrine. In parallel to various animal studies, immunosuppressive actions of catecholamines seem to be co-regulated by the β-adrenoceptor in humans (91,92). Thus, catecholamines clearly contribute to the severe immunodysregulation occurring during septic shock.

It is important to be aware of these adverse effects of catecholamines in critically ill patients. Although catecholamines are textbook drugs for various settings in patients suffering from severe trauma, hemorrhagic shock, sepsis or septic shock, their administration needs to be evaluated carefully on an individual basis to maximize benefit and minimize adverse effects of catecholamine administration.

Or Skilled Hephaestus[§§§§] Going to Work?

Despite all these potentially harmful actions described above, there are several benefits of endogenous catecholamines (Figure 3). First of all, in addition to neuropeptides, the neuro-endocrine-immune network produces powerful mediators enabling rapid communication and fine-tuning of the nervous, endocrine, and immune systems. A recent report allows a brief foretaste of how exquisite this fine-tuning might in fact be. Blockade of diverse adrenoceptors on rat phagocytes variably inhibited expression of different cytokines and chemokines (11). TNFα production was inhibited completely by blockade of the α_2-adrenoceptor or high-dose blockade of the β_2-adrenoceptor, while remaining completely unaffected by α_1- or β_1-adrenoceptor blockade. In sharp contrast, IL-1β levels were suppressed greatly by pharmacological blockade of either α_1-, α_2-, β_1-, or β_2-adrenoreceptors. IL-6 and CINC-1 production by phagocytes was regulated by either α_2-, β_1-, or β_2-adrenoreceptors, respectively. Because norepinephrine has higher affinity for the α-adrenergic receptors and epinephrine for β-adrenoceptors, it might well be that these two catecholamines display dissimilar effects on phagocytes which could define a very distinct inflammatory mediator pattern best suited for a particular inflammatory setting. A better understanding of these observations might provide us with many new pharmacological targets to dampen inflammation. Finally,

Footnote §§: *Ares, son of Zeus and Hera, is the Greek God of savage war, bloodlust and slaughter.*

Footnote §§§: *Ephialtes guided Xerxes' Persian forces around the allied Greek troops who were blocking the pass of Thermophylae in 480 BC, leading to the last stand of the Leonidas and his 500 Spartans. The malicious treacherousness of this ancient character is still being remembered today, as Ephialtes literally means "nightmare" in Modern-Greek.*

Footnote §§§§: *Hephaestus, son of Zeus and Hera, is the Greek God of technology, blacksmiths, metallurgy and fire. His skilled craftsmanship is thought to have created many of the splendid equipment of the Greek Gods, and most of the power-imbued metalworks that appear in Greek mythology: Hermes' winged helmet and sandals, Aegis' breastplate, Aphrodite's legendary girdle, Achilles' armor, Heracles' bronze clappers, Helios' chariot and Eros' famed bow and arrow.*

recent research reports suggest that catecholamines might be cytotoxic for human neuroblastoma cells (93,94). While specific types of cancer might present an appealing new target for catecholamine-dependent immunomodulation, this needs to be further evaluated.

CONCLUSIONS

Besides the adrenomedullary chromaffin cells and neurons, lymphocytes, and phagocytes represent a third category of catecholamine-producing cells. They are able to synthesize and release endogenous catecholamines *de novo* which can modify various pathological responses, all of which challenges traditional paradigms. The wide distribution of immune cells throughout the body, combined with their ability to migrate to the site of inflammation, underscores the dynamic role of immune/inflammatory cells. Targeting lymphocyte/phagocyte-derived catecholamines will pose an extremely challenging quest for researchers. Because catecholamines are not proteins, usage of neutralizing antibodies seem an unlikely strategy. The fact that immune cells utilize the very same molecular pathways as the adrenal medulla and neurons defies classical immunological approaches such as blocking catecholamine-producing enzymes by antibodies or RNA-silencing to inhibit immune/inflammatory cell-derived catecholamines. Moreover, myriad actions of endogenous catecholamines occur inside the cell and perhaps even in the nucleus, further complicating a selective targeting attempt. However, extending our understanding for extra- and intracellular adrenergic regulation of lymphocytes and phagocytes, its implications and its possibilities might deepen our understanding of the pathogenesis of diverse diseases and ultimately might result in great curative advances.

ACKNOWLEDGMENTS

The authors thank Beverly Schumann and Sue Scott for the preparation of this manuscript. This work was supported by NIH grants GM-29507, GM-61656, and HL-31963, and DOD grant W81XWH-06-2-0044 (P.A.W.) and Deutsche Forschungsgemeinschaft grants DFG HU 823/2-1, DFG HU 823/2-2, and DFG HU 823/2-3 (M.H.-L.).

REFERENCES

1. Sternberg EM. (2006) Neural regulation of innate immunity: a coordinated nonspecific host response to pathogens. *Nat. Rev. Immunol.* 6:318-28.
2. Tracey KJ. (2002) The inflammatory reflex. *Nature*. 420:853-9.
3. Elenkov IJ, Wilder RL, Chrousos GP, Vizi ES. (2000) The sympathetic nerve—an integrative interface between two supersystems: the brain and the immune system. *Pharmacol. Rev.* 52:595-638.
4. Blalock JE. (2005) The immune system as the sixth sense. *J. Intern. Med.* 257:126-38.
5. Straub RH. (2004) Complexity of the bi-directional neuroimmune junction in the spleen. *Trends Pharmacol. Sci.* 25:640-6.
6. Swanson MA, Lee WT, Sanders VM. (2001) IFN-gamma production by Th1 cells generated from naive CD4+ T cells exposed to norepinephrine. *J. Immunol.* 166:232-40.
7. Sanders VM *et al.* (1997) Differential expression of the beta2-adrenergic receptor by Th1 and Th2 clones: implications for cytokine production and B cell help. *J. Immunol.* 158:4200-10.
8. Torres KC *et al.* (2005) Norepinephrine, dopamine and dexamethasone modulate discrete leukocyte subpopulations and cytokine profiles from human PBMC. *J. Neuroimmunol.* 166:144-57.
9. Peng YP, Qiu YH, Jiang JL, Wang JJ. (2004) Effect of catecholamines on IL-2 production and NK cytotoxicity of rats in vitro. *Acta Pharmacol. Sin.* 25:1354-60.
10. Spengler RN, Allen RM, Remick DG, Strieter RM, Kunkel SL. (1990) Stimulation of alpha-adrenergic receptor augments the production of macrophage-derived tumor necrosis factor. *J. Immunol.* 145: 1430-4.
11. Flierl MA *et al.* (2007) Phagocyte-derived catecholamines enhance acute inflammatory injury. *Nature*. 449:721-5.
12. Marino F *et al.* (1999) Endogenous catecholamine synthesis, metabolism storage, and uptake in human peripheral blood mononuclear cells. *Exp. Hematol.* 27:489-95.
13. Bergquist J, Tarkowski A, Ekman R, Ewing A. (1994) Discovery of endogenous catecholamines in lymphocytes and evidence for catecholamine regulation of lymphocyte function via an autocrine loop. *Proc. Natl. Acad. Sci. U. S. A.* 91: 12912-6.
14. Josefsson E, Bergquist J, Ekman R, Tarkowski A. (1996) Catecholamines are synthesized by mouse lymphocytes and regulate function of these cells by induction of apoptosis. *Immunology*. 88:140-6.
15. Bergquist J, Silberring J. (1998) Identification of catecholamines in the immune system by electrospray ionization mass spectrometry. *Rapid Commun. Mass Spectrom.* 12:683-8.
16. Bergquist J, Josefsson E, Tarkowski A, Ekman R, Ewing A. (1997) Measurements of catecholamine-mediated apoptosis of immunocompetent cells by capillary electrophoresis. *Electrophoresis*. 18: 1760-6.
17. Freeman JG *et al.* (2001) Catecholamines in murine bone marrow derived mast cells. *J. Neuroimmunol.* 119:231-8.
18. Spengler RN, Chensue SW, Giacherio DA, Blenk N, Kunkel SL. (1994) Endogenous norepinephrine regulates tumor necrosis factor-alpha production from macrophages in vitro. *J. Immunol.* 152:3024-31.
19. Brown SW *et al.* (2003) Catecholamines in a macrophage cell line. *J. Neuroimmunol.* 135:47-55.
20. Warthan MD *et al.* (2002) Phenylethanolamine N-methyl transferase expression in mouse thymus and spleen. *Brain Behav. Immun.* 16:493-9.
21. Cosentino M *et al.* (2000) HPLC-ED measurement of endogenous catecholamines in human immune cells and hematopoietic cell lines. *Life Sci.* 68:283-95.
22. Qiu YH, Cheng C, Dai L, Peng YP. (2005) Effect of endogenous catecholamines in lymphocytes on lymphocyte function. *J. Neuroimmunol.* 167:45-52.
23. Qiu YH, Peng YP, Jiang JM, Wang JJ. (2004) Expression of tyrosine hydroxylase in lymphocytes and effect of endogenous catecholamines on lymphocyte function. *Neuroimmunomodulation*. 11:75-83.
24. Cosentino M *et al.* (2002) Stimulation with phytohaemagglutinin induces the synthesis of catecholamines in human peripheral blood mononuclear cells: role of protein kinase C and contribution of intracellular calcium. *J. Neuroimmunol.* 125:125-33.
25. Musso NR, Brenci S, Setti M, Indiveri F, Lotti G. (1996) Catecholamine content and in vitro catecholamine synthesis in peripheral human lymphocytes. *J. Clin. Endocrinol. Metab.* 81:3553-7.
26. Chritton SL *et al.* (1997) Adrenomedullary secretion of DOPA, catecholamines, catechol metabolites, and neuropeptides. *J. Neurochem.* 69:2413-20.
27. Molinoff PB, Axelrod J. (1971) Biochemistry of catecholamines. *Annu. Rev. Biochem.* 40:465-500.
28. Shore PA. (1972) Transport and storage of biogenic amines. *Annu. Rev. Pharmacol.* 12:209-26.
29. Cosentino M *et al.* (2005) Interferon-gamma and interferon-beta affect endogenous catecholamines in human peripheral blood mononuclear cells: implications for multiple sclerosis. *J. Neuroimmunol.* 162:112-21.
30. Kilpatrick DL, Slepetis RJ, Corcoran JJ, Kirshner N. (1982) Calcium uptake and catecholamine secretion by cultured bovine adrenal medulla cells. *J. Neurochem.* 38:427-35.
31. Musso NR, Brenci S, Indiveri F, Lotti G. (1998) Acetylcholine-induced, calcium-dependent norepinephrine outflow from peripheral human lymphocytes. *J. Neuroimmunol.* 87:82-7.
32. Axelsson J. (1971) Catecholamine functions. *Annu. Rev. Physiol.* 33:1-30.
33. Zhu BT. (2002) Catechol-O-Methyltransferase (COMT)-mediated methylation metabolism of

endogenous bioactive catechols and modulation by endobiotics and xenobiotics: importance in pathophysiology and pathogenesis. *Curr. Drug Metab.* 3:321-49.
34. Balsa MD, Gomez N, Unzeta M. (1989) Characterization of monoamine oxidase activity present in human granulocytes and lymphocytes. *Biochim. Biophys. Acta.* 992:140-4.
35. Faraj BA, Olkowski ZL, Jackson RT. (1991) Binding of [3H]-dopamine to human lymphocytes: possible relationship to neurotransmitter uptake sites. *Pharmacology.* 42:135-41.
36. Faraj BA., Olkowski ZL, Jackson RT. (1995) A cocaine-sensitive active dopamine transport in human lymphocytes. *Biochem. Pharmacol.* 50:1007-14.
37. Mill J, Asherson P, Browes C, D'Souza U, Craig I. (2002) Expression of the dopamine transporter gene is regulated by the 3' UTR VNTR: Evidence from brain and lymphocytes using quantitative RT-PCR. *Am. J. Med. Genet.* 114:975-9.
38. Amenta F *et al.* (2001) Identification of dopamine plasma membrane and vesicular transporters in human peripheral blood lymphocytes. *J. Neuroimmunol.* 117:133-42.
39. Cosentino M *et al.* (2003) Unravelling dopamine (and catecholamine) physiopharmacology in lymphocytes: open questions. *Trends Immunol.* 24:581-2; author reply 582-3.
40. Gordon J, Barnes NM. (2003) Lymphocytes transport serotonin and dopamine: agony or ecstasy? *Trends Immunol.* 24:438-43.
41. Bidart JM, Motte P, Assicot M, Bohuon C, Bellet D. (1983) Catechol-O-methyltransferase activity and aminergic binding sites distribution in human peripheral blood lymphocyte subpopulations. *Clin. Immunol. Immunopathol.* 26:1-9.
42. Madden KS, Sanders VM, Felten DL. (1995) Catecholamine influences and sympathetic neural modulation of immune responsiveness. *Annu. Rev. Pharmacol. Toxicol.* 35:417-48.
43. Sanders VM, Kohm AP. (2002) Sympathetic nervous system interaction with the immune system. *Int. Rev. Neurobiol.* 52:17-41.
44. Sanders VM, Straub RH. (2002) Norepinephrine, the beta-adrenergic receptor, and immunity. *Brain Behav. Immun.* 16:290-332.
45. Ottaway CA, Husband AJ. (1994) The influence of neuroendocrine pathways on lymphocyte migration. *Immunol. Today.* 15:511-7.
46. Loeper M, Crouzon O. (1904) L'action de l'adrenaline sur le sang. *Arch. Med. Exp. Anat. Pathol.* 16:83-108.
47. Zoukos Y *et al.* (1994) Increased expression of high affinity IL-2 receptors and beta-adrenoceptors on peripheral blood mononuclear cells is associated with clinical and MRI activity in multiple sclerosis. *Brain.* 117(Pt 2):307-15.
48. Rouppe van der Voort C, Kavelaars A., van de Pol M, Heijnen CJ. (2000) Noradrenaline induces phosphorylation of ERK-2 in human peripheral blood mononuclear cells after induction of alpha(1)-adrenergic receptors. *J. Neuroimmunol.* 108:82-91.
49. Ghosh MC *et al.* (2003) Dopamine inhibits cytokine release and expression of tyrosine kinases, Lck and Fyn in activated T cells. *Int. Immunopharmacol.* 3: 1019-26.
50. Levite M *et al.* (2001) Dopamine interacts directly with its D3 and D2 receptors on normal human T cells, and activates beta1 integrin function. *Eur. J. Immunol.* 31:3504-12.
51. Cosentino, M *et al.* (2007) Human CD4+CD25+ regulatory T cells selectively express tyrosine hydroxylase and contain endogenous catecholamines subserving an autocrine/paracrine inhibitory functional loop. *Blood.* 109:632-42.
52. Saha B, Mondal AC, Majumder J, Basu S, Dasgupta PS. (2001) Physiological concentrations of dopamine inhibit the proliferation and cytotoxicity of human CD4+ and CD8+ T cells in vitro: a receptor-mediated mechanism. *Neuroimmunomodulation.* 9:23-33.
53. Kipnis J *et al.* (2004) Dopamine, through the extracellular signal-regulated kinase pathway, downregulates CD4+CD25+ regulatory T-cell activity: implications for neurodegeneration. *J. Neurosci.* 24:6133-43.
54. Van Tits LJ *et al.* (1990) Catecholamines increase lymphocyte beta 2-adrenergic receptors via a beta 2-adrenergic, spleen-dependent process. *Am. J. Physiol.* 258:E191-202.
55. Anstead MI, Hunt TA, Carlson SL, Burki NK. (1998) Variability of peripheral blood lymphocyte beta-2-adrenergic receptor density in humans. *Am. J. Respir. Crit. Care Med.* 157:990-2.
56. Besser MJ, Ganor Y, Levite M. (2005) Dopamine by itself activates either D2, D3 or D1/D5 dopaminergic receptors in normal human T-cells and triggers the selective secretion of either IL-10, TNFalpha or both. *J. Neuroimmunol.* 169:161-71.
57. McKenna F *et al.* (2002) Dopamine receptor expression on human T- and B-lymphocytes, monocytes, neutrophils, eosinophils and NK cells: a flow cytometric study. *J. Neuroimmunol.* 132:34-40.
58. Pierce KL, Premont RT, Lefkowitz RJ. (2002) Seven-transmembrane receptors. *Nat. Rev. Mol. Cell Biol.* 3:639-50.
59. Engler KL, Rudd ML, Ryan JJ, Stewart JK, Fischer-Stenger K. (2005) Autocrine actions of macrophage-derived catecholamines on interleukin-1 beta. *J. Neuroimmunol.* 160:87-91.
60. Starkie RL, Rolland J, Febbraio MA. (2001) Effect of adrenergic blockade on lymphocyte cytokine production at rest and during exercise. *Am. J. Physiol. Cell Physiol.* 281:C1233-40.
61. Borovikova LV *et al.* (2000) Vagus nerve stimulation attenuates the systemic inflammatory response to endotoxin. *Nature.* 405:458-62.
62. Wang H *et al.* (2003) Nicotinic acetylcholine receptor alpha7 subunit is an essential regulator of inflammation. *Nature.* 421:384-8.
63. Tracey KJ. (2007) Physiology and immunology of the cholinergic antiinflammatory pathway. *J. Clin. Invest.* 117:289-96.
64. Cosentino M *et al.* (2004) Dopaminergic modulation of oxidative stress and apoptosis in human peripheral blood lymphocytes: evidence for a D1-like receptor-dependent protective effect. *Free Radic. Biol. Med.* 36:1233-40.
65. Del Rio MJ, Velez-Pardo C. (2002) Monoamine neurotoxins-induced apoptosis in lymphocytes by a common oxidative stress mechanism: involvement of hydrogen peroxide (H(2)O(2)), caspase-3, and nuclear factor kappa-B (NF-kappaB), p53, c-Jun transcription factors. *Biochem. Pharmacol.* 63:677-88.
66. Jones DC, Gunasekar PG, Borowitz JL, Isom GE. (2000) Dopamine-induced apoptosis is mediated by oxidative stress and Is enhanced by cyanide in differentiated PC12 cells. *J. Neurochem.* 74: 2296-304.
67. Burke WJ, Kristal BS, Yu BP, Li SW, Lin TS. (1998) Norepinephrine transmitter metabolite generates free radicals and activates mitochondrial permeability transition: a mechanism for DOPEGAL-induced apoptosis. *Brain Res.* 787:328-32.
68. Buu NT. (1993) Uptake of 1-methyl-4-phenylpyridinium and dopamine in the mouse brain cell nuclei. *J. Neurochem.* 61:1557-60.
69. Bergquist J, Ohlsson B, Tarkowski A. (2000) Nuclear factor-kappa B is involved in the catecholaminergic suppression of immunocompetent cells. *Ann. N. Y. Acad. Sci.* 917:281-9.
70. Oberbeck R *et al.* (2002) Influence of beta-adrenoceptor antagonists on hemorrhage-induced cellular immune suppression. *Shock.* 18:331-5.
71. Cunnick JE, Lysle DT, Kucinski BJ, Rabin BS. (1990) Evidence that shock-induced immune suppression is mediated by adrenal hormones and peripheral beta-adrenergic receptors. *Pharmacol. Biochem. Behav.* 36:645-51.
72. Molina PE. (2001) Noradrenergic inhibition of TNF upregulation in hemorrhagic shock. *Neuroimmunomodulation.* 9:125-33.
73. Molina PE, Abumrad NN. (1999) Central sympathetic modulation of tissue cytokine response to hemorrhage. *Neuroimmunomodulation.* 6:193-200.
74. Lyte M, Bailey MT. (1997) Neuroendocrine-bacterial interactions in a neurotoxin-induced model of trauma. *J. Surg. Res.* 70:195-201.
75. Freestone PP *et al.* (2002) Growth stimulation of intestinal commensal Escherichia coli by catecholamines: a possible contributory factor in trauma-induced sepsis. *Shock.* 18:465-70.
76. Lyte M., Frank CD, Green BT. (1996) Production of an autoinducer of growth by norepinephrine cultured Escherichia coli O157:H7. *FEMS Microbiol. Lett.* 139:155-9.
77. Kinney KS, Austin CE, Morton DS, Sonnenfeld G. (2000) Norepinephrine as a growth stimulating factor in bacteria-mechanistic studies. *Life Sci.* 67: 3075-85.
78. Belay T, Sonnenfeld G. (2002) Differential effects of catecholamines on in vitro growth of pathogenic bacteria. *Life Sci.* 71:447-56.
79. Annane D *et al.* (1999) Inappropriate sympathetic activation at onset of septic shock: a spectral analysis approach. *Am J Respir Crit Care Med.* 160: 458-65.

80. Annane D, Bellissant E, Cavaillon JM. (2005) Septic shock. *Lancet*. 365:63-78.
81. Oberbeck R *et al*. (2004) Adrenergic modulation of survival and cellular immune functions during polymicrobial sepsis. *Neuroimmunomodulation*. 11:214-23.
82. Oberbeck R. (2006) Catecholamines: physiological immunomodulators during health and illness. *Curr. Med. Chem*. 13:1979-89.
83. Basu S, Dasgupta PS. (2000) Dopamine, a neurotransmitter, influences the immune system. *J. Neuroimmunol*. 102:113-24.
84. Tsao CW, Lin YS, Cheng JT. (1997) Effect of dopamine on immune cell proliferation in mice. *Life Sci*. 61:PL 361-71.
85. Beck G *et al*. (2004) Clinical review: immunomodulatory effects of dopamine in general inflammation. *Crit. Care*. 8:485-91.
86. McCorkle FM, Taylor RL Jr. (1994) Continuous administration of dopamine alters cellular immunity in chickens. *Comp. Biochem. Physiol. C. Pharmacol. Toxicol. Endocrinol*. 109:289-93.
87. Yang S, Koo DJ, Zhou M, Chaudry IH, Wang P. (2000) Gut-derived norepinephrine plays a critical role in producing hepatocellular dysfunction during early sepsis. *Am. J. Physiol. Gastrointest. Liver Physiol*. 279:G1274-81.
88. Yang S, Zhou M, Chaudry IH, Wang P. (2001) Norepinephrine-induced hepatocellular dysfunction in early sepsis is mediated by activation of alpha2-adrenoceptors. *Am. J. Physiol. Gastrointest. Liver Physiol*. 281:G1014-21.
89. Zhou M, Das P, Simms HH, Wang P. (2005) Gut-derived norepinephrine plays an important role in up-regulating IL-1beta and IL-10. *Biochim. Biophys. Acta*. 1740:446-52.
90. Zhou M, Hank Simms H, Wang P. (2004) Increased gut-derived norepinephrine release in sepsis: up-regulation of intestinal tyrosine hydroxylase. *Biochim. Biophys. Acta*. 1689:212-8.
91. Bergmann M *et al*. (1999) Attenuation of catecholamine-induced immunosuppression in whole blood from patients with sepsis. *Shock*. 12:421-7.
92. Bergmann M, Sautner T. (2002) Immunomodulatory effects of vasoactive catecholamines. *Wien. Klin. Wochenschr*. 114:752-61.
93. Chan AS, Ng LW, Poon LS, Chan WW, Wong YH. (2007) Dopaminergic and adrenergic toxicities on SK-N-MC human neuroblastoma cells are mediated through G protein signaling and oxidative stress. *Apoptosis*. 12:167-79.
94. Moussa CE, Tomita Y, Sidhu A. (2006) Dopamine D1 receptor-mediated toxicity in human SK-N-MC neuroblastoma cells. *Neurochem. Int*. 48:226-34.

animal models of SCA may also be useful for a better understanding of what should or should not be done for resuscitation. Since left ventricular function before VF is a major determinant for successful resuscitation, a model of VF in chronic myocardial infarction with no acute ischemia and a model of VF associated with nonischemic induced heart failure may also be useful (6).

There is no doubt that acute coronary artery occlusion is frequent in SCA, and it may be found in 50% of patients (7). This may affect up to 85% to 90% of patients with both ST segment elevation and chest pain before SCA, but coronary occlusion is poorly predicted in other settings by clinical and electrocardiographic findings. One further question is whether a coronary angiography should be systematically performed early after SCA. Immediate coronary angiography can be followed if necessary by coronary angioplasty. It seems reasonable to perform coronary angiography in patients with a sufficiently high hope of survival. A score using several simple items may help to identify these patients: those with age <75, those with early initial intervention (in the first 10 mins), those with ventricular tachyarrhythmia rather than asystole on initial surface electrocardiogram, and those with no need to use epinephrine (8, 9). Those in whom shock will develop in the first 48 hrs should also undergo coronary angiography. In these latter patients, shock or refibrillation after resuscitation is possibly still related to ischemia rather than to myocardial damage, hypotension, or epinephrine use, and revascularization may bring some benefit.

Treatment of ventricular arrhythmias during acute myocardial infarction has been a controversial topic for several decades. Primary VF accounts for the majority of early deaths in myocardial infarction. VF is a less common cause of death in the hospital with the early use of revascularization strategies in conjunction with β-blockers. Secondary VF occurring in the setting of congestive heart failure or cardiogenic shock can also contribute to death from myocardial infarction. We now hope that the use of targeted models of cardiac arrest will clarify several unsolved issues, improve our strategies of acute management, and decrease the midterm mortality for more patients with SCA.

Laurent Fauchier, MD, PhD
Axel de Labriolle, MD
Services de Cardiologie
Pôle Thorax
Cardiovasculaire
Hémostase
Centre Hospitalier
Universitaire Trousseau
Tours, France

REFERENCES

1. Cobb LA, Fahrenbruch CE, Olsufka M, et al: Changing incidence of out-of hospital ventricular fibrillation. *JAMA* 2002; 288: 3008–3013
2. ECC Committee, Subcommittees and Task Forces of the American Heart Association. 2005 American Heart Association Guidelines for Cardiopulmonary Resuscitation and Emergency Cardiovascular Care. *Circulation* 2005; 112(24 Suppl):IV1–IV203
3. White RD: Waveforms for defibrillation and cardioversion: Recent experimental and clinical studies. *Curr Opin Crit Care* 2004; 10: 202–207
4. Niemann JT, Rosborough JP, Youngquist S, et al: Is all ventricular fibrillation the same? A comparison of ischemically induced and electrically induced ventricular fibrillation in a porcine cardiac arrest and resuscitation model. *Crit Care Med* 2007; 35:1356–1361
5. Zipes DP, Wellens HJ: Sudden cardiac death. *Circulation* 1998; 98:2334–2351
6. Mehta D, Curwin J, Gomes A, et al: Sudden death in coronary artery disease. Acute ischemia versus myocardial substrate. *Circulation* 1997; 96:3215–3233
7. Spaulding CM, Joly L, Rosenberg A, et al: Immediate coronary angiography in survivors of out-of-hospital cardiac arrest. *N Engl J Med* 1997; 336:1629–1633
8. Weaver WD, Hill D, Fahrenbruch CE, et al: Use of the automatic external defibrillator in the management of out-of-hospital cardiac arrest. *N Engl J Med* 1988; 319:661–666
9. Morrison LJ, Visentin LM, Kiss A, et al: Validation of a rule for termination of resuscitation in out-of-hospital cardiac arrest. *N Engl J Med* 2006; 355:478–487

New therapeutic approaches for influenza A H5N1 infected humans*

The article by Dr. Arabi and colleagues (1) in this issue of *Critical Care Medicine* is based on a literature review of papers published in English and featuring humans with avian influenza A (H5N1) virus pulmonary infection. The potential use of a neuraminidase inhibitor to impede viral entry into cells is suggested. Such an approach is based on the known requirements of avian and human influenza A viruses for binding to cell surfaces via sialic acid residues covalently linked to galactose. These structures are found on epithelial cells in respiratory bronchioles and on alveolar epithelial cells (2). It is now fairly clear that, like the severe acute respiratory syndrome coronavirus, the H5N1 influenza A RNA virus proliferates chiefly in the lung for a period of several weeks, although extrapulmonary viral replication may also occur in the intestine and perhaps in other organs (3). The results of viral replication in the lung are alveolar epithelial cell damage and/or destruction, resulting in massive intra-alveolar edema and hemorrhage together with intense fibrin deposition along alveolar walls, all of which lead to serious problems with gas exchange between the vascular and alveolar compartments and severe hypoxemia (4). Collectively, these morphologic changes have been described as diffuse alveolar damage and the adult respiratory distress syndrome. To date, the only therapeutic strategy in such circumstances is the use of supportive interventions (artificial ventilation, vasopressor support).

Not unexpectedly, there is evidence that diffuse alveolar damage caused by the H5N1 virus also triggers up-regulation of

***See also p. 1397.**

Key Words: H5N1 influenza A lung injury; fibrin; alveolar injury; coagulation; tumor necrosis factor-α; activated protein C; acute respiratory distress syndrome

DOI: 10.1097/01.CCM.0000259174.45444.AF

tissue factor, which is a potent procoagulatory factor and may be linked to extensive fibrin deposition along alveolar walls as well as the consumptive coagulopathy occurring during H5N1 infection. There is evidence that H5N1 infection in mouse lung results in generation of multiple cytokines and chemokines (e.g., interleukin-6, interleukin-1β, tumor necrosis factor [TNF]-α, macrophage inflammatory protein-1α). Interestingly, mice genetically deficient in TNF-α-1 receptor have a greatly reduced mortality even though viral replication in the lung is not affected (5).

Such data suggest that two therapeutic strategies might be considered in the case of humans with influenza A H5N1 infection: activated protein C (APC) and blockade of TNF-α or its receptor. APC blocks several different activated coagulation factors and also has anti-inflammatory properties. APC has been approved for use in humans with high-grade sepsis (6). Therapeutic use of APC is contraindicated if there is evidence of severe consumptive coagulopathy, thrombocytopenia, or other signs that the clotting system has been extensively activated. The use of APC might diminish the consumptive coagulopathy occurring during H5N1 infection, especially as it involves the lungs. Blocking antibody to TNF-α and the TNF-α receptor blocking agent, soluble TNFαRI (sTNFαRI), are known to be effective in the treatment of patients with rheumatoid arthritis ((7). In patients with rheumatoid arthritis, sTNFαRI seems to be well tolerated and is largely without evidence of toxicity. If the data in knockout mice can be extrapolated to humans with H5N1 infection, either blockade of TNF-α (with antibody) or use of sTNFαRI might be therapeutically effective. It is clear that there is an urgent need for reliable, specific, and sensitive tests for early detection of H5N1 infection. There is an equally urgent need for highly effective drugs to block H5N1 entry into cells and intracellular replication. In the meantime, in H5N1-infected patients, perhaps the use of APC or sTNFαRI might provide some therapeutic benefit, but clinical trials are obviously required.

Peter A. Ward, MD
Department of Pathology
University of Michigan
Medical School
Ann Arbor, MI

REFERENCES

1. Arabi Y, Gomersall CD, Ahmed QA, et al: The critically ill avian influenza A (H5N1) patient. *Crit Care Med* 2007; 35:1397–1403
2. Shinya K, Ebin M, Yamada S, et al: Influenza virus receptors in the human airway. *Brief Communications, Nature* 2006; 440:435–436
3. Uiprasertkul M, Puthavathana P, Sangsiriwut K, et al: Influenza A H5N1 replication sites in humans. *Emerg Infect Dis* 2005; 11:1036–1041
4. Wai-Fu N, Ka-Fai T, Lam WL, et al: The comparative pathology of severe acute respiratory syndrome and avian influenza A subtype H5N1—A review. *Human Pathol* 2006; 37: 381–390
5. Szretter KJ, Gangappa S, Lu X, et al: Role of host cytokine responses in the pathogenesis of avian H5N1 influenza viruses in mice. *J Virol* 2007; 81:2736–2744
6. Bernard GR, Vincent JL, Laterre PF, et al: Efficacy and safety of recombinant human activated protein C for severe sepsis. *N Engl J Med* 2001; 344:699–709
7. Moreland LW, Baumgartner SW, Schiff MH, et al: Treatment of rheumatoid arthritis with a recombinant human tumor necrosis factor receptor (p75)-Fc fusion protein. *N Engl J Med* 1997; 337:141–147

ANTIOXIDANTS & REDOX SIGNALING
Volume 9, Number 11, 2007

DOI: 10.1089/ars.2007.1785

Forum Review

Role of Oxidants in Lung Injury During Sepsis

REN-FENG GUO and PETER A. WARD

ABSTRACT

The role of oxidative stress has been well appreciated in the development of sepsis-induced acute lung injury (ALI). Oxidative stress in sepsis-induced ALI is believed to be initiated by products of activated lung macrophages and infiltrated neutrophils, promptly propagating to lung epithelial and endothelial cells. This leads to tissue damage and organ dysfunction. On stimulation, neutrophils (PMNs) enable their migration machinery. The lung undergoes changes favoring adhesion and transmigration of PMNs, resulting in PMN accumulation in lung, which is a characteristic of sepsis-induced ALI. Oxidative stress turns on the redox-sensitive transcription factors (NF-κB, AP-1), resulting in a large output of proinflammatory cytokines and chemokines, which further aggravate inflammation and oxidative stress. During the process, transcription factor nuclear factor-erythroid 2-p45–related factor 2 (Nrf2) and heme oxygenase (HO) appear to play the counterbalancing roles to limit the propagation of oxidative stress and inflammatory responses in lung. Many antioxidants have been tested to treat sepsis-induced ALI in animal models and in patients with sepsis. However, the results are inconclusive. In this article, we focus on the current understanding of the pathogenesis of sepsis-induced ALI and novel antioxidant strategies for therapeutic purposes. *Antioxid. Redox Signal.* 9, 1991–2002.

INTRODUCTION

DESPITE TECHNICAL DEVELOPMENTS in intensive care units (ICUs) and advanced supportive treatment, the death rate in septic patients remains high, with a range of lethality ranging from 30 to 50% (3). The acute respiratory distress syndrome (ARDS) has been defined as a severe form of acute lung injury (ALI), featuring pulmonary inflammation and increased capillary leak (98). ARDS may arise in a number of clinical situations, especially in patients with sepsis. As a common complication of sepsis, it has been considered a leading cause for death in sepsis. A well-described pathophysiologic model of ARDS is one form of acute lung inflammation mediated by inflammatory cells and mediators as well as oxidative stress (22).

Oxidative stress is caused by an imbalance between the production of reactive oxygen species (ROS) and the biologic scavenger system, which can readily detoxify the reactive oxygen intermediates under normal physiologic conditions. Oxidative-induced damage has been considered to be one of the underlying mechanisms that contribute to multiple organ failure in sepsis (7, 35, 102). Because of the natural oxidizing nature of the atmosphere and the direct exposure to many atmospheric pollutants, the lung is at high risk of oxidative injury. It has been recognized that oxidative stress can not only directly cause tissue damage, but it also can affect the molecular mechanisms that control lung inflammation. In the healthy lung, airway lining fluids and extracellular spaces are maintained in a highly reduced state (with millimolar levels of reduced glutathione, GSH) to preserve normal physiologic functions. Under normal conditions, the levels of antioxidants and oxidants in lung are balanced in favor of a reducing state. Decreases in antioxidants or increases in oxidants can disrupt this equilibrium and can cause oxidative stress. An imbalance in the oxidant–antioxidant system has been recognized as one of the first events that ultimately lead to inflammatory reactions in the lung (17).

Oxidative stress has been found to occur in many forms of lung disorders, such as pneumonia, ARDS, idiopathic pulmonary fibrosis, lung transplantation, chronic obstructive pul-

Department of Pathology, University of Michigan Medical School, Ann Arbor, Michigan.

monary disease, cystic fibrosis, bronchiectasis ischemia–reperfusion, and lung cancer (10, 18, 79). Based on composition, oxidants can be divided into two main categories, ROS and reactive nitrogen species (RNS). Superoxide, hydroxyl radicals, and hydrogen peroxide are generally classified as ROS in contrast to nitric oxide and peroxynitrite, which are nitrogen based. These molecules naturally function as neurotransmitters, second messengers, and as a part of the chemical host defense against infection. It is only when their concentrations become excessive, especially extracellularly, that the potential for adverse responses can occur. High ROS/RNS levels lead to alterations in normal cell function and eventually compromise local tissue and systemic homeostatic mechanisms. In this review, we focus on the understanding of the roles of oxidative stress in sepsis-induced ALI and potential therapeutic strategies by using antioxidants.

DETECTION OF OXIDATIVE STRESS IN LUNG

It is clear that a better understanding of the oxidative state in the lung is important for the diagnosis and treatment of lung diseases. Many methods have been developed for detection of free radicals from oxygen, ROS, RNS, and their byproducts to assess the presence of oxidative stress. The techniques include established standard protocols and advanced methods using high-performance liquid chromatography (HPLC), mass spectrometry, and electron paramagnetic resonance. Described later are the most frequently used methods for evaluation of lung oxidative status.

Monitoring oxidative stress in live cells

ROS in live cells can be detected by using a fluorogenic marker for ROS and observing under fluorescence microscopy. One frequently used marker is carboxy-H_2DCFDA, a cell-permeable fluorogenic marker, which is oxidized during oxidative stress in live cells and emits bright green fluorescence (97). $NO^{\cdot}$ production by lung cells can be measured by using the $NO^{\cdot}$ fluorescent indicator, DAF-2 (89). On reaction with an active intermediate (N_2O_3) formed during the oxidation of $NO^{\cdot}$ to nitrite, DAF-2 is converted to its fluorescent triazole form, which can be measured by fluorescent plate readers at excitation and emission wavelengths of 485 and 538 nm, respectively..

Hydrogen peroxide (H_2O_2) and superoxide products in bronchoalveolar fluids

H_2O_2 fluids in bronchoalveolar fluids (BALs) can be measured by the simple assay for detecting the presence of peroxides in both aqueous and lipid environments. The basis of these assays is the complexing of ferrous ion (Fe^{2+}) by H_2O_2 in the presence of xylenol orange. Peroxides will oxidize Fe^{2+} to Fe^{3+}, and Fe^{3+} will form a colored complex with xylenol orange that can be read at 560 nm (46, 47). Superoxide radical generation can be estimated by nitroblue-tetrazolium reduction assay (60).

Antioxidant status in lung

The antioxidant status in the lungs can be evaluated by lung levels of superoxide dismutase (SOD) and catalase (CAT) and their activities. SOD activity can be assessed by the OxyScan SOD-525 assay, which measures the activity of all forms of SOD. The method is based on the SOD-mediated increase in the rate of autoxidation of 5,6,6a,11b-tetrahydro-3,9,10-trihydroxybenzôfluorene in aqueous alkaline solution to yield a chromophore with maximum absorbance at 525 nm. Catalase (CAT) activity can be determined by a two-step reaction scheme (catalase-520 assay). First, catalase reacts with a known quantity of H_2O_2 to generate H_2O and $O_2^{\cdot}$. In the presence of horseradish peroxidase (HRP), the remaining H_2O_2 reacts with 3,5-dichloro-2-hydroxybenzenesulfonic acid and 4-aminophenazone to form a chromophore with a color intensity. Lipid peroxidation levels in lung can be measured by thiobarbutiric acid–reactive substances assay (25). The GSH/GSSG ratio, a useful measure of oxidative stress, can be determined by a colorimetric method by using Bioxtech GSH/GSSG-412.

Protein oxidation and lipid peroxidation in lung

The levels of protein carbonyls and nitrotyrosine are widely used for the detection of oxidative modification of proteins. Protein carbonyls are considered to be one of the most reliable methods to evalute the protein damage mediated by oxidative stress. Nitrotyrosine levels in tissues and BAL fluids correlate with oxidant stress in animal and human studies (33). Protein carbonyls can be measured through the reaction with dinitrophenylhydrazine (DNPH) (57). The proteins are first precipitated by the addition of 20% trichloroacetic acid and then redissolved in DNPH. Nitrotyrosine is often determined by enzyme-linked immunosorbent assay (ELISA), Western blotting, and immunohistochemistry with specific antibodies. Lipid peroxidation, oxidized lipids, and lipid mediators are believed to play an important role in lung inflammatory diseases. The detection of products of lipid peroxidation has been widely used to estimate the overall status of oxidative stress in lung. Among them, thiobarbituric acid reactants (TBARs) and malondialdehyde (MDA) are commonly used indicators (16).

DNA damage

The most common type of damage caused by reactive oxygen species in the body is oxidative damage to DNA. Hydroxydeoxyguanosine (8-OHdG), a product of this type of DNA damage, is used as a biomarker for oxidative stress. It can be measured by the immunohistochemical procedure and an HPLC system equipped with an electrochemical detector (HPLC-ECD) (63). More recently, it has been reported that capillary electrophoresis-mass spectrometry (CE/MS) can be also used for the analysis 8-OHdG to study oxidative stress (101).

Analysis of expired air for oxidation products

Studies have shown that expired $NO^{\cdot}$ and CO can serve as biomarkers for oxidative stress, whereas ethane can serve as a marker of lipid peroxidation (73). CO can be detected electrochemically, and it can also be measured by a laser spectrophotometer and near-infrared CO analyzers. The levels of exhaled

$NO^{\cdot}$ can be assessed by chemiluminescence. Ethane content can be detected by using gas chromatography. Oxidative stress in lung appears to be an important factor in predicting or assessing (or both) lung injury. Methods for detection of oxidative stress have a broad range from well-established protocols to newly developed technologies. It is very difficult to measure oxygen free radicals directly because of their short half-lives and reactivity with other molecules. Radical spin-trapping agents have been used to form stable radical adducts, which can be detected by electron paramagnetic resonance spectroscopy (EPR). Trapping agents are generally nitrone- or nitroso-containing molecules, such as 5,5-dimethyl-1-pyrroline-*n*-oxide (DMPO), that react with oxygen free radicals to form stable nitroxide free radicals (72). The sampling procedure to collect exhaled breath condensate can be used to measure H_2O_2, leukotrienes, isoprostanes, and 3-nitrotyrosine in lung inflammation (73). Given the nature of complexity and importance of lung biology, it is essential to develop sensitive and reliable tools to monitor the status of lung oxidative stress. A standardized protocol is also required for clinical application.

EVIDENCE OF OXIDATIVE STRESS IN SEPSIS-INDUCED ALI

Low antioxidant and high plasma levels of oxygen free radicals have been well documented in patients with sepsis and in animal models of sepsis (30, 35, 96). Many oxidative indicators have been reported in lungs from septic patients and animals. In patients with sepsis, protein carbonyls were significantly elevated in both blood and BAL fluids during the initial phase of sepsis, decreasing within a few days but remaining above control values (102). In the same study, myeloperoxidase (MPO) activity was also markedly increased in BAL fluids from septic patients. Strong correlations were found between carbonyl concentrations in BAL fluid and plasma, when compared with protein carbonyls, TBARS, and MPO in lung, suggesting that neutrophil oxidants might be chiefly responsible for oxidative stress in lungs during sepsis. All patients with ARDS had higher levels of hypoxanthine, a prooxidant substrate for xanthine oxidase (75). Hypoxanthine levels were 2 times higher in nonsurvivors than those in survivors. Nonsurvivor ARDS patients appeared to have higher levels of oxidative stress and damage when compared with survivors. Surprisingly, hypoxanthine levels were normal in patients in intensive care with sepsis but no lung injury. These data suggest that oxidative stress plays an essential role in the pathogenesis of ALI in sepsis, and directly contributes to the bad outcome.

Oxidative stress in animal models of sepsis has been also well described. In rodent sepsis models induced by cecal ligation and puncture (CLP), the activities of enzymatic antioxidants, including SOD, CAT, and glutathione peroxidase (GSH-PX), in lung were significantly decreased during the early- and late-sepsis phages (21), indicating that sepsis sets up an environment favorable for oxidative stress in lung. As expected, MDA concentrations and nitrate (NO_3^-)/nitrite (NO_2^-) levels were also elevated in the septic lung. In addition, MPO activity was found to be enhanced, and a large number of neutrophil infiltrates were observed by histology in lungs from septic animals. Many other oxidative indicators in lung, including 8-isoprostane, exhaled $NO^{\cdot}$, superoxide anion, glutathione, protein carbonyls, and TBARS, were all changed in favor of an oxidative-stress status during experimental sepsis (2, 19, 51, 59, 85, 86, 96).

NEUTROPHIL ACCUMULATION IN LUNG DURING SEPSIS

The pathophysiology of the sepsis-induced ALI/ARDS is very complicated and not completely defined. However, increased production of ROS/RNS from PMNs has been proposed as one of the significant mechanisms underlying the development of lung inflammation. Additionally, the contribution by lung macrophages may be an important source for ROS/RNS. Sepsis-induced ALI is characterized by the activation of a variety of cells, including inflammatory cells such as PMNs and macrophages, and increased levels of inflammatory mediators. PMN infiltrates occur in lungs from both humans and animals with sepsis. The number of neutrophils in BAL fluids from patients with ARDS is significantly increased and associated with poor survival (1, 61, 100). Circulating PMNs infiltrate and accumulate in the lung *via* transmigration through the endothelium, interstitium, and alveolar epithelium to enter the alveolar compartment or be sequestered in lung capillaries. Upregulation of chemoattractant molecules (chemokines) occurs, establishing a concentration gradient that directs the neutrophils into the lung. Adhesion molecules, including integrins, selectins, and ICAMs, are also involved in the migration process (40). These events are described in Fig. 1.

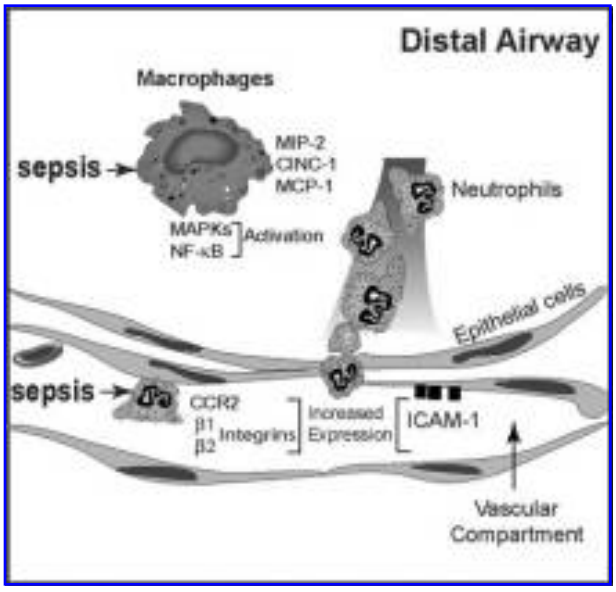

FIG. 1. The mechanism of PMN accumulation in the lung during sepsis. In rat and mouse models of sepsis, activated alveolar macrophages release MIP-2 (rat), CINC-1 (rat), and MCP-1 (mouse), which chemoattract PMNs into the lung. Increased levels of CCR2 as well as β_1 and β_2 integrins on PMNs, together with enhanced expression of ICAM-1 on endothelial cells, facilitate PMN adhesion and migration.

Local production of CXC chemokines is essential for the accumulation of PMNs in the lung under conditions of acute inflammation. For PMN chemoattractants, although sufficient local concentrations of CXC chemokines are necessary for PMN recruitment, the dictating factor is the ratio of lung-to-blood chemokine concentrations (11). In experimental sepsis, lung production of two important CXC chemokines, MIP-2 and CINC-1, increased but lagged behind in comparison with the levels of MIP-2 and CINC in blood (38). As a result, lung levels of CXC chemokines increased when blood levels of those decreased. The discrepancy might be important for CXC chemokines to create a gradient difference between the two compartments (vascular and alveolar), which is necessary for initiation of PMN migration. CXC chemokines have been implicated in all steps in the extravasation process of leukocytes, including rolling, adhesion, and transmigration *in vivo* (104). Thus, the role of blood CXC chemokines may primarily focus on the activation of PMNs and endothelial cells, setting the stage for PMN migration, whereas local CXC chemokines chiefly function chemotactically during sepsis. In addition, blood CXC chemokines produced in the early stage of experimental sepsis may provide vital signals for PMN survival, given the fact that CXC chemokines and C5a reduce PMN apoptosis (23, 39). Under such conditions, the greatly prolonged life span of PMNs may be related to the development of the symptoms of sepsis. The reason for higher BAL levels of CXC chemokines is likely the activation of lung macrophages. It is clear that a phase exists in which alveolar macrophages are prone to activation during the early stage of sepsis, and then may go into a refractory (deactivation) stage (38, 82). Conversely, PMNs quickly enter into this refractory phase, and their capability for producing CXC chemokines and other inflammatory mediators is greatly compromised. It was found that CXC chemokine macrophage-inflammatory protein-2 (MIP-2) production in both alveolar macrophages and PMNs was dependent on mitogen-activated protein (MAP) kinases (p38 and p42/p44) and NF-κB pathways (38). Interestingly, alveolar macrophages still maintain, and even increase, their capacity for activation of p38 and p42/p44 MAPKs during sepsis, whereas septic blood PMNs become nonresponsive to stimulations. Paralysis of signaling pathways in PMNs is likely caused, at least in part, by overproduction of C5a in sepsis. In addition, the CC chemokine, MCP-1, seems to also play an important role in attracting PMNs into lung (89). PMNs in sepsis used a novel migration pathway that is CC chemokine receptor CCR2 dependent. Ordinarily, PMNs do not express CCR2, but in sepsis, this receptor is clearly expressed (88).

Sepsis involves widespread upregulation of both PMN and endothelial adhesion molecules (74). In a rat model of sepsis, it was observed that the content of β_1 and β_2 integrins on circulating PMNs was elevated after CLP. The increased expression of β_1 integrin on blood PMNs followed β_2 integrin elevation, which was seen as early as 3 h after CLP. Rapid elevation of β_2 integrin may represent an important role in host defense by directing PMNs into inflamed organs. Several lines of evidence support such a role for β_2 integrin in the mobilization of PMNs into tissues. Patients with inherited deficiencies of β_2 integrin are much more susceptible to bacterial infection (41). In a canine model of lung inflammation (i.v. infusion of TNF-α), anti-CD11b treatment reduced PMN accumulation early (within the first 24 h), but not later (>24 h) (74), suggesting that leukocyte trafficking may differ between the early and late stages of inflammation. Expression of β_1 integrin in PMN migration is amplified in sepsis. Fully activated β_1 integrin at the later stage of sepsis may alter the balance of integrin cooperativity. It was previously shown that blood PMNs from septic, but not control, patients expressed $\alpha_4\beta_1$ integrin, which caused increased adhesiveness to immobilized VCAM-1 (43). Anti-β_1 integrin antibody interferes with cell motility of septic PMNs from CLP rats, indicating that sepsis alters the trafficking of PMNs into the lung by engaging a β_1 integrin–dependent pathway (37). The adhesion molecule, ICAM-1, is also involved in PMN migration during sepsis. Absence or blockade of this molecule impairs the ability of PMNs to migrate into organ tissues and reduces consequent secondary organ damage, resulting in improved clinical indicators and overall survival (42). We previously demonstrated that PMN migration into lung during sepsis is ICAM-1 dependent, but not VCAM-1 dependent, perhaps related to VCAM-1 shedding that occurs during the course of sepsis development (54).

Figure 1 illustrates a simplified version of pathways for PMN migration in the lung during sepsis. CCR2 and β_1 and β_2 adhesion molecules on PMNs are upregulated during the course of sepsis, whereas PMN capability to produce CXC chemokines is reduced. In lung, activated macrophages release a large amount of PMN chemoattractants and other inflammatory cytokines, whereas ICAM-1 is activated on endothelial cells, setting the stage for PMN migration. These processes are tightly regulated by MAPKs and NF-κB pathways.

ROLE OF OXIDANTS IN SEPSIS-INDUCED ALI

Inflammation occurs after activation of PMNs and macrophages, resulting in ROS/RNS generation and the release of lysosomal enzymes and cationic proteins. Oxidative stress is initiated by ROS such as superoxide ($O_2^{\cdot}$) and hydrogen peroxide (H_2O_2). These oxidants are not very harmful *per se*, but can be converted into more dangerous oxidants, causing harmful reactions in tissues (16). Generation of superoxide-derived products continues to be the main pathway responsible for the production of ROS. $O_2^{\cdot}$ can be generated through various enzymatic systems, including the mitochondrial respiratory chain, xanthine oxidase, cyclooxygenase, and NADPH oxidase (16). The NADPH oxidase pathway is well defined in phagocytic cells. Activation of the oxidase can be initiated by a variety of inflammatory mediators and is likely to be a major source of oxidant generation in sepsis-induced lung injury. Translocation of cytosolic subunits of NADPH oxidase components from the cytoplasm to the cell membrane occurs in PMNs, macrophages, and monocytes on cell stimulation, thus representing a potential therapeutic target in the treatment of ROS-mediated lung injury during sepsis. NADPH oxidase catalyzes the transfer of an additional electron to molecular oxygen (O_2) to form the $O_2^{\cdot}$ anion. Because NADPH oxidase adds single electrons to O_2, oxygen-derived intermediates are also produced. Reduction of Fe^{3+} to Fe^{2+} or Cu^{2+} to Cu^{+} by superoxide in the Fenton re-

action facilitates the generation of hydroxyl radicals (OH^-). In the presence of Fe^{2+}, superoxide is reduced to H_2O_2, which can then be metabolized in the presence of transition metals and chloride to form hypochlorous acid (HOCl). This reaction is catalyzed by MPO and provides a practical marker for PMN accumulation in tissue. Although it is not a free radical, H_2O_2 can permeate cellular membranes, thus extending the damage beyond the originating cell. These products injure cells of the lung and airway and interfere with gas exchange.

$NO^{\cdot}$ is an abundant signaling molecule. Like H_2O_2, it is able to cross cell membranes to alter various physiologic processes through binding and activation of guanylate cyclase. *Via* this intermediate, $NO^{\cdot}$ functions as a secondary messenger in the maintenance of systemic vascular tone. $NO^{\cdot}$ also affects platelet aggregation and can stimulate immune responses, activate genes, and cause apoptosis (32, 50). It is fairly unreactive with bioorganic molecules; however, it does react with aromatic amino acids to form stable nitrotyrosine adducts in proteins and peptides, which may impair cell function. $NO^{\cdot}$ is synthesized by three nitric oxide synthase (NOS) isozymes, so named by the origin of the cell in which they were originally discovered. Two of the three forms (nNOS and eNOS) are constitutively expressed and generate small amounts of $NO^{\cdot}$, which generally are not sufficient to cause cellular damage. Binding to calcium and calmodulin is required for NOS activation, serving as factors that regulate NOS activity. In contrast, the third isoform (iNOS) is an inducible calcium-independent enzyme that produces copious amounts of $NO^{\cdot}$ for several hours to even days after induction. It is during circumstances that initiate induction of this third NOS form that the physiologic roles of $NO^{\cdot}$ are superseded by its implication as the culprit behind various injurious inflammatory responses and potentially cytotoxic events.

In the setting of lung, all three NOS isozymes are present. Various forms of $NO^{\cdot}$ can be observed as *S*-nitrosothiol, nitrate, and nitrite in exhaled air and bronchoalveolar lavage from human lungs (24, 95). Upregulation of iNOS amplifies the conversion of L-arginine to L-citrulline and $NO^{\cdot}$ formation. In the presence of superoxide, $NO^{\cdot}$ is converted to peroxynitrite ($ONOO^-$), which is then protonated to form an unstable species, peroxynitrous acid (ONOOH). The presence of iNOS has been reported in alveolar macrophages, PMNs, and endothelial and lung epithelial cells (99). Accordingly, these cells are all potential sources of peroxynitrite. $ONOO^-$ reacts with protein thiols and is thought to be the predominant mechanism by which $NO^{\cdot}$ production leads to cytotoxicity. Peroxynitrous acid is degraded to form the hydroxy radical, NO_3^- and NO_2^- by hemolytic cleavage, or it can react with CO_2 to form peroxycarboxylate ($ONOOCO_2^-$). Detection of NO_3^- and nitrite NO_2^- serves as a convenient experimental marker for $NO^{\cdot}$ production. Activation of infiltrating and resident phagocytes can cause an increase in both $NO^{\cdot}$ and superoxide, resulting in apoptosis. On a molecular level, the resulting peryoxynitrite interacts with DNA to cause DNA fragmentation, and with membrane lipids to cause peroxidation of the endothelial or alveolar epithelial cell plasma membranes. Low concentrations of $NO^{\cdot}$ suppress peroxidation, but as superoxide levels increase, cell membrane injury becomes intensified. Reduced amounts of $NO^{\cdot}$ serve to decrease endothelial cell membrane permeability, thus limiting PMN transmigration from the vascular compartment into the lung tissue. $NO^{\cdot}$ is an endogenous inhibitor of leukocyte adhesion to endothelial cells, but this phenomenon is reversed by increasing amounts of superoxide anion. The potential pathways that generate oxidants in sepsis-induced ALI are illustrated in Fig. 2.

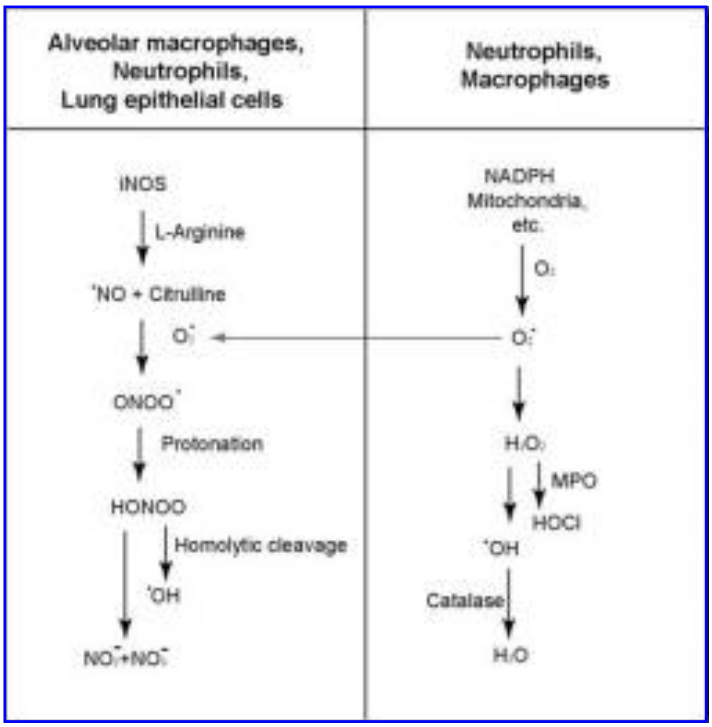

FIG. 2. Mechanisms for production of reactive oxygen species in sepsis-induced ALI.

Role of $NO^{\cdot}$ in sepsis-induced ALI

Sepsis and ALI are associated with a high level of $NO^{\cdot}$ production after activation of iNOS. $NO^{\cdot}$ has been implicated in the pathophysiology of ALI in humans and animal models of ALI. However, NOS inhibition with nonselective inhibitors, such as N^{G}-monomethyl-L-arginine (L-NMMA), in animals with sepsis and ALI has resulted in worsened outcomes (65, 71), suggesting complex roles of $NO^{\cdot}$ in the pathogenesis of sepsis. The results obtained from iNOS-deficient mice have been controversial. In the CLP-induced sepsis model, no pulmonary protein leak developed in iNOS-deficient mice, despite increased pulmonary MPO activity (27). By using the same model, it has been demonstrated that pulmonary oxidant stress is completely iNOS dependent and is associated with tyrosine nitration, and that pulmonary oxidant stress and nitrosative stress are dependent on the presence of iNOS in inflammatory cells (macrophages and PMNs), with no apparent contribution of iNOS in pulmonary parenchymal cells (80, 81). Therefore, the authors proposal that iNOS inhibition targeted specifically to inflammatory cells may be an effective therapeutic approach in sepsis and acute lung injury. In the bacterial lipopolysaccharide (LPS) model of ALI, lung-injury parameters such as MPO levels and albumin leak into lung were not affected by eNOS deficiency, but substantially were intensified in mice with iNOS deficiency. In LPS-indued lung injury in iNOS-deficient mice, BAL levels of CXC chemokines (MIP-2, KC) did not show any difference when compared with wild-type (WT) mice, but CC chemokines (MCP-1, MCP-3) were enhanced. Blockade of MCP-1 in iNOS-deficient mice reduced lung MPO to the levels present in WT mice. Thus, iNOS appears to play a protective role in this ALI model by limiting PMN accumulation in lung (89). Reasons for the discrepancy for iNOS-deficient effects from two ALI models are not clear. Tissue-specific KO conditions and reliable specific inhibitors for iNOS may help clarify the role of $NO^{\cdot}$ in sepsis-induced ALI, thereby assisting in the design of future clinical trials. Nevertheless, the role of $NO^{\cdot}$ in oxidative stress in lung is indisputable.

Role of $O_2^{\cdot}$ in sepsis-induced ALI

Generation of $O_2^{\cdot}$ by the NADPH oxidase complex of PMNs is crucial for host defense responses, and it is essential for killing invading microorganisms. However, $O_2^{\cdot}$ may also exert harmful effect in tissues. NADPH oxidase is a multisubunit complex in which $gp91^{phox}$ and $p47^{phox}$ are essential for $O_2^{\cdot}$ generation. $O_2^{\cdot}$ can work as a "double-edged sword," so it is not surprising that the results from $p47^{phox-/-}$ and $gp91^{phox-/-}$ mice are perplexing in the setting of sepsis (31). More PMN infiltrates and higher bacterial loads were seen in lungs from $p47^{phox-/-}$ and $gp91^{phox-/-}$ mice compared with WT mice after live *Escherichia coli* challenge, whereas lung microvascular injury was prevented in these mice. Thus, PMN infiltration in lung tissue did not result in overt lung microvascular injury, when the $O_2^{\cdot}$ generation was impaired. In the same study, it was found that increased bacterial load in NADPH-deficient mice was a critical factor for activating the release of chemokines, which subsequently enhanced PMN sequestration and migration into lung tissue. A selective SOD mimetic, M40401, was found to be protective in a live *E. coli* model of sepsis, but it improved survival only in severe sepsis and was less effective and even harmful with less-severe sepsis (19). Another SOD mimetic, "Tempol," has been reported to improve survival in CLP-induced septic rats, reduce the plasma levels of $NO^{\cdot}$ and IL-1β, and decrease the levels of organ $O_2^{\cdot}$ and tissue injury (59). It seems that $O_2^{\cdot}$ is indispensable for killing bacteria, but also leads to tissue damage during sepsis.

$NO^{\cdot}$ and $O_2^{\cdot}$ appear to play dual roles in the pathogenesis of sepsis-induced ALI. They may function by totally different mechanisms at different stages of sepsis. Thus, in clinical trials that involve antioxidant inhibitors, a compelling need exists to monitor closely the bacterial load and oxidative status. For example, it might be reasonable to scavenge $O_2^{\cdot}$ at a stage when the systemic bacterial load is partially contained during sepsis.

OXIDANT-RELATED MOLECULAR EVENTS IN SEPSIS-INDUCED ALI

NF-κB and activator protein-1 (AP-1)

NF-κB and AP-1 are two well-defined redox-sensitive transcription factors. Oxidative stress activates multiple stress kinase pathways and transcription factors (NF-κB, AP-1) by modifying cysteine residues subsequently regulating gene expression for proinflammatory cytokines as well as the protective antioxidant molecules (76). Activation of NF-κB occurs in lung macrophages and in lung tissue during sepsis (28, 45, 62). NF-κB is a heteromeric dimer composed of a complex of proteins from the RelA family. NF-κB is constitutively relegated to the cytosolic compartment. The dimer most commonly comprises p50 (NF-κB1) and p65 (RelA) subunits bound to members of the inhibitor κB (IκB) family. Activation of NF-κB occurs in response to an appropriate stimulus. After phosphorylation and ubiquitination of an IκB subunit, it is subsequently degraded by a 28S proteasome. This allows the heterodimer complex to translocate to the nucleus and bind to specific DNA promotor sequences. Access to DNA is dependent on the degree of histone coiling, which is in turn regulated by the degree of acetylation of histone core residues. As the DNA becomes more acetylated, it unwinds, thus allowing binding of transcription factors, initiating gene transcription. H_2O_2 and TNF-α have both been shown to increase histone acetylation, providing a potential mechanism for oxidant-mediated inflammation (56). This effect may be antagonized by $NO^{\cdot}$, which has been shown to be capable of maintaining levels of IκB, thus hindering NF-κB activation (95). Whether this is achieved by decreasing IκB degradation or increasing its synthesis has yet to be determined. Depletion of glutathione leads to ubiquitination of NF-κB and subsequent activation (77, 78). As glutathione levels increase, IκB degradation is inhibited so that NF-κB does not become activated. NF-κB also regulates iNOS and the inducible form of cyclooxygenase (COX-2). Thus, regulation of the inflammatory response may proceed through a negative-feedback loop *via* NF-κB and nitric oxide. An endogenous protease inhibitor, secretory leukocyte protease inhibitor (SLPI), inhibits IκB degradation, suppressing NF-κB activation. PMN accumulation, ROS activity, and levels of IL-1 and IL-8 were shown to decrease in LPS-treated rabbits that in-

haled $NO^{\cdot}$ (48). These decreases correlated with a concomitant decrease in NF-κB activation. Depletion of lung macrophages in rats by airway instillation of liposome-encapsulated dichloromethylene diphosphonate suppressed activation of NF-κB and resultant BAL levels of TNF-α and MIP-2 (55). PMN accumulation and vascular permeability were also decreased, suggesting that activation of alveolar macrophages served as the source of an initial inflammatory stimulus. Activated alveolar macrophages and infiltrated PMNs generate ROS and cytokines, propagating the cycle of oxidant stress and inflammation. This scenario is likely to be the key event that drives pulmonary oxidant stress and inflammation during sepsis-induced ALI.

The promoter regions of various cytokines and chemokines contain binding sites for AP-1, suggesting that AP-1 plays a critical role in coordinating the gene expression of various inflammatory mediators. Like NF-κB, AP-1 activation occurs in lung during sepsis and likely modulates inflammation (4). AP-1 is a complex multisubunit protein composed of members of the Jun and Fos families. Much is known regarding its role in events regulating cell proliferation, transformation, differentiation, and apoptosis (49). AP-1 activation was found to be detectable in alveolar macrophages as well as in whole-lung lysates. Macrophage depletion or anti–TNF-α treatment significantly decreased the level of AP-1 activation in lung after IgG immune complex deposition, but complement depletion had no effect (36). AP-1 also responds to oxidative and cellular stress, DNA damage resulting from UV irradiation, and exposure to proinflammatory cytokines (TNF-α, IFN-γ, and TGF-β). TNF-α has been shown to activate AP-1 upstream of MAPK kinase pathways. Activation of AP-1 appears to occur concurrent with activation of other transcription factors, including Elk-1, ATF-2, and CEBP (58, 78). The AP-1 family of transcription factors has been found to play a critical role in regulating the stress-inducible protein heme oxygenase-1 (HO-1) gene after LPS treatment in rat lung (12), suggesting that AP-1 may also participate in the negative regulatory loop of the inflammatory chain.

Nuclear factor-erythroid 2-p45–related factor 2 (Nrf2)

Nrf2 is a transcription factor that is expressed in many organs, including lung. Nrf2 is directly involved in transcriptional activation of ARE-driven redox-related genes including GST, NADPH/quinine reductase, UDP-glucosyltransferases, epoxide hydrolase, heme oxygenase-1, glutathione peroxidase-2, peroxiredoxins, and glutathione reductase (GSSG-R). Therefore, it appears to be an important modulator in regulation of redox status in cells. Nrf2 has been reported as a critical intracellular molecule for regulation of the innate immune response and survival in mouse models of sepsis. Disruption of Nrf2 dramatically worsened the survival of mice in response to endotoxin and CLP-induced septic shock. Inflammation in these Nrf2-deficient mice was greatly intensified after LPS challenge. In response to LPS, Nrf2-deficient cells showed greater activation of NF-κB, which appeared to be regulated *via* the modulation of the oxidant–antioxidant system (93). In addition, these mice have been shown to be more susceptible to hyperoxic lung injury and lung inflammation induced by the oxidant butylated hydroxytoluene (BHT) (14, 15). Activation of Nrf2 by a chemical agonist, CDDO-Im, attenuated LPS-induced inflammatory responses and oxidative stress in lung, and decreased mortality in Nrf2-sufficient mice (94). Nrf2 appears to be an important transcription factor that limits progression of oxidative stress during sepsis-induced ALI. Therefore, activation or overexpression of this molecule in lung appears to be an attractive strategy for antioxidative defense.

Heme oxygenase-1 (HO-1)

Cumulative evidence has demonstrated that the stress-inducible protein, HO-1, is an auxiliary antioxidant molecule, closely involved in the regulation of lung oxidative status and inflammatory responses. LPS induces high mRNA levels of HO-1 expression in the rat lung, which correlates with increased HO-1 protein levels and enzyme activity (12, 13). Redox-sensitive transcription factor AP-1 plays a critical role in regulating HO-1 gene activation after LPS exposure. In a murine model of sepsis, mice treated with a lethal dose of LPS and subsequently exposed to the HO-1 enzymatic product, CO, had significantly improved survival and lower serum IL-6 and IL-1β levels than controls. The same effect was obtained when endogenous CO was induced through overexpression of HO-1 (68). Interestingly, AP-1 binding was decreased by CO exposure. CO, ferrous iron, and biliverdin are main enzymatic products of HO activation. With the rat model of CLP-induced sepsis, biliverdin treatment offered a potent defense against lethal endotoxemia, as well as in the lungs, and effectively abrogated the lung inflammatory response. Biliverdin administration before a lethal dose of LPS led to a significant improvement in long-term survival, reduced lung permeability and lung alveolitis, and decreased proinflammatory cytokine IL-6. In the same case, augmentation of IL-10, a potent antiinflammatory cytokine in lung injury, occurred (84). Iron (Fe) released as a result of HO-1 activation returns to a transient chelatable pool, where it may potentially promote oxidative stress and inflammation. However, this pathway can be effectively inhibited by ferritin generated through HO-1. Apparently, HO-1 works as a strong negative regulator in the development of oxidative stress and lung inflammatory responses during sepsis-induced ALI. Endogenous CO indeed increased in patients with severe sepsis (103), suggesting that the HO-1 pathway has been activated, and provides a protective role in patients with sepsis.

Other important molecular events in sepsis-induced ALI

Cellular oxidative stress regulates cell function from many perspectives, including receptor function, enzymatic activity, transcription factor activation, and gene expression. As described earlier, it has been documented that protein modifications frequently occur during sepsis. Oxidation-involved molecular events such as tyrosine phosphorylation, activation of MAP kinases, protein kinase C, phospholipase A_2, are found in the lung during sepsis and are likely contribute to the pathogenesis of sepsis (45, 53, 69, 90). Other oxidation-involved events such as protein carbonylation, tyrosine chlorination, and tyrosine nitration are also reported in sepsis (20, 66). How these events regulate the development of sepsis-induced ALI has yet to be defined.

As depicted in Fig. 3, oxidative stress in the lung activates NF-κB and AP-1 pathways during sepsis-induced ALI, which in turn leads to amplified inflammatory responses. AP-1 and Nrf2 activation result in HO-1 expression, leading to CO production in the lung during sepsis. CO together with enzymatic antioxidants generated from Nrf2 activation may play an anti-inflammatory role in sepsis-induced ALI.

ANTIOXIDANT TREATMENT IN SEPSIS-INDUCED ALI

In an earlier study in patients with sepsis-induced ALI, it was found that oral intake of an antioxidant mixture reduced lung microvascular permeability, improved oxygenation and cardiopulmonary function, and reduced proinflammatory eicosanoid synthesis and lung inflammation (29). These findings provide hope for antioxidant strategies in the treatment of sepsis.

Both enzymatic antioxidants and nonenzymatic antioxidants have been widely tested in humans and animals with sepsis. *N*-acetylcysteine (NAC), a nonenzymatic antioxidant, is one of the most extensively tested antioxidants. NAC possesses powerful antioxidative roles by directly scavenging oxygen radicals (H_2O_2, OH , HOCl) and indirectly replenishing the cellular glutathione system. In the models of sepsis-induced ALI, NAC has been shown to be highly protective in lung inflammatory responses by reducing the levels of inflammatory mediators, inhibiting PMN activation and sequestration, suppressing the prothrombotic state, and preventing hypoxic pulmonary vasoconstriction (HPV) (6, 26). However, clinical trails have resulted in controversial findings. Although NAC improves the degree of organ-failure indexes in patients with septic shock, it reduces cardiac performance and tissue oxygenation (5). It was even harmful when initiation of NAC treatment occurred >24 h after hospital admission (67). A later clinical trial suggested that NAC treatment aggravated sepsis-induced organ failure, in particular cardiovascular failure (87). In a recent preclinical trial study using a porcine model of endotoxemia, NAC failed to improve any of the variables of the systemic, pulmonary, or hepatosplanchnic hemodynamics, gas exchange, and metabolism, although it significantly elevated glutathione levels (96). More experimental and clinical studies with new management approaches are required to take advantage of the potential therapeutic utility of NAC.

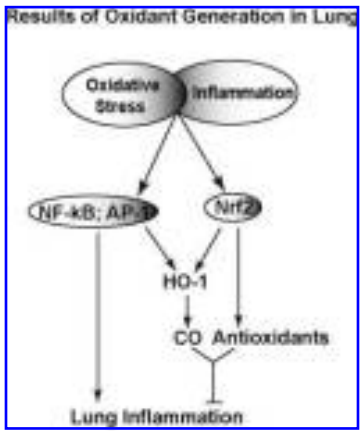

FIG. 3. Molecular events in sepsis-induced ALI. Oxidative stress and inflammation in lung activate the transcription factors, NF-κB and AP-1, leading to amplified inflammatory responses. AP-1 and Nrf2 activation result in HO-1 expression, resulting in CO production. CO, together with enzymatic antioxidants generated from Nrf2 activation, results in an antiinflammatory outcome in sepsis-induced ALI.

Tocopherol (vitamin E) is another nonenzymatic antioxidant that has potential for treatment of sepsis-induced ALI (83, 92). Tocopherol can directly scavenge ROS and upregulate the activities of antioxidant enzymes. It can terminate the chain reaction of lipid peroxidation by scavenging lipid peroxyl radicals. In the mouse model of endotoxin-induced ALI, liposomal tocopherol administration significantly decreased the number of PMNs in airspaces and reduced lung injury, as evidenced by decreased lactate dehydrogenase activity in airways and reduced lung edema. Tocopherol failed to inhibit NF-κB and AP-1 activation, as well as the endotoxin-induced expression of proinflammatory cytokines in lung tissue. In patients with ARDS, the antioxidative system is severely compromised, as evidenced by decreased plasma levels of α-tocopherol, ascorbate, β-carotene, and selenium (64). The early administration of α-tocopherol and ascorbic acid (vitamin C) in humans reduced the incidence of organ failure and shortened the ICU length of stay (70). Vitamin C is known to scavenge $O_2^{\cdot}$ by forming the semi-dehydroascorbate free radical that is subsequently reduced by GSH. Thus, oral intake of combined antioxidants appears to be beneficial in the setting of sepsis-induced ALI.

The antioxidant enzyme SOD, with a biologic function of dismutating $O_2^{\cdot}$ to H_2O_2, holds promise for the treatment of sepsis-induced ALI. Extracellular (EC)-SOD-deficient mice showed increased evidence of ALI that occurs after hemorrhagic shock, accompanied by increased lung PMN accumulation and MPO activity (8). Overexpression of pulmonary EC-SOD in the mouse lung significantly attenuated lung injury that occurs after hemorrhagic shock (9). Overexpression of EC-SOD in lung also attenuated influenza-induced lung injury by both ameliorating inflammation and attenuating oxidative stress (91). Unlike nonenzymatic antioxidants, antioxidant enzymes such SOD and CAT have high affinities and rates of reaction, which can effectively detoxify ROS in numerous cycles, representing a highly efficient mechanism in detoxification. Similar to SOD, CAT provided impressive protection against acute lung injury induced in experimental animals after administration of LPS. EUK-8, a low-molecular-weight salen-manganese complex that exhibits both SOD-like and CAT-like activities *in vitro*, significantly attenuated several features of lung dysfunction caused by endotoxin, including arterial hypoxemia, pulmonary hypertension, decreased dynamic pulmonary compliance, and pulmonary edema (34). Because of the obvious gap between human diseases and animals models, further clinical data are needed to assess the role of the SOD/CAT approach in sepsis-induced ALI.

Other antioxidants that have shown therapeutic merits in the animal models of sepsis-induced ALI include methylene blue (21), resveratrol (52), tempol (59), β-glucan (85), M4041 (19), melatonin (86), and AT1-receptor inhibitor (44). However,

these compounds have been tested only in animals. More experimental and clinical data are expected in the coming years to validate these compounds by using various animal models and eventually in humans with sepsis.

SUMMARY

Sepsis and sepsis-induced ALI represent unsolved clinical problems due to the extremely complicated pathogenesis, which involves an imbalance of the pro- and antiinflammatory networks, complement activation, endothelial cell activation, PMN and macrophage activation, oxidative stress, and transcription factor activation. Blockade of only one of the inflammatory mediators has not resulted in a satisfactory outcome in human clinical trials, perhaps because of the complexity of the inflammatory network and the redundancy of inflammatory mediators. As oxidative stress works through the initiation and progression phases in the development of sepsis, the importance of oxidant stress in sepsis-induced ALI in humans has been appreciated. The disappointing results of NAC clinical trials may reflect the inability to reestablish a redox balance in the setting of sepsis in patients. It has been realized that severity of sepsis alters the effects of $O_2^{\cdot}$ inhibition in sepsis (19). Further improvement of antioxidant interventions requires better understanding of the mechanisms and characteristics of oxidant stress in the specific setting of a disease condition and the development of more-effective delivery strategies. In addition, the redox-sensitive transcription factor, NF-κB, seems to be a logical target for therapy in ARDS patients. However, blockade of NF-κB inevitably turns off some gene expression, which may lead to immunosuppression. To this end, a local inhibition of lung NF-κB activation may be a less detrimental therapeutic strategy. Therapeutic strategies should be directed at the improvement of net proinflammatory, prooxidant, and cytotoxic imbalances that develop in ARDS.

ACKNOWLEDGMENTS

This work is supported by the National Institutes of Health (grants GM-61656, HL-31963, and GM-02507).

ABBREVIATIONS

ALI, acute lung injury; AP-1, activator protein-1; BAL, bronchoalveolar fluid; BHT, butylated hydroxytoluene; CAT, catalase; CE/MS, capillary electrophoresis–mass spectrometry; CLP, cecal ligation and puncture; COX, cyclooxygenase; DMPO, 5,5-dimethyl-1-pyrroline-*n*-oxide; DNPH, dinitrophenylhydrazine; EPR, electron paramagnetic resonance spectroscopy; Fe^{2+}, ferrous ion; GSH-PX, glutathione peroxidase; GSSG-R, glutathione reductase; HO-1, heme oxygenase-1;HPLC, high-performance liquid chromatography; HPV, hypoxic pulmonary vasoconstriction; HRP, horseradish peroxidase; H_2O_2, hydrogen peroxide; HOCl, hypochlorous acid; L-NMMA, NO_3^- nitrate; LPS, lipopolysaccharide; MIP-2, macrophage-inflammatory protein-2; MAP, mitogen-activated protein; MPO, myeloperoxidase; MDA, malondialdehyde; NAC, *N*-acetylcysteine; NO_2^-, nitrite; N^G-monomethyl-L-arginine; NOS, nitric oxide synthase; Nrf2, nuclear factor-erythroid 2-p45–related factor 2; $O_2^{\cdot}$, superoxide; OH^-, hydroxyl radical; 8-OHdG, hydroxydeoxyguanosine; $ONOO^-$, peroxynitrite; ONOOH, peroxynitrous acid; $ONOOCO_2^-$, peroxycarboxylate; RNS, reactive nitrogen species; ROS, reactive oxygen species; SOD, superoxide dismutase; SLPI, secretory leukocyte protease inhibitor; TBARS, thiobarbituric acid-reactive substances; vitamin C, ascorbic acid; vitamin E, tocopherol.

REFERENCES

1. Aggarwal A, Baker CS, Evans TW, and Haslam PL. G-CSF and IL-8 but not GM-CSF correlate with severity of pulmonary neutrophilia in acute respiratory distress syndrome. *Eur Respir J* 15: 895–901, 2000.
2. Andrades M, Ritter C, Moreira JC, and Dal-Pizzol F. Oxidative parameters differences during non-lethal and lethal sepsis development. *J Surg Res* 125: 68–72, 2005.
3. Angus DC, Linde-Zwirble WT, Lidicker J, Clermont G, Carcillo J, and Pinsky MR. Epidemiology of severe sepsis in the United States: analysis of incidence, outcome, and associated costs of care. *Crit Care Med* 29: 1303–1310, 2001.
4. Armstead VE, Opentanova IL, Minchenko AG, and Lefer AM. Tissue factor expression in vital organs during murine traumatic shock: role of transcription factors AP-1 and NF-kappaB. *Anesthesiology* 91: 1844–1852, 1999.
5. Atkinson MC. The use of N-acetylcysteine in intensive care. *Crit Care Resusc* 4: 21–27, 2002.
6. Baboolal HA, Ichinose F, Ullrich R, Kawai N, Bloch KD, and Zapol WM. Reactive oxygen species scavengers attenuate endotoxin-induced impairment of hypoxic pulmonary vasoconstriction in mice. *Anesthesiology* 97: 1227–1233, 2002.
7. Borrelli E, Roux-Lombard P, Grau GE, Girardin E, Ricou B, Dayer J, and Suter PM. Plasma concentrations of cytokines, their soluble receptors, and antioxidant vitamins can predict the development of multiple organ failure in patients at risk. *Crit Care Med* 24: 392–397, 1996.
8. Bowler RP, Arcaroli J, Abraham E, Patel M, Chang LY, and Crapo JD. Evidence for extracellular superoxide dismutase as a mediator of hemorrhage-induced lung injury. *Am J Physiol Lung Cell Mol Physiol* 284: L680–L687, 2003.
9. Bowler RP, Arcaroli J, Crapo JD, Ross A, Slot JW, and Abraham E. Extracellular superoxide dismutase attenuates lung injury after hemorrhage. *Am J Respir Crit Care Med* 164: 290–294, 2001.
10. Bowler RP and Crapo JD. Oxidative stress in allergic respiratory diseases. *J Allergy Clin Immunol* 110: 349–356, 2002.
11. Call DR, Nemzek JA, Ebong SJ, Bolgos GL, Newcomb DE, and Remick DG. Ratio of local to systemic chemokine concentrations regulates neutrophil recruitment. *Am J Pathol* 158: 715–721, 2001.
12. Camhi SL, Alam J, Otterbein L, Sylvester SL, and Choi AM. Induction of heme oxygenase-1 gene expression by lipopolysaccharide is mediated by AP-1 activation. *Am J Respir Cell Mol Biol* 13: 387–398, 1995.
13. Camhi SL, Alam J, Wiegand GW, Chin BY, and Choi AM. Transcriptional activation of the HO-1 gene by lipopolysaccharide is mediated by 5′ distal enhancers: role of reactive oxygen intermediates and AP-1. *Am J Respir Cell Mol Biol* 18: 226–234, 1998.
14. Chan K and Kan YW. Nrf2 is essential for protection against acute pulmonary injury in mice. *Proc Natl Acad Sci U S A* 96: 12731–12736, 1999.
15. Cho HY, Jedlicka AE, Reddy SP, Zhang LY, Kensler TW, and Kleeberger SR. Linkage analysis of susceptibility to hyperoxia. Nrf2 is a candidate gene. *Am J Respir Cell Mol Biol* 26: 42–51, 2002.

16. Christofidou-Solomidou M and Muzykantov VR. Antioxidant strategies in respiratory medicine. *Treat Respir Med* 5: 47–78, 2006.
17. Crapo JD. Oxidative stress as an initiator of cytokine release and cell damage. *Eur Respir J Suppl* 44: 4s–6s, 2003.
18. Crapo JD. Redox active agents in inflammatory lung injury. *Am J Respir Crit Care Med* 168: 1027–1028, 2003.
19. Cui X, Parent C, Macarthur H, Ochs SD, Gerstenberg E, Solomon S, Fitz Y, Danner RL, Banks SM, Natanson C, Salvemini D, and Eichacker PQ. Severity of sepsis alters the effects of superoxide anion inhibition in a rat sepsis model. *J Appl Physiol* 97: 1349–1357, 2004.
20. Dalle-Donne I, Giustarini D, Colombo R, Rossi R, and Milzani A. Protein carbonylation in human diseases. *Trends Mol Med* 9: 169–176, 2003.
21. Demirbilek S, Sizanli E, Karadag N, Karaman A, Bayraktar N, Turkmen E, and Ersoy MO. The effects of methylene blue on lung injury in septic rats. *Eur Surg Res* 38: 35–41, 2006.
22. Demling RH. The modern version of adult respiratory distress syndrome. *Annu Rev Med* 46: 193–202, 1995.
23. Dunican AL, Leuenroth SJ, Ayala A, and Simms HH. CXC chemokine suppression of polymorphonuclear leukocytes apoptosis and preservation of function is oxidative stress independent. *Shock* 13: 244–250, 2000.
24. Dweik RA, Laskowski D, Abu-Soud HM, Kaneko F, Hutte R, Stuehr DJ, and Erzurum SC. Nitric oxide synthesis in the lung: regulation by oxygen through a kinetic mechanism. *J Clin Invest* 101: 660–666, 1998.
25. Erdincler DS, Seven A, Inci F, Beger T, and Candan G. Lipid peroxidation and antioxidant status in experimental animals: effects of aging and hypercholesterolemic diet. *Clin Chim Acta* 265: 77–84, 1997.
26. Fan J, Shek PN, Suntres ZE, Li YH, Oreopoulos GD, and Rotstein OD. Liposomal antioxidants provide prolonged protection against acute respiratory distress syndrome. *Surgery* 128: 332–338, 2000.
27. Farley KS, Wang LF, Razavi HM, Law C, Rohan M, McCormack DG, and Mehta S. Effects of macrophage inducible nitric oxide synthase in murine septic lung injury. *Am J Physiol Lung Cell Mol Physiol* 290: L1164–L1172, 2006.
28. Feng X, Yan W, Liu X, Duan M, Zhang X, and Xu J. Effects of hydroxyethyl starch 130/0.4 on pulmonary capillary leakage and cytokines production and NF-kappaB activation in CLP-induced sepsis in rats. *J Surg Res* 135: 129–136, 2006.
29. Gadek JE, DeMichele SJ, Karlstad MD, Pacht ER, Donahoe M, Albertson TE, Van Hoozen C, Wennberg AK, Nelson JL, and Noursalehi M. Effect of enteral feeding with eicosapentaenoic acid, gamma-linolenic acid, and antioxidants in patients with acute respiratory distress syndrome. Enteral Nutrition in ARDS Study Group. *Crit Care Med* 27: 1409–1420, 1999.
30. Galley HF, Howdle PD, Walker BE, and Webster NR. The effects of intravenous antioxidants in patients with septic shock. *Free Radic Biol Med* 23: 768–774, 1997.
31. Gao XP, Standiford TJ, Rahman A, Newstead M, Holland SM, Dinauer MC, Liu QH, and Malik AB. Role of NADPH oxidase in the mechanism of lung neutrophil sequestration and microvessel injury induced by Gram-negative sepsis: studies in p47phox-/- and gp91phox-/- mice. *J Immunol* 168: 3974–3982, 2002.
32. Gaston B, Drazen JM, Loscalzo J, and Stamler JS. The biology of nitrogen oxides in the airways. *Am J Respir Crit Care Med* 149: 538–551, 1994.
33. Gole MD, Souza JM, Choi I, Hertkorn C, Malcolm S, Foust RF 3rd, Finkel B, Lanken PN, and Ischiropoulos H. Plasma proteins modified by tyrosine nitration in acute respiratory distress syndrome. *Am J Physiol Lung Cell Mol Physiol* 278: L961–L967, 2000.
34. Gonzalez PK, Zhuang J, Doctrow SR, Malfroy B, Benson PF, Menconi MJ, and Fink MP. Role of oxidant stress in the adult respiratory distress syndrome: evaluation of a novel antioxidant strategy in a porcine model of endotoxin-induced acute lung injury. *Shock* 6(suppl 1): S23–S26, 1996.
35. Goode HF, Cowley HC, Walker BE, Howdle PD, and Webster NR. Decreased antioxidant status and increased lipid peroxidation in patients with septic shock and secondary organ dysfunction. *Crit Care Med* 23: 646–651, 1995.
36. Guo RF, Lentsch AB, Sarma JV, Sun L, Riedemann NC, McClintock SD, McGuire SR, Van Rooijen N, and Ward PA. Activator protein-1 activation in acute lung injury. *Am J Pathol* 161: 275–282, 2002.
37. Guo RF, Riedemann NC, Laudes IJ, Sarma VJ, Kunkel RG, Dilley KA, Paulauskis JD, and Ward PA. Altered neutrophil trafficking during sepsis. *J Immunol* 169: 307–314, 2002.
38. Guo RF, Riedemann NC, Sun L, Gao H, Shi KX, Reuben JS, Sarma VJ, Zetoune FS, and Ward PA. Divergent signaling pathways in phagocytic cells during sepsis. *J Immunol* 177: 1306–1313, 2006.
39. Guo RF, Sun L, Gao H, Shi KX, Rittirsch D, Sarma VJ, Zetoune FS, and Ward PA. In vivo regulation of neutrophil apoptosis by C5a during sepsis. *J Leukoc Biol* 80: 1575–1583, 2006.
40. Guo RF and Ward PA. Mediators and regulation of neutrophil accumulation in inflammatory responses in lung: insights from the IgG immune complex model. *Free Radic Biol Med* 33: 303–310, 2002.
41. Hawkins HK, Heffelfinger SC, and Anderson DC. Leukocyte adhesion deficiency: clinical and postmortem observations. *Pediatr Pathol* 12: 119–130, 1992.
42. Hildebrand F, Pape HC, Harwood P, Muller K, Hoevel P, Putz C, Siemann A, Krettek C, and van Griensven M. Role of adhesion molecule ICAM in the pathogenesis of polymicrobial sepsis. *Exp Toxicol Pathol* 56: 281–290, 2005.
43. Ibbotson GC, Doig C, Kaur J, Gill V, Ostrovsky L, Fairhead T, and Kubes P. Functional alpha4-integrin: a newly identified pathway of neutrophil recruitment in critically ill septic patients. *Nat Med* 7: 465–470, 2001.
44. Imai Y, Kuba K, Rao S, Huan Y, Guo F, Guan B, Yang P, Sarao R, Wada T, Leong-Poi H, Crackower MA, Fukamizu A, Hui CC, Hein L, Uhlig S, Slutsky AS, Jiang C, and Penninger JM. Angiotensin-converting enzyme 2 protects from severe acute lung failure. *Nature* 436: 112–116, 2005.
45. Jarrar D, Kuebler JF, Rue LW, 3rd, Matalon S, Wang P, Bland KI, and Chaudry IH. Alveolar macrophage activation after trauma-hemorrhage and sepsis is dependent on NF-kappaB and MAPK/ERK mechanisms. *Am J Physiol Lung Cell Mol Physiol* 283: L799–L805, 2002.
46. Jiang ZY, Hunt JV, and Wolff SP. Ferrous ion oxidation in the presence of xylenol orange for detection of lipid hydroperoxide in low density lipoprotein. *Anal Biochem* 202: 384–389, 1992.
47. Jiang ZY, Woollard AC, and Wolff SP. Lipid hydroperoxide measurement by oxidation of Fe2+ in the presence of xylenol orange: comparison with the TBA assay and an iodometric method. *Lipids* 26: 853–856, 1991.
48. Kang JL, Park W, Pack IS, Lee HS, Kim MJ, Lim CM, and Koh Y. Inhaled nitric oxide attenuates acute lung injury via inhibition of nuclear factor-kappa B and inflammation. *J Appl Physiol* 92: 795–801, 2002.
49. Karamouzis MV, Konstantinopoulos PA, and Papavassiliou AG. The activator protein-1 transcription factor in respiratory epithelium carcinogenesis. *Mol Cancer Res* 5: 109–120, 2007.
50. Kobzik L, Bredt DS, Lowenstein CJ, Drazen J, Gaston B, Sugarbaker D, and Stamler JS. Nitric oxide synthase in human and rat lung: immunocytochemical and histochemical localization. *Am J Respir Cell Mol Biol* 9: 371–377, 1993.
51. Koksal GM, Sayilgan C, Aydin S, Oz H, and Uzun H. Correlation of plasma and tissue oxidative stresses in intra-abdominal sepsis. *J Surg Res* 122: 180–183, 2004.
52. Kolgazi M, Sener G, Cetinel S, Gedik N, and Alican I. Resveratrol reduces renal and lung injury caused by sepsis in rats. *J Surg Res* 134: 315–321, 2006.
53. Kuklin V, Kirov M, Sovershaev M, Andreasen T, Ingebretsen OC, Ytrehus K, and Bjertnaes L. Tezosentan-induced attenuation of lung injury in endotoxemic sheep is associated with reduced activation of protein kinase C. *Crit Care* 9: R211–R217, 2005.
54. Laudes IJ, Guo RF, Riedemann NC, Speyer C, Craig R, Sarma JV, and Ward PA. Disturbed homeostasis of lung intercellular adhesion molecule-1 and vascular cell adhesion molecule-1 during sepsis. *Am J Pathol* 164: 1435–1445, 2004.

55. Lentsch AB, Czermak BJ, Bless NM, Van Rooijen N, and Ward PA. Essential role of alveolar macrophages in intrapulmonary activation of NF-kappaB. *Am J Respir Cell Mol Biol* 20: 692–698, 1999.
56. Lentsch AB and Ward PA. Activation and regulation of NFkappaB during acute inflammation. *Clin Chem Lab Med* 37: 205–208, 1999.
57. Levine RL, Garland D, Oliver CN, Amici A, Climent I, Lenz AG, Ahn BW, Shaltiel S, and Stadtman ER. Determination of carbonyl content in oxidatively modified proteins. *Methods Enzymol* 186: 464–478, 1990.
58. Li QJ, Vaingankar S, Sladek FM, and Martins-Green M. Novel nuclear target for thrombin: activation of the Elk1 transcription factor leads to chemokine gene expression. *Blood* 96: 3696–3706, 2000.
59. Liaw WJ, Chen TH, Lai ZZ, Chen SJ, Chen A, Tzao C, Wu JY, and Wu CC. Effects of a membrane-permeable radical scavenger, Tempol, on intraperitoneal sepsis-induced organ injury in rats. *Shock* 23: 88–96, 2005.
60. Libon C, Forestier F, Cotte-Laffitte J, Labarre C, and Quero AM. Effect of acute oral administration of alcohol on superoxide anion production from mouse alveolar macrophages. *J Leukoc Biol* 53: 93–98, 1993.
61. Martin TR, Pistorese BP, Hudson LD, and Maunder RJ. The function of lung and blood neutrophils in patients with the adult respiratory distress syndrome: implications for the pathogenesis of lung infections. *Am Rev Respir Dis* 144: 254–262, 1991.
62. Meduri GU, Muthiah MP, Carratu P, Eltorky M, and Chrousos GP. Nuclear factor-kappaB- and glucocorticoid receptor alpha-mediated mechanisms in the regulation of systemic and pulmonary inflammation during sepsis and acute respiratory distress syndrome: evidence for inflammation-induced target tissue resistance to glucocorticoids. *Neuroimmunomodulation* 12: 321–338, 2005.
63. Mei N, Tamae K, Kunugita N, Hirano T, and Kasai H. Analysis of 8-hydroxydeoxyguanosine 5′-monophosphate (8-OH-dGMP) as a reliable marker of cellular oxidative DNA damage after gamma-irradiation. *Environ Mol Mutagen* 41: 332–338, 2003.
64. Metnitz PG, Bartens C, Fischer M, Fridrich P, Steltzer H, and Druml W. Antioxidant status in patients with acute respiratory distress syndrome. *Intensive Care Med* 25: 180–185, 1999.
65. Minnard EA, Shou J, Naama H, Cech A, Gallagher H, and Daly JM. Inhibition of nitric oxide synthesis is detrimental during endotoxemia. *Arch Surg* 129: 142–147; discussion 147–148, 1994.
66. Mohiuddin I, Chai H, Lin PH, Lumsden AB, Yao Q, and Chen C. Nitrotyrosine and chlorotyrosine: clinical significance and biological functions in the vascular system. *J Surg Res* 133: 143–149, 2006.
67. Molnar Z, Shearer E, and Lowe D. N-Acetylcysteine treatment to prevent the progression of multisystem organ failure: a prospective, randomized, placebo-controlled study. *Crit Care Med* 27: 1100–1104, 1999.
68. Morse D, Pischke SE, Zhou Z, Davis RJ, Flavell RA, Loop T, Otterbein SL, Otterbein LE, and Choi AM. Suppression of inflammatory cytokine production by carbon monoxide involves the JNK pathway and AP-1. *J Biol Chem* 278: 36993–36998, 2003.
69. Nagase T, Uozumi N, Aoki-Nagase T, Terawaki K, Ishii S, Tomita T, Yamamoto H, Hashizume K, Ouchi Y, and Shimizu T. A potent inhibitor of cytosolic phospholipase A2, arachidonyl trifluoromethyl ketone, attenuates LPS-induced lung injury in mice. *Am J Physiol Lung Cell Mol Physiol* 284: L720–L726, 2003.
70. Nathens AB, Neff MJ, Jurkovich GJ, Klotz P, Farver K, Ruzinski JT, Radella F, Garcia I, and Maier RV. Randomized, prospective trial of antioxidant supplementation in critically ill surgical patients. *Ann Surg* 236: 814–822, 2002.
71. Nava E, Palmer RM, and Moncada S. Inhibition of nitric oxide synthesis in septic shock: how much is beneficial? *Lancet* 338: 1555–1557, 1991.
72. Olea-Azar C, Rigol C, Mendizabal F, Morello A, Maya JD, Moncada C, Cabrera E, Di Maio R, Gonzalez M, and Cerecetto H. ESR spin trapping studies of free radicals generated from nitrofuran derivative analogues of nifurtimox by electrochemical and *Trypanosoma cruzi* reduction. *Free Radic Res* 37: 993–1001, 2003.
73. Paredi P, Kharitonov SA, and Barnes PJ. Analysis of expired air for oxidation products. *Am J Respir Crit Care Med* 166: S31–S37, 2002.
74. Parent C and Eichacker PQ. Neutrophil and endothelial cell interactions in sepsis: the role of adhesion molecules. *Infect Dis Clin North Am* 13: 427–447, 1999.
75. Quinlan GJ, Lamb NJ, Tilley R, Evans TW, and Gutteridge JM. Plasma hypoxanthine levels in ARDS: implications for oxidative stress, morbidity, and mortality. *Am J Respir Crit Care Med* 155: 479–484, 1997.
76. Rahman I, Biswas SK, Jimenez LA, Torres M, and Forman HJ. Glutathione, stress responses, and redox signaling in lung inflammation. *Antioxid Redox Signal* 7: 42–59, 2005.
77. Rahman I, Gilmour PS, Jimenez LA, Biswas SK, Antonicelli F, and Aruoma OI. Ergothioneine inhibits oxidative stress- and TNF-alpha-induced NF-kappa B activation and interleukin-8 release in alveolar epithelial cells. *Biochem Biophys Res Commun* 302: 860–864, 2003.
78. Rahman I, Gilmour PS, Jimenez LA, and MacNee W. Oxidative stress and TNF-alpha induce histone acetylation and NF-kappaB/AP-1 activation in alveolar epithelial cells: potential mechanism in gene transcription in lung inflammation. *Mol Cell Biochem* 234–235: 239-248, 2002.
79. Rahman I and Kelly F. Biomarkers in breath condensate: a promising new non-invasive technique in free radical research. *Free Radic Res* 37: 1253–1266, 2003.
80. Razavi HM, Wang L, Weicker S, Quinlan GJ, Mumby S, McCormack DG, and Mehta S. Pulmonary oxidant stress in murine sepsis is due to inflammatory cell nitric oxide. *Crit Care Med* 33: 1333–1339, 2005.
81. Razavi HM, Wang le F, Weicker S, Rohan M, Law C, McCormack DG, and Mehta S. Pulmonary neutrophil infiltration in murine sepsis: role of inducible nitric oxide synthase. *Am J Respir Crit Care Med* 170: 227–233, 2004.
82. Reddy RC, Chen GH, Newstead MW, Moore T, Zeng X, Tateda K, and Standiford TJ. Alveolar macrophage deactivation in murine septic peritonitis: role of interleukin 10. *Infect Immun* 69: 1394–1401, 2001.
83. Rocksen D, Ekstrand-Hammarstrom B, Johansson L, and Bucht A. Vitamin E reduces transendothelial migration of neutrophils and prevents lung injury in endotoxin-induced airway inflammation. *Am J Respir Cell Mol Biol* 28: 199–207, 2003.
84. Sarady-Andrews JK, Liu F, Gallo D, Nakao A, Overhaus M, Ollinger R, Choi AM, and Otterbein LE. Biliverdin administration protects against endotoxin-induced acute lung injury in rats. *Am J Physiol Lung Cell Mol Physiol* 289: L1131–1137, 2005.
85. Sener G, Toklu H, Ercan F, and Erkanli G. Protective effect of beta-glucan against oxidative organ injury in a rat model of sepsis. *Int Immunopharmacol* 5: 1387–1396, 2005.
86. Sener G, Toklu H, Kapucu C, Ercan F, Erkanli G, Kacmaz A, Tilki M, and Yegen BC. Melatonin protects against oxidative organ injury in a rat model of sepsis. *Surg Today* 35: 52–59, 2005.
87. Spapen HD, Diltoer MW, Nguyen DN, Hendrickx I, and Huyghens LP. Effects of N-acetylcysteine on microalbuminuria and organ failure in acute severe sepsis: results of a pilot study. *Chest* 127: 1413–1419, 2005.
88. Speyer CL, Gao H, Rancilio NJ, Neff TA, Huffnagle GB, Sarma JV, and Ward PA. Novel chemokine responsiveness and mobilization of neutrophils during sepsis. *Am J Pathol* 165: 2187–2196, 2004.
89. Speyer CL, Neff TA, Warner RL, Guo RF, Sarma JV, Riedemann NC, Murphy ME, Murphy HS, and Ward PA. Regulatory effects of iNOS on acute lung inflammatory responses in mice. *Am J Pathol* 163: 2319–2328, 2003.
90. Spitzer JA and Zhang P. Protein tyrosine kinase activity and the influence of gender in phagocytosis and tumor necrosis factor secretion in alveolar macrophages and lung-recruited neutrophils. *Shock* 6: 426–433, 1996.
91. Suliman HB, Ryan LK, Bishop L, and Folz RJ. Prevention of influenza-induced lung injury in mice overexpressing extracellular superoxide dismutase. *Am J Physiol Lung Cell Mol Physiol* 280: L69–L78, 2001.

92. Suntres ZE and Shek PN. The pulmonary uptake of intravenously administered liposomal alpha-tocopherol is augmented in acute lung injury. *J Drug Target* 4: 151–159, 1996.
93. Thimmulappa RK, Lee H, Rangasamy T, Reddy SP, Yamamoto M, Kensler TW, and Biswal S. Nrf2 is a critical regulator of the innate immune response and survival during experimental sepsis. *J Clin Invest* 116: 984–995, 2006.
94. Thimmulappa RK, Scollick C, Traore K, Yates M, Trush MA, Liby KT, Sporn MB, Yamamoto M, Kensler TW, and Biswal S. Nrf2-dependent protection from LPS induced inflammatory response and mortality by CDDO-Imidazolide. *Biochem Biophys Res Commun* 351: 883–889, 2006.
95. Thomassen MJ and Kavuru MS. Human alveolar macrophages and monocytes as a source and target for nitric oxide. *Int Immunopharmacol* 1: 1479–1490, 2001.
96. Vassilev D, Hauser B, Bracht H, Ivanyi Z, Schoaff M, Asfar P, Vogt J, Wachter U, Schelzig H, Georgieff M, Bruckner UB, Radermacher P, and Froba G. Systemic, pulmonary, and hepatosplanchnic effects of N-acetylcysteine during long-term porcine endotoxemia. *Crit Care Med* 32: 525–532, 2004.
97. Wan XS, Zhou Z, Ware JH, and Kennedy AR. Standardization of a fluorometric assay for measuring oxidative stress in irradiated cells. *Radiat Res* 163: 232–240, 2005.
98. Ware LB and Matthay MA. The acute respiratory distress syndrome. *N Engl J Med* 342: 1334–1349, 2000.
99. Warner RL, Paine R 3rd, Christensen PJ, Marletta MA, Richards MK, Wilcoxen SE, and Ward PA. Lung sources and cytokine requirements for in vivo expression of inducible nitric oxide synthase. *Am J Respir Cell Mol Biol* 12: 649–661, 1995.
100. Weiland JE, Davis WB, Holter JF, Mohammed JR, Dorinsky PM, and Gadek JE. Lung neutrophils in the adult respiratory distress syndrome: clinical and pathophysiologic significance. *Am Rev Respir Dis* 133: 218–225, 1986.
101. Weiss DJ and Lunte CE. Detection of a urinary biomarker for oxidative DNA damage 8-hydroxydeoxyguanosine by capillary electrophoresis with electrochemical detection. *Electrophoresis* 21: 2080–2085, 2000.
102. Winterbourn CC, Buss IH, Chan TP, Plank LD, Clark MA, and Windsor JA. Protein carbonyl measurements show evidence of early oxidative stress in critically ill patients. *Crit Care Med* 28: 143–149, 2000.
103. Zegdi R, Perrin D, Burdin M, Boiteau R, and Tenaillon A. Increased endogenous carbon monoxide production in severe sepsis. *Intens Care Med* 28: 793–796, 2002.
104. Zhang XW, Liu Q, Wang Y, and Thorlacius H. CXC chemokines, MIP-2 and KC, induce P-selectin-dependent neutrophil rolling and extravascular migration in vivo. *Br J Pharmacol* 133: 413–421, 2001.

Address reprint requests to:
Ren-Feng Guo, M.D.
Department of Pathology
The University of Michigan Medical School
1301 Catherine Road
Ann Arbor, MI 48109-0602

E-mail: grf@med.umich.edu

Date of first submission to ARS Central, June 15, 2007; date of acceptance, June 23, 2007.

This article has been cited by:

1. Erdogan Ozturk, Semra Demirbilek, Zekine Begec, Murat Surucu, Ersin Fadillioglu, Hale Kırımlıoglu, M. Ozcan Ersoy. 2008. Does leflunomide attenuate the sepsis-induced acute lung injury?. *Pediatric Surgery International* . [CrossRef]
2. Shyam Biswal , Daniel G. Remick . 2007. Sepsis: Redox Mechanisms and Therapeutic Opportunities. *Antioxidants & Redox Signaling* **9**:11, 1959-1962. [Citation] [PDF] [PDF Plus]

The Phosphatidylinositol 3-Kinase Signaling Pathway Exerts Protective Effects during Sepsis by Controlling C5a-Mediated Activation of Innate Immune Functions[1]

Christiane D. Wrann,[2]* Navid A. Tabriz,[2]* Tanja Barkhausen,* Andreas Klos,[‡] Martijn van Griensven,[†] Hans C. Pape,[§] Daniel O. Kendoff,* Renfeng Guo,[¶] Peter A. Ward,[¶] Christian Krettek,* and Niels C. Riedemann[3]*

The PI3K/Akt signaling pathway has been recently suggested to have controversial functions in models of acute and chronic inflammation. Our group and others have reported previously that the complement split product C5a alters neutrophil innate immunity and cell signaling during the onset of sepsis and is involved in PI3K activation. We report in this study that in vivo inhibition of the PI3K pathway resulted in increased mortality in septic mice accompanied by strongly elevated serum levels of TNF-α, IL-6, MCP-1, and IL-10 during sepsis as well as decreased oxidative burst activity in blood phagocytes. PI3K inhibition in vitro resulted in significant increases in TLR-4-mediated generation of various proinflammatory cytokines in neutrophils, whereas the opposite effect was observed in PBMC. Oxidative burst and phagocytosis activity was significantly attenuated in both neutrophils and monocytes when PI3K activation was blocked. In addition, PI3K inhibition resulted in strongly elevated TLR-4-mediated generation of IL-1β and IL-8 in neutrophils when these cells were costimulated with C5a. C5a-induced priming effects on neutrophil and monocyte oxidative burst activity as well as C5a-induced phagocytosis in neutrophils were strongly reduced when PI3K activation was blocked. Our data suggest that the PI3K/Akt signaling pathway controls various C5a-mediated effects on neutrophil and monocyte innate immunity and exerts an overall protective effect during experimental sepsis. ***The Journal of Immunology,*** **2007, 178: 5940–5948.**

During the early inflammatory response to invading microorganisms, crucial innate immune players such as neutrophils and monocytes are set into place to defend the host. During experimental sepsis, neutrophils are activated very early in the onset phase of the inflammatory response as first line of defense, contributing significantly to mediator generation, pathogen phagocytosis, and O^{2-} radical production. In various diseases related to acute inflammation, neutrophils are also thought to be responsible for host tissue damage and organ failure. However, during sepsis it is a well-described phenomenon that neutrophils undergo a status of immune paralysis with regard to their ability to fight invading microorganisms (1), setting the stage for super infection and for high lethality during sepsis (2), whereas the overall $t_{1/2}$ in the serum is prolonged. The latter observation could be explained by activation of the PI3K pathway in neutrophils (3, 4), which, during sepsis, could at least partially be due to generation of the complement split product C5a (5, 6).

During the onset of experimental sepsis, the complement system is activated via three well-known pathways, leading to generation of the potent inflammatory split product C5a. There is growing evidence for various harmful effects of C5a and C5aR activation during the onset of sepsis (1, 7, 8). Blockade of either C5a or C5aR leads to greatly improved survival in septic rodents (9–11). Earlier work suggested that C5a generation during sepsis plays a critical role for suppression of neutrophil innate immune functions (11–14). We recently demonstrated that C5a has a key function for altering intracellular signaling pathways in neutrophils in vitro and during the onset of sepsis in vivo (2, 15, 16), offering an explanation for the above-mentioned suppression of innate immune functions.

The PI3K signaling pathway, including the downstream Akt kinase, has been described as important inhibitory regulator of neutrophil apoptosis (3, 4). Recent work pointed out an important role of this signaling pathway for neutrophil respiratory burst (17, 18) as well as chemotaxis of neutrophils in response to fMLP (17, 19–21). Various studies then reported the importance of PI3K activation for neutrophil sequestration in inflamed tissue in different animal models (22–25). These results implicated an important role of this signaling pathway for the innate immune response during acute inflammation. We thought to investigate the regulatory potential of this pathway for TLR-4- and C5a-mediated activation of neutrophils and monocytes and for outcome in experimental sepsis.

Materials and Methods

Reagents

Human rC5a and other reagents were purchased from Sigma-Aldrich, if not otherwise indicated.

*Department of Trauma Surgery, Hannover Medical School, Hannover, Germany; [†]Ludwig Boltzmann Institute for Experimental and Clinical Traumatology, Vienna, Austria; [‡]Department of Medical Microbiology, Hannover Medical School, Hannover, Germany; [§]Department of Orthopedic Surgery, Division Orthopedic Traumatology, University of Pittsburgh, Pittsburgh, PA 15213; and [¶]Department of Pathology, University of Michigan Medical School, Ann Arbor, MI 48109

Received for publication October 27, 2006. Accepted for publication February 20, 2007.

The costs of publication of this article were defrayed in part by the payment of page charges. This article must therefore be hereby marked *advertisement* in accordance with 18 U.S.C. Section 1734 solely to indicate this fact.

[1] This work was supported by Hochschulinterne Leistungsfoerderung-1 Grant (Hannover Medical School, Hannover, Germany) and by Deutsche Forschungsgemeinschaft Grant RI 1216/4-1 (German Research Council (Deutsche Forschungsgemeinschaft)).

[2] C.D.W. and N.A.T. contributed equally to this work.

[3] Address correspondence and reprint requests to Dr. Niels C. Riedemann, Department of Trauma Surgery, Medizinische Hochschule Hannover, Carl Neuberg Strasse 1, 30625 Hannover, Germany. E-mail address: nriedeman@yahoo.com

Neutrophil and PBMC isolation from whole blood and in vitro stimulation

EDTA/heparin was used as an anticoagulant for the isolation of human neutrophils and PBMC from blood. After Ficoll-Paque gradient centrifugation (Biocoll; Biochrom), PBMC were collected from the buffy coat and neutrophils were separated from the pellet by dextrane (Roth) sedimentation. Hypotonic RBC lysis was achieved, using sterile H_2O. Neutrophils were resuspended in DMEM containing 10% FCS (Biochrom). A final concentration of 6×10^6 cells/ml was used for stimulation at 37°C and 5% CO_2 for the times indicated with C5a (50 or 200 ng/ml) or LPS (20, 50, or 100 ng/ml), or both. Supernatant fluids were collected after pelleting of the cells and frozen at −80°C until used for ELISA analysis. For certain experiments, neutrophils were preincubated for 30 min with 50 μM PI3K inhibitor LY294002 (New Englands Biolabs), which inhibits downstream phosphorylation of the Akt pathway.

Western blot analysis

Neutrophils were isolated from human blood and stimulated at 37°C in vitro with human rC5a (10–100 ng/ml) or LPS (50 ng/ml), or both. Approximately 2×10^6 cells per condition were then used for whole cell lysis using Laemmli buffer containing 5% 2-ME. Lysates were separated on a NuPAGE 4–12% Bis-Tris gel (Invitrogen Life Technologies), and proteins were then transferred to a nitrocellulose membrane. Membranes were incubated overnight with Abs to phosphorylated and nonphosphorylated human/rat Akt, FKHR,[4] glycogen synthase kinase (GSK)-3β, phosphatase and tensin homolog deleted on chromosome 10, and phosphoinositide-dependent protein kinase 1 (New Englands Biolabs). For detection of the protein, ECL plus was used (Amersham Biosciences), according to the manufacturer's instructions.

Quantitation of IL-6, TNF-α, IL-1β, IL-12, IL-10, and IL-8 in cell supernatants

Neutrophils were isolated from human whole blood, as outlined above, and stimulated at 37°C in vitro with human rC5a (50 or 200 ng/ml) or LPS (50 ng/ml), or both for 6 h in an incubator with 5% CO_2 under sterile conditions. Cell supernatants were than isolated and frozen at −80°C until analyzed for various mediators using a commercially available flow cytometric bead assay, according to the manufacturer's instructions (BD Biosciences). For IL-8 ELISA experiments were conducted using a commercially available IL-8 ELISA kit, according to the manufacturer's instructions (BioSource International).

Cecum ligation and puncture (CLP) in mice and inhibition of the PI3K/Akt pathway in vivo

Specific pathogen-free C57BL/6 mice (Own Laboratories, Zentrales Tierlabor Medizinische Hochschule Hannover) were used for all CLP studies. Anesthesia was achieved by i.p. injection of ketamine (Ketanest; Pfizer) and xylazine (Rompun; Bayer). In the CLP model, approximately two-thirds of the cecum was ligated through a 3-cm abdominal midline incision. The ligated part of the cecum was punctured through and through with a 21-gauge needle. After repositioning of the bowel, the abdomen was closed in layers, using a 4.0 surgical suture (Ethicon) and metallic clips. For inhibition of the PI3K/Akt signaling pathway in vivo, a specific inhibitor (LY294002; New Englands Biolabs) was diluted in 200 μl of Dulbecco's PBS (DPBS) solution and injected into the penal vein of mice immediately following CLP to achieve a total blood concentration of 50 μM. Control animals received 200 μl of DPBS, including equal amounts of DMSO, also immediately after CLP. All animal studies were reviewed and approved by the local ethic committee of the state of Lower Saxony, Germany.

Collection of serum samples in mice

After induction of CLP, animals were sacrificed at the indicated time points and blood was drawn from the inferior caval vein. Blood samples were allowed to clot at 5°C for 6 h before centrifugation at 4000 rpm for 15 min at 4°C. Serum was collected and immediately frozen at −80°C until used for ELISA analysis. For experiments using the flow cytometric analysis of oxidative burst in neutrophils and monocytes from whole blood in mice, animals were treated with LY294002, as outlined earlier, and were then sacrificed 90 min thereafter. Next, blood was drawn from the inferior caval vein, and 100 μl of mouse whole blood was used for further flow cytometric analysis of oxidative burst activity, as outlined in the section below. Heparin was used as anticoagulant.

Quantitation of IL-6, TNF-α, IL-10, MCP-1, IL-12, IFN-γ, and keratinocyte-derived chemokine (KC) in serum samples

Serum samples were collected, as outlined above. For quantification of various mediators, a commercially available flow cytometric bead assay was performed, according to the manufacturer's instructions (BD Biosciences). For quantification of mouse KC ELISA experiments were conducted using a commercially available mouse KC ELISA kit, according to the manufacturer's instructions.

Quantitation of oxidative burst and phagocytosis in whole blood cells

To determine the ability of blood neutrophils and monocytes to generate oxygen radicals and to conduct phagocytosis, commercially available flow cytometry-based assays were used, according to the manufacturer′s instructions (Phagoburst, Phagotest; ORPEGEN Pharma). The Phagoburst assays use dihydrorhodamine 123 as a fluorogenic substrate and determine the percentage of active cells and their enzymatic activity/degree of activity. For Phagotest analysis, whole blood samples were incubated with FITC-labeled *Escherichia coli* bacteria (3.3×10^7 bacteria/ml) for 10 min in a 37°C warm water bath. Leukocyte surface-bound bacteria were neutralized using quenching solution. Cells were analyzed in a FACSCalibur flow cytometer (BD Biosciences). In a forward/side scatter dot plot, gates were set on granulocytes and monocytes to analyze each population with regard to mean fluorescence intensity (MFI). For oxidative burst measurement in mouse whole blood, samples were collected after inhibitor treatment, as described earlier, and then stimulated with PMA (1.4 μM) for 10 min in a 37°C water bath and processed according to the same protocol explained in this paragraph.

In vitro stimulation of oxidative burst and phagocytosis in blood phagocytes

Heparinized human whole blood was preincubated for 30 min with 50 μM PI3K inhibitor LY294002 (New England Biolabs) or with an equal amount of the vehicle (DMSO) at 37°C and 5% CO_2. Human rC5a was then added at different concentrations (1–10,000 ng/ml), and the blood was further incubated for different time periods (10, 20, and 60 min). In one set of experiments, the cells were then stimulated with either unlabeled opsonized bacteria (*E. coli*) (6.7×10^8 bacteria/ml), PMA (1.4 μM), or the chemotactic peptide fMLP (0.8 μM) for 10 min in a 37°C water bath and processed afterward, according to the protocol explained above. In another set of experiments, the cells were processed immediately after C5a incubation with no further stimulation.

Assessment of bacterial growth in the peritoneal cavity during CLP-induced sepsis in mice

Sepsis was induced with CLP, and animals were treated with or without LY294002, according to the explained protocol, before being sacrificed at 6 h after CLP. The peritoneal cavity was lavaged with 10 ml of sterile 0.9% NaCl. Samples were diluted serially in 0.9% NaCl and incubated in parallel on Columbia 5% sheep blood plates, McConkey plates, and Slanetz-Bartley *Enterococci*-specific indicator plates for 24 h in aerobic atmosphere. The resulting bacterial colonies were further analyzed by biochemical assays, counted, and expressed as CFU per sample.

Statistical analysis

All values were expressed as the mean ± SEM. Significance was assigned where $p < 0.05$. Data sets were analyzed using Student's t test or using one-way ANOVA, with individual group means being compared with the Tukey multiple comparison test. Statistical analysis for survival studies was performed using proportional hazards modeling. The software used was GraphPad Prism 3.0 (GraphPad).

Results

Impact of PI3K/Akt inhibition on outcome during sepsis in mice

To determine whether inhibition of the PI3K/Akt pathway had effects on outcome during experimental sepsis in rodents, we conducted CLP experiments in mice receiving either 200 μl of DPBS as control or 200 μl of DPBS containing the PI3K inhibitor LY294002 to achieve a serum concentration of 50 μM. Mice were followed up for 7 days and monitored every 6 h for various signs

[4] Abbreviations used in this paper: FKHR, forkhead-related transcription factor; CLP, cecum ligation and puncture; DPBS, Dulbecco's PBS; GSK, glycogen synthase kinase; KC, keratinocyte-derived chemokine; MFI, mean fluorescence intensity.

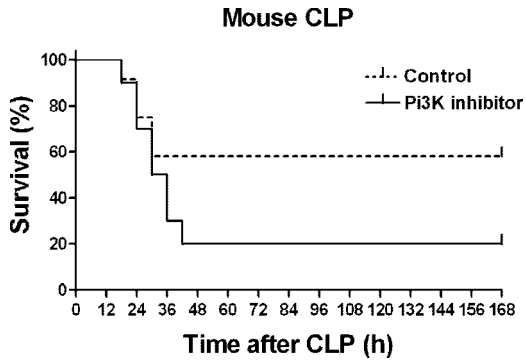

FIGURE 1. Effect of PI3K inhibition on outcome in experimental sepsis CLP study in C57BL/6 mice. CLP was induced with a 21-gauge needle and a two-thirds ligation of the cecum. CLP was induced and mice were treated with LY294002 directly after CLP by penal vein injection with 200 μl of DPBS containing body weight-adjusted concentrations of LY294002 to reach a calculated serum concentration of ~50 μM. Control groups were treated equally with 200 μl of DPBS containing no inhibitor. Experiments were conducted with $n = 12$ animals per group.

of sickness. The group of mice receiving LY294002 demonstrated significantly reduced survival as well as earlier and more severe onset of sepsis (Fig. 1) when compared with the control group. These results demonstrated an overall protective effect mediated by the PI3K/Akt signaling pathway during the onset of sepsis.

Impact of in vivo PI3K/Akt pathway inhibition on cytokine generation during sepsis and on burst activity in phagocytes

We conducted CLP experiments in mice receiving either 200 μl of DPBS as control or 200 μl of DPBS containing the PI3K inhibitor LY294002 to achieve an intravascular concentration of 50 μM, as described in *Materials and Methods*. Six hours after induction of sepsis, blood was drawn from the caval vein, followed by exsanguinations of the animals. Serum samples were prepared and analyzed for presence of various mediators using a flow cytometric bead assay. As depicted in Fig. 2*A*, significantly higher serum levels were found in LY294002-treated animals for TNF-α, IL-6, IL-10, and MCP-1, when compared with control mice. For KC, a tendency toward higher levels in LY294002-treated mice (mean value 33,833 pg/ml) was observed when compared with control mice (mean value 26,998 pg/ml), which was not found to be statistically significant. No differences were found for IL-12 and IFN-γ (data not shown). These results demonstrated an inhibitory function of the PI3K/Akt pathway for generation of crucial inflammatory mediators such as TNF-α and IL-6 during the onset phase of sepsis, suggesting an overall negative feedback mechanism on inflammation in this model. We further investigated the effect of in vivo inhibition of the PI3K pathway on oxidative burst in neutrophils and monocytes in a whole blood assay. Mice were treated with 200 μl of DPBS containing LY294002 (50 μM serum concentration) or no inhibitor. Heparinized whole blood samples were drawn 90 min after treatment and stimulated with PMA (1.4 μM) for 10 min. The inhibitor treatment resulted in a significant decrease of burst activity in both cell populations, neutrophils and monocytes (Fig. 2*B*), demonstrating in vivo activity of the administered PI3K inhibitor. The number of bursting cells was not affected (data not shown).

Effect of PI3K/Akt inhibition on bacterial growth in the peritoneal cavity during sepsis

Six hours after induction of sepsis and inhibitor treatment with or without LY294002, peritoneal lavage fluids were collected from the mice and cultured and bacterial counts were determined as

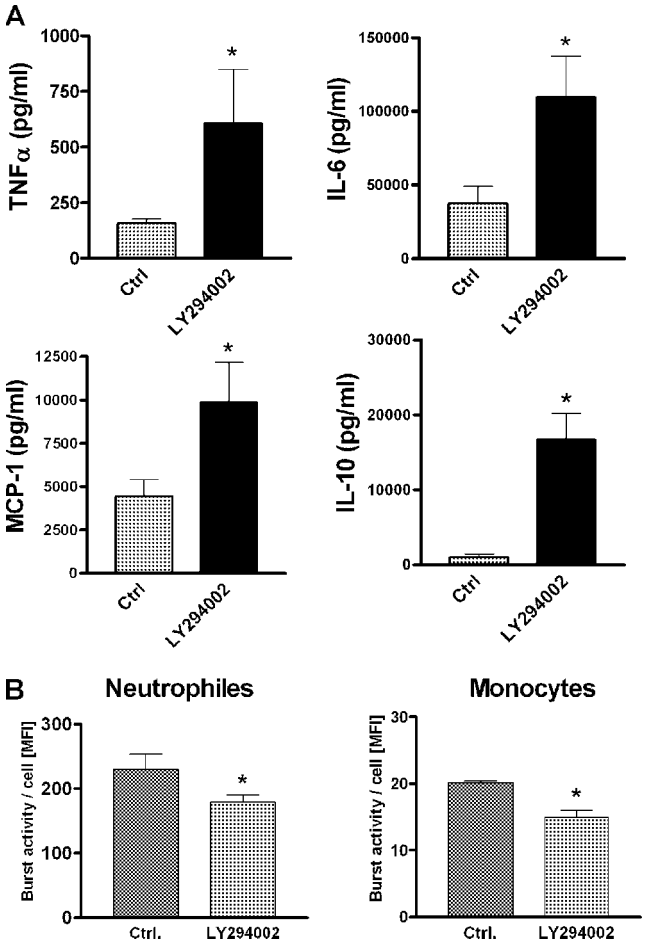

FIGURE 2. Impact of in vivo PI3K/Akt pathway inhibition on cytokine generation during sepsis and on burst activity in phagocytes. *A*, Flow cytometric bead ELISA of serum samples from septic animals. Animals underwent CLP and were treated with 200 μl of DPBS containing LY294002 (50 μM serum concentration) or no inhibitor directly after CLP. Blood serum samples were drawn 6 h after induction of CLP. The symbol * indicates statistical significant difference from the control group. Data are representative for five to seven animals per group. *B*, Flow cytometric analysis of oxidative burst in whole blood samples gated for neutrophil and monocyte cell populations. Animals were treated with 200 μl of DPBS containing LY294002 (50 μM serum concentration) or no inhibitor. Heparinized whole blood samples were drawn 90 min after treatment and stimulated with PMA (1.4 μM) for 10 min. Fifty thousand cells were analyzed for each experimental point. Oxidative burst activity per single cell is depicted as MFI. Neutrophils are shown in the *left panel* and monocytes in the *right panel*. *, Statistical significant difference from the control group. Data are representative for three to five animals per group.

CFU after 24 h of incubation. The dominating bacteria found in all samples were *Enterococci* spp.; *Staphylococci* and *Lactobacillus* spp. were also detected to a lesser extent in most samples. No statistical significant difference in CFU counts of *Enterococci* spp. could be detected in the LY294002-treated group when compared with the vehicle control group (data not shown). Also, no significant differences in the variety of other bacteria were detected. These results suggested that PI3K inhibition resulted in adverse effects on outcome in septic mice most likely triggered by impaired innate immune functions rather than by direct effects on bacterial growth.

Role of the PI3K/Akt pathway on LPS-induced cytokine generation in neutrophils and PBMC

An earlier study has described the involvement of the PI3K pathway in LPS/TLR-4-dependent TNF-α generation in PBMC,

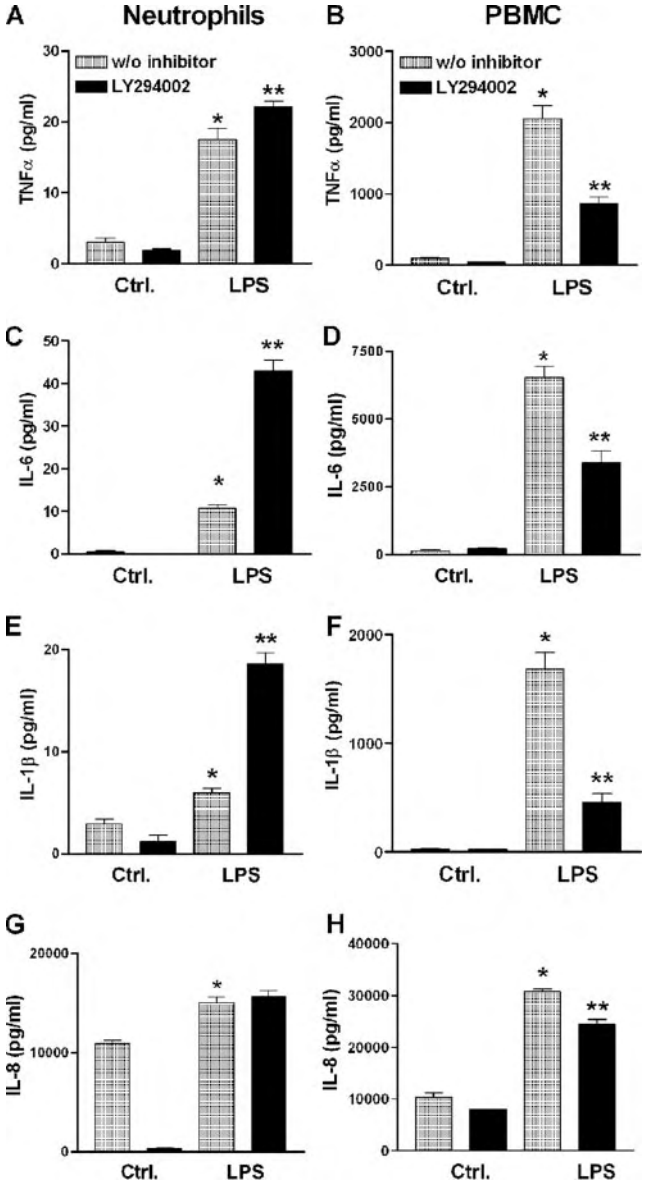

FIGURE 3. Effects of PI3K inhibition on LPS-induced mediator generation in human neutrophils (*A*, *C*, *E*, *G*) and PBMC (*B*, *D*, *F*, *H*) in vitro. Flow cytometric bead ELISA of neutrophil and PBMC supernatant fluids. Neutrophils and PBMC were isolated from whole blood and incubated in vitro with LPS (50 ng/ml) or medium control for 6 h at 37°C at a concentration of 6×10^6 cells/ml. Cells were stimulated in the absence or presence of LY294002 after preincubation for 30 min at a concentration of 50 μM. *, Statistical significant difference from the control group; **, statistical significant difference from the LPS-treated group with no inhibitor. Data are representative of three to four independent experiments, with incubation and analysis being conducted in separate triplicate or quadruplicate samples.

demonstrating reduction of LPS-induced TNF-α generation after PI3K inhibition (26), suggesting a promoting effect of PI3K for TNF-α generation. Because we found in vivo strongly elevated mediator levels 6 h after CLP in serum samples of mice, we thought to investigate LPS-induced in vitro generation of various mediators in neutrophils and PBMC after 6 h of stimulation. Interestingly, we observed that in neutrophils the proinflammatory mediators TNF-α, IL-6, and IL-1β were significantly increased when PI3K activity was inhibited (Fig. 3, *A*, *C*, *E*, and *G*), whereas the opposite effect could be seen in PBMC (Fig. 3, *B*, *D*, *F*, and *H*),

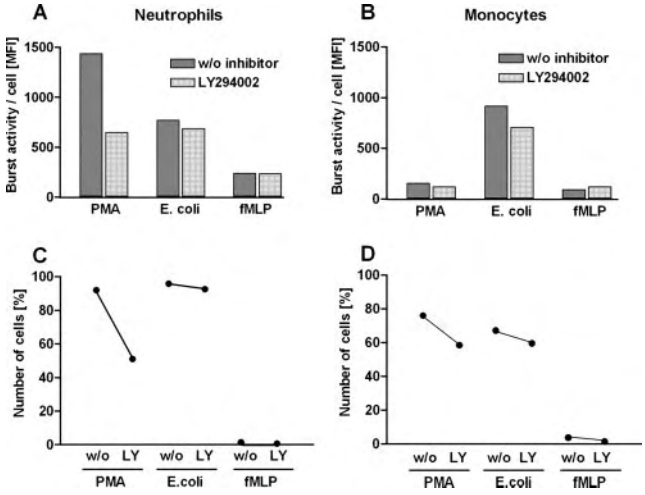

FIGURE 4. Effects of PI3K inhibition on oxidative burst in neutrophils and monocytes in human whole blood. Flow cytometric analysis of oxidative burst in whole blood samples gated for neutrophil and monocyte cell populations. Fifty thousand cells were analyzed for each experimental point. Human whole blood samples were preincubated with LY294002 (50 μM) or equal amounts of vehicle control and then stimulated with either PMA (1.4 μM), *E. coli* bacteria (6.7×10^8/ml), or fMLP (0.8 μM) for 10 min. Oxidative burst activity per single cell is depicted as MFI (*A* and *B*), and numbers of bursting cells are shown in percentages (*C* and *D*). Data are representative of two to three independent experiments per graph.

suggesting an inhibitory potential of this signaling pathway for LPS-induced neutrophil mediator generation and a stimulatory function in PBMC. However, under in vivo conditions as described above, an overall inhibitory function of the PI3K pathway was dominating, with respect to TNF-α, IL-6, but also IL-10 and MCP-1 generation, as described earlier.

Effects of PI3K inhibition on oxidative burst in neutrophils and monocytes in vitro

We investigated the role of the PI3K pathway on oxidative burst in neutrophils and monocytes in a whole blood assay, as described in *Materials and Methods*. Whole blood samples were preincubated with 50 μM LY294002 for 30 min, and oxidative burst was then stimulated with PMA, *E. coli*, as well as fMLP. PI3K inhibition resulted in a strong reduction of PMA- and *E. coli*-induced oxidative burst in neutrophils and in monocytes (Fig. 4, *A* and *B*), as well as in reduction of the number of cells initiating oxidative burst (Fig. 4, *C* and *D*). The latter effect was more apparent in PMA-induced oxidative burst when compared with *E. coli* as stimulus, especially in neutrophils (Fig. 4*C*). PMA appeared to be the strongest stimulus for neutrophils, whereas in monocytes, *E. coli* achieved a stronger stimulation of oxidative burst. The induction of oxidative burst by fMLP resulted in only minor initiation of oxidative burst in neutrophils and monocytes. Also, no inhibitory effects could be seen after PI3K inhibition when cells were stimulated with fMLP. Earlier studies have suggested a stimulatory effect of PI3K for fMLP-induced oxidative burst in isolated neutrophils in vitro (17), which could not be confirmed in this whole blood assay (Fig. 4*A*). Our data suggest an overall promoting effect of the PI3K pathway on PMA- and *E. coli*-induced oxidative burst in neutrophils and monocytes.

Effects of PI3K inhibition on phagocytosis activity in neutrophils and monocytes in vitro

We further thought to investigate whether PI3K inhibition would also affect phagocytosis in neutrophils and monocytes. Whole

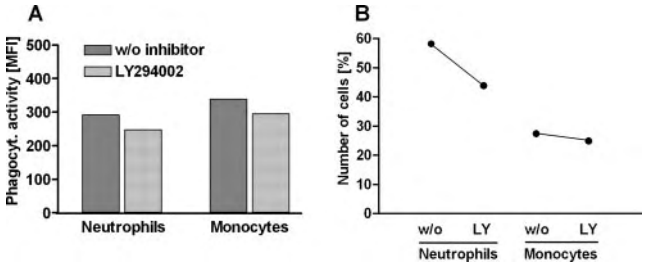

FIGURE 5. Effects of PI3K inhibition on *E. coli*-induced phagocytosis in neutrophils and monocytes in human whole blood. Human whole blood samples were preincubated with LY294002 (50 μM) or equal amounts of vehicle control and then stimulated with opsonized FITC-conjugated *E. coli* bacteria (3.3×10^7/ml) for 10 min. Fifty thousand cells were analyzed for each experimental point. Phagocytosis activity per single cell is depicted as MFI (*A*), and numbers of bursting cells are shown in percentages (*B*). Data are representative of three independent experiments.

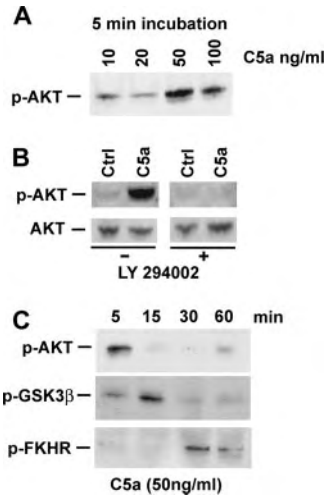

FIGURE 6. Activation of the PI3K pathway in human neutrophils by C5a. Western blot analysis of Akt activation (phosphorylation) in whole cell lysates of human neutrophils. *A*, Cells were stimulated at 37°C for 5 min with various concentrations of C5a, as depicted. *B*, Cells were stimulated for 5 min at 37°C in the absence or presence of 50 μm LY294002. *C*, Western blot analysis of Akt, GSK-3β, and FKHR activation in whole cell lysates of isolated human neutrophils. Cells were stimulated at 37°C with C5a (50 ng/ml) for various time points, as depicted. The blots are representative of two to three independent experiments.

blood samples were collected from healthy donors and subjected to PI3K inhibition by preincubation for 30 min with 50 μM LY249002 or control containing PBS and equal amounts of DMSO. PI3K inhibition clearly attenuated *E. coli*-induced phagocytosis activity in both neutrophils and monocytes (Fig. 5*A*), as well as the total number of phagocytosing cells (Fig. 5*B*), with the latter effect being less prominent in monocytes. Our data suggest a promoting effect of the PI3K signaling pathway for neutrophil and monocyte phagocytosis activity.

Activation of the PI3K/Akt signaling pathway in neutrophils by C5a

It has been described recently that C5a activates the PI3K/Akt signaling pathway in neutrophils in vitro, which could be linked to inhibition of apoptosis in neutrophils (4, 5). In monocytes, LPS-induced phosphorylation of Akt, Raf-1, and GSK-3β has been described before (26). The c-Raf kinase is known to initiate MEK1/2 phosphorylation, thereby initiating activation of the ERK1/2 MAPK pathway. The c-Raf kinase therefore represents an important link between Akt and ERK1/2 MAPK signaling pathways. Another group has described recently that, in macrophages, C5a induces PI3K/Akt activation, leading to downstream activation of ERK1/2 (27). Our group demonstrated earlier rapid phosphorylation of Akt in neutrophils upon stimulation with C5a (2). We thought to investigate in further detail the activation patterns of C5a within the PI3K/Akt signaling pathway in neutrophils. We conducted in vitro studies stimulating isolated human neutrophils with C5a at various time points and various concentrations (Fig. 6). We found that C5a was capable of inducing Akt phosphorylation within 2–15 min, peaking at 5-min activation (data not shown). Concentrations of 50–100 ng/ml C5a demonstrated the strongest Akt phosphorylation potential (Fig. 6*A*). Blockade of the PI3K with LY294002 resulted in complete inhibition of Akt phosphorylation (Fig. 6*B*). We investigated upstream and downstream activation within the Akt signaling pathway induced by C5a. We found that C5a induced phosphorylation of GSK-3β as well as the forkhead kinase family member FKHR in a time-dependent manner (Fig. 6*C*). Induction of the known negative regulator of Akt activation, the so-called phosphatase and tensin homolog deleted on chromosome 10, could also not be detected (data not shown).

Role of PI3K inhibition for C5a-mediated effects on LPS-induced generation of IL-1β and IL-8 in neutrophils

A recent report described C5a as negative regulator for IL-12 generation in human monocytes, with this effect being dependent on C5a-induced PI3K/Akt activation (28). Our group described various regulatory effects of C5a on neutrophil mediator generation in concert with LPS-induced TLR-4 stimulation (2, 15, 16). We thought to investigate in greater detail the involvement of PI3K activation for LPS-induced mediator generation in neutrophils in vitro. Human neutrophils were isolated from blood and incubated for 6 h in vitro with C5a (50 ng/ml), LPS (50 ng/ml), or both in the absence or presence of the PI3K inhibitor LY294002 (Fig. 7). Stimulation of neutrophils with C5a alone did not result in significant generation of IL-1β (Fig. 7*A*). LPS stimulation resulted in minor generation of IL-1β, which was increased when PI3K signaling was absent. Costimulation of neutrophils with C5a and LPS per se did not result in significant increase of IL-1β generation

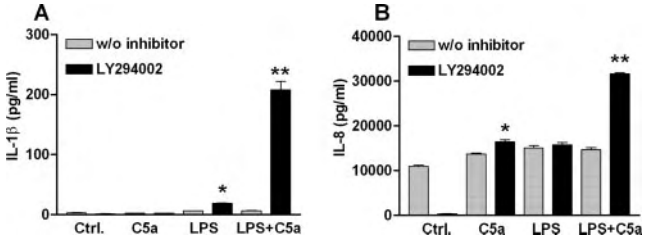

FIGURE 7. Effects of PI3K inhibition on C5a-mediated modulation of TLR-4-dependent generation of IL-1β and IL-8 in human neutrophils. Flow cytometric bead ELISA of neutrophil supernatant fluids for IL-1β (*A*) and IL-8 (*B*). Neutrophils were isolated from whole blood and incubated in vitro with C5a (50 ng/ml), LPS (50 ng/ml), or both for 6 h at 37°C at a concentration of 6×10^6 cells/ml. Cells were stimulated in the absence or presence of LY294002 after preincubation for 30 min at a concentration of 50 μM. *, Statistical significant difference from the corresponding single treatment group (LPS and C5a, respectively) without LY294002. **, Statistical significant difference from the LPS + C5a-costimulated treatment group with no inhibitor. Data are representative of two to three independent experiments, with incubation and analysis being conducted in separate triplicate or quadruplicate samples.

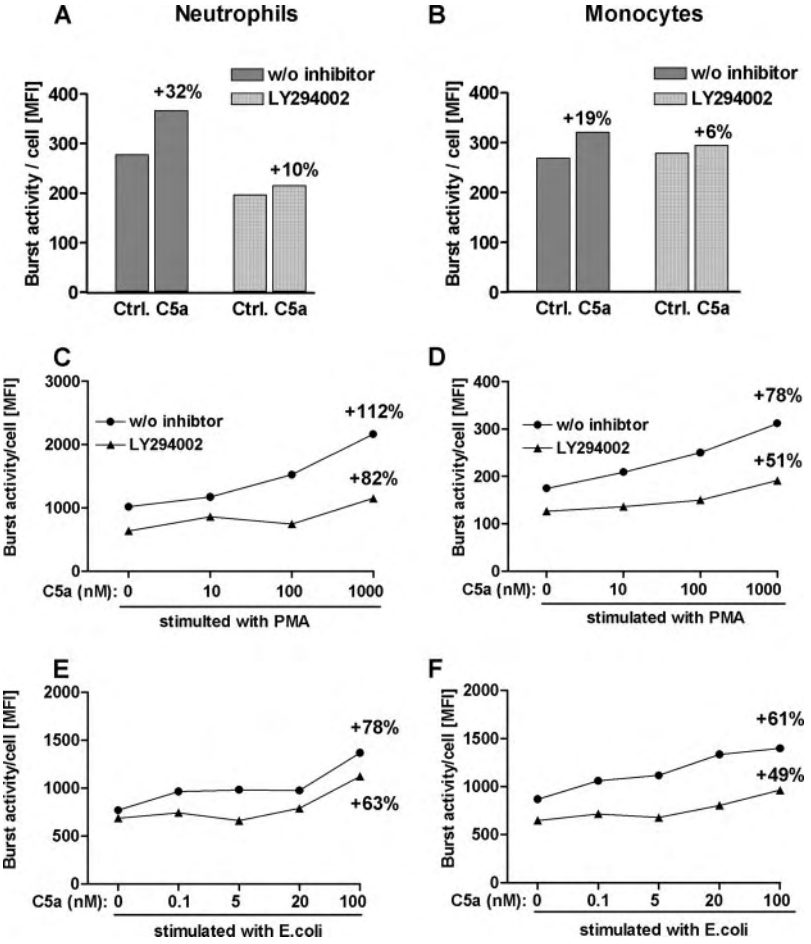

FIGURE 8. Effects of PI3K inhibition on C5a-mediated modulation of oxidative burst in neutrophils and monocytes in human whole blood. Flow cytometric analysis of oxidative burst in whole blood samples gated for neutrophil and monocyte cell populations. Fifty thousand cells were analyzed for each experimental point. *A* and *B*, Human whole blood samples were preincubated with LY294002 (50 μM) or equal amounts of vehicle. Samples were then incubated with or without C5a (100 ng/ml) for 60 min, and oxidative burst was measured with no further stimulation. *C–F*, Whole blood samples were preincubated with or without LY294002 (50 μM) for 30 min and then incubated with different concentrations of C5a (0–10,000 ng/ml) for 20 min before final stimulation with either PMA (1.4 μM) (*C* and *D*) or *E. coli* bacteria (6.7×10^8/ml) (*E* and *F*) for 10 min. Oxidative burst activity per single cell is depicted as MFI. Percentages of the maximum increase in oxidative burst activity are calculated compared with control values (0 C5a) and depicted on the *right panels* of the curves. Data are representative of two to three independent experiments.

when compared with LPS-only stimulated cells. This changed dramatically, under conditions of PI3K inhibition. A similar phenomenon could be observed for generation of IL-8 (Fig. 7*B*). PI3K inhibition attenuated baseline IL-8 generation completely. This effect was counteracted by stimulation with C5a or LPS. The latter stimulation led to small, but significant increases in IL-8 generation after PI3K signaling was inhibited, when compared with C5a- or LPS-stimulated neutrophils undergoing no PI3K inhibition. Costimulation of neutrophils with LPS and C5a after PI3K blockade resulted in significantly enhanced IL-8 generation when compared with cells with intact PI3K signaling. These results suggested that the PI3K signaling pathway exerts an important inhibitory control function for C5a-mediated boost of TLR-4-dependent generation of the proinflammatory mediator IL-1β and the potent chemoattractant IL-8.

Role of PI3K inhibition for C5a-mediated effects on oxidative burst generation in neutrophils and monocytes

Generation of oxidative burst represents a crucial function of the innate immune response to invading microorganisms. We thought to investigate the effect of PI3K inhibition on C5a-mediated oxidative burst and on C5a-mediated priming effects in human neutrophils and monocytes. We found that C5a induced oxidative burst in neutrophils and monocytes with regard to the intensity of burst activity per cell (Fig. 8, *A* and *B*), whereas only small effects could be observed on the total number of bursting cells (data not shown). When PI3K activation was inhibited, the observed increase was almost completely abolished in neutrophils and strongly reduced in monocytes, demonstrating involvement of this signaling pathway in C5a-mediated oxidative burst. We further investigated whether C5a-mediated priming of oxidative burst was dependent on PI3K activation (Fig. 8, *C–F*). Whole blood samples were preincubated with or without LY294002 for 30 min and than treated with various concentrations of C5a for 20 min before being stimulated with either PMA or *E. coli*. PMA-induced oxidative burst was strongly primed by preincubation with C5a in both neutrophils and monocytes (Fig. 8, *C* and *D*). This effect was strongly reduced in both cell populations when PI3K activation was inhibited, suggesting PI3K dependency of this C5a-mediated priming effect for PMA-induced oxidative burst. Similar experiments were conducted using *E. coli* as stimulus for oxidative burst. Low concentrations of C5a (1 ng/ml) achieved a noticeable priming effect for *E. coli*-induced oxidative burst in neutrophils and monocytes (Fig. 8, *E* and *F*). This effect was clearly reduced when PI3K activation was inhibited. However, in neutrophils, preincubation with high doses of C5a (1000 ng/ml) resulted in strongly increased *E. coli*-induced oxidative burst even after inhibition of PI3K activation (Fig. 8*D*), suggesting another pathway being responsible for priming effects induced by high-dose C5a preincubation before *E. coli* stimulation. Similarly, in monocytes, the C5a-induced priming effect for higher doses of C5a (200–1000 ng/ml) was only slightly inhibited when PI3K activation was blocked (Fig. 8*F*).

Role of PI3K inhibition for C5a-mediated effects on phagocytosis in neutrophils and monocytes

The ability of neutrophils and monocytes to conduct phagocytosis represents another crucial function of the innate immune response, which has also been demonstrated to be strongly dependent on C5a/C5aR (29), as well as on C5a and activating FcγR in Kupffer cells (30). We thought to investigate whether C5a effects on

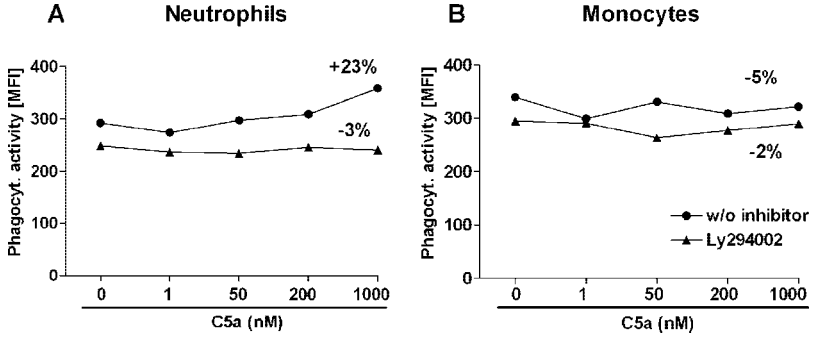

FIGURE 9. Effects of PI3K inhibition on C5a-mediated priming of *E. coli*-induced phagocytosis in neutrophils and monocytes in human whole blood. Flow cytometric analysis of phagocytosis in whole blood samples gated for neutrophil and monocyte cell populations. Fifty thousand cells were analyzed for each experimental point. Samples were preincubated with LY294002 (50 μM) or equal amounts of vehicle control, and then incubated with different concentrations of C5a (0–1000 ng/ml) for 60 min before being stimulated for 10 min with opsonized FITC-conjugated *E. coli* bacteria (3.3×10^6/ml). The phagocytosis activity per single cell of neutrophils (*A*) and monocytes (*B*) is given as MFI. Percentages of the maximum increase in phagocytosis activity are calculated compared with control values (0 C5a) and depicted on the *right panels* of the curves. Data are representative of two to three independent experiments.

E. coli-induced phagocytosis were dependent on PI3K signaling in neutrophils and monocytes. Preincubation of neutrophils with C5a resulted in dose-dependent enhancement of the phagocytic process induced by attenuated *E. coli* bacteria. This effect was completely abolished, when the PI3K signaling pathway was blocked, suggesting a strong dependency of this C5a-mediated priming effect on intact PI3K signaling (Fig. 9*A*). These findings could not be seen in monocytes applying the same experimental setting and assay (Fig. 9*B*). The number of phagocytosing cells was not considerably affected by C5a in both neutrophils and monocytes (data not shown).

Discussion

The PI3K/Akt signaling pathway has been suggested before to exert protective effects in models of acute inflammation (20, 31, 32), but rather harmful effects in models of chronic inflammation such as systemic lupus (33) or rheumatoid arthritis (34). It has also been described as important inhibitory pathway for apoptosis in neutrophils (5, 6, 35) and as important signaling pathway for LPS-induced B cell activation (36). Overexpression of Akt in lymphocytes prolonged their survival and also improved outcome in experimental sepsis (31), suggesting an important role of this signaling pathway during inflammation. However, until now, only little is known about the function of this pathway for innate immunity during acute inflammation. We demonstrate in this study an overall protective role of this pathway in our acute model of polymicrobial sepsis (Fig. 1) and a controlling inhibitory function for generation of various inflammatory mediators during the onset phase of sepsis (Fig. 2*A*). We were able to demonstrate that in vivo injection of LY294002 resulted in significant reduction of oxidative burst activity in blood monocytes and neutrophils in mice, offering a possible explanation for observed adverse effects for outcome during sepsis. Recent data demonstrated that inhibition of PI3K with wortmannin reversed the protective effects of glucan phosphate during experimental sepsis, demonstrating a protective effect of this pathway during acute inflammation (32). Our observations are in line with such earlier findings.

We compared the role of the PI3K pathway for TLR4-dependent generation of cytokines in vitro in neutrophils and monocytes. Interestingly, we were able to demonstrate opposing effects in these two cell populations. In neutrophils, PI3K activation appeared to limit the LPS response for generation of TNF-α, IL-6, IL-1β, and IL-8 (Fig. 3, *A*, *C*, *E*, and *G*), whereas in monocytes PI3K activation appeared to have a significantly promoting function for LPS-dependent generation of these mediators (Fig. 3, *B*, *D*, *F*, and *H*). Similar findings in monocytes have been reported regarding the role of PI3K for LPS-induced TNF-α generation (26). In bone marrow mouse neutrophils, a recent study reported that TLR-2-dependent activation of PI3K occurs, and that inhibitions of this pathway resulted in reduced generation of TNF-α and MIP2. The latter observations are somewhat in contrast to our findings, even though it cannot be excluded that TLR-2-dependent generation of TNF-α in neutrophils is controlled by PI3K differently from the TLR-4-dependent one. Also, another study recently reported crucial differences between mouse and human neutrophils with respect to the importance of various PI3K subunits, making observation regarding PI3K activation in mouse neutrophils difficult to compare with those in humans (18). The same may or may not apply to monocytes.

In the context of mediator generation, the findings in vivo during sepsis in mice (Fig. 2*A*) clearly demonstrate an inhibitory potential of the PI3K pathway. Our in vitro studies reflect these findings only in neutrophils, but not in PBMC (Fig. 3). The question as to which of these two cell populations is responsible for the cytokine storm in vivo during sepsis is puzzling. Complex interactions between various blood phagocytes and also endothelial cells further complicate this matter. Earlier studies of our own group demonstrated that neutrophil depletion clearly diminished the IL-6 generation in the serum of septic mice (15), suggesting a leading role of neutrophils. However, the question outlined above cannot be finally answered as of yet.

Neutrophils are generally regarded as driving force for acute inflammation, whereas monocytes are thought to be more important in chronic inflammation. In this context, our observations may partially explain why PI3K activation appears to be beneficial in acute inflammatory processes, e.g., by limiting neutrophil activation, whereas being harmful in more chronic inflammatory processes, e.g., by promoting monocyte activation.

As outlined earlier, PI3K activation has been reported before to be involved in regulating oxidative burst and phagocytosis in neutrophils and monocytes (17, 18, 20, 37). However, no studies have been conducted to compare these cell populations directly. We report in this study that PI3K inhibition resulted in impaired oxidative burst and phagocytosis activity in both neutrophils and monocytes (Figs. 4 and 5). In neutrophils, this effect was especially strong for PMA-induced oxidative burst, whereas in monocytes the inhibitory effect was more prominent for *E. coli*-induced oxidative

burst. These findings again suggest different regulatory functions of this pathway in neutrophils when compared with monocytes.

The concept of C5a/C5aR interception during sepsis has evolved in recent years, and C5a has become an interesting target for potential clinical interventions in the field of acute inflammation and especially sepsis (1). Our and other groups have suggested that large amounts of C5a are generated early during the onset of sepsis, but the intracellular regulatory mechanisms controlling C5a-induced effects on innate immune functions are not understood in detail. We have found recently that C5a negatively regulates LPS-induced production of TNF-α by rat neutrophils in vitro, but has the opposite effect on macrophages (16). In this study, TNF-α generation in neutrophils was strongly dependent on NF-κB activation, and treatment of CLP mice with anti-C5a caused enhanced serum levels of TNF-α, apparently by protecting the signaling pathways from C5a-induced dysfunction. We also recently demonstrated involvement of p38 and ERK1/2 activation in generation of IL-6 in neutrophils (15) and reported that the PI3K signaling pathway is involved in LPS-mediated macrophage migration inhibitory factor generation in neutrophils (2). A recent report from another group described C5a as negative regulator for IL-12 generation in human monocytes, with this effect being dependent on C5a-induced PI3K/Akt activation (28). We thought to investigate in greater detail the role of the PI3K/Akt signaling pathway for C5a-induced alterations of mediator generation upon TLR4 stimulation in neutrophils. We found that C5a-mediated effects on LPS-induced IL-1β and IL-8 generation were controlled in an inhibitory fashion by the PI3K pathway (Fig. 7), offering a partial explanation for the observed rise of serum inflammatory mediators in CLP mice after PI3K inhibition.

Oxidative burst and phagocytosis represent key players of the innate immune response to invading microorganisms. Recent work has demonstrated the importance of C5a for an intact oxidative burst and phagocytosis in neutrophils and monocytes in response to *E. coli* in a new whole blood assay applying flow cytometric analysis (29). The PI3K/Akt pathway has also been described to be an important mediator of neutrophil oxidative burst in other assays using isolated human neutrophils (17). The ability of Kupffer cells to conduct phagocytosis has been described to be regulated by C5a as well as activating FcγR in recent studies (30). The PI3K pathway appears to be important late in the process of phagocytosis in neutrophils and monocytes, namely during the phagosome closure after cup formation (37, 38). We thought to investigate in how far C5a-dependent regulation of oxidative burst and phagocytosis was dependent on PI3K activation in neutrophils and peripheral blood monocytes. Our results demonstrated that C5a-mediated priming of *E. coli*- and PMA-induced oxidative burst was largely dependent on intact PI3K signaling in both neutrophils and monocytes. C5a-mediated enhancement of phagocytosis appeared also to be dependent on PI3K activation in neutrophils.

Taken together, our results suggest that the PI3K signaling pathway exerts an overall protective role during the onset of sepsis in rodents by limiting C5a-mediated effects on neutrophil cytokine generation, and promoting oxidative burst and phagocytosis. We further propose that this pathway has opposing regulatory mechanisms in TLR-4-mediated cytokine generation in neutrophils when compared with monocytic cells. Inducing the activation of this pathway may represent a therapeutic approach for limiting acute inflammatory diseases such as sepsis.

Acknowledgment

We thank Gerda Bartling for excellent technical assistance with the microbiological analyses of the peritoneal lavage fluids.

Disclosures

The authors have no financial conflict of interest.

References

1. Riedemann, N. C., R. F. Guo, and P. A. Ward. 2003. Novel strategies for the treatment of sepsis. *Nat. Med.* 9: 517–524.
2. Riedemann, N. C., R. F. Guo, H. Gao, L. Sun, M. Hoesel, T. J. Hollmann, R. A. Wetsel, F. S. Zetoune, and P. A. Ward. 2004. Regulatory role of C5a on macrophage migration inhibitory factor release from neutrophils. *J. Immunol.* 173: 1355–1359.
3. Klein, J. B., A. Buridi, P. Y. Coxon, M. J. Rane, T. Manning, R. Kettritz, and K. R. McLeish. 2001. Role of extracellular signal-regulated kinase and phosphatidylinositol-3 kinase in chemoattractant and LPS delay of constitutive neutrophil apoptosis. *Cell. Signal.* 13: 335–343.
4. Hu, Z., and M. M. Sayeed. 2005. Activation of PI3-kinase/PKB contributes to delay in neutrophil apoptosis after thermal injury. *Am. J. Physiol.* 288: C1171–C1178.
5. Perianayagam, M. C., V. S. Balakrishnan, A. J. King, B. J. Pereira, and B. L. Jaber. 2002. C5a delays apoptosis of human neutrophils by a phosphatidylinositol 3-kinase-signaling pathway. *Kidney Int.* 61: 456–463.
6. Perianayagam, M. C., V. S. Balakrishnan, B. J. Pereira, and B. L. Jaber. 2004. C5a delays apoptosis of human neutrophils via an extracellular signal-regulated kinase and Bad-mediated signalling pathway. *Eur. J. Clin. Invest.* 34: 50–56.
7. Ward, P. A. 2004. The dark side of C5a in sepsis. *Nat. Rev. Immunol.* 4: 133–142.
8. Guo, R. F., and P. A. Ward. 2005. Role of C5a in inflammatory responses. *Annu. Rev. Immunol.* 23: 821–852.
9. Czermak, B. J., V. Sarma, C. L. Pierson, R. L. Warner, M. Huber-Lang, N. M. Bless, H. Schmal, H. P. Friedl, and P. A. Ward. 1999. Protective effects of C5a blockade in sepsis. *Nat. Med.* 5: 788–792.
10. Riedemann, N. C., R. F. Guo, T. A. Neff, I. J. Laudes, K. A. Keller, V. J. Sarma, M. M. Markiewski, D. Mastellos, C. W. Strey, C. L. Pierson, et al. 2002. Increased C5a receptor expression in sepsis. *J. Clin. Invest.* 110: 101–108.
11. Huber-Lang, M. S., E. M. Younkin, J. V. Sarma, S. R. McGuire, K. T. Lu, R. F. Guo, V. A. Padgaonkar, J. T. Curnutte, R. Erickson, and P. A. Ward. 2002. Complement-induced impairment of innate immunity during sepsis. *J. Immunol.* 169: 3223–3231.
12. Huber-Lang, M. S., N. C. Riedeman, J. V. Sarma, E. M. Younkin, S. R. McGuire, I. J. Laudes, K. T. Lu, R. F. Guo, T. A. Neff, V. A. Padgaonkar, et al. 2002. Protection of innate immunity by C5aR antagonist in septic mice. *FASEB J.* 16: 1567–1574.
13. Solomkin, J. S., M. K. Jenkins, R. D. Nelson, D. Chenoweth, and R. L. Simmons. 1981. Neutrophil dysfunction in sepsis. II. Evidence for the role of complement activation products in cellular deactivation. *Surgery* 90: 319–327.
14. Guo, R. F., N. C. Riedemann, K. D. Bernacki, V. J. Sarma, I. J. Laudes, J. S. Reuben, E. M. Younkin, T. A. Neff, J. D. Paulauskis, F. S. Zetoune, and P. A. Ward. 2003. Neutrophil C5a receptor and the outcome in a rat model of sepsis. *FASEB J.* 17: 1889–1891.
15. Riedemann, N. C., R. F. Guo, T. J. Hollmann, H. Gao, T. A. Neff, J. S. Reuben, C. L. Speyer, J. V. Sarma, R. A. Wetsel, F. S. Zetoune, and P. A. Ward. 2004. Regulatory role of C5a in LPS-induced IL-6 production by neutrophils during sepsis. *FASEB J.* 18: 370–372.
16. Riedemann, N. C., R. F. Guo, K. D. Bernacki, J. S. Reuben, I. J. Laudes, T. A. Neff, H. Gao, C. Speyer, V. J. Sarma, F. S. Zetoune, and P. A. Ward. 2003. Regulation by C5a of neutrophil activation during sepsis. *Immunity* 19: 193–202.
17. Chen, Q., D. W. Powell, M. J. Rane, S. Singh, W. Butt, J. B. Klein, and K. R. McLeish. 2003. Akt phosphorylates p47^{phox} and mediates respiratory burst activity in human neutrophils. *J. Immunol.* 170: 5302–5308.
18. Condliffe, A. M., K. Davidson, K. E. Anderson, C. D. Ellson, T. Crabbe, K. Okkenhaug, B. Vanhaesebroeck, M. Turner, L. Webb, M. P. Wymann, et al. 2005. Sequential activation of class IB and class IA PI3K is important for the primed respiratory burst of human but not murine neutrophils. *Blood* 106: 1432–1440.
19. Hannigan, M., L. Zhan, Z. Li, Y. Ai, D. Wu, and C. K. Huang. 2002. Neutrophils lacking phosphoinositide 3-kinase γ show loss of directionality during *N*-formyl-Met-Leu-Phe-induced chemotaxis. *Proc. Natl. Acad. Sci. USA* 99: 3603–3608.
20. Hirsch, E., V. L. Katanaev, C. Garlanda, O. Azzolino, L. Pirola, L. Silengo, S. Sozzani, A. Mantovani, F. Altruda, and M. P. Wymann. 2000. Central role for G protein-coupled phosphoinositide 3-kinase γ in inflammation. *Science* 287: 1049–1053.
21. Sadhu, C., K. Dick, W. T. Tino, and D. E. Staunton. 2003. Selective role of PI3Kδ in neutrophil inflammatory responses. *Biochem. Biophys. Res. Commun.* 308: 764–769.
22. Puri, K. D., T. A. Doggett, J. Douangpanya, Y. Hou, W. T. Tino, T. Wilson, T. Graf, E. Clayton, M. Turner, J. S. Hayflick, and T. G. Diacovo. 2004. Mechanisms and implications of phosphoinositide 3-kinase δ in promoting neutrophil trafficking into inflamed tissue. *Blood* 103: 3448–3456.
23. Puri, K. D., T. A. Doggett, C. Y. Huang, J. Douangpanya, J. S. Hayflick, M. Turner, J. Penninger, and T. G. Diacovo. 2005. The role of endothelial PI3Kγ activity in neutrophil trafficking. *Blood* 106: 150–157.
24. Ong, E., X. P. Gao, D. Predescu, M. Broman, and A. B. Malik. 2005. Role of phosphatidylinositol 3-kinase-γ in mediating lung neutrophil sequestration and vascular injury induced by *E. coli* sepsis. *Am. J. Physiol.* 289: L1094–L1103.
25. Sadhu, C., B. Masinovsky, K. Dick, C. G. Sowell, and D. E. Staunton. 2003. Essential role of phosphoinositide 3-kinase δ in neutrophil directional movement. *J. Immunol.* 170: 2647–2654.

26. Guha, M., and N. Mackman. 2002. The phosphatidylinositol 3-kinase-Akt pathway limits lipopolysaccharide activation of signaling pathways and expression of inflammatory mediators in human monocytic cells. *J. Biol. Chem.* 277: 32124–32132.
27. Chiou, W. F., H. R. Tsai, L. M. Yang, and W. J. Tsai. 2004. C5a differentially stimulates the ERK1/2 and p38 MAPK phosphorylation through independent signaling pathways to induced chemotactic migration in RAW264.7 macrophages. *Int. Immunopharmacol.* 4: 1329–1341.
28. La Sala, A., M. Gadina, and B. L. Kelsall. 2005. G_i-protein-dependent inhibition of IL-12 production is mediated by activation of the phosphatidylinositol 3-kinase-protein 3 kinase B/Akt pathway and JNK. *J. Immunol.* 175: 2994–2999.
29. Mollnes, T. E., O. L. Brekke, M. Fung, H. Fure, D. Christiansen, G. Bergseth, V. Videm, K. T. Lappegard, J. Kohl, and J. D. Lambris. 2002. Essential role of the C5a receptor in *E. coli*-induced oxidative burst and phagocytosis revealed by a novel lepirudin-based human whole blood model of inflammation. *Blood* 100: 1869–1877.
30. Kumar, V., S. R. Ali, S. Konrad, J. Zwirner, J. S. Verbeek, R. E. Schmidt, and J. E. Gessner. 2006. Cell-derived anaphylatoxins as key mediators of antibody-dependent type II autoimmunity in mice. *J. Clin. Invest.* 116: 512–520.
31. Bommhardt, U., K. C. Chang, P. E. Swanson, T. H. Wagner, K. W. Tinsley, I. E. Karl, and R. S. Hotchkiss. 2004. Akt decreases lymphocyte apoptosis and improves survival in sepsis. *J. Immunol.* 172: 7583–7591.
32. Williams, D. L., C. Li, T. Ha, T. Ozment-Skelton, J. H. Kalbfleisch, J. Preiszner, L. Brooks, K. Breuel, and J. B. Schweitzer. 2004. Modulation of the phosphoinositide 3-kinase pathway alters innate resistance to polymicrobial sepsis. *J. Immunol.* 172: 449–456.
33. Barber, D. F., A. Bartolome, C. Hernandez, J. M. Flores, C. Redondo, C. Fernandez-Arias, M. Camps, T. Ruckle, M. K. Schwarz, S. Rodriguez, et al. 2005. PI3Kγ inhibition blocks glomerulonephritis and extends lifespan in a mouse model of systemic lupus. *Nat. Med.* 11: 933–935.
34. Camps, M., T. Ruckle, H. Ji, V. Ardissone, F. Rintelen, J. Shaw, C. Ferrandi, C. Chabert, C. Gillieron, B. Francon, et al. 2005. Blockade of PI3Kγ suppresses joint inflammation and damage in mouse models of rheumatoid arthritis. *Nat. Med.* 11: 936–943.
35. Klein, J. B., M. J. Rane, J. A. Scherzer, P. Y. Coxon, R. Kettritz, J. M. Mathiesen, A. Buridi, and K. R. McLeish. 2000. Granulocyte-macrophage colony-stimulating factor delays neutrophil constitutive apoptosis through phosphoinositide 3-kinase and extracellular signal-regulated kinase pathways. *J. Immunol.* 164: 4286–4291.
36. Venkataraman, C., G. Shankar, G. Sen, and S. Bondada. 1999. Bacterial lipopolysaccharide induced B cell activation is mediated via a phosphatidylinositol 3-kinase dependent signaling pathway. *Immunol. Lett.* 69: 233–238.
37. Dewitt, S., W. Tian, and M. B. Hallett. 2006. Localised PtdIns(3,4,5)P_3 or PtdIns(3,4)P_2 at the phagocytic cup is required for both phagosome closure and Ca^{2+} signalling in HL60 neutrophils. *J. Cell Sci.* 119: 443–451.
38. Cox, D., C. C. Tseng, G. Bjekic, and S. Greenberg. 1999. A requirement for phosphatidylinositol 3-kinase in pseudopod extension. *J. Biol. Chem.* 274: 1240–1247.

REPORT DOCUMENTATION PAGE

Form Approved
OMB No. 0704-0188

1. REPORT DATE *(DD-MM-YYYY)*	2. REPORT TYPE	3. DATES COVERED *(From - To)*
8/20/08	Annual	Aug 21,07 – Aug 20, 08

4. TITLE AND SUBTITLE Mechanisms of the Activation of Key Transcription Factors in Mustard Gas Induced Lung Injury and Protection by Antioxidant Liposomes

5a. CONTRACT NUMBER W81XWH-06-2-0044

5b. GRANT NUMBER

5c. PROGRAM ELEMENT NUMBER

6. AUTHOR(S)
Salil K. Das

5d. PROJECT NUMBER

5e. TASK NUMBER

5f. WORK UNIT NUMBER

7. PERFORMING ORGANIZATION NAME(S) AND ADDRESS(ES)

Meharry Medical College, 1005
David Todd Blvd.,Nashville, TN
37208

8. PERFORMING ORGANIZATION REPORT NUMBER

9. SPONSORING / MONITORING AGENCY NAME(S) AND ADDRESS(ES)
US Army Medical Research and
Materiel Command,
Fort Detrick
MD 21702-5012

10. SPONSOR/MONITOR'S ACRONYM(S)

11. SPONSOR/MONITOR'S REPORT NUMBER(S)

12. DISTRIBUTION / AVAILABILITY STATEMENT

Approved for Public Release, Distributions Unlimited

13. SUPPLEMENTARY NOTES

14. ABSTRACT

We have established in our laboratory that intratracheal exposure of 2-chloroethyl ethyl sulfide (CEES), a mustard gas analog to guinea pigs causes reactive oxygen species (ROS) mediated lung injury by stimulation of inflammatory cytokines, such as TNF-α and activation of transcription factor NF-κB. The purpose of the present study was to determine whether CEES-induced activation of TNF-α is followed by activation of other novel transcription factors. Increased expression of these genes may lead to altered expression of proteins that may exacerbate the injury in lung or lung cells. Current studies reveal that CEES exposure causes activation of several transcription factors, such as AP-1. The AP-1 activation was also found to be mediated via activation of MAPk signaling pathway. In addition, we have further established that CEES-induced lung injury is associated with desensitization of beta-adrenergic receptors, a molecular marker for respiratory distress. We have also developed several antioxidant liposomes and some of these have shown promise to protect against CEES-induced lung injury.

15. SUBJECT TERMS

16. SECURITY CLASSIFICATION OF:			17. LIMITATION OF ABSTRACT	18. NUMBER OF PAGES	19a. NAME OF RESPONSIBLE PERSON
a. REPORT	b. ABSTRACT	c. THIS PAGE			19b. TELEPHONE NUMBER *(include area code)*
Unclassified	Unclassified	Unclassified			USAMRMC

Table of Contents

8/21/2007-8/20/2008 Annual DOD Report – W81XWH-06-2-0044 Salil K. Das

Statement of Work

We have established in our laboratory that intratracheal exposure of 2-chloroethyl ethyl sulfide (CEES), a mustard gas analog to guinea pigs causes reactive oxygen species (ROS) mediated lung injury by stimulation of inflammatory cytokines, such as TNF-α. The purpose of the present investigation is to determine whether CEES-induced activation of inflammatory cytokines is followed by the activation of several key transcription factors (nuclear factor- B [NF-κB], activation protein-1 [AP-1], serum accelerator factor [SAF], and CCAAT/enhancer binding protein [C/EBP]). These transcription factors induce expression of many target genes including, alpha 1-antitrypsin [α1-AT], matrix metalloproteinases [MMP], and tissue inhibitors of metalloproteinases [TIMPs]. Increased expression of these genes will lead to altered expression of proteins that may exacerbate the injury in lung or lung cells.

We intend to achieve this goal by conducting the following specific aims:

1. Analysis of the transcripts of target genes (alpha 1-antitrypsin [α1-AT], matrix metalloproteinase [MMP], and tissue inhibitors of metalloproteinases [TIMPs] in the lung by Northern blot or RT-PCR.
2. Analysis of the target proteins in the lung by immunohistochemistry.
3. Analysis of SAF-1, AP-1, NF-κB and C/EBP transcription factor in the lung by immunohistochemistry. Co-localization analysis of transcription factor and target genes.
4. Functional analysis of transcription factor activity in the tracheal epithelial cells by assessing promoter-binding activity.
5. Analysis of the signaling mechanisms (protein kinase A [PKA], protein kinase C [PKC], and mitogen activated protein kinase [MAPK]) involved in the activation of SAF-1 in the lung cells following CEES exposure.
6. Analysis of the effectiveness of the treatment by (a) delivery of a liposome containing an antioxidant, such as N-acetyl cysteine (NAC) either intravenously or subcutaneously, and (b) in combination therapy with a specific inhibitor or inhibitors of transcription factors in abolishing the induction of the transcription factors involved in lung injury.

Introduction

For several years we have been studying in a guinea pig model the molecular mechanisms by which CEES causes lung injury associated with ARDS. Our earlier publication indicated that CEES causes lung injury and significantly decreases expression and activity.of cholinephosphotransferase (CPT), the terminal enzyme in CDP-choline pathway for phosphatidylcholine synthesis (1). This decrease in CPT activity was not associated with any mutation of the CPT gene and is probably mediated by accumulation of ceramides. CEES induced ceramide accumulation may thus play an important role in the development of ARDS by modulating the expression of CPT. We have previously shown that exposure of CEES to guinea pigs causes an increase in the levels of TNF-α, NF-κB and ceramides in the lung (2). However, NF-κB disappeared after 2 hours indicating an intricate interplay of pro- and anti- apoptotic inflammatory cytokines. In subsequent studies, we utilized a state of the art cytokine array technology to identify other cytokines affected by CEES exposure (3). The array of cytokine induction within an hour of CEES exposure and dynamic changes in cytokine profile by one day post CEES exposure reveals that following an initial damage, the lung tissue tries to recover and prevent further damage through self defense mechanisms mediated through various classes of cytokines. We also showed that antioxidant liposomes were protective against acute lung injury induced by exposure to CEES (4-6). We have also observed that CEES exposure causes progressive lung fibrosis (5-7).

Body

1. Activation of MAPK/AP-1 Signaling Pathway in Lung Injury Induced by 2-Chloroehtyl Ethyl Sulfide, a Mustard Gas Analog

We reported earlier that the activation of free-radical-mediated TNF-α cascade is the major pathway in the inflammatory lung disease induced by CEES, a mustard gas analog. TNF-α induces AP-1 activation via phosphorylation of MAPKs. The present study examines the relationship between CEES induced lung injury and MAPKs signaling pathway. Adult guinea pigs received single intratracheal injection of different doses of CEES and were sacrificed at different time points. CEES exposure caused lung injury with evidence of fibrosis. The optimum activation of all members of the MAPKs family (ERK1/2, p38 and JNK1/2) was achieved at 0.5 mg/kg dose and at 1 h (Fig. 2). No significant change was observed beyond that time point. This led to an activation of AP-1 transcription factors associated with an increase in the protein levels of Fos, ATF and Jun family members (Fig. 3). To explore the involvement of AP-1 in cell proliferation, we determined the protein levels of cell cycle protein cyclin D1 and cell differentiation marker PCNA (Fig. 4). An up regulation of these proteins was observed. Hence it is suggested that CEES exposure causes accumulation of TNF-α, which is associated with an activation of MAPK/AP-1 signaling pathway and cell proliferation. Further studies are needed to clarify whether the observed effects are the adaptive responses of the lung or they contribute to the lung injury.

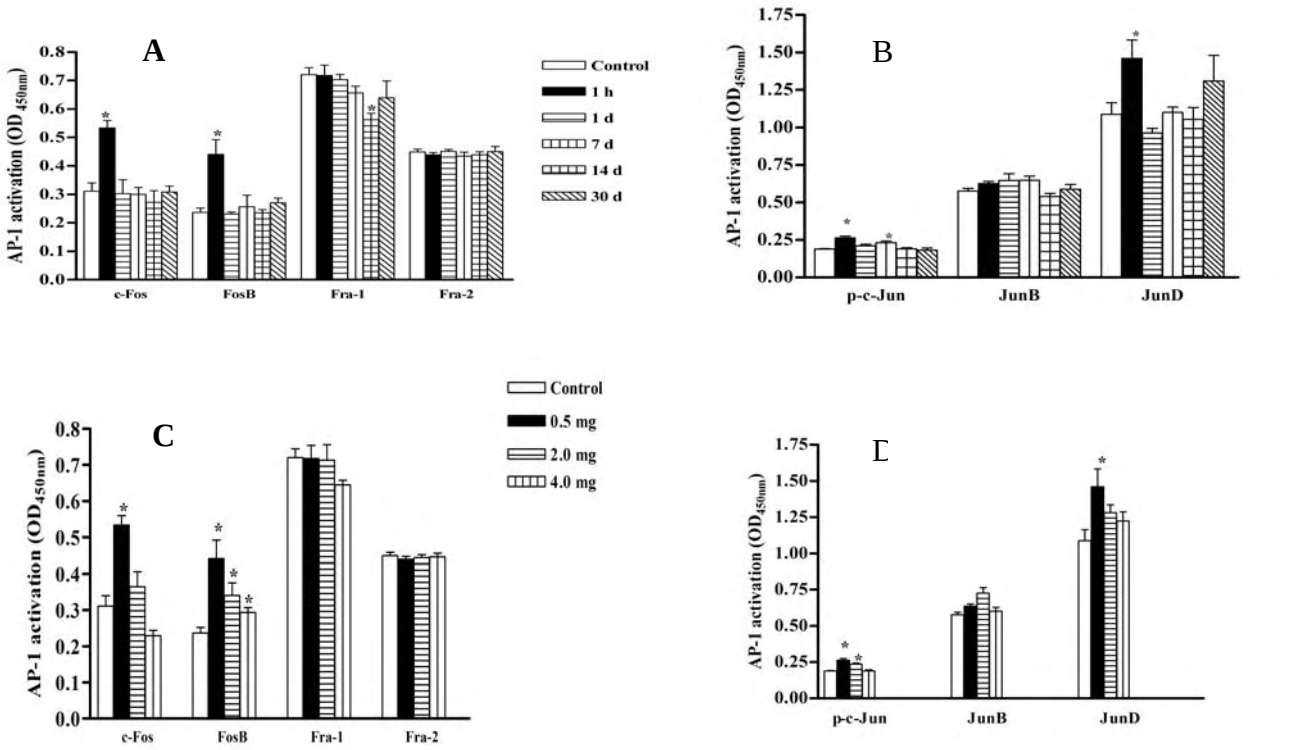

Fig. 1. CEES-induced activation of DNA binding of AP-1 family members in guinea pig lung. (A) Time dependent induction of AP-1 DNA binding activity after intratracheal injection of CEES (0.5 mg / kg body wt.) (B) DNA binding activity of AP-1 1h after exposure to CEES at different doses (ranging from 0.5 to 4.0 mg / kg body wt.). Statistical significance was determined by Dunnett's test after one-way ANOVA. Results are expressed as mean ± SE (N = 3), *p < 0.05 compared to control.

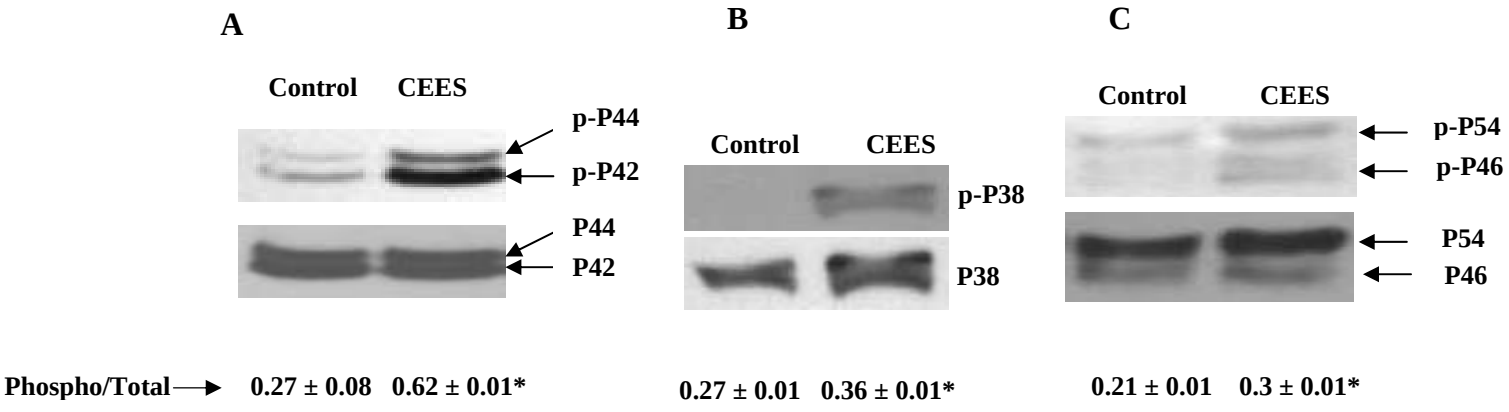

Fig. 2: CEES-induced activation of MAPKs in guinea pig lung. Western blot analysis of ERK 1/2 (A), p38 (B), JNK 1/2(C) (N = 3 in each group). Statistical significance was determined by the Student's *t*-test. Results are expressed as mean ± SE, *p < 0.05 compared to control.

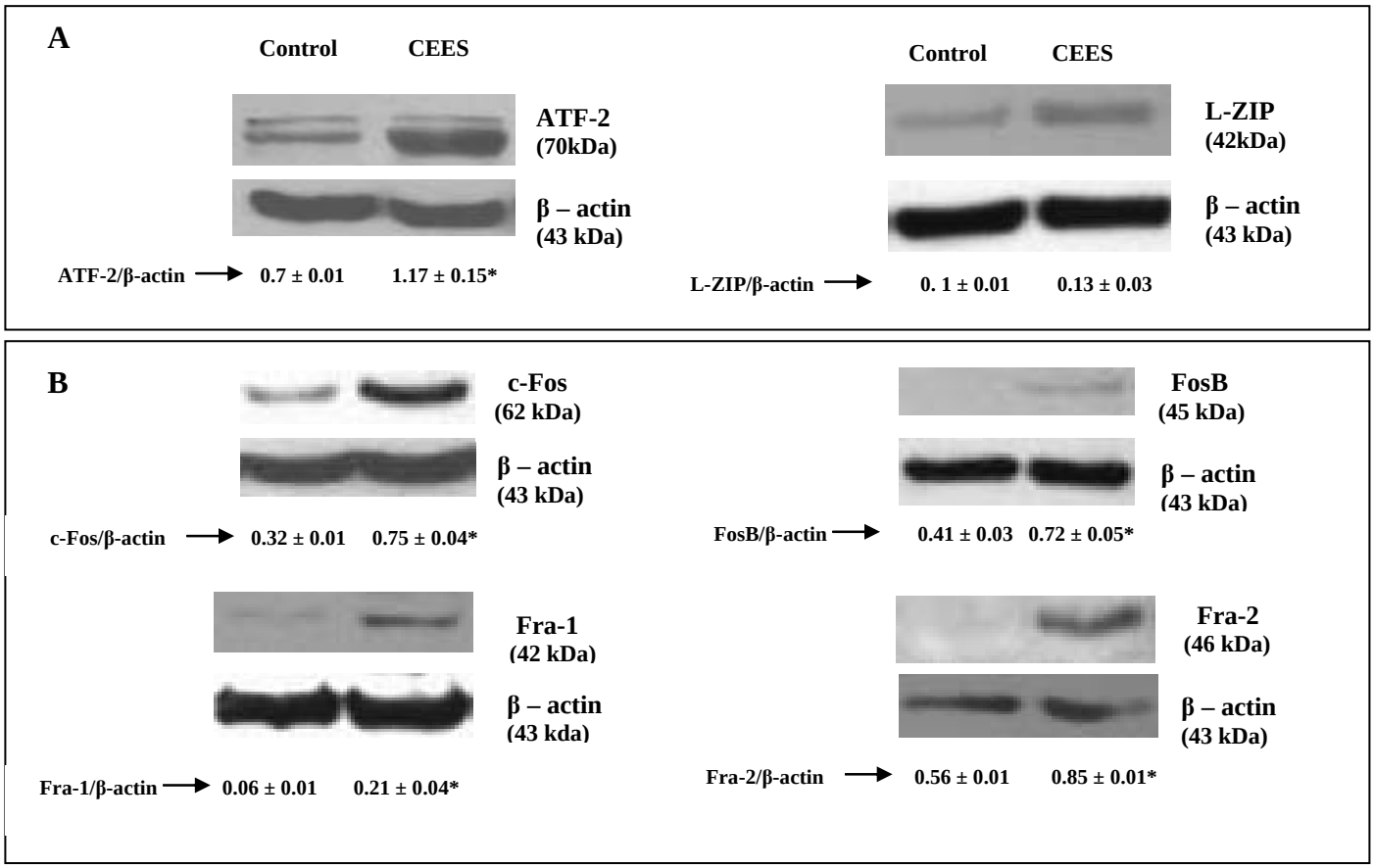

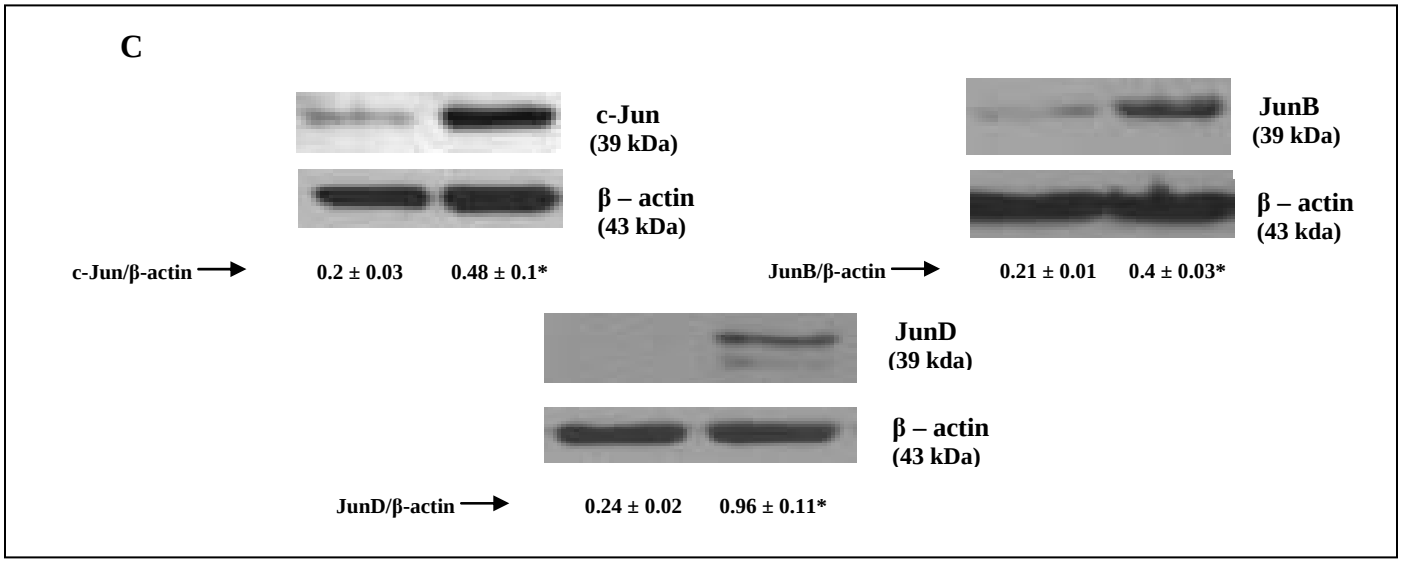

Fig. 3: CEES-induced increase in protein levels of AP-1 transcription factors in guinea pig lung. Western blot analysis of ATF-2 and L-ZIP (A); c-Fos, Fos-B, Fra-1, Fra-2 (B); c-Jun, JunB, JunD (C) (N = 3 in each group). Statistical significance was determined by the Student's *t*-test. Results are expressed as mean ± SE, *p < 0.05 compared to control.

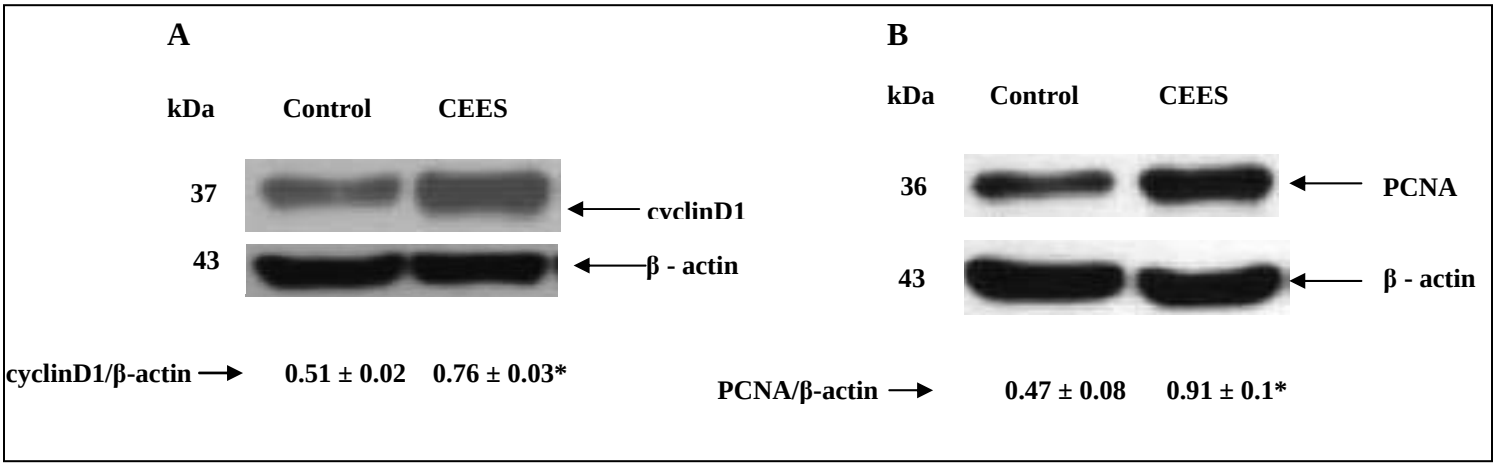

Fig. 4: CEES-induced activation of AP-1 dependent cell cycle protein in guinea pig lung. Western blot analysis of cyclinD1 (A) and PCNA (B) (N = 3 in each group). Statistical significance was determined by the Student's *t*-test. Results are expressed as mean ± SE, *p < 0.05 compared to control.

2. Desensitization of β-Adrenergic Receptors in Lung Injury Induced by 2-Chloroethyl Ethyl Sulfide (CEES), a Mustard Analog

CEES exposure causes inflammatory lung diseases, including acute respiratory distress syndrome and pulmonary fibrosis. This may be associated with oxidative stress, which has been implicated in the desensitization of beta-adrenergic receptors (β-ARs). The objective of this study was to investigate whether lung injury induced by intratracheal CEES exposure (2 mg/kg b.wt) causes desensitization of β-ARs. The animals were sacrificed after 7 days and lungs were removed. Lung injury was established by measuring the leakage of iodinated-BSA into lung tissue. Receptor binding characteristics were determined by measuring the binding of [^{3}H]-dihydroalprenolol (0.5-24 nM) to membrane fraction in the presence and absence of DL-propranolol (10 μM). Both high and low affinity β-ARs were identified in lung. Binding capacity was significantly higher in low affinity site in both control and experimental groups. Although CEES exposure did not change K_D and B_{max} at the high affinity site, it significantly decreased both K_D and B_{max} at low affinity sites (Table 1). A 20% decrease in β_2-AR mRNA level (Fig. 1) and a 60% decrease in membrane protein levels (Fig. 2) were observed in the experimental group. Furthermore, there was significantly less stimulation of adenylate cyclase activity by both cholera toxin and isoproterenol in the experimental group in comparison to the control group (Table 2). Treatment of lungs with IBMX, an inhibitor of phosphodiesterase could not abolish the difference between the control group and experimental group on the stimulation of the adenylate cyclase activity (Fig. 3). Thus, our study indicates that CEES-induced lung injury is associated with desensitization of β_2-AR.

Table 1. Effects of mustard gas exposure on binding characteristics of β-adrenoreceptors

Samples	High Affinity		Low Affinity	
	Kd (nM)	B_{max} (fmol/mg protein)	Kd (nM)	B_{max} (fmol/mg protein)
Control	0.68 ± 0.17	221.2 ± 56.9	6.40 ± 2.1	2087 ± 370
CEES-exposed	0.62 ± 0.15	203.8 ± 69.0	2.85 ± 0.9	765.4 ± 164.1*

*B_{max} at low affinity sites is significantly reduced by mustard gas exposure ($p = 0.03$)
(n =3 for each group)

Table 2. Intracellular level of cAMP in choleratoxin treated guinea pig lung: Role of CEES treatment

Addition	cAMP (fmol/mg of Protein)	
	Vehicle	CEES
Endogenous	98.20 ± 2.65	35.62 ± 0.67
Cholera Toxin (50 ng/ml)	2074.51 + 6.77	1050.34 ± 6.87

The values are Mean ± S.E.M. of 4 samples.

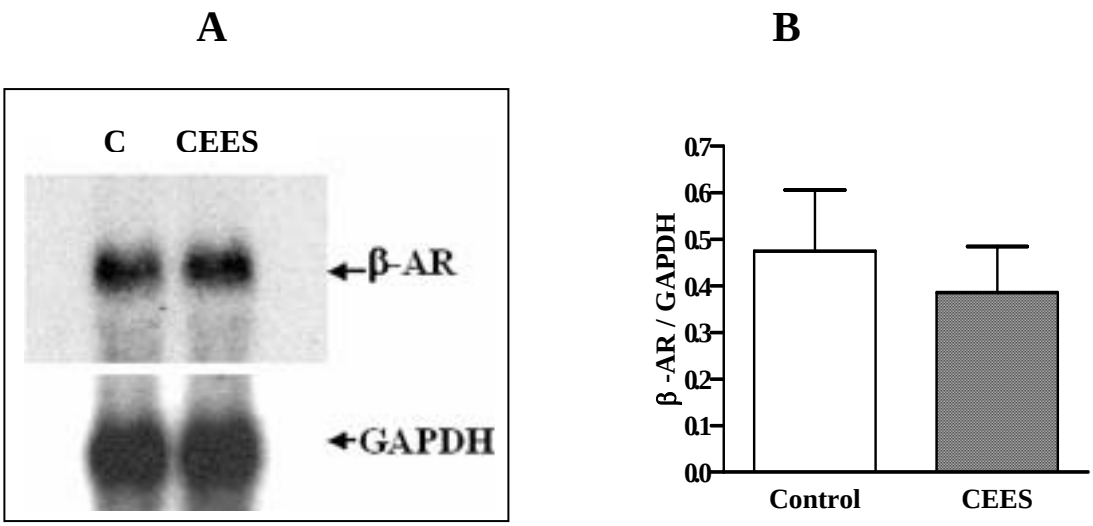

Figure 1. Effect of Mustard Gas on Guinea Pig Lung β_2-AR Receptor Gene Expression
A**.** A representative autoradiogram of Northern blot analysis**.** B**.** Bar graph of normalized densitometric values (n=3).

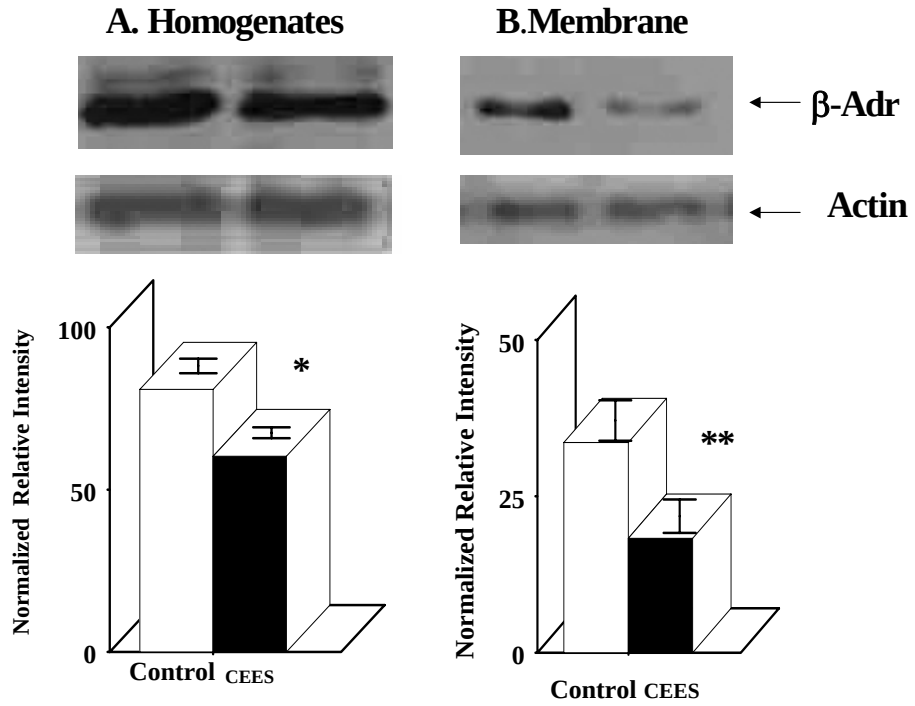

Figure 2. Effect of Mustard Gas on Guinea Pig Lung β_2-AR Receptor Levels
A. Homogenate (n=3); B**.** Membrane (n=3).

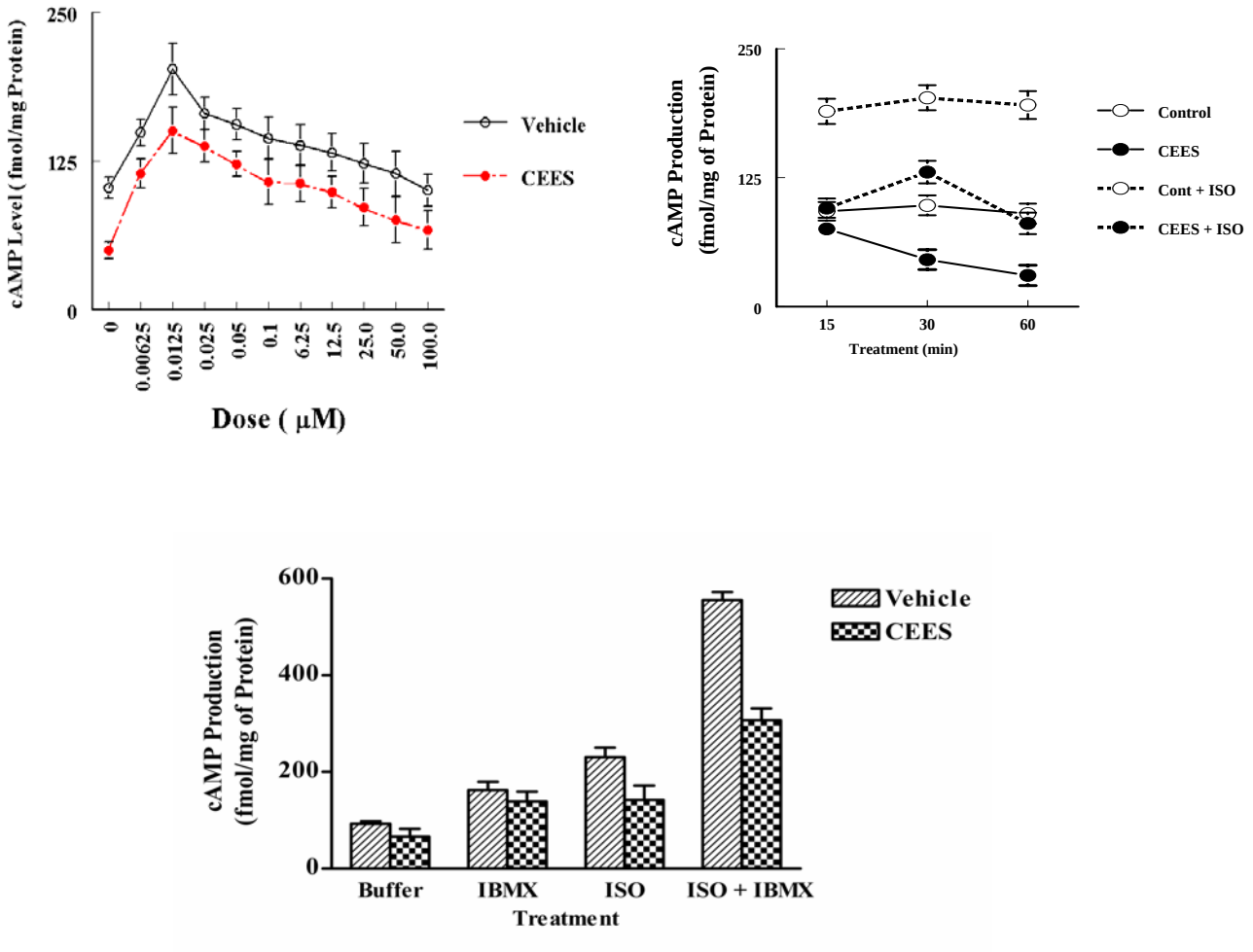

Figure 3. Effects of Mustard Gas Exposure on cAMP Production in Guinea Pig Lung. A. Dose response curve in the presence and absence of isoproterenol (n = 3); B**.** Time response curve in the presence and absence of isoproterenol (n = 3), C. Response in the presence of isoproterol and IBMX singly or in combination (n = 3).

3. Protection of half sulfur mustard gas-induced lung injury in guinea pigs by antioxidant liposomes

This study was to develop antioxidant liposomes as antidotes for mustard gas induced lung injury in guinea pigs. Five antioxidant liposomes (LIP-1, LIP-2, LIP-3, LIP-4 and LIP-5) were prepared differing in the levels of phospholipid, cholesterol, phosphatidic acid, tocopherol (α, γ,δ), N-acetylcysteine (NAC) and GSH (Table 1). A single dose (200 μl per animal) of each liposome was administered intratracheally after 5 min and 1 h of exposure of 2-chloroethyl ethyl sulfide (CEES). The animals were sacrificed either after 2 h (for lung injury study) or after 30 days (for histology study) of CEES exposure. These antioxidant liposomes offered 9 to 76% protection against lung injury as evidenced by leakage of BSA from blood into the lung (Table 2). The maximum protection was achieved with two liposomes, LIP-2 (71.5%) and LIP-4 (75.4%), when administered after 5 minutes of CEES exposure. Delaying the administration of the liposomes after 1 h of CEES exposure decreased the efficacy. Both liposomes contained 11 mM α-tocopherol, 11 mM γ-tocopherol and 75 mM NAC. However, LIP-2 contained additionally 5 mM-δ-tocopherol. Overall, LIP-2 and LIP-4

offered significant prophylactic protection by controlling recruitment of neutrophils, eosinophils, and accumulation of septal and perivascular fibrin and collagen, and parenchymal collapse. However, LIP-2 showed better protection than LIP-4 in terms of the accumulation of aggregated RBCs in the bronchi, alveolar space, arterioles and veins, and fibrin and collagen deposition in the alveolar space. The protection against CEES-induced lung fibrosis by antioxidant liposomes, particularly LIP-2 was further evident by a decrease in lipid peroxidation and hydroxyproline content in lung. Our study clearly suggests that NAC can be used in combination with vitamin E as a liposome for effective antidote against lung injury.

Table 1. Composition of Antioxidant Liposomes

Liposomes	Liposome Content (mM)							
	Phospholiposome (PL90H)	Cholesterol	Phosphatidic Acid (PA)	Tocopherol (Vitamin E)			NAC	GSH
				α	γ	δ		
LIP1 (Blank)	71	28	0.67	-	-	-	-	-
LIP 2	55	22	0.6	11	11	5	75	-
LIP 3	62	25	0.6	6	6	-	75	-
LIP 4	55	22	0.6	11	11	-	75	-
LIP 5	55	22	0.6	11	11	-	-	75

Table 2. Effects of Liposome Treatment on CEES-Induced Lung Injury in Guinea Pigs (Leakage of ^{125}I-BSA from Blood into the Lung).

Treatment	Permeability Index	
	Liposomes injected 5 min after CEES Exposure	Liposomes injected 60 min after CEES Exposure
Control (No CEES)	0.20 ± 0.04	
Control (CEES only)	1.30 ± 0.22	
CEES + LIP 1	1.18 ± 0.03	1.11 ± 0.21
CEES + LIP 2	0.37 ± 0.03	0.74 ± 0.04
CEES + LIP 3	0.60 ± 0.02	0.80 ± 0.06
CEES + LIP 4	0.32 ± 0.01	0.76 ± 0.03
CEES + LIP 5	0.64 ± 0.05	0.83 ± 0.04

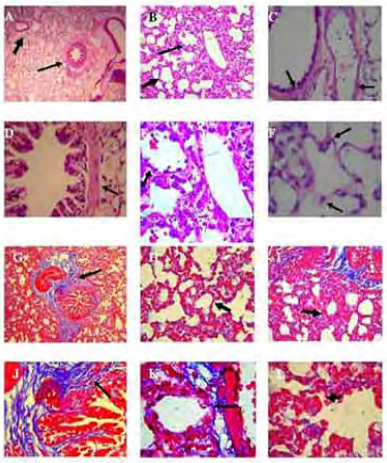

Figure 1. Sections of control lungs with H & E (A-F) and Trichrome stain (G-L). Lungs were obtained after tracheal instillation of vehicle (0.1 ml) at 30 days. (A and G- 10x; B,C,H and I - 40x; D, E, F, J, K and L - 100x)

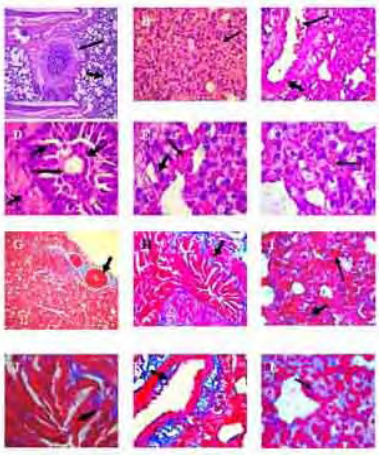

Figure 2. Sections of CEES-exposed lungs with H & E (A-F) and Trichrome stain (G-L). Lungs were obtained after 30 days of single exposure of CEES (2 mg/kg). (A and G - 10 x; B, C, H and I - 40 x; D, E, F, J, K and L - 100x)

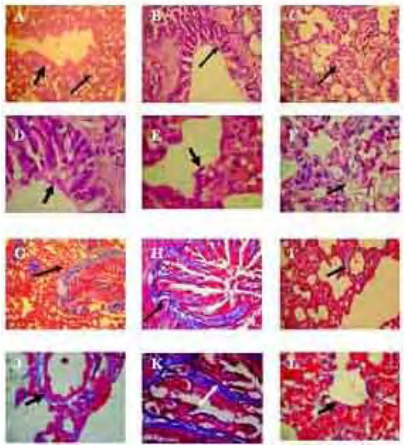

Figure 3. Sections of lungs exposed to CEES and LIP-2. Guinea pigs were exposed to CEES (2mg/kg) intratracheally and 5 minutes later received a single tracheal instillation of 200 µl LIP-2. After 30 days of CEES exposure, lung sections were stained with H & E (A-F) and trichrome stain (G-L) (A and G - 10x ; B, C, H and I - 40x; D, E, F, J, K and L - 100 x)

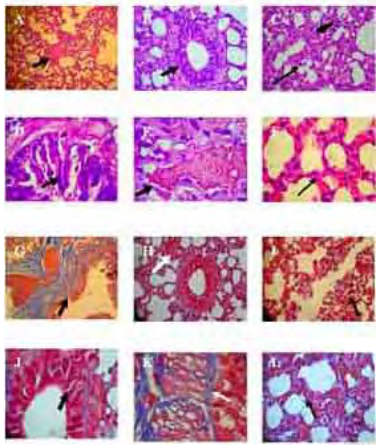

Figure 4. Sections of lungs exposed to CEES and LIP-4. Guinea pigs were exposed to CEES (2mg/kg) intratracheally and 5 minutes later received a single tracheal instillation of 200 µl LIP-4. After 30 days of CEES exposure, lung sections were stained with H & E (A-F) and trichrome stain (G-L) (A and G - 10x ; B, C, H and I - 40x; D, E, F, J, K and L - 100 x)

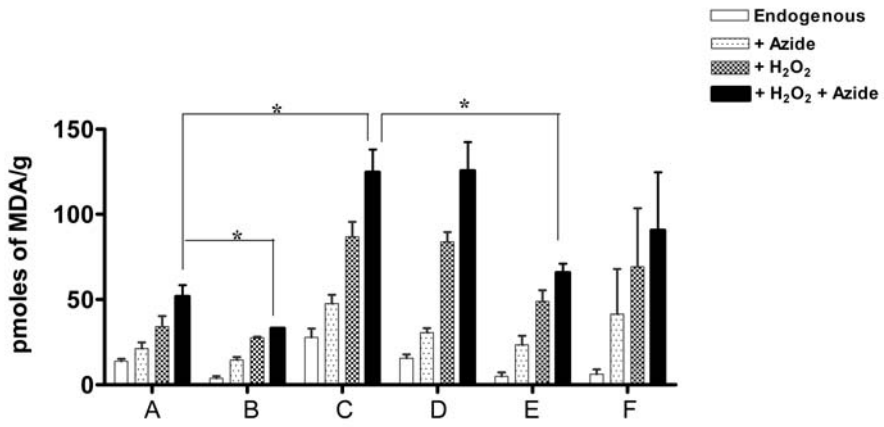

Figure 5. Effect of CEES exposure on *in vitro* lipid peroxidation of lung: Protection by liposome treatment. Guinea pigs were exposed to CEES (2mg/kg) intratracheally and 5 minutes later received a single tracheal instillation of 200 μl of liposomes (LIP-1, LIP-2 and LIP-4) and lungs were removed after 30 days of CEES exposure for measurement of lipid peroxidation. Lipid peroxidation was measured in the presence and absence of Na-azide, an irreversible inhibitor of catalse. A = Vehicle, B = Vehicle + blank liposome (LIP-1), C = CEES, D = CEES + LIP-1, E = CEES + LIP-2, F = CEE + LIP-4. Ateisks indicate statistically different ($P < 0.05$).

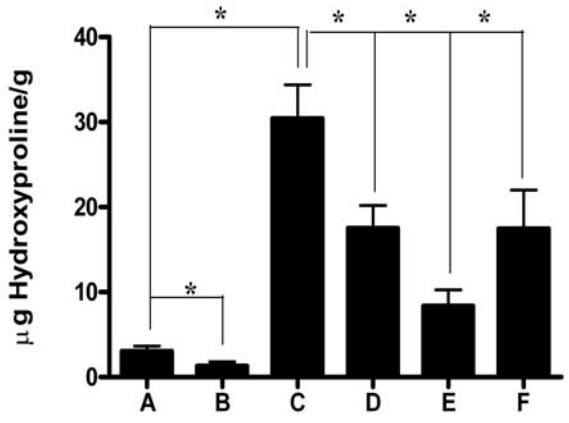

Figure 6. Effect of CEES exposure on the hydroxyproline content of lung: Protection by liposome treatment. Guinea pigs were exposed to CEES (2mg/kg) intratracheally and 5 minutes later received a single tracheal instillation of 200 μl of liposomes (LIP-1, LIP-2 and LIP-4) and lungs were removed after 30 days of CEES exposure for measurement of hydroxyproline A = Vehicle, B = Vehicle + blank liposome (LIP-1), C = CEES, D = CEES + LIP-1, E = CEES + LIP-2, F = CEES + LIP-4. Asterisks indicate statistically different ($P < 0.05$).

.

Reportable Outcomes

Presentations (Aug 21, 07 – Aug 20, 08)

1 Das SK, Activation of AP-1 Transcription Factors in mustard Gas-Induced Lung Injury. Annual Conference of Association of Clinical Biochemists of India, Dec 18-20, 2007, New Delhi, India, Indian J. Clin. Biochem. Vol 22 (Suppl) 19S6.4, 2007

2 Gadsden JL, Mukhopadhyay S, Schaeffer MW, Sinha Roy S, Mukherjee S and Das SK. Effects of 2-Chloroethyl Ethyl Sulfide (CEES), a Mustard Gas Analog, on Serotonin/Dopamine Signaling in Guinea Pig Brain, FASEB Meeting, April 4-9, 2008, San Diego, CA.

3 Schaeffer MW, Sinha Roy S, Mukherjee S and Das SK. Improved High-Performance Liquid Chromatography Method with Diode Array Detection for Simultaneous Analysis of Retinoic Acid Isomers, Retinol, Retinyl Esters, Vitamin E, and Selected Carotenoids in Guinea Pig Tissues, FASEB Meeting, April 5-9, 2008, San Diego, CA.

4 Sinha Roy S, Schaeffer MW, Mukherjee S and Das SK. Mustard Gas-Induced Alteration of Retinoid Metabolism/Signaling in Guinea Pig Lung, FASEB Meeting, April 4-9, 2008, San Diego, CA.

5 Mukhopadhyay S, Mukherjee S, Smith M.G. and Das S.K. Activation of MAPK/AP-1 Signaling and Associated Metalloproteinases and Cell Cycle Protein in Guinea Pig Lung by 2-Chloroethyl Ethyl Sulfide (CEES), a Mustard Gas Analog. 2008 Bioscience Review, page 151, Hunt Valley, MD, June 1-6, 2008.

Manuscripts (Aug 21, 07 – Aug 20, 08)

1. Smith M.G., Stone W., Ren-Feng G., Ward, P. A., Suntress Z., Mukherjee, S. and Das, S. K. Vesicants and Oxidative Stress, In: “Chemical Welfare Agents: Chemistry Pharmacology Toxicology, and Therapeutics, eds: J.A. Romano, B. J. Lukey and H. Salem, Taylor & Francis Publisher, pp 247-292, 2008.
2. Mukhopadhyay S, Mukherjee S, Smith M.G. and Das S.K. Activation of MAPK/AP-1 Signaling Pathway in Lung Injury Induced by 2-Chloroethyl Ethyl Sulfide, a Mustard Gas Analog, Toxicol lett. (2008), doi:10.1016/J.toxlet.2008.07.005..
3. Schaeffer M.W., Sinha Roy S., Mukherjee s. and Das S. K. Identification of lutein, a dietary antioxidant carotenoid in guinea pig tissues, Biochem Biophys. Res. Commun. 374: 378-381, 2008)

Conclusion

1. We have established in our laboratory that intratracheal exposure of 2-chloroethyl ethyl sulfide (CEES), a mustard gas analog to guinea pigs causes reactive oxygen species (ROS) mediated lung injury by stimulation of inflammatory cytokines, such as TNF-α and activation of transcription factor NF-κB. It is now evident that CEES-induced activation of TNF-α is associated with an increase in MAPKs/AP-1 signaling, a stimulation of cell proliferation and lung injury. Further studies are needed to clarify whether the observed effects are the adaptive responses of the lung or they contribute to the lung injury.

2. CEES-induced lung injury is associated with a decrease in the binding capacity of β-adrenergic receptors, inhibition of β2-adrenoreceptors gene expression as well as desensitization, internalization and degradation of β2-adrenoreceptors.

3. Liposomal delivery selectively enhances reducing environment in lung macrophages and thereby protects against CEES toxicity in these cells. This is further evident by our observation that antioxidant liposomes offer a protection against lipid peroxidation induced by CEES. Furthermore, our data clearly indicates that delivery of antioxidant liposomes, particularly LIP-2 which contains δ-tocopherol significantly protect against CEES-induced increase in lung on the levels of hydroxyproline, and thus lung fibrosis.

Pertinent References for Text

1. Sinha Roy, S; Mukherjee, S; Kabir, M; Rajaratnam, V; Smith, M and Das, S.K. Inhibition of Cholinephosphotransferase Activity in Lung Injury Induced by 2-Chloroethyl Ethyl Sulfide, a Mustard Analog, J. Biochem. Molecular Toxicol. 19: 289-297, 2005.
2. Chatterjee, D; Mukherjee, S; Smith M, and Das, S.K. Signal Transduction Events in Lung Injury Induced by 2-Choloroethyl Ethyl Sulfide, a Mustard Analog. J. Biochem. Molecular Toxicol. 17: 114-121, 2003.
3. Rajaratnam VS and Das SK. Array of Cytokine Induction in Early Lung Injury Response to 2-Chloroethyl Ethyl Sulfide, A Mustard Gas Analog. FASEB J., Vol. 19, A852, 2005, FASEB Meeting, April 2-6, 2005, San Diego, CA.
4. Das, S. K., Mukherjee, S., Smith, M and Chatterjee, D. Prophylactic Protection by N-Acetylcysteine Against the Pulmonary Injury Induced by 2-Chloroethyl Ethyl Sulfide, A Mustard Analogue, J. Biochem. Molecular Toxicol. 17: 177-184, 2003
5. Mukherjee S and Das SK. Pulmonary Fibrosis in Guinea Pig Induced by 2-Chloroethyl Ethyl Sulfide. FASEB J., Vol. 19, A280, 2005, FASEB Meeting, April 2-6, 2005, San Diego, CA.
6. McClintock, S.D., Hoesel L.M., Das, S. K., Till, G.O., Neff, T., Kunkel R.G., Smith M.G. and Ward, P.A. Attenuation of Half Sulfur Mustard Gas-Induced Acute Lung Injury in Rats. J. Applied Toxicology. 26: Issue 2, 126-131, 2006.
7. Das SK, Stone WL, Smith M and Mukherjee S. Protection of Mustard Gas-Induced Lung Injury by Antioxidant Liposomes. Proc 5th International SISPAT Symposium on Toxic Substances, Singapore, Nov 27-Dec 2, p 10-15, 2006.
8. Mukhopadhyay S, Rajaratnam V., Mukherjee S., Smith M and Das, S.K. Modulation of the Expression of Superoxide Dismutase Gene in Lung Injury by 2-Chloroethyl Ethyl Sulfide, a Mustard Analog. J. Biochem Mol. Toxicol. 20: 142-149, 2006.

Appendices (reprints in pdf format) (Aug 21, 07 – Aug 20, 08).

Mukhopadhyay S, Mukherjee S, Smith M.G. and Das S.K. Activation of MAPK/AP-1 Signaling Pathway in Lung Injury Induced by 2-Chloroethyl Ethyl Sulfide, a Mustard Gas Analog, Toxicol lett. (2008), doi:10.1016/J.toxlet.2008.07.005.

Schaeffer M.W., Sinha Roy S., Mukherjee s. and Das S. K. Identification of lutein, a dietary antioxidant carotenoid in guinea pig tissues, Biochem Biophys. Res. Commun. 374: 378-381, 2008), doi:10.1016/j.bbrc.2008.07.030.

Toxicology Letters xxx (2008) xxx–xxx

Contents lists available at ScienceDirect

Toxicology Letters

journal homepage: www.elsevier.com/locate/toxlet

Activation of MAPK/AP-1 signaling pathway in lung injury induced by 2-chloroethyl ethyl sulfide, a mustard gas analog

Sutapa Mukhopadhyay[a], Shyamali Mukherjee[a], Milton Smith[b], Salil K. Das[a,*]

[a] Department of Cancer Biology, Meharry Medical College, 1005 David Todd Blvd., Nashville, TN 37208, United States
[b] AMAOX Ltd, Melbourne, FL 32944, USA

ARTICLE INFO

Article history:
Received 7 May 2008
Received in revised form 2 July 2008
Accepted 2 July 2008
Available online xxx

Keywords:
MAPK
AP-1
Lung injury
CEES

ABSTRACT

We reported earlier that the activation of free-radical-mediated tumor necrosis factor-α (TNF-α) cascade is the major pathway in the inflammatory lung disease induced by 2-chloroethyl ethyl sulfide (CEES), a mustard gas analog. TNF-α induces activating protein 1 (AP-1) activation via phosphorylation of mitogen activated protein kinases (MAPKs). The present study examines the relationship between CEES induced lung injury and MAPKs signaling pathway. Adult guinea pigs received single intratracheal injection of different doses of CEES and were sacrificed at different time points. CEES exposure caused lung injury with evidence of fibrosis. The optimum activation of all members of the MAPKs family (ERK1/2, p38 and JNK1/2) was achieved at 0.5 mg/kg dose and at 1 h. No significant change was observed beyond that time point. This led to an activation of AP-1 transcription factors associated with an increase in the protein levels of Fos, activating transcription factor (ATF) and Jun family members. To explore the involvement of AP-1 in cell proliferation, we determined the protein levels of cell cycle protein cyclin D1 and cell differentiation marker proliferating cell nuclear antigen (PCNA). An up regulation of these proteins was observed. Hence it is suggested that CEES exposure causes accumulation of TNF-α, which is associated with an activation of MAPK/AP-1 signaling pathway and cell proliferation. Further studies are needed to clarify whether the observed effects are the adaptive responses of the lung or they contribute to the lung injury.

1. Introduction

Mustard gas is a well-known chemical warfare agent which was extensively used in World War I (Willems, 1989; Mellor et al., 1991). This poisonous chemical agent exerts its effects on eyes, skin, and respiratory tissue, and thereby impairment of nervous, cardiac, and digestive systems in humans and laboratory animals (Elsayed et al., 1989a,b; Momeni et al., 1992; Debrowska et al., 1996; Dacre and Goldman, 1996). Inhalation of mustard gas causes hemorrhagic inflammation to the tracheobronchial tree, with severe pulmonary complications, including adult respiratory distress syndrome (ARDS) (Elsayed et al., 1989a,b). Long-term exposure of mustard gas at low doses may lead to lung cancer (Calvet et al., 1994).

The basis for the tissue injuries caused by mustard gas is not fully understood. Mustard gas belongs to a group of bifunctional alkylating agents that has electrophilic properties. Several studies in rats and mice have shown that the mechanism of mustard gas action on lung, skin, or other organ includes DNA alkylation; cross-linking of DNA (Gross et al., 1985; Elsayed et al., 1992; Yamakido et al., 1996); activation of proteases, resulting in proteolysis of several vital intracellular enzymes and structural proteins (Cowman and Broomfield, 1993); production of free radicals and free radical-mediated oxidative stress (Kopff et al., 1994; Husain et al., 1996).

Mustard gas induced lung injury is associated with pulmonary fibrosis (McClintock et al., 2006). Tumor necrosis factor-α (TNF-α) is an important cytokine involved in the pathogenesis of inflammatory diseases of the lung. We have established earlier that the initiation of free-radical-mediated TNF-α cascade is the major pathway in the mustard gas mediated lung injury in guinea pigs (Chatterjee et al., 2003; Das et al., 2003). TNF-α induces transcriptional factor activating protein 1 (AP-1) activation via phosphorylation and activation of mitogen activated protein kinases (MAPKs) (Cohen et al., 2006). Interestingly, the promoter regions of many inflammatory cytokines and chemokines contain AP-1 binding sites (Koj, 1996; Zagariya et al., 1998; Roebuck et al., 1999) suggesting that AP-1 activation may be necessary for the induction of acute, cytokine-mediated inflammation. However, it is not known whether a similar mechanism is responsible for mustard gas induced lung injury in guinea pigs.

* Corresponding author. Tel.: +1 615 327 6988; fax: +1 615 327 6442.
E-mail address: sdas@mmc.edu (S.K. Das).

0378-4274/$ – see front matter © 2008 Elsevier Ireland Ltd. All rights reserved.
doi:10.1016/j.toxlet.2008.07.005

MAPKs cascades are multi-functional signaling pathways that are evolutionally well conserved in all eukaryotic cells. MAPKs are serine/threonine kinases that are sequentially phosphorylated by upstream kinases. Three major pathways, such as extracellular signal-regulating kinases (ERKs), c-Jun N-terminal kinases (JNKs, also referred to as stress-activated protein kinases), and p38 MAP kinases have been characterized (Kyriakis and Avruch, 2001; Takeda et al., 2003). They mediate signal transduction from the cell surface to the nucleus. Activation of ERK is primarily involved in growth factor- and phorbol ester-stimulated responses. Responses to proinflammatory cytokines, UV radiation, and other stresses are mostly dependent on JNK and p38 activation (Karin, 1995; Shaulian and Karin, 2001).

MAPK signaling pathways have been shown to affect AP-1 activity by direct phosphorylation of AP-1 proteins and by influence on the abundance of individual AP-1 components in a cell (Karin, 1995; Whitmarsh and Davis, 1996). AP-1 is an important regulatory protein involved in cell growth, differentiation, transformation, and apoptosis (Angel and Karin, 1991; Shaulian and Karin, 2001). The AP-1 complex consists of homo- or heterodimers of Fos families (c-Fos, Fos-B, Fra-1 and Fra-2), activating transcription factor families (ATF-1 and ATF-2) and Jun subfamilies (c-Jun, Jun-B and Jun-D) of basic-region leucine-zipper (B-ZIP) proteins (Herdegen and Leah, 1998; Steinmuller et al., 2001; Shaulian and Karin, 2002). These transcription factors act as converging points to MAPK signal transduction pathways activated by toxic or mitogenic stimuli. Upon activation, AP-1 binds to DNA sequences, such as 5′-TGAG/CTCA-3′ [TPA response element (TRE) or AP-1 site], and regulates the transcription of multiple genes, including themselves, in a context (promoter and cell type) - dependent manner (Angel and Karin, 1991; Zhang et al., 2004). Activation of JNK leads to the phosphorylation and activation of c-Jun, and ATF-2, that form heterodimers and preferentially bind to TRE to activate c-Jun transcription, and activation of p38 can also phosphorylate and activate ATF-2 (Karin, 1995). AP-1 proteins have been suggested to play both pro- and anti-regulatory roles in pulmonary defense, injury, and repair (Reddy and Mossman, 2002).

Based on this knowledge, it is important to evaluate the role of MAPK phosphorylation and subsequent AP-1 activation on the mustard gas induced lung injury. We hypothesized that exposure of 2-chloroethyl ethyl sulfide (CEES), a mustard gas analog modulates AP-1 family member expression in lung tissue, thereby altering protein–protein interactions between themselves and other members of the leucine-zipper super family of transcription factors. In this study, we investigated the roles of MAPK signaling pathways in the regulation of AP-1 transcriptional activity as well as AP-1 dependent cell cycle proteins.

2. Materials and methods

2.1. Animals and CEES treatment

Male guinea pigs (Hartley strain, 5–6 weeks old, 400 g body weight) were obtained from Harlan Sprague–Dawley Inc. (Indianapolis, IN). To determine the optimum treatment time, animals were infused intratracheally with a single dose (0.5 mg/kg body wt.) of CEES (Sigma Chemicals, St. Louis, MO) in ethanol (infusion volume was 100 μl/animal). Control animals were infused with 100 μl of ethanol in the same way. The animals were then sacrificed after different time points of 1 h and 1, 7, 14 and 30 days of post-CEES infusion. For dose-dependent studies, animals were intratracheally infused with single injection of different doses (0.5, 2 and 4 mg/kg body wt.) of CEES in ethanol for 1 h. Lungs were perfused with 2.6 mM phosphate buffered saline containing 5.6 mM glucose, removed from the chest cavity and immediately flash frozen in liquid nitrogen and stored at −80 °C for further experiment.

2.2. AP-1 activation assay

The activation of individual family member of AP-1 in the lung tissues was measured by TransAM AP-1 ELISA kits (Active Motif, Carlsbad, CA) according to the manufacturer's protocol.

2.3. Western blot analysis

Lung tissues were homogenized in a 5 volume of ice cold lysis buffer (Biosource, Camarillo, CA) containing protease inhibitor cocktail (0.01%, Sigma Chemicals, St. Louis, MO) by using a Brinkman Polytron (setting 6–7, 30 s). Proteins were measured by Bio-Rad protein assay (Bio-Rad, Hercules, CA) and 50 μg protein was separated by

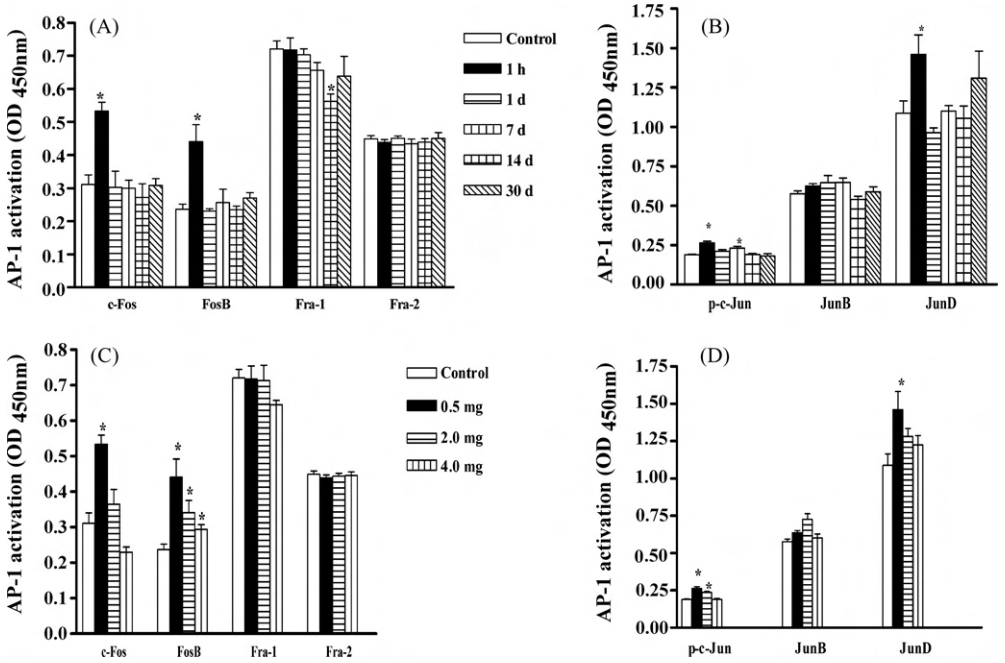

Fig. 1. CEES-induced activation of DNA binding of AP-1 family members in guinea pig lung. (A) Time dependent induction of AP-1 DNA binding activity after intratracheal injection of CEES (0.5 mg/kg body wt.). (B) DNA binding activity of AP-1 1 h after exposure to CEES at different doses (ranging from 0.5 to 4.0 mg/kg body wt.). Statistical significance was determined by Dunnett's test after one-way ANOVA. Results are expressed as mean ± S.E. ($N = 3$), $^{*}p < 0.05$ compared to control.

Please cite this article in press as: Mukhopadhyay, S., et al., Activation of MAPK/AP-1 signaling pathway in lung injury induced by 2-chloroethyl ethyl sulfide, a mustard gas analog. Toxicol. Lett. (2008), doi:10.1016/j.toxlet.2008.07.005

12% SDS polyacrylamide gel electrophoresis (SDS-PAGE). Proteins were transferred electrophoretically onto PVDF membranes Immobilon-P (Millipore, Bedford, MA). The membrane was immunoblotted with primary antibodies: MAPK (Cell Signaling Tech., Danvers, MA), c-Fos, FosB, Fra-1, Fra-2, c-Jun, JunB, JunD, ATF-2, L-ZIP, cyclin D1 and proliferating cell nuclear antigen (PCNA) (Santa Cruz Biotechnology Inc., Santa Cruz, CA) and horseradish peroxidase (HRP)-conjugated anti mouse, anti-goat and anti-rabbit secondary antibodies. Binding of antibodies to the blots was detected with an ECL-detection system (PerkinElmer, Boston, MA) following manufacturer's instructions. Stripped blots were re-probed with β-actin specific polyclonal antibodies (Santa Cruz Biotechnology Inc., Santa Cruz, CA) to enable normalization of signals between samples. Band intensities were analyzed using Bio-Rad Gel Doc (Bio-Rad, Hercules, CA).

2.4. Statistical analysis

Data were expressed as means ± standard error (S.E.). Statistical significance was determined by the Student's *t*-test or by Dunnett's test after one-way analysis of variance (ANOVA), when multiple comparisons were made, using GraphPad prism Version 4.0 (GraphPad software, San Diego, CA). Results were considered statistically significant at $p < 0.05$.

3. Results

3.1. AP-1 family profiling for DNA binding activation after CEES exposure

To determine the time at which maximal activation of AP-1 is expressed, we have given single intratracheal injection (0.5 mg/kg body weight) of CEES to guinea pigs. At different time points, the guinea pigs were sacrificed and lungs were removed after perfusion and AP-1 activation were measured. Fig. 1A shows the effects of CEES on activation of AP-1 over time. The DNA binding activity of c-Fos, FosB, p-c-Jun and JunD was increased within 1 h of CEES exposure, but the activity decreased rapidly after 1 h and came to the normal level up to 30 days. No effect was noticed on Fra-1, Fra-2 and JunB. Fig. 1B shows the dose-dependent effects of CEES on AP-1 activation after 1 h. These studies revealed that optimal DNA activation of c-Fos, Fos B, p-c-Jun and JunD was observed at 0.5 mg/kg dose of CEES exposure.

3.2. Effects of CEES on MAPK activity

The optimum activation of individual family member of AP-1 was achieved at 0.5 mg dose and at 1 h; hence we focused our research on that particular dose and time point. CEES exposure caused a 100%, 33% and 42% increase in the phosphorylation of ERK1/2 (p44/42), p38 and JNK 1/2 (p54/46), respectively (Fig. 2).

3.3. Western blot analysis of AP-1 transcription factors

Since we observed a higher DNA binding activity of AP-1 transcription factor in CEES-exposed lung (Fig. 1), we determined the protein levels of individual members of AP-1 family. First we studied the protein levels of ATF-2 and L-ZIP. CEES exposure caused a significant increase in the protein level of only ATF-2 (68%) and not L-ZIP (Fig. 3A).

Among Fos members of the AP-1 transcription factors family, the optimum activation was achieved at 0.5 mg dose and at 1 h. The protein level was significantly increased in all four members of Fos family (Fig. 3B). CEES exposure caused a 134%, 75%, 250%, and 51% increase in the protein levels of c-Fos, FosB, Fra-1 and Fra-2, respectively. It should be noted however that even though protein levels of Fra-1 and Fra-2 were increased due to CEES exposure, we did not find any increase on their DNA binding activity (Fig. 1).

All members of the Jun family were activated optimally at 0.5 mg dose and at 1 h of CEES exposure. The protein level was significantly increased in all three members of Jun family (Fig. 3C). CEES exposure caused a 140%, 90%, and 300% increase in the protein levels of c-Jun, JunB, and JunD, respectively. DNA binding activity of JunB however was not changed (Fig. 1).

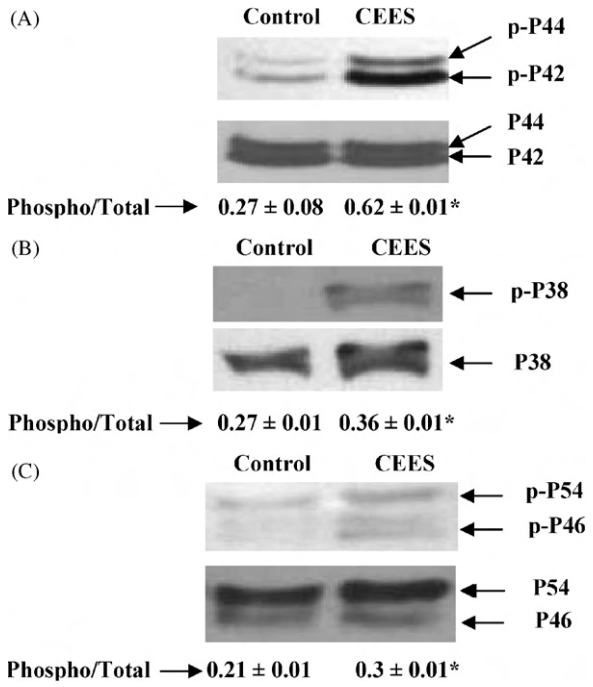

Fig. 2. CEES-induced activation of MAPKs in guinea pig lung. Western blot analysis of ERK 1/2 (A), p38 (B), JNK 1/2 (C) ($N = 3$ in each group). Statistical significance was determined by the Student's *t*-test. Results are expressed as mean ± S.E., $^{*}p < 0.05$ compared to control.

3.4. Up regulation of AP-1 dependent cell cycle proteins by CEES exposure

To further explore the involvement of AP-1 in cell proliferation, we determined the protein levels of cell cycle proteins, PCNA and cyclin D1 (Fig. 4). Both dose-and time-response effects were studied. The optimum effect was observed at 0.5 mg dose for both proteins. The optimum activation was achieved at 1 h (data not shown). Fig. 4 demonstrates that CEES exposure caused a 49% and 93% increase in the protein levels of cyclin D1 and PCNA, respectively.

4. Discussion

We observed that exposure of CEES to guinea pigs resulted an immediate and severe injury to lung epithelium. It is evident from our earlier findings (Sinha Roy et al., 2005) that CEES exposure causes a clear morphological change in the type II alveolar cells and disruption in their secretory function due to accumulation of lamellar bodies. These cells are responsible for the secretion of lung surfactant, and any injury to these cells is expected to cause a modulation in surfactant secretion.

We already reported that the initiation of free-radical-mediated TNF-α cascade is the major pathway in the mustard gas mediated adult respiratory distress syndrome (Chatterjee et al., 2003). TNF-α induces the activation of AP-1 in alveolar epithelial cells (Rahman, 2000). TNF-α promoter itself contains AP-1 binding sites and is subject to positive auto regulation (Baud and Karin, 2001). We found earlier that TNF-α increased within 1 h of CEES exposure (Chatterjee et al., 2003). Similarly, we found that exposure with 0.5 mg/kg dose of CEES after 1 h significantly induced the basal level of AP-1 activation in guinea pig lung (Fig. 1). Thus, we chose this concentration to investigate the possible signaling pathways involved in the regulation of AP-1 activation.

Please cite this article in press as: Mukhopadhyay, S., et al., Activation of MAPK/AP-1 signaling pathway in lung injury induced by 2-chloroethyl ethyl sulfide, a mustard gas analog. Toxicol. Lett. (2008), doi:10.1016/j.toxlet.2008.07.005

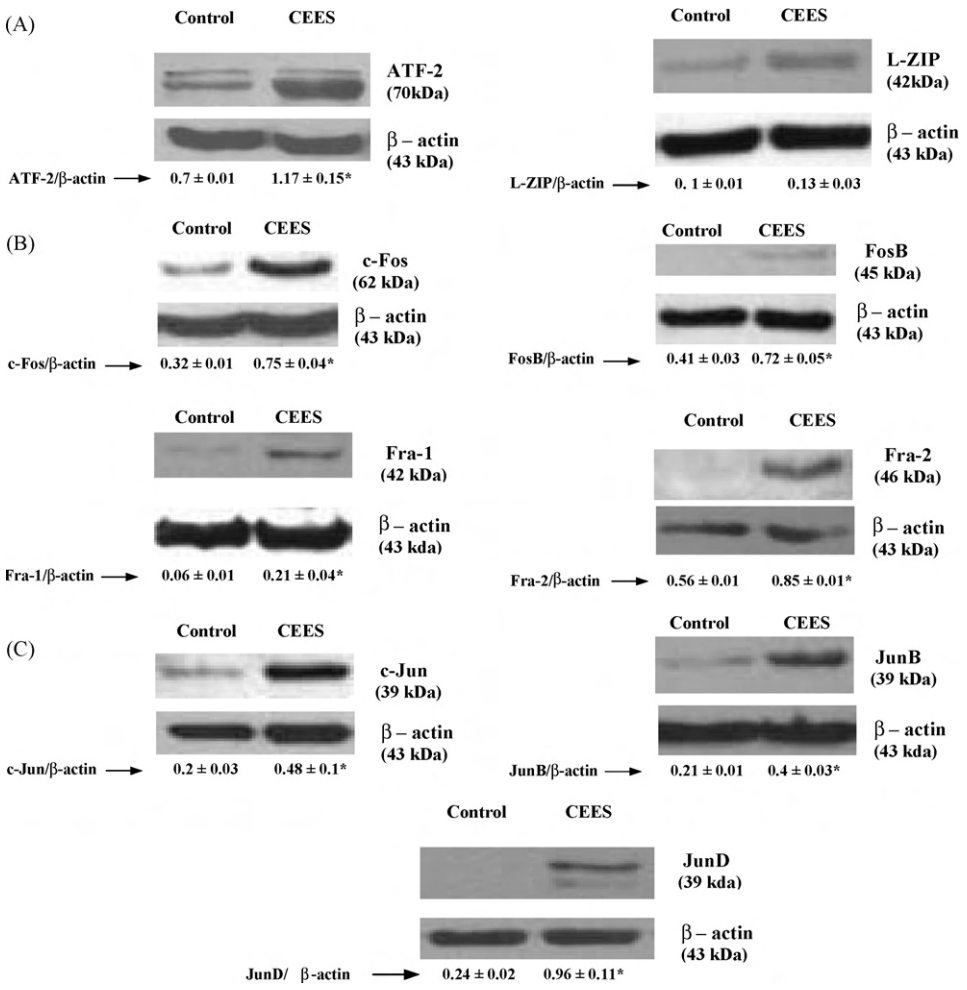

Fig. 3. CEES-induced increase in protein levels of AP-1 transcription factors in guinea pig lung. Western blot analysis of ATF-2 and L-ZIP (A); c-Fos, Fos-B, Fra-1, Fra-2 (B); c-Jun, JunB, JunD (C) ($N = 3$ in each group). Statistical significance was determined by the Student's t-test. Results are expressed as mean ± S.E., $^{*}p < 0.05$ compared to control.

The present study examines the relationship between mustard gas induced lung injury and MAPKs signaling pathway in guinea pig. To elucidate the mechanisms, we measured the activity (total and phospho) of individual members of the MAPK family (p38, JNK1/2, and ERK1/2) in the lung tissues. According to our results, a significant increase was observed in the phosphorylation of all three MAPKs (ERK, JNK and p38) in CEES-exposed animals (Fig. 2). These results are in agreement with previous finding that JNK cascade is activated following exposure to inflammatory cytokines (Karin, 1995). In addition to that, Carter et al. (1999) also demonstrated that activation of both the ERK and p38 kinase pathways is necessary for optimal accumulation of IL-6 and TNF mRNAs and cytokine release from endotoxin (LPS)-stimulated alveolar macrophages (AM). Inhibition of either of these pathways only partially reduced cytokine gene expression, but simultaneous inhibition of both pathways resulted in a marked reduction in expression of these genes. Our result also suggests that mustard gas induced induction of inflammatory cytokines trigger the ERK, JNK and p38 MAPK signal transduction pathways that may cause the ultimate lung damage.

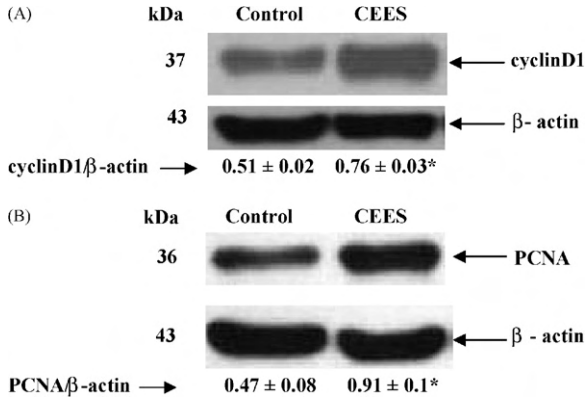

Fig. 4. CEES-induced activation of AP-1 dependent cell cycle protein in guinea pig lung. Western blot analysis of cyclin D1 (A) and PCNA (B) ($N = 3$ in each group). Statistical significance was determined by the Student's t-test. Results are expressed as mean ± S.E., $^{*}p < 0.05$ compared to control.

Distinct MAPK pathways are responsible for the phosphorylation and activation of AP-1 proteins (Zhong et al., 2005). The stress-responsive p38 and JNK MAPK pathways regulate cell cycle and apoptosis (Zhang et al., 2005). MAPKs have significant roles in mediating signals triggered by cytokines, growth factors, and environmental stress; and are involved in controlling cell proliferation, cell differentiation, and death (Franklin et al., 1994; Rincon, 2001).

AP-1 is the down stream signal of MAPKs signaling pathways (Karin, 1995), and the blocking of MAPKs leads to the inhibition of AP-1 transactivation and subsequent cell transformation (Dong et al., 1997). AP-1 activity plays a critical role in the process of tumorigenesis (Angel and Karin, 1991; Sun and Oberley, 1996). AP-1 regulates cellular proliferation, differentiation, apoptosis, cancer

Please cite this article in press as: Mukhopadhyay, S., et al., Activation of MAPK/AP-1 signaling pathway in lung injury induced by 2-chloroethyl ethyl sulfide, a mustard gas analog. Toxicol. Lett. (2008), doi:10.1016/j.toxlet.2008.07.005

cell invasion and oncogene-induced transformation (McDonnell et al., 1990; Szabo et al., 1991; Brown et al., 1993).

To elucidate whether any down stream signal of MAPK pathway is affected by CEES exposure, we monitored the protein levels of AP-1 family. Since AP-1 is a homo or hetero dimers of Fos family, activating transcription factor (ATF) and Jun subfamilies of basic-region leucine-zipper (L-ZIP) proteins, we measured the protein levels of individual components. We observed a significant increase in ATF-2 protein level (Fig. 3A). At the transcription level, ATF-2 is phosphorylated and activated by all three MAPKs, supporting our observation that increased MAPK activity may result in an increase in ATF-2. We measured the protein level of individual family members of both Fos (c-Fos, Fra-1, Fra-2 and Fos-B) and Jun (c-Jun, Jun-B and Jun-D) families. We found a significant increase of c-Fos, FosB, Fra-1 and Fra-2 in the CEES-exposed animals (Fig. 3B). A significant increase in the protein levels of c-Jun, JunB and Jun-D was also observed in animals exposed to CEES in contrast to the control animals (Fig. 3C). Since c-Jun is phosphorylated by JNK, observed increased level of phosphorylated JNK is responsible for the increase in phosphorylated c-Jun level (Figs. 1 and 2). Phosphorylation of c-Jun stimulates their ability to activate transcription, thereby leading to c-Jun induction (Karin, 1995).

Jun and Fos proteins differ significantly in both their DNA binding and transactivation potential as well as their target gene regulation (Zhong et al., 2005). In vitro studies have shown that Jun/Fos heterodimers are more stable and have a stronger DNA binding activity than Jun homodimers (Ryseck and Bravo, 1991). Thus, increased activation of AP-1 in CEES-exposed lung was due to c-Fos and c-Jun dimerization.

PCNA is a cofactor of DNA polymerase delta and is required for DNA synthesis. The PCNA gene contains AP-1 sites in the promoter region and its expression is regulated by AP-1 activity (Yamaguchi et al., 1991; Gillardon et al., 1995). Our result shows an up-regulation of PCNA in CEES-exposed animal compared with control (Fig. 4). Cyclin D1, the regulatory subunit of several cyclin-dependent kinases, is required for, and capable of shortening, the G1 phase of the cell cycle. AP-1 proteins bind the cyclin D1-954 region. Cyclin D1 promoter activity is stimulated by over expression of mitogen-activated protein kinase through the proximal 22 base pairs (Albanese et al., 1995). Several AP-1 proteins are shown to bind these sites and activate cyclin D1 expression (Albanese et al., 1995; Brown et al., 1998; Beier et al., 1999). Our results show that up regulation of AP-1 dependent cell cycle proteins as well as cell differentiation marker occur in the lung of animals exposed to CEES (Fig. 4).

In conclusion, it is evident that CEES-induced activation of TNF-α is associated with an increase in MAPKs/AP-1 signaling, a stimulation of cell proliferation and lung injury. Further studies are needed to clarify whether the observed effects are the adaptive responses of the lung or they contribute to the lung injury.

Conflict of interest

None.

Acknowledgement

This study was supported by the US Army Grant W81XWH-06-2-0044.

References

Albanese, C., Johnson, J., Watanabe, G., Eklund, N., Vu, D., Arnold, A., Pestell, R.G., 1995. Transforming p21ras mutants and c-Ets-2 activate the cyclin D1 promoter through distinguishable regions. J. Biol. Chem. 270, 23589–23597.

Angel, P., Karin, M., 1991. The role of Jun, Fos and the AP-1 complex in cell-proliferation and transformation. Biochim. Biophys. Acta 1072, 129–157.

Baud, V., Karin, M., 2001. Signal transduction by tumor necrosis factor and its relatives. Trends Cell Biol. 11, 372–377.

Beier, F., Lee, R.J., Taylor, A.C., Pestell, R.G., LuValle, P., 1999. Identification of the cyclin D1 gene as a target of activating transcription factor 2 in chondrocytes. Proc. Natl. Acad. Sci. U.S.A. 96, 1433–1438.

Brown, J.R., Nigh, E., Lee, R.J., Te, H., Thompson, M.A., Saudou, F., Pestell, R.G., Greenberg, M.E., 1998. Fos family members induce cell cycle entry by activating cyclin D1. Mol. Cell Biol. 18, 5609–5619.

Brown, P.H., Alani, R., Preis, L.H., Szabo, E., Birrer, M.J., 1993. Suppression of oncogene-induced transformation by a deletion mutant of c-jun. Oncogene 8, 877–886.

Calvet, J.H., Jarrean, P.H., Levame, M., D'ortho, M.P., Lorino, H., Harf, A., Mavier, I.M., 1994. Acute and chronic respiratory effects of sulfur mustard intoxication in guinea pigs. J. Appl. Physiol. 76, 681–688.

Carter, A.B., Monick, M.M., Hunninghake, G.W., 1999. Both Erk and p38 kinases are necessary for cytokine gene transcription. Am. J. Respir. Cell Mol. Biol. 20, 751–758.

Chatterjee, D., Mukherjee, S., Smith, M.G., Das, S.K., 2003. Signal transduction events in lung injury induced by 2-chloroethyl ethyl sulfide, a mustard analog. J. Biochem. Mol. Toxicol. 17, 114–121.

Cohen, M., Meisser, A., Haenggeli, L., Bischof, P., 2006. Involvement of MAPK pathway in TNF-alpha-induced MMP-9 expression in human trophoblastic cells. Mol. Human Reprod. 12, 225–232.

Cowman, F.M., Broomfield, C.A., 1993. Putative roles of inflammation in the dermatopathology of sulfur mustard. Cell Biol. Toxicol. 9, 201–213.

Dacre, J.C., Goldman, M., 1996. Toxicology and pharmacology of the chemical warfare agent sulfur mustard. Pharmacol. Rev. 48, 289–326.

Das, S.K., Mukherjee, S., Smith, M., Chatterjee, D., 2003. Prophylactic protection by N-acetylcysteine against the pulmonary injury induced by 2-chloroethyl ethyl sulfide, a mustard analogue. J. Biochem. Mol. Toxicol. 17, 177–184.

Debrowska, M.I., Becks, L.L., Lelli, J.L., Levee, M.G., Hinshaw, D.B., 1996. Sulfur mustard induces apoptosis and necrosis in endothelial cells. Toxicol. Appl. Pharmacol. 141, 568–583.

Dong, Z., Ma, W., Huang, C., Yang, C.S., 1997. Inhibition of tumor promoter-induced activator protein 1 activation and cell transformation by tea polyphenols, (−)-epigallocatechin gallate, and theaflavins. Cancer Res. 57, 4414–4419.

Elsayed, N.M., Omaye, S.T., Klain, G.J., Inase, J.L., Dahlberg, E.T., Wheeler, C.R., Korte, D.W., 1989a. Response of mouse brain to a single subcutaneous injection of the monofunctional sulfur mustard, butyl-2-chloroethyl sulfide (BCS). Toxocology 58, 11–20.

Elsayed, N.M., Omaye, S.T., Klain, G.J., Korte, D.W., 1992. Free radical mediated lung response to the monofunctional sulfur mustard, butyl-2-chloroethyl sulfide after subcutaneous injection. Toxicology 72, 153–165.

Elsayed, N.M., Ta, P.N., Korte, D.W., 1989b. Biochemical alterations in mouse liver induced by nitrogen mustard. Toxicologist 9, 26–34.

Franklin, R.A., Tordai, A., Patel, H., Gardner, A.M., Johnson, G.L., Gelfand, E.W., 1994. Ligation of the T-cell receptor complex results in activation of the Ras/Raf-1/MEK/MAPK cascade in human T lymphocytes. J. Clin. Invest. 93, 2134–2140.

Gillardon, F., Moll, I., Uhlmann, E., 1995. Inhibition of c-Fos expression in the UV-irradiated epidermis by topical application of antisense oligodeoxynucleotides suppresses activation of proliferating cell nuclear antigen. Carcinogenesis 16, 1853–1856.

Gross, C.L., Meier, H.L., Papirmeister, B., Brinkley, F.B., Johnson, J.B., 1985. Sulfur mustard lowers nicotinamide adenine dinucleotide concentrations in human skin grafted to nude mice. Toxicol. Appl. Pharmacol. 81, 85–90.

Herdegen, T., Leah, J.D., 1998. Inducible and constitutive transcription factors in the mammalian nervous system: control of gene expression by Jun, Fos and Krox, and CREB/ATF proteins. Brain Res. Brain Res. Rev. 28, 370–490.

Husain, K., Dube, S.N., Sugendran, K., Singh, R., DasGupta, S., Somani, S.M., 1996. Effect of topically applied sulphur mustard on antioxidant enzymes in blood cells and body tissues of rats. J. Appl. Toxicol. 16, 245–248.

Karin, M., 1995. The regulation of AP-1 activity by mitogen-activated protein kinases. J. Biol. Chem. 270, 16483–16486.

Koj, A., 1996. Initiation of acute phase response and synthesis of cytokines. Biochim. Biophys. Acta 1317, 84–94.

Kopff, M., Zakrzewska, I., Strzelczyk, M., Klem, J., Dubiecki, W., 1994. Superoxide dismutase and catalase activity in psoriatic patients treated topically with ointment containing 2-chloroethyl-3-chloropropyl sulfide. Pol. J. Pharmacol. 46, 439–444.

Kyriakis, J.M., Avruch, J., 2001. Mammalian mitogen-activated protein kinase signal transduction pathways activated by stress and inflammation. Physiol. Rev. 81, 807–869.

McClintock, S.D., Hoesel, L.M., Das, S.K., Till, G.O., Neff, T., Kunkel, R.G., Smith, M.G., Ward, P.A., 2006. Attenuation of half sulfur mustard gas-induced acute lung injury in rats. J. Appl. Toxicol. 26, 126–131.

McDonnell, S.E., Kerr, L.D., Matrisian, L.M., 1990. Epidermal growth factor stimulation of stromelysin mRNA in rat fibroblasts requires induction of proto-oncogenes c-fos and c-jun and activation of protein kinase C. Mol. Cell Biol. 10, 4284–4293.

Mellor, S.G., Rice, P., Cooper, G.C., 1991. Vesicant burns. Br. J. Plast. Surg. 44, 434–437.

Momeni, A.Z., Enshaeih, S., Meghadadi, M., Amindjavaheri, M., 1992. Skin manifestations of mustard gas: a clinical study of 535 patients exposed to mustard gas. Arch. Dermatol. 128, 775–780.

Rahman, I., 2000. Regulation of nuclear factor-kappa B, activator protein-1, and glutathione levels by tumor necrosis factor-alpha and dexamethasone in alveolar epithelial cells. Biochem. Pharmacol. 60, 1041–1049.

Please cite this article in press as: Mukhopadhyay, S., et al., Activation of MAPK/AP-1 signaling pathway in lung injury induced by 2-chloroethyl ethyl sulfide, a mustard gas analog. Toxicol. Lett. (2008), doi:10.1016/j.toxlet.2008.07.005

Reddy, S.P., Mossman, B.T., 2002. Role and regulation of activator protein-1 in toxicant-induced responses of the lung. Am. J. Physiol. Lung Cell Mol. Physiol. 283, L1161–L1178.
Rincon, M., 2001. MAP-kinase signaling pathways in T-cell. Curr. Opin. Immunol. 13, 339–345.
Roebuck, K.A., Carpenter, L.R., Lakshminarayanan, V., Page, S.M., Moy, J.N., Thomas, L.L., 1999. Stimulus-specific regulation of chemokine expression involves differential activation of the redox-responsive transcription factors AP-1 and NF-kappaB. J. Leukoc. Biol. 65, 291–298.
Ryseck, R.P., Bravo, R., 1991. c-Jun, JunB, JunD differ in their binding affinities to AP-1 and CRE consensus sequences: effects of fos proteins. Oncogene 6, 533–542.
Shaulian, E., Karin, M., 2001. AP-1 in cell proliferation and survival. Oncogene 20, 2390–2400.
Shaulian, E., Karin, M., 2002. AP-1 as a regulator of cell life and death. Nat. Cell Biol. 4, E131–E136.
Sinha Roy, S., Mukherjee, S., Kabir, S., Rajaratnam, V., Smith, M., Das, S.K., 2005. Inhibition of cholinephosphotransferase activity in lung injury induced by 2-chloroethyl ethyl sulfide, a mustard analog. J. Biochem. Molec. Toxicol. 19, 289–297.
Steinmuller, L., Cibelli, G., Moll, J.R., Vinson, C., Thiel, G., 2001. Regulation and composition of activator protein 1 (AP-1) transcription factors controlling collagenase and c-Jun promoter activities. Biochem. J. 360, 599–607.
Sun, Y., Oberley, L.W., 1996. Redox regulation of transcriptional activators. Free Radic. Biol. Med. 21, 335–348.
Szabo, E., Presis, L.H., Brown, P.H., Birrer, M.J., 1991. The role of jun and fos gene family members in 12-*O*-tetradecanoylphorbol-13-acetate induced hemopoietic differentiation. Cell Growth Differ. 2, 475–482.
Takeda, K., Matsuzawa, A., Nishitoh, H., Ichijo, H., 2003. Roles of MAPKKK ASK1 in stress-induced cell death. Cell Struct. Funct. 28, 23–29.
Whitmarsh, A.J., Davis, R.J., 1996. Transcription factor AP-1 regulation by mitogen-activated protein kinase signal transduction pathways. J. Mol. Med. 74, 589–607.
Willems, J.L., 1989. Clinical management of mustard gas casualties. Annal. Med. Milit. Belg. 3, 1–61.
Yamaguchi, M., Hayashi, Y., Hirose, F., Matsuoka, S., Moriuchi, T., Shiroishi, T., Moriwaki, K., Matsukage, A., 1991. Molecular cloning and structural analysis of mouse gene and pseudogenes for proliferating cell nuclear antigen. Nucleic Acids Res. 19, 2403–2410.
Yamakido, M., Ishinka, S., Hiyama, K., Maeda, A., 1996. Former poison gas workers and cancer: Incidence and inhibition of tumor formation by treatment with biological response modifier N-CWS. Environ. Health Perspect. 104, 485–488.
Zagariya, A., Mungre, S., Lovis, R., Birrer, M., Ness, S., Thimmapaya, B., Pope, R., 1998. Tumor necrosis factor alpha gene regulation: enhancement of C/EBPbeta-induced activation by c-Jun. Mol. Cell Biol. 18, 2815–2824.
Zhang, N., Ahsan, M.H., Zhu, L., Sambucetti, L.C., Purchio, A.F., West, D.B., 2005. NF-κB and not the MAPK signaling pathway regulates GADD45β expression during acute inflammation. J. Biol. Chem. 280, 21400–21408.
Zhang, Q., Kleeberger, S.R., Reddy, S.P., 2004. DEP-induced fra-1 expression correlates with a distinct activation of AP-1-dependent gene transcription in the lung. Am. J. Physiol. Lung Cell Mol. Physiol. 286, L427–L436.
Zhong, C.Y., Zhou, Y.M., Douglas, G.C., Witschi, H., Pinkerton, K.E., 2005. MAPK/AP-1 signal pathway in tobacco smoke-induced cell proliferation and squamous metaplasia in the lungs of rats. Carcinogenesis 26, 2187–2195.

Please cite this article in press as: Mukhopadhyay, S., et al., Activation of MAPK/AP-1 signaling pathway in lung injury induced by 2-chloroethyl ethyl sulfide, a mustard gas analog. Toxicol. Lett. (2008), doi:10.1016/j.toxlet.2008.07.005

Biochemical and Biophysical Research Communications 374 (2008) 378–381

Contents lists available at ScienceDirect

Biochemical and Biophysical Research Communications

journal homepage: www.elsevier.com/locate/ybbrc

Identification of lutein, a dietary antioxidant carotenoid in guinea pig tissues

Michael W. Schäffer, Somdutta Sinha Roy, Shyamali Mukherjee, Salil K. Das *

Department of Cancer Biology, Meharry Medical College, 1005 David Todd Boulevard, Nashville, TN 37208, USA

ARTICLE INFO

Article history:
Received 8 July 2008
Available online 16 July 2008

Keywords:
Guinea pig
Tissues
Carotenoids
Lutein
HPLC

ABSTRACT

Lutein, a dietary carotenoid, is a well known antioxidant. The major source of this carotenoid in humans is diet. We report here the presence of lutein, a dietary carotenoid in several guinea pig tissues (in decreasing order: liver > spleen > lung ≫ testis > kidney > plasma > eye but not in white adipose tissue). The presence of lutein in lung and other tissues may be significant in term of its antioxidant capacity of these organs.

Lutein and its stereoisomer zeaxanthin are members of the xanthophyll family of carotenoids. In diet, they can be found in high concentrations in dark green, leafy vegetables, in orange colored fruits and vegetables and in egg yolks [1]. Lutein and zeaxanthin are powerful antioxidants that play an important role in ocular health and in the prevention of cardiovascular disease, stroke, and lung cancer [1].

Rodents are often used as model systems for studies on various metabolic pathways and diseases. Our laboratory uses a guinea pig model system to study the effects of various inhalable environmental toxicants (e.g. tobacco smoke) [2]. Therefore it is of particular interest to monitor levels of different antioxidant vitamins and carotenoids in various tissues of a model rodent system.

Using a recently developed gradient HPLC-method of our laboratory with photodiode-array detection [3], we describe the identification of lutein in selected guinea pig tissues, which is likely to be absorbed and accumulated from food.

Materials and methods

Chemicals and reagents. HPLC-grade acetonitrile, methanol, hexane, tetrahydrofuran (THF), acetic acid (glacial), and ethanol were purchased from Fisher Scientific (Pittsburgh, PA). Standards were purchased from Carotenature GmbH, Lupsingen, Switzerland (Lutein, zeaxanthin, lycopene) or Sigma–Aldrich, St. Louis, MO (β-apo-8′-carotenal, β-carotene). Standard solutions were prepared and handled under protection from light and stored at −80 °C.

HPLC analysis. The HPLC-system (Shimadzu, Norcross, GA) was equipped with an autoinjector SIL-10ADvp (with 20 μL injection loop), an online solvent degasser DGU-14A, a system controller CBM-10AWvp, a low pressure gradient unit FCV-10ALvp, a solvent delivery unit LC-10ADvp, a column oven CTO-10Avp, and a photodiode-array detector SPD-M10Avp, controlled by EZStart v7.3 software. The chromatographic analysis was performed using an analytical scale (Dimensions 300 mm × 4 mm) Nucleosil column C18, with a particle size 3 μm and a pore size of 120 Å (ES Industries, West Berlin, NJ).

The chromatographic conditions were as follows: mobile phase A: acetonitrile/H_2O/glacial acetic acid—90/10/2; mobile phase B: acetonitrile/methanol—90/10; mobile phase C: 100% THF), over a total run time of 26 min. The following gradient program was applied: 0–4.5 min 100% A, 6.5 min 100% B, 12 min 60% B, 40% C, from 15–20 min to 100% B, until 26 min back to 100% A with a constant flow rate of 1 mL/min, and a constant column temperature of 22 °C.

Animals. Guinea pigs (Hartley Strain, *Cavia porcellus*) were obtained from Harlan (Indianapolis, IN) and maintained on a guinea pig diet (#7006), purchased from Harlan Teklad (Madison, WI). Animals received diet and drinking water *ad libitum* and were housed under standard conditions. Animals were sacrificed by decapitation. Organs were taken out, flushed in ice-chilled phosphate buffered saline (PBS) and flash-frozen in liquid nitrogen. Samples were stored at −80 °C away from light until analysis.

Standards and quantification

External calibration. A stock solution was prepared by dissolving the pure chemical in ethanol. The absorption was measured by spectrophotometry (Perkin-Elmer, Shelton, CT) at a wavelength

* Corresponding author. Fax: +1 615 327 6442.
E-mail address: sdas@mmc.edu (S.K. Das).

0006-291X/$ - see front matter © 2008 Elsevier Inc. All rights reserved.
doi:10.1016/j.bbrc.2008.07.030

of 450 nm against ethanol (lutein, zeaxanthin) or hexane (lycopene, β-carotene) and diluted with ethanol or hexane until a value of approximately 0.5 was achieved. The concentration was calculated according to Lambert–Beer's law using the molar extinction coefficients according to Barua et al. [4]. Six different volumes of the diluted solution were dried by evaporation under nitrogen and re-dissolved in 200 μL isopropanol resulting in six different concentrations. These solutions were prepared fresh for every use and applied directly for HPLC.

Internal standard. Retinyl acetate (RAc) was chosen as internal standard since this substance has similar chemical properties as the analytes and in addition RAc is a not a naturally occurring vitamin A-metabolite. The same amount of RAc was added to each sample before the extraction procedure.

Extraction of lutein from the tissue samples. Tissue specimens were homogenized in PBS with a tissue homogenizer, Model PRO 200 (Pro Scientific Inc., Monroe, CT). Equal volume of ethanol, containing 0.1% 2,6-di-*tert*-butyl-4-methylphenol (BHT) and 80 ng of internal standard, was added to the homogenate, and vortexed. An equal volume of *n*-hexane was added to the homogenate/ethanol-mixture and shaken in the dark for 15 min. After centrifugation, the hexane phase was transferred to a glass tube and placed in a TurboVap LV-N_2-Evaporator (Caliper Life Sciences, Hopkinton, MA) for the removal of hexane. The extraction procedure was repeated twice and the pooled hexane-phases were evaporated until dryness. The pellets were resuspended in isopropanol and transferred to amber glass vials. An aliquot of 20 μl was injected onto the HPLC-system. Plasma samples were extracted in a similar fashion; apart that the initial homogenization step was not required.

Statistical analysis. Values for biochemical variables are given as mean ± standard error of the mean (SEM). Statistical analysis was done using GraphPad prism Version 4.0 (GraphPad software, San Diego, CA).

Results

Identification of lutein in guinea pig tissues and diet

Using the features of a diode array detector, HPLC analysis permitted the monitoring over a wide spectral range instead of a fixed wavelength. Our HPLC-method is intended for the analysis of various samples for their vitamin A and E contents. Chromatograms of guinea pig lung extracts showed an unknown peak with the retention time of t_r = 14.16 min (lung, Fig. 1B) at a detection wavelength of λ = 450 nm. The corresponding UV-spectrum of this peak (Fig. 1E) showed two maxima at λ = 447 and 475 nm. To find out whether this substance could originate from the food source, a pellet of the Harlan Tekland guinea pig diet #7006 was extracted and its chromatogram also revealed a peak (a) at t_r = 14.028 min (Fig. 1C). The corresponding UV-spectrum of this peak (Fig. 1F) showed also two maxima at λ = 447 and 475 nm. According to the literature [4], the observed light absorptions point to carotenoids in general, and to lutein in particular, which has absorption maxima at 421, 445, and 475 nm (in ethanol), in contrast to zeaxanthin with 426, 452, and 479 nm (in light petroleum). However, a careful evaluation of this peak revealed the presence of a smaller shoulder with a peak (b) at t_r = 14.128 min. The UV-spectrum of peak (b) differs from the main peak (a). It shows an additional peak between 330 and 340 nm.

In order to confirm the identity of carotenoid in guinea pig diet and lung, we compared the retention times and UV-spectra (data not shown) of several carotenoids (β-apo-8′-carotenal, lutein, lycopene and beta-carotene) to that of diet and lung sample. For the lutein standard, its chromatogram gave a peak signal with the retention time of t_r = 14.627 min (Fig. 1A) and a similar UV-spectrum with two maxima at λ = 447 and 475 nm. The absorption maximum at 421 nm could not be resolved by the diode array detector, but was indicated as a shoulder. The EZStart software of the HPLC-system allows also a comparison of the similarity of UV-spectra. Both UV-spectra of the lutein standard (Fig. 1D) and the lung sample (Fig. 1E) showed a similarity of 99.98% within the wavelength range between 300 and 500 nm (data not shown).

Lutein levels in selected guinea pig tissues and guinea pig diet

In order to find out the distribution pattern of lutein in the guinea pigs, selected tissues were analyzed for their lutein content (Table 1). Analyses revealed that lutein was most abundant in liver (709.38 ± 18.26 ng per g wet weight) followed by spleen (383.45 ± 19.79 ng per g wet weight), lung tissue (140.15 ± 2.95 ng per g wet weight), and to some lesser extend in testis (28.69 ± 0.21 ng per g wet weight), kidney (25.65 ± 1.19 ng per g wet weight), plasma (18.38 ± 0.56 ng per mL), and eye (3.59 ± 1.29 ng per g wet weight). Interestingly, lutein could not be detected in white adipose tissue (WAT). It should be noted that limit of detection was determined to be 0.1159 ng lutein injected onto the HPLC-system. However, WAT samples showed two distinct peaks at similar retention times (t_r = 14.2 min and t_r = 14.6 min). The UV-spectra of these unknown peaks revealed for each a single absorption maximum at 418 nm, not characteristic to lutein.

It should be noted that lutein could not be detected in tissues of other rodents like mice (C57BL6) and rats (Sprague–Dawley) (data not shown). This is likely due to the fact that mice and rats normally receive a different, carnivorous-based diet that usually does not contain any plant extracts and hence, no carotenoids. In contrast, the guinea pig diet contained Lutein (all-*trans* and 13-*cis*) in a concentration of 7.97 ± 0.12 mg/kg.

Discussion

Krinsky et al. [5] reported the UV-spectra of lutein and zeaxanthin and their *cis*-/*trans*-isomers. Their 13-*cis* isomers show additional absorption maxima at 330 and 340 nm, respectively. These missing absorption maxima in our UV-spectra (Fig. 1D–F) and the shorter wavelengths of the absorption maxima point to the all-*trans* isomer of lutein as the major component, rather than all-*trans* zeaxanthin.

According to the manufacturer of the guinea pig diet, one of the main ingredients is dehydrated alfalfa meal. The alfalfa plant (*Medicago sativa*) is known for its high concentration of lutein [6]. Therefore it is likely that lutein found in guinea pig diet and consequently in guinea pig tissues originates from the alfalfa extract. Taken together, it is likely that the major peak consists mainly of all-*trans* lutein and to some lesser extent (<10%) as the 13-*cis* isomer. Because of the incomplete separation of these two isomers, the values are expressed as total lutein content.

Interestingly, we could identify and detect all-*trans* lutein in tissues that rely on a constant supply of vitamin A and have an active vitamin A metabolism. Recently, Matsumoto et al. [7] identified β-cryptoxanthin and lutein as natural ligands for the nuclear retinoic acid receptors (RAR)—especially RARα and RARγ—but not for the retinoid x receptors (RXR). Simultaneously, they have shown that other dietary carotenoids like β-carotene, zeaxanthin, astaxanthin, and lycopene failed to show similar activity. RAR and RXR isoforms (α, β, and γ) have been shown by our laboratory to be well expressed in guinea pig lungs [8]. Furthermore, Aung et al. [9] reported that lutein can counteract cigarette smoke-induced changes of certain genes related to inflammatory-immune responses, transcription factors and cell proliferation in lung of C57BL6 mice.

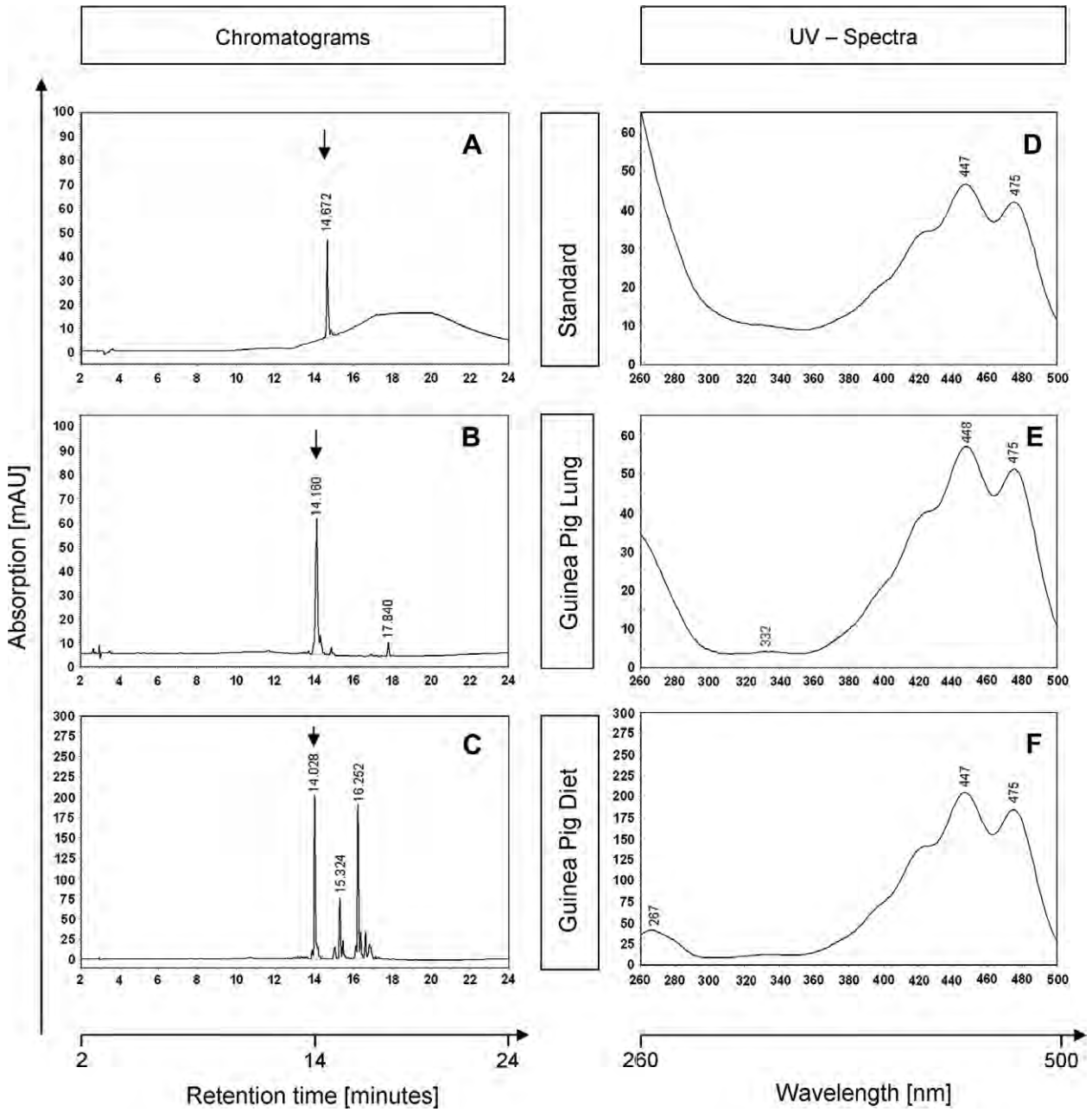

Fig. 1. Chromatograms (left column) of lutein standard (A), guinea pig lung extract (B), guinea pig diet #7006 (C), monitored at λ = 450 nm. UV-spectra (right column, range: 260–500 nm) of peaks of lutein standard (D), guinea lung extract (E), and guinea pig diet #7006 (F), of the corresponding peaks as indicated by arrows.

Taken together, our findings suggest, that guinea pig take up all-*trans* lutein from their diet and distribute it from the liver through the bloodstream to various targets. Lutein concentration was found to be highest in liver and was not detectable in WAT. It is likely that liver serves as a storage for lutein in guinea pigs. Other tissues, including WAT that could potentially serve as storage do not contain any detectable amounts of lutein. With the assumed role of liver as storage for lutein, it is noteworthy that spleen and lung seem to have a preference for the uptake of lutein in comparison to other organs that contain lutein, too (testis, kidney, plasma, and eye).

Table 1
Lutein concentrations in selected guinea pig tissues

Organ	[ng lutein/g wet weight]	*n* (samples)
Liver	709.38 ± 54.79	9
Spleen	383.45 ± 19.79	3
Lung	140.15 ± 8.86	9
Testis	28.69 ± 0.52	6
Kidney	25.65 ± 2.39	4
Plasma[a]	18.38 ± 0.97	3
Eye	3.59 ± 1.29	5
White adipose tissue	Not detected	6

Data represent mean values in [ng lutein/g wet weight] ± SEM.
[a] Plasma values are given in [ng lutein per mL] ± SEM.

Since RAR-isoforms are expressed in guinea pig lung and lutein is accumulated in this tissue, it could potentially serve as a RAR-ligand to activate transcription. Therefore, lutein may not only play a role as antioxidant but also contribute to the vitamin A-related metabolism and influence gene expression. This is supported by our finding that lutein is found in tissues that rely on cellular supply with vitamin A. Itagaki et al. [10] studied the pharmacological action of lutein in rats. They observed a prefer-

ential distribution of lutein to the liver, lung and spleen, but little or no distribution to the brain and fat, which is in agreement with our results.

Among the analyzed tissues, the second highest concentration of lutein was detected in spleen. The spleen accommodates several tasks such as the efficient phagocytosis of erythrocytes and recycling of iron, the capture and the destruction of pathogens and the induction of adaptive immune responses [11]. It is possible that lutein plays an important role in some of these processes. Lutein may protect the spleen tissue from oxidative stress during the degradation of captured pathogens. Furthermore, several epidemiological studies suggest an immunmodulatory role for dietary carotenoids, including lutein [12]. Chen and Ross [13] demonstrated that retinoic acid regulates the gene expression of CD1d, a non-classical antigen-presenting surface molecule that activates natural killer T cells by presenting glycolipid antigens. This process was exclusively mediated through RARα. Since Matsumoto et al. [7] identified β-cryptoxanthin and lutein as natural ligands for the nuclear retinoic acid receptors (RARα and RARγ), it seems likely that lutein could substitute for all-*trans* retinoic action in the course of immune cell activation.

It is known for some time that humans and monkeys are able to take up xanthophylls from diet and to accumulate them in the eye, especially in the macula lutea [14]. The demonstration of lutein in the guinea pig eyes is a novel finding. We are currently investigating whether lutein also accumulates in the macula lutea similar to human and primates.

Our laboratory is actively involved in investigating the molecular mechanisms of cigarette smoke (CS)-induced lung disease with guinea pigs as a model [2]. The guinea pig model system for CS exposure might be superior to any other rodent models since they take up lutein with their regular herbivorous diet and lutein may play an important role in chemoprevention and gene expression in our cigarette smoke model system. In this regard, guinea pig resembles humans than any other rodents. Humans are omnivorous and lutein (amongst other carotenoids) has also been found in different human tissues like lung, colon, breast, skin, and plasma [15]. Furthermore, a continuously growing body of evidence suggests that lutein and zeaxanthin may contribute to the protection against several age-related diseases, including cataract, age-related macular degeneration (AMD), heart disease, and some forms of cancer, including lung cancer [16].

Acknowledgments

This work was supported by FAMRI Clinical Innovator Award # 062415 and US Army Grant W81XWH-06-2-0044.

References

[1] Lutein and zeaxanthin – Monograph, Altern. Med. Rev. 10(2) (2005) 128–135.
[2] S. Mukherjee, T. Nayyar, F. Chytil, S.K. Das, Mainstream and sidestream cigarette smoke exposure increases retinol in guinea pig lungs, Free Radic. Biol. Med. 18 (1995) 507–514.
[3] M.W. Schäffer, S. Sinha Roy, S. Mukherjee, S.K. Das, Improved high-performance liquid chromatography method with diode array detection for simultaneous analysis of retinoic acid isomers, retinol, retinyl esters, vitamin E, and selected carotenoids in guinea pig tissues, FASEB J. 22 (2008) A282. 621.3.
[4] A.B. Barua, H.C. Furr, R.B. van Breemen, Vitamin A and carotenoids, in: A.P. De Lenheer, W.E. Lambert, J.F. Van Bocxlaer (Eds.), Modern Chromatographic Analysis of Vitamins, third ed., Marcel Dekker Inc., New York, 2000, pp. 1–74.
[5] N.I. Krinsky, M.D. Russett, G.J. Handelman, D.M. Snodderly, Structural and geometrical isomers of carotenoids in human plasma, J. Nutr. 120 (1990) 1654–1662.
[6] M. Hoffman, D. Baugh, M. Ahern, D. Walsh, Isolation of lutein from alfalfa, United States Patent 7253294, 2007. Available from: <http://www.freepatentsonline.com/7253294.html>.
[7] A. Matsumoto, H. Mizukami, S. Mizuno, K. Umegaki, J. Nishikawa, K. Shudo, H. Kagechika, M. Inoue, Beta-cryptoxanthin, a novel natural RAR ligand, induces ATP-binding cassette transporters in macrophages, Biochem. Pharmacol. 74 (2007) 256–264.
[8] S. Sinha Roy, M.W. Schäffer, S. Mukherjee, S.K. Das, Modulation of lung retinoid metabolism and signaling by smoking in a guinea pig model, FASEB J. 20 (5) (2006). 630.2.
[9] H.H. Aung, V.T. Vasu, Y. Lee, G. Valacchi, U.C. Obermüller-Jevic, L. Packer, K. Gohil, C.E. Cross, Lutein sensitive genes: modulation by cigarette smoke (CS.), FASEB J. 20 (2006) A611. 398.13.
[10] S. Itagaki, W. Ogura, Y. Sato, T. Noda, T. Hirano, S. Mizuno, K. Iseki, Characterization of the disposition of lutein after i.v. administration to rats, Biol. Pharm. Bull. 29 (10) (2006) 2123–2125.
[11] R.E. Mebius, G.G. Kraal, Structure and function of the spleen, Nat. Rev. Immunol. 5 (8) (2005) 606–616.
[12] B.P. Chew, J.S. Park, Carotenoid action on the immune response, J. Nutr. 134 (2004) 257S–261S.
[13] Q. Chen, A.C. Ross, Retinoic acid regulates CD1d gene expression at the transcriptional level in human and rodent monocytic cells, Exp. Biol. Med. 232 (2007) 488–494.
[14] D.M. Snodderly, Evidence for protection against age-related macular degeneration by carotenoids and antioxidant vitamins, Am. J. Clin. Nutr. 62 (6, Suppl.) (1995) 1448S–1461S.
[15] D.W. Nierenberg, S.L. Nann, A method for determining concentrations of retinol, tocopherol, and five carotenoids in human plasma and tissue samples, Am. J. Clin. Nutr. 56 (1992) 417–426.
[16] J.D. Ribaya-Mercado, J.B. Blumberg, Lutein and zeaxanthin and their potential roles in disease prevention, J. Am. Coll. Nutr. 23 (6, Suppl.) (2004) 567S–587S.

REPORT DOCUMENTATION PAGE

Form Approved
OMB No. 0704-0188

1. REPORT DATE *(DD-MM-YYYY)*	**2. REPORT TYPE**	**3. DATES COVERED** *(From - To)*
12/09/2008	Annual Report	1 Sep 2007 – 30 Aug 2008

4. TITLE AND SUBTITLE

Development of Therapeutic and Diagnostic Countermeasures to WMD

Project 7 – Antioxidant Liposome as a new Adjuvant Therapy for inhalational Anthrax

5a. CONTRACT NUMBER
Subcontract No. 3000619434

5b. GRANT NUMBER
W81XWH-06-2-0044

5c. PROGRAM ELEMENT NUMBER

6. AUTHOR(S)
Dr. Ken Alibek, Caroline Kusuma, Yian Kim Tan, Dr. Svetlana Hopkins

5d. PROJECT NUMBER

5e. TASK NUMBER

5f. WORK UNIT NUMBER

7. PERFORMING ORGANIZATION NAME(S) AND ADDRESS(ES)

AFG Biosolutions, Inc. 9119 Gaither Road, Gaithersburg, MD 20877

8. PERFORMING ORGANIZATION REPORT NUMBER

9. SPONSORING / MONITORING AGENCY NAME(S) AND ADDRESS(ES)

U.S. Army Medical Research and Materiel Command Fort Detrick, Maryland 21702

10. SPONSOR/MONITOR'S ACRONYM(S)

11. SPONSOR/MONITOR'S REPORT NUMBER(S)

12. DISTRIBUTION / AVAILABILITY STATEMENT

Distribution authorized to U.S. Government agencies only (proprietary information, (enter date of report)

13. SUPPLEMENTARY NOTES
ROS, oxidative stress, lethal toxin, anthrax

14. ABSTRACT

The results obtained suggest that lethal toxin induced the production of ROS as measured by the oxidation of carboxy-DCFDA. This overproduction can be partially neutralized by the presence of exogenous antioxidant and was also observed to confer some protection to the cells from the cytotoxic effect of lethal toxin. It is believed that the overproduction of ROS is responsible for the cell lysis in lethal toxin-treated cells (Hanna et al, 1994).

15. SUBJECT TERMS

16. SECURITY CLASSIFICATION OF:			**17. LIMITATION OF ABSTRACT**	**18. NUMBER OF PAGES**	**19a. NAME OF RESPONSIBLE PERSON**
a. REPORT	**b. ABSTRACT**	**c. THIS PAGE**			USAMRMC
U	U	U	UU		**19b. TELEPHONE NUMBER** *(include area code)*

Standard Form 298 (Rev. 8-98)
Prescribed by ANSI Std. Z39.18

TABLE OF CONTENTS:

INTRODUCTION

The purpose of this proposal is to verify the principal of a novel antioxidant therapy in addition to conventional antibiotic treatment (ciprofloxacin) for inhalational anthrax. To achieve this goal, numerous in vitro and in vivo experiments are described and will be performed on a highly expedited schedule by AFG Biosolutions, Inc.

Infection with *Bacillus anthracis* spores through intradermal inoculation, ingestion or inhalation results in three different distinct clinical presentations: cutaneous anthrax, gastro-intestinal anthrax and inhalational anthrax. Inhalational anthrax is the most fatal form of infection and therefore is the most realistic scenario for a bioterrorist attack. Victims of anthrax succumb to septicemia, toxemia, systemic inflammatory response syndrome (SIRS), septic shock, and multiple organ dysfunction syndromes (MODS) within one to seven days post-exposure (Dixon et al, 1999). During the initial infectious process, macrophages play a pivotal role as cellular mediators of infection, particularly in inhalational anthrax.

The involvement of intracellular reduction-oxidation (redox) in the development of sepsis and septic shock has been well-defined. Sufficient evidence indicates that tissue injury associated with severe sepsis and MODS are mediated in part by excessive production of reactive oxygen intermediates (ROIs). Recent studies have shown that ROIs actively contribute to the pathogenesis of anthrax infection in several aspects as described below. Depending on the stage of the infection, oxidative species can: 1). Facilitate germination of engulfed *B. anthracis* spores in macrophages; 2). Alter function of infected cells by oxidizing intracellular and membrane-bound molecules including DNA, proteins, and membrane lipids; 3). Induce over expression of inflammatory mediators by activating transcription factor NFκB; 4). Coordinate with anthrax LeTx to lyse macrophages and induce apoptosis of a variety of immune cells. Considering the aforementioned, blocking reactive oxygen species may ameliorate the inflammation associated with anthrax infection. In addition, modulating oxidative stress-related molecules, such as redox-sensitive transcriptional factors, may be useful for the regulation of these inflammatory responses.

Recently we have successfully developed a signal transduction inhibition antioxidant liposome (STIMAL) which can efficiently remove the overproduced ROIs both *in vitro* and *in vivo*. In this study, we propose to test protective effects of STIMAL in the event of anthrax infection.

In order to fulfill goals of this proposal, the three following specific aims were established as stated in the application:

Aim 1: To determine the protective effect of signal transduction inhibition antioxidant liposomes (STIMAL) on human PBMC from apoptosis and murine macrophages from cytolysis after infection with *B. anthracis* spores or treatment with LeTx.

Aim 2: To determine if STIMAL is able to block or diminish hemolysis and production of inflammatory mediators caused by anthrax infection.

Aim 3: To evaluate the protective efficacy of antioxidant liposome in murine anthrax model.

These aims have not been modified since the original submission.

BODY OF REPORT

Aim 1: To determine the protective effect of signal transduction inhibition antioxidant liposomes (STIMAL) on human PBMC from apoptosis and murine macrophages from cytolysis after infection with *B. anthracis* spores or treatment with LeTx.

Early work conducted by Hanna (Hanna et al, 1994) has shown excessive production of reactive oxidative species by macrophages treated with anthrax LeTx. Treatment of murine macrophages with LeTx *in vitro* resulted in the release of large amounts of superoxide anion and subsequent cytolysis of the macrophages on a consistent basis. The cytolytic effect of LeTx could be blocked by introducing various exogenous antioxidants or by introducing a combination of N-acetyl-L-cysteine and methionine, which promote production of the endogenous antioxidant glutathione.

We have developed cytolytic assay using murine macrophage cell line RAW 264.7 to assess the protective effect of STIMAL against LeTx induced cell lysis. In our study, we investigated the effect of higher concentration of antioxidant liposomes on cell lysis and determine the best treatment method (simultaneous vs preincubation), which gives the best protection against cell lysis due to LeTx challenge. Different concentrations of antioxidant liposomes starting from 25mM to 6.25mM were tested to determine whether it protects or mitigates the cytolytic action of lethal toxin.

Briefly, RAW 264.7 cells were seeded in a 96 well plate at a density of $2.5x10^4$ cells per well in DMEM supplemented with 10% FBS and antibiotic. Cells were grown for 2 days in 37^0C incubator with 5% CO_2. Before treatment, media was aspirated and antioxidant liposomes (25mM, 12.5mM, and 6.25mM) diluted in DMEM with 5% FBS were added to cells 2 hours prior to LeTx challenge. LeTx at PA 500ng/ml : LF 100ng/ml or PA 250ng/ml : LF 50ng/ml was then added to the well. Three hours or two and half hour after LeTx treatment, the cells were rinsed to remove residual liposome and LeTx. Cell cytotoxicity was determined by CellTiter 96 AQueous One Solution Cell Proliferation Assay (Promega).

We consistently observed an increase in cell cytotoxicity in blank liposome with LeTx well compared to LeTx only well (Figure 1) in both LeTx concentration tested. Thus, we could not draw any conclusion about the protective effect of STIMAL due to this phenomenon. Liposome might interact with LeTx and cells and increases cell lysis. We then tested whether washing STIMAL away prior to LeTx challenge will diminish the cytotoxicity effect in blank liposome with LeTx well. The method described above was applied with the following modifications: (a) cells were preincubated with STIMAL for 4 hours instead of 2 hours and (b) antioxidant liposomes were removed and wells were rinsed to remove any residual liposomes before LeTx was added. Figure 2 shows that STIMAL removal prior to LeTx challenge reduces the cytotoxic effect we previously observed. However, in this experiment antioxidant liposomes both NAC- and GSH-liposome at all concentrations tested do not protect cells from LeTx induced cytotoxicity (less than 5%).

We increased STIMAL incubation time with $5x10^5$ cells per well up to 20 hours before LeTx challenge. Figure 3 shows that NAC- and GSH-liposome at 25mM protect LeTx treated cells by 15% (vs blank liposome) and 25% (vs untreated). Lower concentration of STIMAL has lower protection on LeTx treated cells. We conclude that NAC- and GSH- liposome at 25mM (highest concentration we tested) give the best protection on murine macrophages RAW 264.7 from cytolysis after treatment with LeTx. We also made sure that the protective effect of STIMAL was not due to possible residual antioxidant liposome in the wells (data not shown).

The effect of STIMAL treatment on lethal toxin-induced apoptosis were investigated on human PBMCs. Apoptosis is a type of programmed cell death whereby the cell undergo

cellular changes that resulted in eventual death of the cell and is characterized by cell shrinkage and blebbing, nucleus fragments, chromatin condensed, DNA degradation, exteriorization of phosphatidylserine and activation of caspases. Popov et al (2002) demonstrated that cells from human peripheral blood display apoptotic behavior after treated with LeTx.

Whole blood was collected in sodium citrate and subsequently used for the isolation of PBMCs using the ficoll gradient method. Briefly, 10mls of whole blood were mixed with 20mls of DPBS and 10mls of Ficoll were added slowly from the bottom of the tube. The tubes were centrifuged at 2000rpm for 30mins and the buffy coat interphase was transferred to new tube. Cells were further washed twice with media and seeded in 6 well plates at a concentration of 1 X 10^6 cells per well. Cells were activated with 100U/ml of IFN γ for 24-48 hours prior to treatment. Lethal toxin was added at a final concentration of 500µg/ml PA and 100µg/ml LF for 24hours. Cells were detached from the plate, washed and resuspended to 1 x 10^6 cells/ml. 100µl of the suspension were transferred to a FACS tube and 5µl of each Annexin V-FITC and 5µl of propidium iodide were added to the tube and incubated for another 20mins in the dark. 400µl of FACS binding buffer were added and analysed by FACS within 30mins. Annexin V-FITC assay is based on the specific affinity of annexin V to the exposed phosphatidylserine that is externalized to the outside of the cell surface.

PBMC that were treated with lethal toxin showed an 8-10% increase of apoptotic cells after 24 hours as observed by the higher number of cells with Annexin V +, PI – (Figure 4). This effect could be attributed to the mixed population of PBMC and the susceptibility of the various cell types to lethal toxin. We investigated the effect of STIMAL treatment on lethal toxin-induced apoptosis. PBMCs were pre-treated with 12.5mM and 6.25mM blank liposome, NAC-liposome or GSH-liposome for 24 hours prior to LeTx treatment, and then subjected to Annexin V staining assay as mentioned above. Pre-treatment of PBMCs with STIMAL for 24 hours followed by LeTx treatment were found to reduce the number of apoptotic cells as compared to just LeTx treated cells (Figure 5). NAC appears to provide a slightly better protection against apoptosis as compared to GSH. Both GSH and NAC provide protection in a dose-dependent fashion. However, blank liposome controls containing the same concentration of liposome were found to be highly toxic to the cells with more than 90% death (Figure 6). This observation is in contrast with those obtained with RAW 264.7 cells as no toxicity was observed for cells treated with blank liposome for 24 hours.

Aim 2: To determine if STIMAL is able to block or diminish hemolysis and production of inflammatory mediators caused by anthrax infection.

Due to unsuccessful results to reproduce hemolysis induced by lethal toxin in human blood in our hand, we are not able to determine if STIMAL is able to block or diminish hemolysis. Much effort has been devoted to this hemolysis assay (as discussed in previous annual report), but none of them produce positive results. Thus, we take a different approach in our investigation.

Anthrax toxin both lethal toxin and edema toxin inhibit immune cell chemotaxis by perturbing chemokine receptor signaling (Paccani, SR et al, 2007). Another study conducted by Dr. Rest et al also showed that anthrolysin, a newly described toxin of the cholesterol-dependent cytolysin (CDC) family, inhibit immune cell chemotaxis and antioxidant i.e. NAC or GSH were able to reverse the effect (unpublished data). We are currently working on developing neutrophil chemotaxis assay using fresh human neutrophils or HL-60 cells that are differentiated toward PMN-like cells by the addition of 1.25% DMSO to the culture medium. Once the assay is established, we will conduct an experiment to confirm that LeTx

inhibit immune cell chemotaxis Then, we will investigate whether STIMAL is able to restore chemotaxis of immune cells due to lethal toxin.

Popov et al suggests that LeTx can cause a reduction in phagocytic and/or bactericidal activity of macrophages against spores and germinating bacilli (Popov et al, 2002). We would like to investigate whether STIMAL is able to restore the phagocytic activity of human neutrophils or macrophages infected with anthrax spores.

We have developed an in house assay to measure phagocytic activity of murine macrophage cell line RAW 264.7 against *B. anthracis* sterne spores. The assay measures the amount of spores or vegetative bacteria that are taken by RAW 264.7 cells by phagocytosis using Alamar Blue. It is a sensitive, non-toxic and safe assay of cell viability and proliferation for mammalian or microbial cells. Alamar Blue is a redox indicator that yields a colorimetric change and a fluorescent signal in a response to a metabolic activity. The assay is based on the ability of metabolically active cells to convert the reagent into a fluorescent and colorimetric indicator. Damaged and non-viable cells have lower innate metabolic activity and thus generate a proportionally lower signal. We investigated if there was a significant reduction in phagocytosis activity in LeTx treated macrophage cells compared to non LeTx treated cells.

Briefly, RAW 264.7 cells were seeded in a 96 well black fluorescence plate at a density of $1x10^5$ cells per well in DMEM/F12 50:50 without phenol red, FBS or antibiotics. Cells were grown overnight in 37^0C incubator with 5% CO_2. Next day, media was aspirated and cells were treated with different concentrations of LeTx for 3 hours. PA concentration was kept constant at 500ng/ml, and lethal factor was administered at concentrations between 2 and 64ng/ml. Toxin was prepared in DMEM/F12 media immediately before the experiment. At the end of 3 hours incubation, LeTx was removed and cells were washed once with twice volume of media. $2x10^6$ spores were then added to each well, and phagocytosis was allowed to occur for 30 minutes. The supernatant was removed, and cells were washed six times with twice volume of PBS. RAW 264.7 cells were then lysed with 100ul of 1% aqueous saponin in DMEM/F12 media for 5 min (spores or bacteria cells are not affected by 1% saponin). After lysis, 10ul of Alamar Blue (Biosource, USA) was added to each well. The plate was incubated for 5 hours at 37^0C and fluorescence was measured by excitation at 530nm and emission at 590nm.

Cell viability of RAW 264.7 cells after treatment with LeTx was also analyzed using CellTiter 96® Aqueous One Solution Cell Proliferation Assay (MTS, Promega). The assay is similar to MTT assay; the main difference is that this assay utilizes MTS instead of MTT as the tetrazolium reagent. The system also includes PMS, an electron coupling reagent, which facilitates the reduction of MTS. During the assay, MTS is converted into a soluble formazan product, eliminating the need for addition of Solubilization Solution. 20ul of MTS was added to each well (100ul per well) one and a half hour before the end of LeTx treatment. The plate was incubated for 1.5 hours at 37^0C and absorbance was read at 490nm using an ELISA plate reader.

RAW 264.7 cells treated with PA 500ng/ml:LF 8ng/ml and PA 500ng/ml:LF 16ng/ml showed decrease in phagocytosis of *B. anthracis* sterne spores (Figure 7). Cells treated with PA alone, LF alone, PA 500ng/ml:LF 2ng/ml, and PA 500ng/ml:LF 4ng/ml did not show decrease in phagocytosis of *B.anthracis* spores compared to non treated cells. Percent spore phagocytosis of RAW 264.7 cells compared to non treated control was also calculated (Figure 8). Cells treated with PA 500ng/ml:LF 16ng/ml showed 54% viability compare to non treated cells, while other treatments showed greater than 85% viability. We normalized percent spore of phagocytosis to its MTS reading (cell viability) as shown in Figure 8B. We

suggest that 60% reduction in phagocytic activity in cells treated with PA 500ng/ml:LF 8ng/ml is valid (cell viability was 85%), while 70% phagocytic activity reduction in cells treated with PA 500ng/ml:LF 16ng/ml might be due to reduced cell numbers (cell viability was 54%), thus it might not be valid.

We varied the duration of LeTx treatment from 2 hours to 4 hours. Cells treated for 2 hours with LeTx did not show decrease in phagocytosis of *B. anthracis* sterne spores (Figure 9). Cells treated for 4 hours with LeTx showed decrease in phagocytosis of spores but the cells viability was low (data not shown). We confirm that phagocytic activity of macrophages is inhibited by sublytic concentration of lethal toxin at PA 500ng/ml:LF 8ng/ml. We will investigate whether STIMAL is able to restore the phagocytic activity in RAW 264.7 macrophages infected with anthrax spores.

We conducted experiments to measure production of inflammatory mediators from human peripheral blood mononuclear cells (PBMCs) and macrophages caused by anthrax infection. We investigated which inflammatory cytokines were produced by human PBMCs or macrophage after LeTx or cell wall treatment.

PBMCs and monocytes were isolated from human blood that was purchased from Virginia Blood Services. The blood was shipped and stored at 4^0C, and blood components were isolated within 2 days after collection. Human PBMCs and monocytes were isolated before use in assay. Briefly, PBMCs were isolated by centrifuging for 30 minutes at 900g on Fico/Lite-LymphoH (Atlanta Biologicals, GA). The buffy coat containing PBMCs were collected and resuspended in RPMI containing 10% FBS to $5x10^6$/ml. The cells were then plated on a 48 well plate at $1x10^6$/well (200ul volume/well). PBMCs were incubated at 37^0C, 5% CO2 for 1 day or 2 days with media only (control), 1ug/ml *B. anthracis* cell wall, LeTx (500ng/ml PA + 100ng/ml LF), or 10ug/ml lipopolysaccharide (LPS). At the end of incubation, the supernatants were harvested and assayed for the presence of TNF-α, IFN-γ, IL-2, IL-4, IL-5, and IL-10 using the BD Pharmingen CBA kit. This method uses flow cytometry to measure soluble analytes in a particle-based immunoassay.

Monocytes were purified from PBMCs using adherence method. PBMCs were resuspended in DMEM without serum. Adherent monocytes were obtained by culturing PBMCs ($2x10^7$/flask) in serum-free DMEM for 1 hour at 37^0C. Medium containing nonadherent cells was removed by aspiration, and cells were washed twice with 10ml DPBS to remove any residual nonadherent cells. Medium was then replaced with 10ml fresh RPMI (ATCC) supplemented 55uM 2-mercaptoethanol, 0.1mM MEM non-essential amino acids, 1x Penicillin/Streptomycin/Amphotericin, 10% FBS, and 20ng/ml human M-CSF. Following a 5-day incubation period, nonadherent cells were removed, and human macrophages were harvested by trypsin. Macrophages were plated on a 96 well plate at $1x10^5$/well (100ul volume/well). Macrophages were incubated at 37^0C, 5% CO2 for 1 day or 2 days with media only (control), 1ug/ml *B. anthracis* cell wall, LeTx (500ng/ml PA + 100ng/ml LF), 1ug/ml *B. anthracis* cell wall with LeTx, or 10ug/ml lipopolysaccharide (LPS). At the end of incubation, the supernatants were harvested and assayed for the presence of TNF-α, IFN-γ, IL-2, IL-4, IL-5, and IL-10 using the BD Pharmingen CBA kit.

We observed that human macrophages treated with *B. anthracis* cell wall after 24 hour incubation show a slight increase in IL-5, IL-10 and TNF-α compared to media only control (Table 1). However, macrophages treated with LeTx after 24 hour incubation show a significant decrease in IL-5, IL-10 and TNF-α compared to media only control. Figure 10 shows a decrease in TNF-α in LeTx-treated cells compared to cells with media only. Macrophages treated with cell wall, LeTx or combination of cell wall and LeTx did not result in increase production of IL-2, IL-4, or IFN-γ (data shown in Table 1).

We observed that human PBMCs expressed significant levels of TNF-α upon exposure to cell wall and LPS for 24 hour compared to media only control (Figure 11). LPS serves as positive control in this experiment. A slight increase in IL-5 (Figure 12) and IL-10 (Figure 13) production was also observed after cells were treated with cell wall after 24 hours. However, PBMCs treated with LeTx after 24 hour incubation show a significant decrease in IL-5, IL-10 and TNF-α compared to media only control (data shown in Table 2), which is similar to what observed in treated macrophages cells. PBMCs treated with cell wall, or LeTx did not result in increase production of IL-2, IL-4, or IFN-γ (Table 2).

Human PBMCs or macrophage treated with *B. anthracis* cell wall do not increase the production of IL-2, IL-4, and IFN-γ. We also show that LeTx alone does not induce inflammatory cytokine expression. Moreover, it seems that LeTx inhibits certain inflammatory cytokine expression for example TNF-α, IL-5 and IL-10. Thus, in our cytokine study we will choose the model that gives us the most increase in cytokine production, which is human PBMCs treated with *B. anthracis* cell wall. Then we will test whether STIMAL can diminish the production of TNF-α in PBMCs treated with cell wall.

Aim 3: To evaluate the protective efficacy of antioxidant liposome in murine anthrax model.

Animal study to evaluate the protective efficacy of antioxidant liposome has been assessed in our murine anthrax model. Several animal experiments were conducted earlier in the study to conform that the murine anthrax model was established in house. LD50 of *Bacillus anthracis* sterne spores (34F2) was determined. Briefly, *B. anthracis* 34F2 was prepared in a liquid media and the culture was allowed to progress to sporulation. Spores were then purified by gradient centrifugation. 9-10 week age of anthrax-sensitive strain mice DBA2 were used in the study. Female DBA2 mice were injected (200ul) with *B. anthracis* 34F2 spores by intraperitoneal injection. The animals were monitored every day (morning and evening) for 6 days for mortality. The data shown in Table 3 are from a single experiment to determine LD50 of *Bacillus anthracis* 34F2 in DBA2 mice. Ten mice were used in each dose group.

Our results show similar pattern as previously seen in our murine anthrax model. All mice expire within 120-148 hours after infection, some of them start dying within the first 24-48 hours and the death peak is being reached within 48-72 hours after infection. Computation of 50% endpoints (LD50) by method of Reed and Muench yields $4.2x10^5$ cfu/mouse as our LD50 titer. Previous studies show that a delayed treatment with ciprofloxacin 24 hours after *B. anthracis* spores infection gives 50% protection from mortality. A study was conducted to confirm these results and subsequently the animal model is used to evaluate the protective efficacy of antioxidant liposome.

Briefly, 11 week age of female anthrax-sensitive strain DBA2 mice (Harlan) were injected with *B. anthracis* 34F2 spores ranging from $3.12x10^5$ cfu/mouse (~1 LD50) to $1.56x10^7$ cfu/mouse (~ 50 LD50) by intraperitoneal injection. 24 hours after challenge, 50 mg/kg (200ul of 5mg/ml) ciprofloxacin (MP Biomedicals) was administered intraperitoneally. Ciprofloxacin was prepared in sterile water and stored at -20^0C, and thawed each time before use. The animals were monitored every day (morning and evening) for 10 days for mortality. Ten mice were used in each dose group, except for the highest challenge dose (7 mice). Mice survival count was recorded and shown in Table 4. We observed that mice survival counts in $9.36x10^6$ group and $1.25x10^7$ group were higher than expected. However, all animals in $1.56x10^7$ group died by day 6. The 2 previous doses were an anomaly. Thus, we selected $1x10^7$ cfu/mouse as our challenge dose for our anthrax model.

The protective effect of NAC liposome in combination with ciprofloxacin was assessed. Briefly, 8-9 week age of female DBA2 mice were injected with $1x10^7$ cfu of *B. anthracis* 34F2 spores per mouse by intraperitoneal injection. 24 hours after spore challenge, mice were treated with 50 mg/kg ciprofloxacin alone or in combination with different dosages of NAC-liposome (40, 70 and 100 mg/kg) through intraperitoneal injection. The treatments were administered for 10 days. NAC-liposome was administered in the morning, and ciprofloxacin was administered in the evening starting from day 2 to day 10. NAC-liposome was administered simultaneously with ciprofloxacin on day 1 (24 hour post spore challenge). Mice were observed for mortality for 14 days after termination of treatment. The animals were grouped as shown in Table 5. Ten mice were used in each dose group. NAC-liposome and blank liposome were received from Dr. Stone's lab (University of Tennessee) and used one day after being made, and stored at 4^0C for 10 days treatment. The liposome was diluted in PBS and prepared each time before use.

All mice including NAC-liposome treated started to show signs of hemorrhages and accumulation of fluid within the peritoneal cavity (ascites) on day 2 after challenge (Figure 14). All animals had ruffled fur by day 3. Mice survival count was recorded (Table 5) and survival curve was graphed (Figure 15). We observed a delayed death in NAC-liposome treated group especially in 100mg/kg group (Figure 16). Hazard ratio, which is the slope of the survival curve or a measure of how rapidly subjects are dying was calculated. The hazard ratio was 2.5, which means that the ciprofloxacin only group dies 2.5x faster than 100mg/kg NAC-liposome group. There were 6 mice survivors in 100mg/kg NAC-liposome treated group compared to 3 mice survivors in ciprofloxacin only group. However, based on analysis using GraphPad Prism 4, p value was 0.1202 (>0.05) and the survival curves between ciprofloxacin alone and NAC-liposome 100 mg/kg + ciprofloxacin were not significantly different.

Different variables such as timing, duration, and route of STIMAL treatment were investigated to assess the best model that gives the most protective effect against anthrax. We also investigated the new formulated 90G STIMAL, which has smaller vesicles compared to the previous version (85G) of STIMAL, thus has a more stable size distribution over a longer time interval.

Along the course of the study, we switched animal vendor from Harlan to Charles River (as noted). Our usual animal vendor, Harlan had a colony breeding problem (some of their mice do not survive past 5 weeks of age). A small animal study was performed to confirm that mice from Charles River respond the same way as Harlan when infected with *Bacillus anthracis* sterne spores (34F2) and ciprofloxacin. Based on our results (data not shown), Charles River mice were slightly more sensitive to *B. anthracis* sterne spores, and we decided to lower the spore challenge dose to $5x10^6$ cfu/mouse. Animals challenged with this dose without ciprofloxacin all expired within 120 hours after infection, while animals treated with ciprofloxacin 24 hours after *B. anthracis* spores infection gave ~50% protection from mortality.

The protective effect of GSH liposome in combination with ciprofloxacin was also being assessed. The experiment protocol is similar to previous one described above with the following modifications: mice (Charles River) were treated with 50 mg/kg ciprofloxacin alone or in combination with different dosages of GSH-liposome (40, 70 or 100 mg/kg) or pure GSH (100mg/kg) intraperitoneally. The STIMAL or pure GSH (Sigma) treatment was administered for 5 days, and the ciprofloxacin was administered for 10 days. The animals were grouped as shown on Table 6. GSH was tested in this experiment instead of NAC, GSH dosage used was molar equivalent to NAC concentration used in previous experiment (FW

NAC= 163.2, FW L-Glutathione= 307.33). Ten mice were used in each dose group. STIMAL treatment was reduced to five days instead of ten days to eliminate the possibility that prolonged treatment of STIMAL might induce stress to the mice. This is based on our previous observations that mice treated with STIMAL started to crash starting on day 5 of treatment. Thus an experiment to assess whether shortening the duration of STIMAL treatment will improve survival was conducted.

Mice survival count was recorded (Table 6) and Kaplan Meier survival curve was graphed as shown in Figure 17. A delayed death in GSH-liposome treated group was observed both in 187mg/kg (Figure 18) and 132mg/kg group (Figure 19). Based on log rank test, p values were 0.0286 and 0.0429, respectively, and the survival curves were significantly different. Median survival for GSH-liposome at 187mg/kg was 7 and at 132mg/kg was 6.5 compared to 5 for blank liposome. Hazard ratio, which is the slope of the survival curve or a measure of how rapidly subjects are dying was calculated. The hazard ratio was 2.4 for 187mg/kg group, which means that the blank liposome group dies 2.4x faster than 187mg/kg GSH-liposome group. The hazard ratio was 2.1 for 132mg/kg group, which means that the blank liposome group dies 2.1x faster than 132mg/kg GSH liposome group. One thing that needs to be noted, in this experiment the blank liposome displayed higher level of aggregation compare to the GSH liposome, and this might have an effect on our results. We have encountered this inconsistency issue in the previous liposome preparations as well. University of Tennessee has been informed and they are currently working on the aggregation issue.

We conducted an animal experiment to test the new formulated 90G STIMAL from Dr. Stone's lab. The liposome used in this experiment was more pure and has more stable size distribution over a longer time interval. The liposome was diluted in PBS and prepared each time before use. Pure N-Acetyl-L Cysteine (NAC, Sigma) and L-Glutathione (GSH, Sigma) were also tested in this experiment, they were diluted in PBS and sterile filtered. NAC solution or GSH solution were prepared fresh each time before use.

The experiment protocol is similar to previous one described above with the following modifications: 24 hours after spore challenge, mice from Harlan were treated with 50 mg/kg ciprofloxacin alone or in combination with different dosages of NAC- or GSH-liposome through intraperitoneal injection. GSH dosage used was molar equivalent to NAC concentration used in experiment (FW NAC= 163.2, FW L-Glutathione= 307.33). The treatments were administered for 10 days. NAC-liposome was administered in the morning, and ciprofloxacin was administered in the evening starting from day 2 to day 10. NAC-liposome was administered simultaneously with ciprofloxacin on day 1 (24 hour post spore challenge). Mice were observed for mortality for 14 days after termination of treatment. The animals were grouped as shown in Table 7. Ten mice were used in each dose group.

The result shows that mice including GSH-liposome and NAC-liposome groups started to show signs of hemorrhages and ascites on day 2 after challenge. The animals started to look ruffled on day 3, and by day 4 all groups appeared sick. Mice survival count was recorded as shown in Table 7 and Kaplan Meier survival curve was graphed as shown in Figure 20. Mice treated with NAC- or GSH-liposome did not look significantly better than ciprofloxacin only group. GSH- or NAC- liposomes even at highest dose used did not seem to give protection against mortality (Figure 21). One of the possible reasons is that 90G liposome might induce more stress to the macrophages and might induce other inflammatory response.

We then conducted an experiment to investigate whether administering STIMAL through intravenous route is more effective compared to intraperitoneal route. The experiment

protocol is similar to previous one described above with the following modifications: 24 hours after spore challenge ($5x10^6$cfu/mouse), mice (Charles River) were treated with 50 mg/kg ciprofloxacin alone or in combination with different dosages of NAC-liposome (40 or 100 mg/kg) or pure NAC (100mg/kg) through intraperitoneal or intravenous injection. The treatments were administered for 10 days as the following: for the IV group, STIMAL was administered through IV from day 1 to 5 and from day 6 to 10 STIMAL was given IP; for IP group, STIMAL was given IP for total of 10 days. NAC-liposome or pure NAC (Sigma) was administered in the morning, and ciprofloxacin was administered in the evening starting from day 2 to day 10. NAC-liposome or pure NAC was administered simultaneously with ciprofloxacin on day 1 (24 hour post spore challenge). Mice were observed for mortality for 14 days after termination of treatment. The animals were grouped as shown in Table 8. Ten mice were used in each dose group.

Mice survival count was recorded (Table 8) and Kaplan Meier survival curve was graphed as shown in Figure 22. All mice developed symptoms of anthrax infection including hemorrhages, ascites, and ruffled fur by day 3. We did not see significant difference between two routes of administration used (Figure 23). We continue to use IP route to administer STIMAL since it is a more convenient technique compared to IV. Pure NAC itself whether it was given IP or IV did not demonstrate protective efficacy.

In the following experiment, we investigated whether administering STIMAL earlier (<24h post spore challenge) will improve mice survival. We treated anthrax infected mice with first dosage of NAC liposome at 4 or 8 hours after spore challenge. Briefly, 8-9 week age of female DBA2 mice from Harlan were injected with $1x10^7$ cfu of *B. anthracis* 34F2 spores per mouse by intraperitoneal injection. 4 or 8 hours after spore challenge, mice were treated with first dosage of NAC-liposome (100mg/kg or 120mg/kg) through intraperitoneal injection. 30 hours after spore challenge, mice were treated with 50 mg/kg ciprofloxacin alone or in combination with NAC-liposome at 100mg/kg or 120 mg/kg through intraperitoneal injection. The treatments were administered for 10 days. NAC-liposome was administered in the morning, and ciprofloxacin was administered in the evening starting from day 2 to day 10. NAC-liposome was administered simultaneously with ciprofloxacin on day 1. Mice were observed for mortality for 14 days after termination of treatment. The animals were grouped as shown in Table 9. Ten mice were used in each dose group.

All mice including NAC-liposome treated group started to show signs of hemorrhages and accumulation of fluid within the peritoneal cavity (ascites) on day 2 after challenge. All animals had ruffled fur by day 3. Mice survival count was recorded (Table 9) and Kaplan Meier survival curve was graphed (Figure 24). Based on our observation, mice in all NAC treated group looked better and more active between day 1 to 4 post infection compared to blank liposome group, however on day 5 all mice groups appeared sick and inactive. We observed a slight delay of death in NAC-liposome treated group compared to blank liposome group (Figure 25), however the difference was not statistically significant. Median survival for NAC-liposome 4h post at 100mg/kg was 7 compared to 4.5 for blank-liposome 4h post at 120mg/kg. Thus, we concluded that STIMAL administration at the time points earlier than 24 hours after infection did not improve the mice survival.

At this point, we are not able to draw any conclusions based on our animal experiment results that have been performed so far. One of the promising results obtained show that 100mg/kg NAC liposome treated mice died 2.5x slower than the ciprofloxacin only group (Figure 16). There were 6 mice survivors in NAC liposome treated group compared to 3 mice survivors in ciprofloxacin only group. However, this experiment was never been repeated exactly the same way due to vendor change. We also encountered some limitations with the STIMAL we used. STIMAL is not stable for a long period of time, it starts

to lose its activity after more than 1 week stored at 4^0C (data not shown). We also observed an increase in aggregation in few batch of liposomes.

KEY RESEARCH ACCOMPLISHMENTS

- Based on our apoptosis assay, results suggest that NAC- and GSH- liposome provide slight protection against apoptosis in LeTx treated PBMCs.
- NAC- and GSH- liposome partially protect cells from cytotoxic effect of lethal toxin.
- Our in vivo murine anthrax model suggests that antioxidant liposome may prolong survival (delay death) for few days, but not enough to protect mice from mortality.

REPORTABLE OUTCOMES

None during this reporting period

CONCLUSIONS

The results obtained so far suggest that NAC- and GSH- liposome provide protection against apoptosis by reducing number of apoptotic LeTx treated PBMCs. NAC- and GSH- liposome also partially protect cells from cytotoxic effect of lethal toxin. Our results show that NAC- and GSH- liposome at 25mM improve survivability of LeTx treated cells.

Our in vivo murine anthrax model suggests that antioxidant liposome may prolong survival (delay death) for few days, but not enough to protect mice from mortality. It is early to draw a conclusion at this stage, and we will continue our effort to evaluate the protective efficacy of antioxidant liposome in our *in vitro* model. The following experiments will be conducted: (1) To investigate whether STIMAL is able to restore the phagocytic activity of macrophage infected with anthrax spores, (2) To develop neutrophil chemotaxis assay in house, and investigate whether STIMAL is able to restore chemotaxis of immune cells due to lethal toxin, (3) To determine whether STIMAL is able to diminish production of inflammatory cytokines from human PBMC and macrophages caused by anthrax infection, (4) To determine if STIMAL is able to ameliorate the activation of NF-kB which will lead to over production of inflammatory mediators in anthrax infection.

REFERENCES

Dixon TC, Meselson M, Guillemin J, Hanna PC. Anthrax. N Engl J Med. 1999, 341(11):815-26.

Hanna PC, Kruskal BA, Ezekowitz RA, Bloom BR, Collier RJ. Role of macrophage oxidative burst in the action of anthrax lethal toxin. Mol Med. 1994, 1:7-18.

Paccani SR, Tonello F, Patrussi L, Capitani N, Simonato M, Montecucco C, Baldari CT. Anthrax toxins inhibit immune cell chemotaxis by perturbing chemokine receptor signaling. Cellular Microbiology. 2007, 9(4):924-929.

Popov SG, Villasmil R, Bernardi J, Grene E, Cardwell J, Wu A, Alibek D, Bailey C, Alibek K. Lethal toxin of *Bacillus anthracis* causes apoptosis of macrophages. Biochem Biophys Res Comm. 2002, 293:349-355.

APPENDICES

(A)

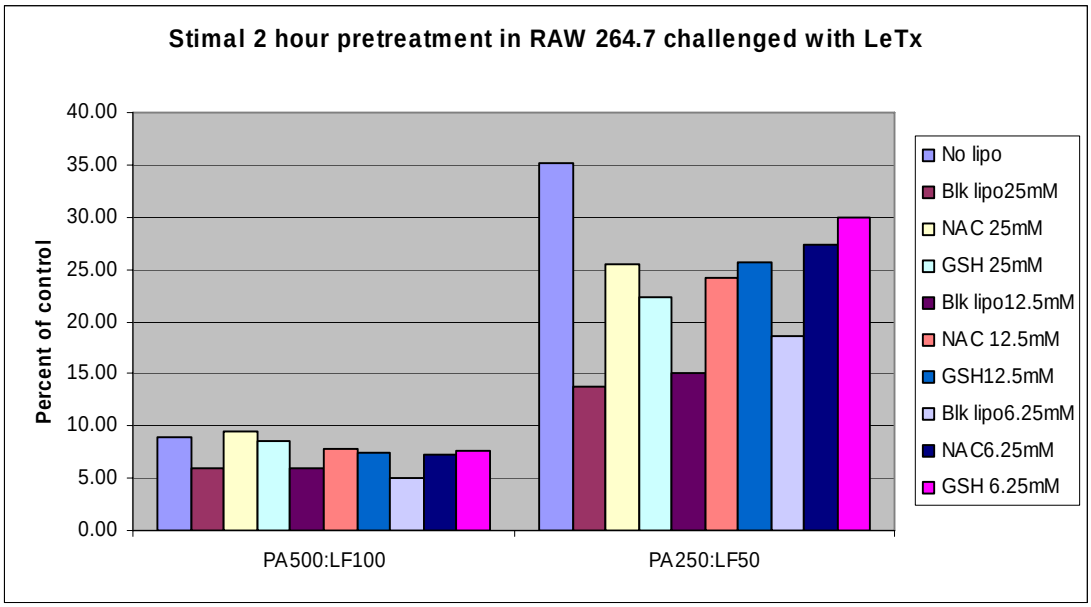

(B)

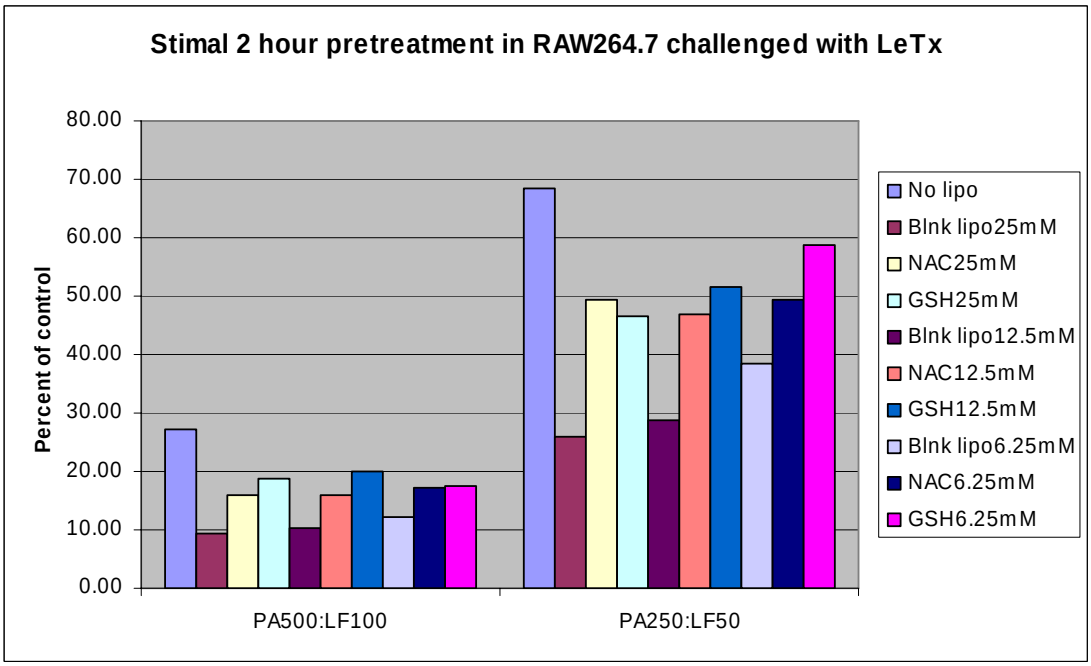

Figure 1. Effects of STIMAL on RAW 264.7 from cytolysis after treatment with LeTx. Antioxidant liposomes at 25mM, 12.5mM, or 6.25mM were added to cells 2 hours prior to LeTx challenge. Then LeTx at PA 500ng/ml : LF 100ng/ml or PA 250ng/ml : LF 50ng/ml was added to the well. Three hours (A) or two and half hour (B) after LeTx treatment, cell cytotoxicity was determined by CellTiter 96 AQueous One Solution Cell Proliferation Assay (Promega).

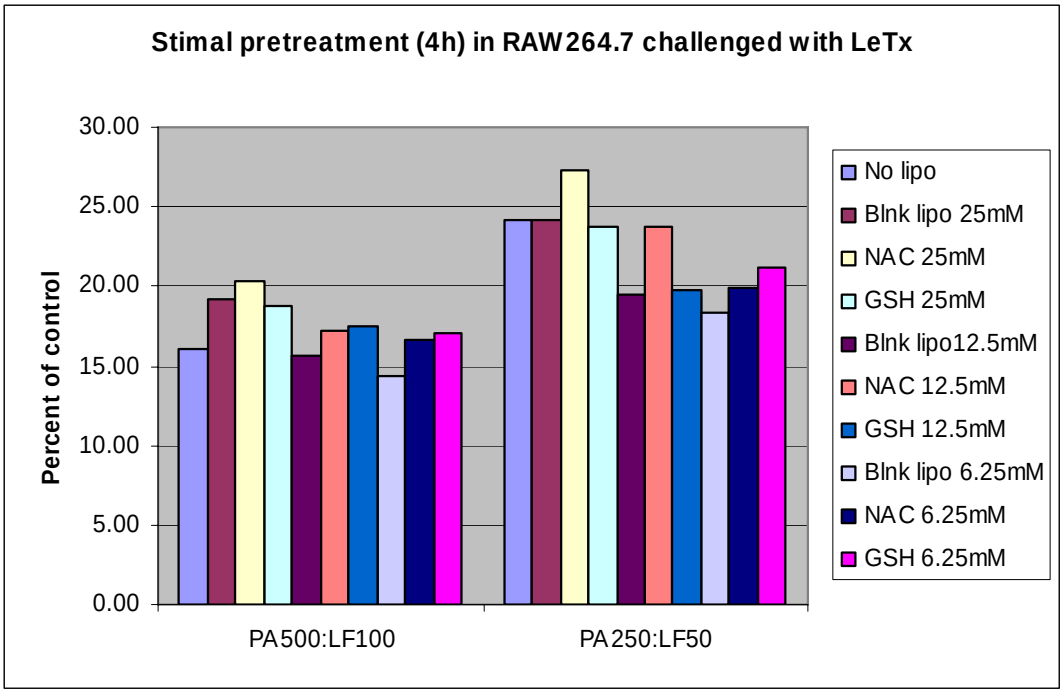

Figure 2. Effects of STIMAL on RAW 264.7 from cytolysis after treatment with LeTx. Antioxidant liposomes at 25mM, 12.5mM, or 6.25mM were added to cells 4 hours prior to LeTx challenge. Before LeTx treatment, antioxidant liposomes were removed and rinsed to remove any residual liposomes. LeTx at PA 500ng/ml : LF 100ng/ml or PA 250ng/ml : LF 50ng/ml was then added to the well. After three hours, cell cytotoxicity was determined by CellTiter 96 AQueous One Solution Cell Proliferation Assay (Promega).

(A)

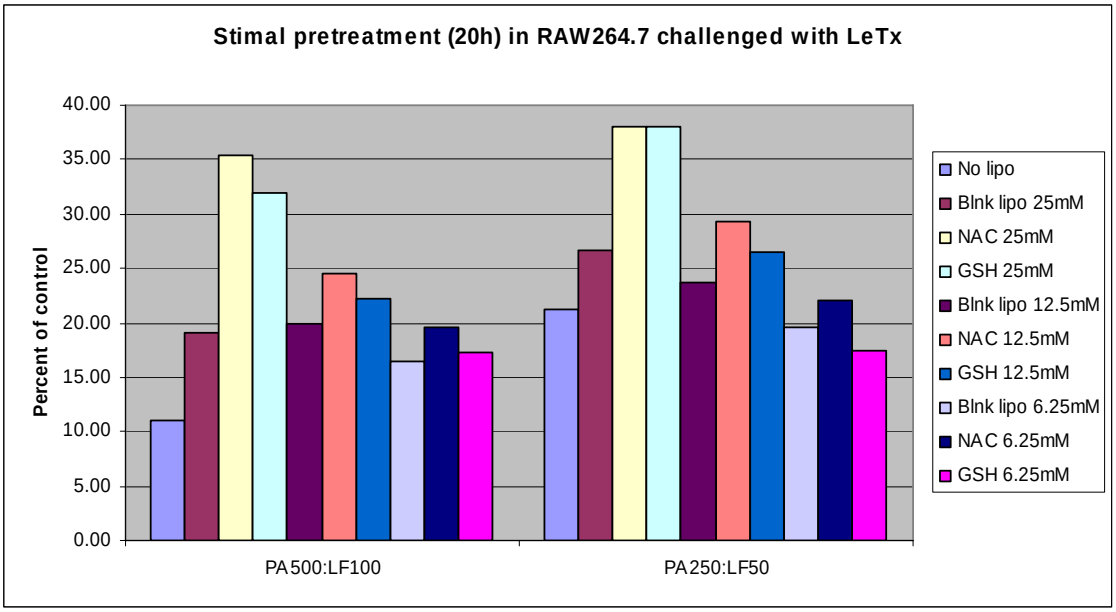

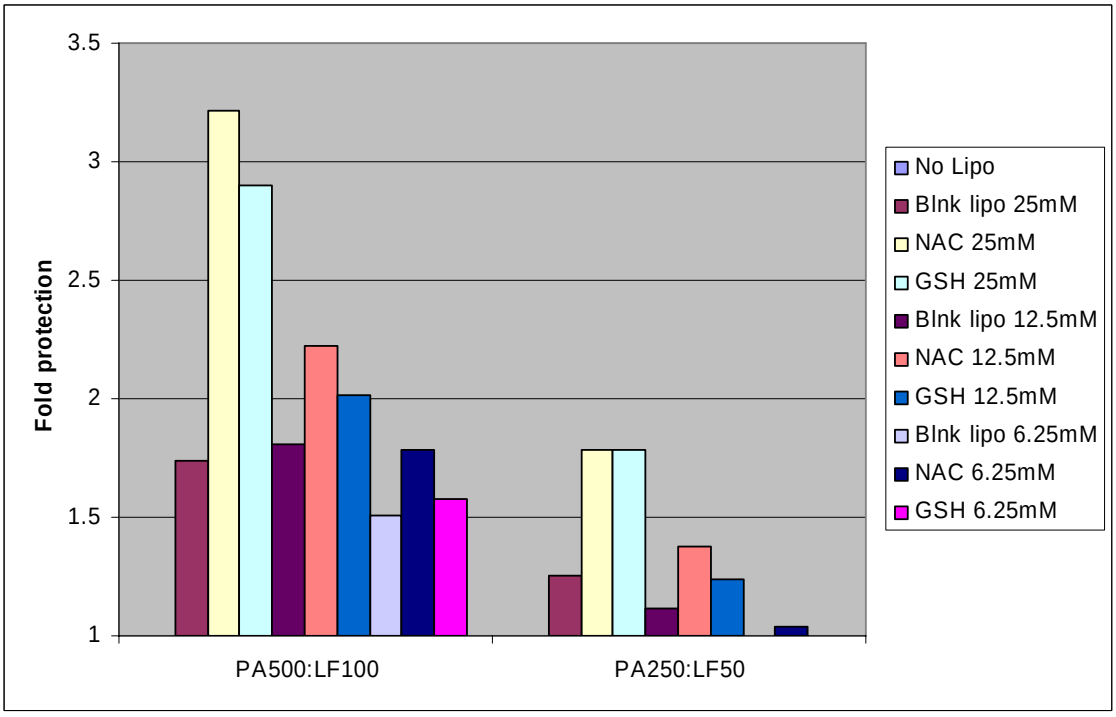

(B)

Figure 3. STIMAL protects RAW 264.7 from cytolysis after treatment with LeTx. Antioxidant liposomes at 25mM, 12.5mM, or 6.25mM were preincubated with cells for 20 hours before LeTx challenge. Before LeTx treatment, antioxidant liposomes were removed and rinsed to remove any residual liposomes. LeTx at PA 500ng/ml : LF 100ng/ml or PA 250ng/ml : LF 50ng/ml was then added to the well. After three hours, cell cytotoxicity was determined by CellTiter 96 AQueous One Solution Cell Proliferation Assay (Promega).

(A) (B)

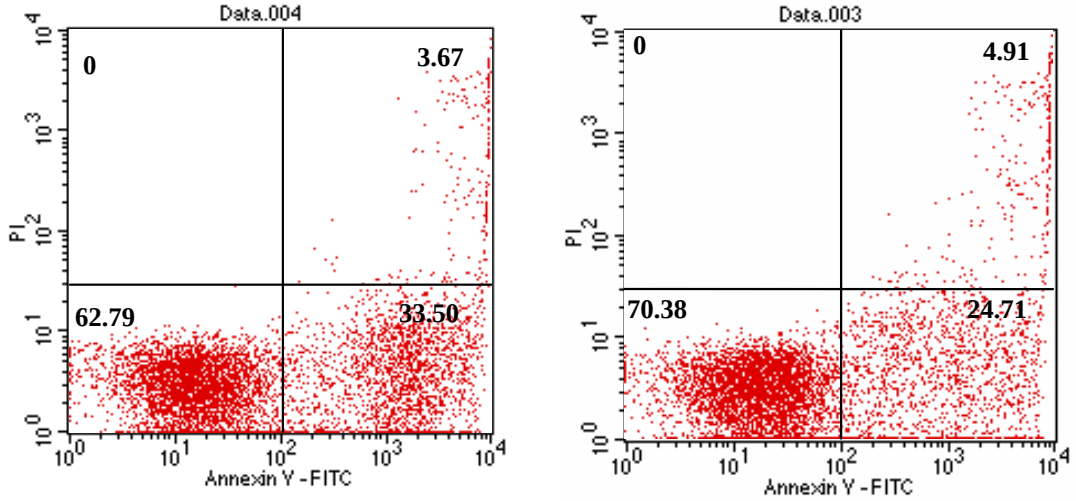

Figure 4. Scatter plot of PBMCs treated with (A) lethal toxin - 500µg/ml PA + 100µg/ml LF for 24hours and (B) PBS control. Live cells (PI -, Annexin -), apoptotic cells (PI -, Annexin +), dead cells (PI +, Annexin +)

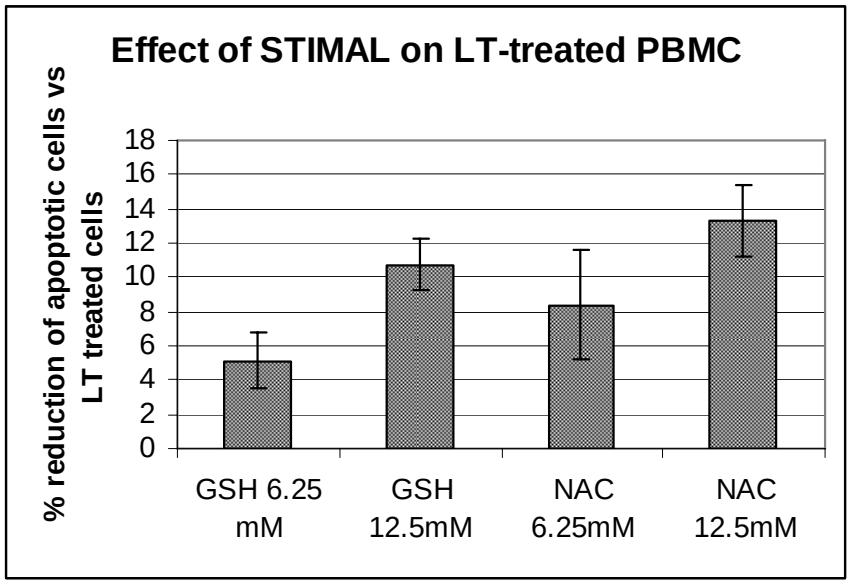

Figure 5. Protective effect of STIMAL against LeTx-induced apoptosis in PBMC.
PBMCs were treated with 12.5mM and 6.25mM NAC- or GSH- liposome for 24 hours prior to LeTx treatment and subject to Annexin V staining assay.

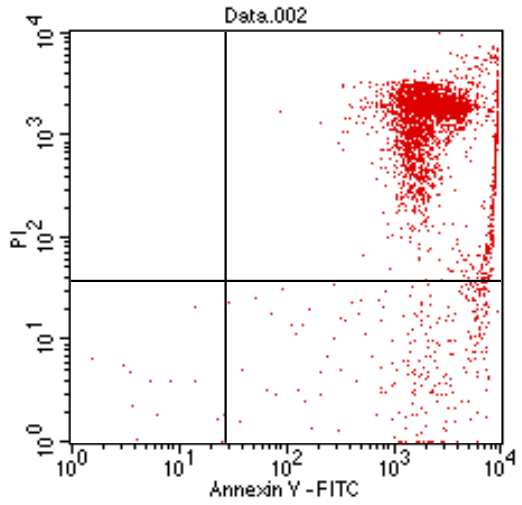

Figure 6. Toxic effects of blank liposome on PBMC.
PBMC were treated with 12.5mM and 6.25mM blank liposome for 24 hours and subject to Annexin V staining assay. Graph shown is representative of 12.5mM. PBMC treated with 6.25mM showed similar profiles (data not shown). Live cells (PI -, Annexin -), apoptotic cells (PI -, Annexin +), dead cells (PI +, Annexin +)

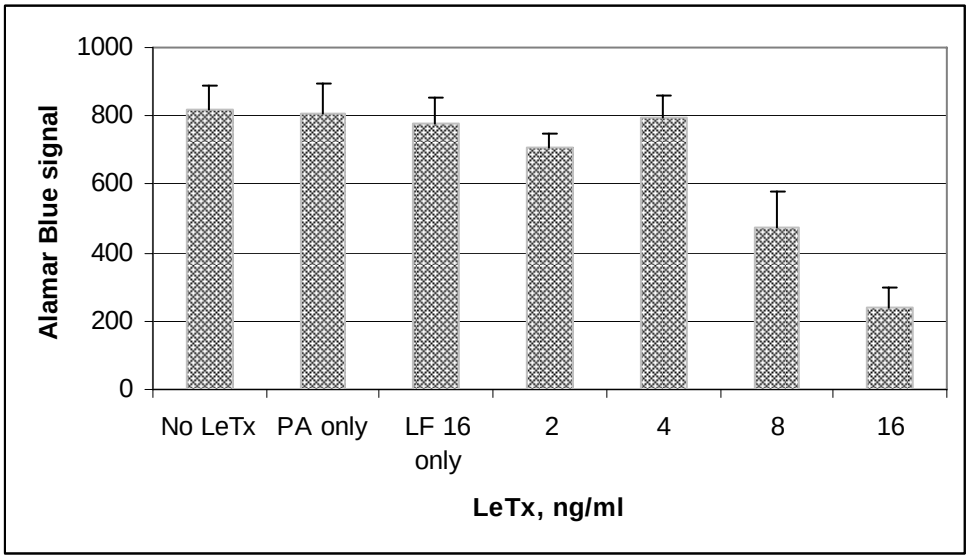

Figure 7. LeTx decreases phagocytic capacity of RAW 264.7 cells.
Cells were treated with LeTx for 3 hours. Spores ($2x10^6$/well) were then added to cells and incubated for 30 min. Cells were lysed and the viability of remaining spores and vegetative bacteria was determined using Alamar Blue.

(A)

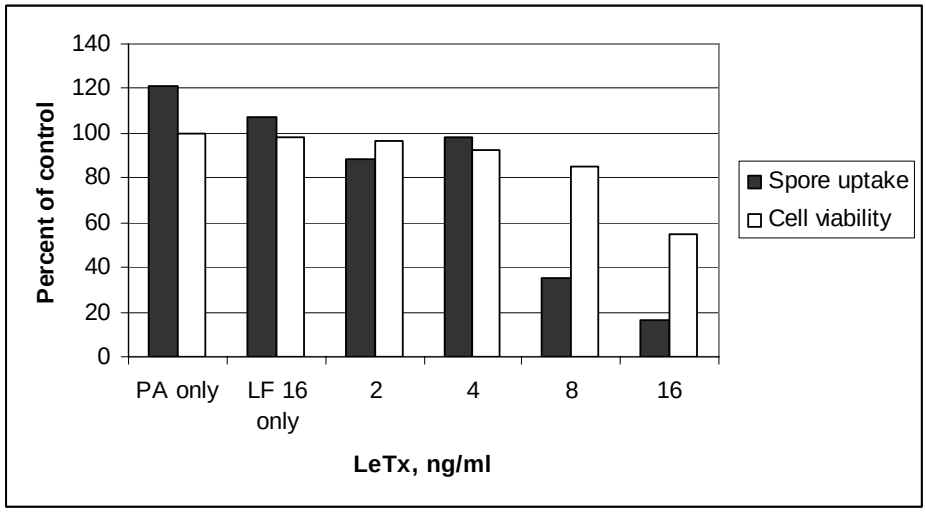

(B)

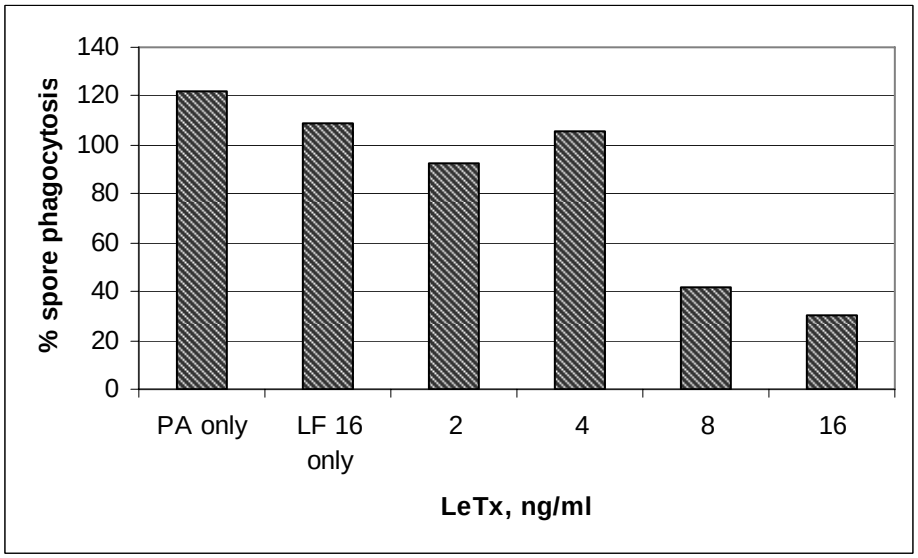

Figure 8. Percent spore phagocytosis of RAW 264.7 cells compared to non treated control. (A) Cells viability was measured after 3 hours LeTx treatment using CellTiter 96® Aqueous One Solution Cell Proliferation Assay (MTS). (B) Percent spore phagocytosis of RAW 264.7 was re-calculated based on its respective cell viability.

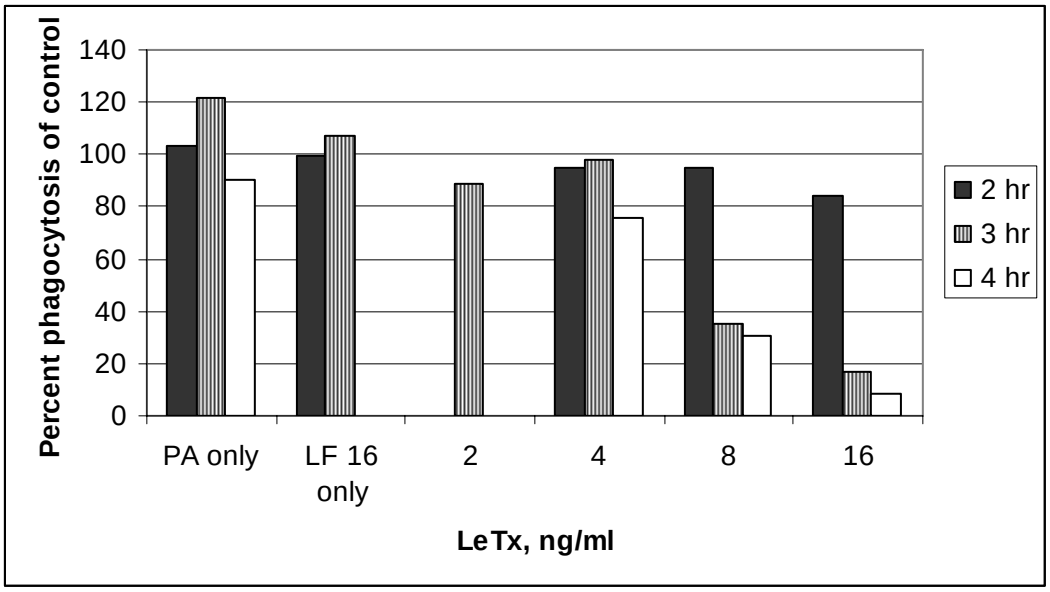

Figure 9. Percent spore phagocytosis of RAW 264.7 cells compared to non treated control after 2, 3 or 4 hours LeTx treatment.

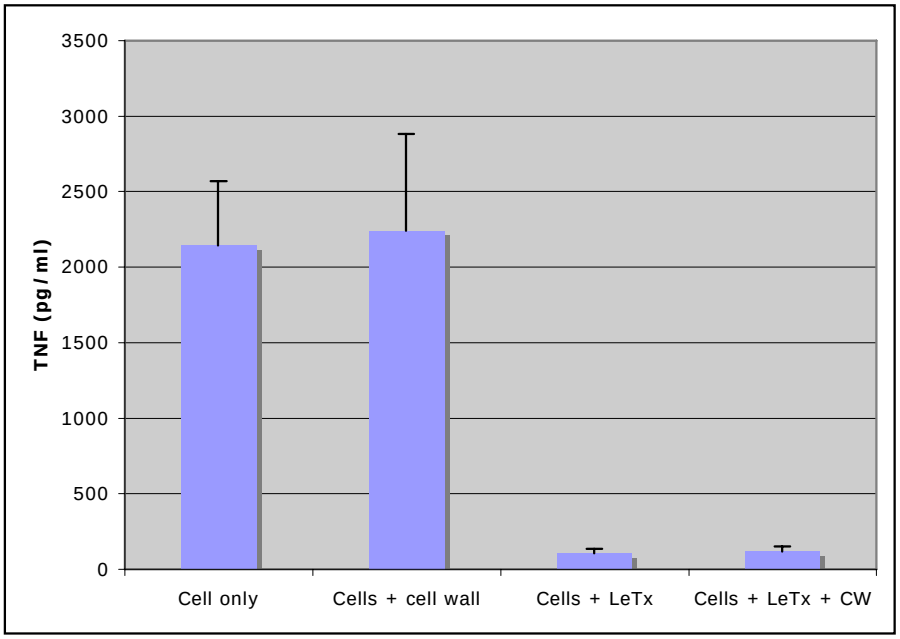

Figure 10. Inhibition of TNF-α expression in human macrophages treated with LeTx. Macrophages were treated with media only, 1ug/ml *B. anthracis* cell wall, LeTx (500ng/ml PA + 100ng/ml LF), or both cell wall and LeTx for 24h. Supernatants were collected and cytokine was quantified by BD Pharmingen CBA kit. Data are means ± standard errors of the results from two separate experiments.

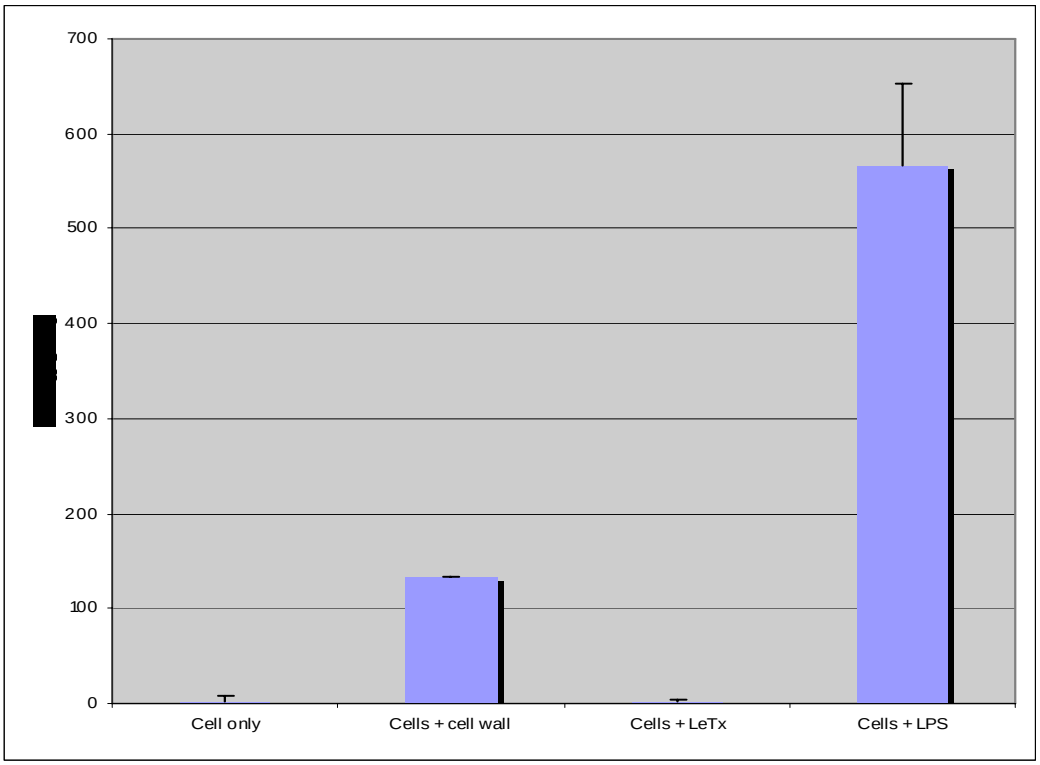

Figure 11. Production of TNF-α by human PBMCs activated by *B. anthracis* cell wall. PBMCs were treated with media only (control), 1ug/ml *B. anthracis* cell wall, LeTx (500ng/ml PA + 100ng/ml LF), or 10ug/ml LPS. At the end of incubation, the supernatants were harvested and assayed for the presence of TNF-α using the BD Pharmingen CBA kit. Data are means ± standard errors of the results from two separate experiments.

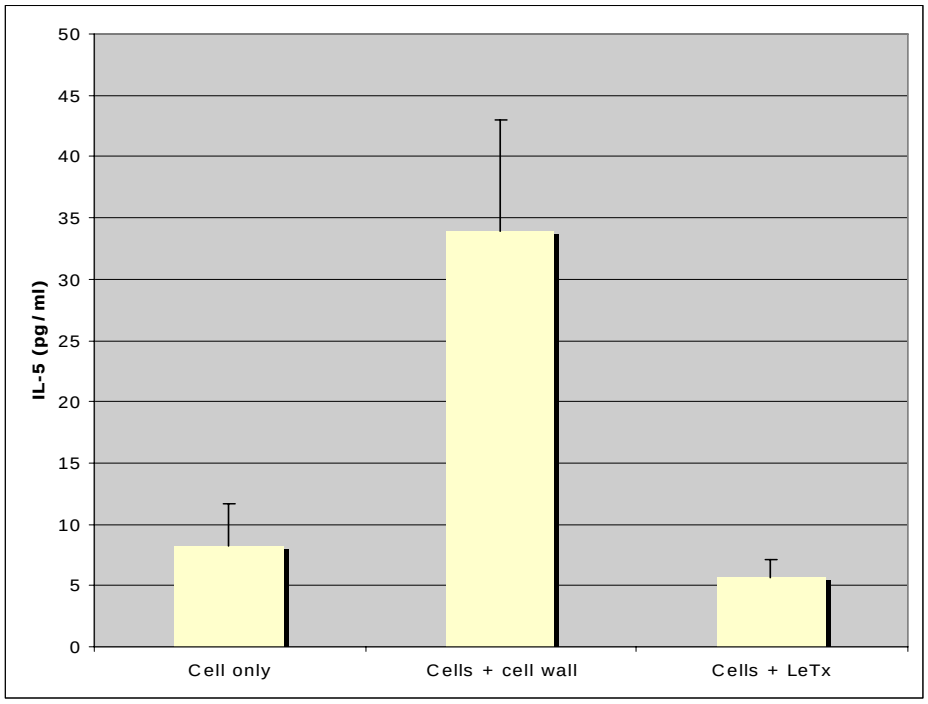

Figure 12. Production of IL-5 by human PBMCs activated by *B. anthracis* cell wall. PBMCs were treated with media only (control), 1ug/ml *B. anthracis* cell wall, or LeTx (500ng/ml PA + 100ng/ml LF). At the end of incubation, the supernatants were harvested and assayed for the presence of IL-5 using the BD Pharmingen CBA kit. Data are means ± standard errors of the results from two separate experiments.

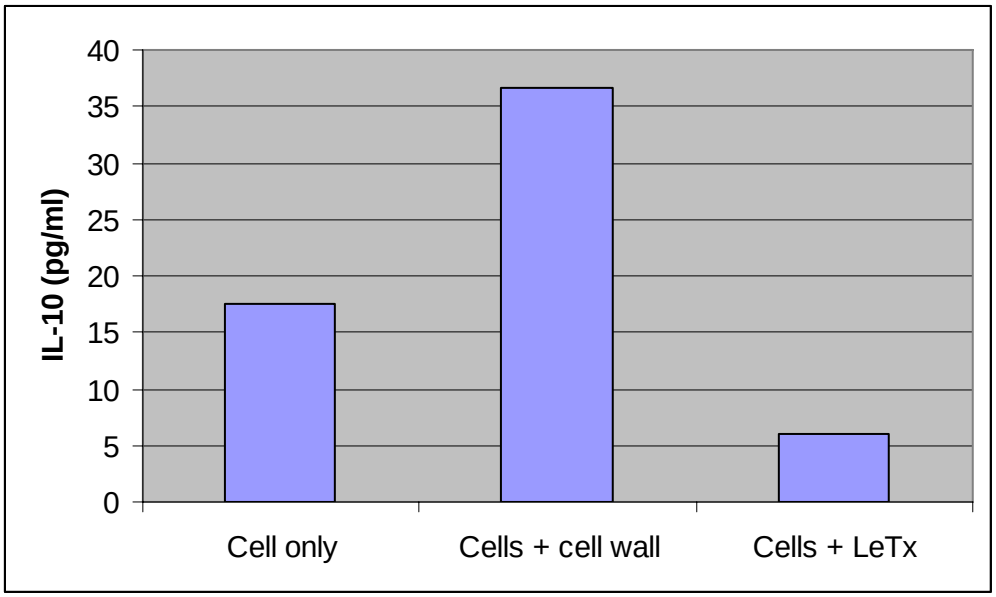

Figure 13. Production of IL-10 by human PBMCs activated by *B. anthracis* cell wall. PBMCs were treated with media only (control), 1ug/ml *B. anthracis* cell wall, or LeTx (500ng/ml PA + 100ng/ml LF). At the end of incubation, the supernatants were harvested and assayed for the presence of IL-10 using the BD Pharmingen CBA kit.

(A)

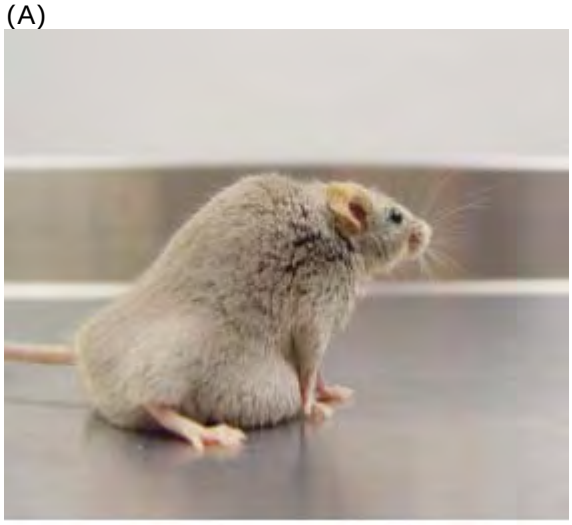

(B)

Figure 14. (A)Accumulation of free fluid within the peritoneal cavity (ascites) and (B) sign of hemorrhages.

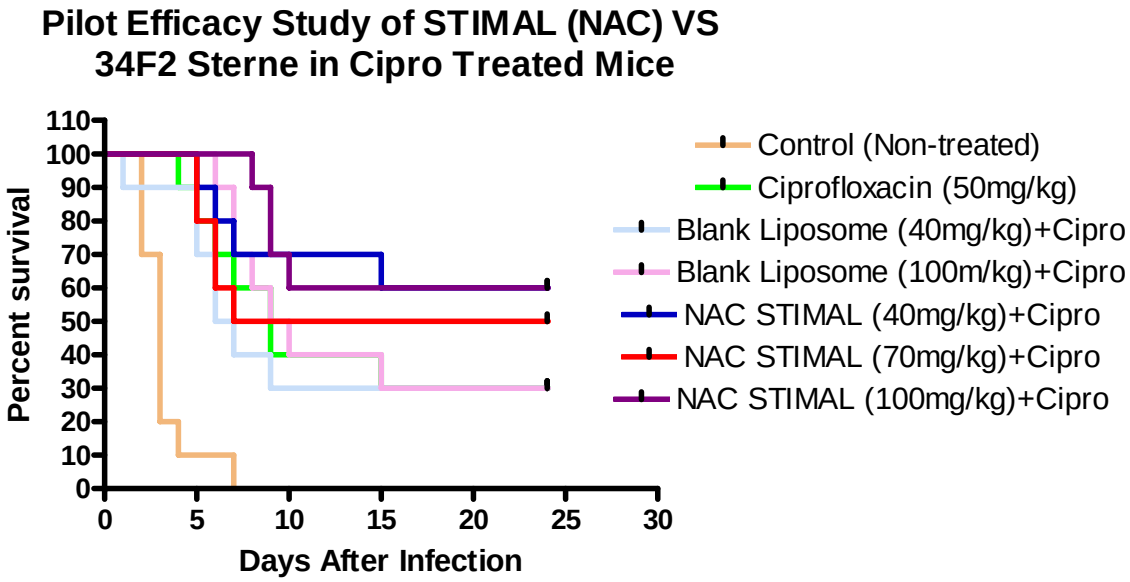

Figure 15. Survival curve for DBA2 mice infected with *B. anthracis* sterne spores and treated with ciprofloxacin alone or in combination with various dosages of NAC-liposome or blank liposome.

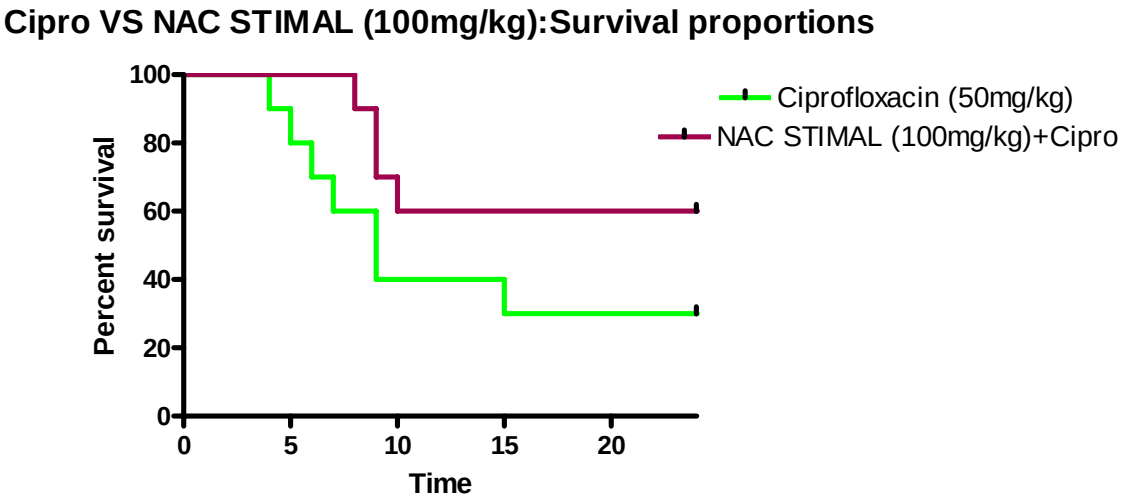

Chi square	2.415
df	1
P value	0.1202
P value summary	ns
Are the survival curves sig different?	No

Figure 16. Survival curve for DBA2 mice infected with *B. anthracis* sterne spores and treated with ciprofloxacin alone or in combination with 100mg/kg NAC-liposome.

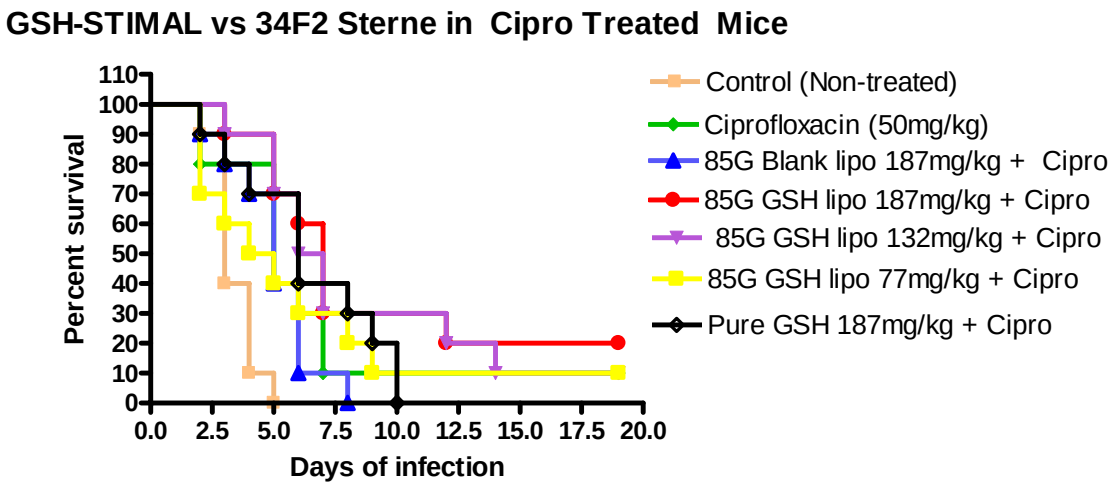

Figure 17. Kaplan Meier survival curve for DBA2 mice infected with *B. anthracis* sterne spores and treated with ciprofloxacin alone or in combination with GSH-liposome or blank liposome.

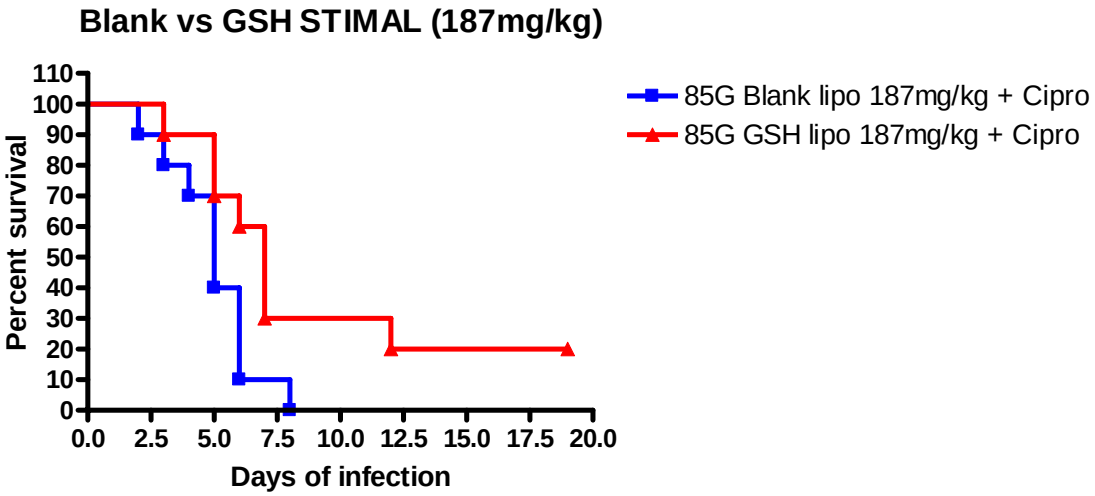

Chi square	4.792
df	1
P value	0.0286
Are the survival curves sig different?	Yes

Figure 18. Survival curve for DBA2 mice infected with *B. anthracis* sterne spores and treated with blank liposome or GSH liposome at 187mg/kg in combination with ciprofloxacin.

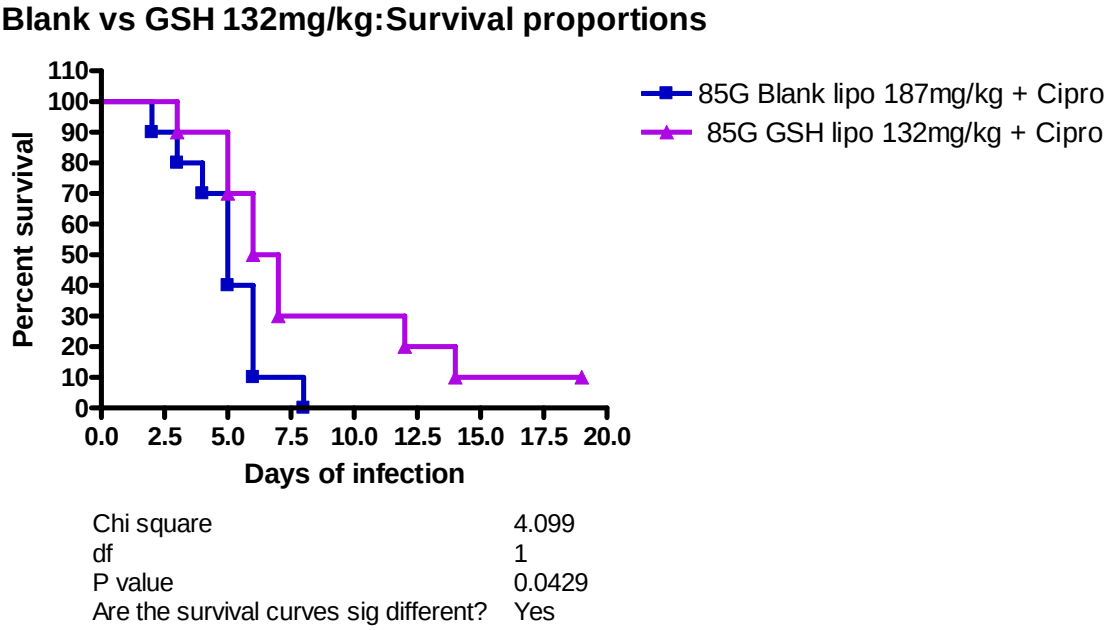

Figure 19. Survival curve for DBA2 mice infected with *B. anthracis* sterne spores and treated with blank liposome or GSH liposome at 132mg/kg in combination with ciprofloxacin.

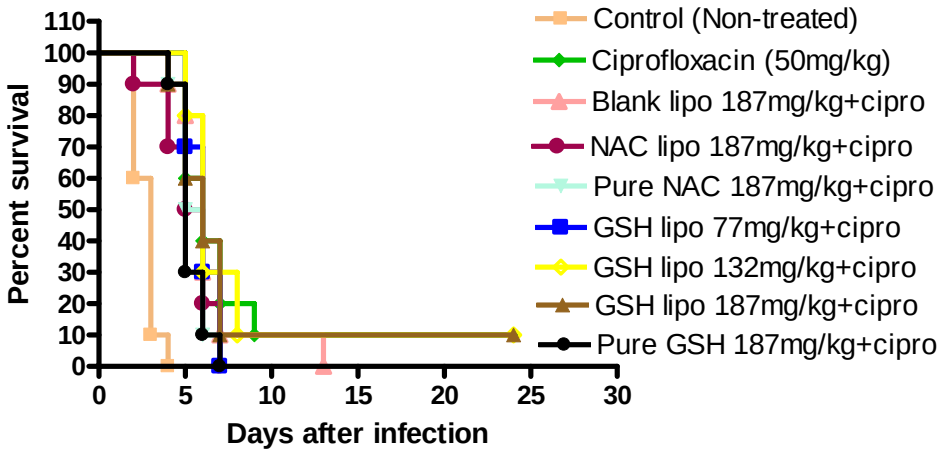

Figure 20. Kaplan Meier survival curve for DBA2 mice infected with *B. anthracis* sterne spores and treated with ciprofloxacin alone or in combination with 90G NAC- or GSH-liposome or blank liposome.

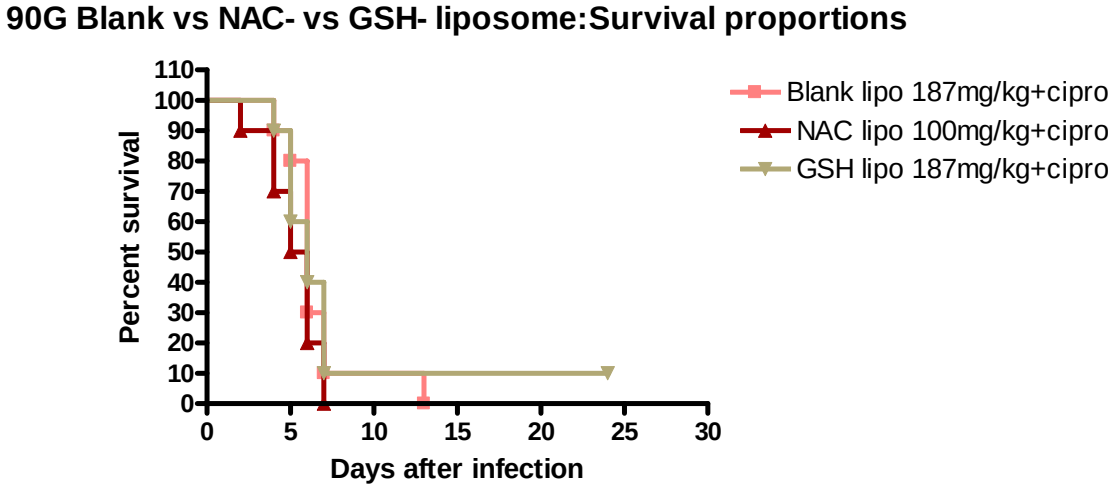

Figure 21. Survival curve for DBA2 mice infected with *B. anthracis* sterne spores and treated with 90G NAC-, GSH- or blank liposome in combination with ciprofloxacin.

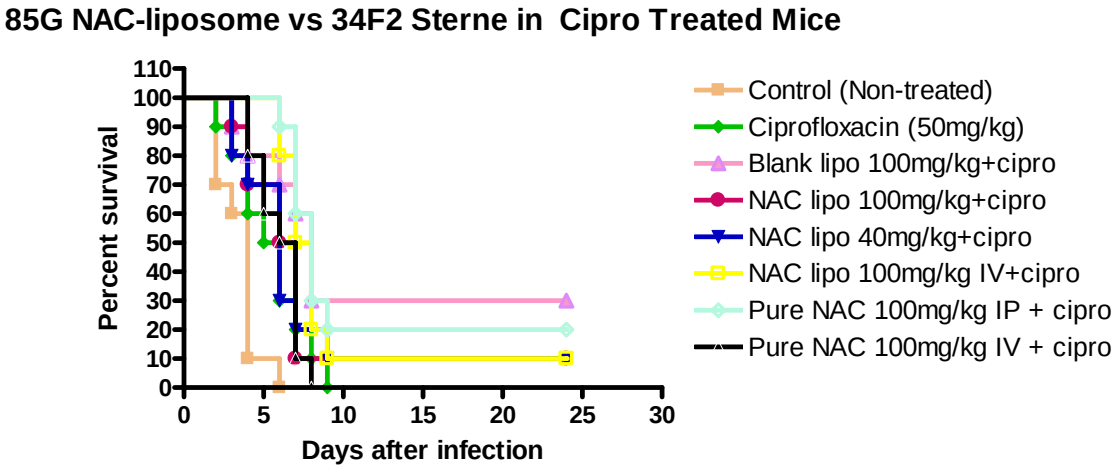

Figure 22. Kaplan Meier survival curve for DBA2 mice infected with *B. anthracis* sterne spores and treated with ciprofloxacin alone or in combination with NAC-liposome or blank liposome. NAC-liposome was given either through the intraperitoneum or intravenous route, the ciprofloxacin was given intraperitoneally.

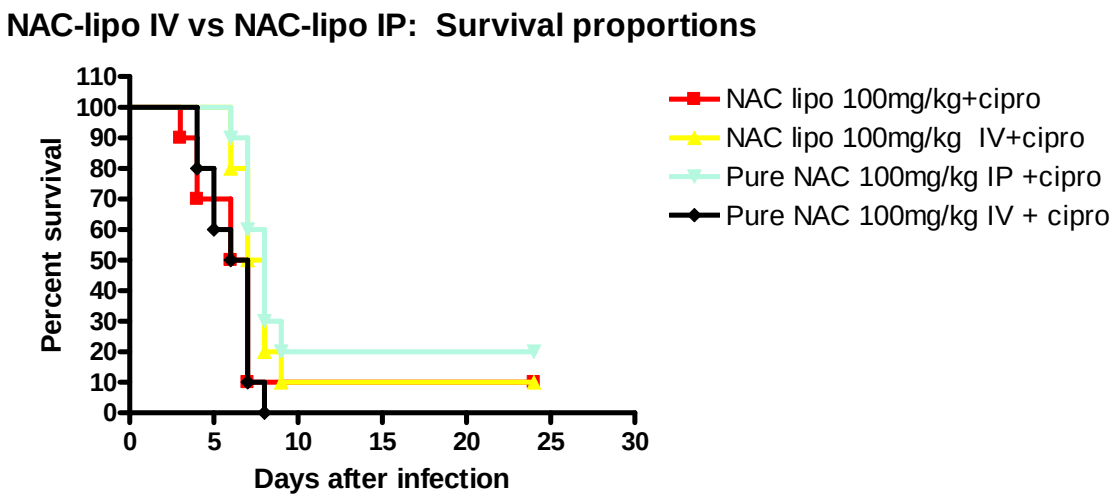

Figure 23. Survival curve for DBA2 mice infected with *B. anthracis* sterne spores and treated with NAC-liposome or pure NAC through intraperitoneal or intravenous route in combination with ciprofloxacin.

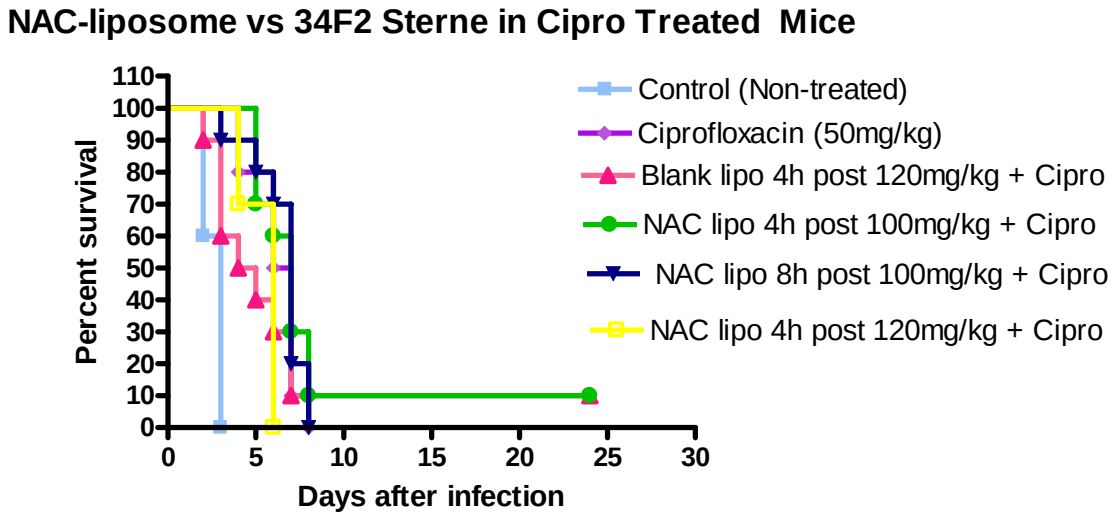

Figure 24. Kaplan Meier survival curve for DBA2 mice infected with *B. anthracis* sterne spores and treated with ciprofloxacin alone or in combination with NAC-liposome or blank liposome.

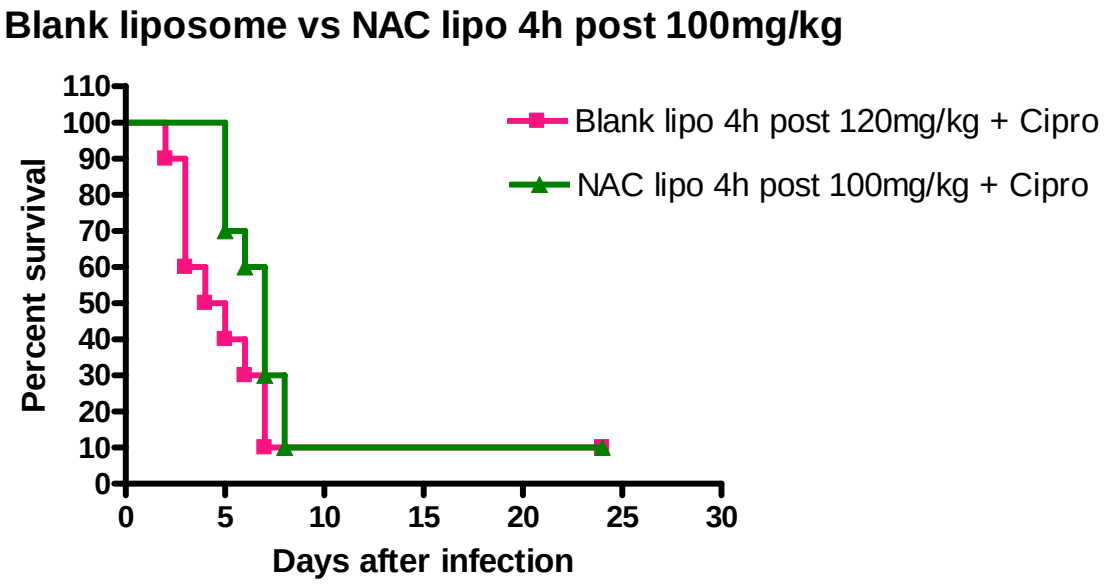

Figure 25. Survival curve for DBA2 mice infected with *B. anthracis* sterne spores and treated with blank liposome or NAC-liposome in combination with 50mg/kg ciprofloxacin.

Samples	IL-2 (pg/ml)	IL-4 (pg/ml)	IL-5 (pg/ml)	IL-10 (pg/ml)	IFN-γ (pg/ml)	TNF-α (pg/ml)
Cell only	10.1	60.6	4419.6	237.1	16	2445.3
Cells + cell wall	9.1	66.2	4573.3	319.6	17.2	2693.1
Cells + LeTx	12.1	57.4	1213.3	152.3	20.3	126.9
Cells + LeTx + CW	7.8	48.1	1294.5	153.6	13.6	140.4

Table 1. Cytokine expression by human macrophage cells after 1 day incubation. Macrophages were treated with media only, 1ug/ml *B. anthracis* cell wall, LeTx (500ng/ml PA + 100ng/ml LF), or both cell wall and LeTx for 24h. Supernatants were collected and cytokine was quantified by BD Pharmingen CBA kit.

Samples	IL-2 (pg/ml)	IL-4 (pg/ml)	IL-5 (pg/ml)	IL-10 (pg/ml)	IFN-γ (pg/ml)	TNF-α (pg/ml)
Cell only	12.4	59.5	10.7	31.8	22.2	6
Cells + cell wall	11	55.3	27.4	47.3	20.6	134.1
Cells + LeTx	8.7	53.1	6.7	9.1	16	3.3
Cells + LPS	11.7	65.1	4234.7	1803.7	35.6	627.1

Table 2. Cytokine expression by human PBMCs after 1 day incubation.
PBMCs were treated with media only, 1ug/ml *B. anthracis* cell wall, LeTx (500ng/ml PA + 100ng/ml LF), or 10ug/ml LPS for 24h. Supernatants were collected and cytokine was quantified by BD Pharmingen CBA kit.

	Mice Surviving (n=10)									
Group (cfu/mouse)	0 hour	24 hour	48 hour	56 hour	72 hour	96 hour	120 hour	128 hour	144 hour	168 hour
4.0x10^7	10	10	7	3	0	0	0	0	0	0
2.0x10^7	10	10	8	5	0	0	0	0	0	0
1.0x10^7	10	10	8	7	2	0	0	0	0	0
5.0x10^6	10	10	9	8	5	3	1	1	0	0
2.5x10^6	10	10	10	10	5	2	1	1	1	1
1.25x10^6	10	10	10	10	9	8	8	8	6	5
6.25x10^5	10	10	10	10	10	7	4	1	1	1
3.13x10^5	10	10	10	10	10	7	6	6	6	6
1.56x10^5	10	10	10	10	10	10	8	8	8	7

Table 3. *Bacillus anthracis* sterne spores (34F2) were administered to DBA2 mice intraperitoneally. The animals were monitored every day for 6 days for mortality. Ten mice were used in each dose group.

	Mice surviving (n=10)										
Group (cfu/mouse)*	Day 0	Day 1	Day 2	Day 3	Day 4	Day 5	Day 6	Day 7	Day 8	Day 9	Day 10
3.12x10^5	10	10	10	10	10	10	9	9	9	9	9
3.12x10^6	10	10	10	10	10	10	8	7	6	6	6
6.24x10^6	10	10	10	10	10	10	9	7	5	5	5
9.36x10^6	10	10	10	10	10	9	8	8	8	8	8
1.25x10^7	10	10	10	10	10	10	10	10	10	10	10
1.56x10^7**	7	7	7	4	4	4	0	0	0	0	0

*All mice groups are treated with 50mg/kg ciprofloxacin
** 7 mice used in this group

Table 4. *Bacillus anthracis* sterne spores (34F2) were administered to DBA2 mice intraperitoneally. 50 mg/kg ciprofloxacin was administered 24 hours post challenge by intraperitoneal injection. The animals were monitored every day for 10 days for mortality.

	Mice surviving (n=10)										
Group*	Day 0	Day 1	Day 2**	Day 3***	Day 4	Day 5	Day 6	Day 7	Day 8	Day 9	Day 10
Control-Non treated	10	10	7	2	1	1	1	0	0	0	0
Cipro alone	10	10	10	10	9	8	7	6	6	4	4
Blank liposome 40mg/kg + cipro	10	9	9	9	9	7	5	4	4	3	3
Blank liposome 100mg/kg + cipro	10	10	10	10	10	10	9	7	6	5	4
NAC-liposome 40mg/kg + cipro	10	10	10	10	10	9	8	7	7	7	7
NAC-liposome 70mg/kg + cipro	10	10	10	10	10	8	6	5	5	5	5
NAC-liposome 100mg/kg + cipro	10	10	10	10	10	10	10	10	9	7	6

Group*	Mice surviving (n=10)									
	Day 11	Day 12	Day 13	Day 14	Day 15	Day 16	Day 18	Day 20	Day 22	Day 24
Control-Non treated	0	0	0	0	0	0	0	0	0	0
Cipro alone	4	4	4	4	3	3	3	3	3	3
Blank liposome 40mg/kg + cipro	3	3	3	3	3	3	3	3	3	3
Blank liposome 100mg/kg + cipro	4	4	4	4	3	3	3	3	3	3
NAC-liposome 40mg/kg + cipro	7	7	7	7	6	6	6	6	6	6
NAC-liposome 70mg/kg + cipro	5	5	5	5	5	5	5	5	5	5
NAC-liposome 100mg/kg + cipro	6	6	6	6	6	6	6	6	6	6

*All mice were challenged with 1x10^7 cfu/mouse *B. anthracis* 34F2 spores
** Signs of hemorrhages and ascites in almost all animals
***Ruffled fur

Table 5. Protective effect of NAC liposome in combination with ciprofloxacin in DBA2 mice infected with *B. anthracis* sterne spores. The treatments were administered for 10 days and observed for mortality up to 24 days. NAC-liposome was administered in the morning, and ciprofloxacin was administered in the evening starting from day 2 to day 10. NAC-liposome was administered simultaneously with ciprofloxacin on day 1 (24 hour post spore challenge).

Group*	Mice surviving (n=10)										
	Day 0	Day 1	Day 2**	Day 3***	Day 4	Day 5	Day 6	Day 7	Day 8	Day 9	Day 10
Control-Non treated	10	10	9	4	1	0	0	0	0	0	0
Ciprofloxacin (50mg/kg) alone	10	10	8	8	8	4	3	1	1	1	1
Blank liposome 187mg/kg + Cipro	10	10	9	8	7	4	1	1	0	0	0
GSH liposome 187mg/kg + Cipro	10	10	10	9	9	7	6	3	3	3	3
GSH liposome 132mg/kg + Cipro	10	10	10	9	9	7	5	3	3	3	3
GSH liposome 77mg/kg + Cipro	10	10	7	6	5	4	3	3	2	1	1
Pure GSH 187mg/kg + Cipro	10	10	9	8	7	7	4	4	3	2	0

Group*	Mice surviving (n=10)									
	Day 11	Day 12	Day 13	Day 14	Day 15	Day 16	Day 18	Day 20	Day 22	Day 24
Control-Non treated	0	0	0	0	0	0	0	0	0	0
Ciprofloxacin (50mg/kg) alone	1	1	1	1	1	1	1	1	1	1
Blank liposome 187mg/kg + Cipro	0	0	0	0	0	0	0	0	0	0
GSH liposome 187mg/kg + Cipro	3	2	2	2	2	2	2	2	2	2
GSH liposome 132mg/kg + Cipro	3	2	2	1	1	1	1	1	1	1
GSH liposome 77mg/kg + Cipro	1	1	1	1	1	1	1	1	1	1
Pure GSH 187mg/kg + Cipro	0	0	0	0	0	0	0	0	0	0

*All mice were challenged with 5x10^6 cfu/mouse *B. anthracis* 34F2 spores
** Signs of hemorrhages and ascites in almost all animals
***Ruffled fur

Table 6. Protective effect of GSH liposome in combination with ciprofloxacin in DBA2 mice infected with *B. anthracis* sterne spores. The GSH liposome treatment was administered for 5 days instead of 10 days. Ciprofloxacin treatment was administered for 10 days and observed for mortality up to 24 days.

Group*	Mice surviving (n=10)										
	Day 0	Day 1	Day 2**	Day 3***	Day 4	Day 5	Day 6	Day 7	Day 8	Day 9	Day 10
Control-Non treated	10	10	6	1	0	0	0	0	0	0	0
Ciprofloxacin (50mg/kg) alone	10	10	10	10	10	6	4	2	2	1	1
Blank liposome 100mg/kg + cipro	10	10	10	10	9	8	3	1	1	1	1
NAC liposome 100mg/kg + cipro	10	10	9	9	7	5	2	0	0	0	0
Pure NAC 100mg/kg + cipro	10	10	10	10	9	5	1	0	0	0	0
GSH-liposome 187mg/kg + cipro	10	10	10	10	10	7	3	0	0	0	0
GSH-liposome 132mg/kg + cipro	10	10	10	10	10	8	3	3	1	1	1
GSH-liposome 77mg/kg + cipro	10	10	10	10	9	6	4	1	1	1	1
Pure GSH 187mg/kg + cipro	10	10	10	10	9	3	1	0	0	0	0

	Mice surviving (n=10)									
Group*	**Day 11**	**Day 12**	**Day 13**	**Day 14**	**Day 15**	**Day 16**	**Day 18**	**Day 20**	**Day 22**	**Day 24**
Control-Non treated	0	0	0	0	0	0	0	0	0	0
Ciprofloxacin (50mg/kg) alone	1	1	1	1	1	1	1	1	1	1
Blank liposome 100mg/kg + cipro	1	1	0	0	0	0	0	0	0	0
NAC liposome 100mg/kg + cipro	0	0	0	0	0	0	0	0	0	0
Pure NAC 100mg/kg + cipro	0	0	0	0	0	0	0	0	0	0
GSH-liposome 187mg/kg + cipro	0	0	0	0	0	0	0	0	0	0
GSH-liposome 132mg/kg + cipro	1	1	1	1	1	1	1	1	1	1
GSH-liposome 77mg/kg + cipro	1	1	1	0	0	0	0	0	0	0
Pure GSH 187mg/kg + cipro	0	0	0	0	0	0	0	0	0	0

*All mice were challenged with 1x10^7 cfu/mouse *B. anthracis* 34F2 spores
** Signs of hemorrhages and ascites in some animals
***Ruffled fur

Table 7. Effect of 90G NAC- and GSH- liposome in combination with ciprofloxacin in DBA2 mice infected with *B. anthracis* sterne spores. The treatments were administered for 10 days and observed for mortality up to 24 days.

	Mice surviving (n=10)										
Group*	**Day 0**	**Day 1**	**Day 2****	**Day 3*****	**Day 4**	**Day 5**	**Day 6**	**Day 7**	**Day 8**	**Day 9**	**Day 10**
Control-Non treated	10	10	7	6	1	1	0	0	0	0	0
Ciprofloxacin (50mg/kg) alone	10	10	9	8	6	5	3	2	1	0	0
Blank liposome 100mg/kg + Cipro	10	10	10	9	8	8	7	6	3	3	3
NAC liposome 100mg/kg + Cipro	10	10	10	9	7	7	5	1	1	1	1
NAC liposome 40mg/kg + Cipro	10	10	10	8	7	7	3	2	2	1	1
NAC liposome 100mg/kg IV + Cipro	10	10	10	10	10	10	8	5	2	1	1
Pure NAC 100mg/kg IP + Cipro	10	10	10	10	10	10	9	6	3	2	2
Pure NAC 100mg/kg IV + Cipro	10	10	10	10	8	6	5	1	0	0	0

	Mice surviving (n=10)									
Group*	**Day 11**	**Day 12**	**Day 13**	**Day 14**	**Day 15**	**Day 16**	**Day 18**	**Day 20**	**Day 22**	**Day 24**
Control-Non treated	0	0	0	0	0	0	0	0	0	0
Ciprofloxacin (50mg/kg) alone	0	0	0	0	0	0	0	0	0	0
Blank liposome 100mg/kg + Cipro	3	3	3	3	3	3	3	3	3	3
NAC liposome 100mg/kg + Cipro	1	1	1	1	1	1	1	1	1	1
NAC liposome 40mg/kg + Cipro	1	1	1	1	1	1	1	1	1	1
NAC liposome 100mg/kg IV + Cipro	1	1	1	1	1	1	1	1	1	1
Pure NAC 100mg/kg IV + Cipro	2	2	2	2	2	2	2	2	2	2
Pure NAC 100mg/kg IP + Cipro	0	0	0	0	0	0	0	0	0	0

*All mice were challenged with 5x10^6 cfu/mouse *B. anthracis* 34F2 spores
** Signs of hemorrhages and ascites in almost all animals
***Ruffled fur

Table 8. Effect of different routes of NAC-liposome administration in DBA2 mice infected with *B. anthracis* sterne spores. NAC-liposome was given either through the intraperitoneum or intravenous route, the ciprofloxacin was given intraperitoneally. The treatments was administered for 10 days and observed for mortality up to 24 days.

	Mice surviving (n=10)										
Group*	**Day 0**	**Day 1**	**Day 2****	**Day 3*****	**Day 4**	**Day 5**	**Day 6**	**Day 7**	**Day 8**	**Day 9**	**Day 10**
Control-Non treated	10	10	6	0	0	0	0	0	0	0	0
Cipro (50mg/kg) alone	10	10	10	10	8	8	5	1	0	0	0
Blank liposome 4h post 120mg/kg + cipro	10	10	9	6	5	4	3	1	1	1	1
NAC- liposome 4h post 100mg/kg + cipro	10	10	10	10	10	7	6	3	1	1	1
NAC-liposome 8h post 100mg/kg + cipro	10	10	10	9	9	8	7	2	0	0	0
NAC-liposome 4h post 120mg/kg + cipro	10	10	10	10	7	7	0	0	0	0	0

	Mice surviving (n=10)									
Group*	**Day 11**	**Day 12**	**Day 13**	**Day 14**	**Day 15**	**Day 16**	**Day 18**	**Day 20**	**Day 22**	**Day 24**
Control-Non treated	0	0	0	0	0	0	0	0	0	0
Cipro (50mg/kg) alone	0	0	0	0	0	0	0	0	0	0
Blank liposome 4h post 120mg/kg + cipro	1	1	1	1	1	1	1	1	1	1
NAC- liposome 4h post 100mg/kg + cipro	1	1	1	1	1	1	1	1	1	1
NAC-liposome 8h post 100mg/kg + cipro	0	0	0	0	0	0	0	0	0	0
NAC-liposome 4h post 120mg/kg + cipro	0	0	0	0	0	0	0	0	0	0

*All mice were challenged with 1x10^7 cfu/mouse *B. anthracis* 34F2 spores
** Signs of hemorrhages and ascites in almost all animals
***Ruffled fur

Table 9. Effect of earlier administration of NAC-liposome in combination with ciprofloxacin in DBA2 mice infected with *B. anthracis* sterne spores. First dose of liposome treatment was given at 4h or 8h after spore challenge. Both liposome and ciprofloxacin treatments were administered for 10 days and observed for mortality up to 24 days.

REPORT DOCUMENTATION PAGE

Form Approved
OMB No. 0704-0188

1. REPORT DATE *(DD-MM-YYYY)*	**2. REPORT TYPE**	**3. DATES COVERED** *(From - To)*
30-08-2008	Annual	01-09-2007 – 30-08-2007

4. TITLE AND SUBTITLE

The Development of Therapeutic and Diagnostic Countermeasures to WMD by the Advanced Medical Countermeasures Consortium:

Effects of Antioxidants on Bacillus anthracis - Macrophage Interactions

5a. CONTRACT NUMBER

5b. GRANT NUMBER
W81XWH-06-2-0044

5c. PROGRAM ELEMENT NUMBER
PE 62384BP

6. AUTHOR(S)

Richard F. Rest, Ph.D.

5d. PROJECT NUMBER

5e. TASK NUMBER

5f. WORK UNIT NUMBER

7. PERFORMING ORGANIZATION NAME(S) AND ADDRESS(ES)

Drexel University College of Medicine
2900 Queen Lane
Philadelphia, PA 19129

8. PERFORMING ORGANIZATION REPORT NUMBER

9. SPONSORING / MONITORING AGENCY NAME(S) AND ADDRESS(ES)
US Army Medical Research and Material Command
Fort Dietrich, Maryland 21702

10. SPONSOR/MONITOR'S ACRONYM(S)

11. SPONSOR/MONITOR'S REPORT NUMBER(S)

12. DISTRIBUTION / AVAILABILITY STATEMENT

Approved for public release; distribution unlimited

13. SUPPLEMENTARY NOTES

14. ABSTRACT

Background STIMAL is a non-toxic anti-oxidant and anti-inflammatory therapeutic based on liposome-encapsulated N-acetylcysteine (NAC). During inhalation anthrax, *B. anthracis* (BA) interacts with alveolar macrophages, and disease is initiated following this critical interaction. In the previous year of funding, we hypothesized that STIMAL would help human macrophages limit the *in vitro* growth of BA. It did, and it also reversibly inhibited BA spore germination *in vitro*. **Methods** We treated BA spores or vegetative BA with STIMAL/NAC *in vitro* in the presence or absence of human macrophages, and quantified BA and macrophage viability and functions, and spore germination. **Results** (i) In the absence of macrophages, STIMAL/NAC reversibly inhibits BA germination , (ii) STIMAL/NAC, in a dose and time-dependent manner, stimulates macrophages to kill intracellular BA by increasing intracellular reduced glutathione. (iii) STIMAL/NAC reversibly inhibits germination of BA spores by chemically reducing specific (not all) surface germination receptors. **Conclusions** NAC has dramatic protective activities regarding macrophage killing of BA, and inhibition of BA spore germination. In case of an anthrax attack, NAC could be used as an immediate adjunctive therapeutic aid to help prevent the initial events of BA-macrophage interactions in humans. STIMAL, could be an ancillary therapeutic agent, as the first multithread treatment countermeasure, in conjunction with vaccines and antimicrobials.

15. SUBJECT TERMS
liposome, anti-oxidants, therapeutic, anthrax, macrophage

16. SECURITY CLASSIFICATION OF:			**17. LIMITATION OF ABSTRACT**	**18. NUMBER OF PAGES**	**19a. NAME OF RESPONSIBLE PERSON**
a. REPORT	**b. ABSTRACT**	**c. THIS PAGE**			USAMRMC
U	U	U	UU		**19b. TELEPHONE NUMBER** *(include area code)*

Table of Contents

Page

STATEMENT OF WORK

1. Continue studies to determine if antioxidants (and antioxidant-loaded liposomes, STIMAL) alter the interactions and outcomes of viable, virulent *B. anthracis* (BA) spores with human macrophages.
   a) Use wild type BA and mutants – lethal factor, protective antigen, capsule biosynthesis, and ALO – to probe BA-macrophage interactions. On the bacterial side, observe and quantify spore germination, toxin expression, intracellular vs extracellular vs cell associated location of BA, and bacterial viability and replication. On the macrophage side, observe and quantify viability, apoptosis, phagocytosis, actin polymerization, oxidative burst, and iNOS expression levels.
   b) Determine the effects of antioxidants and empty or antioxidant-loaded liposomes on the functions measured in 1.a.

2. Determine the effects of antioxidants (and antioxidant-loaded liposomes) on intracellular signal transduction and the release of pro-inflammatory cytokines from human monocyte-derived macrophages and human macrophage-like cell lines incubated with sublethal concentrations of ALO and LT, alone or in combination. In aim 2, parameters to be measured include those associated with intracellular signaling relevant to chemotaxis and chemotaxis inhibition by ALO.
   a) Observe and quantify IL-1α, IL-1β, IL-6, IL-8, IL-10, IL-12 and TNFα mRNA (via RT-PCR) and cytokine release (via ELISA / FACS analysis). Other cytokines will be measured as necessary and for controls.
   b) Observe and quantify key intracellular signal molecules in NFκB activation, including IκB cleavage, p38 phosphorylation, NFκB translocation to the nucleus, and IRAK, TRAF6 and IKK activation.
   c) Measure intracellular calcium concentrations, IP3 concentrations, and the activity and expression of protein kinase Cs.
   d) Determine the effects of antioxidants and empty or antioxidant-loaded liposomes on the functions measured in 2.a.

The overall experimental design for the proposed studies is to treat cultured human macrophages with viable *B. anthracis* spores or ALO/LT, in the absence or presence of antioxidant liposomes, free antioxidant (NAC or glutathione) or empty liposomes, and then measure various parameters. In aim 1, the parameters to be measured include levels of *B. anthracis* germination, viability and replication, and macrophage antibacterial activity, including the ability of macrophages to bind and internalize *B. anthracis*, to limit (or not) spore germination and viability, and to mount an oxidative burst. In aim 2, parameters to be measured include those associated with intracellular signaling relevant to chemotaxis and chemotaxis inhibition by ALO.

INTRODUCTION **SUBJECT**: Oxidative stress, including the production of reduced oxygen products during the interaction of macrophages with pathogens, alters the host response, often exacerbating the host-parasite interaction, leading to more severe inflammation or disease. Inhibiting or dampening the oxidative response can help ameliorate inflammation and reduce disease manifestations. **PURPOSE and SCOPE**: With this in mind, we hypothesized that anti-inflammatory agents, particularly liposome-encapsulated reducing agents such as N-acetylcysteine (NAC), glutathione (GSH), and tocopherols, would help human macrophages limit growth of *Bacillus anthracis* (BA), in an *in vitro* system where BA spores and macrophages are incubated together in small culture dishes. Last year we found that reducing agents have a dramatic effect on helping macrophages control BA spore germination and replication of BA, and that reducing agents inhibit BA spore germination in the absence of macrophages. This past year we began to investigate the cellular and molecular mechanisms of these observations.

BODY This section of the report summarizes what has been presented in each quarterly report. Liposomes for all of our studies were from the laboratory of Dr. William Stone, East Tennessee State University, a member of the consortium.

Mariana Bernui, a full time senior graduate student working on this project, continued her studies, and is writing 2 manuscripts as first author. One ms is on the inhibition of *Bacillus anthracis* (BA) spore germination by NAC/STIMAL, the second ms is on the effects of NAC/STIMAL on the interaction of BA with macrophages. Mariana presented seven posters this last grant year, abstracts of which can be found in the appendix. Mariana was awarded a student travel award to the ASM Biodefense meeting, and her 'poster' presentation was one of just a handful honored as being chosen for an oral presentation.

Task 1. Determine if antioxidant-loaded liposomes alter the cellular functions of human monocyte derived macrophages and human macrophage-like cell lines treated in vitro with sublethal concentrations of anthrolysin O (ALO) and anthrax lethal toxin (LT), alone or in combination.

- ***a) Measure macrophage viability, apoptosis, chemotaxis, phagocytosis, phagosome-lysosome fusion, phagolysosome pH, phagocytic killing and upregulation of surface markers.***
- ***b) Determine the effects of empty or antioxidant-loaded liposomes on the functions measured in 1.a).***

We studied the role of intracellular GSH levels on macrophage chemotaxis in response to the anthrax toxin Anthrolysin O (ALO). We previously showed that ALO inhibits macrophage chemotaxis and that STIMAL or soluble NAC completely reverses or prevents this inhibition. We wished to know the mechanism of action of NAC in this system. To do so, we pretreated (or not) macrophages with BSO (buthionine sulfoximine; a reagent that decreases intracellular GSH) or NAC, then treated (or not) with ALO and measured chemotaxis. Pretreatment with NAC alone, BSO alone or NAC + BSO did not affect chemotaxis of RAW 264.7 mouse macrophages (or THP-1 human macrophages, data not shown) towards fMLP (formyl-methionyl-leucyl-phenylalanine), a standard chemoattractant peptide. This shows that the concentrations of BSO and NAC that we are using were not toxic to macrophages. Since BSO had no effect on macrophage chemotaxis, this also indicates that $[GSH]_i$ does not directly correlate with the ability of macrophages to chemotax. As expected, ALO inhibited chemotaxis, and this chemotaxis inhibition was completely reversed by NAC. Macrophages pretreated with BSO, which decreases $[GSH]_i$, washed, then treated with NAC, which increases $[GSH]_i$, and then treated with ALO, chemotaxed ~70% as much as macrophages treated with BSO alone or BSO and NAC. Taken together, these data indicate that BSO or $[GSH]_i$ has little <u>direct</u> effect on or correlation with macrophage chemotaxis in our system. This is contrary to our observations that $[GSH]_i$ is directly correlated with the ability of macrophages to limit BA spore outgrowth. Thus, NAC apparently has different mechanisms to affect (and effect) different macrophages functions.

Task 2. Determine if antioxidant-loaded liposomes alter the release of pro-inflammatory cytokines from human monocyte-derived macrophages and human macrophage-like cell lines incubated with sublethal concentrations of ALO and LT, alone or in combination (months 3-12).

- ***e) Measure IL-1α, IL-1β, IL-6 and TNFα mRNA and cytokine release. Other cytokines will be measured as necessary and for controls.***
- ***f) Determine the effects of empty or antioxidant-loaded liposomes on the functions measured in 2.a).***

This task was not studied. We propose to begin these studies in the coming year.

Task 3. Determine if antioxidant-loaded liposomes alter the interactions and outcomes of viable, virulent Bacillus anthracis spores with human macrophages (months 5-12).

a) ***Use wild type B. anthracis and mutants – lethal factor, protective antigen, edema factor, capsule biosynthesis, and anthrolysin O – to probe B. anthracis-macrophage interactions. Observe spore germination, B. anthracis viability and replication, and macrophage responses, including viability, apoptosis, upregulation of surface markers, and cytokine release.***
b) ***Determine the effects of empty or antioxidant-loaded liposomes on the functions measured in 3.a).***

We initially investigated the effect of NAC on the interaction of BA spores with macrophages. Brief summary - We treated BA Sterne strain 7702 spores or vegetative cells with various concentrations of NAC or STIMAL *in vitro* in the presence or absence of: (i) human monocyte-derived macrophages, (ii) RAW 264.7 murine macrophages, or (iii) differentiated human THP-1 cells. BA and macrophage viability and BA spore germination were measured at appropriate times. Results: (i) NAC completely and reversibly inhibited BA germination in the absence of macrophages. (ii) NAC had little effect on sporulation rate. (iii) NAC inhibited specific germination receptors, e.g. GerK and GerL. (iv) NAC altered BA germination in the presence of macrophages, which allowed rapid and successful killing of BA after macrophage phagocytosis, in stark contrast to cultures without NAC, and (v) glutathione and dithiothreitol had similar effects. Conclusions: STIMAL and its active component NAC have dramatic protective activities regarding macrophage killing of BA, and reversibly inhibit *B. anthracis* spore germination.

We studied the mechanism by which STIMAL and NAC increase the ability of macrophages to inhibit germination and outgrowth of BA in culture. BSO decreases intracellular reduced glutathione (GSH) by inhibiting its biosynthesis. To determine whether intracellular GSH levels are associated with the ability of macrophages to handle BA spores, we depleted macrophages *in vitro* with BSO for several hours and then infected them with BA spores. We found that BSO-treated macrophages allow more growth of BA in culture than do untreated macrophages. Thus, a decrease in intracellular GSH hinders the ability of macrophages to handle BA infection. We next treated BSO-pretreated macrophages with STIMAL, i.e., liposome encapsulated NAC. We hypothesized that NAC would reverse the effect of BSO by increasing intracellular GSH. Indeed, STIMAL reversed the effects of BSO. Whereas BSO-treated macrophages allowed significant outgrowth of BA spores *in vitro*, subsequent treatment of BSO-preteated macrophages with STIMAL allowed the macrophages once again to significantly limit BA outgrowth. As we have seen before, macrophages treated with STIMAL alone dramatically inhibited the outgrowth of BA spores. Thus, there is a direct correlation between intracellular GSH levels and the ability of macrophages to limit BA outgrowth from spores – the more $[GSH]_i$, the better ability macrophages have to limit BA growth.

We also undertook studies on the mechanism(s) by which NAC inhibits BA spore germination. BA spores have specific germination receptors on their surface that detect small molecules, including amino acids such as alanine, in the environment. We hypothesized that NAC affected the alanine receptors, which are called GerK and GerL. Indeed, spores treated with 5 mM NAC were completely inhibited from germinating in the presence of the potent and specific germinants alanine and inosine. This inhibition is not limited to alanine and inosine, as the activity of the germinants proline and serine is also completely inhibited by 5 mM NAC. BA spores treated with NAC and then washed, show a 30 min delayed germination. Thus, NAC's ability to inhibit germination is reversible, and appears to depend upon the redox state of surface exposed germination receptors.

We showed that NAC inhibition of BA spore germination was reversible. Spores were treated with NAC for 30 minutes, spun down and resuspended in fresh Germination Buffer with or without germinants (1 mM inosine + 0.5 mM proline). Addition of germinants constitutes time zero (t_0). Germination was measured by heating samples at 65C for 30 min, every 20 min for 2 hr. After heat

treatment, only spores remain viable. Vegetative cells are killed. CFU's plated on LB agar plates were counted the next morning. The spores pre-treated with NAC, and then the NAC washed away, had a lag before germination proceeded. To expand the relevance of these studies, we showed that other reducing agents, including glutathione and dithiothreitol, inhibit BA spore germination as well. Spores were suspended in fresh Germination Buffer with 5 mM NAC, GSH, or DTT. Germinants (1 mM inosine + 0.5 mM proline) were added at t_0. Surviving spores were quantified every 15 min for 1 hr by incubating aliquots for 30 min at 65^{o}C to kill vegetative BA, and dilution plating on LB agar plates. The next morning CFUs were counted. We observed that NAC, GSH and DTT chemically reduce (as opposed to oxidize) sensitive sites on some BA spore germination receptors, which inhibits their function. Our newest data in these studies indicate that NAC inhibits only certain germination receptors, specifically receptors for alanine, serine or proline (GerK, GerL, GerX). For instance, proline or serine both readily induce germination, whereas NAC completely but reversibly inhibits the ability of the potent germinants proline and serine to induce germination. On the contrary, NAC does not inhibit the ability of the germinants tryptophan or histidine (GerS, GerH) to induce germination. We will continue to test this hypothesis in the coming year, as indicated in our previously submitted proposal.

Finally, in efforts to determine the mechanism by which NAC inhibits BA spore germination, we treated various concentrations of spores, ranging from 1 X 10^6 to 1 X 10^9 / ml with 5 mM NAC and observed germination for 1 hr. As expected, in buffer alone spore germination was minimal, and in the presence of germinants (1 mM inosine and 0.5 mM alanine) germination was almost complete at 60 min. Our data clearly show that as spore concentration increases above 5 X 10^6 / ml, NAC's anti-germination effects diminish. This supports our hypothesis that NAC isn't directly inhibiting germinants, per se, but rather is chemically reducing (sulfhydral groups within?) germinant receptors on the surface of BA spores.

In the next year, we propose to: (1) Continue to work on the mechanisms by which NAC inhibits the ability of ALO to inhibit neutrophil and macrophage chemotaxis, and by which NAC inhibits the ability of ALO to stimulate neutrophil degranulation; (2) Begin studies on the ability of NAC to modulate stimulation of macrophage cytokine release by ALO and/or LT; (3) Continue to study the mechanisms by which NAC inhibits BA spore germination; (4) Submit 2 or 3 manuscripts on all of our studies to date, and; (5) Continue to work on the ability of NAC to increase the ability of macrophages to limit outgrowth of BA in culture.

KEY RESEARCH ACCOMPLISHMENTS

- STIMAL/NAC completely and reversibly inhibits BA spore germination.
- Reduced glutathione (GSH) and beta-mercaptoethanol (BME) also reversibly inhibit BA spore germination.
- Inhibition of spore germination by reducing agents is due to their reducing capacity.
- STIMAL/NAC increases the ability of macrophages to kill intracellular BA by increasing intracellular GSH concentrations.
- Inhibition of spore germination is specific for and limited to a defined subset of spore surface exposed germination receptors.

REPORTABLE OUTCOMES Six meeting abstracts were submitted and presented as poster or oral presentations. These are listed in the appendix.

CONCLUSION In this second year of funding for my lab, we have made further progress towards our goals, and have made headway into defining the mechanisms for some of the significant observations we made last year.

REFERENCES - NONE

APPENDICES

1. Abstracts (6)
2. updated CV for Richard Rest, PI
3. updated CV for Mariana Bernui, graduate student

==========

Drexel University College of Medicine Discovery Day 2007, Philadelphia, PA (ORAL PRESENTATION)

The Effects of Antioxidants on the Interaction of *Bacillus anthracis* with Macrophages
Mariana E. Bernui, Elise M. Mosser and Richard F. Rest
Department of Microbiology and Immunology, and Institute for Molecular Medicine and Infectious Disease, Drexel University College of Medicine, Philadelphia, PA

N-acetylcysteine (NAC), and antioxidant, induces the up- and down-regulation of macrophage cell surface molecules, as well as remodeling of the macrophage cytoskeleton. However, NAC's interaction with bacterial pathogens such as *Bacillus anthracis* (BA) and its effect upon infection have yet to be elucidated. During inhalation anthrax, BA spores are rapidly phagocytized by alveolar macrophages and germinate into vegetative bacteria, which leads to the onset of infection and disease. We incubated (i) human monocyte-derived macrophages (hMDMs), (ii) RAW 264.7 mouse macrophages or (iii) differentiated THP-1 cells with or without 5 mM NAC and subsequently infected them with BA Sterne strain 7702 spores. At 2 hours post-infection, untreated and treated macrophages had similar numbers of cell-associated spores. However, spores in NAC treated hMDMs began germinating at 3 hours whereas spores in the untreated hMDMs germinated only after 4 hours. Thus pretreatment with NAC affected BA's ability to regulate its highly controlled germination process. In addition, compared to untreated cells, there was a 2 log decrease in the number of extracellular vegetative bacteria 6 hours post-infection in NAC treated hMDMs. Similar observations were made for RAW 264.7 and differentiated THP-1s. A greater percentage of NAC pretreated macrophages were viable 8 hours post-infection compared to untreated cells. Thus, macrophages pretreated with NAC kill BA more effectively than do untreated macrophages. Unexpectedly, in the absence of macrophages, NAC reduced BA spore germination >95%. Therefore, the interplay between the effect of NAC on macrophages and its effect on spores leads to successful alleviation of BA infection *in vitro*.

==========

6th Annal ASM Biodefense and Emerging Diseases Research Meeting, February 24-27, 2008, Baltimore, MD (INVITED ORAL PRESENTATION)

N-acetylcysteine (NAC) or STIMAL (encapsulated NAC) Increase the Ability of Human Macrophages to Kill *Bacillus anthracis*. Mariana Bernui,[1] Milton Smith,[2] William Stone[3], R F Rest[1]
[1]Drexel University College of Medicine, Philadelphia, PA, [2]Amaox, Ltd., Melbourne, FL, [3] East Tennessee State University, Johnson City, TN

Background: STIMAL is a non-toxic, anti-inflammatory therapeutic based on liposome-encapsulated N-acetylcysteine (NAC) which ameliorates the pathophysiology associated CEES, a mustard gas analogue. NAC is a thiol, mucolytic agent, and precursor of intracellular L-cysteine and reduced glutathione. Although it is approved for human use, NAC's interaction with bacterial pathogens such as *Bacillus anthracis* (BA) and its effect upon BA infection have yet to be elucidated. During inhalation anthrax, BA

interacts directly with alveolar macrophages, and infection and disease is initiated. In the present studies, we investigated whether STIMAL and NAC (i) help human macrophages limit in vitro growth of BA and (ii) have any direct effect upon spore or vegetative BA function. **Methods**: We treated BA Sterne strain 7702 spores or vegetative cells with various concentrations of NAC or STIMAL in vitro in the presence or absence of either: (i) human monocyte-derived macrophages (hMDMs), (ii) RAW 264.7 murine macrophages, or (iii) differentiated human THP-1s monolayer. BA and macrophage viability and functions were measured at appropriate time points. Proper controls were included. **Results**: (i) NAC accelerated sporulation. (ii) NAC completely delayed/inhibited BA germination in the absence of macrophages. (iii) NAC, in a dose and time-dependent manner, stimulated the ability of macrophages to kill intracellular BA. (iv) NAC is not directly toxic to BA or macrophages. **Conclusions**: STIMAL and its active component NAC have dramatic protective activities regarding macrophage killing of BA and could be used as an immediate therapeutic aid to help prevent initial intra-alveolar events. Therefore it could be an ancillary therapeutic agent, as the first multithread treatment countermeasure, in conjunction with vaccines and antimicrobials. (This work was supported by DOD contract W81XWH-06-2-00442 (Peter Ward, PI), Drexel University, Drexel University College of Medicine, Eastern Tennessee State University, and NIH grant U54 AI057168, Mike Levine, PI.)

==========

ASM General Meeting, June 1-5, 2008, Boston, MA (POSTER)

N-acetylcysteine (NAC) or STIMAL (encapsulated NAC) inhibit germination of *Bacillus anthracis* spores

Mariana E. Bernui,[1] Milton Smith,[2] William Stone[3], Richard F. Rest[1]
[1]Drexel University College of Medicine, Philadelphia, PA, [2]Amaox, Ltd., Melbourne, FL, [3] East Tennessee State University, Johnson City, TN

Background: Inhalation anthrax is the most severe form of anthrax, which is initiated by introduction of *B. anthracis* (BA) spores to the lower respiratory tract, where they are phagocytosed by alveolar macrophages and dendritic cells. Germination of spores, and an environment allowing rapid out-growth of vegetative cells are essential in the early stages of disease in order to establish infection, and to allow the bacteria to multiply and spread to regional lymph nodes and the blood stream. Finding a therapeutic agent that hampers the spores' ability to germinate could prevent dissemination and disease. STIMAL is a non-toxic, anti-inflammatory therapeutic based on liposome-encapsulated N-acetylcysteine (NAC), which ameliorates the pathophysiology associated with mustard gas analogues. NAC is a thiol, a therapeutic mucolytic agent, and a precursor of intracellular L-cysteine and reduced glutathione. NAC's interaction with bacterial pathogens such as BA has not been studied. **Methods:** We treated BA Sterne strain 7702 spores or vegetative cells with various concentrations of NAC or STIMAL *in vitro* in the presence or absence of: (i) human monocyte-derived macrophages, (ii) RAW 264.7 murine macrophages, or (iii) differentiated human THP-1sr. BA and macrophage viability and functions were measured at appropriate times, and proper controls were performed. **Results**: (i) NAC completely inhibited BA germination in the absence of macrophages. (ii) Pretreatment with and then removal of NAC did not inhibit germination, indicating the need for the presence of NAC. (iii) NAC had little effect on sporulation rate. (iv) NAC inhibited specific germination receptors, e.g. GerK and GerL. (v) NAC altered BA germination in the presence of macrophages, which allowed rapid and successful killing of BA after macrophage phagocytosis, in stark contrast to cultures without NAC. (vi) Glutathione, but no other tested antioxidant, had similar effects. **Conclusions:** STIMAL and its active component NAC have dramatic protective activities regarding macrophage killing of BA and could be used as a therapeutic aid to help prevent initial intra-alveolar events. (This work was supported by DOD contract W81XWH-06-2-00442 (Peter Ward, PI), Drexel University, Drexel University College of Medicine, Eastern Tennessee State University, and NIH grant U54 AI057168, Mike Levine, PI.)

==========

17th Annual Infection and Immunity Forum, May 9th, 2008, Philadelphia, PA (INVITED ORAL PRESENTATION)

N-acetylcysteine (NAC) and STIMAL® (liposome-encapsulated NAC) impair germination of *Bacillus anthracis* spores and increase the ability of macrophages to limit anthrax growth *in vitro*
Mariana Bernui,[1] Milton Smith,[2] William Stone[3], Richard F. Rest[1]
[1]Drexel University College of Medicine, Philadelphia, PA, [2]Amaox, Ltd., Melbourne, FL, [3] East Tennessee State University, Johnson City, TN

Inhalational anthrax is initiated by introduction of *B. anthracis* (BA) spores into the lung where they are phagocytosed by alveolar macrophages. Spore germination and an environment permissive for rapid growth of vegetative bacilli are essential to establish infection in the early stages of anthrax. A therapeutic agent that inhibits spore germination or augments phagocytic killing could help prevent anthrax. STIMAL is an anti-inflammatory therapeutic based on liposome-encapsulated NAC, a powerful biological antioxidant. We treated BA strain Sterne 7702 spores with NAC or STIMAL *in vitro* in the presence or absence of macrophages. NAC or STIMAL completely inhibited BA spore germination (in the absence of macrophages), but were not bactericidal. Pretreatment with and then removal of NAC or STIMAL did not inhibit spore germination to the same extent as when they were present throughout the assay, indicating a reversible redox event. We found that the specific BA spore germination receptors gerK and gerL were targeted by NAC. NAC and STIMAL also altered BA spore germination in the presence of macrophages, which allowed rapid and successful killing of intracellular BA after macrophage phagocytosis, which was in stark contrast to cultures without NAC, where BA overgrew BA cultures. Finally, glutathione, but no other antioxidant tested, had similar effects. Therefore, STIMAL and its active component NAC show dramatic protective activities by inhibiting BA spore germination and by augmenting macrophage killing of BA. They could be used as immediate therapeutic aids to prevent anthrax soon after a bioterrorism attack. (This work was supported by DOD contract W81XWH-06-2-0044 (Peter Ward, PI), Drexel University, Drexel University College of Medicine, Eastern Tennessee State University, and NIH grant U54 AI057168, Mike Levine, PI.)

==========

Biodefense Research Conference November 2007, Philadelphia, PA (POSTER)

STIMAL (Liposome-Encapsulated N-Acetylcysteine) Increases the Ability of Human Macrophages to Kill *Bacillus anthracis*
Drexel University College of Medicine, 2900 Queen Lane, Philadelphia, PA, 19129; 215-991-8382 phone; 215-991-8909 fax; rickrest@drexel.edu
R F Rest,[1] Mariana Bernui,[1] Milton Smith,[2] William Stone[3], [1] Drexel University College of Medicine, Philadelphia, PA, [2] Amaox, Ltd., Melbourne, FL, [3] East Tennessee State University, Johnson City, TN

ACKNOWLEDGMENTS: This work was supported by DOD contract W81XWH-06-2-00442 (Peter Ward, PI), Drexel University, Drexel University College of Medicine, Eastern Tennessee State University, and NIH grant U54 AI057168 (Mike Levine, PI).

Anthrax is caused *by Bacillus anthracis* (BA), a spore-forming, facultative aerobic, Gram positive bacillus. Anthrax in humans and many animals is initiated by introduction of BA spores into the body by penetration of the epidermis, the gut, or the respiratory epithelium. *In vivo* experiments have demonstrated

that once inhaled, anthrax spores can reach the bronchioles and alveoli of the lung, and most spores rapidly and efficiently associate with alveolar macrophages and dendritic cells. The germination of spores and emergence of vegetative bacilli, in an environment allowing rapid out-growth in the body, are essential in the early stages of infection in order to establish disease. After germination, the bacilli multiply and spread to the regional lymph nodes and lymph, and from there to the blood stream where they can reach $>10^8$/ml.

In vitro, there are contradicting studies about how successful macrophages are at clearing anthrax spores. Most agree spore uptake is inefficient, yet there is extensive adherence of spores and vegetative cells to the macrophage surface. Four to six hours post infection, there is extensive germination and vegetative cell outgrowth, with chains of bacteria extending across several macrophages. The degree of BA clearance varies depending on the type of macrophage cell (or cell line) and the methodology used in each study.

In studies presented here, we use (i) human monocyte-derived macrophages (hMDMs), (ii) the RAW 264.7 murine macrophage cell line, or (iii) the differentiated human THP-1 cell line, infected with BA Sterne strain 7702 spores, to study the effect of individual or liposome encased antioxidants (STIMAL) on the interaction between BA and macrophages. Liposomes are cholesterol and fatty-acid rich carriers that can readily fuse with cell membranes and successfully deliver their contents inside the cell. STIMAL is a non-toxic, anti-inflammatory therapeutic based on liposome-encapsulated N-acetylcysteine (NAC). STIMAL ameliorates the pathophysiology associated with *in vivo* and *in vitro* administration of CEES, a mustard gas analogue (J Appl Toxicol. 2002, 22:257). The antioxidants we focused on in the present studies are NAC and glutathione, and the fat soluble tocopherols. NAC is a thiol, a mucolytic agent, a precursor of intracellular L-cysteine and reduced glutathione, and a source of sulfhydryl groups in cells and scavenger of free radicals as it interacts with reactive oxygen species such as OH• and H_2O_2. NAC's interaction with bacterial pathogens like BA and its effect upon BA infection have yet to be elucidated. At the initiation of these studies, we hypothesized that NAC would affect the interplay between BA and macrophages, providing the latter with means to better clear the infection.

We incubated various macrophages or macrophage cell lines in 24 well plates with or without 5 mM NAC and subsequently infected them with BA. At 2 hrs post-infection, untreated and treated macrophages had similar numbers of cell-associated spores. However, starting at 4 hrs, spores germinated 2 hrs earlier in NAC treated hMDMs, compared to untreated cells, and the germinated BA were rapidly killed. In addition, and logically following the intracellular killing of germinated spores, there was a >3-fold decrease in the number of extracellular vegetative bacteria 6 hrs post-infection in NAC treated hMDMs, compared to untreated controls. A similar phenomenon occurred with RAW 264.7 or differentiated THP-1 macrophages. Via *in vitro* viability assays and via light microscopy, a significantly greater percentage of NAC pretreated macrophages were viable at the end of assays (8 hours) compared to untreated macrophages. Thus, macrophages pre-treated with 5 mM NAC kill germinating BA spores more effectively than do untreated macrophages, strictly limit total BA growth, and remain viable. In the absence of macrophages, 5 mM NAC reduced germination of BA spores >95% in a 90 min study. Importantly, NAC was not toxic to spores or vegetative bacilli at the times or concentrations used in our studies. Therefore, the interplay between the effect of NAC on macrophages and its direct effect on BA spores may lead to successful clearance of BA infection. We suggest that STIMAL could be used in conjunction with antibiotics and vaccination in the event of an anthrax attack.

==========

Biotech 2007, Philadelphia, PA, October 2007 (POSTER)

STIMAL (Liposome-Encapsulated N-Acetylcysteine) Increases the Ability of Human Macrophages to Kill *Bacillus anthracis*

R F Rest,[1] Mariana Bernui,[1] Milton Smith,[2] William Stone[3], [1] Drexel University College of Medicine, Philadelphia, PA, [2] Amaox, Ltd., Melbourne, FL, [3] East Tennessee State University, Johnson City, TN

Purpose: After an anthrax attack, combination therapy will likely be used to assure decreased morbidity and mortality. Therapy may include vaccines, antibiotics, and therapeutics, including inhaled or injected antioxidants. STIMAL is a non-toxic, anti-inflammatory therapeutic based on liposome-encapsulated N-acetylcysteine (NAC) that ameliorates the lung pathophysiology associated with CEES, a mustard gas analogue (J Biochem Mol Toxicol 2003 17:177). During inhalation anthrax, *Bacillus anthracis* (BA) spores interact with alveolar macrophages to initiate disease. We hypothesized that STIMAL (and soluble NAC) would increase the ability of human macrophages to kill BA.

Methods: We treated human macrophages and/or BA spores or vegetative cells with STIMAL or NAC *in vitro*, in cell monolayers, and examined macrophage and BA viability. In addition, we measured BA sporulation and germination, and we observed BA-macrophage interactions via Normaski DIC light microscopy.

Results: (i) NAC accelerates sporulation of BA (in the absence of macrophages). (ii) NAC inhibits BA germination (in the absence of macrophages). (iii) NAC is not toxic to BA or macrophages. (iv) NAC significantly increases the ability of macrophages to kill intracellular BA. (v) NAC significantly increases the ability of macrophages to limit intracellular and extracellular BA growth. All observations were time and dose dependent.

Conclusions: NAC and STIMAL have dramatic protective activities regarding macrophage killing of BA and could be used as immediate therapeutic aids to help prevent initial alveolar events. We propose that STIMAL could be an ancillary therapeutic agent, as the first multi-threat treatment countermeasure, in conjunction with vaccines and antimicrobials.

Acknowledgments: This work was supported by DOD contract W81XWH-06-2-00442 (Peter Ward, PI); Drexel University; Drexel University College of Medicine; Eastern Tennessee State University; NIH grant U54 AI057168 (Mike Levine, PI).

September, 2008

RICHARD F. REST, Ph.D.

Department of Microbiology and Immunology
Drexel University College of Medicine
(formerly MCP Hahnemann School of Medicine)
2900 Queen Lane
Philadelphia, PA 19129
(215) 991-8382 - work
(215) 848-2271 - department fax
(610) 519-0265 - home
rickrest@drexelmed.edu

EDUCATIONAL HISTORY

1970-1974, Ph.D., Microbiology, University of Kansas, Lawrence
Advisor: Donald C. Robertson, Ph.D.
1966-1970, B.S., Microbiology, University of Massachusetts, Amherst
Advisor: Martin S. Wilder, Ph.D.

PROFESSIONAL EXPERIENCE & POSITIONS

(Drexel Univ College of Medicine was formerly MCP Hahnemann Univ Sch of Medicine was formerly Hahnemann Univ)
2005-present, Director, Biomed Grad and Postgrad Professional Development, Drexel University College of Medicine
1999-2001, Associate Dean, Biomedical Graduate Studies, MCP Hahnemann University School of Medicine
1994-present, Professor, Dept. of Pathology and Laboratory Medicine, Drexel Univ College of Medicine
1990-present, Professor, Dept. of Microbiology & Immunology, Drexel Univ College of Medicine
1983-1990, Associate Professor, Dept. of Microbiology & Immunology, Hahnemann University School of Medicine
1983, Associate Professor (with tenure), University of Arizona Health Sciences Center
1977-1983, Assistant Professor, Dept. Molecular & Medical Microbiology
University of Arizona Health Sciences Center, Tucson
1974-1977, Post-doctoral Fellow, Department of Bacteriology and Immunology
University of North Carolina, Chapel Hill
Advisor: John K. Spitznagel, M.D.

RESEARCH INTERESTS

I am interested in how *Neisseria gonorrhoeae, N. meningitidis* and *Bacillus anthracis* cause disease. My laboratory personnel have investigated two neisseria virulence factors: Opa proteins and sialyltransferase. (1) Opa proteins, a family of outer membrane proteins, are pluripotent virulence factors, allowing gonococci and meningococci to adhere to, invade and survive within human phagocytes, epithelial cells and endothelial cells. Using the yeast two hybrid system, we showed that intracellular Opa+ gonococci bind at least two human epithelial cell cytosolic proteins, including pyruvate kinase (PK) and thyroid hormone receptor interacting protein 6 (TRIP6). Gonococci bind PK and appear to require pyruvate for optimal intracellular survival and growth. We hypothesize that gonococci bind TRIP6, which is a cytoskeletal-associated protein and a nuclear messenger & transcriptional activator, to signal their presence within the cell, and alter host responses. (2) We have shown sialyltransferase (stase) to be an outer membrane, surface-exposed glycosyltransferase that transfers sialic acid (N-acetylneuraminic acid, Neu5Ac) from CMP-Neu5Ac to terminal galactoses of neisseria lipooligosaccharide (LOS). Sialylation of LOS can render gonococci and meningococci resistant to the bactericidal action of human serum, and modulate how these pathogens interact with host cells. We study regulation of expression of stase by environmental cues including contact with serum and human cells. (3) More recently we have studied the effect of antioxidants, including N-acetylcysteine (NAC), on interactions of *B. anthracis* with human macrophages and neutrophils, focusing on spores and the role of Anthrolysin O (ALO), a pore-forming, cholesterol-dependent cytolysin. ALO has rapid lethal effects and potent sublethal effects on host cells, due at least in part to signaling through TLR4 (Toll like Receptor 4). We are also characterizing a new global transcription regulator, unique to the *B. cereus* group.

ACTIVITIES, COMMITTEES, POSITIONS AND AWARDS

National and International

Research Career Development Award, NIH, 80-85

Ad hoc member, various NIH study sections, 82 – present
Member, Bacteriology and Mycology 2 (BM2) Study Section, NIH, 84-88
Editorial board: Infection and Immunity, 88-present
Editorial Advisory Board, The Journal of Infectious Diseases, 06 – present
Member, NIH Reviewer's Reserve, 89-94
Ad hoc grant proposal review: American Cancer Society, NIH, NSF, US - Israel Cooperative Program, Veterans Administration, The Wellcome Trust (England), US Civilian Research & Development Foundation (CRDF)
Invited referee: Amer J Pathology, Amer J Respiratory Cell & Molecular Biology, Antimicrobial Agents & Chemotherapy, Applied & Environmental Micro, Canadian J Microbiol, Cellular Microbiol, Clin and Vaccine Immunology, Clin Immunol & Immunopath, FEMS Immuno & Med Micro, Gene, Infect & Immun, Int'l J Exptl Pathology, J Bact, J Clin Immunol, J Clin Invest, J Immunol, J Infect Dis, J Leukocyte Biol, J Virology, Life Science, Microbial Pathogenesis, Microbiology, Molec Microbiol, Nature Medicine, PNAS, Scanning Electron Microscopy, Vaccine
Sabbatical leave with Drs. Barry Eisenstein and Laurence Boxer, Univ Mich Med Sch, 8/89-8/90
Member, national ASM Biotechnology Conference Committee, 90-92
Member, national ASM Public and Scientific Affairs Board, 91-97
Co-organizer and co-chair, *Microbial Pathogenesis and Immune Response I & II*; N.Y. Academy of Sciences, sponsor; 9/93, Orlando, FL; 10/95, New York, NY.
Sabbatical leave with Dr. E. Richard Moxon, Oxford Univ, England, 8/96-8/97
Outside Reviewer, FDA Laboratory of Enterics and Sexually Transmitted Diseases, 8/97
Member, USMLE Step 1 Microbiology Test Material Development Committee, 03 – 05
Chair, Microbiology and Immunology Test Committee, US Podiatric Medical Licensing Exam, 06 – present
Contributor, Faculty of 1000, biodefense, infectious disease – 08- present

Local and Regional
President Elect/President, Arizona Branch American Society for Microbiology (ASM), 81-83
Chair, Program Committee, Eastern Pennsylvania Branch ASM, 91-93
Chair and organizer, *92, 93, 94, 96, 02, 03, 04 Phila Infection & Immunity Forum* (Eastern PA Branch ASM)
Volunteer teacher, middle and high school students; STDs and their prevention, 92-96
1994 Teaching Faculty Award (best teacher), from the Hahnemann University Graduate Student Society
President Elect/President, Eastern Pennsylvania Branch ASM, 95-97/97-99
Nominated by MCPHU class of 2000 for the Golden Apple Award, best medical school teacher, 1998
Nominated by MCPHU class of 2004 for the Golden Apple Award, best medical school teacher, 2001
Nominated by DUCOM class of 2008 for the Golden Apple Award, best medical school teacher, 2005
Board of Directors, Families with Children from China – Delaware Valley (FCC-DV), 00-04
Vice President, Families with Children from China – Delaware Valley (FCC-DV), 01-04
Board of Directors, Radnor Elementary School PTO, 01-03
President, Ding Hao Chinese School PTO, 01-03
Board of Directors, Chinese Culture Association of Greater Philadelphia, 02-present
Board of Directors, Ding Hao Chinese School, 02-present

University & Medical School Committees and Positions
University Safety Comm 87-89, 93-95
Comm on Academic Quality, Graduate School 87-89, 93-95, 97-99
Admissions Comm, COM Graduate School 90-91
Admissions Comm, COM doctoral subcommittee, Graduate School 90-91
University Research Comm, University, 90-99, ex officio 99-01
Medical School Research Comm, University, co-chair, 91-96; ad hoc 97-01
MD/PhD Advisory Comm, University, 92 (inception)-95
University Biosafety Comm / Institutional Biosafety Committee, Chair, 93-95
Microbiology & Immunology Dept Graduate Program coordinator, 92-97; co-director 97-99; 01-04
University Council, 96
Department of Microbiology & Immunology Graduate Program course coordinator, 96-03
Committee to Investigate Endowments (appointed by University President) 98
Research Support Services Task Force, chair (appointed by COM Dean) 98-99
University Library Committee 99-00
Associate Dean for Biomedical Graduate Studies 99-01 (appointed by COM Dean)
University Research Finance Committee, co-chair (appointed by University Provost), 01-03
The National Bioterrorism Civilian Medical Response Center, steering committee, 01-present
Medical Student Summer Research Program, Director, 00-present
Research Strategic Planning at COM, Collaborations subcommittee chair (appointed by COM Dean), 02

Strategic Planning Committee, COM, (appointed by COM Dean), co-chair 04-06, member 07-present
Capital Committee, COM, member (appointed by University Provost), 04-07
Institute of Basic and Applied Protein Science (IBAPS), steering comm & member, 03 (inception) - 05
Committee on future of IBAPS (appointed by University Provost), 05
Committee on University Institutes, Centers and Programs (appointed by University Provost), 05-07
Biomed Grad and Postdoc Professional Development, Director (appointed by COM Dean), 05-present
University Committee on Drexel Faculty Diversity (appointed by University Provost), 06 - 08
DUCOM Core Curriculum sub-committee, Biomedical Graduate Studies, 06 - present

University Activities

Organized and wrote grant proposals for Hahnemann, through NIH Shared Instrumentation Program, for: DuPont ultracentrifuge, 88; ABI peptide synthesizer, 91; BioRad molecular imaging system, 93; ABI DNA sequencer, 98

Advise Hahnemann medical and graduate students who volunteer teach middle and high school students about STDs and their prevention, 92-96

Research mentor for:

high school students in HUMRAP (HU Minority Research Apprentice Program): Rosemary Ali, 89 & 90; Jenny Solis, 91 & 92; Nya Lewis 95

>MCPHU/Drexel medical students: Nicolle Lee, 86-87; Christopher Bowden, 87; Bo Hong Yoo, 88-89; Greg Ahearn, 92; Sarah Arnold, 92; Sarah Chang, 01; Karlyn Powell, 02; John Galiote, 03; Steven Boyle, 04; Ben Willenbring, 08

>MCPHU Medical Sciences Track Students: Michael DiMarino, 94; John Merlino,94-95; Yetunde Olesande, 99-00

>Minority high school teachers in HU Summer Research Program: Michael Bailey, 93

>Bucknell Univ. "Jan Plan" work-study program: John Van Kirk, 92; Duane Godshall, 93

>Summer Undergraduate Research Fellowship (SURF): Michael Quayle, 01; Alissa Romano, 03; Amit Prasad, 04

>Other undergraduates: Denise Ireland, Drexel, 01-02; Alexandra Bortnick, Univ Maryland, 02; Krista Kolbach, Penn State Univ, 02; Cassie Gunnis, Bradford Univ (UK), 03

Member, Microbiology and Immunology Graduate Program, 83 (inception)-present; Molecular Biology Graduate Program, 88 (inception)-present; Radiation Sciences Graduate Program, 99-05 (Program disbanded); Molecular Pathobiology Graduate Program, 88 (inception)-present

TEACHING EXPERIENCE

University of Arizona

1977-78: *Pathogenic Microbiology* (MICRO 220); 12 lectures, 75 undergraduates.
1977-83: *Pathogenic Mechanisms*, literature seminar (MMIC 596g), 6-8 graduate students.
1978-79: *Medical Microbiology* (MMIC 801), Initiated and re-designed 10 laboratory exercises; 12 lectures, 88 medical students. MICRO 220; 12 lectures, 40 undergraduate students. *Molecular Mechanisms of Microbial Pathogenesis* (MMIC 550); 20 lectures of 1½ hour each, 8 graduate students.
1979-81: MMIC 801; Course Coordinator, 15 lectures.
1981-83: MMIC 801; Course Coordinator, 12 lectures. MMIC 550; 20 lectures of 1½ hours each, 6-12 graduate students.

Drexel University College of Medicine (formerly MCP and Hahnemann School of Medicine)

1984-85: *Medical Microbiology*; 3-4 hrs/wk laboratory for semester (15 weeks), and four 50 min lectures to 175 medical students.
85-89: As 84-85; plus *Molecular Mechanisms of Microbial Pathogenesis*; ten 2-3 hr lectures, to 3-6 graduate students, annually. 88-89; chaired committee to reorganize the Microbiology Department's M.S. and Ph.D. curricula.
89-90: ***On sabbatical leave***
90-93: 8-12 lectures and 5-10 laboratory sessions in *Medical Microbiology,* annually. 12 2-3 hr lectures in two graduate courses, *Introduction to Infection and Immunity: molecular pathogenesis* and *Advanced Infection and Immunity: molecular pathogenesis*, annually or semi-annually.
93-96: As 90-93, plus, organized, direct and team teach a graduate course, entitled *Microbial Physiology and Genetics*, for 1st/2nd year graduate students, annually or semi-annually.
96-97: ***On sabbatical leave***
97-present: Similar to 90-96. Plus scattered lectures in our graduate core courses, including Molecular Biology & Genetics, and Cell Biology.

2001-2003: Course director, graduate Biomedical Ethics (Research Integrity) core course taken by all Biomed Grad students.

03-04: Course director and lecturer, Biomedical Ethics (Research Integrity), graduate core course; Course director and lecturer, Molecular Biology graduate core course; Course co-director and lecturer; Molecular Pathogenesis, a new 1 year course taken by first year Microbiology & Immunology graduate students; Lecturer, Medical Microbiology taken by ~200 medical students

04-05: Course director and lecturer, Biomedical Ethics graduate core course; Course co-director and lecturer, Molecular Biology and Genetics graduate core course; Course director and lecturer, Microbial and Molecular Pathogenesis I & II, graduate courses; Lecturer, Medical Microbiology, medical student course

05-06: Similar to 04-05.

06-08: Course Director and lecturer, Scientific Integrity (Responsible Conduct of Research), a biomedical graduate student required core course; Course Director and lecturer, Molecular Biology and Genetics, a biomedical graduate student required core course; Course Director and lecturer, Molecular Mechanisms of Microbial Pathogenesis I & II, required core courses for Microbiology and Immunology graduate students; Lecturer, Animal Models in Biomedical Research; Lecturer, Medical Microbiology, a required medical student course.

STUDENT EXAMINATION COMMITTEES (not including my own students)

Mary Pully, MS Nursing/Psychology, 1987; Susan Jordan, PhD Biochemistry, 1989; Brian Finnegan, MS Microbiology and Immunology (M&I), 1989; Michael Autieri, PhD Pathology, 1992; Katie Zaifert, MS M&I, 1992; Peter Kima, PhD Molecular Biology and Biotechnology (MB&B), 1992; Marguerite Dalton, PhD Biochemistry, 1993; Bruce Kuo, PhD MB&B, 1994; Richard Tomko, PhD M&I, 1995; Patrick Farley, PhD MB&B, 1995; Barbara Timblin, PhD M&I, 1996; Dalei Shao, PhD MB&B, 1995; Feng Zhu, MS Radiation Sciences 1996; Thomas Nesspor, MS MB&B, 1996; Terry Rowland, MS Radiation Sciences, 1996; Luan Tao, PhD MB&B 1997; Sumita Bhaduri, PhD MB&B 1997; Norman Waters, MS M&I 1997; Paul Calvo, MS MB&B 1997; Yvette Murley, PhD M&I 1997; Ana Gabrea, PhD M&I 1998; Connie Kang, PhD M&I 1998; Rocio Mulero, PhD M&I 1998; Christopher Hand, PhD Radiation Sciences 2000; Elizabeth Javazon, MS Molecular and Human Genetics; Angela MacIntyre, PhD Molecular Pathobiology; Thomas Caltagirone, PhD Neurosciences 2003; Donghui Zhang, MS Molec Biol 2003; Devrim Eren, PhD Molec Human Genetics 2003; Ajaya Kumar Devabhaktuni, Radiation Sciences 2003; Xin Fan, PhD M&I, Univ of Penn School of Medicine 2004; Jason Stumhofer, PhD M&I 2004; Daniel Woods, Ph.D. M&I, Temple University School of Medicine 2005; Shannon Morgan, Ph.D. M&I, Temple Univ School of Medicine 2006. ***Present*** Jean-Paul McGovern, PhD, Biomedical Engineering, Drexel; Swati Thorat, PhD, M&I; Shriya Raj, PhD, M&I.

POST-DOCTORAL FELLOWS

Linda J. Eaton, Ph.D., 1980-83. Biochemical analysis of human neutrophil phagolysosomes: bactericidal activities and oxidative metabolism. Present position: Director of Research & Development, List Biological Labs, Campbell, CA.

Barbara Belisle, Ph.D., 1986-87. The role of outer membrane protein PII in gonococcal adherence to human cervical and endometrial epithelial cells.

Susan T. Hingley, Ph.D., 1988 - 1991. Interactions of *N. gonorrhoeae with* human epithelial cells: the roles of pili, PII (Opa) proteins and lipooligosaccharide (LOS). Present position: Associate Professor of Biology, Pennsylvania College of Osteopathic Medicine, Philadelphia.

Daniel J. J. Simon, Ph.D., 1991 - 1994. Molecular studies on the interactions of Opa proteins with their neutrophil and epithelial cell receptors. Present position: Senior scientist, Glaxo-Wellcome, Verona, Italy.

Janice (Dobrowolski) Bennett, Ph.D. 1996-1999. Molecular structure-function studies on the interactions of Neisserial Opa proteins with cytosolic epithelial cell proteins - pyruvate kinase (PK-M2) and thyroid hormone interacting protein 6 (TRIP6).

Shi V. Liu, M.D., Ph.D. 1997-2000. Environmental regulation of Neisseria sialyltransferase gene expression, and genomic analysis of complex repeats in the genomes of pathogenic Neisseria. Present position: Scientist, USDA, Research Triangle Park, NC.

Vida Irani, Ph.D.. 2000 – 2001. Environmental regulation of sialyltransferase gene expression. Current position, postdoc, Department of Pathology, University of Pennsylvania.

Dawn (Bell) Shell, Ph.D. 2000–2004. Molecular and functional analysis of sialyltransferase gene expression; human immune response to sialyltransferase. Current position: Assistant Professor of Biology, Pennsylvania College of Osteopathic Medicine, Philadelphia.

Vincent Ng, Ph.D. 2004 – 2005. Interaction of *Bacillus anthracis* with human macrophages and neutrophils; biological role of Anthrolysin O.

GRADUATE STUDENTS

Paul Buck, 1978-80, M.S. Effects of lysosomal enzymes on gonococcal metabolism.

Rosalie A. Fowler, 1978-83, M.S. Biochemical analysis of phagosome-lysosome fusion in neutrophils. Present position, Director, Clinical Microbiology, St. Christopher's Hospital, Tucson, AZ.

Elizabeth E. Vela, 1980-83, M.S. (Research advisor). Biochemical analysis of macrophage maturation.

Joseph R. Mezzatesta, M.S., 1979-83, Ph.D. Phagocytosis and killing of gonococci by human mononuclear phagocytes. Present position: Senior Scientist, Research and Development, Wyeth-Lederle Laboratories, Pearl River, NY.

John P. Rock, 1980-86, Ph.D. Effects of human neutrophil lysosomal enzymes on gonococcal metabolism and physiology. Present position: Manager, Strategic Project Management, AgrEvo Environmental Health, Research Triangle Park, NC.

Steven H. Fischer, 1981-88, MD/PhD. Role of gonococcal outer membrane protein PII (Opa) in phagocytosis by human PMN. Present position: Private practice, Florida.

Christopher Elkins M.S., 1983-88, Ph.D. Role of gonococcal outer membrane PII (Opa) in neutrophil stimulation and adherence. Present position: Research Associate Professor, Dept of Microbiology & Immunology, UNC, Chapel Hill.

Catherine Farrell, 1984-1990, Ph.D. A human neutrophil receptor for gonococcal outer membrane protein PII (Opa). Present position: Senior scientific writer, Sanofi Ltd., Philadelphia, PA.

Fredrick Naids, 1984-1991, Ph.D. Molecular and cellular studies on the role of PII in gonococcal stimulation of human neutrophils. Present position: Vice President for Marketing and Sales, Cerup Corp, US/France.

Joseph V. Frangipane, 1988-1993, Ph.D. Interaction of gonococci with human neutrophils and serum: role of oxygen and CMP-NANA (cytidinemonophosphate N-acetyl-neuraminic acid). Present position: Applications specialist, Life Technologies Corp, Gaithersburg, MD.

David McGee, 1992-1997, Ph.D. Molecular analysis of the regulation of expression of gonococcal and meningococcal sialyltransferase gene(s). Present position: Assistant Professor, Department of Microbiology & Immunology, University of South Alabama.

Janine Ferguson, 1993-1997, M.S. Regulation of gonococcal sialyltransferase activity by *in vivo* signals and substrates. Present position: Nurse Practitioner, New Jersey.

John M. Williams, 1993-1999, M.D./Ph.D. Use of the yeast two hybrid system to identify gonococcal Opa receptors in the cytoplasm of human epithelial cells. Present position: Resident, Harvard Univ.

Dawn (Bell) Shell, 1992-1999, Ph.D. Physical and immunologic characterization of neisserial sialyltransferases; the role of PIII (Rmp) in gonococcal adhesion and invasion. Present position: Assistant Professor of Biology, Pennsylvania College of Osteopathic Medicine, Philadelphia.

Jeff Shannon, 1999-2003, Ph.D. The role of Opa proteins in the intracellular lifestyle of *Neisseria gonorrhoeae* and *Neisseria meningitidis*; Characterization of *Bacillus anthracis* Anthralysin O. Present position: postdoctoral fellow, Rocky Mountain National Laboratories, Montana.

Mathanraj Packiam, 2001-2006, Ph.D. Regulation of sialyltransferase expression by *N. gonorrhoeae* and *N. meningitidis*. Present position: postdoc, USUHS.

Yognandan Pandya, 2003 – 2005, M.S. Biomedical Engineering. The role of Anthrolysin O in the interaction of *Bacillus anthracis* with human macrophages and neutrophils. Present position: biopharma, NJ.

Elise (Bifano) Mosser, 2003-2007, Ph.D. Transcriptional regulation and mechanism of action of Anthrolysin O, a *Bacillus anthracis* virulence factor.

Mariana Bernui, 2005 – present, Ph.D. candidate. The effect of antioxidants on the interaction of *Bacillus anthracis* and its toxins with human macrophages and neutrophils.

Mitali Purohit, M.S. 2006 – present, Ph.D., candidate. The effects of antioxidants on the interaction of *Bacillus anthracis* and its toxins with human macrophages and neutrophils.

Judy Rieger, 2006 – 2007, M.S. candidate. The effects of antioxidants on the interaction of Anthrolysin O with human macrophages and neutrophils. Moved on to another lab.

Meghan Wynosky, 2006 – present, Ph.D. candidate. The role of Arp1 and Arp2 in transcriptional regulation of *B. anthracis v*irulence factors.

RESEARCH SUPPORT (@ = active)

Bactericidal action of cationic proteins from human PMN. Postdoctoral Fellowship, 1 F32 AI01533, NIH ($28,500 total), 6/75-5/77.

Wellcome Research Travel Grant from the Burroughs Wellcome Fund, to study in the laboratory of H. Smith, Ph.D., Head, Department of Microbiology, University of Birmingham, England ($3,450), 5/21/79-7/13/79.

Macrophage maturation and lysosomal adaptations. Co-investigator for bacterial studies, 5% effort, Program No. 821 from the Veterans Administration, 10/78-9/81. S. Axline, M.D., PI.

Effects of phagolysosomal contents on Neisseria gonorrhoeae, R01 AI15881, NIH ($200,000 total direct costs), PI, 4/79-3/82.

Mechanisms of intracellular pathogenesis, K04 AI00594, NIH ($175,000, total direct costs), Research Career Development Award, PI, 7/80-6/85.

Gonococcal surface components in pathogenesis, F32 AI07874, NIH NRSA post-doctoral fellowship to S. T. Hingley, Ph.D., PI and applicant; R. Rest, Sponsor, 4/89-3/91.

Wellcome Research Travel Grant, Burroughs Wellcome Fund, to study with E. R. Moxon, M.D., Dept of Paediatrics, Univ of Oxford, England ($10,400), 8/96 - 8/97.

Gonococcal Opa proteins and intracellular survival, F32 AI10046, NIH NRSA post-doctoral fellowship to Janice (Dobrowolski) Bennett, Ph.D., postdoc; R.F. Rest, Sponsor; 12/97-12/99.

Intracellular fate of Neisseria gonorrhoeae, R01 AI20897, NIH ($175,000 direct, 6/00-5/01). PI at 25% effort, 9/78 - 5/01. To be renewed.

Development of a biodetector for bioterrorism agents. Drexel University Synergy Award ($10,000). Co-investigator, 7/02 – 6/03.

Carbide-derived carbon filters for biohazardous agents. Drexel University Synergy Award ($20,000). Co-investigator, 7/02-6/03.

Active Filtration System for Building Defense Against Chemical/Biological Attacks. N00175-03-C-0024, Collaboration on a DARPA contract with PlasmaSol Corp, Hoboken, NJ ($45,000 to Rest). Co-investigator at 10% effort, 9/03-3/04.

Sialylation of the pathogenic Neisseria, R01 AI33505 supplement, NIH ($50,000 direct annually). This is a minority postdoctoral supplement for Dr. Dawn Shell, 9/01-7/04.

BSL3 Laboratory Renovations. Pennsylvania Tobacco Settlement Act 77 Formula Funds, PI, 1/03-12/04. This grant provided funds to renovate one of my BSL2 labs to a BSL3 lab; PI, $65,000.

Interaction of Bacillus anthracis with Macrophages. Pennsylvania Tobacco Settlement Act 77 Formula Funds, PI, 1/03-6/04, $50,000.

Interaction of Anthrolysin O with other Anthrax Toxins, U54 AI57168, NIH, Mid-Atlantic Regional Center of Excellence in Bioterrorism and Emerging Infectious Diseases, Myron Levine M.D., PI, Univ of Maryland Center for Vaccine Development. Rest, co-I, 10% effort, developmental sub-proposal, 09/03 – 03/05, $150,000 to Rest.

Molecular and Structural Mechanisms, Detection and Antagonism of Anthrax Toxins. Pennsylvania Tobacco Settlement Act 77 Formula Funds, PI, 5/04-4/05, co-PI, 0%, $37,500.

Microbiologic Support for Biosensor Development. Ben Franklin Technology Partners, Nanotechnology Institute, Kambiz Pourrezaei, PI, Drexel University. Rest, co-I, 5%, 8/03 – 12/04, $46,000 to Rest.

Sialylation of the pathogenic Neisseria, R01 AI33505, NIH ($200,000 direct annually). PI at 35% effort, 6/94-6/05.

Piezoelectric Biosensor for Anthrax Detection. Contract number: PA 26-0017-00, recipient ID: 6346, Transportation Security Administration, US Department of Transportation, Department of Homeland Security, Banu Onaral, PI, Drexel University. Rest, co-I, 10%, 10/04 – 3/08, $3,250,000 total, ~$300,000 direct to Rest.

The Advanced Medical Countermeasures Consortium: Use of Free and Liposome-encapsulated Antioxidants as a Countermeasure to Mustards and Anthrax. DOD contract no. W81XWH-06-2-0044, PI, Peter A. Ward, University of Michigan. Rest is co-I at 25% effort, 5/06 – 9/07, $6,000,000 total, $375,000 direct to Rest, "Effects of Antioxidant Liposomes on *Bacillus anthracis* – Macrophage Interactions."

@ *The Advanced Medical Countermeasures Consortium: Use of Free and Liposome-encapsulated Antioxidants as a Countermeasure to Anthrax.* DOD contract no. to be determined, PI, Peter A. Ward, University of Michigan. Rest is co-I at 25% effort, 10/07 – 9/08, $2,200,000 total, $175,000 direct to Rest, "Effects of Antioxidant Liposomes on *Bacillus anthracis* – Macrophage Interactions."

@ *Arp: a Bacillus anthracis transcription regulator*. U54 AI57168, NIH, Mid-Atlantic Regional Center of Excellence in Biodefense and Emerging Infectious Diseases (MARCE), Myron Levine M.D., PI. Rest PI, supplementary funds, at 5% effort. 2007-2008, $35,000.

@ *PDAG: a naturally occurring regulator of inflammation.* TherimuneX Pharmaceuticals, Inc – Drexel University College of Medicine Collaborative. Rest, PI at 25% effort. 10/07 – 9/08, $400,000 direct.

@ The antibacterial activity of Abthrax. Human Genome Sciences, Inc. Rest, PI at 10% effort. 7/08-6/09, $45,000.

@ Efficacy of PDAG in *Salmonella typhimurium* infection of mice. TherimuneX Pharmaceuticals, Inc. Rest, PI, 5% effort, 10/08 – 9/09, $40,000.

Anthrolysin O and Phagocytes. 1 R21 AI073827-01A1, NIH, Rest PI at 15% effort, in revision

Arp: a Bacillus anthracis transcription regulator. 1 R01 AI074999-01A1, NIH. Rest, PI at 25% effort; Daniel Simon, co-I at 25% effort, collaboration with Virginia Bioinformatics Institute, Virginia Tech. in revision

PUBLICATIONS

PRIMARY, PEER-REVIEWED

Rest, R.F. and D.C. Robertson. 1974. Glucose transport in *Brucella abortus.* J. Bacteriol. 118:250-258.

Rest, R.F. and D.C. Robertson. 1975. Characterization of the electron transport system in *Brucella abortus*. J. Bacteriol. 122:139-144.

Rest, R.F. and J.K. Spitznagel. 1977. Subcellular distribution of superoxide dismutases in human neutrophils. Influence of myeloperoxidase on the measurement of superoxide dismutase activity. Bioch. J. 166:145-153.

Rest, R.F., M.H. Cooney, and J.K. Spitznagel. 1977. Susceptibility of lipopolysaccharide mutants to the bactericidal action of human neutrophil lysosomal fractions. Infect. Immun. 16:145-151.

Rest, R.F. and J.K. Spitznagel. 1978. The myeloperoxidase/Cl-/H2O2 bactericidal system. Effect of bacterial membrane structure and growth conditions. Infect. Immun. 19:1110-1112.

Rest, R.F., M.H. Cooney, and J.K. Spitznagel. 1978. Bactericidal activity of specific and azurophil granule contents from human neutrophils. Studies with outer membrane mutants of *Salmonella typhimurium* LT-2. Infect. Immun. 19:131-137.

Rest, R.F., M.H. Cooney, and J.K. Spitznagel. 1978. Subcellular distribution of various glycosidases in human polymorphonuclear leukocytes. Bioch. J. 174:53-59.

Rest, R.F. 1979. Killing of *Neisseria gonorrhoeae* by human polymorphonuclear neutrophil granule extracts. Infect. Immun. 25:574-579.

Buck, P. and **R.F. Rest**. 1981. Effects of human neutrophil granule extracts on macromolecular synthesis in *Neisseria gonorrhoeae*. Infect. Immun. 33:426-433.

Rest, R.F. and E. Pretzer. 1981. Degradation of outer membrane proteins of *Neisseria gonorrhoeae* by human neutrophil lysosomal enzymes. Infect. Immun. 34:62-68.

Rest, R.F., S.H. Fischer, Z.Z. Ingham, and J.F. Jones. 1982. Interactions of *Neisseria gonorrhoeae* with human neutrophils: Effects of serum and gonococcal opacity on killing and chemiluminescence. Infect. Immun. 36:737-744.

Mezzatesta, J.R., and **R.F. Rest.** 1983. Interactions of *Neisseria gonorrhoeae* with human mononuclear phagocytes. Infect. Immun. 42:99-105.

Eaton, L.J., and **R.F. Rest**. 1983. Degradation of gonococcal outer membrane proteins within phagolysosomes of phagocytizing human neutrophils. Infect. Immun. 42:1034-1040.

Speer, C.P., M.J. Pabst, H.B. Hedegaard, **R.F. Rest**, and R.B. Johnston, Jr. 1984. Enhanced release of oxygen metabolites by monocyte-derived macrophages exposed to proteolytic enzymes: Activity of neutrophil elastase and cathepsin G. J. Immun. 133: 2151-2156.

Rest, R.F., N. Lee, and C. Bowden. 1985. Stimulation of human leukocytes by P.II+ gonococci is mediated by lectin-like gonococcal components. Infect. Immun. 50:116-122.

Striker, R., M.E. Kline, R.A. Haak, **R.F. Rest**, and R. S. Rosenthal. 1987. Degradation of gonococcal peptidoglycan by granule extract from human neutrophils: demonstration of N-acetyl-glucosaminidase activity that utilizes peptidoglycan substrates. Infect. Immun. 55:2579-84.

Rest, R.F., C. Farrell, and F. Naids. 1988. Mannose inhibits the human polymorphonuclear neutrophil oxidative burst. J. Leukocyte Biol. 43:158-164.

Rock, J., and **R. F. Rest.** 1988. Rapid damage to membranes of *Neisseria gonorrhoeae* caused by human neutrophil granule extracts. J. Gen. Microbiol. 134:509-519.

Fischer, S.H., and **R. F. Rest**. 1988. Gonococci possessing only certain P.II outer membrane proteins interact with human neutrophils. Infect. Immun. 56:1574-1579.

Elkins, C., and **R. F. Rest**. 1990. Monoclonal antibodies to outer membrane protein PII block interactions of *Neisseria gonorrhoeae* with human neutrophils. Infect. Immun. 58:1078-1084.

Farrell, C., and **R. F. Rest**. 1990. Up-regulation of human neutrophil receptors for *Neisseria gonorrhoeae* expressing PII outer membrane proteins. Infect. Immun. 58:2777-2784.

Blomfield, I. C., V. Vaughn, **R. F. Rest**, and B. I. Eisenstein. 1991. Allelic exchange in *Escherichia coli* using *Bacillus subtilis* sac B gene and a temperature-sensitive pSC101 replicon. Molec. Microbiol. 5:1447-1458.

Naids, F. and **R. F. Rest**. 1991. Stimulation of human neutrophil oxidative metabolism by nonopsonized *Neisseria gonorrhoeae*. Infect. Immun. 59:4383-4390.

Naids, F., B. Belisle, N. Lee and **R. F. Rest**. 1991. Interactions of *Neisseria gonorrhoeae* with human neutrophils. Studies with purified PII (Opa) outer membrane proteins and synthetic Opa peptides. Infect. Immun. 59:4628-4635.

R. F. Rest and J. Frangipane. 1992. Growth of *Neisseria gonorrhoeae* in cytidine-3'-monophosphate-N-acetyl neuraminic acid (CMP-NANA) inhibits their nonopsonic (Opa-mediated) association with human neutrophils. Infect. Immun. 60:989-997.

Frangipane, J.V. and **R. F. Rest**. 1992. Anaerobic growth does not affect Opa-mediated (nonopsonic) association of *Neisseria gonorrhoeae* with human neutrophils. Infect. Immun. 60:1793-1799.

Simon, D. and **R. F. Rest**. 1992. *Escherichia coli* expressing a *Neisseria gonorrhoeae* opacity associated (Opa) outer membrane protein invade human cervical and endometrial epithelial cell lines. P.N.A.S. (USA) 89:55112-55116.

Frangipane, J. and **R. F. Rest**. 1993. Anaerobiosis and cytidine-3'-monophosphate-N-acetyl neuraminic acid (CMP-NANA) act synergistically to induce high level resistance to normal human serum by *Neisseria gonorrhoeae*. Infect. Immun. 61:1657-1666.

McGee, D., and **R. F. Rest**. 1996. Regulation of gonococcal sialyltransferase, lipooligosaccharide and serum resistance by glucose, pyruvate and lactate. Infect. Immun. 64:4630-4637.

McGee, D., and **R. F. Rest**. 1996. Expression of sialyltransferase is not required for interaction of *Neisseria gonorrhoeae* with human epithelial cells and human neutrophils. Infect. Immun. 64:4129-4136.

Williams, J.M., L. Zhu, G.-C. Chen and **R. F. Rest**. 1998. Using the yeast two-hybrid system to identify human epithelial cell proteins that bind gonococcal Opa proteins: Intracellular gonococci bind pyruvate kinase via their Opa proteins and require host pyruvate for growth. Molec Microbiol, 27:171-186.

Hood, D. W., K. Makepeace, M. E. Deadman, **R. F. Rest**, P. Thibault, A. Martin, J. C. Richards, & E. R. Moxon. 1999. Sialic acid in the lipopolysaccharide of *Haemophilus influenzae*: strain distribution, influence on serum resistance and structural characterization. Molec. Microbiol. 33:679-692.

Liu, S. V., N. J. Saunders, A. Jeffries and **R. F. Rest**. 2002. Genome analysis and strain comparison of Correia repeats and Correia Repeat-Enclosed Elements (CREE) in pathogenic neisseria. J. Bacteriology, 184:6163-6173.

Shell, D., D. Chiles, R. Judd, S. Seal and **R. F. Rest**. 2002. Outer membrane localization of sialyltransferase in the pathogenic *Neisseria*. Infect Immun 70:3744-3751.

J. G. Shannon, C. L. Ross, T. M. Koehler and **R. F. Rest.** 2003. Characterization of Anthrolysin O, the *Bacillus anthracis* Cholesterol-Dependent Cytolysin. Infect. Immun. 71:3183-3189.

Park, J. M., V. H. Ng, **R. F. Rest**, S. Maeda and M. Karin. 2004. Anthrolysin O and other Gram-positive cytolysins are Toll-like receptor 4 agonists. J. Exp Med 200:1647-1655.

Packiam, M., D. Shell, D., S. V. Liu, Y.B. Liu, D. J. McGee, R. Srivastava, S. Seal and **R. F. Rest**. 2006. Differential expression and transcriptional analysis of the α-2,3-sialyltransferase gene in pathogenic *Neisseria*. Infect. Immun. 74:2637-2650.

Cocklin, S., M. Jost, N. M. Robertson, S. D. Weeks, H.-W. Weber, E. Young, S. Seal, M. Zhang, P. J. Loll, A. J. Saunders, **R. F Rest,** and I. M. Chaiken. 2006. Real-time monitoring of the membrane-binding and insertion properties of the cholesterol-dependent cytolysin Anthrolysin O from *Bacillus anthracis*. J Molec Recognition 19: 354-362.

Mosser, E. M. and **R. F. Rest**. 2006. The *Bacillus anthracis* cholesterol-dependent cytolysin, Anthrolysin O, kills human neutrophils, monocytes and macrophages. BMC Microbiology, 6:56.

Gogotsi, Y, R. K. Dash, G. Yushin, B. E. Carroll, S. R. Altork, S. Sassi-Gaha and **R. F. Rest**. 2007. Bactericidal activity of chlorine-loaded carbide-derived carbon against *Escherichia coli* and *Bacillus anthracis*. J Biomed Materials Res: Part A, 84:607-613.

McGovern, J.-P., W. Y. Shih, **R. F. Rest**, M. Purohit, Y. Pandya, and W.-H. Shih. 2008. Label-Free Flow-Enhanced Specific Detection of *Bacillus anthracis* Using a Piezoelectric Microcantilever Sensor. The Analyst. 133:649-654.

Viator, R. J., **R. F. Rest**, E. Hildebrandt and D. J. McGee. 2008. Characterization of *Bacillus anthracis* arginase: effects of pH, temperature, and cell viability on metal preference. BMC Biochemistry 9:15

McGovern, J-P, W. Y. Shih, M. Mattiucci, **R. F. Rest**, M. Purohit, K. Pourrezaei, B. Onaral, and W-H Shih. 2008. Array PZT/Glass Piezoelectric Microcantilevers for real-time detection of *Bacillus anthracis* with 10 spores/ml sensitivity and 1/1000 selectivity in bacterial mixtures. The Analyst. in press

Nakouzi, A., J. Rivera, **R. F. Rest** and A. Casadevall. 2008. Passive administration of monoclonal antibodies to Anthrolysin O prolong survival in mice lethally infected with *Bacillus anthracis*. BMC Microbiology. In press.

SUBMITTED

W. Wang, G. Jung, T. Nguyen, P. Ruchala, Y. O. Luyang, E. J. Gillespie, K. A. Bradley, A. J. Ratner, **R. F. Rest**, W. Lu, and R. I. Lehrer. 2008. Inactivation of cholesterol-dependent cytolysins by human β-defensins. submitted

Bourdeau, R. W., E. Malito, A. Chenal, M. W. Musch, M. Villereal, E. B. Chang, E. M. Mosser, **R. F. Rest**, R. K. Tweten, and W.-J. Tang. 2008. Cellular functions and pre-pore structure of Anthrolysin O. submitted

M. Purohit, S. Sassi-Gaha and **R.F. Rest**. 2008. Rapid sporulation of *Bacillus anthracis*. submitted

IN PREPARATION

Shannon, J. F, S. R. Altork, J. Dobrowolski, R. Srivastava, **R. F. Rest**. Characterization of binding of gonococcal Opa proteins to TRIP6 within human cells.

Mosser, E. M., Y. Pandya, **R. F. Rest**. 2008. Effects of the *Bacillus anthracis* toxin Anthrolysin O (ALO) on human neutrophil and macrophage cell signaling.

Mosser, E. M., **R. F. Rest**, O. Crasta, S. Mohapatra, C. Evans, B. Sobral, D. J. Simon. 2008. Anthrolysin Regulatory Protein 1 (Arp1): a unique, global transcription regulator in the *Bacillus cereus* group.

Simon, D., E. Mosser, **R. F. Rest**. 2008. Anthrolysin Regulatory Protein genes 1 and 2 (a*rp1* and *arp2*) are responsible for several phenotypes in *Bacillus anthracis*.

Purohit, M., S. Sassi-Gaha, **R. F. Rest**. 2008. The role of proteases in post-translational modification of *Bacillus anthracis* Anthrolysin O.

Books, Book Chapters, Proceedings, Reviews, Etc.

Rest, R.F. 1974. Dissertation: Metabolite transport and the electron transport system in *Brucella abortus*.

Buck, P. and **R.F. Rest**. 1980. Differential inhibition of colony formation and macromolecular synthesis in *Neisseria gonorrhoeae* by human neutrophil lysosomal contents. In: Proceedings of the EMBO Workshop on Genetics and Immunology of Pathogenic Neisseria, pp. 247-250, Hemavan, Sweden (S. Normark and D. Danielsson, eds).

Johnston, R.B., Jr., M.J. Pabst, C.P. Speer, H.B. Hedegaard, **R.F. Rest** and S.M. Bryant. 1984. In: Mononuclear Phagocytes in Inflammation. R. van Furth, editor. Martinus Nijhof, The Hague.

Rest, R.F., N. Lee, and C. Bowden. 1985. Stimulation of human leukocyte oxidative metabolism by P.II+ gonococci is mediated by lectin like gonococcal surface components, p. 495-501. In G. Schoolnick, (ed), The Pathogenic Neisseria: Proceedings of the Fourth International Symposium. American Society for Microbiology, Washington.

Rock, J.P., and **R.F. Rest**. 1985. Effect of human neutrophil lysosomal contents on peptidoglycan turnover and membrane structure in *Neisseria gonorrhoeae*, p. 344-351. In G. Schoolnick, (ed.), The Pathogenic Neisseria: Proceedings of the Fourth Inter-national Symposium. American Society for Microbiology, Washington.

Elkins, C., C. Wilde, C. Farrell, and **R.F. Rest**. 1988. The role of P.II outer membrane proteins in gonococcus - host cell interactions, pp699-702. In J. T. Poolman et al (Eds), Gonococci and Meningococci. Kluwar Academic Publishers, Dordrecht, Netherlands.

E.L. Thomas, R.I. Lehrer, and **R.F. Rest**. 1988. Human neutrophil antimicrobial activity. Proceedings of a meeting entitled "Microbial Surfaces: Determinants of Virulence and Host Responsiveness". Rev. Infect. Dis. 10:S450-S456.

Rest, R.F. 1988. Chapter 28, Human neutrophil and mast cell proteases implicated in inflammation. IN Meth. in Enzym., Volume 163, Chemotaxis and Inflammation, Part M, G. DiSabato, ed, Academic Press, New York.

Rest, R.F. and W.M. Shafer. 1989. Interaction of *Neisseria gonorrhoeae* with human neutrophils. Clin. Microbiol. Rev. 2:S83-S91.

Shafer, W.M. and **R.F. Rest**. 1989. Interaction of gonococci with phagocytic cells. Annual Rev. Microbiol. 43:121-145.

Farrell, C.F., F.L. Naids and **R.F. Rest**. 1991. Identification of a human neutrophil receptor for gonococcal outer membrane protein PII, pp 579-584. IN "Neisseriae 1990," eds, M Achtman, et al, Walter de Gruyter, publishers, Berlin.

Cassell, G.H., L.A. Miller, and **R.F. Rest**. 1992. Biological warfare: role of biological societies. IN "The Microbiologist and Biological Defense Research: Ethics, Politics and International Security," ed, R. A. Zilinskas. Ann. N. Y. Acad. Sci. 666:230-238.

I. Ofek, **R.F. Rest** and N. Sharon. 1992. Nonopsonic phagocytosis of microorganisms. Phagocytes use several molecular mechanisms to recognize, bind, and eventually kill microorganisms. ASM News 58:429-435.

Rest. R.F. and D. P. Speert. 1994. Chapter 8, Measurement of Nonopsonic Phagocytic Killing by Human and Mouse Phagocytes. IN Meth. Enzym., Volume 236, *Bacterial Pathogenesis,* Part B, Interaction of Pathogenic Bacteria with Host Cells, V.L. Clark and P.M. Bavoil, eds, Academic Press, New York.

Rest, R.F. 1994. Chapter 10, Measurement of the Human Neutrophil Respiratory Burst during Phagocytosis and Killing of Bacteria. IN Meth. Enzym., Volume 236, *Bacterial Pathogenesis*, Part B, Interaction of Pathogenic Bacteria with Host Cells, V. L. Clark and P. M. Bavoil, eds, Academic Press, New York.

Rest, R.F., J. Liu, R. Talukdar, J. V. Frangipane and D. Simon. 1994. "Interaction of Pathogenic *Neisseria* with host defenses: what happens *in vivo*?" IN Microbial Pathogenesis and Immune Response, eds., E. Ades, S. Morse & **R. Rest**, Ann. N. Y. Acad. Sci. 730:182-196.

G. Gorby, D. Simon and **R.F. Rest**. 1994. *Escherichia coli* that express *Neisseria gonorrhoeae* Opacity-associated proteins attach to and invade human fallopian tube epithelium, IN Microbial Pathogenesis and Immune Response , eds., E. Ades, S. Morse & **R. Rest**, Ann. N. Y. Acad. Sci. 730: 286-289.

E.W. Ades, **R.F. Rest**, and S.A. Morse, eds. 1994. Microbial Pathogenesis and Immune Response. Ann. N.Y.A.S. vol. 730.

J.V. Frangipane and **R.F. Rest**. 1994. Anaerobic growth induces increased gonococcal sialyltransferase activity and acts synergistically with CMP-NANA to increase gonococcal serum resistance, IN Pathobiology and

Immunobiology of *Neisseriaceae*, Proceedings of the VIIIth International Pathogenic *Neisseria* conference. C.J. Conde-Glez, S.A. Morse, P. Rice, P.F. Sparling and E. Calderon, eds. INSP, Mexico.

Simon, D.J.J., S.T. Hingley and **R.F. Rest**. 1994. Interaction with human epithelial cell lines and neutrophils of *Escherichia coli* expressing gonococcal Opa proteins, IN Pathobiology and Immunobiology of *Neisseriaceae*, Proceedings of the VIIIth International Pathogenic *Neisseria* conference. C.J. Conde-Glez, S.A. Morse, P. Rice, P.F. Sparling and E. Calderon, eds. INSP, Mexico.

Rest, R.F. 1995. Chapter 2. Association of Bacteria with Phagocytic Cells. IN Methods in Enzymology, Volume 253, *Adhesion of Microbial Pathogens*, R. J. Doyle and I. Ofek, eds, Academic Press, New York.

Rest, R.F. and R.E. Mandrell. 1995. Neisseria sialyltransferases and their role in pathogenesis. Microbial Pathogenesis, 19:379-390.

Ades, E.W., **R.F. Rest**, and S.A. Morse, eds. 1996. Microbial Pathogenesis and Immune Response II. Ann. N.Y.A.S. vol. 797.

Simon, D., J. T. Liu, M. S. Blake, C. R. Blake and **R. F. Rest**. 1996. Structure-function studies with *Neisseria gonorrhoeae* Opa outer membrane proteins expressed in *Escherichia coli*. Annals N. Y. Acad. Sci 797:253-254.

Williams, J. M. and **R. F. Rest.** 1996. Cytoplasmic proteins involved in thyroid hormone response also bind *Neisseria gonorrhoeae* Opa outer membrane proteins. Annals N. Y. Acad. Sci. 797:288-289.

Jerse, A., and **R.F. Rest**. 1997. Adhesion and invasion by the pathogenic neisseria. Trends in Microbiol 5:217-221.

Rest. R.F. and D. P. Speert. 1997. Measurement of Nonopsonic Phagocytic Killing by Human and Mouse Phagocytes. IN *Bacterial Pathogenesis: selected Methods in Enzymology*, V.L. Clark and P.M. Bavoil, eds, Academic Press, New York.

Rest, R.F. 1997. Measurement of the Human Neutrophil Respiratory Burst during Phagocytosis and Killing of Bacteria. IN *Bacterial Pathogenesis: selected Methods in Enzymology*, V. L. Clark and P. M. Bavoil, eds, Academic Press, New York.

Rest, R.F. 2008. Regulation of gene expression leading to resistance to immune response by the pathogenic neisseria. In preparation

ABSTRACTS AND INVITED TALKS

I attend three or four international meetings annually at which I, or more often one of my laboratory personnel, present data. I present invited talks at international meetings once or twice a year. I do not keep formal records of such activities.

PATENT APPLICATIONS

1. Compositions and Methods for Activating Toll-like Receptor 4, 2004
2. Compositions and Methods for Preventing and Treating Anthrax Disease, 2004
3. Chlorine-Loaded Carbide-Derived Carbon with Bactericidal Properties, 2005
4. Regulation of Expression of Anthrolysin O: The *Bacillus anthracis* Cholesterol Dependent Cytolysin, 2006
5. Regulation of Gene Expression by *Bacillus anthracis* Arp, 2007
6. Titania deposited electrospun nanofibrous materials preparation method for advanced filtration systems, 2008

MARIANA ESTRELLA BERNUI

Address: 5555 Wissahickon Ave, Apt. 1001, Philadelphia – PA 19144
Phone: (215)991-8366
Mobile: (215)280-0273
E-mail: mb3532@drexel.edu

EDUCATION

August 1996 – December 1998	**Randolph-Macon Woman´s College (Lynchburg, VA)** GPA : 3.8
March 1999 – December 2002	**Universidad Peruana Cayetano Heredia (Lima, Peru)** Bachelor of Science Major : Biology Ranking : 7th place out of 81
July 2004 – present	**Drexel University College of Medicine (Philadelphia, PA)** Biomedical Graduate Program Microbiology and Immunology Department P.I. Dr. Richard F. Rest

RESEARCH EXPERIENCE

Graduate Student, Drexel University College of Medicine, Department of Microbiology and Immunology, August 2004 – present

Examine the effect of antioxidants on *Bacillus anthracis* infection in vitro.
Determine the effect of antioxidants on the cellular alterations caused by a newly characterized anthracis pore forming toxin, Anthrolysin O (ALO).

Research Assistant, Universidad Peruana Cayetano Heredia, Institute of Tropical Diseases Alexander von Humboldt, January 2002 – July 2004

Evaluate the oxidative stress in blood monocytes and neutrophils of Vitamin A-deficient mice
Investigate the effects of Vitamin A deficiency on murine peritoneal monocytes and neutrophils in an *in vivo* murine model
Study the interaction between Vitamin A deficiency (i.e. anemia) and *Leishmania* infection on murine peritoneal monocytes and neutrophils in an *in vivo* murine model

TEACHING EXPERIENCE

Graduate Student, Drexel University College of Medicine, Department of Microbiology and Immunology, January 2006-present

Trained 3 new lab members as well as 2 rotating graduate students and 2 medical students on techniques such as Westerns, in vitro infection assays, chemotaxis and neutrophil degranulation assays, etc.

Course Coordinator, Universidad Peruana Cayetano Heredia, Psychology Department, March 2004 – July 2004: English for Psychologists, Designed the syllabus and curriculum of the course; Prepared and taught every lesson; Evaluated students
Teaching assistant, Universidad Peruana Cayetano Heredia, Biology Department: Human Parasitology, March – July 2002, In charge of two lectures per month, Evaluated students; General Parasitology Laboratory, March – December 2001, Taught the theoretical and practical lessons of the Practical course, Helped structure the course curriculum, Evaluated students; Neuroscience Laboratory, July – December 1999, In charge of the practical exercises, Help evaluate the students.

Teaching assistant, Universidad Peruana Cayetano Heredia, Medical Technology Department: Equipment and Instrumentation, August – December 2002, Lectures on Microbiological techniques
English teacher, Instituto Cultural Peruano Norteamericano: Basic, Intermediate, and Children levels, January 2000 – August 2001, July 2002 – March 2004, Taught and evaluated 100 adult students daily (25 per class), ages 15 to 50, Taught 30 children (10 per class) from the ages 6 to 14 on the Saturday Program

HONORS AND AWARDS

International Student Representative, Student Government Association of the Biomedical Graduate Program, Drexel University College of Medicine , June 2008-present

Abstract chosen for Oral Presentation, 17th Annual Infection and Immunity Forum, May 9th, 2008

Abstract chosen for Oral Presentation, 6th Annual ASM Biodefense and Emerging Diseases Research Meeting, February 24-27, 2008

Student Travel Award, 6th Annual ASM Biodefense and Emerging Diseases Research Meeting, February 24-27, 2008

Judge for undergraduate/high school posters, Drexel University College of Medicine's Discovery Day, October 3rd, 2007

Graduated with honors, Universidad Peruana Cayetano Heredia, May 2001

Team 1 – NCAA Division II Women's Basketball, Randolph-Macon Women's College, 1998-1999

PROFESSIONAL ASSOCIATIONS:

American Society of Microbiology, 2005-current

Student Chapter of the Eastern Pennsylvania Branch of American Society of Microbiology

Secretary, June 2006 – June 2007

Treasurer, June 2007 – June 2008

MEETINGS ATTENDED:

ASM General Meeting, Boston MA (June 1-5, 2008)

6th Annual ASM Biodefense and Emerging Diseases Research Meeting, Baltimore MD (February 24-27, 2008)

Biodefense Research Conference 2007, Philadelphia PA (November 5-7, 2007)

Biotech 2007, Philadelphia PA (October 9-10, 2007)

Mid-Atlantic Regional Center of Excellence for Biodefense and Emerging Infectious Diseases, Ellicot City MD (October 7-8, 2007, May 10-12, 2007, October 16-17, 200,6, June 7-8, 2006, May 12-13, 2005)

Department of Defense Consortium Meeting, Washington DC (June 4-6 2007)

Mid-Atlantic Regional Center of Excellence of Biodefense and Emerging Infectious Diseases-Anthrax project meeting, USUHS, Bethesda MD, (April 11, 2005)

TRAINING:

BSL-3 Laboratory Safety Course, University of Maryland School of Medicine, Baltimore MD, February 9-11, 2004

PRESENTATIONS:

ASM General Meeting, June 1-5, 2008

N-acetylcysteine (NAC) or STIMAL (liposome-encapsulated NAC) inhibit germination of *Bacillus anthracis* spores (Poster) **M. Bernui, M. Smith, W. Stone, R. Rest**

17th Annual Infection and Immunity Forum, May 9th, 2008

N-acetylcysteine (NAC) and STIMAL® (liposome-encapsulated NAC) impair germination of *Bacillus anthracis* spores and increase the ability of macrophages to limit anthrax growth *in vitro* **(Oral) M. Bernui, M. Smith, W. Stone, R. Rest**

The *Bacillus anthracis* toxin Anthrolysin O stimulates macrophages through multiple pathways (Poster) M. Wynosky, M. Bernui, E.M. Mosser, R. Rest

Research Day, April 22nd, 2008

N-acetylcysteine (NAC) and STIMAL® (liposome-encapsulated NAC) impair germination of Bacillus anthracis spores (Poster**) M. Bernui, M. Smith, W. Stone, R. Rest**

The *Bacillus anthracis* toxin Anthrolysin O stimulates macrophages through multiple pathways (Poster) M. Wynosky, M. Bernui, E.M. Mosser, R. Rest

6th Annual ASM Biodefense and Emerging Diseases Research Meeting, February 24-27, 2008

N-acetylcysteine (NAC) or STIMAL (encapsulated NAC) Increase the Ability of Human Macrophages to Kill *Bacillus anthracis* **(Oral) M. Bernui, M. Smith, W. Stone, R. Rest**

Biodefense Research Conference 2007, November 5-7, 2007

STIMAL (Liposome-Encapsulated N-Acetylcysteine) Increases the Ability of Human Macrophages to Kill *Bacillus anthracis* (Poster) **M. Bernui, M. Smith, W. Stone, R. Rest**

Discovery 2007, October 3rd, 2007

The effects of antioxidants on the interaction of *Bacillus anthracis* with macrophages (Poster) **M. Bernui, E.M. Mosser, R. Rest**

The effects of N-acetylcysteine and Anthrolysin O on phagocyte chemotaxis (Poster) M. Wynosky, M. Bernui, E.M. Mosser, R. Rest

Biotech 2007, October 9-10, 2007

STIMAL (Liposome-Encapsulated N-Acetylcysteine) increases the ability of human macrophages to kill *Bacillus anthracis* (Poster) **M. Bernui, M. Smith, W. Stone, R. Rest**

***Bacillus anthracis* International Meeting (ACT)**, June 17-21, 2007

N-acetylcysteine reverses Anthrolysin O inhibition of human neutrophil chemotaxis and degranulation (Poster) M. Bernui, E.M. Mosser, R. Rest

The effects of antioxidants on the interaction of *Bacillus anthracis* with macrophages (Poster) **M. Bernui, R. Rest**

Anthrolysin O modulates human neutrophils and macrophage chemotaxis and degranulation (Poster) E. Mosser, M. Bernui, R. Rest

16th Annual Infection and Immunity Forum (sponsored by the Eastern PA branch of the American Society for Microbiology), May 11th, 2007

The effects of antioxidants on the interaction of *Bacillus anthracis* with macrophages (Poster) **M. Bernui, E.M. Mosser, R. Rest**

Discovery Day, October 11th, 2006

N-acetylcysteine reverses the effects of Anthrolysin O on human granulocyte chemotaxis and protects macrophages from *B. anthracis* infection (Poster) M. Bernui, E. M. Mosser, Y. Pandya, and R. Rest

Mechanisms of Anthrolysin O Modulation of Human Neutrophil Chemotaxis and Degranulation (Poster**)** E. M. Mosser, M. Bernui, Y. Pandya, R. F. Rest

15th Annual Infection and Immunity Forum (sponsored by the Eastern PA branch of the American Society for Microbiology), June 23, 2006

N-acetylcysteine reverses Anthrolysin O inhibition of human neutrophil chemotaxis and degranulation (Poster) M. Bernui, E. M. Mosser, Y, Pandya, and R. Rest

Mechanisms of Anthrolysin O Modulation of Human Neutrophil Chemotaxis and Degranulation (Poster**)** Elise M. Mosser, Mariana Bernui, Yognandan Pandya, Russel Salter, Simon Watkins, Richard Rest

Drexel University Annual Research Day, April 25, 2006.

Anthrolysin O, the *Bacillus anthracis* cholesterol dependent cytolysin, modulates human neutrophil and macrophage function via TLR-4 dependent and independent mechanisms (Poster) E. Mosser, Y. Pandya, M. Bernui, R. Salter, S. Watkins, and R. Rest

Discovery Day, October 6, 2005

The effect of the antioxidant N-acetylcysteine (NAC) and anthrolysin O on Neutrophil function (Poster) M. Bernui, E. Mosser, Y. Pandya, R. Rest

Discovery Day, October 6, 2004

Differential expression of alpha-2,3-Sialyltransferase of *Neisseria gonorrhoeae* and *Neisseria meningitidis* M. Bernui, D. Pandya, R. Packiam, R. Rest

PUBLICATIONS

Action of the *Bacillus anthracis* cholesterol dependent cytolysin Anthrolysin O on phagocyte function. 2008. E. M. Mosser, Y. Pandya, M. Bernui, R. Rest (Submitted)

N-acetylcysteine inhibits the germination of *Bacillus anthracis* spores. 2008. M. Bernui, W. Stone, M. Smith, R. Rest (In preparation)

The effect of antioxidants in the interaction between *Bacillus anthracis* and macrophages. 2008. M. Bernui, E. Mosser, W. Stone, M. Smith, R. Rest (In preparation)

N-acetylcysteine reverses Anthrolysin O inhibition of human phagocyte chemotaxis and degranulation. 2008. M. Bernui, W. Stone, M. Smith, R. Rest (In preparation)

Table of Contents

Introduction

Sulfur mustard or (bis-2-(chloroethyl) sulfide (military code HD) is a dangerous vesicant and a chemical warfare agent. Inflammation and oxidative stress play key roles in the toxicity of HD and its monofunctional analog 2-chloroethyl-ethyl sulfide (CEES) suggesting that antioxidant liposomes could provide a unique therapeutic strategy [1]. Antioxidant liposomes provide the ability to deliver both nontoxic lipid and water-soluble antioxidants and can thereby provide an effective countermeasure to oxidative stress induced damage caused by HD/CEES. As detailed below, we have found that antioxidant liposomes are effective in preventing CEES damage to **both skin (our work) and lungs (in collaboration with Drs. Ward and Das)** even in a post-exposure situation. In addition, our preliminary data also suggest that antioxidant liposomes can alter the redox status of host cells so as to provide resistance to the growth and invasiveness of a variety of pathogens of military interest. In particular, our *in vitro* studies with Dr. Richard Rest, show that liposomes encapsulated with N-acetyl cysteine (NAC-liposomes) completely inhibit the germination of *B. anthracis* (in the absence of macrophages) and stimulate the ability of macrophages to kill intracellular *B. anthracis* (BA).

Our ongoing molecular studies show that immunostimulators like lipopolysaccaride (LPS), capable of inducing intracellular generation of nitric oxide (NO) and reactive

oxygen species (ROS), greatly enhance CEES toxicity in RAW 264.7 macrophages [2]. Our recent studies show that CEES inhibits NO generation in RAW 264.7 macrophages by down-regulating inducible NO synthase (iNOS) protein expression rather than by inhibiting iNOS activity [3]. The generation of NO by iNOS is known to promote wound healing and the inhibition of iNOS expression could account for the slow wound healing following mustard gas exposure.

Nitric oxide is also known to inhibit mast cell degranulation in various species [4, 5]. Therefore, we hypothesized that CEES, by inducing oxidative stress and potentially decreasing NO production, would promote mast cell degranulation. Mast cell degranulation could release large amounts of TNF-α, IL-1β, and other inflammatory cytokines, which could enhance the toxicity of CEES/HD. Our results to date indicate that *in vitro* exposure of mast cells to CEES does increase mast cell degranulation but does not decrease NO production (in marked contrast to our previous results with RAW 264.7 murine macrophages). Nevertheless, we found that stimulating mast cell degranulation with a Ca^{2+} ionophore does enhance CEES toxicity which is consistent with our original hypothesis.

Proteomics provides a unique opportunity to study CEES/HD induced oxidative stress in biological examples at the detailed molecular level. In our current research, we focused on studying HD/CEES induced oxidative stress related changes in protein expression in various *in vivo* animal and *in vitro* model systems. In particular, we have utilized 2-dimensional gel electrophoresis followed by tandem mass spectrometry to identify the affected proteins. This approach will help define the molecular mechanisms responsible for HD/CEES toxicity and thereby aide in the design of yet more effective countermeasures.

Statement of Work (with summary)

First set of goals require: (1) investigate the effect of CEES on the degranulation of mast cells; (2) determine if CEES inhibits the production of nitric oxide (NO) in mast cells; (3) determine if antioxidant liposomes inhibit mast cell degranulation induced by CEES. The first and second goals are now essentially **completed**.

A second series of goals will focus on utilizing redox proteomics to determine how CEES (or HD/pathogen) treatment influences changes in the levels and distribution of oxidized proteins using either mast cell lines or animal tissue samples obtained from other members of the Consortium. We will also determine the identities and functional significance of the oxidized proteins. The effect of antioxidant liposomes on protein expression and oxidation will be studied in both *in vivo* and *in vitro* model systems with exposed to CEES or HD. This work is **well underway** with all of the underlying methodology now in place (see below)

Our **Specific Goals** are:

Task 1: To determine if mast cell degranulation is induced or inhibited by CEES treatment; and if antioxidant liposomes influence this effect. More specifically we will: (1) investigate the effect of CEES on degranulation/cytokine release of rat basophilic leukemia RBL-2H3 and human HMC-1 mast cell lines; (2) determine if CEES inhibits the production of nitric oxide (NO) in the mast cell lines by use of the cell permeable fluorescent dyes; (3) determine if antioxidant liposomes reduce the effect of CEES on mast cell degranulation.

Task 2: Proteomics of various biological samples exposed to CEES or pathogens will be analyzed by 2-dimensional gel electrophoresis (2D-GE). Oxidized proteins from the 2D-GE gels will be identified using tandem mass spectrometry. Utilizing this proteomics approach we will analyze samples from: (1) the *in vivo* animal models, and (2) *in vitro* cellular studies (mast cell lines and human Epiderm skin samples) exposed and not exposed to CEES/HD. The tissue samples (snap frozen in liquid nitrogen) from the animal models have been obtained from other members of the mustard consortium. In addition, the influence of antioxidant-liposomes on the levels and distribution of oxidized proteins from RBL-2H3 mast cells, HMC-1 mast cells and the human Epiderm skin model (both exposed and not exposed to CEES/HD) will be evaluated by proteomics.

Task 3: Our laboratory has continued to supply well characterized antioxidant-liposomes to all other members of the Research Consortium and provide the analytical methodology and services to measure antioxidant (vitamin E and glutathione) levels in tissues collected from the various animal models used by other members of the mustard consortium. We are continuously improving the stability and effectiveness of the antioxidant liposomes. Our most recent formulations show very long term stability during storage. We are now characterizing lyophilized antioxidant liposomes (in collaboration with Dr. Zach Suntres) which have a very long shelf life.

Body

Specific Tasks 1:

Mast cell degranulation induced by 2-chloroethyl ethyl sulfide (CEES)

The rationale for these mast cell studies is based on our ongoing work with RAW 264.7 macrophages and LPS [3]. LPS is a potent immunostimulator which induces intracellular generation of NO and ROS and greatly enhances CEES toxicity in RAW 264.7 macrophages [2]. Noticing a similarity between the effects Ca-ionophore A23187 and LPS, we hypothesized that CEES could affect NO and/or ROS generation in mast cells.

In particular, we explored the effect of CEES on degranulation in rat RBL-2H3 cells using a colorimetric assay measuring the release of β- hexosaminidase, a component of mast cell granules. Previously, we found that CEES (0.5 to 5 mM) completely inhibited

degranulation induced by Ca-ionophore A23187 (simultaneous treatment). We also found that CEES treatment amplified the toxicity of A23187. This year, we confirmed that lower concentrations of CEES (0.1 and 0.25 mM) also reduce the viability of A23187-treated mast cells (**Fig 1**).

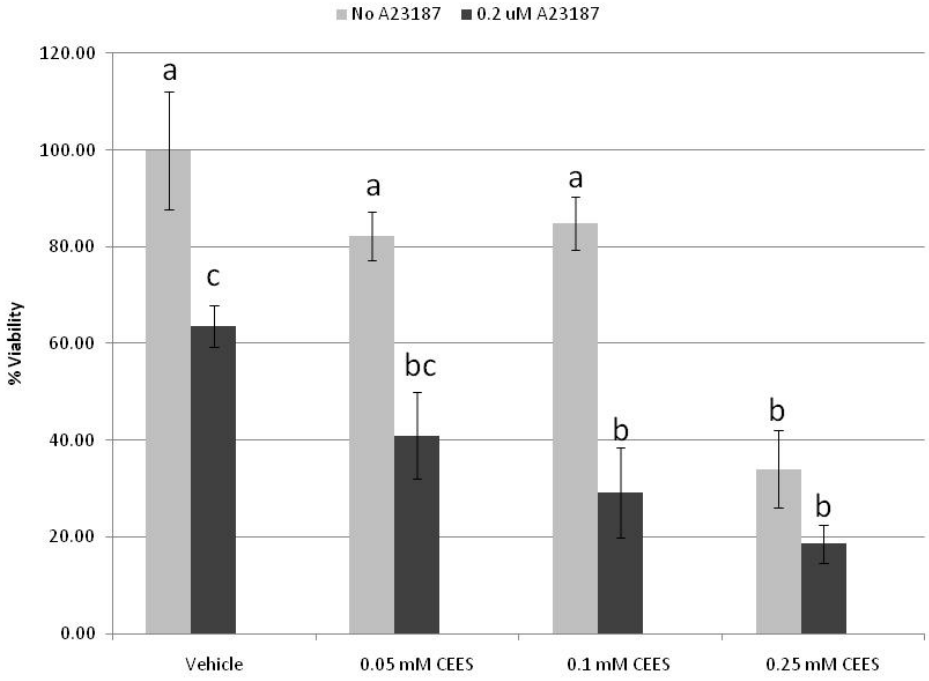

Figure 1: Combined toxic effect of CEES and calcium ionophore A23187. Ca-ionophore A23187 (0.2 μM) was applied to RBL-2H3 cells in the absence or presence of CEES (as indicated). Final concentration of the vehicle (ethanol) was 1.0% (vol/vol). Cell viability was measured by the MTT assay after 24 h incubation. Means not sharing a common letter are significantly different ($P<0.05$).

The data in **Fig 1** support our initial hypothesis that mast cell degranulation (promoted by the Ca-A23187 ionophore) would enhance CEES toxicity.

Since mast cell degranulation is connected to mast cell NO production, we expected that CEES might reduce NO generation in mast cells stimulated with calcium ionophore A23187. We, therefore, initiated studies on the effect of CEES on NO production in mast cell lines by measuring the amount of nitrite accumulation in the cell medium. RBL-2H3 cells stimulated with Ca-ionophore. We found that mast cells release very low NO levels that were barely detectable when measured with Griess reagent. Therefore, it was necessary to use a more sensitive fluorescent substrate, 2,3-diaminonaphthalene (DAN), instead of Griess reagent to detect nitrite in media. Using this more sensitive technique, we found that NO production in RBL-2H3 cells was stimulated with increasing levels of A23187, i.e., 1.25 μM A23187 showed an approximately five-fold increase in NO production compare with 0.5 μM A23187 (see **Fig 2**). CEES did not, however, dramatically alter the levels of nitrite accumulation in marked contrast to the results we

observed with RAW 264.7 macrophages. For the data in Fig 2, we have taken care to normalize the level of NO produced to the level of viable cells.

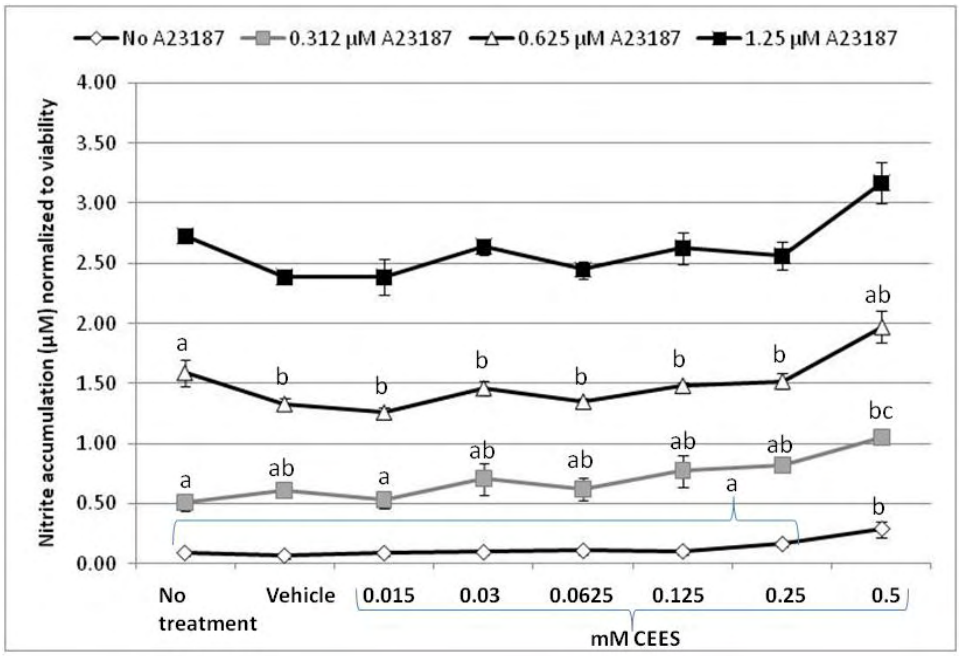

Figure 2: NO generation in RBL-2H3 cells treated with various levels of CEES and stimulated with the calcium ionophore A23187 (as indicated). NO generation was measured as nitrite accumulation in media and normalized to the percentage of viable cells (measured separately by the MTT assay). RBL-2H3 cells were exposed to various levels of CEES (as indicated) in the absence or presence of calcium ionophore A23187 (0 to 1.25 µM) for 22 hours. Nitrite accumulation was measured using the substrate 2,3-diaminonaphthalene. Final concentration of the vehicle (ethanol) was 1.0% (vol/vol). Means not sharing a common letter within a specific A23187 concentration (0, 0.312, 0.625, or 1.25 µM A23187) are significantly different ($P<0.05$).

In the absence of A23187 ionophore, we next found (**see Fig. 3**) that 0.125 mM CEES induced a significant degranulation in RBL-2H3 cells. Although these data are consistent with our initial hypothesis, the experimental data reveal a more complex picture, i.e., CEES at levels greater than 0.125 mM did not promote increased degranulation. Moreover, in the presence of A23187 ionophore, degranulation induced by 0.312 to 0.625 µM A23187 is inhibited at least two-fold when cells are simultaneously treated with 0.5 mM CEES (**Fig. 3**).

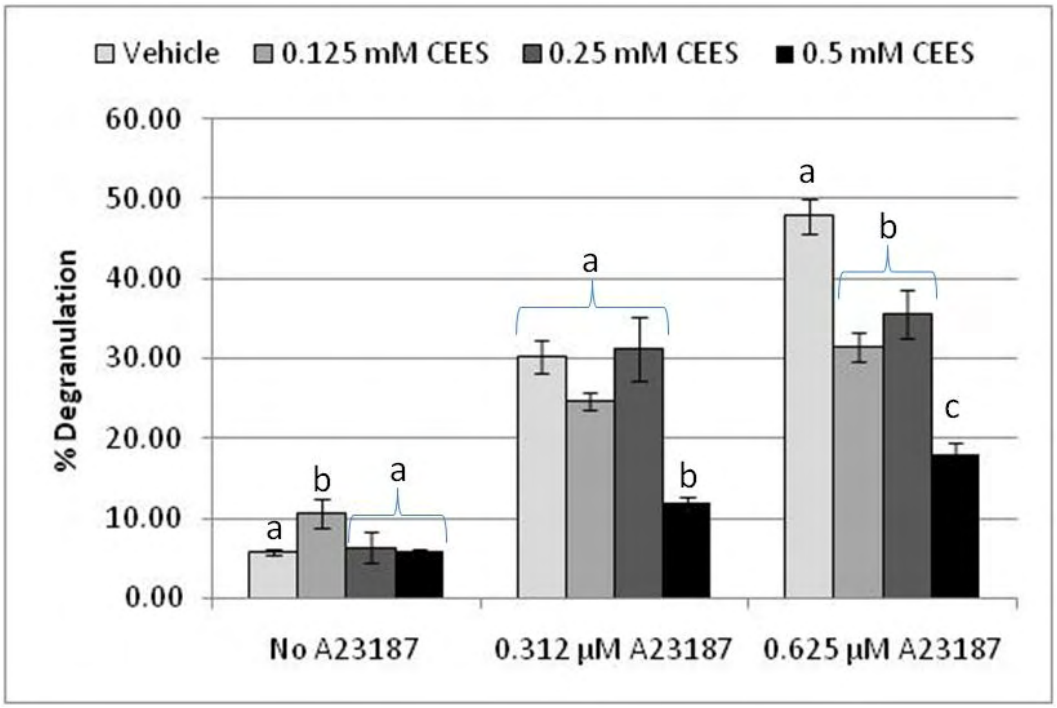

Figure 3: Degranulation of RBL-2H3 cells when simultaneously treated for 1.5 hour with calcium ionophore A23187 (0 to 0.625 µM) **and CEES** (as indicated). Final concentration of the vehicle (ethanol) was 1.0% (vol/vol). A colorimetric assay was used to measure the release (via degranulation) of β-hexosaminidase, one of the major components of mast cell granules. Degranulation percentage was normalized to cell viability. Cell viability was measured by the MTT assay. Means not sharing a common letter within each group of bars (No, 0.312, or 0.625 µM A23187) are significantly different ($P<0.05$).

Specific Tasks 2:

Oxidized proteins (protein carbonyls) will be analyzed by 2-dimensional gel electrophoresis (2D-GE) and identified by mass spectrometry

During 2007, we initiated a series of experiments utilizing proteomic techniques to evaluate differences in protein expression induced by CEES/HD in both *in vivo* and *in vitro* models. We obtained pulmonary tissues samples (stored at -80 ºC) from the USAMRICD for rats exposed to HD (*in vivo*) and treated with antioxidant-liposomes (as well as control samples) after 6 or 24 hours as well as *in vitro* samples from rat mast cells exposed to CEES (as well as control samples). We optimized the 2D-GE separation conditions for rat mast cell samples using narrow range IEF strips (pH 4-7) as well as broad range strips (pH 3-10). We also optimized 2D-GE separation conditions for a number of animal tissue samples treated and not treated with HD.

During 2008, we continued to analyze the rat pulmonary tissues, mast cell samples as well as new Epiderm skin samples (± CEES and ± antioxidant liposomes) utilizing two-dimensional gel electrophoresis (2D-GE).

The Effects of CEES Exposure on Mast Cell Proteomics

We previously reported that RBL-2H3 mast cell viability decreases to 40-20% at CEES concentrations between 0.5 mM – 1.0 mM. In order to study differences in protein expression induced by CEES/HD exposure, we compared the proteomics of non-treated mast cells and cells treated with 0.5 mM CEES. **Fig. 4** shows the 2D-GE separation of cell lysates obtained from non-treated (panel A) or treated (0.5 mM CEES) RBL-2H3 mast cells (panel B). Although we optimized the separation conditions (all the protein spots were sufficiently resolved), we failed to establish equal protein load for the two samples due to some inconsistencies with the measurements of total protein in the cell lysates. We have subsequently discovered that protein concentrations measured with the Quant-iT Protein Assay Kit (Invitrogen) are often erroneous since this assay is interfered by the presence of detergents, urea and thiourea which are present during sample preparation for 2D-GE. We plan to repeat measurement of the total protein in cell lysates using the Bio-Rad RC DC protein assay, a protein assay made specifically to measure protein concentrations in cell lysates prepared for 2D-GE analysis. We then plan to repeat the 2D-GE analyses of the cell lysates loading equal amounts of protein.

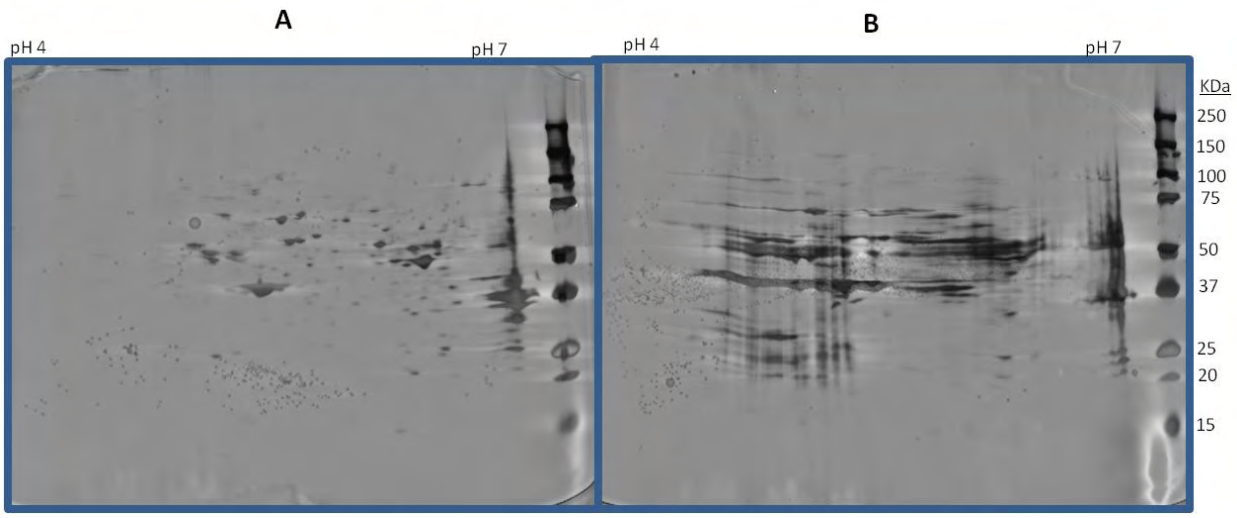

Figure 4: 2D-GE protein separation of cell lysates from RBL-2H3 mast cells exposed to vehicle (A) or 0.5 mM CEES (B). The cells were grown to confluency in 25 cm^2 flasks. Fresh medium containing 0.5 mM CEES or vehicle (1% ethanol) was added. Cell lysates were prepared after 24 hours incubation at 37 C. Lysate samples (approximately 15 µg of total protein) were isoelectrically focused using narrow range (pH 4-7) IEF strips (horizontal separation) and then electrophoresed (vertical separation) using 4-20% SDS PAGE gradient gels. Gels were silver stained. Molecular weights of protein standards are shown on the right.

The Effects of HD Exposure on Rat Lung Proteomics

We also used 2D-GE to analyze rat lung tissue samples (snap frozen in liquid nitrogen) provided by USAMRICD. Prior to lung harvest, these animals had been exposed to CEES or HD and/or treated with antioxidant-liposomes prepared in our laboratory ("Stone" liposomes) or prepared in Dr. Ward's laboratory ("Ward" liposomes) as well as "blank" liposomes containing no antioxidants. We completed the first phase of this study in which we evaluated the potential influence of blank liposomes (not containing any antioxidants) or antioxidant liposome treatment on the levels and distribution of proteins in rat lung tissue.

Fig 5 shows the results from these analyses. Four gels per sample were simultaneously run under identical condition in order to minimize differences resulting from variations in experimental conditions. The replicate gels were aligned by the Dymension-2 software so that consensus spots could be "warped" together. The spots were then detected and 856, 785 and 914 consensus spots were detected in the Blank, Stone and Ward samples respectively. It should be noted that the differences in the number of consensus spots between the different samples does not always mean differences resulting from the different treatments. It can result from differences in the number of permitted absences (spots that are detected even though they are absent in a set number of gels per sample) or the detection of artifacts. The consensus spots from the three samples were then aligned and matched. A total of 819 matching spots resulted. We found no differences in protein expression between the three different treatments, i.e., antioxidant-liposomes do not induce any changes in protein expression compared to blank-liposomes.

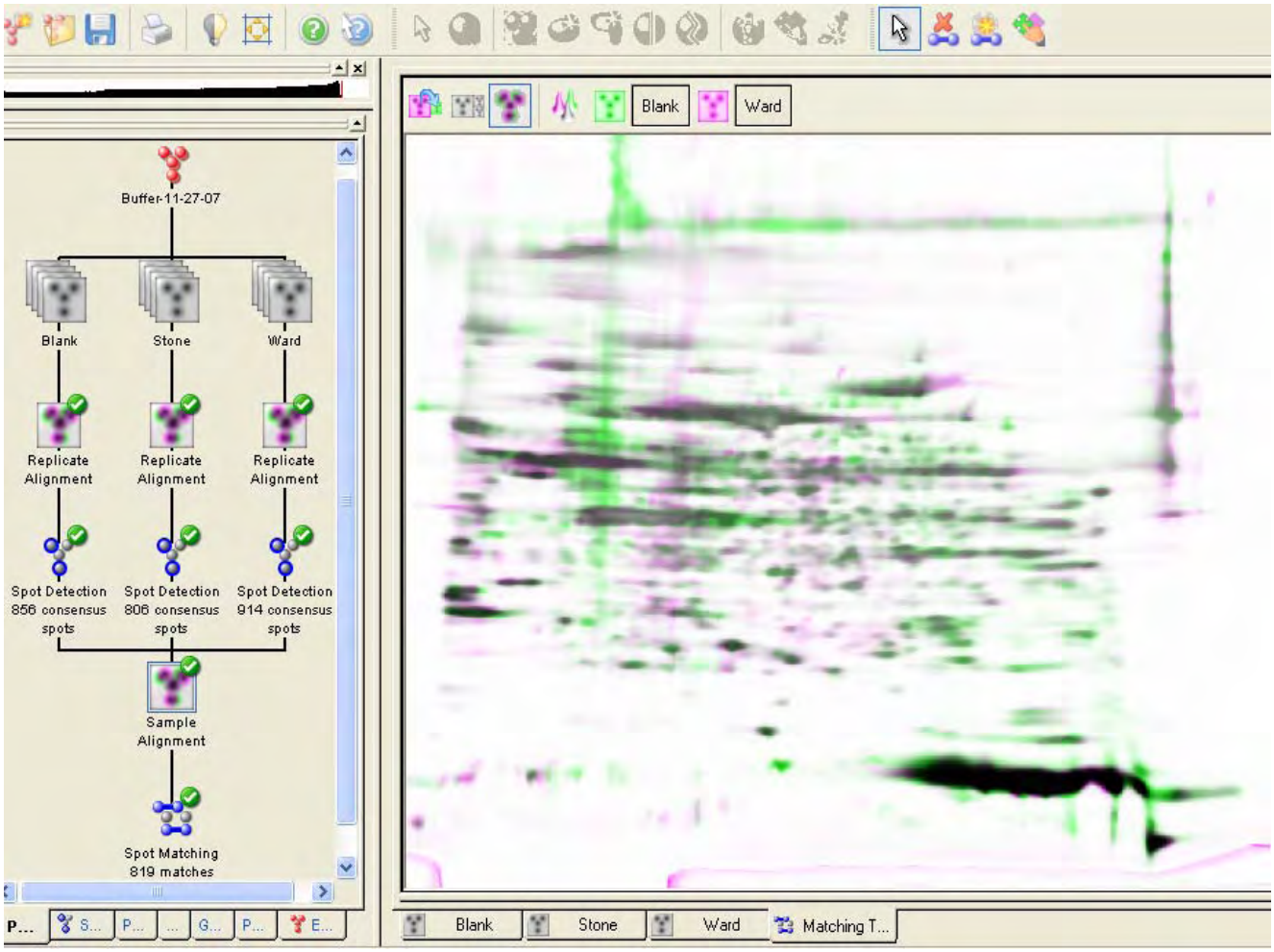

Figure 5: Proteomics Study of the effect of Antioxidant Liposomes in Rat Lung. Frozen tissues samples of rat lungs treated with "Stone" liposomes, "Ward" liposomes or "Blank" liposomes (contain no antioxidants) were obtained from our collaborators. Cell lysates were separated by 2D gel electrophoresis, silver-stained and photographed (three gels per sample). Average differences in protein expression were quantified with Dymension-2 Software. Left panel shows the software sequence for the image comparison and number of consensus spots for each sample and for the final matching. Right panel shows the aligned image for the "Ward" and "Blank" samples ("Stone" sample showed similar result).

Next year, we will analyze (4 samples each group) rat lung tissues untreated with HD/CEES, treated with HD/CEES, untreated plus antioxidant liposomes, and treated with both CEES/HD and antioxidant liposomes. The most affected proteins will be extracted from the gels, trypsinized, and the resulting peptide mixtures analyzed using nanospray LS/MS with our LTQ Linear Ion Trap Mass Spectrometer (Thermo-Fisher). By performing such analyses we will be able to identify oxidized proteins (protein carbonyls) and proteins, expression of which was affected (down-regulated or up-regulated) by CEES or HD.

The Effects of CEES on the EpiDerm™ Skin Proteomics

In addition to the frozen tissue samples supplied by USAMRICD, we generated a set of fresh cellular lyzate samples obtained from EpiDerm skin samples which are an *in vitro* human epidermal model extensively used in toxicology studies. The EpiDerm™ model consists of normal, human-derived epidermal keratinocytes (NHEK) which have been cultured to form a multilayered, highly differentiated model of the human epidermis.

The EpiDerm tissues were treated (or not) with 2.5 mM CEES in the presence or absence of antioxidant liposomes containing reduced glutathione (GSH). In recent experiments (see Bioscience Review 2008 Abstract), we have shown that GSH-liposomes increase the viability of keratinocytes (within EpiDerm) exposed to CEES. We are now performing a series of experiments aimed at discovering the potential alterations in protein expression due to CEES exposure but restored (fully or partially) by GSH-liposome treatment.

Fig. 6 shows differences in the protein expression in EpiDerm due to CEES exposure (red circles) and the differences affected by the GSH-liposomes (green circles). In this experiment, total protein samples from the cellular lysates were separated by the 2D-GE technique and quantitated by using the Dymensions Two software**.** In order to document only significant differences, each sample was run three times (i.e., three separate 2-D-GE runs) and the resulting images then averaged. **Table 1** shows the quantitative differences in protein expression for the types of sample (vehicle, CEES, and CEES+GSH-liposomes). To finalize this set of data, we currently are performing LC/MS identification of the proteins.

The targeted proteins are extracted from the gel, stripped from the silver stain, trypsinized, and resulting peptide mixtures analyzed using nanospray LS/MS on our LTQ Linear Ion Trap Mass Spectrometer (Thermo-Fisher). In order to test this experimental procedure, we analyzed an abundant protein spot from the sample treated with vehicle and separated on 2D gel. The spot appears to contain three merged protein spots. The three spots were, however, unchanged by treatment with CEES or antioxidant liposomes. Raw LC/MS data obtained from the LTQ XL mass spectrometer were analyzed with BioWorks 3.3 software (Thermo-Fisher) in order to determine the best matches to all possible tryptic peptides as determined from a recent UniProt protein database.

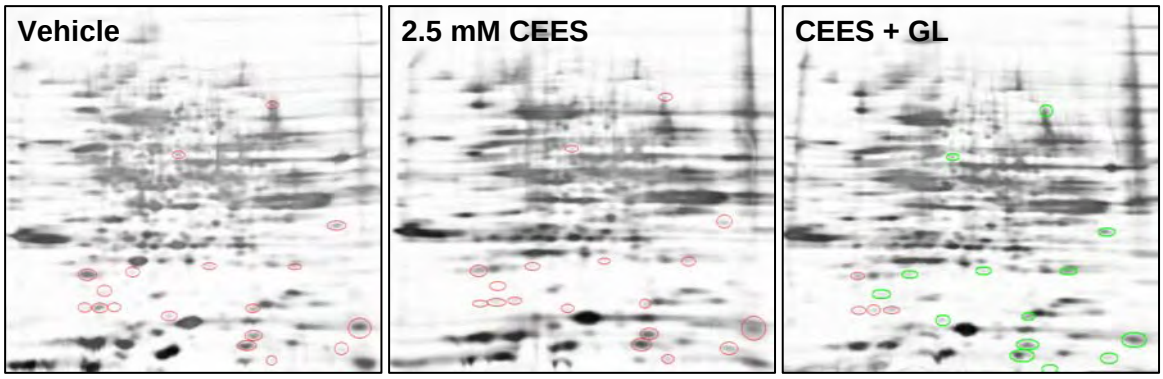

Figure 6. Proteomics Study of CEES toxicity and the effect of GSH-Liposomes in EpiDerm: tissues were exposed to vehicle or 2.5 mM CEES in the absence or presence of GSH-liposomes for 18 h. Cell lysates were separated by 2D gel electrophoresis, silver-stained and photographed (three gels per sample). Average differences in protein expression were quantified with Dymension-2 Software. The proteins differentially expressed after CEES exposure are marked with red circles. The proteins, which expression was partially reversed by GSH-liposomes are marked with green circles.

Table 1 Quantitative differences in protein expression

The differences are expressed as average 2D gel protein spot volume ratios normalized to "Vehicle" samples. Vehicle, exposed to 1% EtOH; CEES, exposed to 2.5 mM CEES; CEES+GL, exposed to CEES and GSH-liposomes simultaneously. Positive values mean that the proteins are up-regulated, negative values mean that the proteins are down-regulated.

Spot	MW (kDa)		Volume Ratio	
		Vehicle	CEES	CEES + GL
1	50.6	1	-3.935	-1.322
2	34.1	1	-2.827	-1.049
3	28.3	1	-1.739	1.174
4	19.5	1	-2.92	-1.224
5	13.4	1	-3.186	-1.403
6	12.2	1	-2.02	1.068
7	11.7	1	1.657	-1.028
8	11.3	1	-1.591	-1.198
9	10.8	1	-2.095	-1.465
10	10.2	1	1.731	-1.219
11	9.3	1	1.761	-1.323

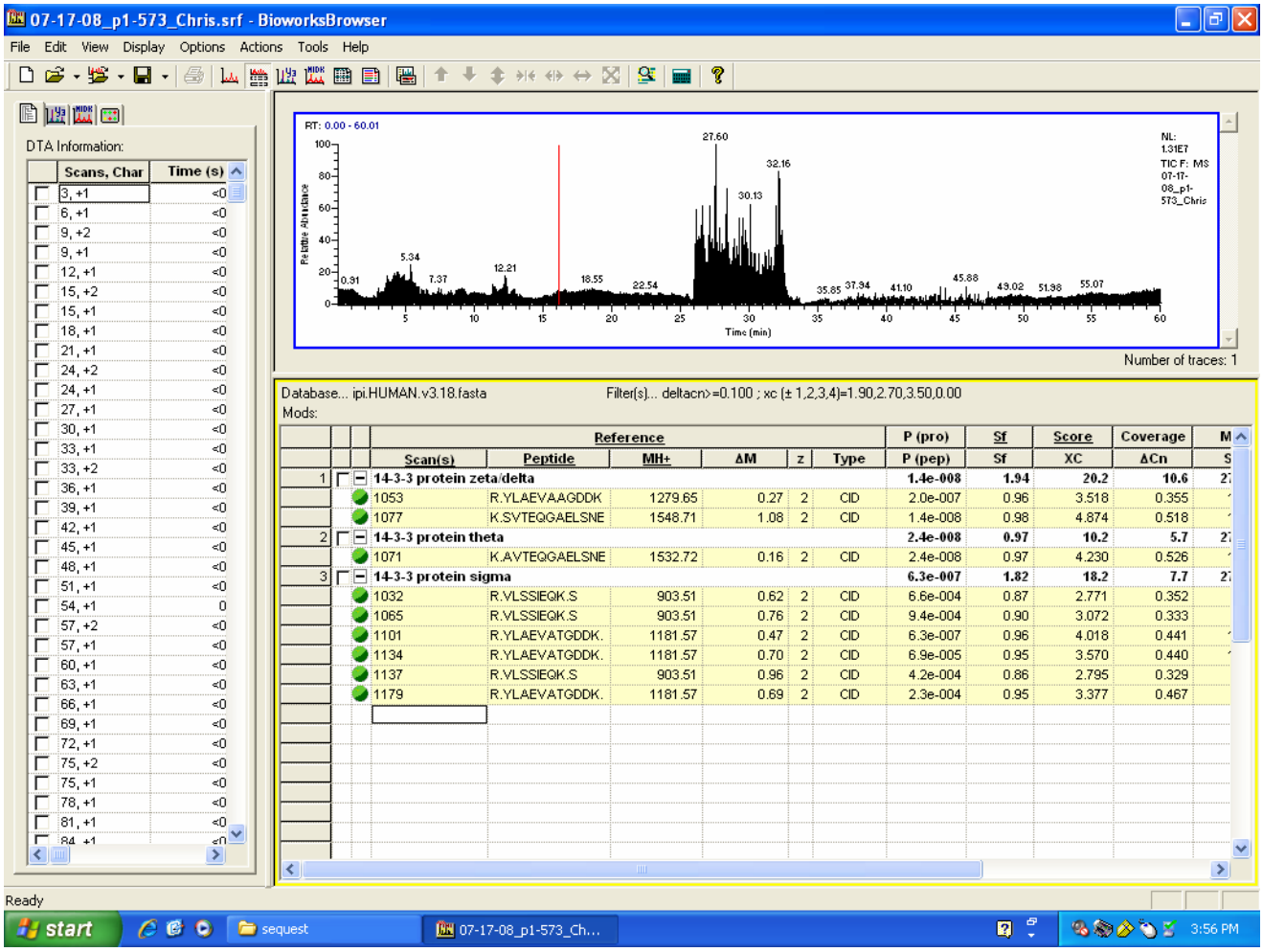

Figure 7: Identification of a set of three proteins from a 2D gel spot (SEQUEST search result). A targeted protein spot from silver stained gel was extracted, distained, and digested by trypsin. Resulting mixture of tryptic peptides was analyzed by LS/MS on the LTQ XL mass spectrometer. Raw data (see the chromatogram at the top right panel) were further analyzed with BioWorks 3.3 software (Thermo-Fisher) in order to determine the best matches to all possible tryptic peptides as determined from a recent UniProt protein database. Computer screen above shows the result of the SEQUEST protein search. Three highly homologous proteins were identified with a high level of significance (see the bottom right panel).

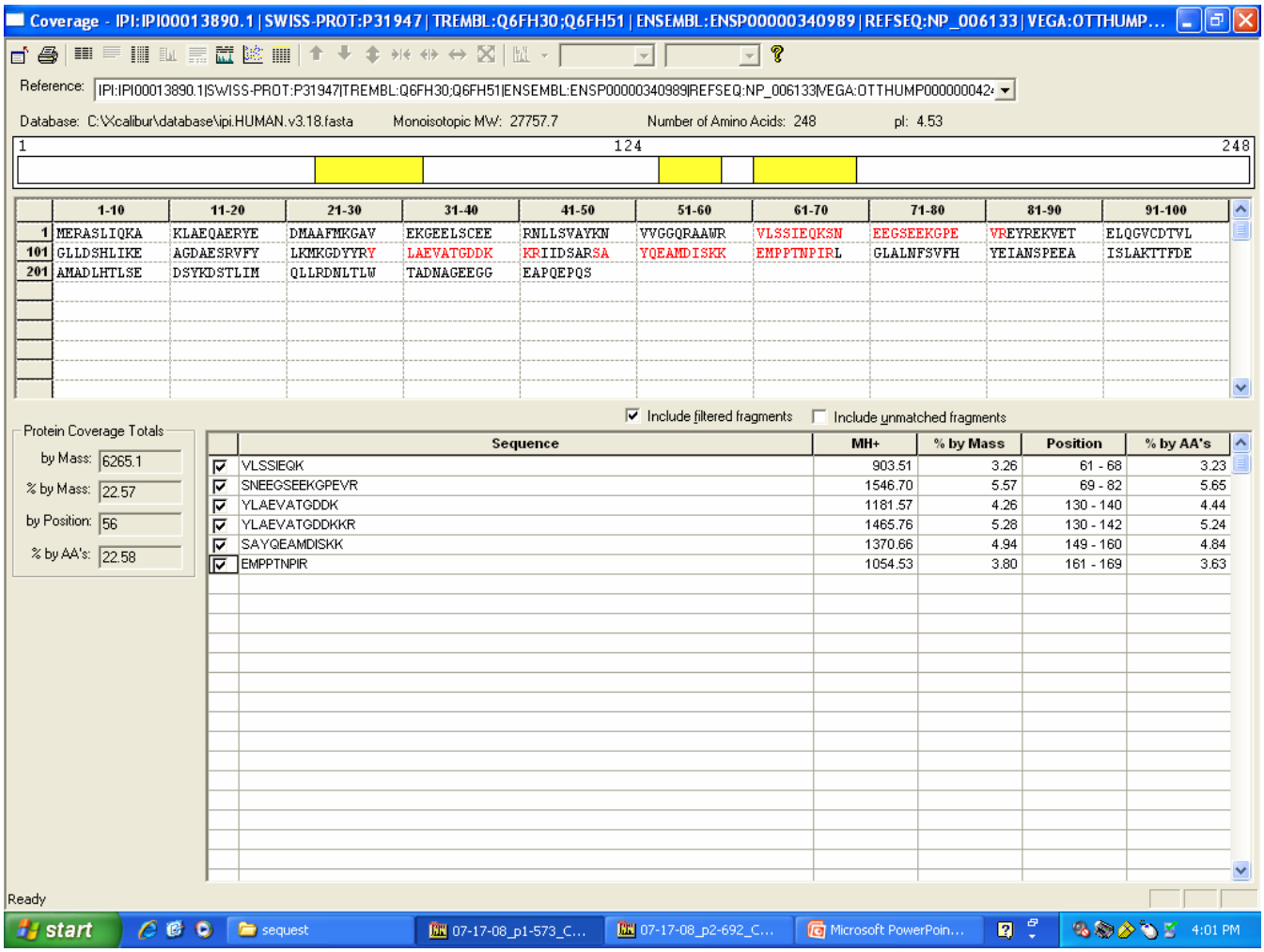

Figure 8: Identification of a set of three proteins from a 2D gel spot (coverage for 14-3-3 Protein Sigma). Raw LC/MS data were analyzed with BioWorks 3.3 software (Thermo-Fisher) in order to determine the best matches to all possible tryptic peptides as determined from a recent UniProt protein database (see Fig.7). Computer screen above shows detailed information for the third protein (14-3-3 Protein Sigma). Specific peptides identified by LC/MS are listed at the bottom panel and are shown in red within the protein sequence at the middle panel.

The database search (**Fig. 7**) revealed the presence of three highly homologous (97%) human proteins, which belong to the 14-3-3 family of regulatory proteins. The **14-3-3 protein sigma** (Stratifin or Epithelial cell marker protein 1) is an adapter protein implicated in the regulation of a large spectrum of signaling pathways. It binds to a large number of partners, usually by recognition of a phosphoserine or phosphothreonine motif. The binding generally results in the modulation of the activity of the binding partner. The main function is p53-regulated inhibition of G2/M progression.
The **14-3-3 protein theta** (or tau, or Protein HS1) is a negative regulator of transcription. It is involved in the protein kinase C signaling pathway. The **14-3-3 protein zeta** (also known as 14-3-3 delta (a phosphorylated form of 14-3-3 zeta); D14Abb1e; KCIP-1;

Tyrosine 3-monooxygenase/tryptophan 5-monooxygenase activation protein, zeta polypeptide; Ywhaz) is another transcription factor involved in the protein kinase C signaling pathway interacting with various serine/threonine protein kinases. It is also an activator of tyrosine 3/tryptophan 5 –monooxygenase.

In skin tissues, it is likely that the **14-3-3 protein zeta** is involved in the synthesis of melanin from tyrosine. **This protein has not, to our knowledge, been identified in human skin and it would be important in preventing skin cancers resulting from prolonged exposure to strong sun light (relevant to military personnel serving in desert environments).**

Fig. 8 shows the protein coverage (the list and sequences of identified peptides) for 14-3-3 protein sigma. **Fig. 9** shows ion matches (comparison of the MS/MS spectrum to theoretically predicted B and Y ions) for one of the identified peptides.

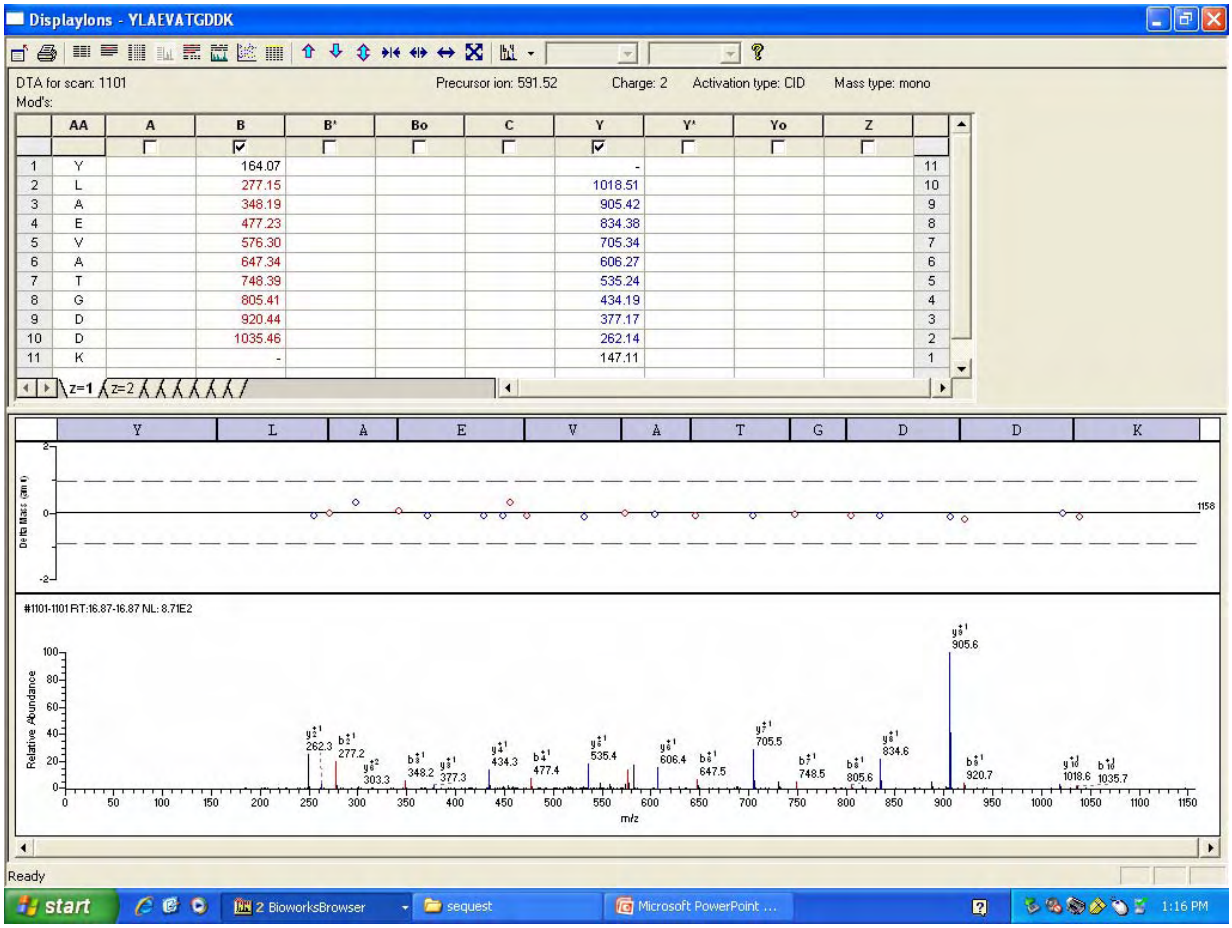

Figure 9: Identification of a set of three proteins from a 2D gel spot (ion matches for peptide YLAEVATGDDK). LS/MS raw data (see Fig. 7 and 8) were further analyzed with BioWorks 3.3 software (Thermo-Fisher) in order to determine the best matches to all possible tryptic peptides as determined from a recent UniProt protein database. Tryptic peptides were identified based upon MS/MS data. Top table shows the list of B and Y ions as they match against the experimental data (matched B ions – red, matched Y ions – blue). The center plot shows the mass errors of the measurement. The bottom panel shows MS/MS data.

Next year, we plan to concentrate our efforts on proteomics changes in various CEES/HD-exposed tissue samples. We will focus on proteins whose expression is altered by CEES exposure but restored (fully or partially) due to the antioxidant liposome treatment.

Specific Tasks 3:

Preparation of well characterized antioxidant-liposomes and collaborations with other members of the AMCC

Work with Dr. Peter Ward on the Ability of Antioxidant-liposomes to Protect against Acute and Long-term CEES-toxicity to Pulmonary Tissues in Rat Model

We have continued to supply well characterized antioxidant liposomes to other members of the AMCC and these efforts have contributed to the overall research productivity of the AMCC (see publications and abstracts by other members of the AMCC).

A key finding of our work with Dr. Peter Ward [6] is that liposomes encapsulated with antioxidants are a superior *in vivo* countermeasure to oxidant inducing vesicants compared to the free or unencapsulated antioxidants. In addition, antioxidant-liposomes are effective in treating pulmonary damage (in a rat model) for at least one and half hour post exposure and can also uniquely suppress progressive lung injury [6].

Work with Dr. Salil Das on the Ability of Antioxidant-Liposomes to Protect Against CEES- Induced Lung Damage in a Guinea Pig Model

In our work with Dr. Salil Das [7], we found that liposomes encapsulated with both vitamin E and N-acetylcysteine (NAC) were effective counter measures to CEES induced lung injury in guinea pigs. Lung damage was measured by albumin leakage from the blood to the lungs (as in our work with Dr. Ward). In addition, the vitamin E, NAC-liposomes also provided protection by controlling recruitment of neutrophils, eosinophils, and accumulation of septal and perivascular fibrin and collagen, and parenchymal collapse. Interestingly, liposomes containing delta-tocopherol were found to be particularly effective as counter measures [7].

Work with Dr. Richard Rest on the Ability of NAC-liposomes to Promote Macrophage Killing of *Bacillus anthracis* (BA)

We have supplied NAC-liposomes to Dr. Richard Rest who is studying the influence of redox modulation on the ability of human macrophages to kill *Bacillus anthracis* (BA). Dr. Rest has found that NAC-liposomes completely delays/inhibits BA germination (in the absence of macrophages) and also stimulates the ability of macrophages to kill intracellular BA. These are clearly results with direct military relevance.

Key Research Accomplishments

1. Antioxidant-liposomes prepared by our laboratory are effective in preventing both acute and long-term *in vivo* damage to the lungs of rats exposed to CEES.

2. Antioxidant-liposomes prepared by our laboratory are effective in preventing *in vivo* CEES-induced damage to the guinea pig lung.

3. *In vitro* experiments with antioxidant-liposomes (with NAC) have shown an ability to prevent *Bacillus anthracis* germination and to enhance the killing of *Bacillus anthracis* by human macrophages.

4. Rat lung tissues treated with blank or antioxidant-liposomes were analyzed by 2D-GE gel analysis and no differences in protein expression were found.

5. RBL-2H3 mast cells treated/untreated with 0.5 mM CEES were analyzed by 2D-GE.

6. The inhibition of calcium ionophore A23187-induced degranulation from various levels (0.039 – 0.5 mM) of CEES was confirmed.

7. NO generation was found to be increased in RBL-2H3 cells treated with the calcium ionophore A23187. Various levels of CEES did not inhibit or stimulate NO generation.

8. A number of human Epiderm skin samples exposed to CEES were analyzed by 2D-GE.

9. Proteomics studies have been initiated in order to reveal changes in protein expression due to CEES exposure and treatment with antioxidant liposomes.

Reportable Outcomes

Presentations:

1. Advanced Medical Countermeasures Consortium Meeting, June 5, 2008, Baltimore, MA: **"Effect of low doses of CEES on degranulation of rat mast cells."**
2. Bioscience Review 2008 Poster (Victor Paromov, Sudha Kumari, Marianne Brannon, Christian Muenyi, and William Stone). "**The Protective Effect of Antioxidant Liposomes in a Human Epidermal Model Exposed to a Vesicating Agent**".
3. Bioscience Review 2008 Poster (Peter A. Ward, Laszlo M. Hoesel, Michael A. Flierl, Daniel Rittirsch, Milton Smith, and William Stone). "**Liposomal Blockade of Lung Injury after Exposure to 2-Chloroethyl Ethyl Sulfide**".

Manuscripts (during the past year of funding):

1. **Viktor Paromov**, Min Qui, **Hongsong Yang**, **Milton Smith**, and **William L. Stone** "The influence of N-acetyl-L-cysteine and polymyxin B on oxidative stress and nitric oxide synthesis in stimulated macrophages treated with a mustard gas analog" in: ***BMC Cell Biology*** 2008, 9:33.

2. **Viktor Paromov**, **Zacharias Suntres, Milton Smith**, **William L. Stone**. "Sulfur Mustard Toxicity in Human Skin: Role of Oxidative Stress and Antioxidant Therapy" in: ***Journal of Burns and Wounds*** 2007, 7:e7.

3. **Milton G. Smith, William L. Stone, Ren-Feng Guo, Peter A. Ward, Zacharias Suntres, Shyamali Mukherjee and Salil K. Das**, Chapter 12 "Vesicants and Oxidative Stress", pp 249-294 in: **Chemical Warfare Agents: Chemistry, Pharmacology, Toxicology and Therapeutics.** Romano editor.

4. **Shyamali Mukherjee, William L Stone, Hongsong Yang, Milton Smith, and Salil K.Das**. "Protection of half sulfur mustard gas-induced lung injury in guinea pigs by antioxidant liposomes" in: **Journal of Applied Toxicology** (submitted).

Conclusion

We found that antioxidant-liposomes are effective in preventing CEES induced lung damage in two *in vivo* models, i.e., rats and guinea pigs. In addition, antioxidant-liposomes can prevent the *in vitro* germination of *Bacillus anthracis* and promote the in intracellular killing of this bacteria by human macrophages.

We have found that toxic doses of CEES impair degranulation in RBL-2H3 rat mast cells. Initially, we proposed that CEES might stimulate mast cell degranulation since CEES was found to inhibit the generation of NO in RAW 264.7 macrophages [3]. Nitric oxide is known to inhibit mast cell degranulation in various species [4, 5]. However, other investigators have found that endogenous nitric oxide does not modulate degranulation of mesenteric or skin mast cells in rats [8]. It is clear, nevertheless that CEES is capable of modulating mast cell degranulation. The molecular mechanisms of this effect and its relation to the oxidative stress will be elucidated in future experiments.

CEES-induced cell injury has a complex molecular mechanism and associated with oxidative stress, gene expression, inflammation, and cell death pathways. The acute phase of injury is an oxidant-mediated process that is associated with intensive inflammatory responses. We found recently that liposomes containing antioxidants (GSH, NAC, in particular) are highly protective in human keratinocytes. We are currently analyzing overall intracellular changes due to the oxidative stress in CEES/HD treated samples utilizing a systems biology approach. We will continue to analyze the differences in protein “finger prints” on the 2D-gels quantitatively using Dymension software (SynGene). The most affected proteins will be extracted from gels, and identified by the nanospray technique on our LTQ Linear Ion Trap Mass Spectrometer (ThermoFisher). By performing such analyses we will be able to identify oxidized proteins (protein carbonyls) and proteins whose expression was affected (down-regulated or up-regulated) by CEES or HD. The effect of antioxidant liposomes on these proteins also will be determined.

References

1. Victor Paromov ZS, Milton Smith, William L. Stone: **Sulfur Mustard Toxicity Following Dermal Exposure: Role of Oxidative Stress, and Antioxidant Therapy**. *Journal of burns and wounds* 2007, **in press**.
2. Stone WL, Qui M, Smith M: **Lipopolysaccharide enhances the cytotoxicity of 2-chloroethyl ethyl sulfide**. *BMC cell biology* 2003, **4**(1):1.
3. Qui M, Paromov VM, Yang H, Smith M, Stone WL: **Inhibition of inducible Nitric Oxide Synthase by a mustard gas analog in murine macrophages**. *BMC cell biology* 2006, **7**:39.
4. Eastmond NC, Banks EM, Coleman JW: **Nitric oxide inhibits IgE-mediated degranulation of mast cells and is the principal intermediate in IFN-gamma-induced suppression of exocytosis**. *J Immunol* 1997, **159**(3):1444-1450.
5. Iikura M, Takaishi T, Hirai K, Yamada H, Iida M, Koshino T, Morita Y: **Exogenous nitric oxide regulates the degranulation of human basophils and rat peritoneal mast cells**. *International archives of allergy and immunology* 1998, **115**(2):129-136.
6. Hoesel LM, Flierl MA, Niederbichler AD, Rittirsch D, McClintock SD, Reuben JS, Pianko MJ, Stone W, Yang H, Smith M *et al*: **Ability of antioxidant liposomes to prevent acute and progressive pulmonary injury**. *Antioxidants & redox signaling* 2008, **10**(5):973-981.
7. Shyamali Mukherjee WLS, Hongsong Yang, Milton Smith, and Salil K.Das: **Protection of half sulfur mustard gas-induced lung injury in guinea pigs by antioxidant liposomes**. *Journal of Applied Toxicology* 2008, **submitted**.
8. Kwasniewski FH, Tavares de Lima W, Bakhle YS, Jancar S: **Endogenous nitric oxide does not modulate mesenteric mast cell degranulation in rats**. *Biochemical pharmacology* 2003, **65**(12):2073-2080.

Appendices (available as PDF files)

1. *BMC Cell Biology* Paper 2008
2. *Journal of Burns and Wounds* Review 2007
3. *BMC Cell Biology* Manuscript 2008

BMC Cell Biology

BioMed Central

Research article

Inhibition of inducible Nitric Oxide Synthase by a mustard gas analog in murine macrophages

Min Qui[†1], Victor M Paromov*[†1], Hongsong Yang[†1], Milton Smith[2] and William L Stone[†1]

Address: [1]Department of Pediatrics, East Tennessee State University, Johnson City, TN, USA and [2]Amox Ltd., Lawton, MI 49605, USA

Email: Min Qui - qui@etsu.edu; Victor M Paromov* - paromov@etsu.edu; Hongsong Yang - yangh@etsu.edu; Milton Smith - mgsmithmd@isp01.net; William L Stone - stone@etsu.edu

* Corresponding author †Equal contributors

Published: 30 November 2006

BMC Cell Biology 2006, **7**:39 doi:10.1186/1471-2121-7-39

Received: 22 September 2006
Accepted: 30 November 2006

This article is available from: http://www.biomedcentral.com/1471-2121/7/39

Abstract

Background: 2-Chloroethyl ethyl sulphide (CEES) is a sulphur vesicating agent and an analogue of the chemical warfare agent 2,2'-dichlorodiethyl sulphide, or sulphur mustard gas (HD). Both CEES and HD are alkylating agents that influence cellular thiols and are highly toxic. In a previous publication, we reported that lipopolysaccharide (LPS) enhances the cytotoxicity of CEES in murine RAW264.7 macrophages. In the present investigation, we studied the influence of CEES on nitric oxide (NO) production in LPS stimulated RAW264.7 cells since NO signalling affects inflammation, cell death, and wound healing. Murine macrophages stimulated with LPS produce NO almost exclusively via inducible nitric oxide synthase (iNOS) activity. We suggest that the influence of CEES or HD on the cellular production of NO could play an important role in the pathophysiological responses of tissues to these toxicants. In particular, it is known that macrophage generated NO synthesised by iNOS plays a critical role in wound healing.

Results: We initially confirmed that in LPS stimulated RAW264.7 macrophages NO is exclusively generated by the iNOS form of nitric oxide synthase. CEES treatment inhibited the synthesis of NO (after 24 hours) in viable LPS-stimulated RAW264.7 macrophages as measured by either nitrite secretion into the culture medium or the intracellular conversion of 4,5-diaminofluorescein diacetate (DAF-2DA) or dichlorofluorescin diacetate (DCFH-DA). Western blots showed that CEES transiently decreased the expression of iNOS protein; however, treatment of active iNOS with CEES *in vitro* did not inhibit its enzymatic activity

Conclusion: CEES inhibits NO production in LPS stimulated macrophages by decreasing iNOS protein expression. Decreased iNOS expression is likely the result of CEES induced alteration in the nuclear factor kappa B (NF-κB) signalling pathway. Since NO can act as an antioxidant, the CEES induced down-regulation of iNOS in LPS-stimulated macrophages could elevate oxidative stress. Since macrophage generated NO is known to play a key role in cutaneous wound healing, it is possible that this work has physiological relevance with respect to the healing of HD induced skin blisters.

Background

HD is a chemical weapon that can produce casualties in military situations and has been used with devastating results against civilian populations [1]. Extensive and slow healing lesions following exposure to HD can place a heavy burden on the medical services of military and public health organizations. The design of effective countermeasures to HD depends upon a detailed understanding of the molecular mechanisms for its toxicity. Important mechanisms of HD induced skin injury are alkylation of DNA and other macromolecules, accompanied by enhanced reactive oxygen species (ROS) generation and depletion of intracellular glutathione (GSH) [2-5]. Depletion of GSH by HD and its metabolites is known to shift the intracellular redox milieu toward a more oxidized state with a subsequent loss of protection against oxidative free radicals and an activation of inflammatory responses[6,7].

It has been shown that HD induces a vast "spectrum" of inflammatory cytokines released from keratinocytes [8,9]. It is likely that CEES cause similar changes in macrophages and leukocytes. We previously found that LPS, as well as inflammatory cytokines, such as tumor necrosis factor-alpha (TNF-α) and interleukin one-beta (IL-1β), significantly amplify the toxicity of CEES in RAW264.7 macrophages [10]. In macrophages, stimulation by LPS, as well as by pro-inflammatory cytokines, leads to the activation and nuclear translocation of NF-κB [11]. One of the major consequences of such activation in macrophages is an induction of iNOS expression with subsequent elevation of intracellular NO [12]. The effect of CEES on NO generation and on the NF-κB pathway is potentially significant since NO signalling plays an important role in inflammation, the mechanisms of cell death NF-κB [13,14], and wound healing [15,16]. The present work describes the inhibition of NO production and iNOS expression in LPS stimulated macrophages treated with CEES.

Results

CEES transiently suppresses NO production and iNOS expression in LPS stimulated cells

In Figure 1a, we examined nitrite secretion into the cell culture medium by RAW 264.7 murine macrophages after 24 hours of treatment with CEES and various levels of LPS. Nitrite level in the cell culture medium, as measured by the Griess reagent, is a reliable indicator of nitric oxide secretion. These data show that CEES (100–500 μM) inhibited the secretion of NO into the cell medium by LPS stimulated macrophages in a dose-dependent manner. Low levels of CEES (≤ 100 μM) only partially inhibited NO production, whereas levels higher than 300 μM completely inhibited NO production. Although CEES does decrease the viability of LPS stimulated macrophages [10], the decreased generation of NO cannot be accounted simply for the loss of viable cells. Figure 1b shows that in case nitrite levels in the culture medium (as measured by OD at 532 nm) are normalized to the amount of viable cells (OD at 580 nm, MTT assay, measured separately) there is still a significant CEES dose dependent inhibition of NO formation.

In order to determine if CEES influenced cellular levels of iNOS, we performed Western blot analyses (Figure 1c) of the cell lysates using highly selective anti-iNOS antibodies with equal amounts of total protein applied to each lane. Control RAW 264.7 macrophages had no detectable iNOS protein, CEES treatment alone did not induce any iNOS protein but LPS (10 ng/ml for 24 hours) produced a marked induction of iNOS protein. When simultaneously treated with LPS (10 ng/ml) and CEES (300 μM) there was a marked reduction in the LPS induction of iNOS protein.

We then examined the influence of 300 μM CEES on the time course of NO production in macrophage stimulated with 10 ng/ml LPS. Figure 2a shows that CEES delays, but does not prevent, the production of NO (as measured by nitrite formation) in LPS-stimulated macrophages. In fact, after 12 hours the rate of NO production is about the same in cells treated with LPS alone compared with cells treated with both LPS and CEES. Western blot data (Figure 2b) from the cells used in Figure 2a show a similar pattern: LPS alone induces robust iNOS protein expression which is completely inhibited by CEES for up to 6 hours. After 12 hours, however, the cells incubated with both CEES and LPS show a rebound in the expression of iNOS and after 24 hours the iNOS protein level in cells treated with both CEES and LPS is very similar to that observed in cells treated with LPS alone. These data show that the influence of CEES on both nitric oxide synthesis and iNOS expression is transient.

CEES does not inhibit iNOS enzymatic activity in vitro

In order to evaluate the possible direct inhibitory effect of CEES on iNOS activity *in vitro*, we measured the intracellular rates of 4,5-diaminofluorescein (DAF-2) or dichlorofluorescin (DCFH) oxidation in intact macrophages. Dichlorofluorescin diacetate (DCFH-DA) is permeable to the cell plasma membrane and intracellular esterases convert it into a membrane impermeable (DCFH) form which is can be oxidized to highly fluorescent dichlorofluorescein (DCF) by free radicals. In macrophages, the oxidation of DCFH has been shown to be a sensitive and relatively selective probe for monitoring intracellular NO formation by iNOS [17].

Using DCFH-DA and DAF-2DA, we were able to continuously monitor NO formation in intact macrophages under a variety of conditions. Previously, we [18] and oth-

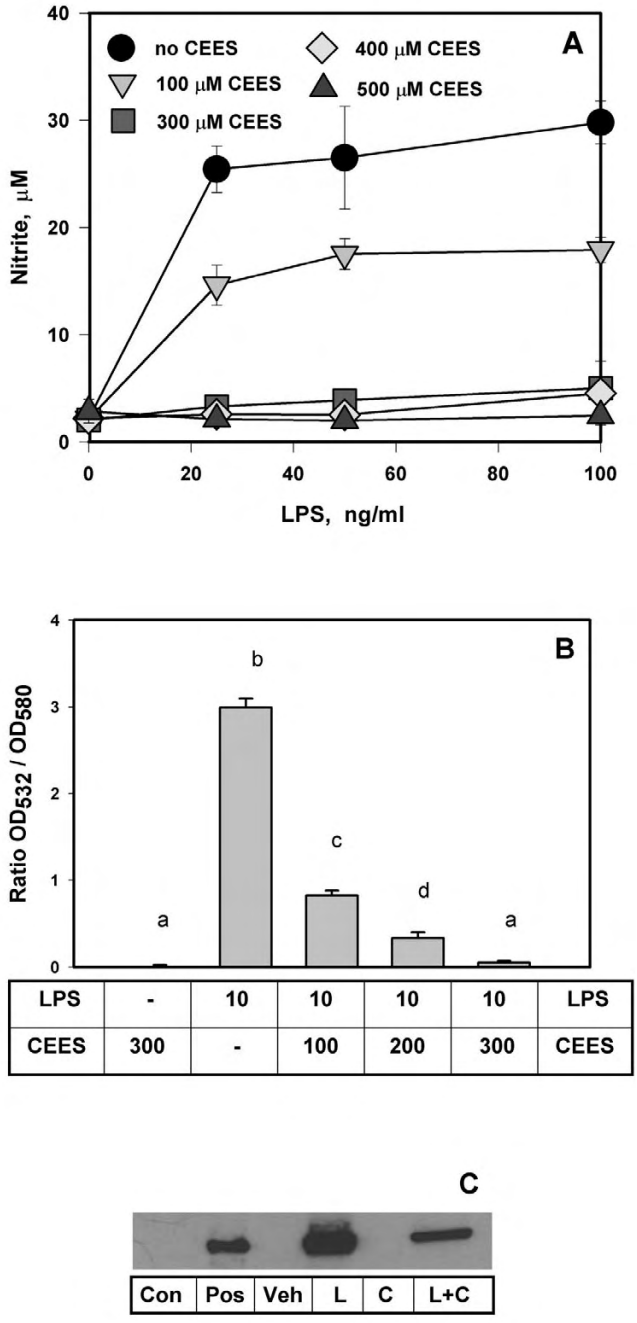

Figure 1

CEES inhibits NO production and iNOS expression in LPS stimulated RAW264.7 macrophages. *Panel A*: Macrophages were simultaneously treated with various levels of CEES (as indicated) and low doses of LPS (as indicated). NO production was monitored as the concentration of nitrite in the culture medium after 24 h. *Panel B*: Cells were treated similarly as for *Panel A*; LPS, 10 ng/ml; CEES, 100, 200, or 300 μM (as indicated). Means not sharing a common letter are significantly different ($p < 0.05$). Nitrite levels in the culture medium (OD at 532 nm) were normalized to the amount of viable cells (OD of the MTT product at 580 nm). *Panel C*: Western blot analysis of iNOS protein from cells simultaneously incubated with 300 μM CEES and/or 10 ng/ml LPS for 24 h; cell lysates were prepared as described in Materials and Methods: Con, control cells; Pos, iNOS protein for positive control; Veh, vehicle; L, 10 ng/ml LPS stimulated cells; C, 300 μM CEES treated cells; L+C, LPS/CEES treated cells.

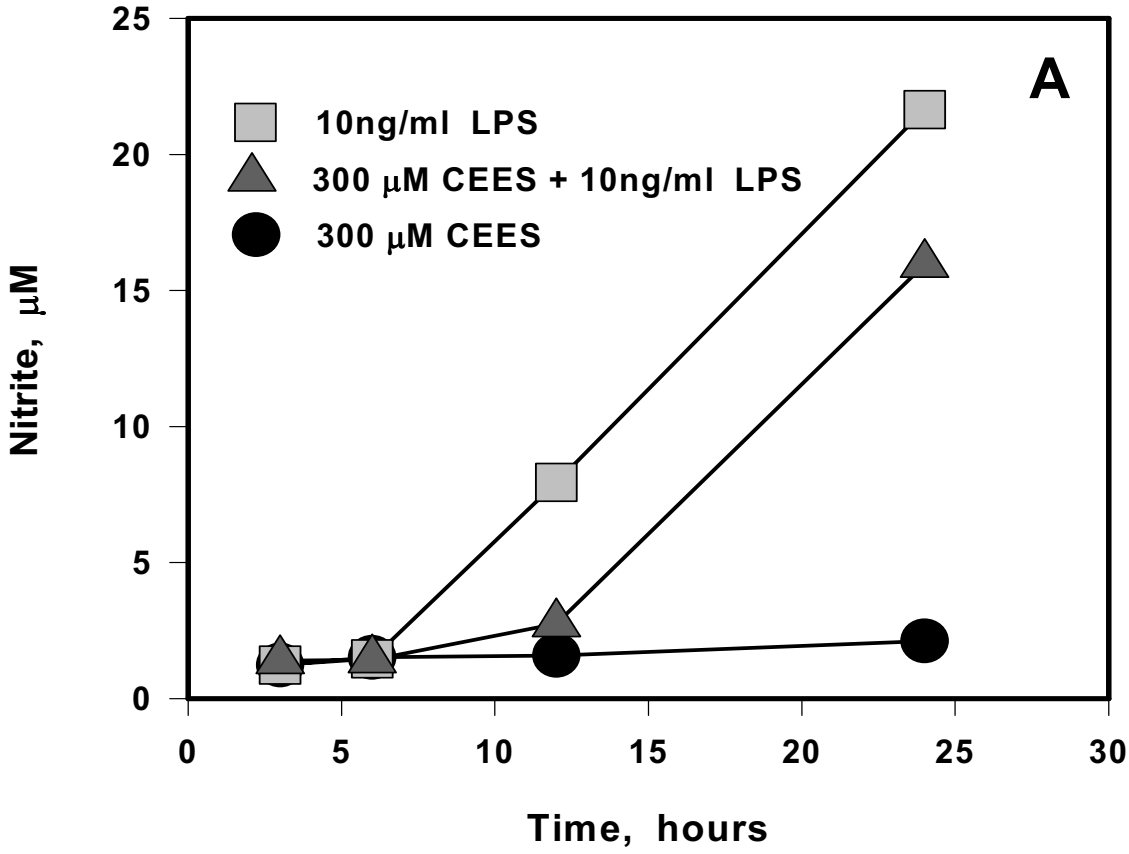

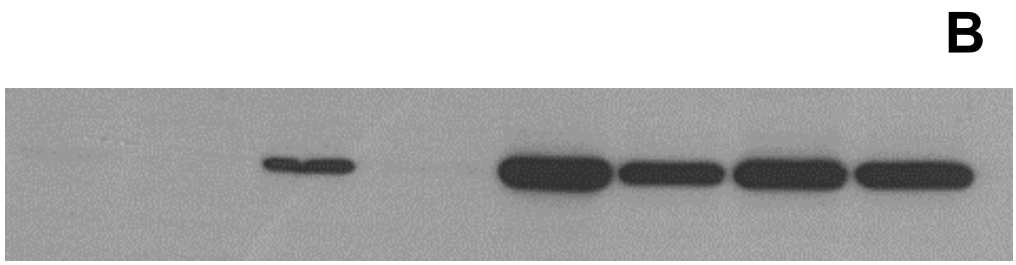

3h	3h	6h	6h	12h	12h	24h	24h
L	L+C	L	L+C	L	L+C	L	L+C

Figure 2
Time course of NO production and iNOS expression in LPS stimulated RAW264.7 macrophages incubated with CEES. *Panel A*: Macrophages were incubated with 10 ng/ml LPS alone, 300 μM CEES alone or simultaneously with both 300 μM CEES 10 ng/ml LPS for various time intervals (as indicated). NO production measured as concentration of nitrite in culture medium. *Panel B*: Western blot analysis of iNOS protein from the cells incubated with 300 μM CEES with or without 10 ng/ml LPS; cell lysates were prepared after 3, 6, 12, or 24 hour incubation (as indicated) as described in Materials and Methods; L, LPS; C, CEES.

ers [19] have shown that LPS exclusively induces the iNOS form of nitric oxide synthase in murine macrophages. Figure 3a shows DCFH oxidation in RAW 264.7 cells stimulated with different levels of LPS for 24 hours. In the absence of LPS, the rate of DCFH oxidation was extremely low but increased with increasing exposure to LPS; however, this effect was nearly saturated at LPS levels above 15 ng/ml.

We then measured the rates of DAF-2 oxidation in RAW 264.7 macrophages stimulated with 20 ng/ml LPS in the presence or absence of 500 μM CEES during 24 hour incubations (Figure 3b). In the absence of LPS or CEES, minimal DAF-2 oxidation was observed. As expected, LPS alone induced a marked increase in DAF-2 oxidation. Next, macrophages incubated with LPS for 24 hours were then exposed (post-treatment) to 500 μM CEES and the rate of DAF-2 oxidation immediately measured. As shown in Figure 3b, there was no change in rate of DAF-2 oxidation compared to cells treated with LPS alone. These data strongly support the notion that CEES does not directly inhibit iNOS enzymatic activity. Similar results were obtained with DCFH-DA staining (data not shown). As expected, macrophages simultaneously treated with both LPS and CEES for 24 hours show a marked decrease in either DAF-2 or DCFH oxidation.

To further confirm that DCFH oxidation is overwhelmingly due to iNOS, we incubated LPS-stimulated macrophages with ebselen (see Figure 3c). Ebselen is a selenoorganic compound that can inhibit both the activity of iNOS [20] and its induction by LPS [21]. Ebselen (25 μM) almost completely inhibited the DCFH oxidation in RAW 264.7 cells treated with 10 ng/ml or 20 ng/ml LPS. Ebselen was not cytotoxic at the levels used in Figure 3 (data not shown).

Discussion

Overall, the experiments detailed in this work show that CEES treatment in LPS-stimulated RAW264.7 murine macrophages transiently inhibits intracellular NO generation by interfering with iNOS expression rather than by direct inhibition of iNOS enzymatic activity. CEES (as well as HD) undergo rapid hydrolysis in aqueous solutions and this may account, in part, for the transitory nature of its inhibiting effect on iNOS induction [22]. LPS is a major component of the cell wall of gram-negative bacteria and is known to trigger a variety of inflammatory reactions in macrophages and other cells expressing CD14 receptors [23,24]. LPS is ubiquitous and is present in serum, tap water, and dust. Military and civilian personnel would, indeed, always have some degree of exposure to environmental LPS.

LPS stimulation of macrophages is known to involve the activation of protein phosphorylation by kinases as well as the activation of nuclear transcription factors such as NF-κB [25-28]. An important consequence of NF-κB activation in macrophages is the induction of iNOS expression followed with highly elevated NO production [12]. Nitric oxide has been demonstrated to have an important role in promoting cell death; however, the precise nature of this role varies with cell type and the dose. Low levels of nitric oxide protect RAW 264.7 macrophages from hydrogen peroxide induced apoptosis [29], however, nitric oxide has also been reported to induce apoptosis in J774 macrophages [14]. Nitric oxide can induce cell death through energy depletion-induced necrosis and oxidant-induced apoptosis.

We are currently exploring the potential molecular mechanism(s) whereby CEES interferes with iNOS expression in LPS stimulated macrophages. It is possible that GSH depletion caused by CEES determines iNOS expression. There are strong evidences suggesting that thiol depletion and iNOS expression are interrelated [30-32]. For example, LPS stimulated macrophages depleted of GSH exhibit a decreased level of iNOS protein and nitrite production [32]. Similarly, both *in vitro* [30] and *in vivo* [31] studies show that hepatocytes depleted of GSH have a diminished production of nitric oxide which is primarily due to a decreased level of iNOS mRNA. Vos et al. [31] have also presented evidence showing that GSH modulation of iNOS expression in hepatocytes is correlated with NF-kB activation, i.e., GSH depletion is associated with a lack of NF-kB activation. The influence of GSH depletion is not, however, consistent in all cell types. Glucose induced reduction of GSH in intestinal epithelial cells is associated with NF-kB activation and upregulation of iNOS gene expression [33].

It is also possible that CEES decreases iNOS expression by interfering with the LPS-induced activation of transcription factor NF-κB and/or signal transducer and activator of transcription-1α (STAT-1α). It is interesting, therefore, that Gray [34] has found that both CEES and HD inhibit the *in vitro* binding of transcription factor activating protein-2 (AP-2) via alkylating the AP-2 DNA consensus binding sequence rather than by direct damage to the AP-2 protein. Furthermore, it is significant that neither CESS nor its hydrolysis products were found to damage the AP-2 transcription factoring in a manner that prevented its DNA binding [35]. Similar experiments have yet to be done with NF-κB. Chen et al. [36] have also found that nitrogen mustard (bis(2-chloroethul) methylamine) similarly inhibits the binding of AP-2 to its consensus sequence. Nitrogen mustard also was shown to inhibit the binding of NF-κB to the GC-rich consensus sequence due to the interactions with DNA [37]. It is possible, therefore,

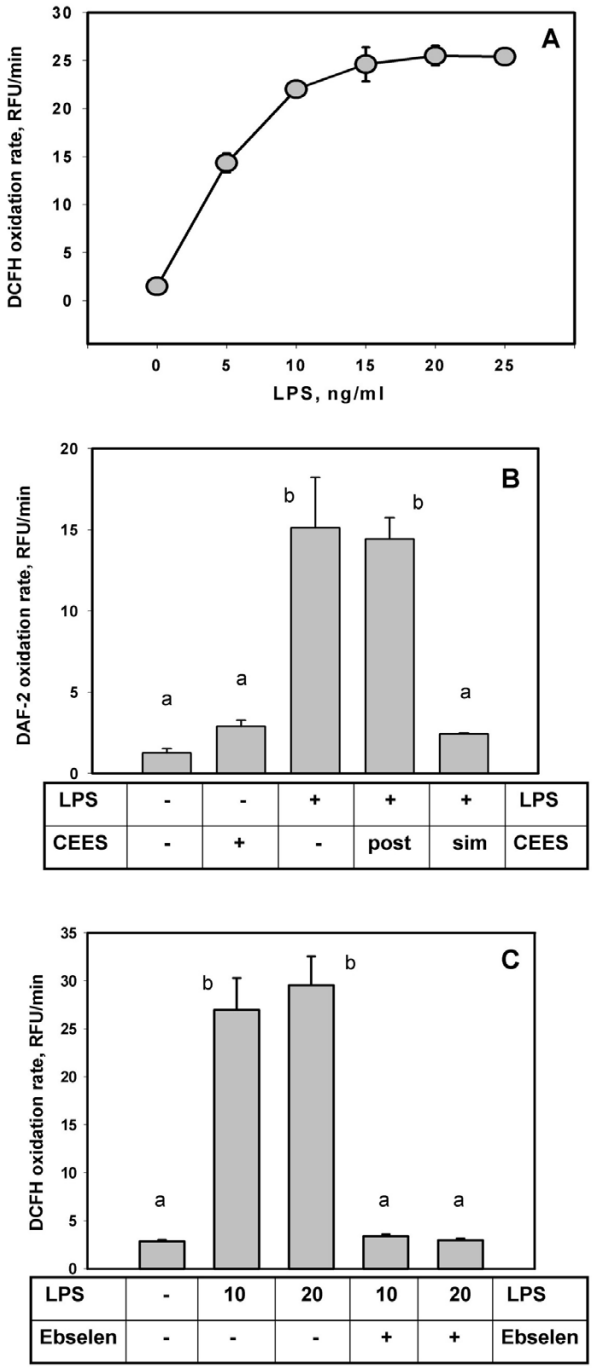

Figure 3

CEES reduces intracellular NO in LPS stimulated RAW264.7 macrophages. *Panel A*: Intracellular DCFH (20 μM) oxidation in LPS stimulated macrophages (as indicated) incubated for 2 h. Fluorescence (excitation 485 nm, emission 520 nm) was measured in Relative Fluorescence Units (RFU); the oxidation rate was expressed as RFU/min. *Panel B*: Macrophages stimulated with 20 ng/ml LPS, were incubated in the presence or absence of 500 μM CEES (as indicated) for 24 h. Post, CEES was applied after the 24 hours of LPS stimulation; Sim, CEES was applied simultaneously with LPS. *Panel C*: LPS stimulated cells were incubated in the presence or absence of 25 μM ebselen, a selective iNOS inhibitor (as indicated). 10, 10 ng/ml LPS; 20, 20 ng/ml LPS. Mean values not sharing a common letter are significantly different ($p < 0.05$).

that CEES also alkylates the NF-κB consensus sequence thereby preventing the binding of the NF-κB to the iNOS promoter. LPS and/or cytokine-inducible NF-κB binding elements of the murine iNOS promoter have been identified [38], and they are rich of guanine, which is the major alkylation site for HD or CEES. The possible effect of CEES on iNOS promoter regulation is currently being explored.

Although the activation of NF-κB due to mustard or CEES exposure have been shown in various cell lines [7,37,39], the detailed mechanism of this event is still unclear. Recent report [39] showed that NF-κB-driven gene expression has maximum at 9 hours in HD treated keratinocytes. In contrast, in a guinea pig model, Chatterjee et al. [40] have shown that NF-κB activation in lung tissues occurs shortly after CEES expose (1 hour), then disappears within 2 hours completely. However, in our experiments we did not observe any short term stimulating effect of CEES on NO production or iNOS expression (data not shown). Notably, the electrophoretic mobility shift assays used by Chatterjee et al. to measure NF-κB activation show only the state of NF-κB protein complex and provide no information regarding its binding to the DNA consensus sequences.

The physiological significance of potentially decreased iNOS expression by exposure to CEES or HD is not known. Considerable evidence, however, supports the view that nitric oxide production via iNOS plays a key role in wound healing [41-43]. Animal studies [16] have shown that the iNOS knockout mice have impaired wound healing that is reversed by iNOS gene transfer. Soneja et al. [44] have suggested that wound healing could be accelerated under circumstances where oxidative stress is minimized and nitric oxide production enhanced. We have initiated work to explore the role of antioxidants in preventing HD induced pathology in skin.

Conclusion

Our results show that CEES transiently inhibits NO production in LPS stimulated macrophages by inhibiting the expression of iNOS protein and not by modulating the enzymatic activity of iNOS. The decreased iNOS expression induced by CEES suggests that this alkylating agent inhibits the LPS stimulated activation of NF-κB and/or STAT-1α transcription factors, and this possibility is being investigated. We cannot directly address the physiological significance of our *in vitro* results, however, both decreased expression of iNOS and decreased production of nitric oxide are associated with impaired wound healing [16,41,43,44]. It is likely that the CEES or HD toxicity is modulated by a complex balance between nitric oxide production, thiol depletion and oxidative stress.

Methods

Materials

RPMI-1640 medium without phenol red and fetal bovine serum with a low endotoxin level were purchased from Life Technologies (Gaithersburg, MD). Rabbit anti-mouse iNOS antibody was obtained from Transduction Laboratory (Lexington, KY). Horseradish peroxidase conjugated anti-rabbit polyclonal antibodies, Escherichia coli lipopolysaccharide serotype 0111:B4, 3-(4,5-dimethylthiazolyl-2)-2,5-diphenyltetrazolium bromide (MTT), and 2-chloroethyl ethyl sulphide were obtained from Sigma Chemical Company (St. Louis, MO).

Cell culture and treatments

RAW264.7 murine macrophage-like cells (American Type Culture Collection, Rockville, MD) were cultured at 37°C in a humidified incubator with 5% CO_2 in RPMI-1640 medium with 10% fetal bovine serum, 50 U/ml penicillin and 50 mg/ml streptomycin (GiBcoBRL Grand Island, NY). CEES was used as a fresh (2 week old or less) 50 mM stock solution in dried ethanol. LPS was prepared as a 1 mg/ml stock solution in PBS and stored at -20°C for up to 3 months.

MTT assay

The MTT (3-(4,5-dimethylthiazool-2yl)-2,5-diphenyltetrazolium bromide) assay was performed by a slight modification of the method described by Wasserman et al. [45,46]. Briefly, at the end of each experiment, cultured cells in 96 well plates (with 200 μl of medium per well) were incubated with MTT (20 μl of 5 μg/ml per well) at 37°C for 4 hours. The formazan product was solubilized by addition of 100 μl of dimethyl sulfoxide (DMSO) and 100 μl of 10% SDS in 0.01 M HCl and the OD measured at 575 nm (Molecular Devices SPECTRAmax Plus microplate reader).

Western blot analysis

Cellular protein lysates were prepared as described in the protocol from Transduction Laboratory (Lexington, KY). Briefly, about 10^6 adherent cells were rinsed once with cold PBS and solublized by boiling in 0.1 ml of SDS-PAGE sample buffer for 5 min. Protein concentration was determined by the BCA protein assay (Pierce Chemical Co., Rockford, IL). A 30 μg aliquot of protein was separated via 8% SDS-PAGE and electrotransferred onto a nitrocellulose membrane. Western blotting was performed with a rabbit polyclonal antiserum against the C-terminal (961 to 1144 amino acids) sequence of mouse iNOS (Transduction Lab, Lexington, KY). The protein was detected using an enhanced chemiluminescence kit from Amersham Life Science (Arlington Heights, IL). Murine iNOS (Calbiochem, CA) was used as a positive control.

Determination of NO production

The production of NO, reflecting cellular NO synthase activity, was estimated from the accumulation of nitrite (NO_2^-), a stable breakdown product of NO, in the medium. Nitrite was measured using the Griess reagent according to the method of Green et al. [47]. Briefly, an aliquot of cell culture medium was mixed with an equal volume of Greiss reagent which reacts with nitrite to form an azo-product. Absorbance of the reaction product was determined at 532 nm using a microplate reader (Molecular Devices Microplate Reader). Sodium nitrite was used as a standard to calculate nitrite concentrations.

Intracellular NO measurement

Assays were performed using 96-well tissue culture plates as described by Imrich and Kobzik [17]. The cell density was adjusted to 2×10^5/ml, and a 100 μl aliquot of the cell suspension in media was placed put in each well. CEES and LPS solutions to achieve desired concentrations were added and the plate incubated for 24 h at 37°C in 5% CO_2. Following the removal of media, serum free 1640 RPMI supplemented with 10 mM HEPES containing 20 μM DCFH-DA or 10 μM DAF-2DA (final concentration) was added, and the plates incubated for 2 h at 37°C. Fluorescence intensity (relative fluorescence unit, RFU) was continuously monitored using 485 nm for excitation and 520 nm emission in a florescence microplate reader (FluoStar Microplate Reader, BMG).

Statistical analyses

Data were analyzed by followed with the Scheffe test for significance with $p < 0.05$. Results were expressed as the mean ± SD. In all the Figures, mean values not sharing a common letter are significantly different ($p < 0.05$). Mean values sharing a common letter are not significantly different. The mean values and standard deviations of at least three independent experiments are provided in all the Figures.

Abbreviations

HD, sulphur mustard gas

CEES, 2-chloroethyl ethyl sulphide

LPS, lipopolysaccharide

NO, nitric oxide

iNOS, inducible nitric oxide synthase

NF-κB, nuclear factor kappa B

STAT-1α, signal transducer and activator of transcription-1α

DCF, dichlorofluorescein

DCFH, dichlorofluorescin

DCFH-DA, dichlorofluorescin diacetate

TNF-α, tumor necrosis factor-alpha

IL-1β, interleukin-1 beta

AP2, activating protein 2

MTT, 3-(4,5-dimethylthiazool-2yl)-2,5-diphenyltetrazolium bromide

DMSO, dimethyl sulfoxide

DEM, diethylmaleate

BSO, buthionine sulfoximine

DAF-2DA, 4,5-diaminofluorescein diacetate

Authors' contributions

WLS supervised the overall conduct of the research, which was performed in his laboratory. MQ and HY carried out all of the experimental work in this study and performed the statistical analyses. WLS and VP analyzed the data and drafted the manuscript. MS (along with WLS) conceived of the study, participated in the study design, and provided continuous evaluation of the experimental data. All authors read and approved the final manuscript.

Acknowledgements

This research was supported by two United States Army Medical Research Command Grants: "The Influence of Antioxidant Liposomes on Macrophages Treated with Mustard Gas Analogues", USAMRMC Grant No. 98164001, and "Topical Application of Liposomal Antioxidants for Protection against CEES Induced Skin Damage", USAMRMC Grant No. W81XWH-05-2-0034.

References

1. Smith KJ, Skelton H: **Chemical warfare agents: their past and continuing threat and evolving therapies. Part I of II.** *Skinmed* 2003, **2(4):**215-221.
2. Yourick JJ, Dawson JS, Benton CD, Craig ME, Mitcheltree LW: **Pathogenesis of 2,2'-dichlorodiethyl sulfide in hairless guinea pigs.** *Toxicology* 1993, **84(1-3):**185-197.
3. Elsayed NM, Omaye ST, Klain GJ, Korte DW Jr.: **Free radical-mediated lung response to the monofunctional sulfur mustard butyl 2-chloroethyl sulfide after subcutaneous injection.** *Toxicology* 1992, **72(2):**153-165.
4. Elsayed NM, Omaye ST: **Biochemical changes in mouse lung after subcutaneous injection of the sulfur mustard 2-chloroethyl 4-chlorobutyl sulfide.** *Toxicology* 2004, **199(2-3):**195-206.
5. Kadar T, Turetz J, Fishbine E, Sahar R, Chapman S, Amir A: **Characterization of acute and delayed ocular lesions induced by sulfur mustard in rabbits.** *Curr Eye Res* 2001, **22(1):**42-53.
6. Gross CL, Innace JK, Hovatter RC, Meier HL, Smith WJ: **Biochemical manipulation of intracellular glutathione levels influences**

cytotoxicity to isolated human lymphocytes by sulfur mustard. *Cell Biol Toxicol* 1993, **9(3):**259-267.
7. Atkins KB, Lodhi IJ, Hurley LL, Hinshaw DB: **N-acetylcysteine and endothelial cell injury by sulfur mustard.** *J Appl Toxicol* 2000, **20 Suppl 1:**S125-8.
8. Arroyo CM, Schafer RJ, Kurt EM, Broomfield CA, Carmichael AJ: **Response of normal human keratinocytes to sulfur mustard (HD): cytokine release using a non-enzymatic detachment procedure.** In *Hum Exp Toxicol Volume 18*. Issue 1 ENGLAND ; 1999:1-11.
9. Sabourin CL, Petrali JP, Casillas RP: **Alterations in inflammatory cytokine gene expression in sulfur mustard-exposed mouse skin.** *J Biochem Mol Toxicol* 2000, **14(6):**291-302.
10. Stone WL, Qui M, Smith M: **Lipopolysaccharide enhances the cytotoxicity of 2-chloroethyl ethyl sulfide.** *BMC Cell Biol* 2003, **4(1):**1.
11. Li YH, Yan ZQ, Brauner A, Tullus K: **Activation of macrophage nuclear factor-kappa B and induction of inducible nitric oxide synthase by LPS.** *Respiratory research* 2002, **3:**23.
12. Kleinert H, Pautz A, Linker K, Schwarz PM: **Regulation of the expression of inducible nitric oxide synthase.** *European journal of pharmacology* 2004, **500(1-3):**255-266.
13. Borutaite V, Brown G: **What else has to happen for nitric oxide to induce cell death?** *Biochem Soc Trans* 2005, **33(Pt 6):**1394-1396.
14. Borutaite V, Brown GC: **Nitric oxide induces apoptosis via hydrogen peroxide, but necrosis via energy and thiol depletion.** *Free Radic Biol Med* 2003, **35(11):**1457-1468.
15. Nakai K, Kubota Y, Kosaka H: **Inhibition of nuclear factor kappa B activation and inducible nitric oxide synthase transcription by prolonged exposure to high glucose in the human keratinocyte cell line HaCaT.** *The British journal of dermatology* 2004, **150(4):**640-646.
16. Yamasaki K, Edington HD, McClosky C, Tzeng E, Lizonova A, Kovesdi I, Steed DL, Billiar TR: **Reversal of impaired wound repair in iNOS-deficient mice by topical adenoviral-mediated iNOS gene transfer.** *J Clin Invest* 1998, **101(5):**967-971.
17. Imrich A, Kobzik L: **Fluorescence-based measurement of nitric oxide synthase activity in activated rat macrophages using dichlorofluorescin.** *Nitric Oxide* 1997, **1(4):**359-369.
18. Huang A, Li C, Kao RL, Stone WL: **Lipid hydroperoxides inhibit nitric oxide production in RAW264.7 macrophages.** *Free Radic Biol Med* 1999, **26:**526-537.
19. Schmidt HH, Warner TD, Nakane M, Forstermann U, Murad F: **Regulation and subcellular location of nitrogen oxide synthases in RAW264.7 macrophages.** *Molecular pharmacology* 1992, **41(4):**615-624.
20. Hattori R, Inoue R, Sase K, Eizawa H, Kosuga K, Aoyama T, Masayasu H, Kawai C, Sasayama S, Yui Y: **Preferential inhibition of inducible nitric oxide synthase by ebselen.** *Eur J Pharmacol* 1994, **267(2):**R1-2.
21. Zhang N, Weber A, Li B, Lyons R, Contag PR, Purchio AF, West DB: **An inducible nitric oxide synthase-luciferase reporter system for in vivo testing of anti-inflammatory compounds in transgenic mice.** In *J Immunol Volume 170*. Issue 12 United States ; 2003:6307-6319.
22. Gray PJ: **Sulphur mustards inhibit binding of transcription factor AP2 in vitro.** In *Nucleic Acids Res Volume 23*. Issue 21 ENGLAND ; 1995:4378-4382.
23. Wright SD, Ramos RA, Tobias PS, Ulevitch RJ, Mathison JC: **CD14, a receptor for complexes of lipopolysaccharide (LPS) and LPS binding protein.** *Science* 1990, **249(4975):**1431-1433.
24. Downey JS, Han J: **Cellular activation mechanisms in septic shock.** *Front Biosci* 1998, **3:**d468-76.
25. Chen CC, Wang JK, Lin SB: **Antisense oligonucleotides targeting protein kinase C-alpha, -beta I, or -delta but not -eta inhibit lipopolysaccharide-induced nitric oxide synthase expression in RAW 264.7 macrophages: involvement of a nuclear factor kappa B-dependent mechanism.** In *J Immunol Volume 161*. Issue 11 UNITED STATES ; 1998:6206-6214.
26. Fujihara M, Connolly N, Ito N, Suzuki T: **Properties of protein kinase C isoforms (beta II, epsilon, and zeta) in a macrophage cell line (J774) and their roles in LPS-induced nitric oxide production.** In *J Immunol Volume 152*. Issue 4 UNITED STATES ; 1994:1898-1906.
27. Shapira L, Takashiba S, Champagne C, Amar S, Van Dyke TE: **Involvement of protein kinase C and protein tyrosine kinase in lipopolysaccharide-induced TNF-alpha and IL-1 beta production by human monocytes.** *J Immunol* 1994, **153(4):**1818-1824.
28. Shapira L, Sylvia VL, Halabi A, Soskolne WA, Van Dyke TE, Dean DD, Boyan BD, Schwartz Z: **Bacterial lipopolysaccharide induces early and late activation of protein kinase C in inflammatory macrophages by selective activation of PKC-epsilon.** *Biochem Biophys Res Commun* 1997, **240(3):**629-634.
29. Yoshioka Y, Kitao T, Kishino T, Yamamuro A, Maeda S: **Nitric oxide protects macrophages from hydrogen peroxide-induced apoptosis by inducing the formation of catalase.** *J Immunol* 2006, **176(8):**4675-4681.
30. Harbrecht BG, Di Silvio M, Chough V, Kim YM, Simmons RL, Billiar TR: **Glutathione regulates nitric oxide synthase in cultured hepatocytes.** *Ann Surg* 1997, **225(1):**76-87.
31. Vos TA, Van Goor H, Tuyt L, De Jager-Krikken A, Leuvenink R, Kuipers F, Jansen PL, Moshage H: **Expression of inducible nitric oxide synthase in endotoxemic rat hepatocytes is dependent on the cellular glutathione status.** *Hepatology* 1999, **29(2):**421-426.
32. Buchmuller-Rouiller Y, Corrandin SB, Smith J, Schneider P, Ransijn A, Jongeneel CV, Mauel J: **Role of glutathione in macrophage activation: effect of cellular glutathione depletion on nitrite production and leishmanicidal activity.** *Cell Immunol* 1995, **164(1):**73-80.
33. Powell LA, Warpeha KM, Xu W, Walker B, Trimble ER: **High glucose decreases intracellular glutathione concentrations and upregulates inducible nitric oxide synthase gene expression in intestinal epithelial cells.** *J Mol Endocrinol* 2004, **33(3):**797-803.
34. Gray PJ: **Sulphur mustards inhibit binding of transcription factor AP2.** *Nucleic Acids Research* 1995, **23(Vol. 23):**4378-4382.
35. Gray PJ: **Sulphur mustards inhibit binding of transcription factor AP2 in vitro.** *Nucleic Acids Res* 1995, **23(21):**4378-4382.
36. Chen XM, Gray PJ, Cullinane C, Phillips DR: **Differential sensitivity of transcription factors to mustard-damaged DNA.** *Chemico-biological interactions* 1999, **118(1):**51-67.
37. Fabbri S, Prontera C, Broggini M, D'Incalci M: **Differential inhibition of the DNA binding of transcription factors NF kappa B and OTF-1 by nitrogen mustard and quinacrine mustard: transcriptional implications.** *Carcinogenesis* 1993, **14(9):**1963-1967.
38. Spink J, Cohen J, Evans TJ: **The cytokine responsive vascular smooth muscle cell enhancer of inducible nitric oxide synthase. Activation by nuclear factor-kappa B.** *The Journal of biological chemistry* 1995, **270(49):**29541-29547.
39. Minsavage GD, Dillman 3d JF: **Protective role of CAPE on bifunctional alkylating agent-induced toxicity in keratinocytes via modulation of NF-kappaB, p53 and ARE/EpRE signaling .** In *Bioscience 2006 Medical Defense Review* ; 2006:94-94.
40. Chatterjee D, Mukherjee S, Smith MG, Das SK: **Signal transduction events in lung injury induced by 2-chloroethyl ethyl sulfide, a mustard analog.** *J Biochem Mol Toxicol* 2003, **17(2):**114-121.
41. Schwentker A, Billiar TR: **Nitric oxide and wound repair.** *Surg Clin North Am* 2003, **83(3):**521-530.
42. Weller R: **Nitric oxide: a key mediator in cutaneous physiology.** *Clin Exp Dermatol* 2003, **28(5):**511-514.
43. Witte MB, Barbul A: **Role of nitric oxide in wound repair.** *Am J Surg* 2002, **183(4):**406-412.
44. Soneja A, Drews M, Malinski T: **Role of nitric oxide, nitroxidative and oxidative stress in wound healing.** *Pharmacol Rep* 2005, **57 Suppl:**108-119.
45. Wasserman TH, Twentyman P: **Use of a colorimetric microtiter (MTT) assay in determining the radiosensitivity of cells from murine solid tumors.** *Int J Radiat Oncol Biol Phys* 1988, **15(3):**699-702.
46. Twentyman PR, Luscombe M: **A study of some variables in a tetrazolium dye (MTT) based assay for cell growth and chemosensitivity.** *Br J Cancer* 1987, **56(3):**279-285.
47. Green LC, Wagner DA, Glogowski J, Skipper PL, Wishnok JS, Tannenbaum SR: **Analysis of nitrate, nitrite, and [15N]nitrate in biological fluids.** In *Anal Biochem Volume 126*. Issue 1 UNITED STATES ; 1982:131-138.

BMC Cell Biology

Research article

The influence of N-acetyl-L-cysteine on oxidative stress and nitric oxide synthesis in stimulated macrophages treated with a mustard gas analogue

Victor Paromov[1], Min Qui[1], Hongsong Yang[1], Milton Smith[2] and William L Stone*[1]

Address: [1]Department of Pediatrics, College of Medicine, East Tennessee State University, Johnson City, TN 37614, USA and [2]AMAOX, Ltd., #208, 6300 N. Wickham Road, Melbourne, FL 32944, USA

Email: Victor Paromov - paromov@etsu.edu; Min Qui - qui@etsu.edu; Hongsong Yang - yangh@etsu.edu; Milton Smith - mgsmithmd@gmail.com; William L Stone* - stone@etsu.edu

* Corresponding author

Published: 20 June 2008

BMC Cell Biology 2008, **9**:33 doi:10.1186/1471-2121-9-33

Received: 14 January 2008
Accepted: 20 June 2008

This article is available from: http://www.biomedcentral.com/1471-2121/9/33

Abstract

Background: Sulphur mustard gas, 2, 2'-dichlorodiethyl sulphide (HD), is a chemical warfare agent. Both mustard gas and its monofunctional analogue, 2-chloroethyl ethyl sulphide (CEES), are alkylating agents that react with and diminish cellular thiols and are highly toxic. Previously, we reported that lipopolysaccharide (LPS) significantly enhances the cytotoxicity of CEES in murine RAW 264.7 macrophages and that CEES transiently inhibits nitric oxide (NO) production via suppression of inducible NO synthase (iNOS) protein expression. NO generation is an important factor in wound healing. In this paper, we explored the hypotheses that LPS increases CEES toxicity by increasing oxidative stress and that treatment with N-acetyl-L-cysteine (NAC) would block LPS induced oxidative stress and protect against loss of NO production. NAC stimulates glutathione (GSH) synthesis and also acts directly as a free radical scavenger. The potential therapeutic use of the antibiotic, polymyxin B, was also evaluated since it binds to LPS and could thereby block the enhancement of CEES toxicity by LPS and also inhibit the secondary infections characteristic of HD/CEES wounds.

Results: We found that 10 mM NAC, when administered simultaneously or prior to treatment with 500 μM CEES, increased the viability of LPS stimulated macrophages. Surprisingly, NAC failed to protect LPS stimulated macrophages from CEES induced loss of NO production. Macrophages treated with both LPS and CEES show increased oxidative stress parameters (cellular thiol depletion and increased protein carbonyl levels). NAC effectively protected RAW 264.7 cells simultaneously treated with CEES and LPS from GSH loss and oxidative stress. Polymyxin B was found to partially block nitric oxide production and diminish CEES toxicity in LPS-treated macrophages.

Conclusion: The present study shows that oxidative stress is an important mechanism contributing to CEES toxicity in LPS stimulated macrophages and supports the notion that antioxidants could play a therapeutic role in preventing mustard gas toxicity. Although NAC reduced oxidative stress in LPS stimulated macrophages treated with CEES, it did not reverse CEES-induced loss of NO production. NAC and polymyxin B were found to help prevent CEES toxicity in LPS-treated macrophages.

Background

Mustard gas (HD) is a chemical weapon that can easily and inexpensively be produced and used against military or civilian populations with both acute and devastating long-term effects [1-3]. It produces rapid damage to eyes, skin and pulmonary tissues as well as subsequent damage to many internal organ systems [1,4]. Despite its long history of use, starting in World War I, the molecular mechanisms for HD toxicity are not fully understood and there is continuing research on the design of optimal countermeasures. Mustard gas acts as an alkylating agent covalently modifying DNA, proteins and other macromolecules. There is increasing evidence that HD or CEES toxicity is due, in part, to an enhanced production of inflammatory cytokines [5-9], increased oxidative stress [10] and the generation of damaging reactive oxygen species (ROS) [8,9,11]. HD and CEES have been shown to shift the intracellular redox milieu toward a more oxidized state by reacting with and depleting the intracellular antioxidant GSH with a subsequent loss of protection against ROS and an activation of inflammatory responses [12-14].

In a previous publication, we showed that the cytotoxicity of CEES towards murine RAW 264.7 macrophages was markedly enhanced by the presence of low levels of LPS (25 ng/ml), or pro-inflammatory cytokines, i.e., 50 ng/ml IL-1β or 50 ng/ml TNF-α [15]. LPS is part of the cell wall of gram negative bacteria: it is ubiquitous and is found in serum, tap water and dust. Both civilian and military personnel would always have some degree of exposure to environmental LPS. HD induced skin lesions often have secondary infections which could markedly increase LPS levels. In macrophages, stimulation by LPS, as well as by pro-inflammatory cytokines, leads to the activation and nuclear translocation of transcription factor NF-κB (nuclear factor-kappa B). One of the major consequences of such activation in macrophages is an induction of iNOS expression with subsequent elevation of intracellular NO [16,17]. In addition to NF-κB activation, the binding of transcription factor STAT-1 (signal transducer and activator of transcription-1) to the inducible nitric oxide synthase (iNOS) promoter is required for optimal induction of the iNOS gene by LPS [17].

In a recent publication, we found that CEES transiently inhibits nitric oxide (NO) production by suppressing iNOS protein expression in LPS stimulated macrophages [18]. NO production is an important factor in promoting wound healing [19,20] and iNOS deficiency impairs wound healing in animal models [21]. RAW 264.7 macrophages have undetectable levels of iNOS or NO production in the absence of LPS and in the presence of LPS they show a marked induction of iNOS and NO production [18].

In the present study, we tested the hypothesis that the synergistic cytotoxic effect of CEES with LPS is due to increased oxidative stress with a subsequent depletion of intracellular GSH levels and an increase in protein carbonyls. In some cell types, GSH has also been found to regulate NO generation with decreased GSH levels associated with decreased NO production [22-24]. Vos et al. [25] found that GSH depletion in hepatocytes prevented iNOS induction by cytokines but this effect could be reversed by the addition of NAC. We, therefore, hypothesized that the addition of NAC to stimulated macrophages would reverse the loss of NO production caused by CEES. We also reasoned that polymyxin B, by binding to LPS, would diminish CEES toxicity in LPS treated macrophages.

Results

The influence of NAC on cell viability and NO production in CEES/LPS treated macrophages

Figure 1a shows the effect of NAC treatment on RAW 264.7 macrophages treated with LPS and/or 500 μM CEES for 24 h. In this experiment, NAC was added simultaneously with LPS and CEES. In the absence of NAC, LPS, at either 50 ng/ml or 100 ng/ml level, markedly decreased cell viability in CEES treated cells compared to cells treated with LPS or CEES alone. This is similar to our previous observations in which cell viability was measured by both the MTT assay and the propidium iodide exclusion assay; the assays were well correlated with each other [15]. The addition of 10 mM NAC increased the viability of macrophages treated with both CEES and LPS (50 ng/ml or 100 ng/ml) to the same level observed for control cells (treated with vehicle alone). It is likely that the differences in the viability of cells treated with NAC and different levels of LPS represent experimental variability since these differences are marginal.

Figure 1b shows NO release, measured as the nitrite levels in the cell culture medium, for the identical cells/treatments used in Figure 1a. As expected, LPS treatment alone resulted in a marked increase of NO generation, and LPS-stimulated macrophages treated with CEES showed a marked reduction in NO production. Surprisingly, NAC treatment did not prevent the decrease in NO production caused by CEES. In cells treated with LPS alone, NAC treatment actually resulted in a decreased production of NO (up to 40% reduction).

In order to further evaluate NAC as a potential protective agent for CEES toxicity in stimulated macrophages, we did two additional experiments in which NAC was added to macrophages 5 h prior to CEES application or 5 h after CEES application. These additional experiments provide a measure of the potential time frame during which NAC could be therapeutically useful. Similar to the previous experiment, LPS and CEES were added simultaneously (as

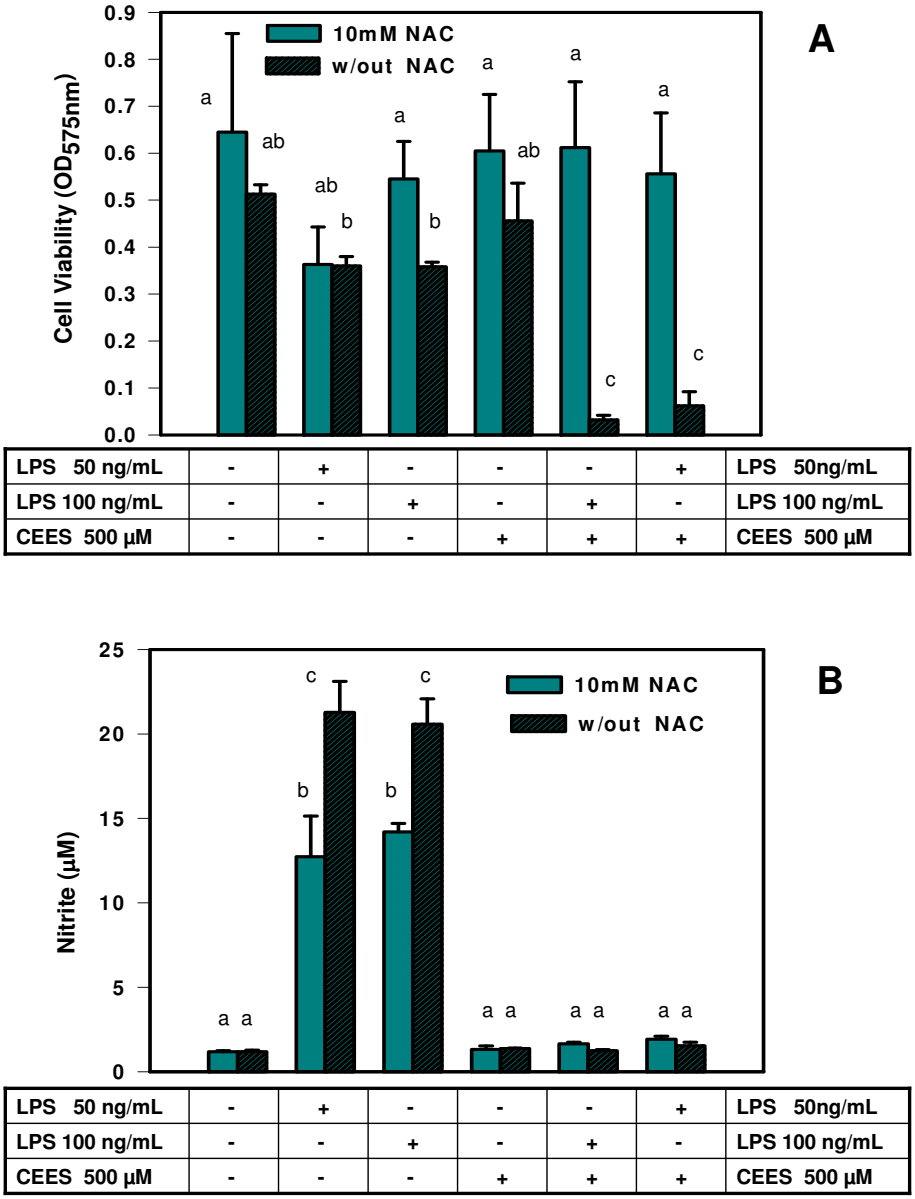

Figure 1

NAC effect on viability and NO production in CEES/LPS treated RAW 264.7 cells (simultaneous NAC/CEES/LPS application). *Panel A:* Macrophages incubated with 50 or 100 ng/ml of LPS or/and 500 μM CEES were simultaneously treated with or without 10 mM NAC (as indicated) for 24 hours. Cell viability was measured using the MTT assay (see Materials and Methods) and expressed as OD at 575 nm. *Panel B:* Macrophages were incubated as described above and NO production measured as the concentration of nitrite in the culture media as described in Materials and Methods. Mean values not sharing a common letter are significantly different ($p < 0.05$).

indicated). As shown in Figure 2a, NAC had a substantial protective effect on cell viability when added 5 h before CEES/LPS; however NAC did not protect against loss of NO production in CEES/LPS-treated cells (Figure 2b). When added 5 h after CEES treatment (Figure 3a), NAC was much less effective in protecting the macrophages but still resulted in at least a doubling of the cell viability compared to the cells not treated with NAC. As shown in Figure 3b, NAC added 5 h after CEES/LPS, also failed to restore NO production.

We believe that the difference in viability of cells stimulated with LPS in the absence or in the presence of NAC (Figure 2A) could represent experimental variation since

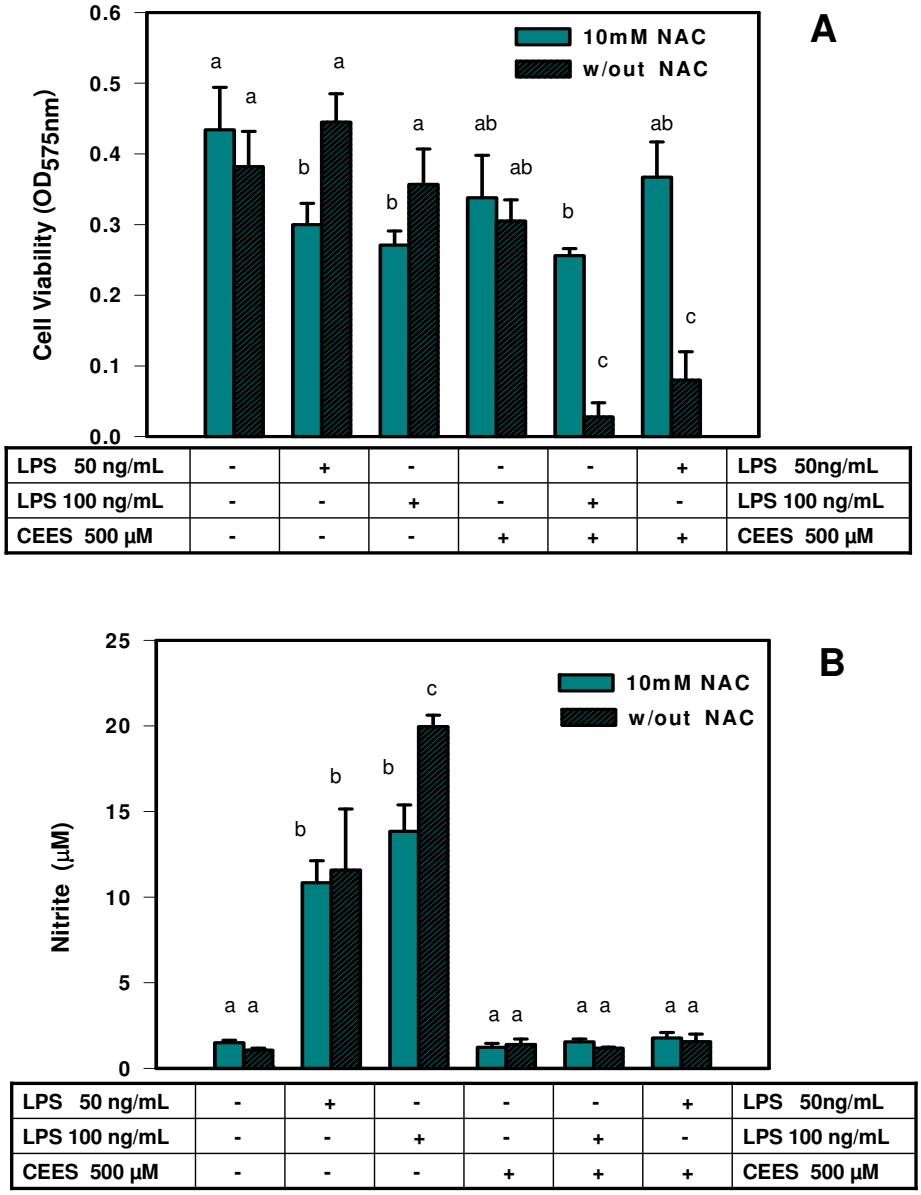

Figure 2

NAC effect on viability and NO production in CEES/LPS incubated RAW 264.7 cells (NAC pre-treatment). *Panel A:* Macrophages were pre-treated with or without 10 mM NAC for 5 hours and then incubated with 50 or 100 ng/ml of LPS or/and 500 μM CEES (as indicated) for 24 hours. Cell viability was measured using the MTT assay (see Materials and Methods) and expressed as OD at 575 nm. *Panel B:* Macrophages were incubated as described above and NO production measured as concentration of nitrite in the culture media as described in Materials and Methods. Mean values not sharing a common letter are significantly different ($p < 0.05$).

relatively small differences are being compared. In the contrast, the protective effect of NAC on CEES+LPS treated macrophages is robust and over seven fold. This point is further reinforced by the data shown in Figure 3A, where viability of cells stimulated with LPS in the absence or in the presence of NAC was not significantly different.

The influence of NAC on oxidative stress and NO production, intracellular GSH and thiols in CEES/LPS treated macrophages by fluorescence microscopy

The influence of NAC on macrophages treated with CEES/LPS was also examined by fluorescent microscopy using three fluorescent probes: a) carboxy-dichlorofluorescin

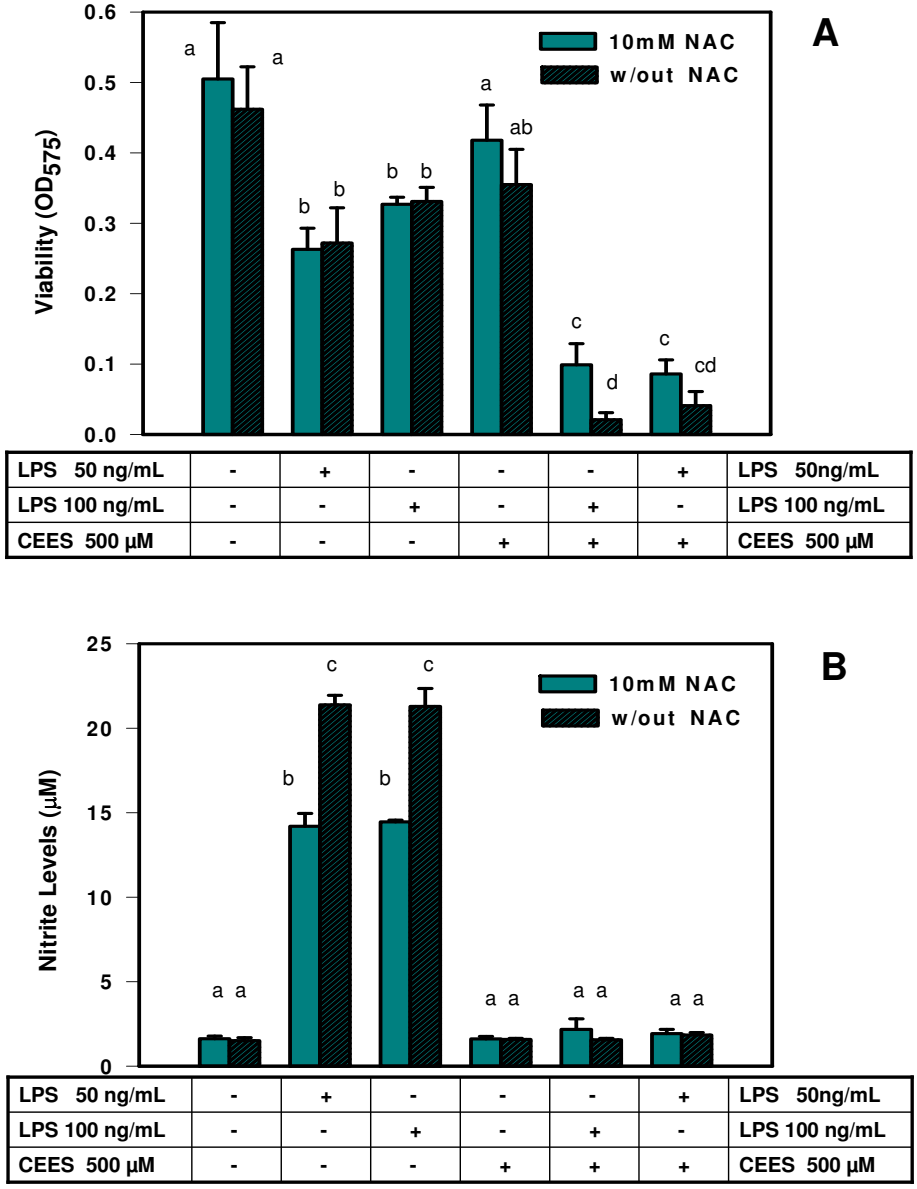

Figure 3

NAC effect on viability and NO production in CEES/LPS treated RAW 264.7 cells (NAC post-treatment). *Panel A:* Macrophages were incubated with 50 or 100 ng/ml of LPS or/and 500 μM CEES (as indicated) for 24 hours and 10 mM NAC was added to the cell culture medium 5 hours after the CEES/LPS application. Cell viability was measured using the MTT assay (see Materials and Methods) and expressed as OD at 575 nm. *Panel B:* Macrophages were incubated as described above and NO production measured as concentration of nitrite in the culture media as described in Materials and Methods. Mean values not sharing a common letter are significantly different ($p < 0.05$).

diacetate (carDCFH-DA), a sensor for combined ROS and reactive nitrogen oxide species (RNOS) generation [26-28]; b) 7-amino-4-chloromethylcoumarin (CMAC), an indicator of intracellular GSH [29], and; c) 5-chloromethylfluorescein diacetate (CMF-DA), a probe for total non-protein cellular thiol levels that lacks specificity for GSH [29,30].

Figure 4a shows the results using the lipid soluble carDCFH-DA probe. This probe enters cells and is trapped after being converted to a nonfluorescent polar derivative by cellular esterases. CarDCFH can then be oxidized by either ROS [26,28] or reactive nitrogen oxide species (RNOS) [26,27] to the fluorescent product carboxydichlorofluorescein (car-DCF) and thereby provide a qualitative index

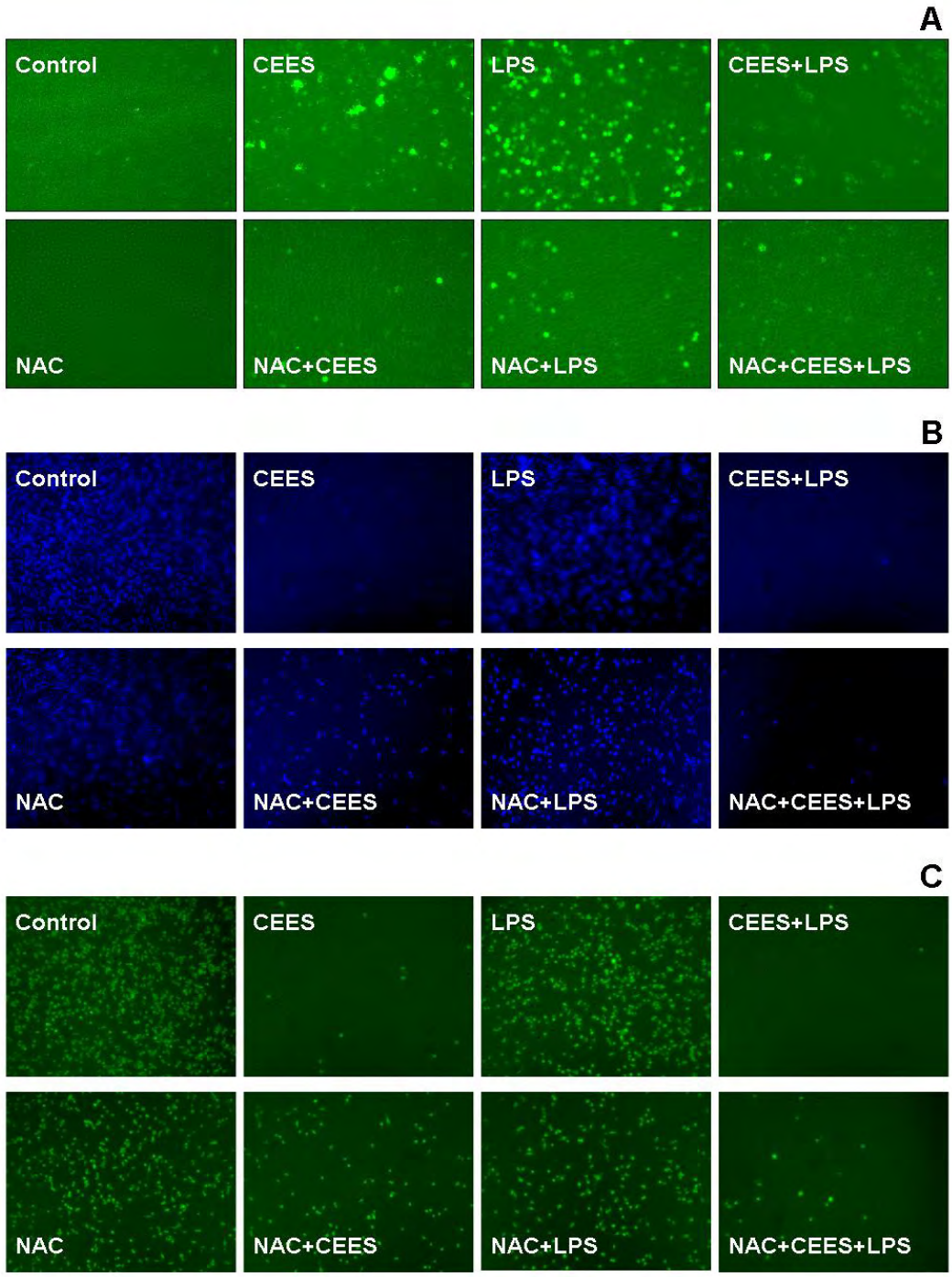

Figure 4

Fluorescent microscopy probes for oxidative stress, GSH and total thiols in RAW 264.7 cells. *Panel A*: Combined generation of ROS and RNOS were monitored using 20 μM carDCFH-DA; *Panel B*: Intracellular GSH levels were examined using 20 μM CMAC; *Panel C*: Levels of non-protein cellular thiols were monitored using 20 μM CMF-DA under a fluorescent microscope. Macrophages were treated with CEES (500 μM) and/or LPS (50 ng/mL) and incubated in the absence of NAC (top row in each panel) or in the presence of 10 mM NAC for 12 h.

of oxidation stress. As expected, treatment with LPS alone (50 ng/ml for 12 h) induced a marked generation of ROS plus RNOS in macrophages. We and others have shown that car-DCF fluorescence in activated macrophages is almost entirely from NO generation rather than ROS generation [18,27]. Figure 4a also shows that a 12 h treatment with CEES alone (500 μM) or simultaneous treatment with 500 μM CEES and 50 ng/ml LPS (CEES+LPS) induces a higher level of car-DCF fluorescence than observed in control cells treated with vehicle alone. We previously reported that CEES markedly reduces NO generation in LPS stimulated cells by reducing the expression of inducible iNOS [18]. The car-DCF fluorescence observed in CEES treated cells or CEES+LPS cells is likely, therefore, to be due to an enhanced generation of ROS alone with a minimal contribution from RNOS.

Simultaneous treatment with 10 mM NAC reduced the car-DCF fluorescence observed in LPS stimulated cells, as well as in CEES or CEES+LPS treated RAW 264.7 macrophages (Figure 4a, compare top row to bottom row). These data qualitatively suggest that CEES and CEES+LPS treatments induce oxidative stress in RAW 264.7 macrophages that can be diminished by NAC treatment.

As a next step we examined intracellular levels of GSH using the CMAC probe (Figure 4b, top row) and levels of total intracellular thiols using the CMF-DA probe (Figure 4c, top row). Both the CMAC and CMF probes revealed similar qualitative patterns: CEES or CEES+LPS treatment for 12 h caused cellular GSH and thiol depletion but treatment with LPS alone did not. These data reinforce the notion that treatment with either CEES alone or treatment with CEES+LPS induces sufficient oxidative stress to reduce intracellular GSH and thiol levels. LPS alone, however, did not induce GSH or thiol depletion. NAC application was found to inhibit the loss of GSH and thiol levels caused by CEES or CEES+LPS treatment (see Figures 4b and 4c, bottom rows).

The microscopic data (Figure 4) show merged visible/fluorescent images, thus allowing cell counting and the monitoring of cell morphology changes. The counts of live (morphologically unchanged) cells under conditions described above (Figure 4) confirmed the major observations from the MTT-derived data (Figure 1a): (1) NAC treatment enhance (3-fold) the viability of CEES+LPS treated macrophages; (2) CEES+LPS is more toxic than CEES alone. The cells count (as percentage of untreated control cells ± SEM) were 57% ± 7, 76% ± 10, 18% ± 4, 84% ± 8, 75% ± 9, 67% ± 6, 54% ± 10, respectively for macrophages treated with CEES (500 μM), LPS (50 ng/ml), CEES+LPS, NAC (10 mM), NAC+CEES, NAC+LPS and NAC+CEES+LPS.

Quantitative effects of CEES on GSH status and protein carbonyl levels in LPS-stimulated RAW 264.7 macrophages

Since the fluorescence microscopy data presented above are primarily qualitative, we wanted to confirm our results by a more quantitative approach. We, therefore, determined the effect of 500 μM CEES on the GSH/GSSG status of RAW 264.7 macrophage treated or untreated with 50 ng/ml LPS for 12 h. Total GSH (GSH+GSSG) and GSSG concentrations were measured in cell lysates using a quantitative GSH assay kit and the values normalized to total protein content of the lysate (see Materials and Methods). Figure 5 shows that both total GSH and GSSG levels in macrophages treated with either vehicle alone or LPS were

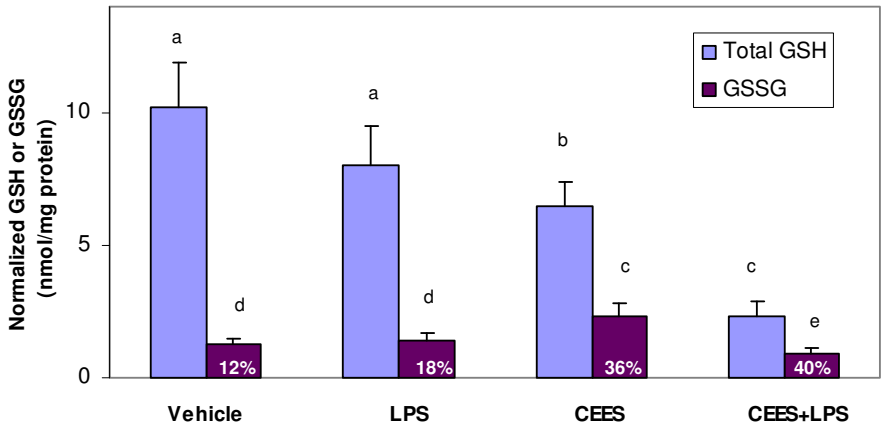

Figure 5
Glutathione status in RAW 264.7 cells incubated with CEES/LPS. Macrophages were incubated with 50 ng/ml LPS or/and 500 μM CEES for 12 h. Total GSH (GSH+GSSG) and GSSG levels were measured using a GSH assay kit (see Materials and Methods section) in cell lysates and normalized to total protein. Numbers show the percentage of GSSG in total GSH. Mean values not sharing a common letter are significantly different ($p < 0.05$).

not significantly different, i.e., similar to our fluorescent microscopy data. However, cells treated with CEES alone showed a depletion in total GSH as well as an increase in GSSG levels; cells treated with both CEES and LPS were further depleted in total GSH and the percentage of GSSG in these cells was the highest (40%). These results show that LPS alone does not induce a significant oxidative stress, CEES alone induces a moderate oxidative stress but the combination of both CEES and LPS induces the highest observed level of oxidative stress.

In addition, we measured the protein carbonyl levels in control cells, cells treated with CEES (500 μM) alone or cells simultaneously treated with both LPS (50 ng/ml) and CEES (500 μM) for 12 h. Protein carbonyls are stable protein oxidation products. The combination of CEES and LPS produced about 1.5 fold increase in protein carbonyl levels, however cells treated with CEES alone were not significantly different from control cells treated with vehicle alone (data not shown). Cells treated with LPS alone were not assayed in this experiment since both our qualitative (Figure 4b and 4c) and quantitative data (Figure 5) showed no evidence of oxidative stress with this treatment.

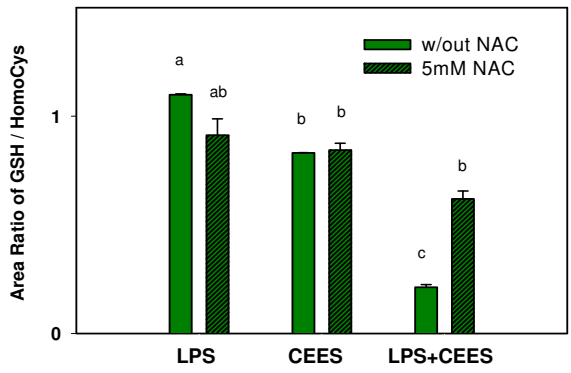

Figure 6
NAC restores intracellular GSH in RAW 264.7 cells incubated with CEES/LPS. Macrophages incubated with 50 ng/ml LPS or/and 500 μM CEES were simultaneously treated with or without 5 mM NAC (as indicated). Cell lysates were measured for reduced GSH after 4 hour incubation using the HPLC technique described in Materials and Methods. The GSH levels were normalized to an internal homocysteine standard. Mean values not sharing a common letter are significantly different ($p < 0.05$).

The inability of NAC to reverse NO loss in CEES/LPS treated cells is not GSH dependent

The data in Figure 1b show that NAC has almost no ability to restore NO production in LPS-stimulated macrophages treated with CEES. An inability of NAC to prevent the depletion of GSH in LPS-stimulated cells treated with CEES could possibly explain these results. In order to explore this possibility, we examined the ability of 5 mM NAC to prevent GSH depletion in LPS (50 ng/ml) stimulated and CEES treated (500 μM for 4 h) RAW 264.7 cells. Figure 6 shows that CEES treatment alone decreased intracellular GSH by only about 10% compared to LPS stimulated cells in the absence NAC. As expected, the decrease in GSH levels was quite large in cells treated with both CEES+LPS (in the absence of NAC) but treatment with 5 mM NAC was effective in preventing this loss. The data shown in Figure 6 were obtained by HPLC analyses of the cell lysates but similar results were obtained by using a fluorometric assay for GSH [31] (data not shown). Despite the fact that NAC can increase the GSH level by three fold in CEES+LPS treated cells it does almost nothing to increase NO production (Figure 1a). These data suggest that the loss of NO production in CEES treated stimulated macrophages is not GSH dependent as has been observed in some other cell lines [22-25].

Polymyxin B diminishes CEES toxicity in LPS-treated macrophages and partially blocks LPS induced NO production

Polymyxin B is an antibiotic drug, which selectively binds and neutralizes LPS. Since LPS enhances CEES toxicity, we tested the ability of polymyxin B to reduce CEES toxicity (500 μM) and decrease NO generation in LPS (50 ng/ml) stimulated macrophages. Figure 7a shows that polymyxin B (10 μg/ml) had no cytotoxic effect on RAW 264.7 macrophages but partially reduced the cytotoxicity of CEES+LPS treated cells (18 h). Nevertheless, polymyxin B produced at least a six fold increase in cell viability compared to cell treated with both LPS and CEES for 18 h. As shown in Figure 7b, polymyxin B effectively blocked the production of NO (measured as nitrite levels) in LPS (50 ng/ml for 18 h) treated macrophages as would be expected if it bound and blocked the action of LPS.

Discussion

The cytotoxic effect of HD, and its analogue CEES, is believed to involve an increased generation of damaging free radicals and ROS [8,11-13,32]. The data presented here show that LPS in combination with CEES induces intracellular GSH and thiol depletion as well as increased levels of protein carbonyls. In experiments with various human cell lines we have found that GSH depletion is relatively rapid as it occurs within first hour of incubation (data not shown). Thus, it is likely that this depletion is due, in large part, by a direct reaction of CEES with GSH. The measurement of protein carbonyls is one of the best

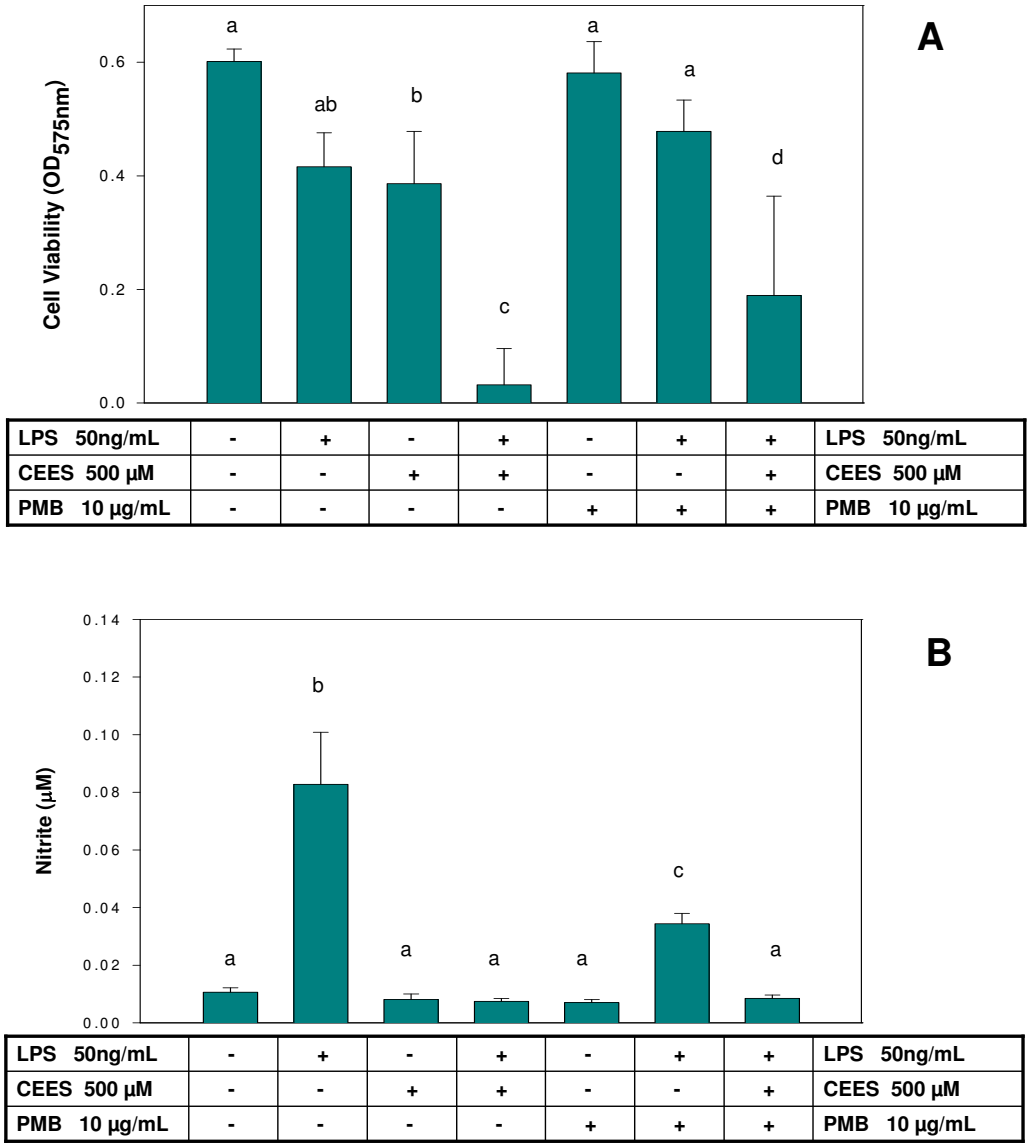

Figure 7

Polmyxin B partially protects LPS stimulated RAW 264.7 cells from CEES toxicity and blocks NO production. *Panel A*: Macrophages incubated with 50 ng/ml LPS or/and 500 μM CEES were simultaneously treated with or without 10 μg/mL polymyxin B (as indicated) for 18 hours. Cell viability was measured using the MTT assay (see Materials and Methods) and expressed as OD at 575 nm. *Panel B:* Macrophages were incubated as described above. NO production was measured as nitrite concentration in the culture media as described in Materials and Methods. Mean values not sharing a common letter are significantly different ($p < 0.05$).

indices for oxidative stress due to the stability of protein carbonyls and sensitivity of the measurement [33]. Cellular thiols are important markers of the redox state of the cell. In particular, GSH is one of the major components of the intracellular redox system and a key intracellular antioxidant that functions as a substrate for glutathione peroxidase which detoxifies both hydrogen peroxide and lipid hydroperoxides [34,35]. Depletion of intracellular stores of GSH plays an important role in the development of oxidative stress [12,13,36]. Recent work also suggests that the anti-apoptotic protein Bcl-2 directly interacts with GSH to regulate an important mitochondrial GSH pool that influences mitochondrial oxidative stress and subsequent apoptosis [37]. It is highly possible that both sulphur and nitrogen mustards possess a similar ability to deplete cellular thiols and induce protein oxidation.

Taken together, our data strongly suggest that CEES induces oxidative stress in stimulated macrophages. Moreover, the pattern of oxidative stress parallels the pattern observed for CEES cytotoxicity, i.e., cytotoxicity and oxidative stress are amplified in cells treated with both CEES and LPS. The addition of 5–10 mM NAC, a well characterized water-soluble antioxidant, was found to be very effective in minimizing CEES toxicity in stimulated macrophages and in preventing GSH depletion. Our data suggests that NAC can be added five hours before or even five hours after CEES and still exert a cytoprotective effect. Das et al. [9] recently found that NAC in drinking water was effective in reducing CEES-induced lung toxicity to Guinea pigs. Fan et al. [38] have shown that liposomal encapsulated NAC delivered intratracheally was more effective than free NAC against acute respiratory distress syndrome in a rat model. It is interesting, therefore, that McClintock et al. [39] have shown that reducing agents (NAC or GSH), as well as some anti-oxidant enzymes, delivered via liposomes, can substantially diminish CEES-induced injury in rat lungs. We are currently formulating an optimal antioxidant liposome preparation for treating either lung or skin induced CEES/HD injury.

We previously reported that CEES induces a transient loss of iNOS protein expression in LPS stimulated RAW 264.7 macrophages but does not inhibit the enzymatic activity of iNOS. Based of the work of others [22-25], we hypothesized that NAC treatment would not only be protective against CEES toxicity but would also restore NO production in LPS stimulated macrophages treated with CEES. Our results indicate, however, that this was not the case. Our data did, however, show that NAC effectively increases cell viability, increases GSH levels and reduces oxidative stress in LPS stimulated macrophages treated with CEES.

CEES could inhibit iNOS protein synthesis by a number of possible molecular mechanisms which we are currently exploring [18]. It is generally accepted that both the transcription factor NF-κB and STAT-1 play central roles in the LPS induction of iNOS [17,40]. It is possible that CEES/HD could inhibit the NF-κB and/or the STAT-1 pathways in RAW 264.7 macrophages and consequently block iNOS gene expression. For instance, CEES could alkylate the NF-κB consensus nucleotide binding sequences thereby preventing the binding of activated NF-κB to the iNOS promoter and block the subsequent production of iNOS mRNA and protein expression. Previous studies *in vitro* have shown that DNA alkylation by CEES [41,42] or by nitrogen mustard [43] can inhibit the DNA binding of transcription factor AP2 or NF-κB.

Alternatively, the DNA binding ability of the NF-κB and/or STAT-1 transcription factors could be reduced by direct covalent modification by CEES or as an indirect result of GSH depletion, i.e., redox regulation. Nishi et al. [44] have found, for example, that the cysteine-62 (Cys-62) residue of the p50 NF-κB protein subunit is oxidized in the cytoplasm but reduced in the nucleus, and that the reduced form is essential for NF-κB DNA binding. It is possible that CEES could rapidly react with Cys-62 of the p50 NF-κB subunit and prevent its DNA binding. However, since NAC was found to restore GSH levels without restoring iNOS activity (see Figures 1 and 7), it is unlikely that a GSH redox modulation of the p50 Cys-62 is the molecular mechanism for CEES induced loss of iNOS protein in LPS-stimulated macrophages. This cannot, however, be completely ruled out based on our current data.

Moreover, there is evidence suggesting that alkylating agents do not inhibit but rather promote NF-κB activation. It is known that CEES or HD treated cells release elevated levels of TNF-α and also show NF-κB activation both *in vitro* and *in vivo* as measured by electrophoretic mobility shift assays (EMSAs)[7,45,46]. Minsavage and Dillman recently demonstrated that NF-κB is activated by HD treatment in human cell lines via nonclassical p53-dependent pathway [47]. Collectively, these data suggest that the inhibition of iNOS expression by CEES or HD could be due to downregulation of the STAT-1 and/or classical NF-κB pathway. We are currently exploring these various molecular mechanisms.

In the work presented here, we also tested the ability of polymyxin B to block the effect of LPS. Polymyxin B binds to the lipid A domain of LPS and neutralizes its activity. Our data show that polymyxin B effectively inhibits CEES toxicity in LPS stimulated cells. *In vivo*, LPS could directly enhance CEES/HD toxicity in cells with functional CD14 receptors or by triggering the release of pro-inflammatory cytokines, such as TNF-α and IL-1β, by immune cells. We have previously demonstrated that inflammatory cytokines also enhance CEES cytotoxicity [15].

Conclusion

Our *in vitro* work presents novel evidence supporting the view that oxidative stress is an important component of CEES/HD toxicity and that antioxidants have therapeutic potential. We anticipated that NAC would prevent GSH depletion and restore the loss of iNOS activity in CEES treated macrophages stimulated with LPS. Although NAC was effective in preventing both CEES toxicity and GSH depletion, it failed to restore iNOS expression. Our results to date indicate that CEES causes a transient decrease in iNOS protein syntheses rather than a direct inhibition of iNOS activity due to covalent modification(s) by CEES. We are currently investigating the molecular mechanism(s) for the down regulation of iNOS expression by CEES.

Inhibition of iNOS and NO production could be an important element in the slow wound healing observed subsequent to CEES/HD injury. Considerable evidence suggests that iNOS is an important component of wound healing [19,20,48]. Although NAC maybe effective at reducing CEES/HD toxicity it is not effective at elevating NO production due to iNOS inhibition by CEES/HD. A more detailed understanding of the molecular mechanism(s) responsible for iNOS inhibition by CEES/HD could, therefore, be useful in the design of more effective countermeasures.

The fact that LPS was found to enhance CEES toxicity highlights the potential importance of preventing secondary infection in the treatment of HD toxicity.

LPS is a component of gram negative bacteria and a ubiquitous environmental contaminant. Its presence at very low levels (ng/ml) amplifies the toxicity of CEES. Polymyxin B, a topically applied antibiotic that binds LPS, was shown to block the iNOS inducing ability of LPS and to reduce CEES toxicity in LPS stimulated cells. Polymyxin B could, therefore, be useful as a supportive treatment in order to prevent secondary infections and to reduce HD toxicity, since it both neutralizes LPS and prevents the growth of gram-negative bacteria in healing wounds.

The path to an optimal countermeasure to CEES/HD exposure may lie in a poly-drug formulation that minimizes oxidative stress, prevents inflammation and secondary infections, and, also, protects iNOS activity. Antioxidant liposomes are currently being investigated as they have unique ability for targeted delivery of both water-soluble and lipid soluble antioxidants [49] or other drugs, for instance, polymyxin B (personal communications, Dr. Zach Suntres) as well as anti-inflammatory agents.

Methods

Materials

RPMI-1640 medium without phenol red and fetal bovine serum with a low endotoxin level were purchased from Life Technologies (Gaithersburg, MD). *Escherichia coli* lipopolysaccharide serotype 0111:B4, 3-(4,5-dimethylthiazolyl-2)-2,5-diphenyltetrazolium bromide (MTT), CEES, NAC, Greiss reagent, GSH, BHT, EDTA, and all organic solvents used were obtained from Sigma Chemical Company (St. Louis, MO). Fluorescent dyes carDCFH-DA, CMAC, and CMF-DA were purchased from Molecular Probes (Invitrogen Corp., Carlsbad, CA).

Cell culture and treatments

RAW264.7 murine macrophage-like cells (American Type Culture Collection, Rockville, MD) were cultured at 37°C in a humidified incubator with 5% CO_2 in RPMI-1640 medium with 10% fetal bovine serum, 100 U/ml penicillin and 100 mg/ml streptomycin (GiBcoBRL Grand Island, NY). Adherent cells were subcultured in 96 well Costar tissue culture plates and treated with CEES and/or LPS in the presence or absence of various concentrations of NAC as indicated in the Figure legends. CEES was used only as a fresh 50 mM stock solution in anhydrous ethanol. LPS was prepared as a 0.5 μg/ml stock solution in PBS, filter-sterilized and stored at -20°C for up to 6 months. NAC was prepared as a 0.5 M stock solution in PBS (pH adjusted to 7.4), filter-sterilized and stored at 4°C for up to two weeks.

MTT assay

MTT assay was performed by a slight modification of the method described by Wasserman et al. [50,51]. Briefly, at the end of each experiment, cultured cells in 96 well plates (with 200 μl of medium per well) were incubated with MTT (20 μl of 5 μg/ml per well) at 37°C for 4 h. The formazan product was solubilized by addition of 100 μl of dimethyl sulfoxide (DMSO) and the OD measured at 575 nm with a Spectramax Plus 384 microplate reader (Molecular Devices Corp, Sunnyvale, CA)

NO generation in RAW264.7 macrophages

The production of NO, reflecting cellular NO synthase activity, was estimated from the accumulation of nitrite (NO_2^-), a stable breakdown product of NO, in the medium. NO_2^- was assayed by the method of Green et al. [52]. Briefly, an aliquot of cell culture medium was mixed with an equal volume of Greiss reagent which reacts with NO_2^- to form an azo-product. Absorbance of the reaction product was determined at 532 nm using a Spectramax Plus 384 microplate reader (Molecular Devices Corp, Sunnyvale, CA). Sodium nitrite was used as a standard to calculate NO_2^- concentrations.

Quantitative GSH analyses

RAW264.7 macrophages incubated in 96-well plate (~10^6 adherent cells/well) and treated with LPS/CEES/NAC as indicated in the Figure legends was assayed for total GSH (GSH plus GSSG) using the GSH assay kit (World Precision Instruments, Sarasota, FL) according to the company's protocol. This assay uses the Tietze's enzymatic recycling method [53]. In order to measure just GSSG, 2-vinylpyridine was first used to derivatize GSH alone [54]. Total GSH and GSSG levels were normalized to the total protein (as determined by the standard BCA assay). Alternatively, GSH analyses of the cell lysates were analyzed by isocratic HPLC with electrochemical detector composed of Coulochem II model 5200A and a Coulochem 5011 analytical cell (ESA Inc, Chelmsford, MA) as described by [55]. Since the cell lysates contained no measurable levels of homocysteine, this aminothiol was used as an internal standard.

Protein carbonyl measurement

Protein carbonyl levels were measured by an enzyme immunoassay kit from Cell Biolabs (San Diego, CA) according to the manufacture's instructions. In this assay, the protein samples are derivatized by making use of the reaction between 2,4-dinitrophenylhydrazine (DNPH) and protein carbonyls to form a DNP hydrazone which is assayed using an anti-DNP antibody and a HRP conjugated secondary antibody. A standard curve from the oxidized BSA standards was run with each microplate. This kit assay is essentially a modification [56] of the method described by Buss et al. [57].

Fluorescent microscopic analyses

The cell density was adjusted to 2×10^5/ml, and a 100 μl aliquot of the cell suspension in media was placed in each well of an 8-well Lab-Tek chamber glass slide (Nunc, Rochester, NY). Vehicle alone, CEES alone (500 μM), CEES+LPS (50 ng/ml) in the presence or absence of NAC (10 mM) were simultaneously added to chamber slides and incubated for 12 h at 37°C in 5% CO_2. At the end of the treatment a stock solution of desired fluorescent probe in DMSO was added and the slides incubated for an additional 30 min at 37°C. The cells were washed with fresh PBS twice, observed and digitally photographed using a MOTIC inverted phase contrast fluorescence microscope equipped with a Nikon Coolpix E4300 4-megapixel camera (Martin Microscope, Easley, SC). A 20 μM carDCFH-DA and a standard FITC filter were used to monitor combined ROS and RNOS generation; a 20 μM CMAC and a standard DAPI filter were used to monitor intracellular GSH; a 20 μM CMF-DA and a standard FITC filter were used to monitor cellular thiol levels. All the optical filters were obtained from Chroma Technology Corp (Rockingham, VT).

Statistical analyses

Data were analyzed ANOVA followed with the Scheffe test for significance with $p < 0.05$ using SPSS 14.0 for Windows (Chicago, IL). Results were expressed as the mean ± SD. In all the Figures, mean values not sharing a common letter are significantly different ($p < 0.05$). Mean values sharing a common letter are not significantly different. The mean values and standard deviations of at least three independent experiments are provided in all the Figures.

Abbreviations

AP2, activating protein 2; CEES, 2-chloroethyl ethyl sulphide; carDCFH-DA, carboxy-dichlorofluorescin diacetate; CMAC, 7-amino-4-chloromethylcoumarin; CMF-DA, 5-chloromethylfluorescein diacetate; DNPH, 2,4-dinitrophenylhydrazine; GSH, reduced glutathione; GSSG, oxidized glutathione; HD, sulphur mustard gas; IL-1β, interleukin-1 beta; LPS, lipopolysaccharide; MTT, 3-(4,5-dimethylthiazool-2yl)-2,5-diphenyltetrazolium bromide; NAC, N-acetyl-L-cysteine; NO, nitric oxide; iNOS, inducible nitric oxide synthase; NF-κB, nuclear factor kappa B; RNOS, reactive nitrogen oxide species; ROS, reactive oxygen species; STAT-1, signal transducer and activator of transcription-1; TNF-α, tumor necrosis factor-alpha

Authors' contributions

VP and WLS analyzed the data and drafted the manuscript. WLS supervised the overall conduct of the research, which was performed in his laboratory. VP, MQ and HY carried out the experimental work in this study and performed the statistical analyses. MS (along with WLS) conceived of the study, participated in the study design, and provided continuous evaluation of the experimental data. All authors read and approved the final manuscript.

Acknowledgements

This research was supported by three United States Army Medical Research Command (USAMRMC) Grants: "The Influence of Antioxidant Liposomes on Macrophages Treated with Mustard Gas Analogues", Grant No. 98164001; "Topical Application of Liposomal Antioxidants for Protection against CEES Induced Skin Damage", Contract No. W81XWH-05-2-0034 and; "A Proteomic Approach for Studying the Therapeutic Use of Antioxidant Liposomes", Contract No. W81XWH-06-2-044.

References

1. Paromov V, Suntres Z, Smith M, Stone WL: **Sulfur mustard toxicity following dermal exposure: role of oxidative stress, and antioxidant therapy.** *J Burns Wounds* 2007, **7:**e7.
2. Balali-Mood M, Hefazi M: **The pharmacology, toxicology, and medical treatment of sulphur mustard poisoning.** *Fundam Clin Pharmacol* 2005, **19(3):**297-315.
3. Smith KJ, Casillas R, Graham J, Skelton HG, Stemler F, Hackley BE Jr.: **Histopathologic features seen with different animal models following cutaneous sulfur mustard exposure.** *Journal of dermatological science* 1997, **14(2):**126-135.
4. Dacre JC, Goldman M: **Toxicology and pharmacology of the chemical warfare agent sulfur mustard.** *Pharmacological reviews* 1996, **48(2):**289-326.
5. Arroyo CM, Burman DL, Kahler DW, Nelson MR, Corun CM, Guzman JJ, Smith MA, Purcell ED, Hackley BE Jr., Soni SD, Broomfield CA: **TNF-alpha expression patterns as potential molecular biomarker for human skin cells exposed to vesicant chemical warfare agents: sulfur mustard (HD) and Lewisite (L).** *Cell biology and toxicology* 2004, **20(6):**345-359.
6. Arroyo CM, Schafer RJ, Kurt EM, Broomfield CA, Carmichael AJ: **Response of normal human keratinocytes to sulfur mustard (HD): cytokine release using a non-enzymatic detachment procedure.** In *Human & experimental toxicology Volume 18*. Issue 1 ENGLAND ; 1999:1-11.
7. Arroyo CM, Schafer RJ, Kurt EM, Broomfield CA, Carmichael AJ: **Response of normal human keratinocytes to sulfur mustard: cytokine release.** In *J Appl Toxicol Volume 20 Suppl 1*. England ; 2000:S63-72.
8. Arroyo CM, Von Tersch RL, Broomfield CA: **Activation of alpha-human tumour necrosis factor (TNF-alpha) by human monocytes (THP-1) exposed to 2-chloroethyl ethyl sulphide (H-MG).** In *Hum Exp Toxicol Volume 14*. Issue 7 ENGLAND ; 1995:547-553.
9. Das SK, Mukherjee S, Smith MG, Chatterjee D: **Prophylactic protection by N-acetylcysteine against the pulmonary injury induced by 2-chloroethyl ethyl sulfide, a mustard analogue.** *Journal of biochemical and molecular toxicology* 2003, **17(3):**177-184.
10. Mukhopadhyay S, Rajaratnam V, Mukherjee S, Smith M, Das SK: **Modulation of the expression of superoxide dismutase gene in**

lung injury by 2-chloroethyl ethyl sulfide, a mustard analog. *Journal of biochemical and molecular toxicology* 2006, **20(3):**142-149.
11. Elsayed NM, Omaye ST, Klain GJ, Korte DW Jr.: **Free radical-mediated lung response to the monofunctional sulfur mustard butyl 2-chloroethyl sulfide after subcutaneous injection.** *Toxicology* 1992, **72(2):**153-165.
12. Elsayed NM, Omaye ST: **Biochemical changes in mouse lung after subcutaneous injection of the sulfur mustard 2-chloroethyl 4-chlorobutyl sulfide.** *Toxicology* 2004, **199(2-3):**195-206.
13. Han S, Espinoza LA, Liao H, Boulares AH, Smulson ME: **Protection by antioxidants against toxicity and apoptosis induced by the sulphur mustard analog 2-chloroethylethyl sulphide (CEES) in Jurkat T cells and normal human lymphocytes.** *British journal of pharmacology* 2004, **141(5):**795-802.
14. Naghii MR: **Sulfur mustard intoxication, oxidative stress, and antioxidants.** *Mil Med* 2002, **167(7):**573-575.
15. Stone WL, Qui M, Smith M: **Lipopolysaccharide enhances the cytotoxicity of 2-chloroethyl ethyl sulfide.** *BMC cell biology* 2003, **4(1):**1.
16. Ganster RW, Taylor BS, Shao L, Geller DA: **Complex regulation of human inducible nitric oxide synthase gene transcription by Stat 1 and NF-kappa B.** *Proceedings of the National Academy of Sciences of the United States of America* 2001, **98(15):**8638-8643.
17. Gao J, Morrison DC, Parmely TJ, Russell SW, Murphy WJ: **An interferon-gamma-activated site (GAS) is necessary for full expression of the mouse iNOS gene in response to interferon-gamma and lipopolysaccharide.** *The Journal of biological chemistry* 1997, **272(2):**1226-1230.
18. Qui M, Paromov VM, Yang H, Smith M, Stone WL: **Inhibition of inducible Nitric Oxide Synthase by a mustard gas analog in murine macrophages.** *BMC cell biology* 2006, **7:**39.
19. Schwentker A, Billiar TR: **Nitric oxide and wound repair.** *The Surgical clinics of North America* 2003, **83(3):**521-530.
20. Witte MB, Kiyama T, Barbul A: **Nitric oxide enhances experimental wound healing in diabetes.** *The British journal of surgery* 2002, **89(12):**1594-1601.
21. Yamasaki K, Edington HD, McClosky C, Tzeng E, Lizonova A, Kovesdi I, Steed DL, Billiar TR: **Reversal of impaired wound repair in iNOS-deficient mice by topical adenoviral-mediated iNOS gene transfer.** *The Journal of clinical investigation* 1998, **101(5):**967-971.
22. Duval DL, Sieg DJ, Billings RE: **Regulation of hepatic nitric oxide synthase by reactive oxygen intermediates and glutathione.** *Archives of biochemistry and biophysics* 1995, **316(2):**699-706.
23. Harbrecht BG, Di Silvio M, Chough V, Kim YM, Simmons RL, Billiar TR: **Glutathione regulates nitric oxide synthase in cultured hepatocytes.** *Ann Surg* 1997, **225(1):**76-87.
24. Tirmenstein MA, Nicholls-Grzemski FA, Schmittgen TD, Zakrajsek BA, Fariss MW: **Glutathione-dependent regulation of nitric oxide production in isolated rat hepatocyte suspensions.** *Antioxidants & redox signaling* 2000, **2(4):**767-777.
25. Vos TA, Van Goor H, Tuyt L, De Jager-Krikken A, Leuvenink R, Kuipers F, Jansen PL, Moshage H: **Expression of inducible nitric oxide synthase in endotoxemic rat hepatocytes is dependent on the cellular glutathione status.** *Hepatology* 1999, **29(2):**421-426.
26. Myhre O, Andersen JM, Aarnes H, Fonnum F: **Evaluation of the probes 2',7'-dichlorofluorescin diacetate, luminol, and lucigenin as indicators of reactive species formation.** *Biochemical pharmacology* 2003, **65(10):**1575-1582.
27. Imrich A, Kobzik L: **Fluorescence-based measurement of nitric oxide synthase activity in activated rat macrophages using dichlorofluorescin.** *Nitric Oxide* 1997, **1(4):**359-369.
28. LeBel CP, Ischiropoulos H, Bondy SC: **Evaluation of the probe 2',7'-dichlorofluorescin as an indicator of reactive oxygen species formation and oxidative stress.** *Chemical research in toxicology* 1992, **5(2):**227-231.
29. Sebastia J, Cristofol R, Martin M, Rodriguez-Farre E, Sanfeliu C: **Evaluation of fluorescent dyes for measuring intracellular glutathione content in primary cultures of human neurons and neuroblastoma SH-SY5Y.** *Cytometry A* 2003, **51(1):**16-25.
30. Poot M, Kavanagh TJ, Kang HC, Haugland RP, Rabinovitch PS: **Flow cytometric analysis of cell cycle-dependent changes in cell thiol level by combining a new laser dye with Hoechst 33342.** *Cytometry* 1991, **12(2):**184-187.
31. Kamencic H, Lyon A, Paterson PG, Juurlink BH: **Monochlorobimane fluorometric method to measure tissue glutathione.** *Analytical biochemistry* 2000, **286(1):**35-37.
32. Elsayed NM, Omaye ST, Klain GJ, Inase JL, Dahlberg ET, Wheeler CR, Korte DW Jr.: **Response of mouse brain to a single subcutaneous injection of the monofunctional sulfur mustard, butyl 2-chloroethyl sulfide (BCS)*.** *Toxicology* 1989, **58(1):**11-20.
33. Berlett BS, Stadtman ER: **Protein oxidation in aging, disease, and oxidative stress.** *The Journal of biological chemistry* 1997, **272(33):**20313-20316.
34. Stone WL, Smith M: **Therapeutic uses of antioxidant liposomes.** *Mol Biotechnol* 2004, **27(3):**217-230.
35. Droge W: **Free radicals in the physiological control of cell function.** *Physiological reviews* 2002, **82(1):**47-95.
36. Kadar T, Turetz J, Fishbine E, Sahar R, Chapman S, Amir A: **Characterization of acute and delayed ocular lesions induced by sulfur mustard in rabbits.** *Current eye research* 2001, **22(1):**42-53.
37. Zimmermann AK, Loucks FA, Schroeder EK, Bouchard RJ, Tyler KL, Linseman DA: **Glutathione binding to the Bcl-2 homology-3 domain groove: a molecular basis for Bcl-2 antioxidant function at mitochondria.** *The Journal of biological chemistry* 2007, **282(40):**29296-29304.
38. Fan J, Shek PN, Suntres ZE, Li YH, Oreopoulos GD, Rotstein OD: **Liposomal antioxidants provide prolonged protection against acute respiratory distress syndrome.** *Surgery* 2000, **128(2):**332-338.
39. McClintock SD, Hoesel LM, Das SK, Till GO, Neff T, Kunkel RG, Smith MG, Ward PA: **Attenuation of half sulfur mustard gas-induced acute lung injury in rats.** *J Appl Toxicol* 2006, **26(2):**126-131.
40. Kleinert H, Pautz A, Linker K, Schwarz PM: **Regulation of the expression of inducible nitric oxide synthase.** *Eur J Pharmacol* 2004, **500(1-3):**255-266.
41. Chen XM, Gray PJ, Cullinane C, Phillips DR: **Differential sensitivity of transcription factors to mustard-damaged DNA.** *Chemico-biological interactions* 1999, **118(1):**51-67.
42. Gray PJ: **Sulphur mustards inhibit binding of transcription factor AP2 in vitro.** *Nucleic Acids Res* 1995, **23(21):**4378-4382.
43. Fabbri S, Prontera C, Broggini M, D'Incalci M: **Differential inhibition of the DNA binding of transcription factors NF kappa B and OTF-1 by nitrogen mustard and quinacrine mustard: transcriptional implications.** *Carcinogenesis* 1993, **14(9):**1963-1967.
44. Nishi T, Shimizu N, Hiramoto M, Sato I, Yamaguchi Y, Hasegawa M, Aizawa S, Tanaka H, Kataoka K, Watanabe H, Handa H: **Spatial redox regulation of a critical cysteine residue of NF-kappa B in vivo.** *The Journal of biological chemistry* 2002, **277(46):**44548-44556.
45. Atkins KB, Lodhi IJ, Hurley LL, Hinshaw DB: **N-acetylcysteine and endothelial cell injury by sulfur mustard.** *J Appl Toxicol* 2000, **20 Suppl 1:**S125-8.
46. Chatterjee D, Mukherjee S, Smith MG, Das SK: **Signal transduction events in lung injury induced by 2-chloroethyl ethyl sulfide, a mustard analog.** *Journal of biochemical and molecular toxicology* 2003, **17(2):**114-121.
47. Minsavage GD, Dillman JF: **BIFUNCTIONAL ALKYLATING AGENT-INDUCED p53 AND NONCLASSICAL NUCLEAR FACTOR-KAPPA B (NF-{kappa}B) RESPONSES AND CELL DEATH ARE ALTERED BY CAFFEIC ACID PHENETHYL ESTER (CAPE): A potential role for antioxidant/electrophilic response element (ARE/EpRE) signaling.** *J Pharmacol Exp Ther* 2007, **321(1):**202-212.
48. Soneja A, Drews M, Malinski T: **Role of nitric oxide, nitroxidative and oxidative stress in wound healing.** *Pharmacol Rep* 2005, **57 Suppl:**108-119.
49. Stone WL, Mukherjee S, Smith M, Das SK: **Therapeutic uses of antioxidant liposomes.** *Methods Mol Biol* 2002, **199:**145-161.
50. Wasserman TH, Twentyman P: **Use of a colorimetric microtiter (MTT) assay in determining the radiosensitivity of cells from murine solid tumors.** *Int J Radiat Oncol Biol Phys* 1988, **15(3):**699-702.
51. Twentyman PR, Luscombe M: **A study of some variables in a tetrazolium dye (MTT) based assay for cell growth and chemosensitivity.** *Br J Cancer* 1987, **56(3):**279-285.
52. Green LC, Wagner DA, Glogowski J, Skipper PL, Wishnok JS, Tannenbaum SR: **Analysis of nitrate, nitrite, and [15N]nitrate in**

biological fluids. In *Analytical biochemistry Volume 126*. Issue 1 UNITED STATES ; 1982:131-138.
53. Tietze F: **Enzymic method for quantitative determination of nanogram amounts of total and oxidized glutathione: applications to mammalian blood and other tissues.** *Analytical biochemistry* 1969, **27(3):**502-522.
54. Griffith OW: **Determination of glutathione and glutathione disulfide using glutathione reductase and 2-vinylpyridine.** *Analytical biochemistry* 1980, **106(1):**207-212.
55. Houze P, Gamra S, Madelaine I, Bousquet B, Gourmel B: **Simultaneous determination of total plasma glutathione, homocysteine, cysteinylglycine, and methionine by high-performance liquid chromatography with electrochemical detection.** *Journal of clinical laboratory analysis* 2001, **15(3):**144-153.
56. Alamdari DH, Kostidou E, Paletas K, Sarigianni M, Konstas AG, Karapiperidou A, Koliakos G: **High sensitivity enzyme-linked immunosorbent assay (ELISA) method for measuring protein carbonyl in samples with low amounts of protein.** *Free radical biology & medicine* 2005, **39(10):**1362-1367.
57. Buss H, Chan TP, Sluis KB, Domigan NM, Winterbourn CC: **Protein carbonyl measurement by a sensitive ELISA method.** *Free radical biology & medicine* 1997, **23(3):**361-366.

JOURNAL OF BURNS AND WOUNDS WWW.JOURNALOFBURNSANDWOUNDS.COM

Sulfur Mustard Toxicity Following Dermal Exposure

Role of Oxidative Stress, and Antioxidant Therapy

Victor Paromov,[a] *Zacharias Suntres,*[b] *Milton Smith,*[c] *and William L. Stone*[a]

[a]Department of Pediatrics, East Tennessee State University, Johnson City; [b]Northern Ontario School of Medicine, Advanced Technology and Academic Centre, 955 Oliver Road Thunder Bay, ON P7B 5E1; and [c]AMAOX, Ltd., #208, 6300 N. Wickham Rd, Melbourne, Fla.

Correspondence: stone@etsu.edu

Published October 30, 2007

Objective: Sulfur mustard (bis-2-(chloroethyl) sulfide) is a chemical warfare agent (military code: HD) causing extensive skin injury. The mechanisms underlying HD-induced skin damage are not fully elucidated. This review will critically evaluate the evidence showing that oxidative stress is an important factor in HD skin toxicity. Oxidative stress results when the production of reactive oxygen (ROS) and/or reactive nitrogen oxide species (RNOS) exceeds the capacity of antioxidant defense mechanisms. **Methods:** This review will discuss the role of oxidative stress in the pathophysiology of HD skin toxicity in both in vivo and in vitro model systems with emphasis on the limitations of the various model systems. Evidence supporting the therapeutic potential of antioxidants and antioxidant liposomes will be evaluated. Antioxidant liposomes are effective vehicles for delivering both lipophilic (incorporated into the lipid bilayers) and water-soluble (encapsulated in the aqueous inner-spaces) antioxidants to skin. The molecular mechanisms interconnecting oxidative stress to HD skin toxicity are also detailed. **Results:** DNA repair and inflammation, in association with oxidative stress, induce intracellular events leading to apoptosis or to a programmable form of necrosis. The free radical, nitric oxide (NO), is of considerable interest with respect to the mechanisms of HD toxicity. NO signaling pathways are important in modulating inflammation, cell death, and wound healing in skin cells. **Conclusions:** Potential future directions are summarized with emphasis on a systems biology approach to studying sulfur mustard toxicity to skin as well as the newly emerging area of redox proteomics.

SULFUR MUSTARD: A CENTURY OF THREAT

Sulfur mustard (SM) or mustard gas (bis-2-(chloroethyl) sulfide, military code: HD) is a chemical warfare agent classified as a weapon of mass destruction. Mustard gas was one of the first chemical weapons deployed against troops on a battlefield during World War I, almost hundred years ago. Since then, the military use of mustard gas has been documented in a number of situations. In 1988, HD was used with devastating results

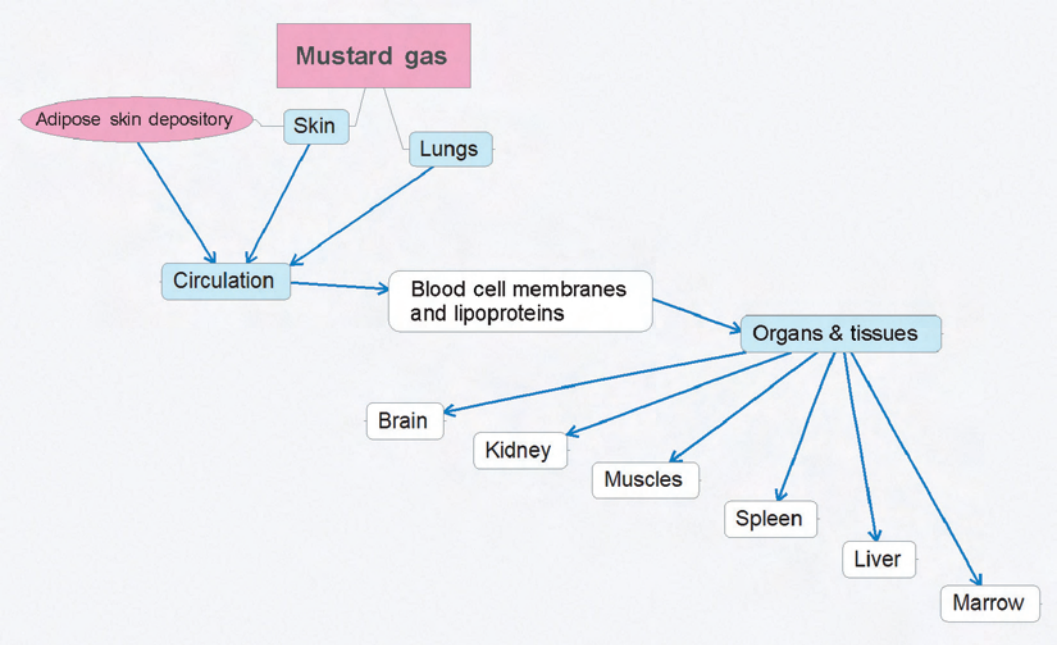

Figure 1. Distribution and accumulation of HD via circulation after dermal/inhalation exposure.

by Saddam Hussein's military forces against civilian targets in Halabja and later during the Iran-Iraq war. Mustard gas produces casualties in the battlefield and forces opposing troops to wear full protective equipment thus slowing the tempo of military operations. It is highly probable that mustard gas could be used by terrorists since it is a simple chemical compound readily synthesized without elaborate technology. Moreover, as a "persistent agent" (US Army classification) aerosolized mustard gas presents a threat for up to 1 week under dry and warm weather conditions because it remains in the environment until fully hydrolyzed. Along with nerve agents, mustard gas presents a major threat as a potential and effective chemical weapon. The possibility of low technology production, easy stockpiling, and difficulty in verifying its storage makes mustard gas a continuing worldwide threat. Presently, there is no antidote or effective treatment for mustard gas intoxication.

PATHOPHYSIOLOGY OF SULFUR MUSTARD ON SKIN

Clinical and physiological characteristics

Mustard gas is lethal in high doses and causes severe damage to the interface organs, that is, skin, lungs, respiratory tract, and eyes. The most prominent toxic effects of HD are on skin where it produces severe damage including extremely slow healing lesions and blisters which can ulcerate, vesicate, and promote secondary infections. Because of its hydrophobic nature, mustard gas easily penetrates and accumulates in the lipid component of exposed tissues. Upon contact with the skin, about 80% of HD evaporates and only about 20% is absorbed by the skin. Skin not only accumulates but also distributes HD to other tissues. Only about 10%–12% of the initially absorbed HD is retained in the skin, whereas up to 90% of HD enters circulation as indicated in Figure 1[1] Extractable skin reservoirs of HD can be

found in the dermis and epidermis even 24 to 48 hours postexposure.[2] In the case of a lethal poisoning, HD concentration in skin blisters remains very high even 7 days after exposure.[3] Consequently, even after the initial exposure, skin reservoirs continue to distribute HD via circulation to the body tissues thereby increasing damage to several organs. Figure 1 schematically shows the distribution pathway of HD toxicity throughout the human body. We would like to point that, although skin is the initial accumulator of HD, its toxic effect is also prominent in distal organs. Therefore, the effect of HD after dermal exposure is not limited only to skin tissues

While the epidermis contains no blood vessels, both the dermis and the subcutaneous regions are rich in blood vessels. Adipose cells in the subcutaneous skin layer are likely to be a depository for HD due to their high lipid content (as indicated in Figure 1). Moreover, HD solublized in adipose cells would be out of contact with water and thereby resistant to hydrolysis. After acute skin exposure, HD would be systemically delivered to various tissues in the body via lipid rich blood cell membranes and plasma lipoproteins and accumulate in lipid rich tissues (adipose tissues, brain, and skin). Chemical analyses following acute HD exposure show a high accumulation in thigh fat, brain, abdominal skin, kidney, and muscle tissues, in decreasing order.[3] In addition, HD can be found in the spleen, liver, and bone marrow.[4] The organs acquiring the most damage after dermal and/or respiratory exposure are indicated in Figure 1.

Skin damage caused by aerosolized HD appears after a latent period of up to 24 hours. First symptoms, such as itching, burning, and erythema, are followed by hyperpigmentation, tissue necrosis, and blister formation in warm moist areas of the body. When a large skin area is exposed to HD, medical conditions can be complicated by fluid imbalance, general inflammation, systemic intoxication, and secondary infection. At high doses, HD can also produce systemic effects with gastrointestinal symptoms (nausea and vomiting), respiratory distress due to the bronchospasm, temporary blindness as well as corneal damage. In most lethal cases, massive skin burns and wounds, as well as lung damage, are the primary causes of death. Since it damages DNA, mustard gas promotes mutagenesis and carcinogenesis.[1,5–7] Acute and severe exposures to HD have been shown to produce skin cancers.[8,9]

A few limited cases of HD exposure in humans provide some evidence for oxidative stress. HD metabolites derived from hydrolysis (thiodiglycol, thiodiglycol sulphoxide), as well as HD metabolites from glutathione (GSH) conjugates by the beta-lyase pathway, can be found in human urine after HD exposure.[10,11] Both thiodiglycol sulphoxide and beta-lyase metabolites can be detected indicating GSH conjugation. Thiodiglycol has also been detected in urine samples from individuals not exposed to HD and is therefore not useful as a definitive marker for HD exposure.[11] In contrast, HD metabolites from the glutathione (GSH)/beta-lyase pathway are specific for HD exposure.[10,11] These observations suggest that GSH depletion occurs in humans, and that GSH-HD/beta-lyase pathway metabolites provide a specific and useful biomarker for diagnosing HD exposure. GSH is a key intracellular antioxidant and its depletion by HD would be expected to increase oxidative stress.

The effects of HD in humans are very complicated and not fully elucidated. Figure 2 summarizes some of the key potential molecular mechanisms for HD toxicity in skin cells (as discussed in more detail below). Macromolecular damage and thiol depletion are primary and presumably the most dangerous intracellular events following HD exposure to

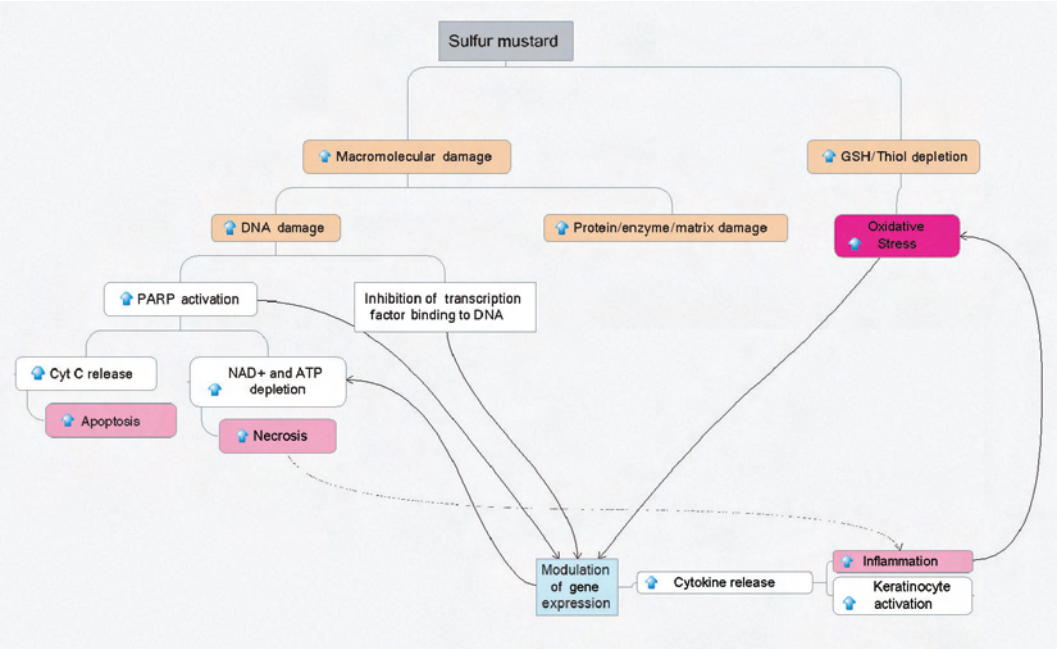

Figure 2. Schematic representation of the hypothesized molecular mechanisms of HD toxicity in skin cells.

skin cells. Macromolecular damage includes DNA damage as well as covalent modification of proteins and inactivation of enzymes. HD can affect cellular proteins indirectly by influencing expression and directly by altering the function of various enzymes and causing fragmentation of the extracellular matrix and cell detachment. GSH and total cellular thiol depletion is considered to be the major source of the oxidative stress. These primary damaging events modulate gene expression and induce inflammation and oxidative stress, which finally leads to apoptosis and/or necrosis (see Fig 2).

GENERAL COUNTERMEASURES

Presently, elimination of contact, decontamination, and supportive therapies are the only primary treatments for vesicant exposure. Respirators and protective masks are effective in preventing inhalation, and special protective clothing can be used to eliminate skin exposure. Various decontaminating agents can eliminate or effectively reduce the toxic effect of HD if used immediately after the exposure. Ambergard XE-555 Resin reactive powder, hypochlorite neutralizing solutions, reactive skin lotions, and absorbent powders can be used to remove HD from human skin. Substantial HD reservoirs can be found in human skin even 24 hours after exposure.[12] These reservoirs can account for up to 35% of the total dose, and it is important, therefore, to develop decontaminating techniques capable of the removing such reservoirs thereby reducing further skin and systemic damage. Graham et al[13] have provided an excellent review of the strategies and current therapies for treating

cutaneous HD toxicity and promoting wound healing. An optimal therapeutic approach is, however, still lacking.

In this review, we will focus on the potential role of antioxidant therapy; we will review the data from in vivo and in vitro models suggesting that oxidative stress is an important molecular mechanism underlying HD toxicity and that antioxidants can be therapeutically useful. The strengths and limitations of the in vivo and in vitro models will be detailed.

MUSTARD GAS/ANALOG-INDUCED OXIDATIVE STRESS IN ANIMAL MODELS AND THE EFFECTS OF ANTIOXIDANTS

Detailed information about HD toxicity to human skin, especially at the molecular level, is very limited. Animal models are, therefore, the major source of information about the pharmacokinetics and the molecular mechanisms of HD skin toxicity. Unfortunately, there is no animal model that exactly mimics the development of HD injury in human skin. Young swine and miniature swine skin are, however, considered to be the best models since they have a similar skin structure (epidermis, dermis, and subcutaneous tissue) and barrier function. Furred animals are poor models probably because their skin is not as well keratinized as human skin, thereby permitting more rapid penetration of drugs or toxins.

Despite limitations, the mouse ear model, the rabbit, the hairless guinea pig, the nude mouse, and the weanling swine have all been useful for studying the (1) pathophysiology, (2) molecular mechanism of action, and (3) efficacy of countermeasures for HD injury. Studies on the Yucatan mini-pig have demonstrated that laminin in the dermo-epithelial junction is a target for partial protease degradation following HD exposure. The protease cleavage of laminin networks may account for the blistering effect of HD.[14] The logistics of dealing with even miniature swine has, however, limited their use in HD studies.

In 2002, Naghii[15] reviewed much of the existing literature connecting HD toxicity and oxidative stress and suggested that further studies in animal models were well justified. Direct evidence for free radical formation in rat lung lavage following inhalation of HD vapor has been obtained by using electron paramagnetic resonance (EPR) and spin trapping techniques.[16] These studies show a rapid formation of ascorbyl radicals followed by the formation of carbon-centered radicals.[16]

Elsayed et al[17,18] have demonstrated that subcutaneous injections of either a butyl 2-chloroethyl sulfide (a monofunctional mustard analog) or 2-chloroethyl 4-chlorobutyl sulfide (a bifunctional mustard gas analog) in animal models caused an elevation in lung tissue lipid peroxidation as assayed by the thiobarbituric acid (TBA) assay. The TBA assay is, however, not very specific: rather then directly measuring levels of lipid hydroperoxide, this assay is generally considered a measure of total "thiobarbituric acid reactive substances" (TBARS). Total (GSH+GSSG) and oxidized (GSSG) glutathione contents in lung tissue were found to increase 1 hour and 24 hours after subcutaneous injection of butyl 2-chloroethyl sulfide.[18] Subcutaneous injection of 2-chloroethyl 4-chlorobutyl sulfide was associated with increased GSSG and decreased GSH at 1 hour postexposure. The increased formation of GSSG and TBARS in lung tissues following subcutaneous injection of mustard analogs is consistent with oxidative stress and suggests that dermal exposure can impact distal organs. This notion is supported by the work of Vijayaraghavan et al,[19] who found that dermally applied HD induces hepatic lipid peroxidation and GSH depletion in mice. In

this study, the generation of malondialdehyde (MDA) was used as an indirect measure of lipid peroxidation Vitamin E or flavonoids, while not influencing hepatic GSH depletion, did reduce MDA levels, suggesting a therapeutic potential.[19]

The effects of topically applied HD on key antioxidant enzymes have been measured but with conflicting results. For example, Husain et al[20] found that HD decreased the levels of glutathione peroxidase in white blood cells, spleen, and liver compared to control. Elsayed et al,[18] however, found an increased level of glutathione peroxidase compared to controls. Elsayed[17] interpreted the increased level of glutathione peroxidase (and other antioxidant enzymes) as an upregulation in response to oxidative stress, whereas Husain et al[20] interpreted the decreased levels of glutathione peroxidase as a potential cause of oxidative stress. Careful in vitro work with purified enzymes may help clarify these issues.

Despite the importance of skin itself as a primary target for HD toxicity, this organ has not been extensively studied with respect to oxidative stress. Yourick et al,[21] using the hairless guinea pig model, analyzed the skin NAD+ and NADP+ content as a function of time after HD exposure. Skin NAD+ content was found to decrease to a minimum after 16 hours (20% of control) whereas NADP+ levels increased (260%) between 1 and 2 hours and returned to control levels at 4 hours. This marked increase in NADP+ levels was thought to be an early marker of oxidative stress and a contributory factor for HD toxicity.[21] Increased NADP+ levels are a result of increased NADPH consumption: NADPH is a major source of reducing equivalents for key antioxidant enzymes such as glutathione reductase/peroxidase and thioredoxine reductase/peroxidase and lack of NADPH would be a source of oxidative stress.

The data presented above support the view that diminished antioxidant protective mechanisms are a consequence of HD exposure. It is less clear, however, whether or not the resulting oxidative stress is a direct contributing factor to mustard toxicity or a secondary effect due to inflammation. In any event, the ability of exogenous antioxidants (as discussed below) to decrease HD toxicity supports the hypothesis that decreasing oxidative stress and/or inflammation is a viable therapeutic strategy.

Antioxidant protection in animal models

As early as 1985, work by Vojvodic et al[22] demonstrated that vitamin E was very effective in extending the survival time of rats acutely poisoned by HD. Vitamin E is, however, a generic term referring to at least 4 different tocopherols (alpha-, beta-, gamma-, and delta-) and 4 tocotrienols (alpha-, beta-, gamma-, and delta-). The particular form of vitamin E used in the Vojvodic et al experiments was not specified.[22] Vitamin E is generally considered to be the primary lipid soluble antioxidant but it is now recognized that vitamin E has important "nonantioxidant" roles in modulating various signal transduction and gene regulation pathways.[23–25] Moreover, the different chemical forms of vitamin E are now known to have distinct chemical and biological properties.[26,27] It is important, therefore, to specify the particular chemical and stereochemical form of vitamin E used in a given experiment.

Superoxide dismutase (SOD, EC 1.15.1.1) is a key antioxidant enzyme that catalyzes the dismutation of superoxide radicals into oxygen and hydrogen peroxide. Eldad et al[28] studied the therapeutic role of both Cu-Zn-SOD (cytosolic form) and Mn-SOD (mitochondrial form) in HD skin damage, using the Hartley guinea pig model. Pretreatment of the animals

by intraperitoneal injection with either form of SOD resulted in a dramatically reduced skin lesion area induced by HD.[28] Treatment with SOD was, however, not effective when given 1 hour after HD poisoning.[28] These data strongly suggest that superoxide radicals play a key role in HD-induced skin toxicity. Superoxide radicals alone are not a particularly damaging form of free radicals but they rapidly react with nitric oxide radicals to form peroxynitrite, which is a potent oxidant capable of causing tissue damage.[29–31]

HD and its analogs are alkylating agents that chemically react with and deplete biological thiols such as GSH, which is a key intracellular antioxidant. By promoting ROS generation and lipid peroxidation (as discussed above), HD will also promote the consumption of GSH and a reduced level of NADPH (see above) will inhibit the regeneration of GSH from GSSG. It is reasonable, therefore, that exogenous GSH or *N*-acetyl-L-cysteine (NAC) would help minimize oxidative stress induced by HD or its analogs. Kumar et al[32] tested the potential protective effect of GSH given to Swiss albino female mice following acute exposure to HD by either inhalation or percutaneous routes. GSH was administered by intraperitoneal injection and the dose was 400 mg/kg of body weight, which translates into about a 20 mM concentration in blood. Survival time following inhalation exposure to HD was increased by GSH administration as well as 2 other antioxidants: trolox (6-hydroxy-2,5,7,8-tetramethylchroman-2-carboxylic acid), which is a water-soluble derivative of alpha-tocopherol, and quercetin, which a flavonoid.[32] Inhalation exposure to HD depleted hepatic GSH levels, and increased hepatic and lung lipid peroxidation (as indirectly measured by MDA levels), and exogenous GSH was able to reduce lung and hepatic lipid peroxidation as well as prevent GSH depletion in these tissues.[32] None of the 3 antioxidants tested were able to significantly increase survival time following percutaneous exposure to HD but exogenous GSH was effective in preventing GSH depletion in blood and liver. Surprisingly, lung levels of GSH were not altered by percutaneous HD exposure.[32] The data present in work by Kumar et al[32] show that the potential effectiveness of antioxidant therapy is dependent on the route of HD exposure.

The role of GSH and NAC (and other antioxidants) in attenuating acute lung injury by 2-chloroethyl ethyl sulfide (CEES) has recently been studied in a rat model in which lung damage was quantitatively measured by the extravasation of ^{125}-I-bovine serum albumin into the extravascular compartment.[33,34] CEES is a monofunctional analog of HD that has proven very useful in mimicking HD exposure. When the experimental animals were depleted of either complement or neutrophils prior to CEES exposure (by intrapulmonary injection) lung damage was significantly decreased.[34] Neutrophil depletion was accomplished by IP injection of rabbit anti-serum to rat polymorphonuclear neutrophils and complement depletion by IP injections cobra venom factor.[34] Antioxidants such as catalase, dimethyl sulfoxide, dimethyl urea, resveratrol, and NAC all provided significant protection in this animal model.[34] NAC (an acetylated form of L-cysteine) can directly function as free radical scavenger and its metabolites are capable of stimulating GSH synthesis.[35] NAC was found to be the most effective antioxidant among those tested[33,34] and was effective even when given up to 90 minutes after lung exposure to CEES.

In the work of McClintock et al,[33] NAC was superior to GSH. In vitro work by Gross et al[36] found that pretreatment of human peripheral blood lymphocytes (PBL) with 10 mM NAC elevated GSH level to 122% of untreated control but caused only a partial protective effect on HD-induced cytotoxicity. These researches also noted work by Meister and Anderson, suggesting[37] that exogenously added GSH does not appear to enter the cell very

effectively. This may help explain why NAC is superior to GSH in the work by McClintock et al.[33]

Bhat et al[38] have studied the potential therapeutic use of lipoic acid to decrease oxidative stress and mustard gas toxicity in a rat model. Lipoic acid is a disulphide derivative of octanoic acid, and it is known to be a crucial prosthetic group for various cellular enzymatic complexes. Lipoic acid has been identified as a potent antioxidant and a potential therapeutic agent for the prevention or treatment of pathological conditions mediated via oxidative stress, as in the case of ischemia-reperfusion injury, diabetes, radiation injury, and oxidative damage of the central nervous system.[39–43] Lipoic acid is taken up and reduced by cells to dihydrolipoate, a more powerful antioxidant than the parent compound, which is also exported to the extracellular medium; hence, protection is affected in both extracellular and intracellular environments. Both lipoic acid and dihydrolipoate, in addition to their direct antioxidant properties, have been shown to regenerate, through redox cycling, other antioxidants such as vitamin C and vitamin E, and to raise intracellular glutathione levels.[44,45] Bhat et al[38] found that lipoic acid pretreatment decreased the levels of lipid peroxidation (measured as MDA) in lung, skin, and eyes in HD treated rats but was not effective posttreatment.

Antioxidant liposomes as a potential countermeasure

Antioxidant liposomes may represent an optimal means of treating HD-induced skin lesions. The authors' laboratory is currently testing this hypothesis. The term "antioxidant liposome" is relatively new and refers to liposomes containing lipid soluble chemical antioxidants, water-soluble chemical antioxidants, enzymatic antioxidants, or combinations of these various antioxidants. Antioxidant liposomes hold great promise in the treatment of many diseases and conditions in which oxidative stress plays a prominent role.[46,47] The relative ease of incorporating hydrophilic and lipophilic therapeutic agents into liposomes; the possibility of directly delivering liposomes to an accessible body site; and the relative nonimmunogenicity and low toxicity of liposomes have rendered this system highly attractive for drug delivery. Moreover, several studies have clearly indicated that the liposomal antioxidant formulations, compared to that of the free nonencapsulated antioxidants, exert a far superior protective effect against oxidative stress-induced tissue injuries.[48]

Experimental studies have shown that liposomes and their constituents effectively penetrate skin.[49,50] Topical application of antioxidant-liposomes is likely, therefore, to be particularly effective in enhancing the antioxidant status of skin. Work by Kirjavainen et al[49] suggests that liposomes containing dioleylphosphatidyl ethanolamine (DOPE) are better able to penetrate into the stratum corneum than liposomes without DOPE. Similarly, ultradeformable liposomes, lipid vesicles with special membrane flexibility due to incorporation of an edge activator such as sodium cholate, have been shown to be superior in comparison to ordinary phosphatidylcholine liposomes (see http://www.skinforum.org.uk/abstracts/ebtassam-essa.php).

At present there are no data on the potential use of antioxidant liposomes in treating HD-induced skin lesions but McClintock et al[33] have found that liposomes containing pegylated (PEG) catalase, PEG-SOD, or the combination were very effective in reducing

CEES-induced lung injury in a rat model. Similarly, liposomes containing NAC, GSH, or resveratrol also were effective according to this study.

In vitro studies using human skin models

Keratinocyte cell lines

In vivo models are essential for testing countermeasures to HD or its analogs, however, in vitro models are also critical for rapid screening of potential therapeutic agents and for detailed studies at the molecular level. Skin is the largest organ of the human body with a complicated multilayer multicell type structure. As mentioned above, there is no model system perfectly mimicking human skin. Normal or immortalized human keratinocytes cultured on plastic as a monolayer represent the simplest and least inexpensive model and are suitable for an initial approach for HD toxicity studies. Normal human epidermal keratinocytes (NHEK) isolated from adult or infant fetal skin tissue are available commercially. These cells are easy to handle, can be frozen for long-term storage but require special medium containing a mixture of growth factors.[51] Even then, NHEK cells spontaneously transform after 3–5 passages as they continuously undergo terminal differentiation.

Nevertheless, NHEK remains the only commercially available normal cell line possessing all of the structural and functional features of normal skin keratinocytes and is being used by many investigators to study mustard gas toxicity.[52] However, the requirement of special growth medium and a short lifespan make this model more expensive than immortalized human keratinocytes such as human pappiloma virus (HPV)–immortalized cell lines or spontaneously immortalized HaCaT cells. There are also a number of commercially available human keratinocyte cell lines immortalized via transfection with DNA coding E6 and/or E7 viral oncoproteins. All of these cell lines still require special medium with growth factors and, like NHEK, have a limited lifespan since they spontaneously transform after 10 to 15 passages.[53]

The HaCaT cell line, originating in Germany, has recently become commercially available; it represents spontaneously immortalized adult human keratinocytes.[54] HaCaT cells are extremely easy to handle and do not require special medium. Theoretically, HaCaT cells have an unlimited lifespan but they do show morphological changes after 10 to 20 passages. Despite the altered growth potential, HaCaT cells still express differentiation-specific markers[54] and unlike HPV-immortalized cell lines, HaCaT cells are not tumorigenic when transplanted into nude mice.[54]

It is well known that HD, like UV radiation, affects mostly proliferating keratinocytes within the lower dermis and basement membrane. Differentiating keratinocytes of the epidermis are much less susceptible to toxicity since they do not undergo apoptosis and respond weakly to inflammatory stimuli. Normal keratinocytes undergo terminal differentiation (so-called "cornification") in response to a high (1 mM) exogenous Ca^{++} concentration.[51] Normal keratinocytes in vivo start to differentiate when they detach from the basement membrane and migrate to the suprabasal layers.[55] Thus, NHEK and HPV-immortalized keratinocytes, unlike HaCaT cells, spontaneously differentiate when subcultured in response to the cell detachment. Therefore, only the first passages of NHEK cells are truly proliferating, whereas every passage of HaCaT culture consists of proliferating cells. On the other hand, HaCaT cells show impaired production and release of IL-1[56] which is crucial for normal

keratinocyte proliferation and also plays an important role in keratinocyte activation and keratinocyte/fibroblast crosstalk in normal skin.[57]

As previously acknowledged, HD-induced depletion of intracellular glutathione (GSH) is a triggering event for oxidative stress in skin. Smith et al[58] have shown that pretreatment of the human keratinocyte cell line, SVK-14, with GSH markedly increases the resistance to HD-induced cytotoxicity. Conversely, pretreatment with buthionine sulfoximine (BSO) increases the sensitivity of G361, SVK14, HaCaT, and NCTC 2544 human keratinocytes to HD toxicity.[59] BSO lowers intracellular GSH by irreversibly inhibiting the rate-limiting GSH synthesis enzyme γ-glutamylcysteine synthetase. Surprisingly, there is no reported direct evidence to date for the enhanced generation of ROS and/or RNOS in HD-treated keratinocytes.

As pointed out earlier, HD and its chemical analogs cause massive leukocyte infiltration in animal skin and lungs[60,61] It is likely that lymphocytes and macrophages, attracted to the burned area by cytokines released from keratinocytes/fibroblasts, could be a major source of oxidative stress to skin cells. It has been demonstrated that HD-exposed NHEK cells express chemoattractants and cytokine.[62–64] Moreover, an enhanced ability of NHEK cells to attract lymphocytes in vitro was demonstrated in an experiment in which the media from HD-treated keratinocytes was tested for chemoattractant activity to polymorphonuclear leukocytes purified from human blood.[65]

Multilayer keratinocyte tissues

Multilayer skin tissues (so-called "3D skin models") are a more realistic model for toxicological studies. The simplest models of this class consist only of keratinocytes such as the commercially available Epiderm, which is a few millimeters thick structure of human NHEK cells grown on top of a wet membrane. Epiderm provides the possibility of applying HD (or other gaseous agents) in vapor or aerosol form which closely simulates a real HD attack. However, this model represents differentiating keratinocytes on a collagen matrix and practically all of the cells within the tissue start to cornify at the moment they are fully grown. Blaha et al[66–68] have characterized the ultrastructural, histological, and molecular response of the Epiderm model to CEES. The Epiderm system not only has great potential for identifying and developing sulfur mustard therapeutic agents but also has limitations. In vivo, skin damage would be accompanied by the rapid leakage of serum, leukocyte infiltration, and perhaps mast cell degranulation (see below) but these events will not occur in any of the available in vitro skin models.

More advanced tissue models, like EpidermFT full thickness skin tissue model, consist of 2 cell types: a bottom layer of human fibroblasts imbedded in gelatin and an upper multilayer of human keratinocytes. This particular model is particularly valuable for studies involving paracrine signaling (keratinocyte/fibroblast interactions). HaCaT cells, with normal human or mouse fibroblasts, have also been used to construct 3D models of human skin. However, the impaired IL-1 production in these cells presents some technical difficulties that can be overcome with the addition of human growth factors.[56] These multilayer skin models morphologically mimic the dermis and epidermis of human skin including the cuboidal appearance of the basal cell layer, the presence of the stratum spinosum and stratum granulosum with typical stellate-shaped keratohyalin granules, and the presence of numerous lamellar bodies that are extruded at the stratum granulosum–stratum corneum interface.

In a key experiment, Blaha et al[67] compared the effects of CEES on the secretion of key inflammatory mediators using 2 model human skin systems, the Epiderm system (from MatTek Corporation) and the Skin2 system (a 3D skin model) from Advanced Tissue Sciences, which consists of differentiating keratinocytes on a fibroblast-collagen matrix. In the Skin2 system, the proinflammatory cytokine IL-1alpha increased in response to CEES but the proinflammatory cytokine IL-6 decreased: the Epiderm showed undetectable levels of IL-6 and the levels of IL-1alpha did not change in response to CEES.[67] These data show that the presence of fibroblasts in the Skin2 model dramatically changes the cytokine secretion response to CEES.

More recently, Hayden et al[69] evaluated the effects of HD on the EpiDermFT skin model which has a 3D, highly differentiated human skin-like structure with an epidermis and a dermis. This in vitro model permits the study of dermal phenomena in which fibroblast-keratinocyte cell interactions are important as appears to be the case for CEES-induced skin injury (see above). Hayden et al[69] treated the EpiDerm-FT model with HD for 8 minutes and evaluated the structural effects at 6 and 12 hours postexposure. Histological analyses showed typical HD targeting of basal keratinocytes (cytopathology, condensed chromatin, pyknotic nuclei, and increased eosinophilia) and epidermal cleavage at the dermal/epidermal junction. Transmission electron microscopy showed that lamina densa of the basement membrane to be largely intact. The EpiDerm-FT model represents a major advance in the development of human skin models and its use in studying the molecular mechanisms/proteomics for HD/CEES toxicity is just beginning to be exploited.

Human skin allografts in immunodeficient mice

A third class of human skin model is provided by the use of human skin allografts in immunodeficient mice. Human skin cells, either genetically modified[70] or normal,[71] were grafted onto nude mice and successfully used to examine HD-induced biochemical alterations in skin. In 1995, Rosenthal et al[70] described an engineered human skin model, in which human keratinocyte clones, with some genetic modifications, were grafted onto nude mice, where they formed histologically normal human skin. Later, the same group reported an advanced model developed in immunodeficient nude mice, where a pellet of cells containing human keratinocytes and fibroblasts were placed on top of the muscular layer at the graft site and grown for 1 week.[71] Glass bulbs filled with HD can be directly applied to the sections of mouse skin containing the human skin allograft. Although these in vivo models are expensive and complicated, they possess a number of advantages over any of the in vitro cultured skin models. Grafted human skin models make it possible to obtain a detailed picture of HD-induced morphological, ultrastructural, and inflammatory alterations in various layers of skin cells possessing the realistic complexity of multiple cell–cell interactions. Recently, 3D human skin allografts in mice have allowed investigators to identify distinctive prevesication and postvesication phases and to monitor both dermal-epidermal separation and basal membrane alterations in response to HD exposure.[72,73] However, a limitation of this model is the lack of a functional immune response in the recipient mice.

In spite of the ever higher degrees of physiological complexity, there is not a single model that reflects all the features of human skin. The choice of a particular model may, therefore, be dictated by the particular experimental design and goals. Wound healing studies, for example, would require an in vivo system with an intact immune system since

immune cells are known to contribute to skin regeneration. Moreover, immune cells are thought to play important roles both in HD-induced skin inflammation and in postexposure wound healing through the expression of proinflammatory cytokines (such as Il-1β, TNF-α, IL-6, and GM-CSF) within the first hour after exposure and proceeding through vesication and blister formation.[64] Leukocyte infiltration always starts shortly after HD treatment in mice, rabbits, or guinea pigs. In wound healing, leukocytes and macrophages provide many of the molecular signals regulating fibroblast and keratinocyte proliferation.

The effects of HD on all of the various cell types that come in contact with skin, including macrophages and mast cells, are also important in understanding the overall effects of HD on skin in vivo. Rikimaru et al[74] have used full-thickness human skin explants to study inflammatory mediators in response to topically applied HD. These investigators found that culture fluids from the HD-treated skin contained increased levels of histamine, plasminogen-activating activity, and prostaglandin E2 compared to control explants. It was concluded that both mast cells and epidermal cells were apparently involved in early mediation of the inflammatory response to HD.[74] In contrast, Inoue et al[75] found that the inflammatory response of the mouse ear to HD did not differ in mast cell deficient mice compared to normal mice. At present, there is no obvious explanation for the differences observed between the work of Rikimaru et al[74] and that of Inoue et al[75] It may well be that the mouse ear is not an optimal model for human skin. It is critically important to determine whether HD, or other toxic vesicants, degranulate mast cells since this process could be a major source of inflammatory mediators and, therefore, a major factor in modulating the immune response to HD. In particular, mast cell degranulation would release large amounts of TNF-alpha, which is an inflammatory cytokine.

We have previously reported that lipopolysaccharide (LPS) as well as other inflammatory factors such as TNF-alpha and IL-1-beta amplify the toxicity of CEES[76] and that CEES is a potent inhibitor of nitric oxide production from inducible nitric oxide synthase (iNOS).[77] LPS is a major component of the cell wall of gram-negative bacteria and is known to trigger a variety of inflammatory reactions in macrophages and other cells having CD14 receptors.[78,79] In particular, LPS is known to stimulate the macrophage secretion of nitric oxide[80] and inflammatory cytokines such as tumor TNF-alpha and IL-1-beta[81] Figure 3 shows that RAW 264.7 macrophages stimulated with LPS at 100 ng/mL are markedly more susceptible ($P < .05$) to CEES cytotoxicity (24 hours with 500 μM) than resting macrophages as indicated by a dramatic drop in dehydrogenase activity as measured by the MTT ((3-(4,5-dimethylthiazol-2-yl)-2,5-diphenyltetrazolium bromide) assay. In the absence of LPS, CEES at a level of 500 μM did not significantly affect cell viability.[76] Figure 4 shows that CEES (100–500 μM for 24 hours) inhibits the secretion of nitric oxide into the cell medium by LPS stimulated macrophages in a dose-dependent manner[77] In these experiments, nitrite secretion into the cell culture medium was used as a measure of nitric oxide synthesis. Macrophages (and mast cells) are both present in dermal tissues.

IgE-mediated mast cell degranulation is known to be inhibited by nitric oxide production.[82] NO is a powerful antioxidant[83] and increased intracellular levels of NO are known to inhibit mast cell degranulation.[84] Significantly, mast cell degranulation and histamine release are stimulated by membrane lipid peroxidation and inhibited by antioxidants such as alpha-tocopherol.[85] Collectively, the information presented above suggests that HD/CEES could induce mast cell degranulation by increasing oxidative stress and/or

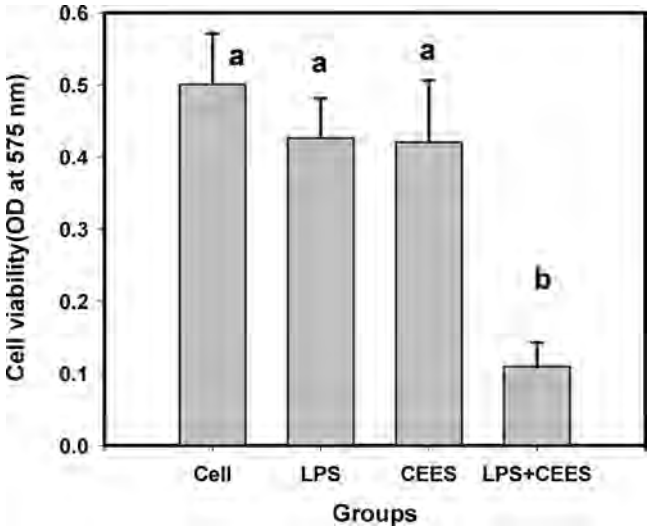

Figure 3. LPS (100 ng/mL) enhances the cytotoxicity of CEES (500 μM). Means not sharing a common letter are significantly different ($P < .05$). Cytotoxicity was measured after 24 hours by the MTT assay.

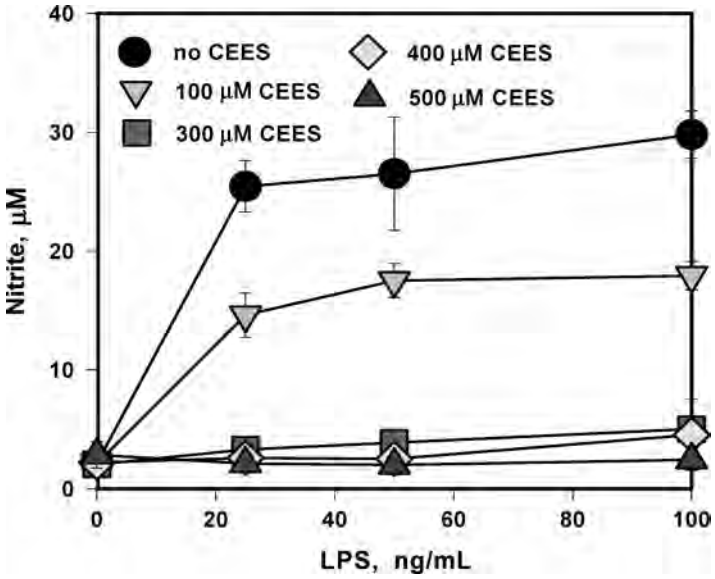

Figure 4. CEES inhibits NO production in LPS stimulated RAW 264.7 macrophages. Cells were simultaneously treated with various levels of CEES (as indicated) and low doses of LPS (as indicated). NO production was monitored as the concentration of nitrite in the culture media after 24 hours.

decreasing nitric oxide production. The subsequent release of TNF-alpha could enhance the cellular toxicity of HD/CEES.

NO generation, mediated by iNOS, is also crucial for the rapid healing of human skin wounds. Although, keratinocytes are known to express iNOS and generate NO in wound healing, it is likely that macrophages, known for their ability to express iNOS and generate high levels of NO, also contribute to the healing stimuli. Thus, it is tempting to suggest that the development of a 3-cell-type (macrophages/fibroblasts/keratinocytes) model would provide a unique and optimal model for studying skin vesication, blistering, and wound healing under very reproducible experimental conditions.

MOLECULAR MECHANISMS FOR MUSTARD TOXICITY

The molecular mechanisms of HD skin toxicity are complex and not yet fully understood. We will focus on 3 major types of interrelated events: primary macromolecule damage, oxidative stress, and inflammation. All of these processes are tightly interconnected and play central roles in HD toxicity. The hypothesized mechanisms of HD toxic effect in skin cells are summarized in Figure 2. In addition, we will discuss the importance of NO signaling modulation in HD toxicity since it is likely to be important for the postexposure wound healing process in skin.

Primary macromolecule damage

HD easily penetrates both cellular and nuclear membranes due to its hydrophobic nature. In the cytosol, it reacts with water forming a highly electrophilic ethylene episulfonium derivative that is the ultimate alkylating agent. DNA alkylation and crosslinking are well-documented primary intracellular damaging reactions of HD. Extensive DNA damage, due to alkylating agents, activates and overloads the DNA repair machinery. In particular, DNA damage induces expression of poly (ADP-ribose) polymerase (PARP), the key regulatory enzyme involved in DNA repair and hypothesized to regulate cell fate by modulating death and survival transcriptional programs.[86] HD induces PARP expression in normal human keratinocytes and the possible involvement of this nuclear enzyme in the regulation of HD cell death mechanisms has been extensively studied.[87–91]

PARP-1 is the most abundant member of the of PARP protein family. PARP-1 binds to DNA structures that have single- and double-strand breaks, crossovers, cruciforms, or supercoils[92]; it signals DNA rupture and facilitates base-excision repair.[93,94] Normally, the intracellular level of PARP-1 is very low, and this enzyme can be detected in the cytosol only under stressful conditions. Upon binding to the damaged DNA sites, PARP-1 metabolizes β-nicotinamide adenine dinucleotide (NAD^+) into branched polymers of ADP-ribose that are transferred to a set of nuclear proteins. This process also results in a very large decrease in the pyridine nucleotide pool. Poly(ADP-ribosyl)ation is thought to be beneficial for genome repair since modifications of proteins proximal to the DNA breaks facilitate multiple local openings of the condensed chromatin structure allowing the binding of the repair protein complex.[93,95]

Despite the beneficial effect, PARP can induce apoptosis or necrosis in skin cells treated with HD[91] or other alkylating agents.[86,96] Thus, limited expression of PARP proteins helps in DNA repair and promotes cell survival but its overexpression (as in case of massive DNA damage) can induce cell death.[97] PARP overproduction, especially in cells utilizing aerobic glycolysis, can lead to the depletion of cellular NAD^+ and ATP (see Fig 2) which rapidly promotes general intracellular bioenergetic collapse and oxidative stress resulting in a regulated form of necrosis.[86,96,98–100] HD is cytotoxic to both dermal fibroblasts and epidermal keratinocytes. It has been suggested that PARP determines the mode of HD-induced cell death in skin fibroblast but not in keratinocytes.[91] In mouse skin fibroblast the absence of PARP shifts the mode of HD-induced cell death shifts from necrosis to apoptosis,[91] whereas keratinocytes, with or without PARP, primarily express an apoptotic form of cell death.[91] HD-treated human keratinocytes show a PARP activation, an upregulation of proapoptotic p53 accompanied by a downregulation of antiapoptotic Bcl-2, and, finally, to caspase activation and apoptosis.[87,90] This pathway was found to be Ca^{++} and calmodulin dependent.[90]

Necrosis due to PARP-induced depletion of NAD^+ and ATP exhaustion during aerobic glycolysis is thought to be the main mechanism of cell death induced by DNA damaging agents, especially in proliferating cells.[96] However, these observations may vary with the dose of alkylating agent, with cell type and perhaps the particular composition of the culture medium (see below) in the case of in vitro studies. HD promotes apoptosis in HeLa cells (10–100 μM),[101] peripheral blood lymphocytes (6–300 μM),[102] keratinocytes (50–300 μM),[53,87] and endothelial cells (<250 μM).[103] A time-dependent shift to necrosis was observed in HD-treated lymphocytes.[102] but a shift toward necrosis is observed at higher levels of HD in endothelial cells (>500 μM)[103] and HeLa (1 mM)[101] Interestingly, human fibroblasts undergo necrosis even at lower concentrations of HD (100–500 μM).[91] In most human cell types, apoptosis predominates within 6–12 hours of postexposure time, whereas necrotic events markedly increase after 12–24 hours.

Countermeasures capable of preventing rapid ATP depletion and mitochondrial dysfunction could be protective against HD-induced necrosis. Unfortunately, this approach would not eliminate cell death completely since apoptosis would likely proceed. However, a shift from necrosis to the less inflammatory apoptotic pathway could possibly be beneficial by helping eliminate secondary infections and improving wound healing. PARP activation causes NAD^+ depletion and NAD+ is required for glycolysis and pyruvate synthesis.[104] In the absence of pyruvate, mitochondrial respiration fails causing bioenergetic collapse and cell death via necrosis.[86] Therefore, the addition of a mitochondria substrate, such as pyruvate, glutamate, or glutamine, to the cell medium could be protective against necrosis.[104] A protective effect of pyruvate treatment has, indeed, been documented in genotoxic stress caused by nitrogen mustard or *N*-methyl-*N*′-nitro-*N*-nitrosoguanidine (MNNG), a chemical analog of HD used as anticancer drugs.[96,100,104]

Alkyl pyruvates, such as methyl pyruvate and ethyl pyruvate, are excellent alternative mitochondrial substrates since they (unlike pyruvate) are stable in solution. In aqueous solutions, pyruvate spontaneously undergoes a series of chemical reactions yielding 2, 4-dihydroxy-2-methylglutarate, which is a mitochondrial poison.[105] In addition, alkyl pyruvates also function as effective and potent scavengers of free radicals. Pyruvates are capable of scavenging hydrogen peroxide (H_2O_2) and the hydroxyl radical (OH&rad;$^-$).[106,107] Administration of pyruvates was shown to protect against various types of oxidant-mediated

cellular and organ injuries in numerous in vitro and in vivo studies.[108,109] These data further suggest that HD activation of PARP and the subsequent depletion of pyruvate is also a contributing factor for HD-induced oxidative stress.

In preliminary results, the authors' laboratory has observed that methyl pyruvate provides protection to human keratinocytes (HaCaT cell line) treated with CEES and a similar effect was observed with ethyl pyruvate (unpublished data). It is worth noting that commercially available serum-free media, formulated to culture NHEK cells, contains 0.5 mM sodium pyruvate. Keratinocyte media from Gibco, Sigma, and Cambrex all contain 0.5 mM pyruvate. It is possible, therefore, that necrosis has not been observed in HD-treated NHEK cells due to the protective effect of sodium pyruvate in the culture media.

In our experiments (unpublished data), however, we used immortalized HaCaT keratinocytes, which proliferate continuously but do not differentiate. Actively proliferating cells utilizes aerobic glycolysis and are more susceptible to mitochondrial dysfunction and necrosis.[86,96,100] After limited number of passages NHEK cells, unlike HaCaT cells, undergo terminal differentiation which is a form of cell death different from either apoptosis or necrosis.[55] This difference between HaCaT and NHEK cells theoretically could cause discrepancies in the cell death pathway caused by HD. Parallel experiments are now being done with NHEK and HaCaT cells to further characterize the protective effect of pyruvate to HD/CEES.

Inflammation

HD-treated normal human keratinocytes release proinflammatory TNF-α, IL-6, IL-1β in a dose-dependent manner[62] but the particular cytokine profiles observed differ depending on the skin model used and the dose of HD.[63,64,110] Cytokine production and responses are known to be regulated by the activation of nuclear transcription factor-kappaB (NF-kappaB) and this activation also plays a key role in determining the fate of a damaged cell. There are numerous activators of NF-kappaB such as bacterial and viral infections, chemical damage, radiation, and oxidative stress. In response to these stimuli, an active NF-kappaB protein complex is liberated in the cytoplasm and it subsequently translocates to the nucleus and triggers selective gene expression. Among the genes regulated by NF-kappaB are adhesion molecules, pro-inflammatory mediators (IL-1 beta, TNF-alpha, interleukin 6), chemokines, IL-8, iNOS, E-selectin, vascular cell adhesion molecule 1 (ICAM-1), and granulocyte-macrophage colony stimulating factor (GM-CSF).[34,111–114] In general, NF-kappaB activation also triggers antiapoptotic genes and promotes cell survival.

Although the precise mechanism(s) of HD-induced gene expression has not yet been fully described in skin cells, it is very likely connected to the DNA damaging effect of HD (see Fig 2) and could, therefore, be PARP-dependent. PARP-1 is known to be a coactivator of NF-kappaB.[115]; however, this pathway has not been fully explored in HD-treated keratinocytes or fibroblasts. It is also possible that HD modulates NF-kappaB and other nuclear factors by covalently modifying DNA binding sequences for transcription factors. Grey et al[116] have shown that HD inhibits the in vitro binding of transcription factor activating protein-2 (AP-2) via alkylating the AP-2 DNA consensus binding sequence rather than by direct damage to the AP-2 protein.

In addition, it is highly possible that HD-induced oxidative stress also can stimulate inflammatory responses via transcription factors. Many of the activators of NF-kappaB can

be blocked with the use of antioxidants.[117,118] Transcription factors AP-1,[119,120] MAF and NRL,[121,122] and NF-IL6[123,124] are regulated by oxygen-dependent mechanisms, and sensitive to ROS. Interestingly, chemical compounds indirectly disrupting NF-kappaB activation induce apoptosis in cancer cells,[125–130] whereas inhibitors of NF-kappaB activation protect HD-treated human keratinocytes.[131,132]

It is also unclear how exactly the proinflammatory cytokines, such as IL-6, contribute to the HD-induced skin damage. It is known, however, that inflammatory processes contribute to the skin damage. In animal models, both skin and lung exposure to HD or CEES causes massive leukocyte infiltration, which starts shortly after the exposure and builds up continuously.[60,61] The fact that skin burns and blistering have a latent period also suggests that secondary responses in skin cells/immune cells also contribute to the mechanisms of HD toxicity. HD treatment is known to induce NF-kappaB activation and release of inflammatory cytokines in both keratinocytes and macrophages.[63,110,133–135] TNF-alpha, in general, induces apoptosis in keratinocytes and treatment with anti-TNF-alpha antibodies is protective against UV-induced skin lesions.[136] However, the effect of TNF-alpha in HD-treated skin is complex and an attempt to reduce cell death in normal human keratinocytes by blocking TNFR1, the major cell receptor for TNH-alphas was not successful.[71]

It is likely that keratinocyte activation (see Fig 2) plays an important role in HD toxicity. Activation of keratinocytes is a multistep pathway induced in response to skin injury. Activated keratinocytes are hyperproliferative and able to migrate to the site of injury in order to form layers of fresh cells in the dermis and epidermis. Activation is regulated by various cell signaling pathways including TNF-alpha.[57,137] Since HD-treated keratinocytes release high levels of TNF-alpha in the medium,[133] we suggest that HD promotes keratinocyte activation, subsequent hyperproliferation, and an enhanced susceptibility to the PARP-mediated bioenergetic collapse. This series of molecular events would cause a shift from apoptosis to necrosis. Although a time- or concentration-dependent shift from apoptosis to necrosis has been well documented for HD-treated lymphocytes,[102] endothelial cells,[103] and HeLa cells,[101] such changes have not been noted for human keratinocytes. As discussed above, this may be due to the fact that NHEK cells are always protected from necrosis by pyruvate-containing media. The recently documented protective effect of NF-kappaB inhibitors in NHEK and HaCaT cells treated with HD[131,132] also supports our speculation since these inhibitors downregulate TNF-alpha which would impair keratinocyte activation.

WOUND HEALING

NO signaling plays a key role in the inflammation and wound healing.[138–140] Animal studies[141] have shown that in iNOS knockout mice, wound healing is impaired but restored by iNOS gene transfer. Lack of NO and impaired expression of iNOS after the HD exposure are thought to be important events promoting skin burns and blistering. We have shown that HD treatment inhibits iNOS expression and NO synthesis (see Fig 4) in LPS-stimulated murine macrophages.[77] Suppression of iNOS expression and several protein activators of wound healing have also been found in human keratinocytes treated with HD.[142]

In keratinocytes, the beginning stage of the wound healing process is determined by the activation process. Under conditions of physical injury, the keratinocyte cell cycle is activated and the cells become hyperproliferative and migrate to the site of injury in response to chemokines.[57,137] Activation of keratinocytes, as well as their return to the healthy basal phenotype, is controlled by cytokines and growth factors produced by various cutaneous cell types, including keratinocytes and lymphocytes infiltrated at the wound site. Various intracellular signaling pathways are involved at the different stages of activation. Interestingly, NF-kappaB activation and consequent autocrine TNF-alpha production occur at the initial stages of the activation and allow keratinocytes to become hyperproliferative and migratory.[57,137] Activation is terminated when lymphocytes, present at the wound site, release interferon-gamma (IFN-gamma), which induces the activation of STAT-1 and makes keratinocytes contract newly deposit fibronectin-rich basement membrane. Finally, transforming growth factor-beta (TGF-beta) secreted by fibroblasts induces the expression of K5 and K14, fully reverting the keratinocytes to a healthy basal phenotype and making them responsive to differentiation stimuli.[57]

In human cells, expression of iNOS, which is the main NO-generating protein in keratinocytes,[143] is regulated synergistically by 2 major pathways: NF-kappaB and STAT-1.[144] As pointed above, both HD and its chemical analog CEES downregulate iNOS expression in murine macrophages[77]and human keratinocytes.[142] Since NF-kappaB activation is well documented in NHEK cells,[131–133] it is possible that the impaired expression of iNOS in HD-treated cells could be attributed to a STAT-1-dependent mechanisms. In addition, the possible STAT-1 inhibition by HD could disrupt the IFN-gamma signaling pathway resulting in keratinocytes unable to terminate their wound healing state.[57] Thus, simultaneous HD-induced NF-kappaB activation and STAT-1 inhibition could alter necrosis, inhibit NO generation, prevent wound healing, and possibly affect vesication and blistering.

The molecular mechanisms whereby HD alters transcription factors activation are not fully elucidated. However, it is highly possible that the ability of mustards to alkylate DNA is involved. As pointed above, HD is capable of chemically modifying both proteins (via crosslinking of Cys residues) and DNA (via alkylation of guanine rich sequences, and crosslinking). It seems likely that HD would more effectively damage "more exposed" regions of DNA with accessibility to transcription factors. Interestingly, Gray[116] had shown that HD inhibits the in vitro binding of transcription factor AP-2 via alkylation of the guanine-rich consensus DNA sequences but not by directly damaging the AP-2 protein. It is tempting to assume that other transcription factor functions could be affected by HD in a similar manner. However, the effects of HD on NF-kappaB and STAT-1α have not been elucidated and AP-2 remains the only transcription factor studied in relation to HD toxicity.

Since some transcription factors are sensitive to ROS and to the redox state of the cell in general, it is likely that oxidative stress, inflammation, and NO signaling are tightly interconnected in skin and its dynamic responses to toxic agents. Soneja et al[145] have suggested that wound healing could be accelerated under circumstances in which oxidative stress is minimized but NO production remains elevated. On the other hand, under conditions elevating oxidative stress, the toxicity of mustards can be greatly enhanced. For instance, the HD analog CEES shows much higher toxicity in cells stimulated by LPS, TNF-alpha, or IL-1beta, which enhance inflammation and oxidative stress.[76]

FUTURE DIRECTIONS

A systems biology approach to mustard toxicity

As discussed above, HD toxicity in skin results from a multistep complex mechanism involving a number of signaling cascades and various cell types. It is extremely difficult to follow each step in this mechanism even in a simple in vitro model. A systems biology approach would view HD toxicity as time-dependent disruption of an integrated and interacting network of genes, proteins, and biochemical reactions. This approach would emphasize integrating data obtained from transcriptomics, metabolomics, and proteomics with the purpose of constructing and validating a comprehensive model of HD toxicity. The computational tools for this task would include network mapping as well as correlation, logical, and kinetic modeling.[146] This comprehensive model would be the best way to address the question: "how relevant to the HD-induced cell death pathways are the direct chemical alterations caused by HD to various cellular proteins (oxidation, cross-linking, and fragmentation) and the indirect chemical protein alterations caused by ROS and RNOS?"

A transcriptomic approach to studying HD toxicity is already yielding useful results. In NHEK cells, DNA array techniques have been applied to studying HD-altered gene expression,[147,148] and mRNA differential display has been used to examine HD-induced transcriptional modulations in human epidermal keratinocytes.[149] Microarray analyses of gene expression in CEES- or HD-exposed mouse skin in vivo have also been accomplished.[147,150] These studies are providing a deeper insight into the mechanism of HD toxicity since they have identified a number of genes upregulated at the early (0.5–4 hours) and intermediate (24 hours) stages of postexposure. DNA array analyses are capable of providing crucial information regarding the changes in transcriptional activity in the cell and are useful in the search for "the key" signaling pathways involved in HD toxicity. These studies will help in the design of evermore effective countermeasures and help identify key biomarkers for therapeutic efficacy. Proteomic data on HD toxicity are currently very limited but this approach would complement the previously accumulated microarray data by helping identify all the key proteins involved in HD toxicity at different stages.

Collectively, the literature reviewed here supports the notion that oxidative stress, free radical damage to biomolecules, and alterations in redox sensitive signaling pathways are key factors in understanding vesicant toxicology. It is likely, therefore, that the newly emerging area of redox proteomics would be particularly useful in understanding HD damage to skin. Redox proteomics is focused on characterizing (1) the chemical modifications of specific proteins induced by ROS and RNOS; (2) alterations in specific proteins induced by changes in redox sensitive transcription factors; and (3) alterations in the function/structure of specific proteins caused by redox sensitive posttranslational modifications.[151–153] In this regard, small thiols, like GSH, are no longer viewed just as protective antioxidants but as redox regulators of proteins via glutathionylation or by oxidation of protein cysteine residue.[152] Redox proteomics is rapidly emerging as a very powerful tool for characterizing and identifying proteins based on their redox state.[153] This approach has recently been used to specifically identify oxidized proteins in Alzheimer's disease and this information has proven useful in identifying new therapeutic targets and in providing new molecular insights into disease etiology.[154]

Multicomponent antioxidant liposomes

HD, due to its hydrophobic nature, effectively penetrates deep into the skin and affects mostly proliferating cells within basement membrane, that is, the lowest layer of proliferating keratinocytes. These growing cells would be highly susceptible to the PARP-mediated bioenergetic collapse since they actively utilize aerobic glycolysis. HD is likely, therefore, to induce necrosis rather than apoptosis in these cells, which would subsequently promote severe inflammation, skin blistering, and vesication. Thus, it is critically important to provide fast and efficient delivery of the desired drugs to the deeper skin layers and liposomes hold promise in this regard. By encapsulating a lipid soluble thiol, antioxidant liposomes could also effectively diminish (by direct covalent reaction) the stores of HD in skin lipid depots. Although this review has emphasized antioxidants, there is practically no limit to the possible encapsulated agents that can be incorporated into liposomes and delivered to the skin cells. These agents could include PARP inhibitors, protease inhibitors, anti-inflammatory agents, and chemical or enzymatic antioxidants. Currently, we are testing novel formulations of multiagent antioxidant liposomes containing both antiapoptotic (NAC) and antinecrotic (ethyl pyruvate) agents. Liposomes can also be formulated with agents designed to accelerate wound healing such as epidermal growth factor, transforming growth factor-β, platelet-derived growth factor, insulin-like growth factor, keratinocyte growth factor, and fibroblast growth factor.

ACKNOWLEDGMENTS

This research was supported by three United States Army Medical Research Command (USAMRMC) Grants: "The Influence of Antioxidant Liposomes on Macrophages Treated with Mustard Gas Analogues", Grant No. 98164001; "Topical Application of Liposomal Antioxidants for Protection against CEES Induced Skin Damage", Contract No. W81XWH-05-2-0034, and; "A Proteomic Approach for Studying the Therapeutic Use of Antioxidant Liposomes", Contract No. W81XWH-06-2-044.

REFERENCES

1. Somani SM, Babu SR. Toxicodynamics of sulfur mustard. *Int J Clin Pharmacol Ther Toxicol*. 1989;27:419–435.
2. Sinclair DC. Disability produced by exposure of skin to mustard-gas vapour. *Br Med J*. 1950;1:346–349.
3. Drasch G, Kretschmer E, Kauert G, von Meyer L. Concentrations of mustard gas [bis(2-chloroethyl)sulfide] in the tissues of a victim of a vesicant exposure. *J Forensic Sci*. 1987;32:1788–1793.
4. Vijayaraghavan R, Kulkarni A, Pant SC, et al. Differential toxicity of sulfur mustard administered through percutaneous, subcutaneous, and oral routes. *Toxicol Appl Pharmacol*. 2005;202:180–188.
5. Papirmeister B, Gross CL, Meier HL, Petrali JP, Johnson JB. Molecular basis for mustard-induced vesication. *Fundam Appl Toxicol*. 1985;5:S134–S149.
6. Langenberg JP, van der Schans GP, Spruit HE, et al. Toxicokinetics of sulfur mustard and its DNA-adducts in the hairless guinea pig. *Drug Chem Toxicol*. 1998;21(suppl 1):131–147.
7. Wormser U. Toxicology of mustard gas. *Trends Pharmacol Sci*. 1991;12:164–167.
8. Hay A. Effects on health of mustard gas. *Nature*. 1993;366:398.
9. Pearson GS. Veterans at risk: the health effects of mustard gas and lewisite. *Nature*. 1993;365:218.
10. Black RM, Read RW. Biological fate of sulphur mustard, 1,1′-thiobis(2-chloroethane): identification of beta-lyase metabolites and hydrolysis products in human urine. *Xenobiotica*. 1995;25:167–73.

11. Boyer AE, Ash D, Barr DB, et al. Quantitation of the sulfur mustard metabolites 1,1′-sulfonylbis[2-(methylthio)ethane] and thiodiglycol in urine using isotope-dilution Gas chromatography-tandem mass spectrometry. *J Anal Toxicol*. 2004;28:327–332.
12. Chilcott RP, Jenner J, Carrick W, Hotchkiss SA, Rice P. Human skin absorption of bis-2-(chloroethyl)sulphide (sulphur mustard) in vitro. *J Appl Toxicol*. 2000;20:349–355.
13. Graham JS, Chilcott RP, Rice P, Milner SM, Hurst CG, Maliner BI. Wound healing of cutaneous sulfur mustard injuries: strategies for the development of improved therapies. *J Burns Wounds*. 2005;4:e1.
14. Lindsay CD, Rice P. Changes in connective tissue macromolecular components of Yucatan mini-pig skin following application of sulphur mustard vapour. *Hum Exp Toxicol*. 1995;14:341–348.
15. Naghii MR. Sulfur mustard intoxication, oxidative stress, and antioxidants. *Mil Med*. 2002;167:573–575.
16. Anderson DR, Yourick JJ, Arroyo CM, Young GD, Harris LW. Use of EPR spin-trapping techniques to detect radicals from rat lung lavage fluid following sulfur mustard vapor exposure. *Med Defense Biosci Rev Proc*. 1993;1:113–121.
17. Elsayed NM, Omaye ST. Biochemical changes in mouse lung after subcutaneous injection of the sulfur mustard 2-chloroethyl 4-chlorobutyl sulfide. *Toxicol*. 2004;199:195–206.
18. Elsayed NM, Omaye ST, Klain GJ, Korte DW Jr. Free radical-mediated lung response to the monofunctional sulfur mustard butyl 2-chloroethyl sulfide after subcutaneous injection. *Toxicol*. 1992;72:153–165.
19. Vijayaraghavan R, Sugendran K, Pant SC, Husain K, Malhotra RC. Dermal intoxication of mice with bis(2-chloroethyl)sulphide and the protective effect of flavonoids. *Toxicol*. 1991;69:35–42.
20. Husain K, Dube SN, Sugendran K, Singh R, Das Gupta S, Somani SM. Effect of topically applied sulphur mustard on antioxidant enzymes in blood cells and body tissues of rats. *J Appl Toxicol*. 1996;16:245–248.
21. Yourick JJ, Dawson JS, Benton CD, Craig ME, Mitcheltree LW. Pathogenesis of 2,2′-dichlorodiethyl sulfide in hairless guinea pigs. *Toxicol*. 1993;84:185–197.
22. Vojvodic V, Milosavljevic Z, Boskovic B, Bojanic N. The protective effect of different drugs in rats poisoned by sulfur and nitrogen mustards. *Fundam Appl Toxicol*. 1985;5:160–168.
23. Azzi A, Gysin R, Kempna P, et al. Vitamin E mediates cell signaling and regulation of gene expression. *Ann N Y Acad Sci*. 2004;1031:86–95.
24. Ricciarelli R, Zingg JM, Azzi A. Vitamin E: protective role of a Janus molecule. *Faseb J*. 2001;15:2314–2325.
25. Zingg JM, Azzi A. Non-antioxidant activities of vitamin E. *Curr Med Chem*. 2004;11:1113–1133.
26. Cooney RV, Franke AA, Harwood PJ, Hatch-Pigott V, Custer LJ, Mordan LJ. Gamma-tocopherol detoxification of nitrogen dioxide: superiority to alpha-tocopherol. *Proc Natl Acad Sci U S A*. 1993;90:1771–1775.
27. Samandari E, Visarius T, Zingg JM, Azzi A. The effect of gamma-tocopherol on proliferation, integrin expression, adhesion, and migration of human glioma cells. *Biochem Biophys Res Commun*. 2006;342:1329–1333.
28. Eldad A, Ben Meir P, Breiterman S, Chaouat M, Shafran A, Ben-Bassat H. Superoxide dismutase (SOD) for mustard gas burns. *Burns*. 1998;24:114–119.
29. Alvarez MN, Trujillo M, Radi R. Peroxynitrite formation from biochemical and cellular fluxes of nitric oxide and superoxide. *Methods Enzymol*. 2002;359:353–366.
30. Beckman JS, Koppenol WH. Nitric oxide, superoxide, and peroxynitrite: the good, the bad, and ugly. *Am J Physiol*. 1996;271:1424–1437.
31. Fukuyama N, Nakazawa H. [Superoxide, nitric oxide and peroxynitrite]. *Nippon Yakurigaku Zasshi*. 1998;112:169–176.
32. Kumar O, Sugendran K, Vijayaraghavan R. Protective effect of various antioxidants on the toxicity of sulphur mustard administered to mice by inhalation or percutaneous routes. *Chem Biol Interact*. 2001;134:1–12.
33. McClintock SD, Hoesel LM, Das SK, et al. Attenuation of half sulfur mustard gas-induced acute lung injury in rats. *J Appl Toxicol*. 2006;26:126–131.
34. McClintock SD, Till GO, Smith MG, Ward PA. Protection from half-mustard-gas-induced acute lung injury in the rat. *J Appl Toxicol*. 2002;22:257–262.
35. Kelly GS. Clinical applications of *N*-acetylcysteine. *Altern Med Rev*. 1998;3:114–127.
36. Gross CL, Innace JK, Hovatter RC, Meier HL, Smith WJ. Biochemical manipulation of intracellular glutathione levels influences cytotoxicity to isolated human lymphocytes by sulfur mustard. *Cell Biol Toxicol*. 1993;9:259–267.

37. Meister A, Anderson ME. Glutathione. *Annu Rev Biochem*. 1983;52:711–760.
38. Bhat S, Gulati S, Husain K, Milner SM. Lipoic acid decreases oxidative stress in sulphur mustard toxicity. Proceedings of American Burn Association, 38th Annual Meeting, S139. Las Vegas, Nevada: *J Burn Care Res*, 27(2, suppl):S139, 2006.
39. Bast A, Haenen GR. Lipoic acid: a multifunctional antioxidant. *Biofactors*. 2003;17:207–213.
40. Dincer Y, Telci A, Kayali R, Yilmaz IA, Cakatay U, Akcay T. Effect of alpha-lipoic acid on lipid peroxidation and anti-oxidant enzyme activities in diabetic rats. *Clin Exp Pharmacol Physiol*. 2002;29:281–284.
41. Ernst A, Stolzing A, Sandig G, Grune T. Antioxidants effectively prevent oxidation-induced protein damage in OLN 93 cells. *Arch Biochem Biophys*. 2004;421:54–60.
42. Maritim AC, Sanders RA, Watkins JB, III. Effects of alpha-lipoic acid on biomarkers of oxidative stress in streptozotocin-induced diabetic rats. *J Nutr Biochem*. 2003;14:288–294.
43. Wollin SD, Jones PJ. Alpha-lipoic acid and cardiovascular disease. *J Nutr*. 2003;133:3327–3330.
44. Busse E, Zimmer G, Schopohl B, Kornhuber B. Influence of alpha-lipoic acid on intracellular glutathione in vitro and in vivo. *Arzneimittelforschung*. 1992;42:829–831.
45. Han D, Handelman G, Marcocci L, et al. Lipoic acid increases de novo synthesis of cellular glutathione by improving cystine utilization. *Biofactors*. 1997;6:321–338.
46. Stone WL, Mukherjee S, Smith M, Das SK. Therapeutic uses of antioxidant liposomes. *Methods Mol Biol*. 2002;199:145–161.
47. Stone WL, Smith M. Therapeutic uses of antioxidant liposomes. *Mol Biotechnol*. 2004;27:217–230.
48. Fan J, Shek PN, Suntres ZE, Li YH, Oreopoulos GD, Rotstein OD. Liposomal antioxidants provide prolonged protection against acute respiratory distress syndrome. *Surg*. 2000;128:332–338.
49. Kirjavainen M, Urtti A, Jaaskelainen I, et al. Interaction of liposomes with human skin in vitro—the influence of lipid composition and structure. *Biochim Biophys Acta*. 1996;1304:179–189.
50. Kirjavainen M, Urtti A, Valjakka-Koskela R, Kiesvaara J, Monkkonen J. Liposome-skin interactions and their effects on the skin permeation of drugs. *Eur J Pharm Sci*. 1999;7:279–286.
51. Boyce ST, Ham RG. Calcium-regulated differentiation of normal human epidermal keratinocytes in chemically defined clonal culture and serum-free serial culture. *J Invest Dermatol*. 1983;81:33s–40s.
52. Smith WJ, Gross CL, Chan P, Meier HL. The use of human epidermal keratinocytes in culture as a model for studying the biochemical mechanisms of sulfur mustard toxicity. *Cell Biol Toxicol*. 1990;6:285–291.
53. Stoppler H, Stoppler MC, Johnson E, et al. The E7 protein of human papillomavirus type 16 sensitizes primary human keratinocytes to apoptosis. *Oncogene*. 1998;17:1207–1214.
54. Boukamp P, Petrussevska RT, Breitkreutz D, Hornung J, Markham A, Fusenig NE. Normal keratinization in a spontaneously immortalized aneuploid human keratinocyte cell line. *J Cell Biol*. 1988;106:761–771.
55. Lippens S, Denecker G, Ovaere P, Vandenabeele P, Declercq W. Death penalty for keratinocytes: apoptosis versus cornification. *Cell Death Differ*. 2005;12(suppl 2):1497–1508.
56. Maas-Szabowski N, Starker A, Fusenig NE. Epidermal tissue regeneration and stromal interaction in HaCaT cells is initiated by TGF-alpha. *J Cell Sci*. 2003;116:2937–2948.
57. Freedberg IM, Tomic-Canic M, Komine M, Blumenberg M. Keratins and the keratinocyte activation cycle. *J Invest Dermatol*. 2001;116:633–640.
58. Smith CN, Lindsay CD, Upshall DG. Presence of methenamine/glutathione mixtures reduces the cytotoxic effect of sulphur mustard on cultured SVK-14 human keratinocytes in vitro. *Hum Exp Toxicol*. 1997;16:247–253.
59. Simpson R, Lindsay CD. Effect of sulphur mustard on human skin cell lines with differential agent sensitivity. *J Appl Toxicol*. 2005;25:115–128.
60. Wormser U, Sintov A, Brodsky B, Nyska A. Topical iodine preparation as therapy against sulfur mustard-induced skin lesions. *Toxicol Appl Pharmacol*. 2000;169:33–39.
61. Das SK, Mukherjee S, Smith MG, Chatterjee D. Prophylactic protection by *N*-acetylcysteine against the pulmonary injury induced by 2-chloroethyl ethyl sulfide, a mustard analogue. *J Biochem Mol Toxicol*. 2003;17:177–184.
62. Arroyo CM, Schafer RJ, Kurt EM, Broomfield CA, Carmichael AJ. Response of normal human keratinocytes to sulfur mustard: cytokine release. *J Appl Toxicol. Jat*. 2000;20(suppl 1):S63–S72.
63. Ricketts KM, Santai CT, France JA, et al. Inflammatory cytokine response in sulfur mustard-exposed mouse skin. *J Appl Toxicol. Jat*. 2000;20(suppl 1):73–76.

64. Sabourin CL, Petrali JP, Casillas RP. Alterations in inflammatory cytokine gene expression in sulfur mustard-exposed mouse skin. *J Biochem Mol Toxicol*. 2000;14:291–302.
65. Vavra AK, Laurent CJ, Ngo V, Sweeney JF, Levitt JM. Sulfur mustard primes phagocytosis and degranulation in human polymorphonuclear leukocytes. *Int Immunopharmacol*. 2004;4:437–445.
66. Blaha M, Bowers W, Kohl J, DuBose D, Walker J. Il-1-related cytokine responses of nonimmune skin cells subjected to CEES exposure with and without potential vesicant antagonists. 2000;13:99–111.
67. Blaha M, Bowers W, Kohl J, et al. Effects of CEES on inflammatory mediators, heat shock protein 70A, histology and ultrastructure in two skin models. *J Appl Toxicol. Jat*. 2000;20(suppl 1):S101–S108.
68. Blaha M, Kohl J, DuBose D, Bowers W Jr, Walker J. Ultrastructural and histological effects of exposure to CEES or heat in a human epidermal model. *In Vitr Mol Toxicol*. 2001;14:15–23.
69. Hayden PJ, Petrali JP, Hamilton TA, Kubilus J, Smith WJ, Klausner M. Development of a full thickness in vitro human skin equivalent (EpiDerm-FT) for sulfur mustard research, SID Abstract #174. 2005 Society for Investigative Dermatology Annual Meeting, 2005.
70. Rosenthal DS, Shima TB, Celli G, De Luca LM, Smulson ME. Engineered human skin model using poly(ADP-ribose) polymerase antisense expression shows a reduced response to DNA damage. *J Invest Dermatol*. 1995;105:38–43.
71. Rosenthal DS, Velena A, Chou FP, et al. Expression of dominant-negative Fas-associated death domain blocks human keratinocyte apoptosis and vesication induced by sulfur mustard. *J Biol Chem*. 2003;278:8531–8540.
72. Greenberg S, Margulis A, Garlick JA. In vivo transplantation of engineered human skin. *Methods Mol Biol*. 2005;289:425–430.
73. Greenberg S, Kamath P, Petrali J, Hamilton T, Garfield J, Garlick JA. Characterization of the initial response of engineered human skin to sulfur mustard. *Toxicol Sci*. 2006;90:549–557.
74. Rikimaru T, Nakamura M, Yano T, et al. Mediators, initiating the inflammatory response, released in organ culture by full-thickness human skin explants exposed to the irritant, sulfur mustard. *J Invest Dermatol*. 1991;96:888–897.
75. Inoue H, Asaka T, Nagata N, Koshihara Y. Mechanism of mustard oil-induced skin inflammation in mice. *Eur J Pharmacol*. 1997;333:231–240.
76. Stone WL, Qui M, Smith M. Lipopolysaccharide enhances the cytotoxicity of 2-chloroethyl ethyl sulfide. *BMC Cell Biol*. 2003;4:1.
77. Qui M, Paromov VM, Yang H, Smith M, Stone WL. Inhibition of inducible nitric oxide synthase by a mustard gas analog in murine macrophages. *BMC Cell Biol*. 2006;7:39.
78. Wright SD, Ramos RA, Tobias PS, Ulevitch RJ, Mathison JC. CD14, a receptor for complexes of lipopolysaccharide (LPS) and LPS binding protein. *Sci*. 1990;249:1431–1433.
79. Downey JS, Han J. Cellular activation mechanisms in septic shock. *Front Biosci*. 1998;3:d468–d476.
80. Tepperman BL, Chang Q, Soper BD. Protein kinase C mediates lipopolysaccharide- and phorbol-induced nitric-oxide synthase activity and cellular injury in the rat colon. *J Pharmacol Exp Ther*. 2000;295:1249–1257.
81. Shapira L, Takashiba S, Champagne C, Amar S, Van Dyke TE. Involvement of protein kinase C and protein tyrosine kinase in lipopolysaccharide-induced TNF-alpha and IL-1 beta production by human monocytes. *J Immunol*. 1994;153:1818–1824.
82. Eastmond NC, Banks EM, Coleman JW. Nitric oxide inhibits IgE-mediated degranulation of mast cells and is the principal intermediate in IFN-gamma-induced suppression of exocytosis. *J Immunol*. 1997;159:1444–1450.
83. Wink DA, Miranda KM, Espey MG, et al. Mechanisms of the antioxidant effects of nitric oxide. *Antioxid Redox Signal*. 2001;3:203–213.
84. McCauley SD, Gilchrist M, Befus AD. Nitric oxide: a major determinant of mast cell phenotype and function. *Mem Inst Oswaldo Cruz*. 2005;100(suppl 1):11–14.
85. Masini E, Palmerani B, Gambassi F, et al. Histamine release from rat mast cells induced by metabolic activation of polyunsaturated fatty acids into free radicals. *Biochem Pharmacol*. 1990;39:879–889.
86. Chiarugi A. Poly(ADP-ribose) polymerase: killer or conspirator? The "suicide hypothesis" revisited. *Trends Pharmacol Sci*. 2002;23:122–129.

87. Rosenthal DS, Simbulan-Rosenthal CM, Iyer S, et al. Sulfur mustard induces markers of terminal differentiation and apoptosis in keratinocytes via a Ca^{2+}-calmodulin and caspase-dependent pathway. *J Invest Dermatol*. 1998;111:64–71.
88. Hinshaw DB, Lodhi IJ, Hurley LL, Atkins KB, Dabrowska MI. Activation of poly [ADP-Ribose] polymerase in endothelial cells and keratinocytes: role in an in vitro model of sulfur mustard-mediated vesication. *Toxicol Appl Pharmacol*. 1999;156:17–29.
89. Bhat KR, Benton BJ, Rosenthal DS, Smulson ME, Ray R. Role of poly(ADP-ribose) polymerase (PARP) in DNA repair in sulfur mustard-exposed normal human epidermal keratinocytes (NHEK). *J Appl Toxicol*. 2000;20(suppl 1):S13–S17.
90. Rosenthal DS, Simbulan-Rosenthal CM, Iyer S, Smith WJ, Ray R, Smulson ME. Calmodulin, poly(ADP-ribose)polymerase and p53 are targets for modulating the effects of sulfur mustard. *J Appl Toxicol*. 2000;20(suppl 1):S43–S49.
91. Rosenthal DS, Simbulan-Rosenthal CM, Liu WF, et al. PARP determines the mode of cell death in skin fibroblasts, but not keratinocytes, exposed to sulfur mustard. *J Invest Dermatol*. 2001;117:1566–1573.
92. Kim MY, Zhang T, Kraus WL. Poly(ADP-ribosyl)ation by PARP-1: "PAR-laying" NAD+ into a nuclear signal. *Genes Dev*. 2005;19:1951–1967.
93. D'Amours D, Desnoyers S, D'Silva I, Poirier GG. Poly(ADP-ribosyl)ation reactions in the regulation of nuclear functions. *Biochem J*. 1999;342(Pt 2):249–268.
94. Herceg Z, Wang ZQ. Functions of poly(ADP-ribose) polymerase (PARP) in DNA repair, genomic integrity and cell death. *Mutat Res*. 2001;477:97–110.
95. Shall S, de Murcia G. Poly(ADP-ribose) polymerase–1: what have we learned from the deficient mouse model? *Mutat Res*. 2000;460:1–15.
96. Zong WX, Ditsworth D, Bauer DE, Wang ZQ, Thompson CB. Alkylating DNA damage stimulates a regulated form of necrotic cell death. *Genes Dev*. 2004;18:1272–1282.
97. Burkle A. PARP-1: a regulator of genomic stability linked with mammalian longevity. *Chembiochem*. 2001;2:725–728.
98. Bouchard VJ, Rouleau M, Poirier GG. PARP-1, a determinant of cell survival in response to DNA damage. *Exp Hematol*. 2003;31:446–454.
99. Decker P, Muller S. Modulating poly (ADP-ribose) polymerase activity: potential for the prevention and therapy of pathogenic situations involving DNA damage and oxidative stress. *Curr Pharm Biotechnol*. 2002;3:275–283.
100. Ying W, Alano CC, Garnier P, Swanson RA. NAD+ as a metabolic link between DNA damage and cell death. *J Neurosci Res*. 2005;79:216–223.
101. Sun J, Wang YX, Sun MJ. Apoptosis and necrosis induced by sulfur mustard in Hela cells. *Zhongguo Yao Li Xue Bao*. 1999;20:445–448.
102. Meier HL, Millard CB. Alterations in human lymphocyte DNA caused by sulfur mustard can be mitigated by selective inhibitors of poly(ADP-ribose) polymerase. *Biochim Biophys Acta*. 1998;1404:367–376.
103. Dabrowska MI, Becks LL, Lelli JL Jr, Levee MG, Hinshaw DB. Sulfur mustard induces apoptosis and necrosis in endothelial cells. *Toxicol Appl Pharmacol*. 1996;141:568–583.
104. Ying W, Chen Y, Alano CC, Swanson RA. Tricarboxylic acid cycle substrates prevent PARP-mediated death of neurons and astrocytes. *J Cereb Blood Flow Metab*. 2002;22:774–779.
105. Willems JL, de Kort AF, Vree TB, Trijbels JM, Veerkamp JH, Monnens LA. Non-enzymic conversion of pyruvate in aqueous solution to 2,4-dihydroxy-2-methylglutaric acid. *FEBS Lett*. 1978;86:42–44.
106. O'Donnell-Tormey J, Nathan CF, Lanks K, DeBoer CJ, de la Harpe J. Secretion of pyruvate. An antioxidant defense of mammalian cells. *J Exp Med*. 1987;165:500–514.
107. Dobsak P, Courderot-Masuyer C, Zeller M, et al. Antioxidative properties of pyruvate and protection of the ischemic rat heart during cardioplegia. *J Cardiovasc Pharmacol*. 1999;34:651–659.
108. Das UN. Pyruvate is an endogenous anti-inflammatory and anti-oxidant molecule. *Med Sci Monit*. 2006;12:RA79–RA84.
109. Mallet RT, Sun J, Knott EM, Sharma AB, Olivencia-Yurvati AH. Metabolic cardioprotection by pyruvate: recent progress. *Exp Biol Med (Maywood)*. 2005;230:435–443.
110. Sabourin CL, Danne MM, Buxton KL, Casillas RP, Schlager JJ. Cytokine, chemokine, and matrix metalloproteinase response after sulfur mustard injury to weanling pig skin. *J Biochem Mol Toxicol*. 2002;16:263–272.

111. Akira S, Kishimoto T. NF-IL6 and NF-kappa B in cytokine gene regulation. *Adv Immunol*. 1997;65:1–46.
112. Brennan P, O'Neill LA. Effects of oxidants and antioxidants on nuclear factor kappa B activation in three different cell lines: evidence against a universal hypothesis involving oxygen radicals. *Biochim Biophys Acta*. 1995;1260:167–175.
113. Barnes PJ, Adcock IM. Transcription factors and asthma. *Eur Respir J*. 1998;12:221–234.
114. Rahman I, MacNee W. Role of transcription factors in inflammatory lung diseases. *Thorax*. 1998;53:601–612.
115. Martin-Oliva D, O'Valle F, Munoz-Gamez JA, et al. Crosstalk between PARP-1 and NF-kappaB modulates the promotion of skin neoplasia. *Oncog*. 2004;23:5275–5283.
116. Gray PJ. Sulphur mustards inhibit binding of transcription factor AP2 in vitro. *Nucleic Acids Res*. 1995;23:4378–4382.
117. Schulze-Osthoff K, Bauer MK, Vogt M, Wesselborg S. Oxidative stress and signal transduction. *Int J Vitam Nutr Res*. 1997;67:336–342.
118. Schwager J, Schulze J. Influence of ascorbic acid on the response to mitogens and interleukin production of porcine lymphocytes. *Int J Vitam Nutr Res*. 1997;67:10–16.
119. Xanthoudakis S, Miao GG, Curran T. The redox and DNA-repair activities of Ref-1 are encoded by nonoverlapping domains. *Proc Natl Acad Sci U S A*. 1994;91:23–27.
120. Yao KS, Xanthoudakis S, Curran T, O'Dwyer PJ. Activation of AP-1 and of a nuclear redox factor, Ref-1, in the response of HT29 colon cancer cells to hypoxia. *Mol Cell Biol*. 1994;14:5997–6003.
121. Kerppola TK, Curran T. A conserved region adjacent to the basic domain is required for recognition of an extended DNA binding site by Maf/Nrl family proteins. *Oncogene*. 1994;9:3149–3158.
122. Kerppola TK, Curran T. Maf and Nrl can bind to AP-1 sites and form heterodimers with Fos and Jun. *Oncogene*. 1994;9:675–684.
123. Klampfer L, Lee TH, Hsu W, Vilcek J, Chen-Kiang S. NF-IL6 and AP-1 cooperatively modulate the activation of the TSG-6 gene by tumor necrosis factor alpha and interleukin-1. *Mol Cell Biol*. 1994;14:6561–6569.
124. Hsu W, Kerppola TK, Chen PL, Curran T, Chen-Kiang S. Fos and Jun repress transcription activation by NF-IL6 through association at the basic zipper region. *Mol Cell Biol*. 1994;14:268–276.
125. Crispen PL, Uzzo RG, Golovine K, et al. Vitamin E succinate inhibits NF-kappaB and prevents the development of a metastatic phenotype in prostate cancer cells: implications for chemoprevention. *Prostate*. 2007;67:582–590.
126. Campbell SE, Stone WL, Lee S, et al. Comparative effects of RRR-alpha- and RRR-gamma-tocopherol on proliferation and apoptosis in human colon cancer cell lines. *BMC Cancer*. 2006;6:13.
127. Smirnov AS, Ruzov AS, Budanov AV, Prokhortchouk AV, Ivanov AV, Prokhortchouk EB. High constitutive level of NF-kappaB is crucial for viability of adenocarcinoma cells. *Cell Death Differ*. 2001;8:621–630.
128. Dhanalakshmi S, Singh RP, Agarwal C, Agarwal R. Silibinin inhibits constitutive and TNFalpha-induced activation of NF-kappaB and sensitizes human prostate carcinoma DU145 cells to TNFalpha-induced apoptosis. *Oncogene*. 2002;21:1759–1767.
129. Ma Z, Otsuyama K, Liu S, et al. Baicalein, a component of Scutellaria radix from Huang-Lian-Jie-Du-Tang (HLJDT), leads to suppression of proliferation and induction of apoptosis in human myeloma cells. *Blood*. 2005;105:3312–3318.
130. Taguchi T, Takao T, Iwasaki Y, Nishiyama M, Asaba K, Hashimoto K. Suppressive effects of dehydroepiandrosterone and the nuclear factor-kappaB inhibitor parthenolide on corticotroph tumor cell growth and function in vitro and in vivo. *J Endocrinol*. 2006;188:321–331.
131. Minsavage GD, Dillman JF 3rd. Protective role of CAPE on bi-functional alkylating agent-induced toxicity in keratinocytes via modulation of NF-kappaB, p53 and ARE/EpRE signaling. *Biosci 2006 Med Defense Rev*, 2006;94–94.
132. Minsavage GD, Dillman JF 3rd. Bifunctional alkylating agent-induced p53 and nonclassical nuclear factor-kappa b (nf-{kappa}b) responses and cell death are altered by caffeic acid phenethyl ester (cape): A potential role for antioxidant/electrophilic response element (ARE/EpRE) signaling. *J Pharmacol Exp Ther*. 2007;321:202–212.
133. Arroyo CM, Burman DL, Kahler DW, et al. TNF-alpha expression patterns as potential molecular biomarker for human skin cells exposed to vesicant chemical warfare agents: sulfur mustard (HD) and Lewisite (L). *Cell Biol Toxicol*. 2004;20:345–359.

134. Atkins KB, Lodhi IJ, Hurley LL, Hinshaw DB. *N*-acetylcysteine and endothelial cell injury by sulfur mustard. *J Appl Toxicol*. 2000;20(suppl 1):S125–S128.
135. Chatterjee D, Mukherjee S, Smith MG, Das SK. Signal transduction events in lung injury induced by 2-chloroethyl ethyl sulfide, a mustard analog. *J Biochem Mol Toxicol*. 2003;17:114–121.
136. Duthie MS, Kimber I, Dearman RJ, Norval M. Differential effects of UVA1 and UVB radiation on Langerhans cell migration in mice. *J Photochem Photobiol B*. 2000;57:123–131.
137. Steffensen B, Hakkinen L, Larjava H. Proteolytic events of wound-healing–coordinated interactions among matrix metalloproteinases (MMPs), integrins, and extracellular matrix molecules. *Crit Rev Oral Biol Med*. 2001;12:373–398.
138. Schwentker A, Billiar TR. Nitric oxide and wound repair. *Surg Clin North Am*. 2003;83:521–530.
139. Weller R. Nitric oxide: a key mediator in cutaneous physiology. *Clin Exp Dermatol*. 2003;28:511–514.
140. Witte MB, Barbul A. Role of nitric oxide in wound repair. *Am J Surg*. 2002;183:406–412.
141. Yamasaki K, Edington HD, McClosky C, et al. Reversal of impaired wound repair in iNOS-deficient mice by topical adenoviral-mediated iNOS gene transfer. *J Clin invest*. 1998;101:967–971.
142. Ishida H, Ray R, Cao Y, Ray P. Role of nitric oxide (NO) in wound healing. *Biosci 2006 Med Defense Rev.* 2006;1:112.
143. Arany I, Brysk MM, Brysk H, Tyring SK. Regulation of inducible nitric oxide s ynthase mRNA levels by differentiation and cytokines in human keratinocytes. *Biochem Biophys Res Commun*. 1996;220:618–622.
144. Kleinert H, Schwarz PM, Forstermann U. Regulation of the expression of inducible nitric oxide synthase. *Biol Chem*. 2003;384:1343–1364.
145. Soneja A, Drews M, Malinski T. Role of nitric oxide, nitroxidative and oxidative stress in wound healing. *Pharmacol Rep*. 2005;57(suppl):108–119.
146. Perkel JM. What can systems biology do for you? Four computational modeling strategies and the data that build them. *Scientist*. 2007;21:68.
147. Rogers JV, Choi YW, Kiser RC, et al. Microarray analysis of gene expression in murine skin exposed to sulfur mustard. *J Biochem Mol Toxicol*. 2004;18:289–299.
148. Sabourin CL, Rogers JV, Choi YW, et al. Time- and dose-dependent analysis of gene expression using microarrays in sulfur mustard-exposed mice. *J Biochem Mol Toxicol*. 2004;18:300–312.
149. Platteborze PL. Effects of sulfur mustard on transcription in human epidermal keratinocytes: analysis by mRNA differential display. *J Appl Toxicol*. 2003;23:249–254.
150. Dillman JF, III, Hege AI, Phillips CS, et al. Microarray analysis of mouse ear tissue exposed to bis-(2-chloroethyl) sulfide: gene expression profiles correlate with treatment efficacy and an established clinical endpoint. *J Pharmacol Exp Ther*. 2006;317:76–87.
151. Sultana R, Boyd-Kimball D, Poon HF, et al. Redox proteomics identification of oxidized proteins in Alzheimer's disease hippocampus and cerebellum: an approach to understand pathological and biochemical alterations in AD. *Neurobiol Aging*. 2006;27:1564–1576.
152. Ghezzi P, Bonetto V, Fratelli M. Thiol-disulfide balance: from the concept of oxidative stress to that of redox regulation. *Antioxid Redox Signal*. 2005;7:964–972.
153. Ghezzi P, Bonetto V. Redox proteomics: identification of oxidatively modified proteins. *Proteomics*. 2003;3:1145–1153.
154. Butterfield DA. Proteomics: a new approach to investigate oxidative stress in Alzheimer's disease brain. *Brain Res*. 2004;1000:1–7.

TABLE OF CONTENTS

Page

REPORT DOCUMENTATION PAGE

Form Approved
OMB No. 0704-0188

1. REPORT DATE *(DD-MM-YYYY)*	**2. REPORT TYPE**	**3. DATES COVERED** *(From - To)*
30/08/2007	Annual	1 Sept 2006- 30 August 2007

4. TITLE AND SUBTITLE

The Toxicological Evaluation of Liposomal Antioxidant Formulations

5a. CONTRACT NUMBER
3000627138

5b. GRANT NUMBER
W81XH-06-2-0044

5c. PROGRAM ELEMENT NUMBER

6. AUTHOR(S)

Dr. Zach Suntres

5d. PROJECT NUMBER

5e. TASK NUMBER

5f. WORK UNIT NUMBER

7. PERFORMING ORGANIZATION NAME(S) AND ADDRESS(ES)

Northern Ontario School of Medicine
955 Oliver Road
Thunder Bay, Ontario
Canada
P7B-5E1

8. PERFORMING ORGANIZATION REPORT NUMBER

9. SPONSORING / MONITORING AGENCY NAME(S) AND ADDRESS(ES)

U.S. Army Medical Research And Material Command
Fort Detrick, Maryland
21702-5012

10. SPONSOR/MONITOR'S ACRONYM(S)

11. SPONSOR/MONITOR'S REPORT NUMBER(S)

12. DISTRIBUTION / AVAILABILITY STATEMENT

Approved for public release; distribution unlimited

13. SUPPLEMENTARY NOTES

14. ABSTRACT

The main objective of this work was to evaluate the safety of a liposomal formulation (STIMAL) containing combinations of the antioxidants α-tocopherol, γ-tocopherol, and/or N-acetylcysteine under Good Laboratory Practices (GLP) conditions. Liposomal formulations containing NAC with/out alpha- or gamma-tocopherols were found to be stable in the presence of body fluids (plasma and bronchoalveolar lavage [BAL]) suggesting that STIMAL can be effective for intravenous or intratracheal administration for the treatment of oxidant-induced tissue injuries because they can overcome structural destabilization from interaction with components in blood (following iv injection) and BAL (following inhalation). The liposomal antioxidant formulations were also found to be non-mutagenic and non-clastogenic. The dosage range finding studies used to determine the maximum tolerated doses (MTD), as well as the acute toxicity studies, in male and female Sprague-Dawley rats and beagle dogs showed that that the highest dose by a single intravenous administration of STIMAL used (consisting of: 660 mg DPPC, 200 mg NAC, 83 mg α-T, and 83 mg γ-T) failed to produce any adverse reactions as evidenced by the histopathological, hematological, and clinical assessments. The factor that limited the administration of higher levels of antioxidants via the liposome delivery system was found to be the viscocity of the preparation. Data from the *in vivo* and *in vitro* studies indicated that the liposomal antioxidant formulations did not demonstrate any potential for toxicity.

15. SUBJECT TERMS

liposomes, antioxidants, toxicity, N-acetylcysteine, alpha-tocopherol, gamma-tocopherol

16. SECURITY CLASSIFICATION OF:			**17. LIMITATION OF ABSTRACT**	**18. NUMBER OF PAGES**	**19a. NAME OF RESPONSIBLE PERSON** USAMRMC
a. REPORT U	**b. ABSTRACT** U	**c. THIS PAGE** U	UU		**19b. TELEPHONE NUMBER** *(include area code)*

Statement of Work

The overall objective of this work was to evaluate the pre-clinical safety of three different liposomal formulations containing combinations of the antioxidants α-tocopherol, γ-tocopherol, and/or N-acetylcysteine under Good Laboratory Practices (GLP) conditions. The preclinical safety studies covered the establishment of the pharmacokinetic and the toxicological profile as well as the assessment of the acute toxicity of liposomal antioxidants containing N-acetylcysteine or N-acetylcysteine and α-tocopherol or N-acetylcysteine and γ-tocopherol in both *in vivo* models (rodent [Sprague-Dawley rat] and non-rodent [beagle dog]) and *in vitro* systems (mutagenicity, genotoxicity). At the end of the preclinical safety evaluation, we were set to identify an initial safe dose, recognize possible target organs for toxicity, and, distinguish safety parameters for clinical monitoring. Briefly, results from the *in vivo* and *in vitro* studies demonstrated that the liposomal antioxidant formulations did not demonstrate any potential for toxicity.

Introduction

The Advanced Medical Countermeasures Consortium (AMCC) was set up to investigate the role of liposomal antioxidant formulations (STIMAL) as an effective antidote/therapeutic product to protect from exposure to chemical warfare agents, such as mustard gas. Mustard gas-induced organ and tissue injuries are mediated through mechanisms that also involve the activation of the inflammatory response and the inducement of oxidative stress (1,2,3). Recent studies have focused on the use of antioxidants as a treatment modality for ameliorating the injurious effects of mustard gas. So far, many natural antioxidants exhibit poor bioavailability and cannot easily cross biological barriers such as membranes. Lipophilic compounds are insoluble in water and are located almost exclusively within membranes. Hydrophilic compounds cannot penetrate many biological compartments enclosed by membranes through passive diffusion and largely remain in extracellular compartments. We have demonstrated that the protective effects of antioxidants against several experimental models of oxidant-induced tissue and organ injuries were significantly enhanced following their delivery as liposomal formulations (4-8). Liposomes are phospholipid vesicles composed of lipid bilayers enclosing an aqueous compartment. Hydrophilic molecules (ie. N-acetylcysteine [NAC]) can be encapsulated in the aqueous spaces and lipophilic molecules (α-Tocopherol, γ-Tocopherol) can be incorporated into the lipid bilayers. The relative ease in incorporating hydrophilic and lipophilic antioxidants in liposomes; the possibility of directly delivering liposomes to an accessible body site; and the relative non-immunogenicity and low toxicity of liposomes have rendered the liposomal system highly attractive for drug delivery (4, 8).

Body

1. Report on *in vitro* studies involving the characterization of liposomal N-acetylcysteine (NAC) formulation.

Experiments were carried out to identify the best possible liposomal antioxidant formulation to be used in the preclinical safety studies. Results from studies described by the consortium collaborators suggested that liposomes containing N-acetylcysteine (NAC) or glutathione (GSH) and/or alpha/gamma-tocopherol are effective against CEES and other oxidant-induced organ injuries. We have validated the preparation and characterization of liposomes containing different antioxidants.

1.a. Stability of liposomal NAC in PBS buffer, plasma, and bronchoalveolar lavage (BAL).

In order for liposomes to be effective in the treatment of oxidant-induced tissue injuries, liposomes have to overcome structure destabilization as a result of interaction with certain serum components present in blood (following iv injection) and bronchoalveolar lavage (following inhalation). Thus, the stability of liposomal NAC formulation in biological fluids such as plasma and bronchoalveolar lavage, as well as PBS buffer as a control, was examined and the results are shown in figures 1 and 2. Liposomal NAC with alpha- or gamma-tocopherols showed better stability in PBS buffer than plasma, but the differences were not great. Inclusion of alpha- or gamma-tocopherol in liposomes improved the retention of NAC under all conditions examined.

Figure 1

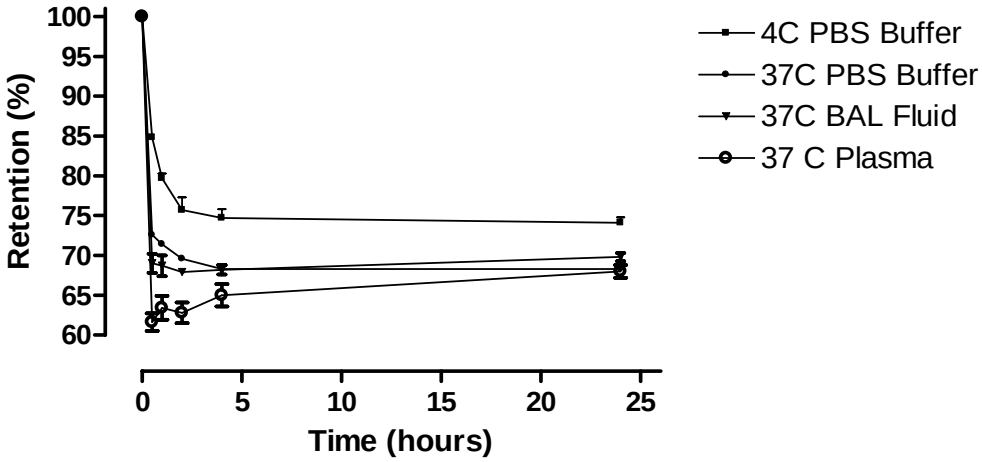

Figure 2

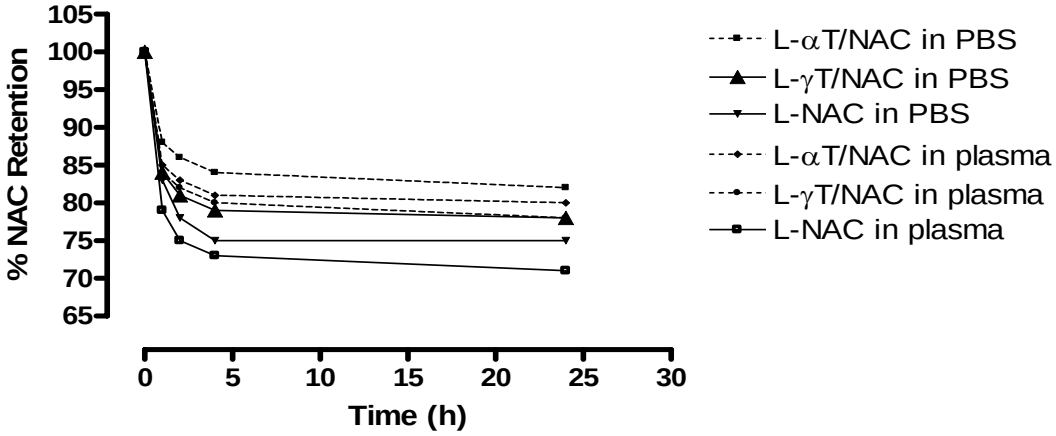

1.b. Improvement of liposomal stability by lyophilization for prolonged storage or shipment purposes.

(i) Storage of lyophilized liposomes

We have found that the stability of the liposomal formulations can be improved significantly when prepared in the powder form following lyophilization. Lyophilization refers to the process whereby a substance is prepared in dry form by freezing and dehydration. Briefly, preformed liposomal formulations can be dehydrated by freeze-drying using a lyophilizator at -45ºC (time of freeze-drying depends on volume of sample). The vials containing the liposomal formulations can be stored at -20°C for months or shipped in dry ice.

(ii) Reconstitution Procedure for lyophilized liposomes

In the reconstitution procedure, the vials containing the liposomal formulations can be rehydrated with sterile Phosphate Buffer Saline (PBS) at pH 6.5 as follows (for a 1 ml final solution): An initial volume of 150 μL of PBS is added to the vial until all the liposomal powder is dissolved (vortexing is highly recommended if liposomes are aggregated); the vial is placed in a pre-heated water bath set at 45°C (this temperature should be maintained throughout the rehydration process) for 15 min. Then, an additional volume of 700 μL of PBS is added to the vial, vortexed well, and placed to the water bath at 45C for an additional 30 min. After heating in the water bath, the mixture is vortexed once more to dissolve any remaining aggregated liposomes. Finally, the sample is centrifuged at 4°C (28000x*g* or higher) for 30 minutes in order to separate lipids that did not form into liposomes, free drug dispersed in supernatant, and any foam produced during the vortex process. After centrifugation, the supernatant is discarded and the pellet formed (liposomes) can be reconstituted with the required buffer of choice (ex. PBS, 0.9% saline) and diluted to the concentration of preference. The liposomes are ready for use.

1.c. (i) Chromosomal Abberations of liposomal antioxidant formulations in Chinese Hamster Ovary Cells

The purpose of the *in vitro* chromosomal aberration test is to identify agents that cause structural chromosomal aberrations in cultured mammalian cells. Structural aberrations may be of two types, chromosome or chromatid. With the majority of chemical mutagens, induced aberrations are of the chromatid type, but chromosome type aberrations also occur. Chromosomal aberrations are the cause of many human genetic diseases and there is substantial evidence that chromosomal damage and related events causing alterations in oncogenes and tumor suppressor genes of somatic cells are involved in cancer induction in humans and experimental animals.

An increase in polyploidy may indicate that a chemical has the potential to induce numerical aberrations. The *in vitro* chromosomal aberration test may employ cultures of established cell lines, cell strains or primary cell cultures. In our studies, the

test substances (empty liposomes (DPPC), liposomal NAC, liposomal α-tocopherol/NAC and liposomal γ-tocopherol/NAC) were investigated in an *in vitro* chromosome aberration test for their potential to induce structural chromosome aberrations in Chinese hamster ovary cell line WB_L. The experimental design followed the *OECD Guideline for the Testing of Chemicals – 473, In Vitro Mammalian Chromosome Aberration Test* (1997). The liposomal antioxidant formulations consisting of DPPC lipids, with NAC, NAC/alpha-tocopherol or NAC/gamma-tocopherol are not clastogenic in cultured Chinese hamster ovary WB_L cells under the conditions of the test (see Appendix 1 for draft report and results).

(ii) Ames test of mutagenicity (preliminary results have shown that STIMAL is not mutagenic. The results and analysis regarding the mutagenicity of STIMAL under GLP conditions will be completed by the end of Sept 2008 and can be made available by mid-October 2008).

1.d. Development of Ultrapressure Liquid Chromatography (UPLC) method for the measurement of N-acetylcysteine and other thiols.

We have developed a simple, sensitive, and rapid method that will be used to determine the levels of NAC/GSH in the different organs and tissues of animals. The method uses the Ellman's reagent derivatization procedure. The mobile phase consists of a mixture of methanol and ammonium formate (20:80 v/v) with a C18 reverse phase column as the stationary phase. Ellman's reagent can react stoichiometrically with thiols giving rise to mixed disulphides which have different retention times. The method was found to yield a quantitative recovery of GSH and NAC of more than 96%, to be sensitive (20 pmole/10 ul injection) and rapid (less than 3 min).

1.e Antioxidant effectiveness of liposomal NAC *in vitro*.

To assess the effectiveness of lipid-encapsulated and free antioxidants, the uptake and antioxidant properties of liposomal NAC and free NAC were examined in an *in vitro* model consisting of cells (hepG2 cell culture) exposed to the oxidant hydrogen peroxide (H_2O_2). The uptake of NAC in cells was assessed by measuring the cellular non-protein thiols (NPSH). The toxicity of liposomal NAC and free NAC as well as the protective effects of the antioxidant formulations against H_2O_2-induced cell injury was assessed by measuring the leakage of lactate dehydrogenase (LDH), an indicator of loss in cell permeability.

Pre-treatment of cells with either NAC or L-NAC (2 or 4 mM NAC for up to 24 h) did not produce any LDH leakage from Hep G2 cells suggesting that both formulations, at the concentrations used, are not toxic.

Exposure of hep G2 cells to free NAC was not effective in increasing the cellular thiol levels. On the other hand, cellular thiol levels were significantly increased, in a concentration-dependent and time-dependent manner,

when cells were treated with liposomal NAC. Pretreatment of cells with L-NAC conferred protection against H_2O_2-induced cell membrane injury, a treatment effect not seen in cells pretreated with L-NAC. These data suggest that delivery of NAC as a liposomal formulation increases the intracellular thiol content and decreases cellular susceptibility to oxidative stresses. (see figures below).

Effect of NAC or L-NAC on cellular Non-protein thiols (NPSH)

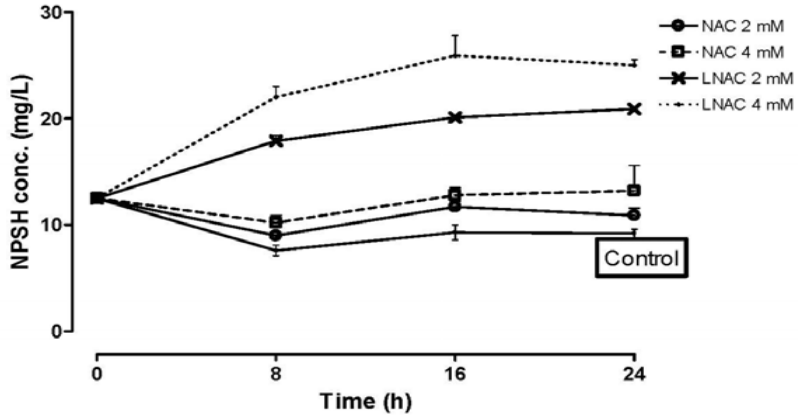

Effect of H2O2 on cells pretreated with NAC or L-NAC

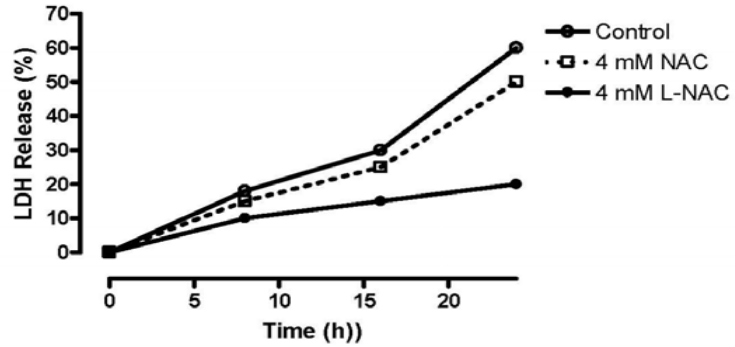

2. Maximum Tolerated Dose studies for four liposomal antioxidant formulations in rodents (rat) and non-rodents (dog)

The up-and-down procedure was used to determine the maximum tolerated dose in both, male and female Sprague-Dawley rats and beagle dogs, respectively. The liposomal formulations tested were: Liposomes consisting of dipalmitoylphosphatidylcholine (DPPC); Liposomal NAC; Liposomal alpha-tocopherol/NAC; and, Liposomal gamma-tocopherol/NAC. The treatments were tested as outlined in the following chart:

Range Finding Chart

Dose *Sequence*	Dose Level (mg/kg)		Number of Animals and Sex (male / female)
	Severe toxic effect or mortality seen at preceding dose	No effect seen at preceding dose	
1st	-	a	1 male / 1 female
2nd	a : m	a x m	1 male / 1 female
3rd	b : m	b x m	1 male / 1 female
4th	c : m	c x m	1 male / 1 female
5th	d : m	d x m	1 male / 1 female

a = initial dose
m = multiplier (1.5 – 3)

The objective of the procedure is that if the first group of animals survives and does not show severe toxic effect, the second group of animals will receive a higher dose. If any animals in the first group die or appear moribund, then the second group of animals will receive a lower dose. The next dose level will be chosen based on the same criteria. Based on the reaction of the previous group, the following group will be dosed at 24 to 72 hour intervals.

Findings.

The dosage range finding study used to determine the maximum tolerated doses (MTD) in male and female Sprague-Dawley rats showed that that the highest dose by a single intravenous administration of STIMAL used (consisting of: 660 mg DPPC, 200 mg NAC, 83 mg α-T, and 83 mg γ-T) failed to produce any adverse reactions. Gross necropsy findings were unremarkable.

The dosage range finding study used to determine the maximum tolerated doses (MTD) in male and female beagle dogs was similar to those for the rats. However, during the initial studies, it was decided to reduce the volume of the liposomal formulations administered to dogs by 50% since some dogs experienced emesis (most likely due to the high rate of a large volume/viscocity of the liposomal formulations).

Due to the high viscosity of the dosing formulations the dose level of 200 mg/kg (NAC) (doses for all formulations are based on NAC, the antioxidant encapsulated in liposomes at the highest levels; IV administration to humans is approximately 150 mg/kg NAC) was considered to be the maximum feasible dose (MFD) that can be injected safely to rats by an intravenous route of administration.

3. Single dose acute intravenous toxicity study for four preparations in rodents (Appendix 2)

For the single dose acute intravenous toxicity study, male and female Sprague-Dawley rats were challenged intravenously with the following liposomal formulations:

1. Liposomes (660 mg/kg DPPC) (control)
2. Liposomal NAC (660 mg DPPC/200 mg NAC/kg)
3. Liposomal alpha-tocopherol/NAC (660 mg/83 mg alpha-tocopherol/200 mg NAC/kg)
4. Liposomal gamma-tocopherol/NAC (660 mg/83 mg gamma-tocopherol/200 mg NAC/kg).

Animals were monitored on a daily basis within the 14-day experimental period. This study examined a safe dose range of three liposomal antioxidant formulations with plain liposomes being determined as a control group (liposomes/ NAC; liposomes/α-tocopherol and NAC; and liposomes/γ-tocopherol and NAC) administered by a single intravenous dose in Sprague-Dawley rats. Endpoints included daily clinical observations, weekly general physical examinations, body weights, food consumption, clinical pathology, gross necropsy and histopathology.

Injections were well-tolerated by animals (for all four formulations), and there were no clinical origins of toxicity associated with the treatment regiments either during injections, after injections or during the 14-day post treatment period.

Rats in all groups gained body weight during the two week observation period, and statistical analysis (ANOVA, $p=0.05$) showed that there was no difference in body weights and body weight gain between the control group (empty liposomes) and the three antioxidant formulations, or amongst antioxidant formulations groups.

Hematology results indicated that RBC counts, reticulocytes, hemoglobin and RBC indices (MCV, MCH and MCHC) were all within the normal ranges for both genders for all test groups. The exception was hematocrit (Hct), which was slightly below the lower limit of the normal historical ranges in males and females, for three test groups and control group which received empty liposomes. These slight decreases in Hct were not considered to be significant as they were just marginally below the normal historical ranges. These differences were most likely due to physiological variations since the control animals appeared to be similarly affected as the test animals.

Platelet counts were within normal ranges for both genders and all groups. WBC counts and differential counts were within the normal physiological range in groups which received empty liposomes, liposome/NAC and α-tocopherol, for both genders. WBC counts, in male rats which were dosed with liposome/NAC and γ-tocopherol were slightly below the lower limit of the normal range, and were also slightly lower than WBC counts in the remaining groups. Neutrophils, lymphocytes and monocytes were within the normal range, but were slightly lower than the counts for these parameters in other groups. This is consistent with the anti-inflammatory properties of γ-tocopherol. However, it cannot be excluded that this finding is not treatment related but because of its low magnitude, this observation is of limited toxicological significance.

Prothrombin time, APTT and fibrinogen were all within the normal ranges for all groups and both genders, with the exception that APTT for female rats treated with liposomes NAC and γ-tocopherol was approximately one second below the low end of normal range. This finding is not clinically significant.

Mean total protein, albumin and globulin were within the normal ranges in all groups and both genders. A/G ratio was marginally increased in female rats treated with empty liposomes and γ-tocopherol.

Cholesterol, triglycerides and glucose levels were all within the normal ranges for all groups and both genders.

Electrolytes (Na^+, Cl^- and K^+), calcium and phosphorus values were essentially within the normal ranges for all groups and both genders. There was however a slight “increase” in Cl^- levels in some groups. This finding is mostly likely an artifact known as a “great chloride shift”, and it is not considered treatment related.

Hepatocellular / hepatobiliary panel showed that ALP, Bil(T) and ALT were within normal ranges for all groups and both genders. AST was slightly increased in males which received liposome/NAC and γ-tocopherol. AST is tissue non-specific, and most likely originated from erythrocytes.

BUN and creatinine were within the normal ranges for all groups and both genders.

LDH and CK were increased in some animals in all groups. There were substantial inter-group and intra-group variabilities in the levels of lactate dehydrogenase (LDH) and creatine kinase (CK), including the control group. These differences are nevertheless known variabilities with these enzymes and are related to their release during regular handling of rats, grasping, dosing, etc. (Yerroum *et al*, 1999), blood collection procedures (Friedel *et al*, 1974), or their release from cellular elements during clotting (Friedel *et al*, 1970).

Gross pathology findings were unremarkable.

Histopathology: The tissues listed under Tissue Preservation from all animals were prepared for microscopic examination by embedding in paraffin wax, sectioning and staining with hematoxylin and eosin and evaluated histopathologically.

Tissue Preservation

During necropsy, the following tissues and organs were retained, from all Main Study animals. Neutral buffered 10% formalin was used for fixation and preservation unless otherwise indicated.

Abnormal Tissues	Kidneys	Skin (inguinal)
Adrenals	Liver (sample of central & left lobes)	Spinal Cord
Lungs	Spleen	
Aorta (Thoracic)	Lymph Node (Mandibular)	Sternum & Marrow
Brain	Lymph Node (Mesenteric)	Stomach
Cecum	Mammary Gland (inguinal)	Testes**
Colon	Nasal Turbinates	Thymus
Duodenum	Optic Nerves**+	Thyroid/Parathyroids +
Epididymes**	Ovaries	Tongue
Esophagus	Pancreas	Trachea
Eyes**	Pituitary	Urinary Bladder
Femur & Marrow	Prostate	Uterus (horns, cervix, body)
Heart***	Salivary Glands (Mandibular)	Vagina
Ileum	Seminal Vesicles	
Jejunum	Sciatic Nerve	
	Skeletal Muscle (quadriceps)	

** *Fixed in Acid Alcohol (euthanized animals only)*

*** *Sections of left and right ventricles and atria, septum with papillary muscle*

\+ *Parathyroids & optic nerves examined only if present in routine sections*

@ *Lungs of euthanized animals infused with formalin*

Three femoral bone marrow smears were prepared from each sacrificed animal, and were retained for possible future examination.

No histological findings were considered to be toxicologically significant. Various known background or incidental conditions were noted in the test and control groups.

Several animals in each group had lesions that were considered to be background changes because they occurred in control animals or because they were known spontaneous conditions in rats.

Lung: Some animals in each group had pulmonary granulomas that are attributed to intravenous injections with embolism of hair fibers and keratinocytes into the pulmonary veins and capillaries.

Kidney: Small foci of interstitial nephritis or atrophic basophilic tubules occur spontaneously in rats. Small tubular deposits of crystalline material (nephrocalcinosis) commonly occurs, especially in female rats on some diets. Pyelonephritis and cystitis occurred sporadically in response to urinary tract infections, most common in female rats.

4. Toxicokinetic Study of liposomal NAC, liposomal alpha-T/NAC and liposomal gamma-T/NAC in rats.

This study examined the pharmacokinetics of test articles LNAC (liposomes consisting of DPPC lipids and N-acetylcysteine; NAC), L-αT/NAC NAT (LNAC and α-tocopherol), L-γT/NAC (LNAC and γ-tocopherol) and control article EL (empty liposomes consisting of DPPC) when administered to rats. Test and control articles were prepared at the Northern Ontario School of Medicine and were provided to Nucro-Technics lyophilized in microcentrifuge and 15 mL polypropylene tubes. Dosing formulations of all articles were prepared at Nucro-Technics as per written instructions from Dr. Suntres. Animals were dosed with test articles by single intravenous injection (lateral tail vein) equivalent to 200 mg/kg of NAC. An equivalent dose of liposomes (EL) was used as a control dose.

Four groups of rats, each with sub-groups A and B, were used in the study. Each study group consisted of 12 rats (6 male, 6 female), with each sub-group consisting of 3 males and 3 females [strain: Crl:CD®(SD)BR-Sprague-Dawley (Charles River Canada)]. Group 1 was treated with empty liposomes, group 2 with L-NAC, group 3 with L-αT/NAC and group 4 with L-γT/NAC. All groups received an equivalent dose of liposomes. Test groups were administered the equivalent of 200 mg/kg NAC (L-NAC), 200 mg/kg NAC and 83.3 mg/kg α-tocopherol (L-αT/NAC) or 200 mg/kg NAC and 71.4 mg/kg γ-tocopherol (L-γT/NAC) in liposomes. Dosing formulations contained test or control article in sterile PBS, pH 6.5.

Animals were fasted the evening before dosing. Animal body weights were measured and recorded on the day of dosing (pre-dose). Clinical observations of animals were performed during dosing and up to 4 hours post-dose. Animals that appeared in

poor health were monitored for a longer duration. Blood samples were collected on 13 occasions for all dosing groups. Samples were collected from all sub-group A animals pre-dose and at 15 minutes, 1, 4, 8, 24 and 72 hours post-dose. Samples were collected from all sub-group B animals at 5 and 30 minutes and at 2, 6, 12 and 48 hours post-dose. Blood plasma was isolated from samples and frozen until plasma analysis. After the final blood collection, surviving animals were sacrificed. Liver, kidneys, lung, spleen, pancreas and heart from these rats were collected and frozen until tissue analysis.

Section 3: Figure 1: Plasma NAC

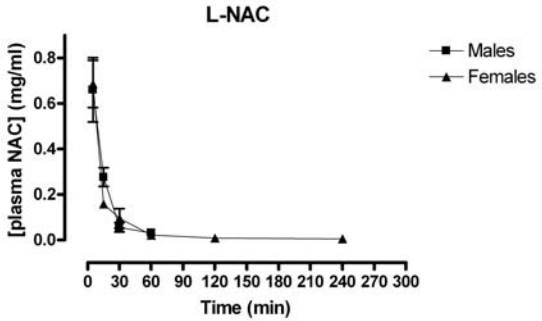

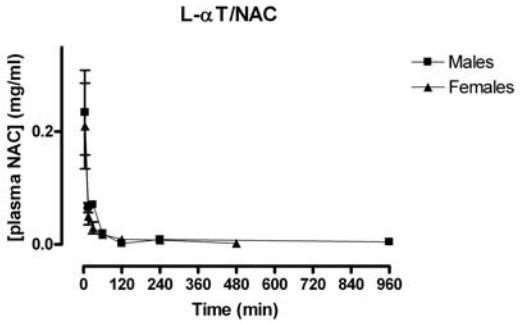

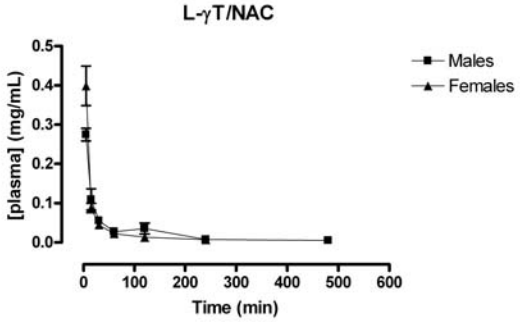

SS

Section 3: Figure 2: Half-life and $K_{elimination}$

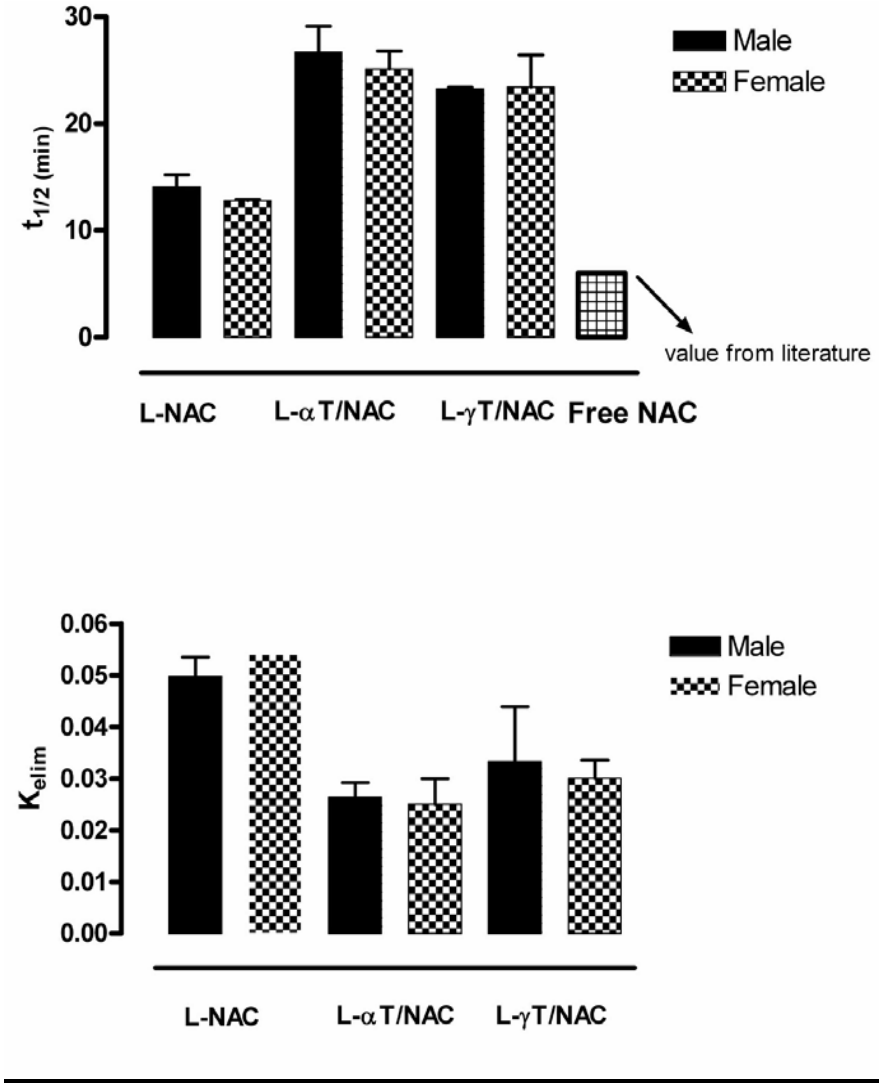

Results.

NAC disappeared faster from the plasma of animals administered with L-NAC (4 hrs) than animals treated with L-αT/NAC (8 hrs) or L-γT/NAC (6 hrs) (Section 3: Figure 1). The half-life of NAC in L-NAC, L-αT/NAC or L-γT/NAC-treated animals

was approximately 13 min, 29 min or 26 min, respectively (Section 3: Figure 2). The approximate half-life of free NAC reported in the literature is approximately 6 min. These data suggest that administration of NAC as a liposomal formulation increases the availability of NAC by 2-fold while inclusion of tocopherols in the formulation increases the availability of NAC by 4-5-fold. This is consistent with data reported in previous work where inclusion of tocopherols in liposomes increases the stability of liposomes and decreases solute leakage (Suntres et al, 1994). Observations from both in vitro and in vivo studies have shown that in most cases after parenteral administration, the entrapped agent may be released from liposomes prematurely upon encountering the biological milieu. Such instability of liposomal membranes, resulting in the leakage of the entrapped solute (ie. NAC) has been attributed to interactions of the liposomal lipid bilayers with various destabilizing serum proteins, degradative enzymes, and oxidative stress. Alpha-tocopherol is known to influence the permeability of phospholipids vesicles by decreasing their vulnerability to the destructive action of plasma proteins and enzymes (Suntres et al., 1994). Consequently, the incorporation of tocopherols in the lipid bilayers of liposomes, not only increases the antioxidant potential of the liposomal formulation (due to their inherent antioxidant properties), but also may enhance the duration of NAC's antioxidant effect.

5. Single dose acute intravenous toxicity study for four preparations in beagle dogs (Appendix 3)

For the single dose acute intravenous toxicity study, male and female beagle dogs were challenged intravenously with the following liposomal formulations:

1. Liposomes (330 mg/kg DPPC) (control)
2. Liposomal NAC (330 mg DPPC/60 mg NAC/kg)
3. Liposomal alpha-tocopherol/NAC (330 mg/25 mg alpha-tocopherol/60 mg NAC/kg)
4. Liposomal gamma-tocopherol/NAC (330 mg/25 mg gamma-tocopherol/60 mg NAC/kg).

Although beagle dogs were able to survive doses of liposomal antioxidants similar to those used in the rat study, the doses were reduced because after the intravenous administration of the formulations, the animals experienced vomiting, an effect from which animals recovered completely after 1 hr post-administration. The most probable cause for this effect was, most likely, the large volume of liposomal formulations administered to the animals and not due to the components of the formulation. A decrease in the injectable volume and rate of administration of the liposomal formulations alleviated the side effect but it resulted in a decrease in the amount of antioxidants delivered to the animals.

The experimental procedures on dogs, carried by technical staff at Nucro-technics (GLP facility), were audited on-site by COL. Peter Schultheiss, Director, Animal Care and Use Review Office, US Army Veterinary Corps on March 14, 2008. Briefly, COL. Schultheiss was satisfied with the experimental protocol and procedures and a full report was communicated to Dr. Peter Ward, Dr. Z. Suntres, and Nucro-Technics.

During the acute study, animals were monitored on a daily basis within the 14-day experimental period. This study examined a safe dose range of three liposomal antioxidant formulations with plain liposomes being determined as a control group (liposomes/ NAC; liposomes/α-tocopherol and NAC; and liposomes/γ-tocopherol and NAC) administered by a single intravenous dose in Sprague-Dawley rats. Endpoints included daily clinical observations, weekly general physical examinations, body weights, food consumption, clinical pathology (Appendix 3), gross necropsy and histopathology.

Injections were well-tolerated by animals (for all four formulations), and there were no clinical origins of toxicity associated with the treatment regiments either during injections, after injections or during the 14-day post treatment period. All data is included in Appendix 3.

Histopathology in male and female dogs (APPENDIX 4)

Results:

A list of grades for all tissues examined, with means are provided in Table 1.

Conditions of possible toxicological significance:
There were no conditions of possible toxicological significance.

Conditions of uncertain significance:
A single female treated with Liposomes/γ-tocopherol and NAC had a temporary increase in ALT. There were no tissue changes that indicated any unresolved injury.

Conditions lacking toxicological significance:
Hypotension which was rapidly resolved occurred during and immediately following treatment in animals in all dose groups.

Conclusions:
The intravenous administration of a single 60 mg/kg dose of Liposomes and NAC or Liposomes/α-tocopherol and NAC, or Liposomes/γ-tocopherol and NAC to beagle dogs caused no substantive clinical or pathological effects during the 14-day observation period.

5.**Toxicokinetic Study of liposomal NAC, liposomal α-T/NAC and liposomal γ-T/NAC in beagle dogs.**

As with the rats, iv administration of the STIMAL significantly improved the retention of antioxidants in the circulation by decreasing the rate of elimination. The incorporation of tocopherols in the liposomal formulation further improve the stability of the formulation, preventing the leakage of NAC and consequently increasing the retention and circulation of NAC in the blood.

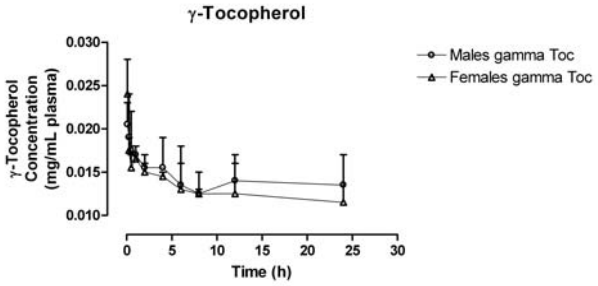

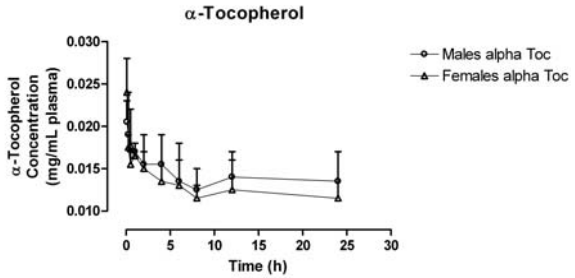

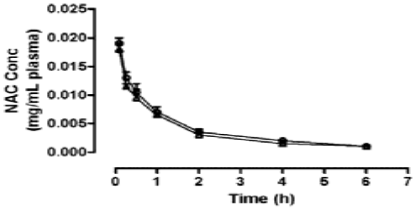

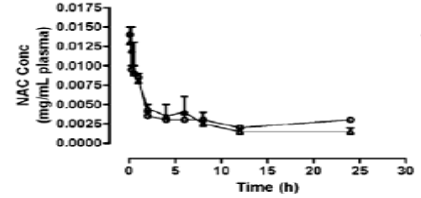

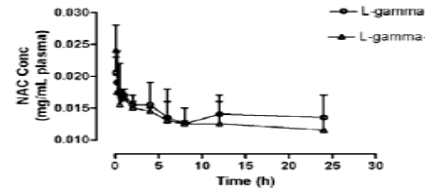

N-Acetylcysteine Pharmacokinetics

	L-NAC		L-αT/NC		L-γT/NAC	
	Male	Female	Male	Female	Male	Female
Half-Life (hr)	0.304	0.285	0.81	0.75	1.15	1.10
K elim	2.28	2.43	0.856	0.925	0.600	0.632
Vd	2610	2720	2790	2680	2720	2860

Pharmacokinetics of Tocopherols

	L-αT/NC		L-γT/NAC	
	Male	Female	Male	Female
Half-Life (hr)	13.60	13.30	18.10	16.90
K elim	0.051	0.052	0.038	0.041
Vd	3390	2970	1420	1500

Key Research Accomplishments:

- Characterization of liposomal antioxidant formulations (STIMAL formulations: liposomal NAC, liposomal alpha-tocopherol/NAC, liposomal gamma-tocopherol/NAC) with regards to their size, entrapment efficiencies, and stability in buffers and body fluids (plasma, bronchoalveolar lavage) at 4Cor 37C.
- Methodology for improving the stability of the liposomal formulation by lyophilization for prolonged storage or shipment purposes.
- Validation of the non-mutagenic properties of the liposomal antioxidant formulations.
- Determination of maximum tolerated dose of the liposomal antioxidant formulations in rodents and non-rodents.
- Determination of acute toxicity of liposomal antioxidant formulations in rodents.
- Determination of the uptake and antioxidant properties of liposomal NAC and free NAC in an *in vitro* model consisting of cells (hepG2 cell culture) exposed to oxidants.
- Development of Ultrapressure Liquid Chromatography (UPLC) method for the measurement of N-acetylcysteine and other thiols.
- Acute toxicity studies in male and female rodents and non-rodents showed that the intravenous administration of the STIMAL formulations are safe under the conditions investigated.
- Encapsulation of antioxidants within liposomes increases their circulation in both rodents and non-rodents.

Reportable Outcomes.

Presentations:

1. Advanced Medical Countermeasures Consortial Meeting, June 28, 2007, Crystal City, VA. "Safety of liposomal antioxidants (STIMAL).
2. Progress report, presented at Advanced Medical Countermeasures Consortium, Hunt Valley (MD), June 4-5, 2008.
3. Attended Biosciences Conference 2008 (Hunt Valley, MD).
4. Presented at the Department of Biomolecular Sciences, Laurentian University, 2007 (invited speaker)
5. Training of two graduate students.

Publications:

1. Paromov, V., **Suntres, Z.,** Stone, W., Smith, M. Sulfur Mustard Toxicity if Human Skin: Role of Oxidative Stress and Antioxidant Therapy. *Journal of Burns and Wounds*, 2007.
2. Smith, M.G., Stone, W., Guo, R.F., Ward, P.A., **Suntres, Z**., Mukherjee, S., and Das, S.K. Vesicants and Oxidative Stress. In Chemical Warfare Agents. Chemistry, Pharmacology, Toxicology, and Therapeutics, J.A. Romano, Jr., B.J. Lukey, H. Salem (eds). 2nd Edition, CRC Press, Boca Raton, FL. pp.247 – 312, 2007.
3. **Suntres, Z.E**., Smith, M.G., Alipour, M., Omri, A., Pucaj, K. Acute toxicity of liposomal antioxidants in rodents (in preparation).
4. **Suntres, Z.E.,** Smith, M.G., Alipour, M., Omri, A., Pucaj, K. Acute toxicity of liposomal antioxidants in beagle dogs (in preparation).
5. Alipour M., Mitsopoulos, P., Omri, A., Smith, M.G., **Suntres, Z.E.** Antioxidant properties of liposomal antioxidants in vitro. Toxicol. (in preparation)

Conclusion.

Liposomal formulations containing NAC with alpha- or gamma-tocopherols are stable in the presence body fluids such as plasma and bronchoalveolar lavage suggesting that the liposomal antioxidant formulations can be effective in the treatment of oxidant-induced tissue injuries because they can overcome structure destabilization as a result of interaction with certain serum components present in blood (following iv injection) and bronchoalveolar lavage (following inhalation). The liposomal antioxidant formulations were non mutagenic. The dosage range finding study used to determine the maximum tolerated doses (MTD) in male and female Sprague-Dawley rats and beagle dogs, as well as the acute toxicity studies, showed that the liposomal antioxidant formulations did not produced any adverse

effects assessed clinically, biochemically, and histopathologically and deemed to be potentially safe for their use in Phase I clinical trials. Pharmacokinetic studies showed that intravenous administration of antioxidants as liposomal formulations dramatically increased their circulation time.

References

1. Naghii MR. Sulfur mustard intoxication, oxidative stress, and antioxidants. Mil. Med. 2002; 167:573-5.
2. Paromov V, Suntres Z, Stone W, Smith M. Sulfur Mustard Toxicity if Human Skin: Role of Oxidative Stress and Antioxidant Therapy. Journal of Burns and Wounds, 2007 (in press).
3. Paromov, V., Suntres, Z., Stone, W., Smith, M. Sulfur Mustard Toxicity if Human Skin: Role of Oxidative Stress and Antioxidant Therapy. *Journal of Burns and Wounds*, 7:60-85, 2007.
4. Stone WL, Smith MG, Therapeutic uses of antioxidant liposomes. Mol. Biotechnol 2004; 27:217-30.
5. Suntres ZE, Hepworth SR, Shek PN, Protective effecct of liposome-associated α-tocopherol against paraquat-induced acute lung toxicity. Biochem. Pharmacol. 1992; 44:1811-18.
6. Suntres ZE, Shek PN, Prevention of phorbol myristate acetate-induced lung injury by α-tocopherol liposomes. J. Drug Targeting 1995; 3:201-8.
7. Suntres ZE, Shek PN, Alleviation of paraquat-induced lung injury by pretreatment with bifunctional liposomes containing α-tocopherol and glutathione. Biochem. Pharmacol. 1996; 52: 1515-20.
8. Suntres ZE, Role of Antioxidants in Paraquat Toxicity. Toxicology 2002; 180: 65-77.

APPENDIX 1: Chromosomal Abberation Test

DRAFT

CHROMOSOME ABERRATION TEST OF

Empty liposomes (DPPC), Liposomal NAC, Liposomal alpha-tocopherol/NAC and Liposomal gamma-tocopherol/NAC

IN CULTURED CHINESE HAMSTER OVARY CELLS

Nucro-Technics Project No.:

For Study Sponsor

Northern Ontario School of Medicine

955 Oliver Road

Thunder Bay, Ontario

P7B 5E1

Contacting Facility and Sponsorship

TESTING FACILITY:

Nucro-Technics

2000 Ellesmere Road, Unit #16

Scarborough, Ontario, Canada

M1H 2W4

SPONSOR:

Northern Ontario School of Medicine
955 Oliver Road
Thunder Bay, Ontario
P7B 5E1

STUDY MONITOR:

Zack Suntres, Ph.D.
Northern Ontario School of Medicine
Tel. No.: (807) 766-7395
Fax No.: (807) 766-7370
Email: zacharias.suntres@normed.ca

SPONSOR'S REPRESENTATIVE:

Dr. Greg Ross
Associate Dean-Research
Northern Ontario School of Medicine

SUMMARY

The test substances, empty liposomes (DPPC), liposomal NAC, liposomal α-tocopherol/NAC and liposomal γ-tocopherol/NAC were investigated in an *in vitro* chromosome aberration test for their potential to induce structural chromosome aberrations in Chinese hamster ovary cell line WB_L. The experimental design followed the *OECD Guideline for the Testing of Chemicals – 473, In Vitro Mammalian Chromosome Aberration Test* (1997).

1. Test and Control Articles

Test Article #1:

Identity:	Liposomes consisting of DPPC lipids
Color/Form:	Lyophilized white powder
Batch / Lot No.:	will be documented in the report
Purity:	will be documented in the report
Storage Conditions:	-10 to -25°C lyophilized (room temperature reconstituted; see directions for reconstitution)
Handling Precautions:	Handle aseptically, standard laboratory procedures
Supplier:	Northern Ontario School of Medicine

Test Article #2:

Identity:	Liposomes consisting of DPPC lipids and N-acetylcysteine (NAC)
Color/Form:	Lyophilized white powder
Batch / Lot No.:	will be documented in the report
Purity:	will be documented in the report
Storage Conditions:	-10 to -25°C lyophilized (room temperature reconstituted; see directions for reconstitution)
Handling Precautions:	Handle aseptically, standard laboratory procedures
Supplier:	Northern Ontario School of Medicine

Test Article #3:

Identity:	Liposomes consisting of DPPC lipids and ∝-tocopherol and NAC
Color/Form:	Lyophilized white powder
Batch / Lot No.:	will be documented in the report
Purity:	will be documented in the report
Storage Conditions:	-10 to -25°C lyophilized (room temperature reconstituted; see directions for reconstitution)
Handling Precautions:	Handle aseptically, standard laboratory procedures
Supplier:	Northern Ontario School of Medicine

Test Article #4:

Identity:	Liposomes consisting of DPPC lipids and γ-tocopherol and NAC
Color/Form:	Lyophilized white powder
Batch / Lot No.:	will be documented in the report
Purity:	will be documented in the report
Storage Conditions:	-10 to -25°C lyophilized (room temperature reconstituted; see directions for reconstitution)
Handling Precautions:	Handle aseptically, standard laboratory procedures
Supplier:	Northern Ontario School of Medicine

Test Article Properties

The Sponsor will provide documentation on the strength, stability, and purity on each batch of test article, unless otherwise noted.

Test and Control Article Preparation

The test articles were prepared by Medical Sciences Division of Northern Ontario School of Medicine and provided in lyophilized form.

In Experiments 1 and 2, cultures were exposed to the liposomal formulations for 3 hours in the absence and presence of an S9 metabolic

activation system, respectively. S9 was prepared from the livers of rats pre-treated with a combination of phenobarbital and benzoflavone. Cells were harvested at 18 hours, approximately 1.5 normal cell cycle lengths. In Experiment 3, the exposure was extended until harvest time at 18 hours without S9.

Exposure to DPPC liposomes, Liposomal NAC, Liposomal α-tocopherol/NAC or Liposomal γ-tocopherol/NAC for 3 hours with and without S9 did not result in detectable cytotoxicity when evaluated by cell count and mitotic index. Extending exposure to 18 hours without S9 did not significantly produce any cytotoxicity. One hundred metaphase cells from each of the duplicate cultures of each of the 4 dilutions were analyzed for chromosome aberrations (16 formulations in total). All results were negative.

It was thus concluded that exposure to DPPC liposomes, Liposomal NAC, Liposomal α-tocopherol/NAC or Liposomal γ-tocopherol/NAC did not induce chromosome aberrations in cultured WB_L Chinese hamster ovary cells under the conditions of the test.

Table of Contents

List of Tables (pages 13-36)

List of Appendices (pg 38-40)

CHROMOSOME ABERRATION TEST OF LIPOSOMAL ANTIOXIDANT FORMULATIONS IN CULTURED CHINESE HAMSTER OVARY CELLS

1. Introduction

The objective of the study was to test Empty liposomes consisting of DPPC lipids, Liposomal NAC, Liposomal α-tocopherol/NAC or Liposomal γ-tocopherol/NAC for their potential to induce aberrant chromosomes in cultured Chinese hamster ovary (CHO) cell line WB_L. The study design followed the *OECD Guideline for the Testing of Chemicals – 473, In Vitro Mammalian Chromosome Aberration Test* (OECD, 1997).

2. Materials

2.1. Test substance

Liposomes were prepared from dipalmitoylphosphatidylcholine and contained NAC, α-tocopherol/NAC or γ-tocopherol/NAC.

2.2. Cells

Cells grow as an adherent monolayer, with a doubling time of approximately 12 hours (Galloway, S.M., *et al*, 1987). Health status of the cultures was determined by observation under a microscope. The cultures were free of mycoplasma.

2.3. Media and culture conditions

Cells were cultured in McCoy's 5A Medium Modified with 2 mM L-glutamine and 25 mM HEPES supplemented with 10% heat-inactivated fetal bovine serum (Invitrogen Corporation, Burlington, ON, Canada). Sterile Falcon tissue culture flasks (BD Biosciences Bedford, MA, U.S.A.) were used. The cells were incubated in a humidified tissue culture incubator at 37 ± 2°C and 5 ± 2% CO_2. When cells reached approximately 50 - 70 % confluency, they were dislodged with 0.05% trypsin (Invitrogen Corporation, Burlington, ON, Canada), collected by centrifugation, and seeded in fresh medium. Each trypsinization was recorded as one passage. For long-term preservation in liquid nitrogen, a freezing medium containing 8% dimethyl sulfoxide (DMSO) (CASRN: 67-68-5) (Sigma Chemical Co., St. Louis, MO, U.S.A.) was used.

2.4. Controls

A sterile 0.1 M phosphate buffer solution, pH 7.4 (PBS), was prepared at the testing facility and was used to re-constitute the lyophilized liposomal test articles and was used as the negative control. Mitomycin C (MMC), (CASRN: 50-07-7), Lot No. 103K0498 (Sigma Chemical Co., St. Louis, MO, U.S.A.) was used at 0.5 µg/ml as a positive control for cultures not treated with S9. Cyclophosphamide (CP), (CASRN: 6055-19-2), Lot No. 113K1406, (Sigma Chemical Co., St. Louis, MO, U.S.A.) was used at 7.5 µg/ml as a positive control for treatment with S9.

2.5. Metabolic activation system

S9 used in the study was the microsomal fraction of a liver homogenate from rats treated with phenobarbital-5, 6-benzoflavone (Moltox Inc. Boone, NC, U.S.A.). Cofactors for the microsomal enzymes include β-nicotinamide adenine dinucleotide phosphate (NADP) and isocitric acid (Sigma Chemical Co., St. Louis, MO, U.S.A.). A 10 x concentrated S9 mix was freshly prepared. The final culture contained 2.4 mg/ml NADP, 4.5 mg/ml isocitric acid and 25 µl/ml S9 (Galloway, S.M., *et al*, 1987).

3. Procedure

3.1. Preparation of cultures

A continuous culture from passage 13 to 14 was used for Experiments 1 and 2 and a separate culture, passage 10, was used for Experiment 3. On the day before each experiment, approximately 5 x 10^5 cells were seeded into each T-25 cm^2 Falcon flask. The cultures were incubated overnight. Duplicate cultures were prepared for each exposure concentration. When examined under an inverted microscope the next day, the cultures appeared healthy, evenly distributed and approximately 20-30 % confluent.

3.2. Test substance preparation and treatment

On each day of an experiment, solutions of each liposomal test article were first prepared separately in 0.1 M phosphate buffer, pH 7.4. The treatment proceeded in a humidified incubator at 37 ± 2°C and 5 ± 2% CO2 for 3 hours in Experiments 1 and 2 or for 18 hours in Experiment 3. At the end of a three-hour treatment, the cells were washed with phosphate buffered saline and the incubation continued in fresh culture medium until harvest time.

The treatment media of the negative control, 5 mg/ml and 10 mg/ml were sampled for measurement of pH and osmolality, using the US Pharmacopeia methods as a reference (USP, 2006a and 2006b).

3.3. Harvest

For all experiments, cultures were harvested 18 hours after the initiation of treatment. Approximately two hours prior to harvesting, Colcemid® (Invitrogen Corporation, Burlington, ON, Canada) was added at 0.1 μg/ml to arrest cells in metaphase. The cells were then harvested and the number of cells was counted using the trypan blue exclusion method. Relative Cell Growth (RCG) was calculated as follows:

$$\text{RCG (\%)} = \frac{\text{Viable cell count in test flask}}{\text{Viable cell count in solvent control flask}} \times 100$$

3.4. Preparation of chromosome slides

The cells were collected by centrifugation, swelled in 0.075 M KC1 and fixed in a 3:1 mixture of methanol and glacial acetic acid. They were dripped on to coded slides, air-dried and stained in 10% Giemsa stain (Evans, H.J., 1976).

For each duplicate culture, 500 cells were examined to score mitotic index. The mitotic index (MI) was calculated as the percent of cells at the mitotic stage. Relative mitotic index (RMI) was calculated as:

$$\text{RMI (\%)} = \frac{\text{Test concentration MI}}{\text{Solvent control MI}} \times 100$$

3.5. Analysis of chromosome aberrations

All slides were randomly coded. Well-spread metaphase cells with 19 - 23 chromosomes were analysed for chromosome aberrations as defined in Protocol TOP/176914 (Scott, *et al*., 1990; OECD, 1997). One hundred cells from each negative control and DPPC liposomes-, liposomal NAC-, liposomal α-tocopherol/NAC- or liposomal γ-tocopherol/NAC-treated culture or 50 cells from a positive control culture were examined (OECD, 1997). The number of each type of aberration, number of aberrations per cell and percent of cells with aberrations were recorded and summarized. If a cell contained >10 aberrations, it counted as ten under "severely damaged cells (s*d*)" (Scott, D., *et al*., 1990). The number of endoreduplicated and polyploidy cells, chromatid gaps and chromosome gaps were recorded when encountered, but not included in the calculations.

4. Results

Three experiments for each of the four formulations were performed. Scores of structural chromosome aberrations in metaphase cells are summarized in Tables 3-1, 3-2 and 3-3 as percentages of cells with aberrations for each corresponding formulation. In Experiments 1 and 2, the cultures were exposed to DPPC liposomes, liposomal NAC, liposomal α-tocopherol/NAC or liposomal γ-tocopherol/NAC for 3 hours in the absence and the presence of S9, respectively. In Experiment 3, the exposure time was extended to 18 hours without S9.

No precipitation of the test article was observed in the culture media throughout the experiments. All treatment media maintained a neutral pH (Appendix I). Osmolality measurements of the treatment media were similar to those of the negative controls and were within a physiological range (Appendix I). Under these conditions, the cells appeared healthy during and after DPPC liposomes-, liposomal NAC-, liposomal α-tocopherol/NAC- or liposomal γ-tocopherol/NAC- treatment for 3 hours with and without S9. The cell growth was normal throughout the testing period at all dilutions tested.

The mitotic indices showed no cytotoxic effects in all three different experiments. (Tables 2).

One hundred metaphase cells from each culture were analyzed for chromosome aberrations. As shown in Tables 3-3, the results confirmed a non-mutagenic response under the test conditions.

All concurrent positive controls induced significant numbers of cells with chromosome aberrations. Without S9, mitomycin C at 0.5 μg/ml induced chromosome aberrations in 85-95 % of cells after three hours of exposure (Tables 3-1) and in 66-67 % of cells after 18 hours of exposure (Tables 3-3). In the presence of S9, treatment with 7.5 μg/ml of cyclophosphamide for three hours resulted in 65-66 % cells with chromosome aberrations (Table 3-2).

5. Discussion

In each of the three experiments, at least four exposure concentrations were analyzed for structural chromosome aberrations. This complied with the requirement of the current guidelines in terms of the number of concentrations to be scored (OECD, 1997).

In Experiments 1 and 2, the liposomal formulations were considered to be non-toxic. After exposure for three hours with and without S9, no cytotoxicity was observed, as evaluated by cell count and mitotic index and by examining the cultures under an inverted microscope.

In Experiment 3, when extending the exposure time to 18 hours without S9, no cytotoxicity was observed.

6. Conclusion

The liposomal antioxidant formulations consisting of DPPC lipids, with NAC, NAC/alpha-tocopherol or NAC/gamma-tocopherol are not clastogenic in cultured Chinese hamster ovary WB_L cells under the conditions of the test.

Results for DPPC

Table 1. Relative Cell Growth for DPPC Control

	Experiment 1, - S9			Experiment 2, + S9			Experiment 3, - S9		
DPPC (mg/ml)	**Cells per flask (x 10^6)**	Mean (x 10^6)	Relative Cell Growth (%)	**Cells per flask (x 10^6)**	Mean (x 10^6)	Relative Cell Growth (%)	**Cells per flask (x 10^6)**	Mean (x 10^6)	Relative Cell Growth (%)
0	2.65 2.70	2.68	100	1.80 1.65	1.73	100	3.15 3.65	3.40	100
5	2.60 2.50	2.55	95	1.60 1.40	1.50	86	3.25 3.55	3.40	100
10	2.75 2.80	2.77	103	1.40 2.05	1.73	100	4.00 3.85	3.93	115
25	2.50 2.35	2.43	91	1.75 1.25	1.50	87	2.65 3.45	3.05	90
50	3.35 2.95	3.15	118	1.55 2.00	1.78	103	3.25 3.40	3.33	98

Table 2. Relative Mitotic Index for DPPC Control

	Experiment 1, - S9			Experiment 2, + S9			Experiment 3, - S9		
DPPC (mg/ml)	**No. of dividing cells**	Mitotic index (%)	Relative mitotic index (%)	**No. of dividing cells**	Mitotic index	Relative mitotic index (%)	**No. of dividing cells**	Mitotic index (%)	Relative mitotic index (%)
0	145 153	29.8	100	145 140	28.5	100	56 43	9.9	100
5	160 163	32.3	108	175 157	33.2	116	55 49	10.4	105
10	146 164	31.0	104	156 127	28.3	99	50 38	8.8	89
25	154 175	32.9	110	139 125	26.4	83	48 40	8.8	89
50	154 135	28.9	97	140 125	26.5	93	51 46	9.7	98

Note: *No. of Dividing Cells* is counted from a total of 500 cells;
Mitotic Index is calculated as the number of dividing cells per hundred cells observed;
Relative Mitotic Index is mitotic index normalized against that of the negative control culture.

Table 3-1. Summary of Chromosome Aberrations - Experiment 1, - S9, 3 hr. exposure for DPPC Control

DPPC (mg/ml)	Cells	Not Computed				Chromatid Type						Chromosome Type					Other Types		No. of Aberrations Per Cell	% of Cel with Aberra
						Simple		Complex				Simple		Complex						
		tg	*sg*	*e*	*pp*	*tb*	*isb*	*tr*	*qr*	*cr*	*id*	*ci*	*sb*	*d*	*r*	*dm*	*pu*	*sd*		
0	100																		0	0
	100				1														0	0
	%				.5														0	0
5	100																		0	0
	100																		0	0
	%																		0	0
10	100																		0	0
	100																		0	0
	%																		0	0
25	100																		0	0
	100																		0	0
	%																		0	0
50	100				1														0	0
	100				1														0	0
	%				1.0														0	0
Mitomycin C 0.5 g/ml	50					10	1	30	8	4	5	8	30		2	1		2	2.08	96
	50	3	1		1	24	3	32	7	4	5	10	20		4	1		4	2.87	88
	%	3.0	1		1	34	4	62	15	8	10	18	50		6	2		6	2.45	92

Note: *sd* = 10 aberrations in calculations

Table 3-2. Summary of Chromosome Aberrations - Experiment 2, +S9, 3 hr. exposure for DPPC Control

DPPC (mg/ml)	Cells	Not Computed				Chromosome Type											Other Types		No. of Aberrations Per Cell	% of Cells with Aberrations
						Simple			Complex				Simple		Complex					
		tg	*sg*	*e*	*pp*	*tb*	*isb*	*tr*	*qr*	*cr*	*id*	*ci*	*sb*	*d*	*r*	*dm*	*pu*	*sd*		
0	100			1	2										1				0.01	1.0
	100	1		1	2														0	0
	%	0.5		1.0	2.0										0.5				0.005	0.5
5	100	2			4														0	0
	100				1														0	0
	%	1.0			2.5														0	0
10	100	1			2														0	0
	100	1			4														0	0
	%	1.0			3.0														0	0
25	100				3														0	0
	100				2														0	0
	%				2.5														0	0
50	100				2														0	0
	100			1	2														0	0
	%			0.5	2.0														0	0
Cyclophosphamide 7.5 g/ml	50	4	3		0	10	6	10	8	3	4	9	5		2	2		2	1.60	68.0
	50	2	2		1	10	4	8	4	1	3	4	7		1	2		1	1.12	62.0
	%	6	5		1	20	10	18	12	4	7	13	13		3	4		3	1.36	65.0

Note: *sd* = 10 aberrations in calculations

Table 3-3. Summary of Chromosome Aberrations - Experiment 3, - S9, 18 hr. exposure for DPPC Control

DPPC (mg/ml)	Cells	Not Computed				Chromatid Type						Chromosome Type					Other Types		No. of Aberrations Per Cell	% of Cells with Aberrations
						Simple		Complex				Simple		Complex						
		tg	*sg*	*e*	*pp*	*tb*	*isb*	*tr*	*qr*	*cr*	*id*	*ci*	*sb*	*d*	*r*	*dm*	*pu*	*sd*		
0	100				1														0	0
	100				1														0	0
	%				1.0														0	0
5	100				2														0	0
	100	1			2														0	0
	%	0.5			2.0														0	0
10	100				4														0	0
	100	2	1		2														0	0
	%	1.0	0.5		3.0														0	0
25	100	1	1		1						1								0.01	1.0
	100				3														0	0
	%	0.5	0.5		2.0						0.5								0.005	0.5
50	43																		0	0
	157	2		1	3														0	0
	%	1.0		0.5	1.5														0	0
Mitomycin C 0.5 g/ml	50	3	1			14	4	20	4	5	6	2	5	2	5	1		1	1.74	69.0
	50	3	1		1	6	2	11	4	2	6	1	5	1	4	1			0.98	63.0
	%	6	2		1	20	6	31	8	7	12	3	10	3	9	2		1	1.36	66.0

sd = 10 aberrations in calculations

DPPC NAC

Table 1. Relative Cell Growth for DPPC/NAC

	Experiment 1, - S9			Experiment 2, + S9			Experiment 3, - S9		
DPPC/NAC (mg/ml)	**Cells per flask (x 10^6)**	Mean (x 10^6)	Relative Cell Growth (%)	**Cells per flask (x 10^6)**	Mean (x 10^6)	Relative Cell Growth (%)	**Cells per flask (x 10^6)**	Mean (x 10^6)	Relative Cell Growth (%)
0	2.70 2.85	2.78	100	2.80 2.65	2.73	100	3.00 3.50	3.25	100
5/1.5	2.60 2.70	2.65	95	2.60 2.50	2.55	91	3.25 3.15	3.20	98
10/3.0	2.65 2.90	2.78	100	2.70 2.65	2.68	98	3.45 3.35	3.40	105
25/7.5	2.60 2.80	2.70	97	2.60 2.45	2.52	92	3.20 3.50	3.35	103
50/15	2.65 2.65	2.65	95	2.55 2.75	2.65	97	3.15 3.00	3.08	95

Table 2. Relative Mitotic Index **for DPPC Control**

	Experiment 1, - S9			Experiment 2, + S9			Experiment 3, - S9		
DPPC (mg/ml)	**No. of dividing cells**	Mitotic index (%)	Relative mitotic index (%)	**No. of dividing cells**	Mitotic index	Relative mitotic index (%)	**No. of dividing cells**	Mitotic index (%)	Relative mitotic index (%)
0	145 153	29.8	100	145 140	28.5	100	56 43	9.9	100
5	160 163	32.3	108	175 157	33.2	116	55 49	10.4	105
10	146 164	31.0	104	156 127	28.3	99	50 38	8.8	89
25	154 175	32.9	110	139 125	26.4	83	48 40	8.8	89
50	154 135	28.9	97	140 125	26.5	93	51 46	9.7	98

Note: *No. of Dividing Cells* is counted from a total of 500 cells;
Mitotic Index is calculated as the number of dividing cells per hundred cells observed;
Relative Mitotic Index is mitotic index normalized against that of the negative control culture.

Table 3-1. Summary of Chromosome Aberrations - Experiment 1, - S9, 3 hr. exposure for DPPC Control/NAC

DPPC/NAC (mg/ml)	Cells	Not Computed				Chromatid Type						Chromosome Type					Other Types		No. of Aberrations Per Cell	% of Cel with Aberra
						Simple		Complex				Simple		Complex						
		tg	*sg*	*e*	*pp*	*tb*	*isb*	*tr*	*qr*	*cr*	*id*	*ci*	*sb*	*d*	*r*	*dm*	*pu*	*sd*		
0	100																		0	0
	100																		0	0
	%																		0	0
5/1.5	100																		0	0
	100																		0	0
	%																		0	0
10/3.0	100																		0	0
	100																		0	0
	%																		0	0
25/7.5	100																		0	0
	100																		0	0
	%																		0	0
50/15	100																		0	0
	100																		0	0
	%																		0	0
Mitomycin C 0.5 g/ml	50					10	1	30	8	4	5	8	30		2	1		2	2.08	96
	50	3	1		1	24	3	32	7	4	5	10	20		4	1		4	2.87	88
	%	3.0	1		1	34	4	62	15	8	10	18	50		6	2		6	2.45	92

Note: *sd* = 10 aberrations in calculations

Table 3-2. Summary of Chromosome Aberrations - Experiment 2, +S9, 3 hr. exposure for DPPC/NAC

DPPC/NAC (mg/ml)	Cells	Not Computed				Chromatid Type						Chromosome Type					Other Types		No. of Aberrations Per Cell	% of Cells with Aberrations
						Simple		Complex				Simple		Complex						
		tg	*sg*	*e*	*pp*	*tb*	*isb*	*tr*	*qr*	*cr*	*id*	*ci*	*sb*	*d*	*r*	*dm*	*pu*	*sd*		
0	100			1	1														0	0
	100		1	1	2														0	0
	%		0.5	1.0	1.5														0	0
5/1.5	100				1														0	0
	100				1														0	0
	%				1														0	0
10/3.0	100				2														0	0
	100				1														0	0
	%				1.5														0	0
25/7.5	100				2														0	0
	100				2														0	0
	%				2.0														0	0
50/15.0	100				1														0	0
	100				1														0	0
	%				1.0														0	0
Cyclophosphamide 7.5 g/ml	50	4	3		0	10	6	10	8	3	4	9	5		2	2		2	1.60	68.0
	50	2	2		1	10	4	8	4	1	3	4	7		1	2		1	1.12	62.0
	%	6	5		1	20	10	18	12	4	7	13	13		3	4		3	1.36	65.0

Note: *sd* = 10 aberrations in calculations

Table 3-3. Summary of Chromosome Aberrations - Experiment 3, - S9, 18 hr. exposure for DPPC?NAC

DPPC/NAC (mg/ml)	Cells	Not Computed				Chromatid Type						Chromosome Type					Other Types		No. of Aberrations Per Cell	% of Cells with Aberrations
						Simple		Complex				Simple		Complex						
		tg	*sg*	*e*	*pp*	*tb*	*isb*	*tr*	*qr*	*cr*	*id*	*ci*	*sb*	*d*	*r*	*dm*	*pu*	*sd*		
0	100				2														0	0
	100				2														0	0
	%				2.0														0	0
5/1.5	100	1																	0	0
	100	1																	0	0
	%	1.0																	0	0
10/3.0	100				1														0	0
	100				1														0	0
	%				1.0														0	0
25/7.5	100				1														0	0
	100				1														0	0
	%				1.0														0	0
50/15	43																		0	0
	157			1	1														0	0
	%			0.5	0.5														0	0
Mitomycin C 0.5 g/ml	50	3	1			14	4	20	4	5	6	2	5	2	5	1		1	1.74	69.0
	50	3	1		1	6	2	11	4	2	6	1	5	1	4	1			0.98	63.0
	%	6	2		1	20	6	31	8	7	12	3	10	3	9	2		1	1.36	66.0

sd = 10 aberrations in calculations

DPPC-NAC/αT

Table 1. Relative Cell Growth for DPPC/NAC/alpha-tocopherol

	Experiment 1, - S9			Experiment 2, + S9			Experiment 3, - S9		
DPPC/NAC/α-T (mg/ml)	**Cells per flask (x 10^6)**	Mean (x 10^6)	Relative Cell Growth (%)	**Cells per flask (x 10^6)**	Mean (x 10^6)	Relative Cell Growth (%)	**Cells per flask (x 10^6)**	Mean (x 10^6)	Relative Cell Growth (%)
0	2.75 2.80	2.78	100	2.00 1.95	1.97	100	3.15 3.30	3.23	100
5/1.5/1.0	2.80 2.70	2.75	98	1.90 1.85	1.87	95	3.15 3.25	3.20	99
10/3.0/2.0	2.75 2.80	2.78	100	1.90 2.00	1.95	99	3.25 3.155	3.20	99
25/7.5/5.0	2.65 2.75	2.70	97	1.75 1.95	1.85	93	3.30 3.20	3.25	101
50/15/10	2.75 2.90	2.83	102	1.85 2.95	1.90	96	3.20 3.05	3.13	97

Table 2. Relative Mitotic Index for DPPC/NAC/α-T

	Experiment 1, - S9			Experiment 2, + S9			Experiment 3, - S9		
DPPC/NAC/αT (mg/ml)	**No. of dividing cells**	Mitotic index (%)	Relative mitotic index (%)	**No. of dividing cells**	Mitotic index	Relative mitotic index (%)	**No. of dividing cells**	Mitotic index (%)	Relative mitotic index (%)
0	150 155	30.5	100	140 130	27.0	100	70 55	12.5	100
5/1.5/1.0	160 145	30.5	100	150 135	28.5	105	55 60	11.5	92
10/3.0/2.0	140 160	30.0	98	145 150	29.5	109	60 70	13.0	104
25/7.5/5.0	140 150	29.0	95	135 165	29.5	109	60 55	11.5	92
50/15/10	130 150	28.0	92	160 145	30.5	112	60 60	12.0	96

Note: *No. of Dividing Cells* is counted from a total of 500 cells;
Mitotic Index is calculated as the number of dividing cells per hundred cells observed;
Relative Mitotic Index is mitotic index normalized against that of the negative control culture.

Table 3-1. Summary of Chromosome Aberrations - Experiment 1, - S9, 3 hr. exposure for DPPC Control/NAC/α-T

DPPC/NAC/αT (mg/ml)	Cells	Not Computed				Chromatid Type						Chromosome Type					Other Types		No. of Aberrations Per Cell	% of Cel with Aberra
						Simple		Complex				Simple	Complex							
		tg	*sg*	*e*	*pp*	*tb*	*isb*	*tr*	*qr*	*cr*	*id*	*ci*	*sb*	*d*	*r*	*dm*	*pu*	*sd*		
0	100																		0	0
	100																		0	0
	%																		0	0
5/1.5/1.0	100																		0	0
	100																		0	0
	%																		0	0
10/3.0/2.0	100																		0	0
	100																		0	0
	%																		0	0
25/7.5/5.0	100																		0	0
	100																		0	0
	%																		0	0
50/15/10	100																		0	0
	100																		0	0
	%																		0	0
Mitomycin C 0.5 g/ml	50					8	1	28	7	3	4	9	27		2			1	1.98	86
	50	2	1		1	24	3	27	6	4	5	12	15		4	1		3	2.62	84
	%	2.0	1		1	32	4	55	13	7	9	21	42		6	1		4	2.30	85

Note: *sd* = 10 aberrations in calculations

Table 3-2. Summary of Chromosome Aberrations - Experiment 2, +S9, 3 hr. exposure for DPPC/NAC/α-T

DPPC/NAC/γ-T (mg/ml)	Cells	Not Computed				Chromatid Type						Chromosome Type					Other Types		No. of Aberrations Per Cell	% of Cells with Aberrations
						Simple			Complex				Simple		Complex					
		tg	*sg*	*e*	*pp*	*tb*	*isb*	*tr*	*qr*	*cr*	*id*	*ci*	*sb*	*d*	*r*	*dm*	*pu*	*sd*		
0	100				1														0	0
	100				1														0	0
	%				1.0														0	0
5/1.5/1.0	100				1														0	0
	100																		0	0
	%				0.5														0	0
10/3.0/2.0	100																		0	0
	100				1														0	0
	%				0.5														0	0
25/7.5/5.0	100																		0	0
	100																		0	0
	%																		0	0
50/15.0/10	100		1																0	0
	100		0.5																0	0
	%																		0	0
Cyclophosphamide 7.5 g/ml	50	3	3		1	10	8	12	7	3	3	2	4		1	1		2	1.42	66.0
	50	2	1		1	7	5	6	3	3	4	11	12		1	2			1.08	66.0
	%	5	4		2	17	13	18	10	6	7	13	16		2	3		2	1.25	66.0

Note: *sd* = 10 aberrations in calculations

Table 3-3. Summary of Chromosome Aberrations - Experiment 3, - S9, 18 hr. exposure for DPPC/NAC/α-T

DPPC/NAC/γT (mg/ml)	Cells	Not Computed				Chromatid Type						Chromosome Type						Other Types		No. of Aberrations Per Cell	% of Cells with Aberrations
						Simple		Complex				Simple		Complex							
		tg	*sg*	*e*	*pp*	*tb*	*isb*	*tr*	*qr*	*cr*	*id*	*ci*	*sb*	*d*	*r*	*dm*	*pu*	*sd*			
0	100				1															0	0
	100	1			1															0	0
	%	0.5			1.0															0	0
5/1.5/1.0	100	1																		0	0
	100																			0	0
	%	0.5																		0	0
10/3.0/2.0	100				1															0	0
	100				1															0	0
	%				1.0															0	0
25/7.5/5.0	100				1															0	0
	100				1															0	0
	%				1.0															0	0
50/15/10	43				2															0	0
	157				1															0	0
	%				1.5															0	0
Mitomycin C 0.5 g/ml	50	3	1			18	4	22	4	6	5	2	5	1	4	1		1		1.64	66.0
	50	2			1	8	4	13	3	2	6	2	4	1	2					0.90	68.0
	%	5	1		1	26	8	35	7	8	11	4	9	2	6	1		1		1.27	67.0

sd = 10 aberrations in calculations

DPPC-NAC/γT

Table 1. Relative Cell Growth for DPPC/NAC/gamma-tocopherol

	Experiment 1, - S9			Experiment 2, + S9			Experiment 3, - S9		
DPPC/NAC/γ-T (mg/ml)	**Cells per flask (x 10^6)**	Mean (x 10^6)	Relative Cell Growth (%)	**Cells per flask (x 10^6)**	Mean (x 10^6)	Relative Cell Growth (%)	**Cells per flask (x 10^6)**	Mean (x 10^6)	Relative Cell Growth (%)
0	2.82 2.78	2.80	100	2.10 2.00	2.05	100	3.00 3.04	3.02	100
5/1.5/1.0	2.81 2.83	2.82	101	1.90 2.06	1.98	97	3.10 2.96	3.03	100
10/3.0/2.0	2.76 2.74	2.75	98	2.03 1.99	2.02	98	3.15 2.97	3.06	101
25/7.5/5.0	2.76 2.68	2.72	97	1.90 1.94	1.92	94	2.90 2.89	2.90	96
50/15/10	2.79 2.85	2.82	101	1.98 2.08	2.04	99	3.00 3.10	3.05	101

Table 2. Relative Mitotic Index **for DPPC/NAC/γ-T**

	Experiment 1, - S9			Experiment 2, + S9			Experiment 3, - S9		
DPPC/NAC/γ-T (mg/ml)	**No. of dividing cells**	Mitotic index (%)	Relative mitotic index (%)	**No. of dividing cells**	Mitotic index	Relative mitotic index (%)	**No. of dividing cells**	Mitotic index (%)	Relative mitotic index (%)
0	162 154	31.6	100	159 142	30.1	100	80 75	15.5	100
5/1.5/1.0	160 150	31.0	98	150 145	29.5	98	85 80	16.5	106
10/3.0/2.0	155 149	30.4	96	155 150	30.5	101	76 74	15.0	97
25/7.5/5.0	156 170	32.6	103	146 158	30.4	101	80 75	15.5	100
50/15/10	148 152	30.0	95	150 155	30.5	101	78 76	15.4	100

Note: *No. of Dividing Cells* is counted from a total of 500 cells;
Mitotic Index is calculated as the number of dividing cells per hundred cells observed;
Relative Mitotic Index is mitotic index normalized against that of the negative control culture.

Table 3-1. Summary of Chromosome Aberrations - Experiment 1, - S9, 3 hr. exposure for DPPC Control/NAC/γ-T

DPPC/NAC/γT (mg/ml)	Cells	Not Computed				Chromatid Type						Chromosome Type					Other Types		No. of Aberrations Per Cell	% of Cel with Aberra
						Simple		Complex				Simple		Complex						
		tg	*sg*	*e*	*pp*	*tb*	*isb*	*tr*	*qr*	*cr*	*id*	*ci*	*sb*	*d*	*r*	*dm*	*pu*	*sd*		
0	100				1														0	0
	100																		0	0
	%				0.5														0	0
5/1.5/1.0	100																		0	0
	100																		0	0
	%																		0	0
10/3.0/2.0	100																		0	0
	100																		0	0
	%																		0	0
25/7.5/5.0	100				1														0	0
	100				1														0	0
	%				1														0	0
50/15/10	100																		0	0
	100																		0	0
	%																		0	0
Mitomycin C 0.5 g/ml	50					8	1	28	7	3	4	9	27		2			1	1.98	86
	50	2	1		1	24	3	27	6	4	5	12	15		4	1		3	2.62	84
	%	2.0	1		1	32	4	55	13	7	9	21	42		6	1		4	2.30	85

Note: *sd* = 10 aberrations in calculations

Table 3-2. Summary of Chromosome Aberrations - Experiment 2, +S9, 3 hr. exposure for DPPC/NAC/γ-T

DPPC/NAC/γ-T (mg/ml)	Cells	Not Computed				Chromatid Type							Chromosome Type				Other Types		No. of Aberrations Per Cell	% of Cells with Aberrations
						Simple		Complex					Simple		Complex					
		tg	*sg*	*e*	*pp*	*tb*	*isb*	*tr*	*qr*	*cr*	*id*	*ci*	*sb*	*d*	*r*	*dm*	*pu*	*sd*		
0	100																		0	0
	100				1														0	0
	%				0.5														0	0
5/1.5/1.0	100				1														0	0
	100																		0	0
	%				0.5														0	0
10/3.0/2.0	100				1														0	0
	100				1														0	0
	%				1.0														0	0
25/7.5/5.0	100																		0	0
	100																		0	0
	%																		0	0
50/15.0/10	100				1														0	0
	100				1														0	0
	%				1.0														0	0
Cyclophosphamide 7.5 g/ml	50	3	3		1	10	8	12	7	3	3	2	4		1	1		2	1.42	66.0
	50	2	1		1	7	5	6	3	3	4	11	12		1	2			1.08	66.0
	%	5	4		2	17	13	18	10	6	7	13	16		2	3		2	1.25	66.0

Note: *sd* = 10 aberrations in calculations

Table 3-3. Summary of Chromosome Aberrations - Experiment 3, - S9, 18 hr. exposure for DPPC/NAC/γ-T

DPPC/NAC/γT (mg/ml)	Cells	Not Computed				Chromatid Type						Chromosome Type					Other Types		No. of Aberrations Per Cell	% of Cells with Aberrations
						Simple		Complex				Simple		Complex						
		tg	*sg*	*e*	*pp*	*tb*	*isb*	*tr*	*qr*	*cr*	*id*	*ci*	*sb*	*d*	*r*	*dm*	*pu*	*sd*		
0	100				2														0	0
	100				1														0	0
	%				1.5														0	0
5/1.5/1.0	100	1																	0	0
	100																		0	0
	%	0.5																	0	0
10/3.0/2.0	100				2														0	0
	100				2														0	0
	%				2.0														0	0
25/7.5/5.0	100																		0	0
	100				1														0	0
	%				0.5														0	0
50/15/10	100																		0	0
	100																		0	0
	%																		0	0
Mitomycin C 0.5 g/ml	50	3	1			18	4	22	4	6	5	2	5	1	4	1		1	1.64	66.0
	50	2			1	8	4	13	3	2	6	2	4	1	2				0.90	68.0
	%	5	1		1	26	8	35	7	8	11	4	9	2	6	1		1	1.27	67.0

sd = 10 aberrations in calculations

LITERATURE

Evans, H.J., Cytological Methods for Detecting Chemical Mutagens. In*: Chemical Mutagens, Principles and Methods for their Detection*, Vol. 4, Ed. A. Hollaender, Plenum Press, New York and London, pp. 1-29, 1976;

Galloway, S.M., Aardema, M.J., Ishidate, M.Jr., Ivett, J.L., Kirkland, D.J., Morita, T., Mosesso, P., Sofuni, T. Report From Working Group On *In Vitro* Tests For Chromosomal Aberrations. *Mutation Res*., 312:241-261, 1994;

Galloway, S.M., Armstrong, M.J., Reuben, C., Colman, S., Brown, B., Cannon, C., Bloom, A.D., Nakamura, F., Ahmed, M., Duk, S., Rimpo, J., Margolin, G.H., Resnick, M.A., Anderson, G. and Zeiger, E. Chromosome Aberrations and Sister Chromatid Exchanges in Chinese Hamster Ovary Cells: Evaluations of 108 Chemicals. *Environ. Mol. Mutagen* 10 (suppl. 10), 1-175, 1987;

FDA, 21 CFR, Part 58, Good Laboratory Practice for Nonclinical Laboratory Studies, National Archives and Records Administration, 2004;

OECD Guideline for the Testing of Chemicals. - 473. *In Vitro* Mammalian Chromosome Aberration Test., Adopted 21st July 1997;

OECD Principles of Good Laboratory Practice, 1998;

Scott, D., Dean, B.J., Danford, N.D. and Kirkland, D.J. Metaphase Chromosome Aberration Assays *In Vitro* In: *Basic Mutagenicity Tests: UKEMS Recommended Procedures*. Cambridge University Press, pp. 62-86, 1990;

Scott, D., Galloway, S.M., Marshall, R.R., Ishidate, M. Jr., Brusick, D., Ashby, J. and Myhr, B.C.Genotoxicity Under Extreme Culture Conditions. A Report from ICPEMC Task Group 9. *Mutation Res*., 257:147-204, 1991;

US Pharmacopeia 29. <791> pH, 2730-2731, 2006a;

US Pharmacopeia 29. <785> Osmolality and Osmolarity, 2718-2720, 2006b.

Appendix I. pH and Osmolality of Treatment Media for DPPC

Treatment medium	Experiment	S9	pH	Osmolality (mOsmol/kg)
Negative control	1	-	7.35	265
	2	+	7.42	314
	3	-	7.29	273
25 mg/ml	1	-	7.39	264
	2	+	7.47	319
	3	-	7.27	281
50 mg/ml	1	-	7.41	264

	2	+	7.50	320
	3	-	7.14	290

Note: The method used as reference: *US Pharmacopeia* (2006) 29 <791> for pH; <785> for osmolality.

Appendix I. pH and Osmolality of Treatment Media for DPPC/NAC

Treatment medium	Experiment	S9	pH	Osmolality (mOsmol/kg)
Negative control	1	-	7.37	260
	2	+	7.44	305
	3	-	7.25	279
25/7.5 mg/ml	1	-	7.40	267
	2	+	7.44	311
	3	-	7.28	280

50/15 mg/ml	1	-	7.43	269
	2	+	7.44	328
	3	-	7.25	305

Note: The method used as reference: *US Pharmacopeia* (2006) 29 <791> for pH; <785> for osmolality.

Appendix I. pH and Osmolality of Treatment Media for DPPC/NAC/αT

Treatment medium	Experiment	S9	pH	Osmolality (mOsmol/kg)
Negative control	1	-	7.34	266
	2	+	7.40	299
	3	-	7.30	283
25/7.5/5.0 mg/ml	1	-	7.38	262
	2	+	7.45	303

	3	-	7.31	290
50/15/10 mg/ml	1	-	7.41	262
	2	+	7.38	324
	3	-	7.27	298

Note: The method used as reference: *US Pharmacopeia* (2006) 29 <791> for pH; <785> for osmolality.

Appendix I. pH and Osmolality of Treatment Media for DPPC/NAC/γT

Treatment medium	Experiment	S9	pH	Osmolality (mOsmol/kg)
Negative control	1	-	7.35	268
	2	+	7.39	296
	3	-	7.31	286

25/7.5/5.0 mg/ml	1	-	7.39	265
	2	+	7.40	298
	3	-	7.32	292
50/15/10 mg/ml	1	-	7.40	265
	2	+	7.40	315
	3	-	7.33	294

Note: The method used as reference: *US Pharmacopeia* (2006) 29 <791> for pH; <785> for osmolality.

Appendix 2: Single dose acute intravenous toxicity study for four preparations in rodents

Haematology Group Summaries – End of Treatment Period – Males

Parameters	Unit	Group Means ± S.D. (n = 5)				
		Group 1 Control (Empty Liposome)	**Group 2 Liposome/NAC**	**Group 3 Liposome/α-toxopherol/NAC**	**Group 4 Liposome/γ-toxopherol/NAC**	**Normal Ranges**
RBC	$x10^{12}$ / L	6.88 ± 0.47	7.30 ± 0.20	7.11 ± 0.38	6.93 ± 0.28	4.9 – 9.8
Hb	g / L	143 ± 5	145 ± 6	145 ± 7	141 ± 2	131 – 184
Hct	%	39.6 ± 1.5	40.5 ± 1.7	40.5 ± 2.0	39.1 ± 0.4	42 – 52
MCV	fL	57.7 ± 2.7	55.5 ± 1.0	57.0 ± 1.4	56.5 ± 1.9	50 – 67
MCH	pg	20.9 ± 1.0	19.8 ± 0.4	20.3 ± 0.4	20.4 ± 0.7	17 – 23
MCHC	g / L	361 ± 5	357 ± 2	357 ± 2	362 ± 3	320 – 366
Platelets	$x10^{9}$ / L	1104 ± 38	1332 ± 93	1134 ± 64	1094 ± 189	474 – 1535
WBC	$x10^{9}$ / L	7.96 ± 1.33	5.58 ± 2.36	9.13 ± 2.76	4.17 ± 0.94	5.0 – 14.0
Neutrophils	$x10^{9}$ / L	0.96 ± 0.19	0.93 ± 0.33	1.31 ± 0.78	0.61 ± 0.10	0.3 – 2.1
Lymphocytes	$x10^{9}$ / L	6.73 ± 1.16	4.44 ± 2.05	7.57 ± 2.51	3.41 ± 0.82	2.5 – 12.8
Monocytes	$x10^{9}$ / L	0.16 ± 0.03	0.11 ± 0.05	0.15 ± 0.03	0.08 ± 0.02	0.1 – 0.4
Eosinophils	$x10^{9}$ / L	0.04 ± 0.02	0.05 ± 0.02	0.04 ± 0.01	0.03 ± 0.02	0 – 0.2
Basophils	$x10^{9}$ / L	0.02 ± 0.01	0.02 ± 0.01	0.03 ± 0.01	0.02 ± 0.01	0 – 0.1
LUC	$x10^{9}$ / L	0.05 ± 0.04	0.03 ± 0.02	0.03 ± 0.01	0.02 ± 0.01	0 – 0.2
Reticulocytes	$x10^{9}$ / L	365.0 ± 26.7	309.9 ± 27.5	338.3 ± 42.4	361.0 ± 69.8	Up to 400

Haematology Group Summaries – End of Treatment Period – Females

Parameters	Unit	Group Means ± S.D. (n = 5)				
		Group 1 Control (Empty Liposome)	**Group 2 Liposome/NAC (**	**Group 3 Liposome/α-toxopherol/NAC**	**Group 4 Liposome/γ-toxopherol/NAC**	**Normal Ranges**
RBC	$x10^{12}$ / L	7.31 ± 0.23	7.30 ± 0.40	7.25 ± 0.05	7.26 ± 0.40	6.6 – 8.7
Hb	g / L	146 ± 5	145 ± 5	146 ± 2	143 ± 4	133 – 157
Hct	%	39.6 ± 1.5	40.1 ± 1.9	39.7 ± 0.6	39.4 ± 0.9	40 – 50
MCV	fL	54.1 ± 2.0	54.9 ± 1.1	54.8 ± 0.5	54.3 ± 2.3	53 – 63
MCH	pg	20.0 ± 0.7	19.9 ± 0.5	20.2 ± 0.3	19.7 ± 0.7	18 – 22
MCHC	g / L	369 ± 5	362 ± 9	369 ± 6	363 ± 3	329 – 374
Platelets	$x10^{9}$ / L	1238 ± 93	1133 ± 75	882 ± 257	1020 ± 164	651 – 1567
WBC	$x10^{9}$ / L	5.23 ± 1.33	5.92 ± 2.05	5.54 ± 1.05	5.59 ± 3.19	4.3 – 15.0
Neutrophils	$x10^{9}$ / L	0.72 ± 0.53	0.72 ± 0.38	0.95 ± 0.36	1.25 ± 0.96	0.1 – 1.6
Lymphocytes	$x10^{9}$ / L	4.27 ± 1.03	5.02 ± 1.66	4.31 ± 1.10	4.06 ± 2.09	2.4 – 10.7
Monocytes	$x10^{9}$ / L	0.12 ± 0.07	0.08 ± 0.06	0.16 ± 0.04	0.16 ± 0.11	0 – 0.3
Eosinophils	$x10^{9}$ / L	0.08 ± 0.03	0.07 ± 0.03	0.08 ± 0.03	0.07 ± 0.04	0 – 0.2
Basophils	$x10^{9}$ / L	0.01 ± 0.00	0.01 ± 0.01	0.02 ± 0.01	0.02 ± 0.01	0 – 0.1
LUC	$x10^{9}$ / L	0.03 ± 0.02	0.02 ± 0.02	0.03 ± 0.01	0.04 ± 0.02	0 – 0.4
Reticulocytes	$x10^{9}$ / L	245.7 ± 20.8	206.7 ± 31.4	240.9 ± 34.6	263.7 ± 32.9	Up to 400

Coagulation Group Summaries – End of Treatment Period

Group	Parameter – Mean ± S.D. (n=5)		
	Prothrombin Time (sec.)	**APTT (sec.)**	**Fibrinogen (g/L)**
Group 1 Control (Empty Liposome) Male	17.9 ± 0.6	13.1 ± 2.0	2.92 ± 0.39
Group 2 Liposome/NAC Male	17.5 ± 0.5	15.4 ± 2.6	2.76 ± 0.08
Group 3 Liposome/α-toxopherol/NAC Male	17.9 ± 0.8	14.3 ± 1.9	2.88 ± 0.18
Group 4 Liposome/γ-toxopherol/NAC Male	17.4 ± 0.5	12.4 ± 0.8	2.51 ± 0.91
Group 1 Control (Empty Liposome) Female	16.3 ± 0.9	13.2 ± 2.8	2.49 ± 0.25
Group 2 Liposome/NAC Female	17.1 ± 1.6	13.4 ± 1.0	2.08 ± 0.76
Group 3 Liposome/α-toxopherol/NAC Female	17.2 ± 0.7	13.2 ± 2.7	2.08 ± 0.52
Group 4 Liposome/γ-toxopherol/NAC Female	16.2 ± 0.7	11.4 ± 1.9	2.50 ± 0.65
Normal Ranges	14.8 - 22.8	12.9 – 29.3	1.5 - 3.9

Serum Chemistry Group Summaries – Males – End of Treatment Period

Parameters	Unit	Group Means ± S.D. (n=5)				
		Group 1 Control (Empty Liposome)	**Group 2 Liposome/NAC**	**Group 3 Liposome/α-toxopherol/NAC**	**Group 4 Liposome/γ-toxopherol/NAC**	**Normal Ranges**
A/G	-	1.2 ± 0.0	1.3 ± 0.1	1.3 ± 0.1	1.3 ± 0.1	0.9 – 1.3
ALB	g / L	28 ± 1	29 ± 1	29 ± 1	29 ± 1	24 – 48
GLOB	g / L	23 ± 1	24 ± 1	23 ± 1	23 ± 1	22 – 39
ALP	u / L	191 ± 45	206 ± 42	207 ± 45	239 ± 35	75 – 435
Bil(T)	µmol / L	3.2 ± 1.6	2.1 ± 0.6	2.0 ± 0.4	2.8 ± 2.2	0.9 – 7.0
BUN	mmol / L	4.6 ± 0.9	4.1 ± 0.6	4.6 ± 0.4	4.4 ± 0.6	2.8 – 8.8
Ca	mmol / L	2.50 ± 0.05	2.49 ± 0.07	2.41 ± 0.05	2.52 ± 0.03	2.5 – 3.1
Cl	mmol / L	113 ± 1	112 ± 2	106 ± 1	105 ± 1	97 – 109
Creatinine	µmol / L	40 ± 3	35 ± 2	36 ± 3	34 ± 4	30 – 65
Glucose	mmol / L	5.8 ± 0.7	5.5 ± 0.6	6.7 ± 0.8	6.7 ± 0.4	1.0 – 8.6
LDH	u / L	3660 ± 1576	5621 ± 1555	4505 ± 574	3334 ± 2041	2127 - 6401
P	mmol / L	2.70 ± 0.15	2.79 ± 0.12	2.54 ± 0.08	2.95 ± 0.07	1.5 – 4.4
K	mmol / L	4.5 ± 0.2	4.7 ± 0.2	4.5 ± 0.1	4.6 ± 0.3	3.8 – 7.4
Protein (T)	g / L	51 ± 2	52 ± 2	52 ± 2	52 ± 2	52 – 80
AST	u / L	104 ± 16	128 ± 15	108 ± 9	125 ± 44	53 – 113
ALT	u / L	51 ± 4	50 ± 3	53 ± 3	55 ± 5	19 – 60
Na	mmol / L	142 ± 1	142 ± 1	141 ± 1	143 ± 1	140 – 153
Triglycerides	mmol / L	0.51 ± 0.20	0.38 ± 0.12	0.36 ± 0.21	0.35 ± 0.26	0.2 – 2.0
CK	u / L	534 ± 165	713 ± 152	594 ± 90	446 ± 290	228 - 529
Cholesterol	mmol / L	1.26 ± 0.10	1.41 ± 0.07	1.41 ± 0.23	1.28 ± 0.27	1.3 – 3.2

Serum Chemistry Group Summaries – Females – End of Treatment Period

Parameters	Unit	Group Means ± S.D. (n=5)				
		Group 1 Control (Empty Liposome)	**Group 2 Liposome/NAC**	**Group 3 Liposome/α-toxopherol/NAC**	**Group 4 Liposome/γ-toxopherol/NAC**	**Normal Ranges**
A/G	-	1.5 ± 0.1	1.3 ± 0.2	1.4 ± 0.1	1.3 ± 0.2	0.9 – 1.3
ALB	g / L	35 ± 1	34 ± 4	34 ± 2	35 ± 3	26 – 55
GLOB	g / L	24 ± 1	25 ± 1	24 ± 1	26 ± 1	23 – 36
ALP	u / L	132 ± 34	152 ± 31	116 ± 15	140 ± 51	74 – 435
Bil(T)	µmol / L	3.7 ± 1.0	4.8 ± 3.2	3.8 ± 2.4	5.0 ± 3.3	0.9 – 7.0
BUN	mmol / L	4.7 ± 0.4	4.3 ± 0.5	4.2 ± 0.2	5.5 ± 0.8	2.9 – 8.8
Ca	mmol / L	2.54 ± 0.05	2.55 ± 0.05	2.51 ± 0.07	2.59 ± 0.03	2.5 – 3.1
Cl	mmol / L	115 ± 2	114 ± 2	108 ± 3	106 ± 1	99 – 110
Creatinine	µmol / L	35 ± 4	33 ± 4	32 ± 3	34 ± 7	31 – 68
Glucose	mmol / L	7.1 ± 0.7	8.9 ± 2.1	6.6 ± 1.0	7.2 ± 2.1	1.0 – 8.1
LDH	u / L	3038 ± 1247	3321 ± 541	3039 ± 1245	3812 ± 1932	1455 - 3081
P	mmol / L	2.43 ± 0.09	2.73 ± 0.17	2.20 ± 0.09	2.41 ± 0.09	1.5 – 3.6
K	mmol / L	4.3 ± 0.2	4.7 ± 0.5	4.3 ± 0.3	4.7 ± 0.5	4.0 – 6.7
Protein (T)	g / L	59 ± 1	59 ± 3	58 ± 2	62 ± 3	54 – 85
AST	u / L	90 ± 14	103 ± 16	101 ± 31	119 ± 37	30 - 140
ALT	u / L	43 ± 4	33 ± 17	45 ± 3	46 ± 6	19 – 60
Na	mmol / L	142 ± 1	143 ± 1	143 ± 1	142 ± 1	140 – 150
Triglycerides	mmol / L	0.14 ± 0.05	0.10 ± 0.00	0.11 ± 0.03	0.10 ± 0.00	0.2 – 2.2
CK	u / L	528 ± 151	751 ± 455	553 ± 482	665 ± 653	158 - 556
Cholesterol	mmol / L	1.46 ± 0.25	1.64 ± 0.27	1.54 ± 0.21	1.64 ± 0.43	1.2 – 3.8

Appendix 3

APPENDIX 3- Acute toxicity effects following a single administration of the STIMAL formulations in male or female beagle dogs

Body Weights

Haematology Group Summaries – Prestudy

Parameters	Unit	Group Means ± S.D. (n = 9)			
		Males	Male Normal Ranges	Females	Female Normal Ranges
RBC	$x10^{12}$ / L	6.60 ± 0.42	5.24 - 7.63	6.51 ± 0.45	5.34 - 7.54
Hb	g / L	148 ± 9	116 - 175	146 ± 7	119 - 174
Hct	%	45.0 ± 2.9	34.3 - 51.0	44.2 ± 2.5	35.1 - 51.0
MCV	fL	68.2 ± 1.4	61.7 - 71.1	67.9 ± 1.9	61.7 - 71.9
MCH	pg	22.4 ± 0.4	21.0 - 24.3	22.4 ± 0.7	21.1 - 24.4
MCHC	g / L	329 ± 3	322 - 362	330 ± 5	323 - 358
Platelets	$x10^{9}$ / L	358 ± 64	187 - 626	419 ± 51	223 - 545
WBC	$x10^{9}$ / L	12.31 ± 2.15	5.47 - 17.95	13.25 ± 4.20	6.39 - 17.09
Neutrophils	$x10^{9}$ / L	6.92 ± 1.46	2.48 - 11.15	7.95 ± 3.84	3.01 - 10.44
Lymphocytes	$x10^{9}$ / L	4.30 ± 1.03	1.54 - 6.09	4.01 ± 1.24	1.63 - 6.38
Monocytes	$x10^{9}$ / L	0.66 ± 0.16	0.16 - 1.23	0.82 ± 0.31	0.23 - 1.16
Eosinophils	$x10^{9}$ / L	0.23 ± 0.12	0 - 0.62	0.26 ± 0.10	0 - 0.51
Basophils	$x10^{9}$ / L	0.15 ± 0.07	0 - 0.13	0.16 ± 0.08	0 - 0.13
LUC	$x10^{9}$ / L	0.06 ± 0.02	0 - 0.10	0.06 ± 0.03	0 - 0.10
Reticulocytes	$x10^{9}$ / L	78.6 ± 23.1	10 - 128.4	99.5 ± 22.5	10 - 123.2

Haematology Group Summaries – Male – 24 hours post-dose

Parameters	Unit	Group Means ± S.D. (n = 2)				
		Group 1 Empty Liposomes (60 mg/kg)	**Group 2 Liposomes + N-acetylcystein (60 mg/kg)**	**Group 3 Liposomes + α-tocopherol and NAC (60 mg/kg)**	**Group 4 Liposomes + γ-tocopherol and NAC (60 mg/kg)**	**Normal Ranges**
RBC	$x10^{12}$ / L	5.85 ± 0.24	5.84 ± 0.47	6.60 ± 1.12	6.50 ± 1.22	5.24 - 7.63
Hb	g / L	133 ± 7	134 ± 8	151 ± 23	148 ± 25	116 - 175
Hct	%	39.5 ± 2.7	38.9 ± 2.9	44.2 ± 6.2	43.9 ± 7.6	34.3 - 51.0
MCV	fL	67.5 ± 1.7	66.6 ± 0.5	67.2 ± 1.9	67.6 ± 0.8	61.7 - 71.1
MCH	pg	22.7 ± 0.3	23.0 ± 0.4	23.0 ± 0.5	22.8 ± 0.4	21.0 - 24.3
MCHC	g / L	337 ± 4	345 ± 3	342 ± 3	336 ± 1	322 - 362
Platelets	$x10^{9}$ / L	153 ± 62	215 ± 7	181 ± 10	156 ± 16	187 - 626
WBC	$x10^{9}$ / L	16.99 ± 2.99	15.62 ± 0.20	15.88 ± 5.34	10.29 ± 0.96	5.47 - 17.95
Neutrophils	$x10^{9}$ / L	12.24 ± 1.97	10.29 ± 0.45	13.28 ± 4.88	8.07 ± 1.47	2.48 - 11.15
Lymphocytes	$x10^{9}$ / L	3.65 ± 0.96	4.11 ± 0.59	2.01 ± 0.35	1.52 ± 0.40	1.54 - 6.09
Monocytes	$x10^{9}$ / L	0.53 ± 0.06	0.82 ± 0.04	0.27 ± 0.11	0.34 ± 0.01	0.16 - 1.23
Eosinophils	$x10^{9}$ / L	0.40 ± 0.04	0.25 ± 0.02	0.20 ± 0.09	0.20 ± 0.04	0 - 0.62
Basophils	$x10^{9}$ / L	0.12 ± 0.01	0.09 ± 0.01	0.08 ± 0.04	0.06 ± 0.05	0 - 0.13
LUC	$x10^{9}$ / L	0.05 ± 0.00	0.07 ± 0.00	0.05 ± 0.05	0.11 ± 0.11	0 - 0.10
Reticulocytes	$x10^{9}$ / L	238.0 ± 34.2	262.1 ± 63.9	327.8 ± 147.6	346.8 ± 122.3	10 - 128.4

Haematology Group Summaries – Male – Week 2

Parameters	Unit	Group Means ± S.D. (n = 2)				
		Group 1 Empty Liposomes (60 mg/kg)	**Group 2 Liposomes + N-acetylcystein (60 mg/kg)**	**Group 3 Liposomes + α-tocopherol and NAC (60 mg/kg)**	**Group 4 Liposomes + γ-tocopherol and NAC (60 mg/kg)**	**Normal Ranges**
RBC	$x10^{12}$ / L	6.11 ± 0.59	6.65 ± 0.18	6.21 ± 0.44	6.43 ± 0.36	5.24 - 7.63
Hb	g / L	133 ± 14	145 ± 6	137 ± 7	141 ± 6	116 - 175
Hct	%	42.0 ± 4.2	45.5 ± 2.1	42.0 ± 1.4	43.5 ± 2.1	34.3 - 51.0
MCV	fL	68.6 ± 0.9	68.0 ± 1.4	67.4 ± 2.0	68.3 ± 0.4	61.7 - 71.1
MCH	pg	21.8 ± 0.1	21.7 ± 0.3	22.1 ± 0.5	22.0 ± 0.4	21.0 - 24.3
MCHC	g / L	318 ± 1	319 ± 1	327 ± 3	322 ± 3	322 - 362
Platelets	$x10^{9}$ / L	422 ± 97	520 ± 41	426 ± 51	427 ± 156	187 - 626
WBC	$x10^{9}$ / L	12.01 ± 1.05	21.38 ± 0.83	16.61 ± 0.27	17.68 ± 3.86	5.47 - 17.95
Neutrophils	$x10^{9}$ / L	5.91 ± 0.21	12.82 ± 0.52	10.74 ± 1.66	10.26 ± 2.28	2.48 - 11.15
Lymphocytes	$x10^{9}$ / L	4.78 ± 0.73	6.39 ± 0.74	4.28 ± 1.52	5.58 ± 1.23	1.54 - 6.09
Monocytes	$x10^{9}$ / L	0.74 ± 0.19	1.58 ± 0.26	0.98 ± 0.01	1.25 ± 0.02	0.16 - 1.23
Eosinophils	$x10^{9}$ / L	0.45 ± 0.27	0.37 ± 0.32	0.47 ± 0.34	0.40 ± 0.17	0 - 0.62
Basophils	$x10^{9}$ / L	0.08 ± 0.05	0.11 ± 0.01	0.08 ± 0.02	0.08 ± 0.08	0 - 0.13
LUC	$x10^{9}$ / L	0.07 ± 0.03	0.13 ± 0.01	0.09 ± 0.05	0.12 ± 0.06	0 - 0.10
Reticulocytes	$x10^{9}$ / L	47.5 ± 3.5	76.5 ± 3.5	47.5 ± 0.7	67.5 ± 19.1	10 - 128.4

Haematology Group Summaries – Female – 24 hours post-dose

Parameters	Unit	Group Means ± S.D. (n = 2)				
		Group 1 Empty Liposomes (60 mg/kg)	**Group 2 Liposomes + N-acetylcystein (60 mg/kg)**	**Group 3 Liposomes + α-tocopherol and NAC (60 mg/kg)**	**Group 4 Liposomes + γ-tocopherol and NAC (60 mg/kg)**	**Normal Ranges**
RBC	$x10^{12}$ / L	6.25 ± 0.49	5.9 ± 0.66	6.88 ± 0.13	6.55 ± 0.04	5.34 - 7.54
Hb	g / L	141 ± 5	136 ± 16	157 ± 6	146 ± 4	119 - 174
Hct	%	41.2 ± 2.0	40.4 ± 4.1	45.7 ± 2.0	43.0 ± 0.4	35.1 - 51.0
MCV	fL	66.0 ± 2.1	68.6 ± 0.6	66.4 ± 1.7	65.6 ± 1.0	61.7 - 71.9
MCH	pg	22.5 ± 1.0	23.1 ± 0.1	22.8 ± 0.3	22.4 ± 0.5	21.1 - 24.4
MCHC	g / L	341 ± 4	336 ± 4	344 ± 4	341 ± 13	323 - 358
Platelets	$x10^{9}$ / L	197 ± 66	244 ± 82	145 ± 81	185 ± 49	223 - 545
WBC	$x10^{9}$ / L	11.63 ± 0.76	15.52 ± 4.24	8.45 ± 1.64	11.85 ± 0.02	6.39 - 17.09
Neutrophils	$x10^{9}$ / L	7.87 ± 1.12	9.23 ± 0.97	5.17 ± 0.34	8.65 ± 0.50	3.01 - 10.44
Lymphocytes	$x10^{9}$ / L	3.01 ± 0.23	4.89 ± 3.34	2.64 ± 1.17	2.31 ± 0.58	1.63 - 6.38
Monocytes	$x10^{9}$ / L	0.41 ± 0.02	0.68 ± 0.15	0.29 ± 0.09	0.32 ± 0.04	0.23 - 1.16
Eosinophils	$x10^{9}$ / L	0.23 ± 0.13	0.53 ± 0.28	0.20 ± 0.10	0.41 ± 0.00	0 - 0.51
Basophils	$x10^{9}$ / L	0.08 ± 0.02	0.12 ± 0.01	0.09 ± 0.02	0.10 ± 0.02	0 - 0.13
LUC	$x10^{9}$ / L	0.05 ± 0.01	0.09 ± 0.04	0.07 ± 0.04	0.06 ± 0.01	0 - 0.10
Reticulocytes	$x10^{9}$ / L	289.4 ± 59.1	268.7 ± 93.2	359.9 ± 8.8	327.5 ± 11.1	10 - 123.2

Haematology Group Summaries – Female – Week 2

Parameters	Unit	Group Means ± S.D. (n = 2)				
		Group 1 Empty Liposomes (60 mg/kg)	**Group 2 Liposomes + N-acetylcystein (60 mg/kg)**	**Group 3 Liposomes + α-tocopherol and NAC (60 mg/kg)**	**Group 4 Liposomes + γ-tocopherol and NAC (60 mg/kg)**	**Normal Ranges**
RBC	$x10^{12}$ / L	6.87 ± 0.40	6.66 ± 0.64	6.51 ± 0.77	6.42 ± 0.74	5.34 - 7.54
Hb	g / L	148 ± 3	149 ± 14	143 ± 17	141 ± 14	119 - 174
Hct	%	46.5 ± 0.7	46.5 ± 4.9	43.0 ± 4.2	41.5 ± 6.4	35.1 - 51.0
MCV	fL	67.7 ± 2.1	69.9 ± 0.2	66.0 ± 0.6	65.2 ± 2.5	61.7 - 71.9
MCH	pg	21.6 ± 0.9	22.4 ± 0.1	22.0 ± 0.0	22.1 ± 0.4	21.1 - 24.4
MCHC	g / L	319 ± 4	320 ± 0	334 ± 2	339 ± 18	323 - 358
Platelets	$x10^{9}$ / L	515 ± 86	489 ± 62	492 ± 32	431 ± 11	223 - 545
WBC	$x10^{9}$ / L	12.92 ± 2.81	14.12 ± 3.83	11.29 ± 0.41	12.46 ± 0.78	6.39 - 17.09
Neutrophils	$x10^{9}$ / L	7.33 ± 2.09	7.65 ± 1.99	6.36 ± 0.08	6.82 ± 0.31	3.01 - 10.44
Lymphocytes	$x10^{9}$ / L	4.18 ± 0.69	5.09 ± 2.22	3.71 ± 0.30	4.50 ± 0.42	1.63 - 6.38
Monocytes	$x10^{9}$ / L	1.10 ± 0.08	0.89 ± 0.18	0.88 ± 0.14	0.69 ± 0.05	0.23 - 1.16
Eosinophils	$x10^{9}$ / L	0.15 ± 0.01	0.29 ± 0.18	0.17 ± 0.04	0.31 ± 0.00	0 - 0.51
Basophils	$x10^{9}$ / L	0.08 ± 0.06	0.10 ± 0.00	0.08 ± 0.04	0.08 ± 0.00	0 - 0.13
LUC	$x10^{9}$ / L	0.10 ± 0.06	0.10 ± 0.01	0.10 ± 0.05	0.06 ± 0.01	0 - 0.10
Reticulocytes	$x10^{9}$ / L	42.0 ± 0.0	96.5 ± 78.5	20.0 ± 5.7	47.0 ± 4.2	10 - 123.2

Coagulation Group Summaries – 24 hours post-dose

Group	Parameter – Mean ± S.D. (n=2)		
	Prothrombin Time (sec.)	**APTT (sec.)**	**Fibrinogen (g/L)**
Group 1 Empty Liposomes (60 mg/kg) Male			
Group 2 Liposomes + N-acetylcystein (60 mg/kg) Male			
Group 3 Liposomes + α-tocopherol and NAC (60 mg/kg) Male			
Group 4 Liposomes + γ-tocopherol and NAC (60 mg/kg) Male			
Group 1 Empty Liposomes (60 mg/kg) Female			
Group 2 Liposomes + N-acetylcystein (60 mg/kg) Female			
Group 3 Liposomes + α-tocopherol and NAC (60 mg/kg) Female			
Group 4 Liposomes + γ-tocopherol and NAC (60 mg/kg) Female			
Normal Ranges	11.6 – 23.3	4.7 – 37.4	1.55 – 3.38

Coagulation Group Summaries – Week 2

Group	Parameter – Mean ± S.D. (n=2)		
	Prothrombin Time (sec.)	**APTT (sec.)**	**Fibrinogen (g/L)**
Group 1 Empty Liposomes (60 mg/kg) Male			
Group 2 Liposomes + N-acetylcystein (60 mg/kg) Male			
Group 3 Liposomes + α-tocopherol and NAC (60 mg/kg) Male			
Group 4 Liposomes + γ-tocopherol and NAC (60 mg/kg) Male			
Group 1 Empty Liposomes (60 mg/kg) Female			
Group 2 Liposomes + N-acetylcystein (60 mg/kg) Female			
Group 3 Liposomes + α-tocopherol and NAC (60 mg/kg) Female			
Group 4 Liposomes + γ-tocopherol and NAC (60 mg/kg) Female			
Normal Ranges	11.6 – 23.3	4.7 – 37.4	1.55 – 3.38

Serum Chemistry Group Summaries – Prestudy

Parameters	Unit	Group Means ± S.D. (n = 9)			
		Males	Male Normal Ranges	Females	Female Normal Ranges
A/G	-	1.3 ± 0.1	0.9 - 1.4	1.1 ± 0.1	0.7 - 1.5
ALB	g / L	29 ± 2	23 - 34	27 ± 2	21 - 33
GLOB	g / L	23 ± 2	21 - 29	23 ± 2	19 - 32
ALP	u / L	142 ± 24	69 - 176	129 ± 26	20 - 248
Bil(T)	µmol / L	< 1.7	0 - 5.5	2.0 ± 0.6	0 - 6.8
BUN	mmol / L	4.0 ± 0.9	2.5 - 7.0	4.1 ± 0.4	2.1 - 7.7
Ca	mmol / L	2.71 ± 0.06	2.54 - 2.92	2.61 ± 0.09	2.54 - 2.92
Cl	mmol / L	113 ± 2	108 - 122	113 ± 2	108 - 121
Creatinine	µmol / L	54 ± 5	44 - 73	54 ± 3	42 - 76
Glucose	mmol / L	5.1 ± 0.1	4.6 - 6.5	4.8 ± 0.5	4.3 - 6.7
LDH	u / L	296 ± 158	30 - 749	305 ± 100	30 - 675
P	mmol / L	2.38 ± 0.15	1.33 - 3.10	2.15 ± 0.10	1.37 - 3.08
K	mmol / L	4.7 ± 0.2	4.0 - 5.5	4.4 ± 0.3	3.9 - 5.4
Protein (T)	g / L	52 ± 2	47 - 60	50 ± 3	29 - 72
AST	u / L	42 ± 4	21 - 57	49 ± 14	23 - 55
ALT	u / L	29 ± 7	22 - 63	27 ± 7	25 - 56
Na	mmol / L	143 ± 1	139 - 152	144 ± 2	140 - 150
Triglycerides	mmol / L	0.19 ± 0.05	0.10 - 0.55	0.16 ± 0.06	0.04 - 0.56
CK	u / L	419 ± 236	100 - 519	456 ± 391	100 - 489
Cholesterol	mmol / L	4.02 ± 0.44	2.62 - 5.19	3.08 ± 0.42	2.39 - 5.19

Serum Chemistry Group Summaries – Male – 24 hours post-dose

Parameters	Unit	Group Means ± S.D. (n = 2)				
		Group 1 Empty Liposomes (60 mg/kg)	**Group 2 Liposomes + N-acetylcystein (60 mg/kg)**	**Group 3 Liposomes + α-tocopherol and NAC (60 mg/kg)**	**Group 4 Liposomes + γ-tocopherol and NAC (60 mg/kg)**	**Normal Ranges**
A/G	-	1.1 ± 0.1	1.1 ± 0.1	1.1 ± 0.1	0.9 ± 0.0	0.9 - 1.4
ALB	g / L	26 ± 0	26 ± 0	28 ± 1	26 ± 3	23 - 34
GLOB	g / L	25 ± 0	24 ± 1	26 ± 2	29 ± 4	21 - 29
ALP	u / L	194 ± 7	136 ± 27	132 ± 1	184 ± 58	69 - 176
Bil(T)	µmol / L	1.9 ± 0.3	< 1.7	2.4 ± 0.9	2.7 ± 0.4	0 - 5.5
BUN	mmol / L	3.7 ± 0.1	4.3 ± 1.0	3.3 ± 0.5	2.4 ± 0.0	2.5 - 7.0
Ca	mmol / L	2.68 ± 0.08	2.70 ± 0.06	2.56 ± 0.04	2.67 ± 0.23	2.54 - 2.92
Cl	mmol / L	115 ± 1	113 ± 2	113 ± 2	117 ± 1	108 - 122
Creatinine	µmol / L	53 ± 5	60 ± 5	50 ± 1	48 ± 6	44 - 73
Glucose	mmol / L	5.0 ± 0.1	5.2 ± 0.1	5.2 ± 0.5	5.2 ± 0.6	4.6 - 6.5
LDH	u / L	490 ± 421	215 ± 60	590 ± 560	482 ± 194	30 - 749
P	mmol / L	2.28 ± 0.02	2.15 ± 0.18	2.14 ± 0.15	2.04 ± 0.25	1.33 - 3.10
K	mmol / L	4.2 ± 0.1	4.2 ± 0.1	4.6 ± 0.8	4.3 ± 0.2	4.0 - 5.5
Protein (T)	g / L	51 ± 0	50 ± 1	54 ± 1	55 ± 6	47 - 60
AST	u / L	83 ± 13	50 ± 3	54 ± 1	54 ± 17	21 - 57
ALT	u / L	105 ± 57	35 ± 4	60 ± 31	35 ± 8	22 - 63
Na	mmol / L	140 ± 0	138 ± 0	140 ± 0	140 ± 2	139 - 152
Triglycerides	mmol / L	0.34 ± 0.01	0.23 ± 0.01	0.26 ± 0.08	0.24 ± 0.06	0.10 - 0.55
CK	u / L	299 ± 83	580 ± 245	220 ± 178	198 ± 63	100 - 519
Cholesterol	mmol / L	5.13 ± 0.37	5.39 ± 0.30	4.41 ± 0.62	6.04 ± 0.96	2.62 - 5.19
GGT	u / L	9 ± 3	7 ± 1	8 ± 2	7 ± 1	4 - 15

Serum Chemistry Group Summaries – Male – Week 2

Parameters	Unit	Group Means ± S.D. (n = 2)				
		Group 1 Empty Liposomes (60 mg/kg)	**Group 2 Liposomes + N-acetylcystein (60 mg/kg)**	**Group 3 Liposomes + α-tocopherol and NAC (60 mg/kg)**	**Group 4 Liposomes + γ-tocopherol and NAC (60 mg/kg)**	**Normal Ranges**
A/G	-	1.1 ± 0.1	1.0 ± 0.1	1.0 ± 0.2	1.1 ± 0.1	0.9 - 1.4
ALB	g / L	28 ± 0	27 ± 1	25 ± 2	26 ± 4	23 - 34
GLOB	g / L	26 ± 2	28 ± 2	28 ± 4	25 ± 1	21 - 29
ALP	u / L	177 ± 1	144 ± 18	123 ± 9	136 ± 23	69 - 176
Bil(T)	µmol / L	< 1.7	< 1.7	< 1.7	< 1.7	0 - 5.5
BUN	mmol / L	4.1 ± 1.2	4.7 ± 0.6	3.6 ± 0.1	3.7 ± 0.8	2.5 - 7.0
Ca	mmol / L	2.67 ± 0.04	2.73 ± 0.01	2.75 ± 0.01	2.75 ± 0.12	2.54 - 2.92
Cl	mmol / L	113 ± 1	113 ± 0	114 ± 0	116 ± 1	108 - 122
Creatinine	µmol / L	52 ± 1	62 ± 2	55 ± 1	57 ± 2	44 - 73
Glucose	mmol / L	4.8 ± 0.0	4.7 ± 0.1	4.8 ± 0.3	4.9 ± 0.1	4.6 - 6.5
LDH	u / L	304 ± 54	526 ± 79	265 ± 22	355 ± 284	30 - 749
P	mmol / L	2.22 ± 0.08	2.26 ± 0.23	2.23 ± 0.01	2.30 ± 0.13	1.33 - 3.10
K	mmol / L	4.6 ± 0.0	5.1 ± 0.1	4.8 ± 0.1	4.6 ± 0.1	4.0 - 5.5
Protein (T)	g / L	53 ± 1	54 ± 1	52 ± 1	51 ± 5	47 - 60
AST	u / L	50 ± 4	49 ± 6	40 ± 4	42 ± 1	21 - 57
ALT	u / L	36 ± 1	24 ± 2	24 ± 14	27 ± 4	22 - 63
Na	mmol / L	137 ± 1	138 ± 1	140 ± 0	139 ± 1	139 - 152
Triglycerides	mmol / L	0.22 ± 0.13	0.13 ± 0.01	0.14 ± 0.04	0.18 ± 0.08	0.10 - 0.55
CK	u / L	340 ± 125	336 ± 204	191 ± 40	260 ± 35	100 - 519
Cholesterol	mmol / L	3.89 ± 0.10	4.35 ± 0.00	3.51 ± 0.35	4.25 ± 0.26	2.62 - 5.19

Serum Chemistry Group Summaries – Female – 24 hours post-dose

Parameters	Unit	Group Means ± S.D. (n = 2)				
		Group 1 Empty Liposomes (60 mg/kg)	**Group 2 Liposomes + N-acetylcystein (60 mg/kg)**	**Group 3 Liposomes + α-tocopherol and NAC (60 mg/kg)**	**Group 4 Liposomes + γ-tocopherol and NAC (60 mg/kg)**	**Normal Ranges**
A/G	-	1.1 ± 0.0	1.1 ± 0.1	1.1 ± 0.1	1.2 ± 0.0	0.7 - 1.5
ALB	g / L	26 ± 1	26 ± 4	26 ± 0	29 ± 3	21 - 33
GLOB	g / L	24 ± 0	24 ± 0	25 ± 4	25 ± 2	19 - 32
ALP	u / L	151 ± 50	125 ± 28	130 ± 21	157 ± 13	20 - 248
Bil(T)	µmol / L	2.2 ± 0.3	< 1.7	< 1.7	4.0 ± 1.7	0 - 6.8
BUN	mmol / L	4.0 ± 0.3	4.2 ± 0.5	4.4 ± 0.2	3.5 ± 0.2	2.1 - 7.7
Ca	mmol / L	2.65 ± 0.05	2.68 ± 0.01	2.65 ± 0.01	2.67 ± 0.08	2.54 - 2.92
Cl	mmol / L	115 ± 1	118 ± 1	114 ± 1	112 ± 0	108 - 121
Creatinine	µmol / L	57 ± 3	54 ± 2	58 ± 0	49 ± 3	42 - 76
Glucose	mmol / L	5.2 ± 0.1	5.3 ± 0.5	5.1 ± 0.2	5.3 ± 0.4	4.3 - 6.7
LDH	u / L	360 ± 69	250 ± 4	325 ± 90	254 ± 125	30 - 675
P	mmol / L	2.06 ± 0.04	2.10 ± 0.04	2.00 ± 0.06	1.90 ± 0.12	1.37 - 3.08
K	mmol / L	4.0 ± 0.1	4.2 ± 0.4	4.2 ± 0.1	4.3 ± 0.1	3.9 - 5.4
Protein (T)	g / L	50 ± 0	50 ± 4	51 ± 3	54 ± 5	29 - 72
AST	u / L	77 ± 5	54 ± 8	46 ± 1	74 ± 44	23 - 55
ALT	u / L	52 ± 6	45 ± 8	28 ± 1	225 ± 274	25 - 56
Na	mmol / L	141 ± 1	140 ± 2	142 ± 2	140 ± 2	140 - 150
Triglycerides	mmol / L	0.33 ± 0.04	0.22 ± 0.02	0.34 ± 0.11	0.17 ± 0.00	0.04 - 0.56
CK	u / L	413 ± 120	399 ± 179	344 ± 45	200 ± 91	100 - 489
Cholesterol	mmol / L	3.90 ± 0.58	4.45 ± 0.51	3.87 ± 0.42	4.60 ± 0.33	2.39 - 5.19
GGT	u / L	7 ± 0	5 ± 0	6 ± 1	10 ± 3	3 - 9

Serum Chemistry Group Summaries – Female – Week 2

Parameters	Unit	Group Means ± S.D. (n = 2)				
		Group 1 Empty Liposomes (60 mg/kg)	**Group 2 Liposomes + N-acetylcystein (60 mg/kg)**	**Group 3 Liposomes + α-tocopherol and NAC (60 mg/kg)**	**Group 4 Liposomes + γ-tocopherol and NAC (60 mg/kg)**	**Normal Ranges**
A/G	-	1.2 ± 0.1	1.3 ± 0.0	1.1 ± 0.1	1.1 ± 0.0	0.7 - 1.5
ALB	g / L	29 ± 1	29 ± 3	25 ± 2	27 ± 3	21 - 33
GLOB	g / L	25 ± 1	23 ± 2	23 ± 0	25 ± 1	19 - 32
ALP	u / L	153 ± 42	122 ± 33	95 ± 3	123 ± 6	20 - 248
Bil(T)	µmol / L	2.2 ± 0.6	< 1.7	< 1.7	< 1.7	0 - 6.8
BUN	mmol / L	4.5 ± 0.7	4.9 ± 0.5	4.8 ± 1.4	4.2 ± 0.6	2.1 - 7.7
Ca	mmol / L	2.68 ± 0.02	2.62 ± 0.02	2.61 ± 0.18	2.71 ± 0.06	2.54 - 2.92
Cl	mmol / L	115 ± 2	116 ± 1	117 ± 4	115 ± 3	108 - 121
Creatinine	µmol / L	57 ± 2	49 ± 6	53 ± 1	54 ± 1	42 - 76
Glucose	mmol / L	4.7 ± 0.1	4.7 ± 1.2	4.8 ± 0.1	5.2 ± 0.6	4.3 - 6.7
LDH	u / L	465 ± 190	240 ± 175	184 ± 47	155 ± 25	30 - 675
P	mmol / L	2.18 ± 0.15	2.27 ± 0.00	1.96 ± 0.01	2.04 ± 0.01	1.37 - 3.08
K	mmol / L	4.8 ± 0.1	5.1 ± 0.6	4.3 ± 0.1	4.5 ± 0.1	3.9 - 5.4
Protein (T)	g / L	53 ± 0	51 ± 6	48 ± 1	53 ± 5	29 - 72
AST	u / L	52 ± 3	42 ± 3	40 ± 1	44 ± 1	23 - 55
ALT	u / L	39 ± 4	20 ± 1	26 ± 6	35 ± 12	25 - 56
Na	mmol / L	137 ± 0	138 ± 1	140 ± 1	140 ± 2	140 - 150
Triglycerides	mmol / L	0.15 ± 0.04	0.16 ± 0.04	0.12 ± 0.03	0.12 ± 0.01	0.04 - 0.56
CK	u / L	422 ± 149	226 ± 1	274 ± 139	188 ± 46	100 - 489
Cholesterol	mmol / L	2.90 ± 0.52	3.59 ± 0.15	2.78 ± 0.26	3.27 ± 0.23	2.39 - 5.19

APPENDIX 4

HISTOPATHOLOGY REPORT

Nucro-Technics Project: 197253

DETERMINATION OF THE MAXIMUM TOLERATED DOSE FOLLOWED BY AN ACUTE INTRAVENOUS TOXICITY STUDY OF THREE LIPOSOMAL ANTIOXIDANT FORMULATIONS IN BEAGLE DOGS

Study Design

Group	Treatment	Regimen	Days	Sex	Count	Slide Numbers
1	Control (Empty Liposomes)	0 mg/kg	15	Male Female	2 2	080149 – 080150 080151 – 080152
2	Test 1 (Liposomes and NAC)	60 mg/kg	15	Male Female	2 2	080153 – 080154 080155 – 080156
3	Test 2 (Liposomes/ αtocopherol and NAC)	60 mg/kg	15	Male Female	2 2	080157 – 080158 080159 – 080160
4	Test 3 (Liposomes/ γ-tocopherol and NAC)	60 mg/kg	15	Male Female	2 2	080161 – 080162 080163 – 080164

The test article was administered once via the *vena cephalica*. Animals were observed for 14 days and necropsy was performed on day 15.

Clinical Observations: Animals in all groups including Empty Liposomes control animals experienced substantial hypotension during and immediately after dosing, but all completely recovered within 15 – 30 minutes after dosing.

Clinical Pathology: Clinical pathology parameters were unremarkable with the exception of one single female dog (#016) dosed with the formulation of Liposomes, γ-tocopherol and NAC, which had approximately a 6-fold increase in ALT at 24 hours after dosing. On Day 5 post-dosing the ALT was approximately 3-fold the normal range, and at the end of the study it was normal.

Gross Necropsy: Necropsy finding
were unremarkable.

Histological Methods:
Hematoxylin and Eosin stained sections were provided from all the following tissues: Adrenal Gland; Aorta (thoracic); Brain; Cecum; Colon; Duodenum; Epididymides; Esophagus; Eyes; Heart; Ileum; Jejunum; Kidneys; Liver (sample of central and left lobes); Lungs (left and right diaphragmatic lobes); Lymph Node (Mandibular); Lymph Node (Mesenteric); Mammary Gland (inguinal); Optic Nerves (if present in routine sections); Ovaries; Pancreas; Pituitary; Prostate; Salivary Glands (Mandibular); Sciatic Nerve; Skeletal Muscle (quadriceps); Skin (inguinal); Spinal Cord; Spleen; Sternum and Marrow; Stomach; Testes; Thymus; Thyroid; Parathyroid; Tongue; Trachea; Urinary Bladder; Uterus (horns, cervix, body); Vagina.

Changes observed in tissues were graded on a scale of: None = 0; Minimal = 1; Mild = 2; Moderate = 3; Marked = 4; Severe = 5.

Results:

A list of grades for all tissues examined, with means are provided in Table 1.

Conditions of possible toxicological significance:
There were no conditions of possible toxicological significance.

Conditions of uncertain significance:
A single female treated with Liposomes/γ-tocopherol and NAC had a temporary increase in ALT. There were no tissue changes that indicated any unresolved injury.

Conditions lacking toxicological significance:
Hypotension which was rapidly resolved occurred during and immediately following treatment in animals in all dose groups.

Conclusions:
The intravenous administration of a single 60 mg/kg dose of Liposomes and NAC or Liposomes/α-tocopherol and NAC, or Liposomes/γ-tocopherol and NAC to beagle dogs caused no substantive clinical or pathological effects during the 14-day observation period.

Lawrence F. Fisher
Lawrence F. Fisher, DVM, PhD, DACVP

01 July 2008
Date

Histopathology Findings

Project: 197253 **Animal:** 002 **Sex:** Male **Pathology No.:** 080150 **Duration:** 15 Days

Group: 1 **Treatment:** Empty Liposomes

Regimen: 0 mg/kg

Tissue	Result	Slide No.	Grade	Description (i.e. No significant findings)
Brain (Hindbrain + Brain Stem)	Normal	-1	0	No significant findings
Brain (Forebrain + Mid Brain)	Normal	-2	0	No significant findings
Adrenals	Normal	-3	0	No significant findings
Pituitary	Normal	-3	0	No significant findings
Sciatic Nerve	Normal	-4	0	No significant findings
Cervical Spinal Cord	Normal	-5	0	No significant findings
Thoracic Spinal Cord	Normal	-6	0	No significant findings
Eye (Left)	Normal	-7	0	No significant findings
Optic Nerve - Left (if present)	Normal	-7	0	No significant findings
Eye (Right)	Normal	-8	0	No significant findings
Optic Nerve - Right (if present)	Normal	-8	0	No significant findings
Heart	Normal	-9	0	No significant findings
Lungs (left & right diaphragmatic lobes)	Normal	-10	0	No significant findings
Liver (sample of central & left lobes)	Normal	-11	0	No significant findings
Kidney (Left)	Normal	-12	0	No significant findings
Kidney (Right)	Normal	-13	0	No significant findings
Pancreas	Normal	-14	0	No significant findings
duodenum	Normal	-14	0	No significant findings
Spleen	Normal	-15	0	No significant findings
Jejunum	Normal	-15	0	No significant findings
Stomach	Normal	-16	0	No significant findings
Ileum	Normal	-17	0	No significant findings
Colon	Normal	-17	0	No significant findings
Mesenteric Lymph Nodes	Normal	-18	0	No significant findings
Cecum	Normal	-18	0	No significant findings
Mandibular Lymph Nodes	Normal	-19	0	No significant findings
Muscle (Quadriceps)	Normal	-20	0	No significant findings
Tongue	Normal	-20	0	No significant findings
Skin	Normal	-21	0	No significant findings
Thymus	Normal	-22	0	No significant findings
Lumbar Cord	Normal	-22	0	No significant findings
Thyroid (Left)	Normal	-23	0	No significant findings
Parathyroid - Left	Normal	-23	0	No significant findings
Thyroid (Right)	Normal	-24	0	No significant findings
Parathyroid - Right	Normal	-24	0	No significant findings
Sterum & Marrow	Normal	-25	0	No significant findings
Salivary Glands	Normal	-26	0	No significant findings
Testis - Left	Normal	-27	0	Immature
Epididymis - Left	Normal	-27	0	No significant findings
Testis - Right	Normal	-28	0	Immature
Epididymis - Right	Normal	-28	0	No significant findings
Prostate	Normal	-29	0	Immature
Bladder	Normal	-29	0	No significant findings
Esophagus	Normal	-30	0	No significant findings
Aorta	Normal	-30	0	No significant findings
Trachea	Normal	-31	0	No significant findings
Mediastinal Lymph Nodes	Abnormal	-32	3	Hemorrhage

Histopathology Findings

Project: 197253 **Animal:** 003 **Sex:** Male **Pathology No.:** 080153 **Duration:** 15 Days

Group: 2 **Treatment:** Liposomes and NAC

Regimen: 60 mg/kg

Tissue	Result	Slide No.	Grade	Description (i.e. No significant findings)
Brain (Hindbrain + Brain Stem)	Normal	-1	0	No significant findings
Brain (Forebrain + Mid Brain)	Normal	-2	0	No significant findings
Adrenals	Normal	-3	0	No significant findings
Pituitary	Normal	-3	0	No significant findings
Sciatic Nerve	Normal	-4	0	No significant findings
Cervical Spinal Cord	Normal	-5	0	No significant findings
Thoracic Spinal Cord	Normal	-6	0	No significant findings
Eye (Left)	Normal	-7	0	No significant findings
Optic Nerve - Left (if present)	Normal	-7	0	No significant findings
Eye (Right)	Normal	-8	0	No significant findings
Optic Nerve - Right (if present)	Normal	-8	0	No significant findings
Heart	Normal	-9	0	No significant findings
Lungs (left & right diaphragmatic lobes)	Abnormal	-10	3	Suppurative pneumonia
Liver (sample of central & left lobes)	Normal	-11	0	No significant findings
Kidney (Left)	Normal	-12	0	No significant findings
Kidney (Right)	Normal	-13	0	No significant findings
Pancreas	Normal	-14	0	No significant findings
duodenum	Normal	-14	0	No significant findings
Spleen	Normal	-15	0	No significant findings
Jejunum	Normal	-15	0	No significant findings
Stomach	Normal	-16	0	No significant findings
Ileum	Normal	-17	0	No significant findings
Colon	Normal	-17	0	No significant findings
Mesenteric Lymph Nodes	Normal	-18	0	No significant findings
Cecum	Normal	-18	0	No significant findings
Mandibular Lymph Nodes	Normal	-19	0	No significant findings
Muscle (Quadriceps)	Normal	-20	0	No significant findings
Tongue	Normal	-20	0	No significant findings
Skin	Normal	-21	0	No significant findings
Thymus	Normal	-22	0	No significant findings
Lumbar Cord	Normal	-22	0	No significant findings
Thyroid (Left)	Normal	-23	0	No significant findings
Parathyroid - Left	Normal	-23	0	No significant findings
Thyroid (Right)	Normal	-24	0	No significant findings
Parathyroid - Right	Normal	-24	0	No significant findings
Sterum & Marrow	Normal	-25	0	No significant findings
Salivary Glands	Normal	-26	0	No significant findings
Testis - Left	Normal	-27	0	Immature
Epididymis - Left	Normal	-27	0	No significant findings
Testis - Right	Normal	-28	0	Immature
Epididymis - Right	Normal	-28	0	No significant findings
Prostate	Normal	-29	0	Immature
Bladder	Normal	-29	0	No significant findings
Esophagus	Normal	-30	0	No significant findings
Aorta	Normal	-30	0	No significant findings
Trachea	Normal	-31	0	No significant findings

Histopathology Findings

Project: 197253 **Animal:** 004 **Sex:** Male **Pathology No.:** 080154 **Duration:** 15 Days

Group: 2 **Treatment:** Liposomes and NAC

Regimen: 60 mg/kg

Tissue	Result	Slide No.	Grade	Description (i.e. No significant findings)
Brain (Hindbrain + Brain Stem)	Normal	-1	0	No significant findings
Brain (Forebrain + Mid Brain)	Normal	-2	0	No significant findings
Adrenals	Normal	-3	0	No significant findings
Pituitary	Normal	-3	0	No significant findings
Sciatic Nerve	Normal	-4	0	No significant findings
Cervical Spinal Cord	Normal	-5	0	No significant findings
Thoracic Spinal Cord	Normal	-6	0	No significant findings
Eye (Left)	Normal	-7	0	No significant findings
Optic Nerve - Left (if present)	Normal	-7	0	No significant findings
Eye (Right)	Normal	-8	0	No significant findings
Optic Nerve - Right (if present)	Normal	-8	0	No significant findings
Heart	Normal	-9	0	No significant findings
Lungs (left & right diaphragmatic lobes)	Normal	-10	0	No significant findings
Liver (sample of central & left lobes)	Normal	-11	0	No significant findings
Kidney (Left)	Normal	-12	0	No significant findings
Kidney (Right)	Normal	-13	0	No significant findings
Pancreas	Normal	-14	0	No significant findings
duodenum	Normal	-14	0	No significant findings
Spleen	Normal	-15	0	No significant findings
Jejunum	Normal	-15	0	No significant findings
Stomach	Normal	-16	0	No significant findings
Ileum	Normal	-17	0	No significant findings
Colon	Normal	-17	0	No significant findings
Mesenteric Lymph Nodes	Normal	-18	0	No significant findings
Cecum	Normal	-18	0	No significant findings
Mandibular Lymph Nodes	Normal	-19	0	No significant findings
Muscle (Quadriceps)	Normal	-20	0	No significant findings
Tongue	Normal	-20	0	No significant findings
Skin	Normal	-21	0	No significant findings
Thymus	Normal	-22	0	No significant findings
Lumbar Cord	Normal	-22	0	No significant findings
Thyroid (Left)	Normal	-23	0	No significant findings
Parathyroid - Left	Normal	-23	0	No significant findings
Thyroid (Right)	Normal	-24	0	No significant findings
Parathyroid - Right	Normal	-24	0	No significant findings
Sterum & Marrow	Normal	-25	0	No significant findings
Salivary Glands	Normal	-26	0	No significant findings
Testis - Left	Normal	-27	0	Immature
Epididymis - Left	Normal	-27	0	No significant findings
Testis-Right	Normal	-28	0	Immature
Epididymis - Right	Normal	-28	0	No significant findings
Prostate	Normal	-29	0	Immature
Bladder	Normal	-29	0	No significant findings
Esophagus	Normal	-30	0	No significant findings
Aorta	Normal	-30	0	No significant findings
Trachea	Normal	-31	0	No significant findings

Histopathology Findings

Project: 197253 **Animal:** 005 **Sex:** Male **Pathology No.:** 080157 **Duration:** 15 Days

Group: 3 **Treatment:** Liposomes and α-tocopherol and NAC

Regimen: 60 mg/kg

Tissue	Result	Slide No.	Grade	Description (i.e. No significant findings)
Brain (Hindbrain + Brain Stem)	Normal	-1	0	No significant findings
Brain (Forebrain + Mid Brain)	Normal	-2	0	No significant findings
Adrenals	Normal	-3	0	No significant findings
Pituitary	Normal	-3	0	No significant findings
Sciatic Nerve	Normal	-4	0	No significant findings
Cervical Spinal Cord	Normal	-5	0	No significant findings
Thoracic Spinal Cord	Normal	-6	0	No significant findings
Eye (Left)	Normal	-7	0	No significant findings
Optic Nerve - Left (if present)	Normal	-7	0	No significant findings
Eye (Right)	Normal	-8	0	No significant findings
Optic Nerve - Right (if present)	Normal	-8	0	No significant findings
Heart	Normal	-9	0	No significant findings
Lungs (left & right diaphragmatic lobes)	Normal	-10	0	No significant findings
Liver (sample of central & left lobes)	Normal	-11	0	No significant findings
Kidney (Left)	Normal	-12	0	No significant findings
Kidney (Right)	Normal	-13	0	No significant findings
Pancreas	Normal	-14	0	No significant findings
duodenum	Normal	-14	0	No significant findings
Spleen	Normal	-15	0	No significant findings
Jejunum	Normal	-15	0	No significant findings
Stomach	Normal	-16	0	No significant findings
Ileum	Normal	-17	0	No significant findings
Colon	Normal	-17	0	No significant findings
Mesenteric Lymph Nodes	Normal	-18	0	No significant findings
Cecum	Normal	-18	0	No significant findings
Mandibular Lymph Nodes	Normal	-19	0	No significant findings
Muscle (Quadriceps)	Normal	-20	0	No significant findings
Tongue	Normal	-20	0	No significant findings
Skin	Normal	-21	0	No significant findings
Thymus	Abnormal	-22	2	Involution
Lumbar Cord	Normal	-22	0	No significant findings
Thyroid (Left)	Abnormal	-23	3	Cyst
Parathyroid - Left	Normal	-23	0	No significant findings
Thyroid (Right)	Abnormal	-24	2	C-cell hyerplasia
Parathyroid - Right	Normal	-24	0	No significant findings
Sterum & Marrow	Normal	-25	0	No significant findings
Salivary Glands	Normal	-26	0	No significant findings
Testis - Left	Normal	-27	0	Immature
Epididymis - Left	Normal	-27	0	No significant findings
Testis-Right	Normal	-28	0	Immature
Epididymis - Right	Normal	-28	0	No significant findings
Prostate	Normal	-29	0	Immature
Bladder	Normal	-29	0	No significant findings
Esophagus	Normal	-30	0	No significant findings
Aorta	Normal	-30	0	No significant findings
Trachea	Normal	-31	0	No significant findings

Histopathology Findings

Project: 197253 **Animal:** 006 **Sex:** Male **Pathology No.:** 080158 **Duration:** 15 Days

Group: 3 **Treatment:** Liposomes and α-tocopherol and NAC

Regimen: 60 mg/kg

Tissue	Result	Slide No.	Grade	Description (i.e. No significant findings)
Brain (Hindbrain + Brain Stem)	Normal	-1	0	No significant findings
Brain (Forebrain + Mid Brain)	Normal	-2	0	No significant findings
Adrenals	Normal	-3	0	No significant findings
Pituitary	Normal	-3	0	No significant findings
Sciatic Nerve	Normal	-4	0	No significant findings
Cervical Spinal Cord	Normal	-5	0	No significant findings
Thoracic Spinal Cord	Normal	-6	0	No significant findings
Eye (Left)	Normal	-7	0	No significant findings
Optic Nerve - Left (if present)	Normal	-7	0	No significant findings
Eye (Right)	Normal	-8	0	No significant findings
Optic Nerve - Right (if present)	Normal	-8	0	No significant findings
Heart	Normal	-9	0	No significant findings
Lungs (left & right diaphragmatic lobes)	Normal	-10	0	No significant findings
Liver (sample of central & left lobes)	Normal	-11	0	No significant findings
Kidney (Left)	Normal	-12	0	No significant findings
Kidney (Right)	Normal	-13	0	No significant findings
Pancreas	Normal	-14	0	No significant findings
duodenum	Normal	-14	0	No significant findings
Spleen	Normal	-15	0	No significant findings
Jejunum	Normal	-15	0	No significant findings
Stomach	Normal	-16	0	No significant findings
Ileum	Normal	-17	0	No significant findings
Colon	Normal	-17	0	No significant findings
Mesenteric Lymph Nodes	Normal	-18	0	No significant findings
Cecum	Normal	-18	0	No significant findings
Mandibular Lymph Nodes	Normal	-19	0	No significant findings
Muscle (Quadriceps)	Normal	-20	0	No significant findings
Tongue	Normal	-20	0	No significant findings
Skin	Abnormal	-21	2	Hyperkeratosis, focal
Thymus	Abnormal	-22	2	Involution
Lumbar Cord	Normal	-22	0	No significant findings
Thyroid (Left)	Normal	-23	0	No significant findings
Parathyroid - Left	Normal	-23	0	No significant findings
Thyroid (Right)	Normal	-24	0	No significant findings
Parathyroid - Right	Normal	-24	0	No significant findings
Sterum & Marrow	Normal	-25	0	No significant findings
Salivary Glands	Normal	-26	0	No significant findings
Testis - Left	Normal	-27	0	Immature
Epididymis - Left	Normal	-27	0	No significant findings
Testis-Right	Normal	-28	0	Immature
Epididymis - Right	Normal	-28	0	No significant findings
Prostate	Normal	-29	0	Immature
Bladder	Normal	-29	0	No significant findings
Esophagus	Normal	-30	0	No significant findings
Aorta	Normal	-30	0	No significant findings
Trachea	Normal	-31	0	No significant findings

Histopathology Findings

Project: 197253 **Animal:** 007 **Sex:** Male **Pathology No.:** 080161 **Duration:** 15 Days

Group: 4 **Treatment:** Liposomes and γ-tocopherol and NAC

Regimen: 60 mg/kg

Tissue	Result	Slide No.	Grade	Description (i.e. No significant findings)
Brain (Hindbrain + Brain Stem)	Normal	-1	0	No significant findings
Brain (Forebrain + Mid Brain)	Normal	-2	0	No significant findings
Adrenals	Normal	-3	0	No significant findings
Pituitary	Normal	-3	0	No significant findings
Sciatic Nerve	Normal	-4	0	No significant findings
Cervical Spinal Cord	Normal	-5	0	No significant findings
Thoracic Spinal Cord	Normal	-6	-	
Eye (Left)	Normal	-7	0	No significant findings
Optic Nerve - Left (if present)	Normal	-7	0	No significant findings
Eye (Right)	Normal	-8	0	No significant findings
Optic Nerve - Right (if present)	Normal	-8	0	No significant findings
Heart	Normal	-9	0	No significant findings
Lungs (left & right diaphragmatic lobes)	Normal	-10	0	No significant findings
Liver (sample of central & left lobes)	Normal	-11	0	No significant findings
Kidney (Left)	Normal	-12	0	No significant findings
Kidney (Right)	Normal	-13	0	No significant findings
Pancreas	Normal	-14	0	No significant findings
duodenum	Normal	-14	0	No significant findings
Spleen	Normal	-15	0	No significant findings
Jejunum	Normal	-15	0	No significant findings
Stomach	Normal	-16	0	No significant findings
Ileum	Normal	-17	0	No significant findings
Colon	Normal	-17	0	No significant findings
Mesenteric Lymph Nodes	Normal	-18	0	No significant findings
Cecum	Normal	-18	0	No significant findings
Mandibular Lymph Nodes	Normal	-19	0	No significant findings
Muscle (Quadriceps)	Normal	-20	0	No significant findings
Tongue	Normal	-20	0	No significant findings
Skin	Normal	-21	0	No significant findings
Thymus	Normal	-22	0	No significant findings
Lumbar Cord	Normal	-22	0	No significant findings
Thyroid (Left)	Normal	-23	0	No significant findings
Parathyroid - Left	Absent	-23	-	
Thyroid (Right)	Normal	-24	0	No significant findings
Parathyroid - Right	Normal	-24	0	No significant findings
Sterum & Marrow	Normal	-25	0	No significant findings
Salivary Glands	Normal	-26	0	No significant findings
Testis - Left	Normal	-27	0	Immature
Epididymis - Left	Normal	-27	0	No significant findings
Testis-Right	Normal	-28	0	No significant findings
Epididymis - Right	Normal	-28	0	No significant findings
Prostate	Normal	-29	0	Immature
Bladder	Normal	-29	0	No significant findings
Esophagus	Normal	-30	0	No significant findings
Aorta	Normal	-30	0	No significant findings
Trachea	Normal	-31	0	No significant findings

Histopathology Findings

Project: 197253 **Animal:** 008 **Sex:** Male **Pathology No.:** 080162 **Duration:** 15 Days

Group: 4 **Treatment:** Liposomes and γ-tocopherol and NAC

Regimen: 60 mg/kg

Tissue	Result	Slide No.	Grade	Description (i.e. No significant findings)
Brain (Hindbrain + Brain Stem)	Normal	-1	0	No significant findings
Brain (Forebrain + Mid Brain)	Normal	-2	0	No significant findings
Adrenals	Normal	-3	0	No significant findings
Pituitary	Absent	-3	-	
Sciatic Nerve	Normal	-4	0	No significant findings
Cervical Spinal Cord	Normal	-5	0	No significant findings
Thoracic Spinal Cord	Normal	-6	0	No significant findings
Eye (Left)	Normal	-7	0	No significant findings
Optic Nerve - Left (if present)	Normal	-7	0	No significant findings
Eye (Right)	Normal	-8	0	No significant findings
Optic Nerve - Right (if present)	Absent	-8	-	
Heart	Normal	-9	0	No significant findings
Lungs (left & right diaphragmatic lobes)	Normal	-10	0	No significant findings
Liver (sample of central & left lobes)	Normal	-11	0	No significant findings
Kidney (Left)	Normal	-12	0	No significant findings
Kidney (Right)	Normal	-13	0	No significant findings
Pancreas	Normal	-14	0	No significant findings
duodenum	Normal	-14	0	No significant findings
Spleen	Normal	-15	0	No significant findings
Jejunum	Normal	-15	0	No significant findings
Stomach	Normal	-16	0	No significant findings
Ileum	Normal	-17	0	No significant findings
Colon	Normal	-17	0	No significant findings
Mesenteric Lymph Nodes	Normal	-18	0	No significant findings
Cecum	Normal	-18	0	No significant findings
Mandibular Lymph Nodes	Normal	-19	0	No significant findings
Muscle (Quadriceps)	Normal	-20	0	No significant findings
Tongue	Normal	-20	0	No significant findings
Skin	Normal	-21	0	No significant findings
Thymus	Normal	-22	0	No significant findings
Lumbar Cord	Normal	-22	0	No significant findings
Thyroid (Left)	Abnormal	-23	2	C-cell hyperplasia
Parathyroid - Left	Normal	-23	0	No significant findings
Thyroid (Right)	Normal	-24	0	No significant findings
Parathyroid - Right	Normal	-24	0	No significant findings
Sterum & Marrow	Normal	-25	0	No significant findings
Salivary Glands	Normal	-26	0	No significant findings
Testis - Left	Normal	-27	0	Immature
Epididymis - Left	Normal	-27	0	No significant findings
Testis-Right	Normal	-28	0	Immature
Epididymis - Right	Normal	-28	0	No significant findings
Prostate	Normal	-29	0	Immature
Bladder	Normal	-29	0	No significant findings
Esophagus	Normal	-30	0	No significant findings
Aorta	Normal	-30	0	No significant findings
Trachea	Normal	-31	0	No significant findings

Histopathology Findings

Project: 197253 **Animal:** 009 **Sex:** Female **Pathology No.:** 080151 **Duration:** 15 Days

Group: 1 **Treatment:** Empty Liposomes

Regimen: 0 mg/kg

Tissue	Result	Slide No.	Grade	Description (i.e. No significant findings)
Brain (Hindbrain + Brain Stem)	Normal	-1	0	No significant findings
Brain (Forebrain + Mid Brain)	Normal	-2	0	No significant findings
Adrenals	Normal	-3	0	No significant findings
Pituitary	Absent	-3	-	
Sciatic Nerve	Normal	-4	0	No significant findings
Cervical Spinal Cord	Normal	-5	0	No significant findings
Thoracic Spinal Cord	Normal	-6	0	No significant findings
Eye (Left)	Normal	-7	0	No significant findings
Optic Nerve - Left (if present)	Normal	-7	0	No significant findings
Eye (Right)	Normal	-8	0	No significant findings
Optic Nerve - Right (if present)	Absent	-8	-	
Heart	Normal	-9	0	No significant findings
Lungs (left & right diaphragmatic lobes)	Normal	-10	0	No significant findings
Liver (sample of central & left lobes)	Normal	-11	0	No significant findings
Kidney (Left)	Normal	-12	0	No significant findings
Kidney (Right)	Normal	-13	0	No significant findings
Pancreas	Normal	-14	0	No significant findings
duodenum	Normal	-14	0	No significant findings
Spleen	Normal	-15	0	No significant findings
Jejunum	Normal	-15	0	No significant findings
Stomach	Normal	-16	0	No significant findings
Ileum	Normal	-17	0	No significant findings
Colon	Normal	-17	0	No significant findings
Mesenteric Lymph Nodes	Normal	-18	0	No significant findings
Cecum	Normal	-18	0	No significant findings
Mandibular Lymph Nodes	Normal	-19	0	No significant findings
Muscle (Quadriceps)	Normal	-20	0	No significant findings
Tongue	Normal	-20	0	No significant findings
Skin	Normal	-21	0	No significant findings
Mammary Gland	Normal	-21	0	No significant findings
Thymus	Normal	-22	0	No significant findings
Lumbar Cord	Normal	-22	0	No significant findings
Thyroid (Left)	Normal	-23	0	No significant findings
Parathyroid - Left	Normal	-23	0	No significant findings
Thyroid (Right)	Normal	-24	0	No significant findings
Parathyroid - Right	Normal	-24	0	No significant findings
Sterum & Marrow	Normal	-25	0	No significant findings
Salivary Glands	Normal	-26	0	No significant findings
Uterus (Horns, Cervix, Body)	Normal	-27	0	Immature
Vagina	Normal	-29	0	Immature
Ovaries	Normal	-29	0	Immature
Bladder	Normal	-29	0	No significant findings
Esophagus	Normal	-30	0	No significant findings
Aorta	Normal	-30	0	No significant findings
Trachea	Normal	-31	0	No significant findings

Histopathology Findings

Project: 197253 **Animal:** 010 **Sex:** Female **Pathology No.:** 080152 **Duration:** 15 Days

Group: 1 **Treatment:** Empty Liposomes

Regimen: 0 mg/kg

Tissue	Result	Slide No.	Grade	Description (i.e. No significant findings)
Brain (Hindbrain + Brain Stem)	Normal	-1	0	No significant findings
Brain (Forebrain + Mid Brain)	Normal	-2	0	No significant findings
Adrenals	Normal	-3	0	No significant findings
Pituitary	Normal	-3	0	No significant findings
Sciatic Nerve	Normal	-4	0	No significant findings
Cervical Spinal Cord	Normal	-5	0	No significant findings
Thoracic Spinal Cord	Normal	-6	0	No significant findings
Eye (Left)	Normal	-7	0	No significant findings
Optic Nerve - Left (if present)	Normal	-7	0	No significant findings
Eye (Right)	Normal	-8	0	No significant findings
Optic Nerve - Right (if present)	Normal	-8	0	No significant findings
Heart	Normal	-9	0	No significant findings
Lungs (left & right diaphragmatic lobes)	Normal	-10	0	No significant findings
Liver (sample of central & left lobes)	Normal	-11	0	No significant findings
Kidney (Left)	Normal	-12	0	No significant findings
Kidney (Right)	Normal	-13	0	No significant findings
Pancreas	Normal	-14	0	No significant findings
duodenum	Normal	-14	0	No significant findings
Spleen	Normal	-15	0	No significant findings
Jejunum	Normal	-15	0	No significant findings
Stomach	Normal	-16	0	No significant findings
Ileum	Normal	-17	0	No significant findings
Colon	Normal	-17	0	No significant findings
Mesenteric Lymph Nodes	Normal	-18	0	No significant findings
Cecum	Normal	-18	0	No significant findings
Mandibular Lymph Nodes	Normal	-19	0	No significant findings
Muscle (Quadriceps)	Normal	-20	0	No significant findings
Tongue	Normal	-20	0	No significant findings
Skin	Normal	-21	0	No significant findings
Mammary Gland	Normal	-21	0	No significant findings
Thymus	Normal	-22	0	No significant findings
Lumbar Cord	Normal	-22	0	No significant findings
Thyroid (Left)	Normal	-23	0	No significant findings
Parathyroid - Left	Normal	-23	0	No significant findings
Thyroid (Right)	Abnormal	-24	2	C-cell hyperplasia
Parathyroid - Right	Normal	-24	0	No significant findings
Sterum & Marrow	Normal	-25	0	No significant findings
Salivary Glands	Normal	-26	0	No significant findings
Uterus (Horns, Cervix, Body)	Normal	-27	0	Immature
Vagina	Normal	-29	0	Immature
Ovaries	Normal	-29	0	Immature
Bladder	Normal	-29	0	No significant findings
Esophagus	Normal	-30	0	No significant findings
Aorta	Normal	-30	0	No significant findings
Trachea	Normal	-31	0	No significant findings

Histopathology Findings

Project: 197253 **Animal:** 011 **Sex:** Female **Pathology No.:** 080155 **Duration:** 15 Days

Group: 2 **Treatment:** Liposomes and NAC

Regimen: 60 mg/kg

Tissue	Result	Slide No.	Grade	Description (i.e. No significant findings)
Brain (Hindbrain + Brain Stem)	Normal	-1	0	No significant findings
Brain (Forebrain + Mid Brain)	Normal	-2	0	No significant findings
Adrenals	Normal	-3	0	No significant findings
Pituitary	Normal	-3	0	No significant findings
Sciatic Nerve	Normal	-4	0	No significant findings
Cervical Spinal Cord	Normal	-5	0	No significant findings
Thoracic Spinal Cord	Normal	-6	0	No significant findings
Eye (Left)	Normal	-7	0	No significant findings
Optic Nerve - Left (if present)	Normal	-7	0	No significant findings
Eye (Right)	Normal	-8	0	No significant findings
Optic Nerve - Right (if present)	Normal	-8	0	No significant findings
Heart	Normal	-9	0	No significant findings
Lungs (left & right diaphragmatic lobes)	Normal	-10	0	No significant findings
Liver (sample of central & left lobes)	Normal	-11	0	No significant findings
Kidney (Left)	Normal	-12	0	No significant findings
Kidney (Right)	Normal	-13	0	No significant findings
Pancreas	Normal	-14	0	No significant findings
duodenum	Normal	-14	0	No significant findings
Spleen	Normal	-15	0	No significant findings
Jejunum	Normal	-15	0	No significant findings
Stomach	Normal	-16	0	No significant findings
Ileum	Normal	-17	0	No significant findings
Colon	Normal	-17	0	No significant findings
Mesenteric Lymph Nodes	Normal	-18	0	No significant findings
Cecum	Normal	-18	0	No significant findings
Mandibular Lymph Nodes	Normal	-19	0	No significant findings
Muscle (Quadriceps)	Normal	-20	0	No significant findings
Tongue	Normal	-20	0	No significant findings
Skin	Normal	-21	0	No significant findings
Mammary Gland	Absent	-21	-	
Thymus	Normal	-22	0	No significant findings
Lumbar Cord	Normal	-22	0	No significant findings
Thyroid (Left)	Normal	-23	0	No significant findings
Parathyroid - Left	Absent	-23	-	
Thyroid (Right)	Abnormal	-24	2	C-cell hyperplasia
Parathyroid - Right	Absent	-24	-	
Sterum & Marrow	Normal	-25	0	No significant findings
Salivary Glands	Normal	-26	0	No significant findings
Uterus (Horns, Cervix, Body)	Normal	-27	0	Immature
Vagina	Normal	-28	0	Immature
Ovaries	Normal	-29	0	No significant findings
Bladder	Normal	-29	0	No significant findings
Esophagus	Normal	-30	0	No significant findings
Aorta	Normal	-30	0	No significant findings
Trachea	Normal	-31	0	No significant findings

Histopathology Findings

Project: 197253 **Animal:** 012 **Sex:** Female **Pathology No.:** 080156 **Duration:** 15 Days

Group: 2 **Treatment:** Liposomes and NAC

Regimen: 60 mg/kg

Tissue	Result	Slide No.	Grade	Description (i.e. No significant findings)
Brain (Hindbrain + Brain Stem)	Normal	-1	0	No significant findings
Brain (Forebrain + Mid Brain)	Normal	-2	0	No significant findings
Adrenals	Normal	-3	0	No significant findings
Pituitary	Abnormal	-3	3	Cyst
Sciatic Nerve	Normal	-4	0	No significant findings
Cervical Spinal Cord	Normal	-5	0	No significant findings
Thoracic Spinal Cord	Normal	-6	0	No significant findings
Eye (Left)	Normal	-7	2	No significant findings
Optic Nerve - Left (if present)	Absent	-7	-	
Eye (Right)	Normal	-8	2	No significant findings
Optic Nerve - Right (if present)	Normal	-8	0	No significant findings
Heart	Normal	-9	0	No significant findings
Lungs (left & right diaphragmatic lobes)	Normal	-10	0	No significant findings
Liver (sample of central & left lobes)	Normal	-11	0	No significant findings
Kidney (Left)	Normal	-12	0	No significant findings
Kidney (Right)	Normal	-13	0	No significant findings
Pancreas	Normal	-14	0	No significant findings
duodenum	Normal	-14	0	No significant findings
Spleen	Normal	-15	0	No significant findings
Jejunum	Normal	-15	0	No significant findings
Stomach	Normal	-16	0	No significant findings
Ileum	Normal	-17	0	No significant findings
Colon	Normal	-17	0	No significant findings
Mesenteric Lymph Nodes	Normal	-18	0	No significant findings
Cecum	Normal	-18	0	No significant findings
Mandibular Lymph Nodes	Normal	-19	0	No significant findings
Muscle (Quadriceps)	Normal	-20	0	No significant findings
Tongue	Normal	-20	0	No significant findings
Skin	Normal	-21	0	No significant findings
Mammary Gland	Normal	-21	0	Immature
Thymus	Normal	-22	0	No significant findings
Lumbar Cord	Normal	-22	0	No significant findings
Thyroid (Left)	Normal	-23	0	No significant findings
Parathyroid - Left	Normal	-23	0	No significant findings
Thyroid (Right)	Normal	-24	0	No significant findings
Parathyroid - Right	Normal	-24	0	No significant findings
Sterum & Marrow	Normal	-25	0	No significant findings
Salivary Glands	Normal	-26	0	No significant findings
Uterus (Horns, Cervix, Body)	Normal	-27	0	Immature
Vagina	Normal	-28	0	Immature
Ovaries	Normal	-29	0	No significant findings
Bladder	Normal	-29	0	No significant findings
Esophagus	Normal	-30	0	No significant findings
Aorta	Normal	-30	0	No significant findings
Trachea	Normal	-31	0	No significant findings

Histopathology Findings

Project: 197253 **Animal:** 013 **Sex:** Female **Pathology No.:** 080159 **Duration:** 15 Days

Group: 3 **Treatment:** Liposomes and α-tocopherol and NAC

Regimen: 60 mg/kg

Tissue	Result	Slide No.	Grade	Description (i.e. No significant findings)
Brain (Hindbrain + Brain Stem)	Normal	-1	0	No significant findings
Brain (Forebrain + Mid Brain)	Normal	-2	0	No significant findings
Adrenals	Normal	-3	0	No significant findings
Pituitary	Normal	-3	0	No significant findings
Sciatic Nerve	Normal	-4	0	No significant findings
Cervical Spinal Cord	Normal	-5	0	No significant findings
Thoracic Spinal Cord	Normal	-6	0	No significant findings
Eye (Left)	Normal	-7	0	No significant findings
Optic Nerve - Left (if present)	Normal	-7	0	No significant findings
Eye (Right)	Normal	-8	0	No significant findings
Optic Nerve - Right (if present)	Normal	-8	0	No significant findings
Heart	Normal	-9	0	No significant findings
Lungs (left & right diaphragmatic lobes)	Normal	-10	0	No significant findings
Liver (sample of central & left lobes)	Normal	-11	0	No significant findings
Kidney (Left)	Normal	-12	0	No significant findings
Kidney (Right)	Abnormal	-13	2	Multifocal hemorrhage
Pancreas	Normal	-14	0	No significant findings
duodenum	Normal	-14	0	No significant findings
Spleen	Normal	-15	0	No significant findings
Jejunum	Normal	-15	0	No significant findings
Stomach	Normal	-16	0	No significant findings
Ileum	Normal	-17	0	No significant findings
Colon	Normal	-17	0	No significant findings
Mesenteric Lymph Nodes	Normal	-18	0	No significant findings
Cecum	Normal	-18	0	No significant findings
Mandibular Lymph Nodes	Normal	-19	0	No significant findings
Muscle (Quadriceps)	Normal	-20	0	No significant findings
Tongue	Normal	-20	0	No significant findings
Skin	Normal	-21	0	No significant findings
Mammary Gland	Normal	-21	0	No significant findings
Thymus	Normal	-22	0	No significant findings
Lumbar Cord	Normal	-22	0	No significant findings
Thyroid (Left)	Normal	-23	0	No significant findings
Parathyroid - Left	Normal	-23	0	No significant findings
Thyroid (Right)	Normal	-24	0	No significant findings
Parathyroid - Right	Normal	-24	0	No significant findings
Sterum & Marrow	Normal	-25	0	No significant findings
Salivary Glands	Normal	-26	0	No significant findings
Uterus (Horns, Cervix, Body)	Normal	-27	0	Immature
Vagina	Normal	-28	0	Immature
Ovaries	Normal	-29	0	No significant findings
Bladder	Normal	-29	0	No significant findings
Esophagus	Normal	-30	0	No significant findings
Aorta	Normal	-30	0	No significant findings
Trachea	Normal	-31	0	No significant findings

Histopathology Findings

Project: 197253 **Animal:** 014 **Sex:** Female **Pathology No.:** 080160 **Duration:** 15 Days

Group: 3 **Treatment:** Liposomes and α-tocopherol and NAC

Regimen: 60 mg/kg

Tissue	Result	Slide No.	Grade	Description (i.e. No significant findings)
Brain (Hindbrain + Brain Stem)	Normal	-1	0	No significant findings
Brain (Forebrain + Mid Brain)	Normal	-2	0	No significant findings
Adrenals	Normal	-3	0	No significant findings
Pituitary	Normal	-3	0	No significant findings
Sciatic Nerve	Normal	-4	0	No significant findings
Cervical Spinal Cord	Normal	-5	0	No significant findings
Thoracic Spinal Cord	Normal	-6	0	No significant findings
Eye (Left)	Normal	-7	0	No significant findings
Optic Nerve - Left (if present)	Normal	-7	0	No significant findings
Eye (Right)	Normal	-8	0	No significant findings
Optic Nerve - Right (if present)	Normal	-8	0	No significant findings
Heart	Normal	-9	0	No significant findings
Lungs (left & right diaphragmatic lobes)	Normal	-10	0	No significant findings
Liver (sample of central & left lobes)	Normal	-11	0	No significant findings
Kidney (Left)	Normal	-12	0	No significant findings
Kidney (Right)	Normal	-13	0	No significant findings
Pancreas	Normal	-14	0	No significant findings
duodenum	Normal	-14	0	No significant findings
Spleen	Normal	-15	0	No significant findings
Jejunum	Normal	-15	0	No significant findings
Stomach	Normal	-16	0	No significant findings
Ileum	Normal	-17	0	No significant findings
Colon	Normal	-17	0	No significant findings
Mesenteric Lymph Nodes	Normal	-18	0	No significant findings
Cecum	Normal	-18	0	No significant findings
Mandibular Lymph Nodes	Normal	-19	0	No significant findings
Muscle (Quadriceps)	Normal	-20	0	No significant findings
Tongue	Normal	-20	0	No significant findings
Skin	Normal	-21	0	No significant findings
Mammary Gland	Normal	-21	0	No significant findings
Thymus	Normal	-22	0	No significant findings
Lumbar Cord	Normal	-22	0	No significant findings
Thyroid (Left)	Abnormal	-23	2	C-cell hyperplasia
Parathyroid - Left	Normal	-23	0	No significant findings
Thyroid (Right)	Normal	-24	0	No significant findings
Parathyroid - Right	Normal	-24	0	No significant findings
Sterum & Marrow	Normal	-25	0	No significant findings
Salivary Glands	Normal	-26	0	No significant findings
Uterus (Horns, Cervix, Body)	Normal	-27	0	No significant findings
Vagina	Normal	-28	0	No significant findings
Ovaries	Normal	-29	0	No significant findings
Bladder	Normal	-29	0	No significant findings
Esophagus	Normal	-30	0	No significant findings
Aorta	Normal	-30	0	No significant findings
Trachea	Normal	-31	0	No significant findings

Histopathology Findings

Project: 197253 **Animal:** 015 **Sex:** Female **Pathology No.:** 080163 **Duration:** 15 Days

Group: 4 **Treatment:** Liposomes and γ-tocopherol and NAC

Regimen: 60 mg/kg

Tissue	Result	Slide No.	Grade	Description (i.e. No significant findings)
Brain (Hindbrain + Brain Stem)	Normal	-1	0	No significant findings
Brain (Forebrain + Mid Brain)	Normal	-2	0	No significant findings
Adrenals	Normal	-3	0	No significant findings
Pituitary	Normal	-3	0	No significant findings
Sciatic Nerve	Normal	-4	0	No significant findings
Cervical Spinal Cord	Normal	-5	0	No significant findings
Thoracic Spinal Cord	Normal	-6	0	No significant findings
Eye (Left)	Normal	-7	0	No significant findings
Optic Nerve - Left (if present)	Absent	-7	-	
Eye (Right)	Normal	-8	0	No significant findings
Optic Nerve - Right (if present)	Normal	-8	0	No significant findings
Heart	Normal	-9	0	No significant findings
Lungs (left & right diaphragmatic lobes)	Normal	-10	0	No significant findings
Liver (sample of central & left lobes)	Normal	-11	0	No significant findings
Kidney (Left)	Normal	-12	0	No significant findings
Kidney (Right)	Normal	-13	0	No significant findings
Pancreas	Normal	-14	0	No significant findings
duodenum	Normal	-14	0	No significant findings
Spleen	Normal	-15	0	No significant findings
Jejunum	Normal	-15	0	No significant findings
Stomach	Normal	-16	0	No significant findings
Ileum	Normal	-17	0	No significant findings
Colon	Normal	-17	0	No significant findings
Mesenteric Lymph Nodes	Normal	-18	0	No significant findings
Cecum	Normal	-18	0	No significant findings
Mandibular Lymph Nodes	Normal	-19	0	No significant findings
Muscle (Quadriceps)	Normal	-20	0	No significant findings
Tongue	Normal	-20	0	No significant findings
Skin	Normal	-21	0	No significant findings
Mammary Gland	Normal	-21	0	No significant findings
Thymus	Normal	-22	0	No significant findings
Lumbar Cord	Normal	-22	0	No significant findings
Thyroid (Left)	Normal	-23	0	No significant findings
Parathyroid - Left	Normal	-23	0	No significant findings
Thyroid (Right)	Normal	-24	0	No significant findings
Parathyroid - Right	Normal	-24	0	No significant findings
Sterum & Marrow	Normal	-25	0	No significant findings
Salivary Glands	Normal	-26	0	No significant findings
Uterus (Horns, Cervix, Body)	Normal	-27	0	No significant findings
Vagina	Normal	-28	0	No significant findings
Ovaries	Normal	-29	0	No significant findings
Bladder	Normal	-29	0	No significant findings
Esophagus	Normal	-30	0	No significant findings
Aorta	Normal	-30	0	No significant findings
Trachea	Normal	-31	0	No significant findings

Histopathology Findings

Project: 197253 **Animal:** 016 **Sex:** Female **Pathology No.:** 080164 **Duration:** 15 Days

Group: 4 **Treatment:** Liposomes and γ-tocopherol and NAC

Regimen: 60 mg/kg

Tissue	Result	Slide No.	Grade	Description (i.e. No significant findings)
Brain (Hindbrain + Brain Stem)	Normal	-1	0	No significant findings
Brain (Forebrain + Mid Brain)	Normal	-2	0	No significant findings
Adrenals	Normal	-3	0	No significant findings
Pituitary	Abnormal	-3	3	Cyst
Sciatic Nerve	Normal	-4	0	No significant findings
Cervical Spinal Cord	Normal	-5	0	No significant findings
Thoracic Spinal Cord	Normal	-6	0	No significant findings
Eye (Left)	Normal	-7	0	No significant findings
Optic Nerve - Left (if present)	Normal	-7	0	No significant findings
Eye (Right)	Normal	-8	0	No significant findings
Optic Nerve - Right (if present)	Absent	-8	-	
Heart	Normal	-9	0	No significant findings
Lungs (left & right diaphragmatic lobes)	Normal	-10	0	No significant findings
Liver (sample of central & left lobes)	Normal	-11	0	No significant findings
Kidney (Left)	Normal	-12	0	No significant findings
Kidney (Right)	Normal	-13	0	No significant findings
Pancreas	Normal	-14	0	No significant findings
duodenum	Normal	-14	0	No significant findings
Spleen	Normal	-15	0	No significant findings
Jejunum	Normal	-15	0	No significant findings
Stomach	Normal	-16	0	No significant findings
Ileum	Normal	-17	0	No significant findings
Colon	Normal	-17	0	No significant findings
Mesenteric Lymph Nodes	Normal	-18	0	No significant findings
Cecum	Normal	-18	0	No significant findings
Mandibular Lymph Nodes	Normal	-19	0	No significant findings
Muscle (Quadriceps)	Normal	-20	0	No significant findings
Tongue	Normal	-20	0	No significant findings
Skin	Normal	-21	0	No significant findings
Mammary Gland	Absent	-21	-	
Thymus	Normal	-22	0	No significant findings
Lumbar Cord	Normal	-22	0	No significant findings
Thyroid (Left)	Normal	-23	0	No significant findings
Parathyroid - Left	Normal	-23	0	No significant findings
Thyroid (Right)	Normal	-24	0	No significant findings
Parathyroid - Right	Normal	-24	0	No significant findings
Sterum & Marrow	Normal	-25	0	No significant findings
Salivary Glands	Normal	-26	0	No significant findings
Uterus (Horns, Cervix, Body)	Normal	-27	0	Immature
Vagina	Normal	-28	0	Immature
Ovaries	Normal	-29	0	Immature
Bladder	Normal	-29	0	No significant findings
Esophagus	Normal	-30	0	No significant findings
Aorta	Normal	-30	0	No significant findings
Trachea	Normal	-31	0	No significant findings

REPORT DOCUMENTATION PAGE

Form Approved
OMB No. 0704-0188

1. REPORT DATE *(DD-MM-YYYY)*	**2. REPORT TYPE**	**3. DATES COVERED** *(From - To)*
30/08/2008	Annual	1 Sept 2007- 30 August 2008

4. TITLE AND SUBTITLE

Development of the APC Biosensor as a diagnostic tool for infectious disease

5a. CONTRACT NUMBER
3000627138

5b. GRANT NUMBER
W81XH-06-2-0044

5c. PROGRAM ELEMENT NUMBER

6. AUTHOR(S)

Keith D. Crawford M.D., Ph.D.

5d. PROJECT NUMBER

5e. TASK NUMBER

5f. WORK UNIT NUMBER

7. PERFORMING ORGANIZATION NAME(S) AND ADDRESS(ES)

Brigham and Women's Hospital 75 Francis Street
Boston, MA 02115

8. PERFORMING ORGANIZATION REPORT NUMBER

9. SPONSORING / MONITORING AGENCY NAME(S) AND ADDRESS(ES)

U.S. Army Medical Research And Material Command Fort Detrick, Maryland 21702-5012

10. SPONSOR/MONITOR'S ACRONYM(S)

11. SPONSOR/MONITOR'S REPORT NUMBER(S)

12. DISTRIBUTION / AVAILABILITY STATEMENT

Approved for public release; distribution unlimited

13. SUPPLEMENTARY NOTES

14. ABSTRACT

Antigen presenting cells (APCs) are being utilized as a method to diagnose an infection. APCs characteristically search out "danger signals", (e.g. Infections, cancerous growth). Once in contact with pathogens, APC generate specific gene and protein signals (biomarkers), which when translated allow for the identification of the disease state and offending pathogen. It is the objective of this group to identify the anthrax-induced biomarkers and to develop a high-throughput platform for detection of exposure to anthrax.
Ideally, once completed the platform, over 24,000 potential victims can be screened in a day, compared to 3 weeks for 5,000 victims with current technology.

15. SUBJECT TERMS

Antigen presenting cells, dendritic cells, and biomarkers

16. SECURITY CLASSIFICATION OF:			**17. LIMITATION OF ABSTRACT**	**18. NUMBER OF PAGES**	**19a. NAME OF RESPONSIBLE PERSON**
a. REPORT	**b. ABSTRACT**	**c. THIS PAGE**			USAMRMC
U	U	U	UU		**19b. TELEPHONE NUMBER** *(include area code)*

Standard Form 298 (Rev. 8-98)
Prescribed by ANSI Std. Z39.18

TABLE OF CONTENTS

Page

Introduction

Infectious agents have been and will continue to be used as inexpensive weapons by bioterrorist. Advancing molecular biology techniques will allow easy manipulation of wild type or genetically modified pathogens into more harmful agents. The body's first line of defense against such agents is the immune system, which innately or adaptively protects against pathogens. A subset of immune cells, dendritic cells (DC) and monocytes (Mo) are APCs (Steinman 1991). These specialized immune cells are in all tissues of the body, especially at mucosal barriers. Once exposed to infectious or noninfectious agents, they phagocytize and transport pathogens to primary immune tissue. Once localized at this site, pathogen are degraded into peptides and presented to T cells. These antigen-specific T cells induce antibody production by B cells and directly prevent pathogen expansion in the host. In some case, pathogens evade the immune response and use the APCs as a replication site, as described for Marburg virus (Lambrecht 2001, Bosio 2004).

By sequestering antigens, APCs act as bio-concentrators rendering them an ideal immune cell for molecular analysis of gene and protein profiles. Previous studies have demonstrated, that DCs respond to pathogen exposure by altering gene expression. This altered gene expression is unique to the pathogen to which the DCs are exposed (Huang 2001). Thus, these unique changes in gene expression can be used to discriminate different pathogens (Reis & Sousa, 2001). We have taken this concept one step further and have successfully demonstrated the existence of pathogen-specific gene profiles with a nanoliter high throughput quantitative PCR. This technology is nanoliter fluidics technology platform for massively parallel and low-volume solution-phase reactions including analysis microarrays and PCR.

This nanoliter technology enables the processing of over 3000 assays on one microarray in 3.5 hours. Our preliminary data demonstrates that DC and Mo exposed to anthrax, Yesinia pestis, and various viruses have distinctive protein/peptide profiles. These profiles can be used to identify early exposure to a pathogen, preclinical state, as well as identify the pathogen. Future research involving the analysis of pathogen-

immune cell genes or proteins will lays the foundation for the development high throughput diagnostic chip, which will allow for the accurate and rapid detection of early pathogen exposure. Host response monitoring will undoubtfully improve our understanding of disease pathogenesis and assist in the development of possible new immunotherapeutic targets.

BODY

Key Research Accomplishments

The over all focus of our research efforts for this reporting period (September 2007-August 2008) has been on the characterization of the host-response evoked in antigen presenting cell populations by biological Category 1 agents.

Significant progress has been made on the remaining tasks: The results of these studies will allow us to design and test diagnostic RNA/DNA/protein microchips for large-scale screening and to determine the effect of antioxidant liposome preparations on cytokine profiles.

As to task 3: Determine whether the APC biosensor can be used as a diagnostic tool for infectious disease. Can one identify the type of pathogen from the genomic profiles caused by the infection? We have identified sets of genes whose transcripts are characteristically expressed by specific pathogens and characterized the biological basis of the pathogen specific signatures. Our findings improve our understanding of the role of B. anthracis toxins in anthrax pathogenesis. In addition, we have identified 6 candidate genes, which can serve as biomarkers for the rapid detection of exposure to B. anthracis exposure (Figure 4).

As to task 4: Determine whether APC cell population produces cytokine profiles that are distinctive of the infecting pathogen. Our finding real that the monitoring of the cytokine profile can serve as a means of demonstrating evidence of infection but these profiles are not pathogen specific. We have also been able to identify two new cytokines MIP-1α and MIP-1β, which when monitored in conjunction with IL-6, IL-8, and TNFα may serve as specific indicator of infection by extremely pathogenic organisms.

Reportable Outcomes

We have exposed APC populations to 4 pathogens (NERCE approved, YP, BA$^{+/-}$ (+ALO), BA$^{+/-}$(-ALO);B subtilis.) and obtained microarray data which define the gene networks turned on by specific pathogens at specific time points (Figure 1) and have defined the genes that are specifically induced for certain pathogens (Figure 2).

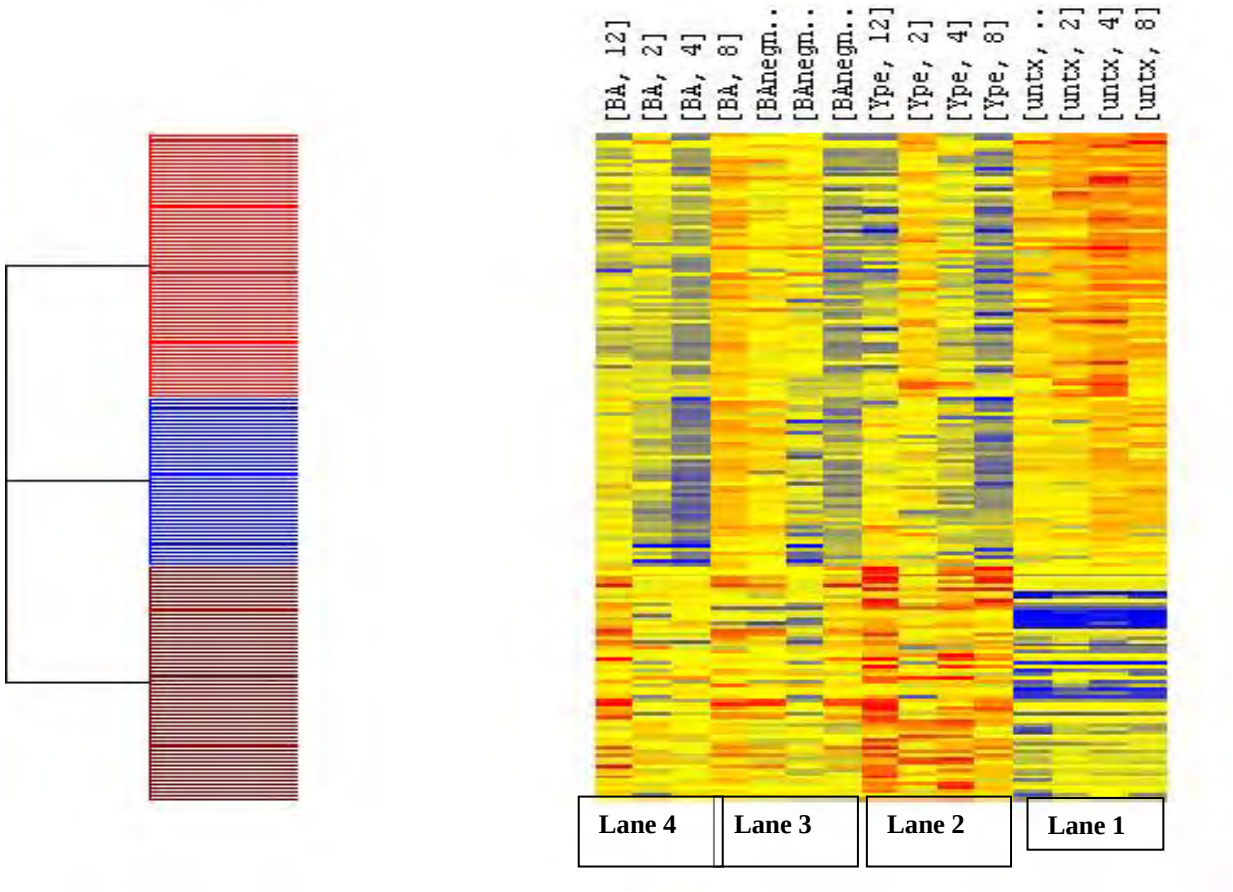

Figure 1. Overview of hierarchical clustering of all samples. Hierarchically clustered gene expression profile of DCs unexposed (lane 1) or exposed to

To assess the pathogen induce global transcription response, we used DNA microarrays containing 37,632 elements representing ~25,000 genes to characterize transcriptome of DC exposed to B. anthracis and Y. *pestis*. As shown in figure 2,

hierarchical clustering groups the samples into 4 major groups: infection-specific down regulated genes, Y. pestis upregulated genes, infection-specific up regulated genes, and B. anthracis-specific down regulated genes. This analysis demonstrated sets of gene whose transcripts are characteristically expressed by specific pathogens.
The results demonstrate high variation in transcript levels among the samples. Genes from the DC samples are organized by hierarchical clustering based on overall similarity in expression patterns. Expression patterns are represented by a color key in which bright red represents the highest level and bright blue represents the lowest levels, and darker shades represent intermediate levels of expression. Values were centered across all samples to a mean of zero. Gene clusters were labeled according to which samples have the highest relative gene expression.

Pathogen-Specific Differential Gene Expression

Gene regulation, which appears to be pathogen specific, was verified using Genespring software (Silicon Genetics, Redwood City, CA). A fold change analysis was performed on the normalized intensities of global genes expression in DCs treated with Y. *Pestis* , B. *anthracis* pOX$^{+/-}$ (+ALO), and B. *anthracis* pOX$^{+/-}$ (-ALO) versus the untreated DCs. Genes with at least a 5-fold increase or decrease between the untreated and treated DCs were deemed significant. Further analysis of the data revealed that 453 genes were uniquely modulated in DCs exposed to B. *anthracis* pOX$^{+/-}$ (+ALO), while 1206 genes were uniquely modulated in DCs exposed to B. *anthracis* pOX$^{+/-}$ (-ALO). Also, 1227 genes were uniquely modulated in DCs exposed to Y. *pestis* and 368 genes were uniquely modulated in DCs exposed to B. *anthracis* pOX$^{+/-}$ (+ALO).See (Figure 2)

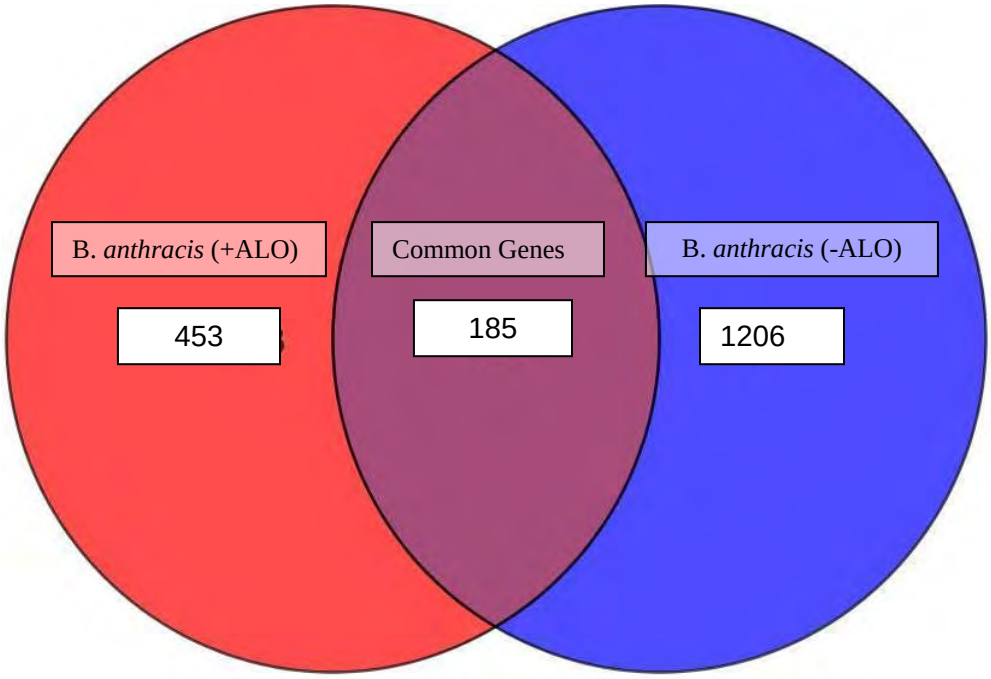

(A)

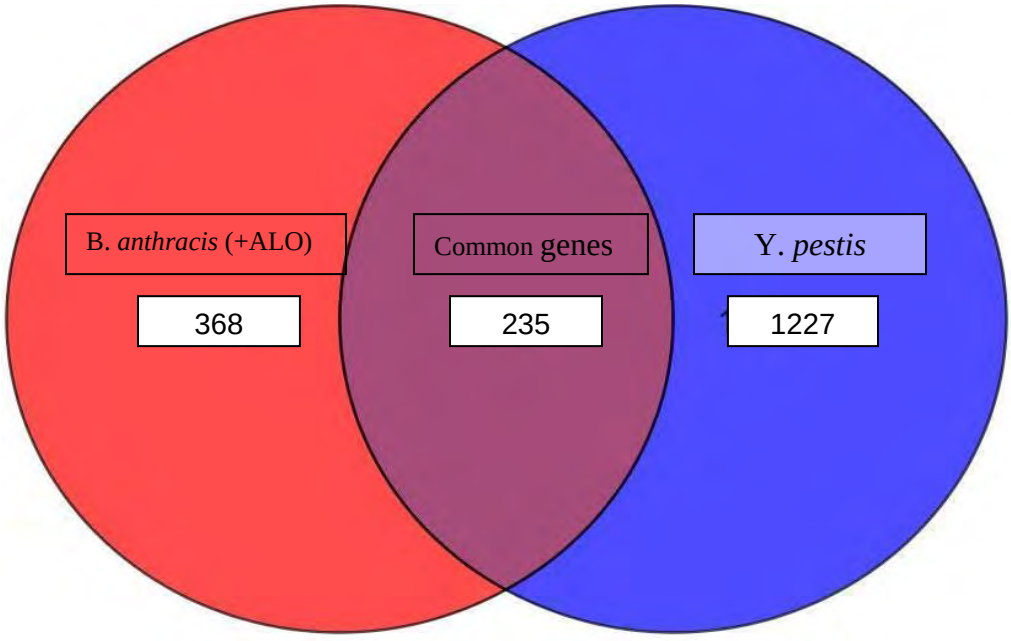

(B)

Figure 2. Comparative Gene Expression between Treated DCs. **(A)** B. *anthracis* pOX$^{+/-}$ (+ALO) and B. *anthracis* pOX$^{+/-}$ (-ALO) **(B)** B. *anthracis* pOX$^{+/-}$ (+ALO) and Y. *pestis*; at 8h pot exposure.

Biological Pathway Analysis

We also characterized the biological basis of the pathogen specific gene signatures with Ingenuity Pathway Analysis tool. This tool allow for the visualization of complex co-regulatory networks accompanying gene expression. We extracted disease and disorder networks from genes which were found specifically upregulated or downregulated in either B. *anthracis* pOX$^{+/-}$ (+ALO) or B. *anthracis* pOX$^{+/-}$ (-ALO) treated samples versus untreated samples (Figure 3). Genes that are associated with immunological diseases were subjected to further analysis (Table1-3).

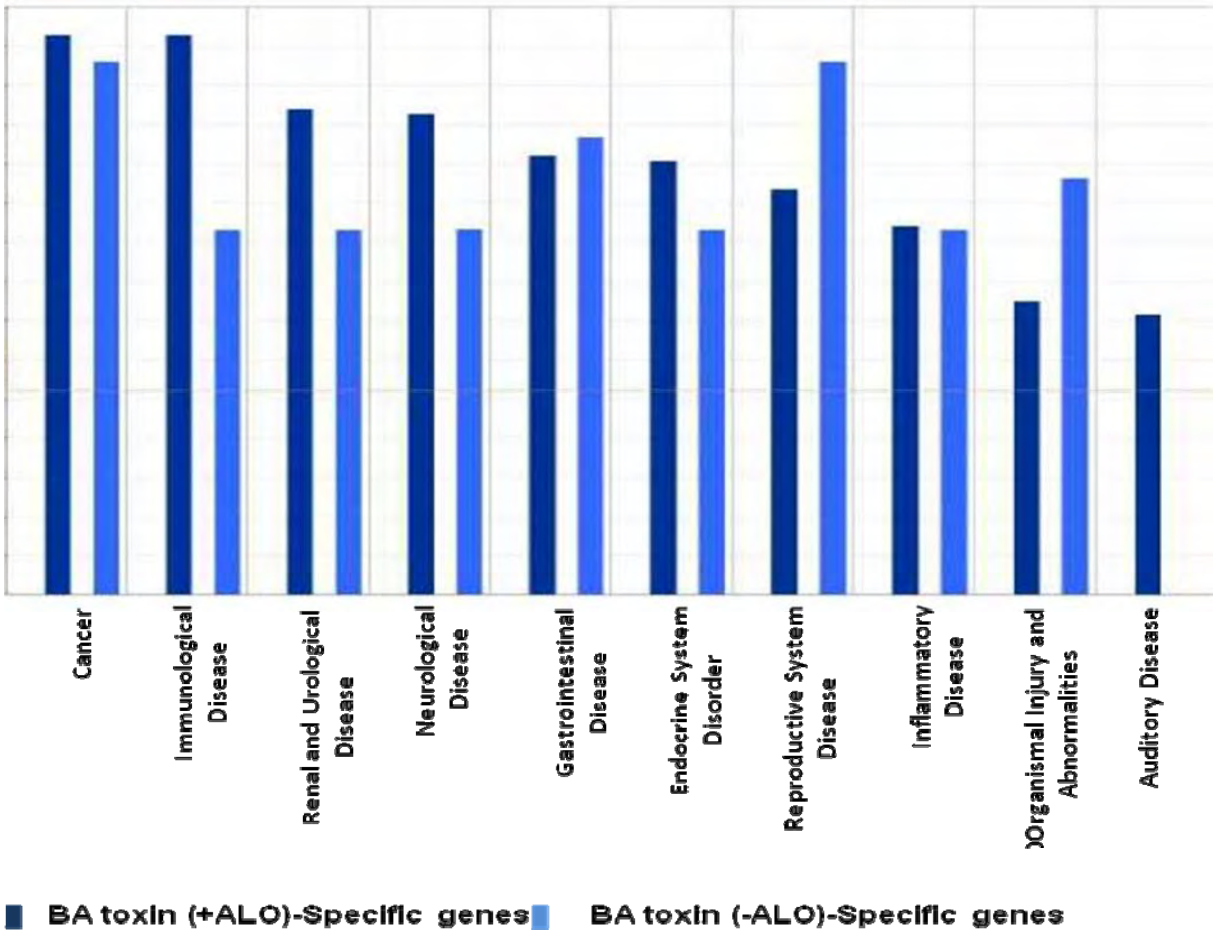

Figure 3. Biological Pathway Analysis of immunological disease associated genes uniquely induced in B. *anthracis* pOX$^{+/-}$ (+ALO) and B. *anthracis* pOX$^{+/-}$ (+ALO) treated DCs at 8h.

Table.1. Fold Changes of BA toxin (+ALO)-Specific induced Genes at 8h post exposure.

BA toxin (+ALO)	Fold Change	Up/Down regulation
MYBL1	7.1924047	up
PTEN	5.2649646	up
CDKN1A	6.7830853	up
SFRS3	10.0770645	down
VDR	7.8245826	down
KIT	7.329635	up
COL7A1	8.297253	up
IGKC	8.142859	up
SKP2	61.597275	up
KIT	7.329635	up
NTF5	5.5585203	up
PTAFR	6.5057373	up

Table 2. Fold Changes of BA toxin (-ALO)-Specific Induced Genes at 8h post exposure.

BA toxin (-ALO)	Fold Change	Up/Down regulation
ABCA1	9.949979	up
MARK2	8.470571	up
p27Kip1	6.082203	up
NPM1 (includes EG:4869)	9.188878	up
PTPN1	8.218369	up
WWOX	12.447507	up
XRCC5	15.596756	up
ABL1	19.132711	up
BGN	53.67799	up
BRCA1	99.70046	up
CCL3	7.964843	up
CHUK	14.251514	up
CSF1	5.843195	up
CSF2RA (includes EG:1438)	11.002402	up
DICER1	7.5122943	up
GH1	6.0626917	up
ICAM1	23.065355	up
IRF8	5.077209	down
ITGA2	16.192371	up
LGALS3	6.465258	up
MAPK14	6.0216446	up
PLCG2	9.017279	up
PML	168.18582	up
RIPK1	5.501172	up
SIGLEC12	5.603798	up
TOP2A	8.521007	up
TRAF1	6.496585	down
APAF1	7.455977	up
BIRC5	5.269616	down

Table 3. Roles of BA toxin (-ALO) -specific Induced Genes in the Process of Immunological Diseases

Molecules	Process	Process Annotation	P-value
ABCA1, MARK2	membranoproliferative glomerulonephritis	membranoproliferative glomerulonephritis	4.68E-03
p27Kip1, NPM1 (includes EG:4869), PTPN1, WWOX, XRCC5	formation	formation of lymphoma	8.32E-03
p27Kip1, PTPN1, XRCC5	formation	formation of non-hodgkin lymphoma	2.86E-02
ABL1, APAF1, BGN, BIRC5, BRCA1,	cell death	cell death of lymphatic system cells	2.26E-02
CCL3, p27Kip1, CHUK, CSF1, CSF2RA (includes EG:1438),		cell death of lymphatic system cells	2.26E-02
DICER1, GH1, ICAM1, IRF8, ITGA2, LGALS3,	cell death	cell death of lymphatic system cells	2.26E-02
MAPK14, PLCG2, PML, RIPK1, SIGLEC12, TOP2A, TRAF1, XRCC5	cell death	cell death of lymphatic system cells	2.26E-02
ABL1, BGN, BRCA1, CCL3, p27Kip1, CHUK, CSF1, CSF2RA (includes EG:1438),,	apoptosis	apoptosis of lymphatic system cells	2.33E-02
IRF8, ITGA2, LGALS3, MAPK14, PLCG2, PML, DICER1, GH1, ICAM1	apoptosis	apoptosis of lymphatic system cells	2.33E-02
RIPK1, SIGLEC12, TOP2A, TRAF1, XRCC5	apoptosis	apoptosis of lymphatic system cells	2.30E-02

Table 4. Roles of BA toxin (+ALO) -Specific Genes in the Process of Immunological Diseases

Molecules	Process	Process Annotation	P-value
MYBL1, PTEN	hyperplasia	hyperplasia of lymph node	2.67E-04
MYBL1	hyperplasia	hyperplasia of spleen	1.64E-02
MYBL1, PTEN	tumorigenesis	tumorigenesis of lymph node	3.84E-03
CDKN1A, MYBL1	growth	arrest in growth of lymphoma cell lines	8.93E-03
CDKN1A, MYBL1, SFRS3	growth	growth of lymphoma cell lines	3.12E-02
CDKN1A, MYBL1	developmental process	arrest in developmental process of lymphoma cell lines	1.10E-02
CDKN1A, MYBL1, SFRS3, VDR	developmental process	developmental process of lymphoma cell lines	2.07E-02
KIT	depletion	depletion of mast cells	1.64E-02
COL7A1	epidermolysis bullosa acquisita	epidermolysis bullosa acquisita	1.64E-02
MYBL1	hypoplasia	hypoplasia of white pulp	1.64E-02
SKP2	latency	latency of T-cell non-hodgkin lymphoma	1.64E-02
KIT	neoplasia	neoplasia of mast cells	1.64E-02
SKP2	penetrance	penetrance of T-cell non-hodgkin lymphoma	1.64E-02
KIT	urticaria pigmentosa	urticaria pigmentosa	1.64E-02
MYBL1, PTEN	disease	disease of lymph node	2.76E-02
IGKC, KIT, NTF5, PTAFR	hypersensitive reaction	hypersensitive reaction of rodents	2.78E-02

IGKC, KIT, NTF5, PTAFR	hypersensitive reaction	hypersensitive reaction of mammalia	2.90E-02

Table 5. RT-PCR validation of Immunological disease associated genes significantly altered in response to $BA^{+/-}$ (+ALO).

		Fold change	
GenBank ID	**Gene name**	**4h**	**12h**
NM_003017.3	splicing factor, arginine/serine-rich 3 (SFRS3)	3.07	5.02
NM_000376.2	vitamin D (1,25- dihydroxyvitamin D3) receptor (VDR), transcript variant 1	-8.57	12.74
NM_001017535.1	vitamin D (1,25- dihydroxyvitamin D3) receptor (VDR), transcript variant 2	-4.43	7.78
NM_139012.1	mitogen-activated protein kinase 14 (MAPK14), transcript variant 2	-3.19	0.95
NM_005983.2	S-phase kinase-associated protein 2 (p45) (SKP2), transcript variant 1	-4.31	1.08
NM_032637.2	S-phase kinase-associated protein 2 (p45) (SKP2), transcript variant 2	-4.61	0.56

Validation of gene transcription by real-time PCR

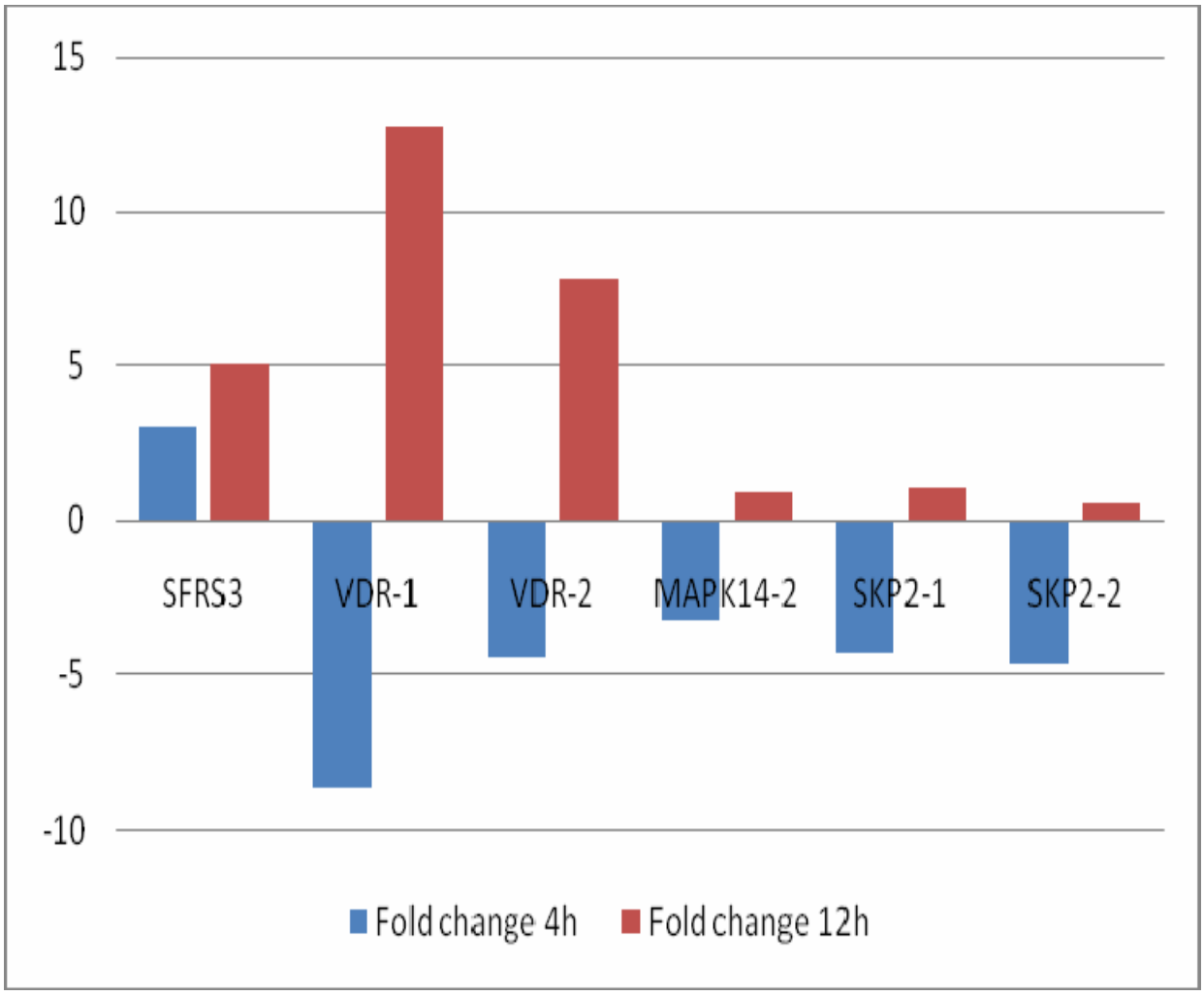

Figure 4. RT-PCR array analysis of DCs treated with $BA^{+/-}$(+ ALO) at 4h and 8h.

As to task 4: Determine whether APC cell population produces cytokine profiles that are distinctive of the infecting pathogen.

Extensive cytokine analysis has been performed on supernant obtained from pathogen exposed dendritic cells. Both innate and adaptive inflammatory cytokines were assessed (Figure 5). Whether dendritic cells were exposed to Y. pestis, B. anthracis, or B. substilis, no change in IL-2, IL-4, IL-5, and γ-IFN was noted (Figure 5a). In contrast, when the supernants were analyzed for the presence of a wide variety of inflammatory cytokines, significant changes in the expression levels of the cytokine production was noted after 8 hours. Next we assess the level of cytokine released and demonstrated that IL-1beta, IL-6, IL-8, IL-10, TNFα and TNFβ were expressed at various levels with IL-8 released at the highest level (Figure 5b). However, no change in the IL-beta and IL-12 cytokine production was noted. In contrast to Y. pestis treated-DC, DC exposed to B. anthracis and B. subtilis expressed comparable levels of IL-8 a lower ratios of B. anthracis (1:1,000 ratio). Of the 7 cytokines assessed, only IL-8 product was notably higher when DC were exposed to lower concentrations of the B. anthracis and subtlis. We next elected to increase the number of inflammatory mediator evaluated and assessed various more inflammatory cytokines, chemokines, and regulatory cytokines. Of the additional cytokines tested, only MIP-1α, MIP-1βIL-6 and TNFα found expressed at low levels in the first 4 hours but increased several fold over the base line. When treated samples were treated with liposome antioxidant, the level of cytokine production was suppress.